

**THE G PROTEIN-COUPPLING  
SPECIFICITY OF D<sub>2</sub>-LIKE DOPAMINE  
RECEPTORS**

**BY**

**JONATHAN ROBERT DAVID LANE**



**UNIVERSITY  
*of*  
GLASGOW**

**VOLUME 1**

**This thesis is presented for the degree of doctor of philosophy**

**May 2007**

**Institute of Biomedical and Life Sciences**

**University of Glasgow**

**© J. Robert Lane, 2007**

## Abstract

The G-protein coupling specificity of D<sub>2</sub>-like dopamine receptors was investigated using both receptor-G protein fusions and membranes of cells in which pertussis toxin-resistant mutants of individual G $\alpha_i$ -family G proteins could be expressed in an inducible fashion. A range of ligands displayed agonism at the long isoform of the human dopamine D<sub>2</sub> receptor. However, varying degrees of efficacy were observed for individual ligands as monitored by their capacity to load [<sup>35</sup>S] GTP $\gamma$ S onto each of G $\alpha_{i1}$ , G $\alpha_{i2}$ , G $\alpha_{i3}$  and G $\alpha_{o1}$ . By contrast, S-(-)-3-(3-hydroxyphenyl)-N-propylpiperidine (S-(-)-3PPP) was a partial agonist when G $\alpha_{o1}$  was the target G protein but an antagonist/inverse agonist at G $\alpha_{i1}$ , G $\alpha_{i2}$ , G $\alpha_{i3}$ . In ligand binding assays dopamine identified both high and low affinity states at each of the dopamine D<sub>2</sub> receptor-G protein fusion proteins and the high affinity state was eliminated by guanine nucleotide. S-(-)-3PPP bound to an apparent single state of the constructs where the D<sub>2</sub> receptor was fused to G $\alpha_{i1}$ , G $\alpha_{i2}$  or G $\alpha_{i3}$ . However, it bound to distinct high and low affinity states of the D<sub>2</sub> receptor-G $\alpha_{o1}$  fusion with the high affinity state being eliminated by guanine nucleotide. Similarly, although dopamine identified guanine nucleotide-sensitive high affinity states of the D<sub>2</sub> receptor when expression of pertussis toxin-resistant forms of either G $\alpha_{i2}$  or G $\alpha_{o1}$  was induced, S-(-)-3PPP identified a high affinity site only in the presence of G $\alpha_{o1}$ . These results demonstrate S-(-)-3PPP to be a protean agonist at the D<sub>2</sub> receptor and may explain *in vivo* actions of this ligand. Furthermore, in agreement with previous studies, the ability of the dopamine D<sub>2</sub> receptor to couple promiscuously to G $\alpha_{i1-3}$ , and G $\alpha_{o1}$  was demonstrated. However, despite high homology between dopamine D<sub>2</sub> and D<sub>3</sub> receptors, the G protein-coupling specificity of the D<sub>3</sub> receptor has not been well characterised. Again using both receptor-G protein fusions and membranes of cells in which pertussis toxin-resistant mutants of individual G $\alpha_i$ -family G proteins could be expressed in an inducible fashion, we confirmed the selective coupling of the D<sub>3</sub> receptor to G $\alpha_{o1}$ . A range of ligands displayed agonism at the

D<sub>21</sub> receptor and the D<sub>3</sub> receptor when coupled to G $\alpha_{o1}$ . As a general trend, agonists, including dopamine, displayed a higher potency at the D<sub>3</sub> receptor. This perhaps reflects the role of D<sub>3</sub> as an autoreceptor. Of particular interest was the demonstration that S-(-)-3PPP has both a higher efficacy and potency at the D<sub>3</sub> receptor when coupled to G $\alpha_{o1}$ .

The investigations into dopamine receptor-G protein coupling highlighted the utility of the [<sup>35</sup>S]GTP $\gamma$ S binding assay as a method of directly measuring receptor catalysed nucleotide exchange on the  $\alpha$  subunit of G proteins. However, the expense associated with the use of radiolabels makes this assay less attractive, particularly for high-throughput screening programmes. In an attempt to develop a non-radioactive assay equivalent to the [<sup>35</sup>S]GTP $\gamma$ S assay an immunisation programme was initiated to generate antibodies selective against the active (GTP bound) conformation of G proteins. 4 way primary screening of 1632 hybridomas generated from mice immunized with GTP $\gamma$ S-loaded G $\alpha_{i1}$  and isolated using an automated robotic colony picker, identified 3 antibodies that interacted with the constitutively active Q<sup>204</sup>L but neither the constitutively inactive G<sup>203</sup>A nor wild type form of G $\alpha_{i1}$ . This profile extended to other closely related G<sub>i</sub>-family G proteins but not to the less closely related G $\alpha_s$  and G $\alpha_q$ /G $\alpha_{11}$  families. Each of these antibodies was, however, also able to identify wild type, GDP-bound G<sub>i</sub>-family G proteins in the presence of AlF<sub>4</sub><sup>-</sup> which mimics the presence of the terminal phosphate of GTP and hence generates an active conformation of the G protein. Stimulation of cells co-expressing a wild type G<sub>i</sub> $\alpha$  subunit and the dopamine D<sub>2</sub> receptor with the agonist ligand nor-apomorphine also allowed these conformation selective antibodies to bind the G protein. Such reagents allow the development of label-free assays for G protein-coupled receptor-mediated activation of G<sub>i</sub>-family G proteins.

# Table of Contents

Abstract .....	II
Table of Contents .....	IV
List of Tables .....	XI
List of Figures .....	XIII
Acknowledgements .....	XX
Author's Declaration.....	XXI
Definitions.....	XXII
1 Introduction.....	1
1.1 G protein-coupled receptors.....	1
1.1.1 Structural features of G protein-coupled receptors .....	2
1.1.2 Classification of G protein-coupled receptors .....	4
1.1.3 Quaternary structure of GPCRs .....	6
1.2 Diversity of heterotrimeric G proteins and their effectors.....	7
1.2.1 Structural features of heterotrimeric G proteins.....	10
1.3 Structural basis of receptor-G protein interactions .....	13
1.3.1 Conformational changes associated with receptor activation .....	13
1.3.2 The receptor-G protein interface.....	14
1.3.3 Structural basis of receptor G protein coupling selectivity.....	15
1.3.4 Receptor domains involved in G protein coupling .....	16
1.3.5 Regions of G protein $\alpha$ subunits predicted to interact with GPCRs .....	22
1.3.6 Regions of G protein $\beta\gamma$ subunits predicted to interact with GPCRs.....	24
1.3.7 Strategies used to study receptor-G protein coupling .....	25
1.3.8 Molecular basis of G protein activation.....	31
1.4 Receptor theory, agonist directed receptor trafficking and protean agonism .....	38
1.4.1 Examples of functional selectivity.....	40

1.4.2	Evidence from kinetic & binding studies.....	41
1.4.3	Evidence from reversal of efficacy (protean agonism).....	42
1.4.4	Evidence from differential phosphorylation, desensitisation, internalisation and palmitoylation.....	42
1.5	Dopamine receptors .....	44
1.5.1	Classification of dopamine receptors.....	44
1.5.2	Localisation of dopamine receptor subtypes.....	46
1.5.3	Functions of dopamine receptors in the brain.....	47
1.5.4	Dopamine and disease.....	47
1.5.5	Dopamine receptor structure.....	50
1.5.6	Dopamine receptor pharmacology.....	53
1.5.7	Signal transduction of dopamine receptors.....	56
1.6	Project Aims.....	65
2	Materials and Methods.....	79
2.1	Materials.....	79
2.1.1	General Reagents, enzymes and kits.....	79
2.1.2	Pharmacological compounds .....	81
2.1.3	Radiochemicals .....	81
2.1.4	Tissue Culture .....	82
2.1.5	Antisera .....	83
2.2	Buffers and Reagents .....	83
2.2.1	Buffers and Reagents for molecular biology .....	83
2.2.2	Buffers and Reagents for biochemical assays.....	85
2.3	Molecular Biology .....	86
2.3.1	LB plates .....	86
2.3.2	Preparation of competent bacteria.....	86
2.3.3	Transformation of competent cell with plasmid DNA.....	87

2.3.4	Preparation of plasmid DNA.....	87
2.3.5	Quantification of DNA.....	89
2.3.6	Digestion of DNA with restriction endonucleases.....	89
2.3.7	Electrophoresis of agarose gels.....	90
2.3.8	Purification of DNA from agarose gels .....	90
2.3.9	Dephosphorylation of Vector DNA .....	91
2.3.10	Ligation of DNA fragments .....	91
2.3.11	Polymerase Chain Reaction .....	92
2.3.12	PCR for Mutagenesis (introduction of mutations using QuikChange site directed mutagenesis kit) .....	93
2.4	Generation of Dopamine receptor constructs.....	95
2.4.1	Dopamine Receptor subcloning into pcDNA3 .....	95
2.4.2	Construction of the Myc-Dopamine Receptor: G-protein $\alpha$ subunit fusion proteins 96	
2.4.3	Construction of Myc-D <sub>21</sub> -YFP fusion protein .....	99
2.5	G protein $\alpha$ subunit constructs .....	100
2.5.1	Generation of G protein mutants.....	100
2.6	Expression of G $\alpha_i$ family G-proteins in <i>E Coli</i> .....	102
2.7	Cell culture.....	103
2.7.1	Routine cell culture .....	103
2.7.2	Cell subculture .....	103
2.7.3	Coating of coverslips and 24 well plates with poly-D-lysine .....	104
2.7.4	Transient transfection using lipofectamine .....	104
2.7.5	Transfections using Effectene® for immunocytochemistry experiments..	105
2.7.6	Generation and maintenance of Flp-In T-REx cell lines inducibly expressing pertussis toxin insensitive G protein $\alpha$ subunits.....	106

2.7.7	Generation and maintenance double cell lines stably expressing Dopamine receptor and expressing pertussis toxin insensitive G protein $\alpha$ subunits from the inducible Flp-In locus .....	107
2.7.8	Induction of inducible gene of interest in Flp-In T-REx cells .....	107
2.7.9	Pertussis Toxin Treatment .....	107
2.7.10	Cell harvesting .....	108
2.7.11	Preparation of cell membranes.....	108
2.8	Protein Biochemistry.....	108
2.8.1	BCA protein quantification assay .....	108
2.8.2	Preparation of samples for SDS gel electrophoresis.....	109
2.8.3	SDS polyacrylamide gel electrophoresis (SDS PAGE).....	109
2.8.4	Western blotting.....	109
2.9	Pharmacological Assays .....	111
2.9.1	Radioligand binding.....	111
2.9.2	[ <sup>35</sup> S] GTP $\gamma$ S binding assays .....	112
2.9.3	Data analysis .....	113
2.10	Antibody Generation and Characterisation Protocols.....	114
2.10.1	Immunisation, hybridoma generation, tissue culture and antibody purification .....	114
2.10.2	ELISA assay.....	115
2.10.3	FMAT assay for screening of hybridoma clones.....	116
2.10.4	General FMAT assay protocol.....	117
2.10.5	Hybridoma expansion and immunoglobulin purification .....	118
2.10.6	Epitope Mapping of Antibodies using PepSet <sup>TM</sup> from Mimotopes .....	119
2.10.7	Immunocytochemistry .....	121
2.10.8	Epifluoresence Microscopy.....	123
3	Protean agonism at the dopamine D <sub>2</sub> receptor .....	124

3.1	Introduction.....	124
3.2	Results.....	127
3.2.1	Generation and characterisation of dopamine D <sub>21</sub> receptor: Cys→Ile G protein alpha subunit fusion proteins.....	127
3.2.2	The ligands p-tyramine and S-(-)-3-PPP only stimulate [ <sup>35</sup> S] GTPγS binding at the D <sub>21</sub> -Cys <sup>351</sup> Ile Gα <sub>o1</sub> fusion protein.....	130
3.2.3	S-(-)-3-PPP only shows a high affinity binding site in competition with [ <sup>3</sup> H] spiperone at D <sub>21</sub> -Cys <sup>351</sup> Ile Gα <sub>o1</sub> fusion protein.....	132
3.2.4	S-(-)-3-PPP acts as an antagonist or inverse agonist at D <sub>21</sub> -Cys→Ile Gα <sub>i1</sub> , Gα <sub>i2</sub> , Gα <sub>i3</sub> , but as a partial agonist at D <sub>21</sub> -Cys <sup>351</sup> Ile Gα <sub>o1</sub> .....	133
3.2.5	Generation and characterisation of stable cell lines expressing Gα <sub>i1</sub> , Gα <sub>i2</sub> , Gα <sub>i3</sub> , and Gα <sub>o1</sub> in an inducible manner.....	134
3.2.6	S-(-)-3-PPP stimulates the binding of [ <sup>35</sup> S] GTPγS upon induction of Cys <sup>351</sup> Ile Gα <sub>o1</sub> expression but not Cys <sup>352</sup> Ile Gα <sub>i2</sub> expression.....	137
3.2.7	S-(-)-3-PPP shows a high affinity binding site in competition with [ <sup>3</sup> H] spiperone binding but only in the presence of Cys <sup>351</sup> Ile Gα <sub>o1</sub> expression and not Cys <sup>352</sup> Ile Gα <sub>i2</sub> expression.....	138
3.2.8	S-(-)-3-PPP acts as a partial agonist at the D <sub>21</sub> receptor upon induction of expression of Cys <sup>351</sup> Ile Gα <sub>o1</sub> but as an antagonist upon induction of Cys <sup>352</sup> Ile Gα <sub>i2</sub> expression.....	140
3.3	Discussion.....	171
4	An investigation of the G protein-coupling specificity of D <sub>2</sub> and D <sub>3</sub> dopamine receptors.....	180
4.1	Introduction.....	180
4.2	Results.....	183
4.2.1	The use of a chimeric D <sub>3/2</sub> receptor to investigate regions of D <sub>21</sub> and D <sub>3</sub> important for G protein coupling selectivity.....	183

4.2.2	Investigation of D2-like dopamine receptor coupling using transient co-transfection of receptor and pertussis toxin insensitive $G\alpha_{i/o}$ subunits .....	184
4.2.3	Generation of dopamine receptor-pertussis toxin-insensitive Cys $\rightarrow$ Ile variant G protein alpha subunit fusions .....	189
4.2.4	The action of various dopamine D <sub>2l</sub> -like agonists at dopamine receptor: Cys $\rightarrow$ Ile G protein alpha subunit variant fusion proteins.....	194
4.2.5	Generation and characterisation of cell lines stably and constitutively expressing D <sub>3</sub> or chimeric D <sub>3/2</sub> receptor and expressing $G\alpha_{i1}$ , $G\alpha_{i2}$ , $G\alpha_{i3}$ , or $G\alpha_{o1}$ Cys $\rightarrow$ Ile mutants from the inducible Flp-In locus.....	199
4.2.6	Characterisation of Flp-In T-REx cells expressing Cys <sup>352</sup> Ile $G\alpha_{i2}$ or Cys <sup>351</sup> Ile $G\alpha_{o1}$ from the inducible Flp-In locus and constitutively expressing the D <sub>3</sub> dopamine receptor.....	200
4.2.7	Agonist-dependent [ <sup>35</sup> S] GTP $\gamma$ S binding is observed in membranes of the D <sub>3</sub> + Cys <sup>351</sup> Ile $G\alpha_{o1}$ cell line only upon induction of expression of Cys <sup>351</sup> Ile $G\alpha_{o1}$ . No stimulation of [ <sup>35</sup> S] GTP $\gamma$ S binding above basal is observed in membranes of the D <sub>3</sub> + Cys <sup>352</sup> Ile $G\alpha_{i2}$ cell line with or without the induced expression of Cys <sup>352</sup> Ile $G\alpha_{i2}$ ....	201
4.2.8	Characterisation of Flp-In T-REx cells expressing Cys <sup>352</sup> Ile $G\alpha_{i2}$ or Cys <sup>351</sup> Ile $G\alpha_{o1}$ from the inducible Flp-In locus and constitutively expressing the chimeric D <sub>3/2</sub> dopamine receptor.....	202
4.2.9	Agonist-dependent [ <sup>35</sup> S] GTP $\gamma$ S binding is observed in membranes of the expressing D <sub>3/2</sub> upon induction of expression of Cys <sup>351</sup> Ile $G\alpha_{o1}$ or Cys <sup>352</sup> Ile $G\alpha_{i2}$ ....	204
4.3	Discussion .....	239
5	The generation and characterisation of antibodies that identify only the active conformation of G <sub>i</sub> -family G protein $\alpha$ subunits .....	247
5.1	Introduction.....	247
5.2	Results.....	252
5.2.1	Antisera raised against C-terminal decapeptide of G protein $\alpha$ subunits .....	252

5.2.2	Characterisation of antisera raised against the C-terminal ten amino acids of $G\alpha_t$	256
5.2.3	Characterisation of antisera generated against a decapeptide corresponding to the C-terminal decapeptide of $G\alpha_q$	258
5.2.4	Characterisation of antisera generated against a decapeptide corresponding to the C-terminal decapeptide of $G\alpha_s$	259
5.2.5	Generation of antibodies selective to the active conformation of $G\alpha_{i1}$	261
5.2.6	Outline of hybridoma generation	261
5.2.7	The FMAT assay system	262
5.2.8	Test bleed ELISAs against recombinant $G\alpha_{i1}$	268
5.2.9	Test bleed ELISAs against human IgG	269
5.2.10	Hybridoma Screen	270
5.2.11	Non-conformation selective antibodies show selectivity to $G\alpha_{i1}$ . Conformation selective antibodies do not pick up $G\alpha_{i1}$ , $G\alpha_{i2}$ , $G\alpha_{i3}$ or $G\alpha_{o1}$ when denatured on a SDS-PAGE gel	277
5.2.12	Immunocytochemistry using antibodies selective against the active conformation of $G\alpha_{i1}$	278
5.2.13	Immunocytochemistry using antibodies not selective for the active conformation of $G\alpha_{i1}$	280
5.2.14	Epitope mapping of anti- $G\alpha_{i1}$ antibodies	281
5.2.15	Further characterisation of conformation selective antibodies	283
5.3	Discussion	363
6	General discussion	375
	Appendices	391
	List of References	393
	Additional Material	427

## List of Tables

Table 1.1: The family of mammalian heterotrimeric G protein subunits: function and expression.....	9
Table 1.2: Chimeric GPCRs that showed a change in G protein-coupling specificity. ....	29
Table 1.3: The dopamine receptor subtypes, their principal signal transduction pathway, and pharmacological profiles .....	55
Table 3.1: [ <sup>3</sup> H] spiperone binds with similar and high affinity to various D <sub>21</sub> receptor-G protein fusions.....	129
Table 3.2: The potency and efficacy of ligands at D <sub>21</sub> receptor-G protein fusions.....	131
Table 3.3: The binding characteristics of dopamine and S-(-)-3-PPP with D <sub>21</sub> receptor-G protein fusions.....	133
Table 3.4: Expression levels of the D <sub>21</sub> receptor are unaffected by expression of various G proteins.....	136
Table 3.5: The binding characteristics of dopamine and S-(-)-3-PPP at the D <sub>21</sub> receptor with and without the induction of Cys <sup>352</sup> Ile Gα <sub>i2</sub> or Cys <sup>351</sup> Ile Gα <sub>o1</sub> .....	139
Table 4.1: [ <sup>3</sup> H] spiperone binds with similar affinity to D <sub>3</sub> and the chimeric D <sub>3/2</sub> receptor when co-expressed with either Cys <sup>352</sup> Ile Gα <sub>i2</sub> or Cys <sup>351</sup> Ile Gα <sub>o1</sub> .....	186
Table 4.2:[ <sup>3</sup> H] spiperone binds with similar and high affinity to various D <sub>3</sub> or D <sub>3/2</sub> receptor-G protein fusions.....	191
Table 4.3: The potency and efficacy of ligands at D <sub>3</sub> receptor-G protein fusions.....	197
Table 4.4: The potency and efficacy of ligands at D <sub>3/2</sub> receptor-G protein fusions.....	198
Table 4.5:Expression levels of the D <sub>3</sub> receptor are unaffected by tetracycline-induced expression of Cys <sup>352</sup> Ile Gα <sub>i2</sub> or Cys <sup>351</sup> Ile Gα <sub>o1</sub> expression .....	201
Table 4.6: Expression levels of the D <sub>3/2</sub> receptor are unaffected by tetracycline induced expression of Cys <sup>352</sup> Ile Gα <sub>i2</sub> .....	203
Table 5.1: Percentage sequence homologies of various G protein α subunits .....	253

Table 5.2: The C-terminal ten amino acids of various G protein $\alpha$ subunits.....	254
Table 5.3: Antisera against $G\alpha_s$ , $G\alpha_{q/11}$ and $G\alpha_{i1/2}$ were generated by CRL Laboratories Ltd. (Cambridge, UK) using the peptides below. ....	255
Table 5.4: A simple characterisation of a high throughput screening assay by calculation of $Z'$ .....	267
Table 5.5: Summary of results from initial hybridoma screen .....	272
Table 5.6: Summary of results from screen of sub-cloned hybridoma .....	275

## List of Figures

Figure 1.1: The G protein cycle .....	67
Figure 1.2: The structure of G protein-coupled receptors (GPCRs).....	69
Figure 1.3: Classification and diversity of GPCRs.....	71
Figure 1.4: Structure of the G protein heterotrimer .....	73
Figure 1.5: GPCR-G protein fusion proteins .....	75
Figure 1.6: Proposed mechanisms of GDP release .....	77
Figure 3.1: The multiple signalling states of GPCRs.....	141
Figure 3.2: The use of pertussis toxin insensitive variants of G <sub>i</sub> family G-proteins to study specific interactions between a receptor and a G <sub>i</sub> G-protein of interest.....	143
Figure 3.3: Generation and characterisation of dopamine D <sub>21</sub> receptor-Cys→Ile variant G protein $\alpha$ subunit fusion proteins.....	145
Figure 3.4: Characterisation of the actions of various D <sub>2</sub> agonists at D <sub>21</sub> receptor-G protein fusion proteins.....	147
Figure 3.5: In ligand binding studies S-(-)-3PPP displays both low and high affinity states only at the D <sub>21</sub> -G $\alpha_{01}$ fusion protein .....	149
Figure 3.6: S-(-)-3PPP is an agonist at D <sub>21</sub> -G $\alpha_{01}$ but an antagonist/inverse agonist for the other D <sub>21</sub> -G protein fusion proteins .....	151
Figure 3.7: The Flp-In <sup>TM</sup> T-REx <sup>TM</sup> HEK293 system can be used to express a gene of interest by induction of expression upon treatment of the cells with tetracycline.....	153
Figure 3.8: Characterisation of Flp-In T-REx cells harbouring pertussis toxin-insensitive mutant G proteins at the Flp-In locus.....	155
Figure 3.9: Characterisation of Flp-In T-REx cells constitutively expressing the D <sub>21</sub> receptor and harbouring pertussis toxin-insensitive mutant G proteins at the inducible Flp-In locus.....	157

Figure 3.10: Characterisation of Flp-In T-REx cells harbouring pertussis toxin-insensitive mutant G proteins at the Flp-In locus and constitutively and stably expressing the D <sub>21</sub> receptor.....	159
Figure 3.11: D <sub>21</sub> receptor stimulates [ <sup>35</sup> S] GTPγS binding to Cys <sup>352</sup> Ile Gα <sub>i2</sub> in membranes of pertussis toxin-treated Flp-In T-REx cells only when G protein expression is induced	161
Figure 3.12: D <sub>21</sub> receptor stimulates [ <sup>35</sup> S] GTPγS binding to Cys <sup>351</sup> Ile Gα <sub>o1</sub> in membranes of pertussis toxin-treated Flp-In T-REx cells only when G protein expression is induced .....	163
Figure 3.13: A high affinity binding site for dopamine but not for S-(-)-3PPP appears with induced expression of Cys <sup>352</sup> Ile Gα <sub>i2</sub> .....	165
Figure 3.14: A high affinity binding site for both dopamine and for S-(-)-3PPP appears with induced expression of Cys <sup>352</sup> Ile Gα <sub>o1</sub> .....	167
Figure 3.15: S-(-)-3PPP is an antagonist of D <sub>21</sub> -mediated activation of Cys <sup>351</sup> Ile Gα <sub>i2</sub> but a partial agonist for Cys <sup>351</sup> Ile Gα <sub>o1</sub> .....	169
Figure 4.1: Schematic representation of the chimeric dopamine receptor (D <sub>3/2</sub> ) consisting of a dopamine D <sub>3</sub> receptor with twelve amino acids in the c-terminus of intracellular loop 3 exchanged by the equivalent region in the D <sub>2</sub> receptor.....	205
Figure 4.2: Characterisation of HEK293T transiently co-transfected with pertussis toxin-insensitive Cys <sup>352</sup> Ile Gα <sub>i2</sub> or Cys <sup>351</sup> Ile Gα <sub>o1</sub> cDNA and dopamine receptor (D <sub>21</sub> , D <sub>3</sub> or D <sub>3/2</sub> ) cDNA. ....	207
Figure 4.3: 10 μM GDP was the optimal concentration for [ <sup>35</sup> S] GTPγS assays using membranes from HEK293T cells co-transfected with dopamine D <sub>3</sub> receptor and Cys <sup>351</sup> Ile Gα <sub>o1</sub> cDNA.....	209
Figure 4.4: The Chimeric D <sub>3/2</sub> dopamine receptor can couple to both Cys <sup>352</sup> Ile Gα <sub>i2</sub> and Cys <sup>351</sup> Ile Gα <sub>o1</sub> .....	211
Figure 4.5: Generation of dopamine D <sub>3</sub> receptor or chimeric D <sub>3/2</sub> receptor-Cys→Ile variant G protein α subunit fusion proteins.....	213

Figure 4.6: Characterisation of dopamine D <sub>3</sub> receptor and chimeric D <sub>3/2</sub> receptor-Cys→Ile variant G protein α subunit fusion proteins: addition of increasing amounts of fusion protein into [ <sup>35</sup> S] GTPγS reactions results in a proportional increase in [ <sup>35</sup> S] GTPγS bound .....	215
Figure 4.7: Dopamine stimulated [ <sup>35</sup> S] GTPγS binding above basal levels was observed only when the dopamine D <sub>3</sub> receptor was fused to Gα <sub>o1</sub> .....	217
Figure 4.8: G protein fusion proteins identify agonists at the D <sub>3</sub> receptor but only when coupled to Gα <sub>o1</sub> .....	219
Figure 4.9: G protein fusion proteins identify agonists at the D <sub>3/2</sub> receptor when coupled to all four pertussis-toxin resistant Gα <sub>i/o</sub> subunits .....	221
Figure 4.10: Comparison of the potency and efficacy at the D <sub>21</sub> -Gα <sub>o1</sub> fusion protein and D <sub>3</sub> -Gα <sub>o1</sub> fusion protein receptor of various agonists reveals a trend towards both higher potency and efficacy at the D <sub>3</sub> receptor. ....	223
Figure 4.11: Comparison of the potency and efficacy at the D <sub>3</sub> -Gα <sub>o1</sub> fusion protein and D <sub>3/2</sub> -Gα <sub>o1</sub> fusion protein of various agonists shows no significant differences in efficacy. ....	225
Figure 4.12: Comparison of the potency and efficacy of various agonists at the D <sub>3/2</sub> -Gα <sub>i3</sub> and D <sub>3/2</sub> -Gα <sub>o1</sub> fusion proteins.....	227
Figure 4.13: Characterisation of Flp-In T-REx cells harbouring pertussis toxin-insensitive mutant G proteins at the Flp-In locus.....	229
Figure 4.14: Characterisation of Flp-In T-REx cells harbouring pertussis toxin-insensitive mutant G proteins at the Flp-In locus.....	231
Figure 4.15: Characterisation of Flp-In T-REx cells harbouring pertussis toxin-insensitive mutant G proteins at the Flp-In locus and constitutively expressing either the D <sub>3</sub> or D <sub>3/2</sub> receptor.....	233

Figure 4.16: Significant agonist-stimulated binding of [ <sup>35</sup> S] GTPγS is observed in Flp-In T-REx HEK293 cells constitutively expressing the dopamine D <sub>3</sub> receptor, only upon expression of Cys <sup>351</sup> Ile Gα <sub>o1</sub> .....	235
Figure 4.17: Significant agonist-stimulated binding of [ <sup>35</sup> S] GTPγS is observed in Flp-In T-REx HEK293 cells constitutively expressing the chimeric dopamine D <sub>3/2</sub> receptor, upon expression of Cys <sup>352</sup> Ile Gα <sub>i2</sub> and Cys <sup>351</sup> Ile Gα <sub>o1</sub> .....	237
Figure 5.1: Characterisation of antisera raised against the C-terminal decapeptide of Gα <sub>t</sub> . .....	287
Figure 5.2: The glycine eluate of antiserum from animal 1319 was used successfully to immunoprecipitate Gα <sub>i2</sub> as part of a [ <sup>35</sup> S] GTPγS binding assay with immunoprecipitation step .....	289
Figure 5.3: The glycine eluate of antiserum from animal 1318 was used to immunoprecipitate Gα <sub>i3</sub> as part of a [ <sup>35</sup> S] GTPγS binding assay with immunoprecipitation step .....	291
Figure 5.4: Antisera from animals 1316 and 1317 raised against the C-terminal decapeptide of Gα <sub>q</sub> selectively recognise Gα <sub>q</sub> when this Gα subunit is transiently expressed in Gα <sub>q/11</sub> null EF88 cells. ....	293
Figure 5.5: The glycine eluate of antiserum from animal 1317 was used to immunoprecipitate Gα <sub>11</sub> as part of a [ <sup>35</sup> S] GTPγS binding assay with immunoprecipitation step. ....	295
Figure 5.6: Antiserum from animal 1314, raised against the C-terminal decapeptide of Gα <sub>s</sub> shows a cholera toxin-induced down-regulation of Gα <sub>s</sub> in HEK293T cells.....	297
Figure 5.7: The glycine eluate antiserum from animal 1314 was used to immunoprecipitate Gα <sub>s</sub> as part of a [ <sup>35</sup> S] GTPγS binding assay with immunoprecipitation step .....	299
Figure 5.8: Outline of the various stages of hybridoma generation. Adapted from ‘Antibodies: A Laboratory Manual’ (Harlow, 1988).....	301

Figure 5.9: Schematic diagram of FMAT assay for the screening of hybridoma raised against $G\alpha_{i1}$ .....	303
Figure 5.10: Permeabilisation of cells using a PBS / 1% BSA / 0.1% sodium azide buffer proved the most effective method for use in an FMAT assay to screen for hybridoma producing antibodies selective against the active conformation of $G\alpha_{i1}$ . .....	305
Figure 5.11: An FMAT assay using a polyclonal antiserum raised against the C-terminal tail of $G\alpha_{i1/2}$ remains robust after a 23 hour incubation .....	307
Figure 5.12: The storage of aliquots of pre-transfected HEK293T cells at $-80^{\circ}\text{C}$ prior to use in FMAT assay has no effect on fluorescent signal or robustness of assay .....	309
Figure 5.13: ELISA using test bleeds from both r $G\alpha_{i1}$ rapid immunisation and plasmid immunisation strategies against r $G\alpha_{i1}$ . All animals immunised with r $G\alpha_{i1}$ showed an affinity for r $G\alpha_{i1}$ . No signal above background was observed for test bleeds from plasmid immunised animals. ....	311
Figure 5.14: ELISA using test bleeds from plasmid immunisation strategies against human IgG. No signal above background was observed for test bleeds from plasmid immunised animals. ....	313
Figure 5.15: Diagram illustrating the four conditions used in the whole cell FMAT assay to screen each hybridoma clone tissue culture supernatant. ....	315
Figure 5.16: Initial hybridoma screen identifies three hybridoma clones producing antibody which showed selectivity towards the active conformation of $G\alpha_{i1}$ .....	317
Figure 5.17: Secondary FMAT screen of hybridoma clones: The three clones identified as showing selectivity towards the active (GTP bound) conformation of $G\alpha_{i1}$ showed a similar selectivity upon repetition of the screen .....	319
Figure 5.18: FMAT screen of hybridoma clones following re-cloning of the three clones identified as showing selectivity towards the active (GTP bound) conformation of $G\alpha_{i1}$ : Displayed are daughter clones that showed the best profile, selected from each of the three parental hybridoma cell lines. ....	321

Figure 5.19: Titration experiment using purified non-conformation selective antibodies produced by hybridoma clones 8F5 and 6B4.....	323
Figure 5.20: Titration experiment using purified conformation selective antibodies produced by hybridoma clones 8A5/1C1, 6F12/1E5 and 8D11/1H1 .....	325
Figure 5.21: Non-conformation selective antibodies 6B4 and 8F5 selectively recognise $G\alpha_{i1}$ over other members of the $G\alpha_{i/o}$ family on a Western blot.....	327
Figure 5.22: Conformation selective antibodies 8A5/1C1, 6F12/1E5 and 8D11/1H1 do not recognise members of the $G\alpha_{i/o}$ family denatured by SDS PAGE.....	329
Figure 5.23: Immunocytochemistry using the conformation selective antibody 8A6/1H1 .....	331
Figure 5.24: Immunocytochemistry using the conformation selective antibody 6F12/1E5 .....	333
Figure 5.25: Immunocytochemistry using the conformation selective antibody 8D11/1C1 .....	335
Figure 5.26: Immunocytochemistry using the non-conformation-selective antibody 6B4 .....	337
Figure 5.27: Immunocytochemistry using the non-conformation selective antibody 8F5339	
Figure 5.28: Immunocytochemistry using an anti- $G\alpha_{i1/2}$ polyclonal antiserum raised against a decapeptide corresponding to the C-terminal ten amino acids of $G\alpha_t$ (1319 Glycine).....	341
Figure 5.29: Epitope mapping of non-conformation selective antibodies using a set of overlapping 16mer peptides corresponding to the amino acid sequence of human $G\alpha_{i1}$ ....	343
Figure 5.30: Epitope mapping of conformation selective antibodies using a set of overlapping 16mer peptides corresponding to the amino acid sequence of human $G\alpha_{i1}$ ....	345
Figure 5.31: The conformation-selective antibody 6F12/1E5 shows selectivity for the constitutively active mutant $Gln^{205}Leu G\alpha_{i2}$ .....	347

Figure 5.32: The conformation-selective antibody 6F12/1E5 shows selectivity for the constitutively active mutant Gln <sup>204</sup> Leu Gα <sub>o1</sub> .....	349
Figure 5.33: The conformation-selective antibody 6F12/1E5 does not show selectivity for the constitutively active mutant Gln <sup>227</sup> Leu Gα <sub>s</sub> .....	351
Figure 5.34: The conformation-selective antibody 6B12/1E5 does not show selectivity for the constitutively active mutant Q <sup>209</sup> L Gα <sub>q</sub> .....	353
Figure 5.35: The conformation-selective antibody 6F12/1E5 does not show selectivity for the constitutively active mutant R <sup>178</sup> C Gα <sub>i2</sub> .....	355
Figure 5.36: AlF <sub>4</sub> <sup>-</sup> is a substitute for and mimic of the γ phosphate of GTP .....	357
Figure 5.37: The conformation-selective antibody 6F12/1E5 recognises the complex Gα <sub>i2</sub> .GDP.AlF <sub>4</sub> <sup>-</sup> .....	359
Figure 5.38: The conformation-selective antibody 6F12/1E5 recognises the agonist induced complex Gα <sub>i2</sub> .GTPγS .....	361

## Acknowledgements

I would like to extend warm thanks to the many people who have contributed, directly or otherwise, to the completion of this research project. Firstly, to my supervisor Professor Graeme Milligan for giving me the opportunity undertake this project and for his helpful advice during the course of my studies. I am also indebted to my fellow colleagues in Lab 253, both past and present, for providing constant assistance and advice. In particular I would like to thank Meritxell Canals for assistance with the immunocytochemistry experiments and Juan Lopez-Giminez for his advice on all matters pharmacological. As part of this research project I enjoyed a useful and productive placement at GlaxoSmithKline. I should like to express my gratitude to those with whom I worked during this period, in particular Steve Rees, Alan Wise and Ben Powney who all provided excellent supervision and support. I would also like to thank Ian Kinghorn, Chris Plumpton and all in the Antibody Technology Group at GSK for their hard work and expertise during the antibody generation project. Katy Gearing, Dion Daniels and all members of the 7TM Receptor Group, Gene Expression and Protein Biochemistry, GSK, were extremely kind in allowing me to become a temporary member of their excellent team and deserve special thanks. I thank the BBSRC and GSK for providing me with funding for my studentship. I am grateful to my friends and family for their support during the last three years, in particular to Oliver Sturm who has let me sleep on his floor for the last six months. Finally I would like to thank David Henderson for his enthusiasm, skill, and hard work during his Master's Project.

## Author's Declaration

The author declares that the following work presented in this volume was written by none other than himself. Apart from where indicated all work was performed by the author.

Experiments described by **Figures 5.10** and **5.11** were performed by Ben Powney and Dion Daniels (Screening and Compound Profiling, GSK, Harlow, UK and Bio-reagents and Assay Development, GSK, Stevenage, UK respectively). Experiments described by **Figures 5.31-5.38** were performed by David Henderson. All immunisations, hybridoma generation and antibody purification was performed by Ian Kinghorn (Antibody Generation, Biological Reagents and Assay Development (BRAD), GSK )

## Definitions

**7-OH-DPAT**, R (+)-7-Hydroxy-DPAT hydrobromide;

**BRET**, bioluminescence resonance energy transfer

**BSA**, bovine serum albumin

**cAMP**, adenosine 3',5' cyclic monophosphate

**D<sub>1</sub>**, human dopamine D<sub>1</sub> receptor

**D<sub>2L</sub>**, long isoform of the human dopamine D<sub>2</sub> receptor;

**D<sub>2S</sub>**, short isoform of the human dopamine D<sub>2</sub> receptor

**D<sub>3</sub>**, human dopamine D<sub>3</sub> receptor

**D<sub>3/2</sub>**, chimeric dopamine receptor in which a twelve amino acid sequence in the C-terminus of the third intracellular loop of D<sub>3</sub> was exchanged with the equivalent region of the dopamine D<sub>2</sub> receptor.

**D<sub>4</sub>**, human dopamine D<sub>4</sub> receptor

**D<sub>5</sub>**, human dopamine D<sub>5</sub> receptor

**ECL 1-3**, Extracellular loop 1-3

**eYFP**, enhanced yellow fluorescent protein

**FMAT**, Fluorometric Microvolume Assay Technology<sup>7</sup>

**FRET**, fluorescence resonance energy transfer

**G $\alpha$** , G protein alpha subunit

**GAP**, GTPase activating protein

**G protein**, GTP-binding protein

**GPCR**, G protein-coupled receptor;

**GRK**, G protein receptor kinase

**GTP**, guanosine triphosphate

**GTP $\gamma$ S**, guanosine 5'-O-(thiotriphosphate);

**GDP**, guanosine diphosphate

**GDP $\beta$ S**, guanosine 5'-[beta-thio] diphosphate

**HBS**, HEPES buffered saline

**HEK**, human embryonic kidney

**ICL 1-3**, Intracellular loop 1-3

**LB medium**, Luri-Bertani medium

**LH**, lutenising hormone

**MAPK**, mitogen activated kinase

**NPA**, *R*-(-)-10, 11-dihydroxy-*N-n*-propylnorapomorphine

**PBS**, phosphate buffered saline

**PCR**, polymerase chain reaction

**PKA**, protein kinase A

**PKC**, protein kinase C

**RGS**, regulator of G protein signalling

**R-(+)-3-PPP**, *R* (+) 3-(3-hydroxyphenyl)-*N*-propylpiperidine;

**SDS**, sodium dodecyl sulphate

**SDS-PAGE**, sodium dodecyl sulphate polyacrylamide gel electrophoresis

**S-(-)-3-PPP**, *S*-(-)-3-(3-hydroxyphenyl)-*N*-propylpiperidine

**7 TM**, seven transmembrane

**TM (I-VII)**, transmembrane domain 1-7

# 1 Introduction

## 1.1 G protein-coupled receptors

The G protein coupled receptor (GPCR) family represents the largest and most versatile group of cell surface receptors, which can detect a diverse array of chemical signals in a highly selective way. As a family of proteins, GPCRs share common structural features including seven transmembrane spanning domains. They can couple to specific guanine nucleotide binding proteins (G proteins) thereby transducing an extracellular signal to an intracellular effector, although more recently several GPCRs have been demonstrated to signal via G protein-independent mechanisms (Hall and Lefkowitz, 2002). GPCRs are the largest superfamily of cell-surface receptors making up nearly 2% of the human genome, with 865 genes that have easily identifiable seven transmembrane characteristics (Vassilatis et al., 2003). Approximately half of these are odorant receptors. Of the remaining 360 receptors, the natural ligand has been identified for approximately 210 receptors, leaving 150 so-called orphan GPCRs with no known ligand or function.

As a family of proteins, GPCRs have the highest impact from a social, therapeutic and economic point of view. Drugs active at these receptors have therapeutic actions across a wide range of human diseases ranging from allergic rhinitis to pain, hypertension and schizophrenia and it has been estimated that approximately 30% of all modern drugs are targeted at these receptors. Interestingly, however, the majority of GPCR-targeted drugs exert their effects on approximately only 30 GPCRs (Wise et al., 2004). GPCRs are involved in all major disease areas such as cardiovascular, metabolic, neurodegenerative, psychiatric, cancer and infectious diseases (Lundstrom, 2006). It is also evident that drugs have still only been developed to affect a very small number of the GPCRs, and the potential for drug discovery within this field is enormous.

GPCRs are thought to operate through a similar molecular mechanism. The binding of extracellular ligands or light activation to GPCRs causes as yet poorly defined conformational changes in the receptor protein, which promotes association of the receptor with distinct classes of heterotrimeric G proteins. These G proteins consist of  $\alpha$  subunits bound to  $\beta\gamma$  complexes and are attached to the cytoplasmic surface of the plasma membrane. Interaction of the ligand-activated receptor with the G protein triggers the exchange of GTP for GDP on the  $\alpha$  subunit and results in the dissociation of the G protein  $\alpha$  subunit from the  $\beta\gamma$  dimer or alternatively a conformational rearrangement between the two (**Figure 1.1**) (Bunemann et al., 2003). These are then able to interact with distinct effector enzymes and ion channels thereby transmitting an extracellular signal into the cell. The  $G\alpha$  subunit has an intrinsic GTPase activity and the bound GTP is hydrolysed to GDP resulting in the inactivation of the  $G\alpha$  subunit.  $G\alpha$ .GDP binds with the  $\beta\gamma$  dimer and the system is returned to the resting state (Milligan and Kostenis, 2006).

In this chapter I will give a general overview of the diversity and structure of both GPCRs and their heterotrimeric G protein signalling partners. I will summarise the current understanding of the structural changes occurring upon receptor-mediated G protein activation, focusing particularly on the structural determinants of receptor/G protein coupling specificity. The final part of this chapter will focus on dopamine receptors, their structure and G protein coupling specificity.

### **1.1.1 Structural features of G protein-coupled receptors**

Despite the remarkable structural diversity of the activating ligands and their amino acid sequences, all GPCRs are predicted to share a common three dimensional fold consisting of seven transmembrane helices (TMI-TMVII) linked by alternating intracellular (ICL I -

III) and extracellular (ECL I - III) loops (**Figure 1.2A**). The extracellular receptor surface including the extracellular N-terminal domain, different extracellular loops, and/or the exofacial portions of various TM domains is known to be critically involved in ligand binding. On the other hand, the intracellular surface (the intracellular loops, the intracellular C-terminal domain, and the cytoplasmic ends of different TM helices) is known to be important for G protein recognition and activation (Wess, 1998). This seven-transmembrane domain structure was predicted by hydrophobicity analysis of the primary sequence of GPCRs. This structure has been confirmed by the determination of the crystal structure of rhodopsin, archetypal class I GPCR (Palczewski et al., 2000) and to date the only solved GPCR structure (**Figure 1.2B**).

The rhodopsin structure provides a useful model for the prediction of other class I receptor structures. The seven transmembrane domains form  $\alpha$  helices of different lengths with TM III being the longest and TMVI and VII being relatively short (Teller et al., 2001; Wess, 1998). The helices are organised in a counter-clockwise arrangement (**Figure 1.2C-D**). In family I receptors the C-terminal end of TM III contains a highly conserved DRY (Asp-Arg-Tyr) motif, that has been implicated in the receptor/G protein coupling (Wess, 1998). In the crystal structure of bovine rhodopsin the transmembrane domains were found to be distorted or kinked due to the presence of proline residues within the transmembrane domains (Palczewski et al., 2000). The helices of TM I and II were found to be tilted from the plane of the membrane by  $25^\circ$  while TM III displayed a  $33^\circ$  tilt. TM IV and VI were shown to be almost perpendicular to the membrane whilst TM V is tilted by  $26^\circ$ . A highly conserved NPXXXY motif in TM VII was shown to be important in stabilising the inactive state of the receptor (Teller et al., 2001). Interestingly the structure also resolved an amphipathic cytoplasmic helix located in the C-terminal domain extending from TM VII. This helix is tilted at  $90^\circ$  to the membrane and forms one of the binding sites for the  $G_t \alpha$ -subunit and plays a role in the regulation of  $G\gamma$  binding (Ernst et al., 2000). A cysteine residue located in the membrane proximal C-terminal region of several GPCRs has been

identified as a potential site for palmitoylation, the attachment of the fatty carbon chain palmitic acid via a thioester bond. This serves as an anchor into the membrane, and effectively creates a fourth intracellular loop. The C-terminal tail is an important site for receptor phosphorylation by receptor kinases following receptor activation, inducing receptor desensitisation (Teller et al., 2001).

The N-terminal region of GPCRs varies considerably in length between individual receptors and can be important for ligand binding. Virtually all GPCRs possess one or more N-linked glycosylation sites (Asn-X-Ser/Thr) where X is any amino acid except proline or asparagine (Wess, 1998). For several GPCRs, prevention of receptor glycosylation results in reduced cell surface expression but has no effect on the function or pharmacology of these receptors. Conserved cysteine residues within this region are thought to be important for protein folding. The extracellular loops of rhodopsin possess two highly conserved cysteine residues in ECL I and the N-terminus of TM III (Cys 110 and Cys 197, respectively) that form a disulphide bond that have been shown to stabilise the receptor structure. The mutation of analogous residues within the  $\beta_2$ -adrenoceptor gives a variant with reduced ability to bind ligand and a destabilised tertiary structure.

### 1.1.2 Classification of G protein-coupled receptors

GPCRs can be divided phylogenetically into six classes. Schematic representations of receptor monomers showing some key structural aspects of the three main families are shown. Family I (**Figure 1.3A**, also referred to as family A or the rhodopsin-like family) is by far the largest subgroup and contains receptors for odorants, small molecules such as the catecholamines and amines, some peptides and glycoprotein hormones. Receptors of Family I are characterized by ~20 highly conserved amino acids (some of which are indicated in the diagram by red circles) and a disulphide bridge that connects the first and

second extracellular loops (ECL1 and 2). Most of the conserved residues, including several conserved proline residues and a conserved DRY (aspartic acid, arginine, tyrosine) motif adjacent to transmembrane domain III (TM III), are located in the cytoplasmic half of the transmembrane domain. Mutagenesis data suggests that these residues are required for protein stability and/or mediating the conformational changes that accompany receptor activation.

Family II or family B GPCRs are characterized by a relatively long amino terminus that contains several cysteines, which presumably form a network of disulphide bridges. Their morphology is similar to some family 1 receptors, but they do not share any sequence homology (**Figure 1.3B**). For example, the family 2 receptors also contain a disulphide bridge that connects ECL1 and ECL2, but the palmitoylation site is missing, the conserved prolines are different from the conserved prolines in the family 1 receptors and the DRY (aspartic acid, arginine, tyrosine) motif adjacent to TM III is absent. Little is known about the orientation of the TM domains, but, given the divergence in amino acid sequence, it is probably quite dissimilar from that of rhodopsin. Ligands for family 2 GPCRs include hormones, such as glucagon, gonadotropin-releasing hormone and parathyroid hormone.

Family III (**Figure 1.3C**) contains the metabotropic glutamate, the  $\text{Ca}^{2+}$  sensing and the  $\gamma$ -aminobutyric acid (GABA) B receptors. These receptors are characterized by a long N-terminus and C-tail. The ligand binding domain is located in the amino terminus, which is often described as being like a 'Venus fly trap'. Except for two cysteines in extracellular loop 1 and extracellular loop 2 that form a putative disulphide bridge, class III receptors do not have any of the key features that characterize class I and II receptors. A unique characteristic of the class III receptors is that the third intracellular loop is short and highly conserved. Although the structure of the amino terminus is well characterized, similar to the class II receptors, little is known about the orientation of the transmembrane domains.

Of the smaller, less characterized GPCR families, family IV comprises pheromone receptors (VNs) associated with the  $G\alpha_{i/o}$  G protein family, while family V includes the ‘frizzled’ and the ‘smoothened’ (Smo) receptors involved in embryonic development and in particular in cell polarity and segmentation. Finally, the cAMP receptors have only been found in *D.discoideum* but possible expression in vertebrate has not yet been reported (Bockaert and Pin, 1999; Lee et al., 2003a).

### 1.1.3 Quaternary structure of GPCRs

GPCR homo and hetero-oligomerisation has been well described for a multitude of GPCRs (Milligan, 2007). Although the work in this thesis does not investigate this area, the perceived importance of quaternary structure for both expression and function of GPCRs warrants a brief discussion in this introduction. The use of atomic force microscopy to visualise discs from mouse rod outer segments and the use of cryo-electron microscopy on 2 dimensional crystals of squid rhodopsin have shown higher order organisation of these proteins (Davies et al., 2001; Fotiadis et al., 2003). In images obtained by atomic force microscopy rhodopsin is organised within para-crystalline arrays with densely packed double rows of the receptor. Models were subsequently generated that optimised the packing arrangements. These models have suggested that the interactions between rows of dimers are provided by the contacts involving elements of TM I. Key interactions between monomers are provided by contacts involving TM IV and V (Fotiadis et al., 2004). Similarly, although no direct biophysical evidence exists, due to lower expression levels, both homo-oligomersation and hetero-oligomerisation has been demonstrated for a diverse range of other GPCRs in a vast range of studies (Angers et al., 2002; George et al., 1998; Milligan, 2007). Similarly, contacts between transmembrane domains have been shown to

be crucial for organisation of these quaternary structures, for example cysteine cross linking studies in the dopamine D<sub>2</sub> receptor highlighted residues within TM IV as being contact points between the dimer (Guo et al., 2005). Dimerisation or oligomerisation has been implicated in a wide variety of functions or roles. These include the formation of dimers/oligomers as an early step in GPCR protein folding, maturation, cell surface delivery and functional expression of the receptor (Milligan, 2007). Functional consequences of hetero-oligomerisation include modulation of signal transduction, for example, the co-expression of the orexin-1 and cannabinoid CB<sub>1</sub> receptor has been reported to enhance the potency of the peptide orexin-A to stimulate phosphorylation of the ERK 1 and 2 MAP kinases 100 fold, an effect that was blocked by the CB<sub>1</sub> receptor antagonist/inverse agonist rimonabant (Ellis et al., 2006). Perhaps most pertinent to this body of work is that hetero-oligomerisation can alter receptor/G protein selectivity. For example, both  $\mu$ -opioid and  $\delta$  opioid receptors are generally considered to be highly selective for G $\alpha_{i/o}$  family subunits. However, upon co-expression it was reported that signals insensitive to pertussis toxin were generated, and interestingly, a switch in G protein coupling selectivity to G $\alpha_z$  has been implicated (George et al., 2000).

## 1.2 Diversity of heterotrimeric G proteins and their effectors

Although nearly 900 heptahelical receptors have been identified, they interact with a relatively small number of G proteins. To date, 21 G $\alpha$  subunits have been identified and these are encoded by 16 genes. Heterotrimeric G proteins are typically divided into four main classes: G<sub>i/o</sub>, G<sub>s</sub>, G<sub>q/11</sub>, and G<sub>12/13</sub> based on sequence homology of the G $\alpha$  subunits. Members of this family range from 39-52 kDa and share between 35% and 95% sequence identity (Downes and Gautam, 1999). The G $\alpha$  subunit families, subtypes, effectors and expression are described in **Table 1.1**. The G $\alpha_s$  family includes several splice variants of

$\alpha_s$ , as well as  $\alpha_{olf}$ , which is largely expressed in olfactory epithelia. Typically,  $G\alpha_s$  subunits enhance the function of adenylate cyclase. The cholera toxin-catalysed ADP ribosylation of an arginine residue leads to the constitutive activation of this family of  $G\alpha$  subunits. The  $G\alpha_{i/o}$  family consists of three distinct  $\alpha_i$  species,  $\alpha_o$ , two retinal transducins ( $\alpha_{t1}$  and  $\alpha_{t2}$ ), an  $\alpha$ -subunit found in the gustatory epithelium ( $\alpha_{gust}$ ) and  $\alpha_z$ . Downstream actions of  $\alpha$ -subunits in this family include the inhibition of adenylate cyclase and the stimulation of  $K^+$  channels. Pertussis toxin-catalysed ADP ribosylation of a cysteine residue 4 amino acids from the c-terminus prevents functional interaction of these all  $\alpha$ -subunits, apart from  $G\alpha_z$  with the receptor. The  $G\alpha_{q/11}$  family activate isoforms of phospholipase C $\beta$  and consist of  $G\alpha_q$ ,  $G\alpha_{11}$ ,  $G\alpha_{14}$ , and  $G\alpha_{16}$ .

In humans 6  $G\beta$  subunits are encoded by 5 genes and 12  $G\gamma$  subunits are expressed (Downes and Gautam, 1999). There is then, the potential for a substantial number of pairings, although a number of possible pairings have been indicated not to form, and tissue expression patterns may further limit the actual number of pairings in particular cells and tissues.  $\beta_1$ - $\beta_4$  are highly homologous but  $\beta_5$  is less so, and unlike the other  $\beta$  subunits it dissociates from the  $\gamma$  subunit.  $\gamma$  subunits are structurally more diverse compared to the  $\beta$  subunits.  $\beta\gamma$  subunits can bind to and influence a wide variety of effectors as summarised in Table 1.1 (Milligan and Kostenis, 2006).

Because of the diversity of G protein subunits and downstream effector molecules, the pattern of physiological responses of a particular cell following stimulation of a given GPCR is quite complex. The nature of the observed responses critically depends on which G protein heterotrimers are recognised by the receptor and which specific effector molecules are present in the cell or tissue. Furthermore, the magnitude of the response will depend on the relative concentration of all molecules involved in the signalling pathway (Wess, 1998).

**Table 1.1: The family of mammalian heterotrimeric G protein subunits: function and expression**

Adapted from Milligan and Kostenis, (2006)

Family	Subtype	Effectors	Expression
$G\alpha_s$	$G\alpha_{s(S)}$	Adenylyl cyclases $\uparrow$ ( $G\alpha_{s,(XL),olf}$ )	$G\alpha_s$ : ubiquitous $G\alpha_{olf}$ : olfactory neurons, certain CNS ganglia; digestive and urogenital tract
	$G\alpha_{s(L)}$	Maxi $K^+$ channel $\uparrow$ ( $G\alpha_s$ )	
	$G\alpha_{s(XL)}$	Src tyrosine kinases (c-Src, Hck) $\uparrow$ ( $G\alpha_s$ )	
	$G\alpha_{olf}$		
$G\alpha_{i/o}$	$G\alpha_{o1}$	Adenylyl cyclase $\downarrow$ ( $G\alpha_{i,o,z}$ )	$G\alpha_{o1-2}$ : neurons, neuroendocrine cells, astroglia, heart $G\alpha_{i1-13}$ : neurons and many others $G\alpha_z$ : platelets, neurons, adrenal chromaffin cells, neurosecretory cells $G\alpha_{i1}$ : rod outer segments, taste buds $G\alpha_{i2}$ : cone outer segments $G\alpha_{gust}$ : sweet and/or bitter taste buds, chemoreceptor cells in the airways
	$G\alpha_{o2}$	Rap1GAPII-dependent ERK/MAPkinase activation $\uparrow$ ( $G\alpha_i$ )	
	$G\alpha_{i1-13}$	$Ca^{2+}$ channels $\downarrow$ ( $G\alpha_{i,o,z}$ )	
	$G\alpha_z$	$K^+$ channels $\uparrow$ ( $G\alpha_{i,o,z}$ )	
	$G\alpha_{i1/2}$	Src tyrosine kinases (c-Src, Hck) $\uparrow$ ( $G\alpha_i$ )	
	$G\alpha_{gust}$	Rap1GAP $\uparrow$ ( $G\alpha_z$ )	
		GRIN1-mediated activation of Cdc42 $\uparrow$ ( $G\alpha_{i,o,z}$ ) cGMP-PDE $\uparrow$ ( $G\alpha_i$ ) $G\alpha_{gust}$ : ?	
$G\alpha_{q/11}$	$G\alpha_q$	Phospholipase C $\beta$ isoforms $\uparrow$	$G\alpha_{q/11}$ : ubiquitous $G\alpha_{15/16}$ : hematopoietic cells
	$G\alpha_{11}$	p63-RhoGEF $\uparrow$ ( $G\alpha_{q/11}$ )	
	$G\alpha_{14}$	Bruton's tyrosine kinase $\uparrow$ ( $G\alpha_q$ )	
	$G\alpha_{15}$	$K^+$ channels $\uparrow$ ( $G\alpha_q$ )	
	$G\alpha_{16}$		
$G\alpha_{12/13}$	$G\alpha_{12}$	Phospholipase D $\uparrow$	Ubiquitous
	$G\alpha_{13}$	Phospholipase C $\epsilon$ $\uparrow$	
		NHE-1 $\uparrow$	
		iNOS $\uparrow$	
		p115RhoGEF $\uparrow$	
		PDZ-RhoGEF $\uparrow$	
	Leukaemia-associated RhoGEF (LARG) $\uparrow$		
	Radixin $\uparrow$		
	Protein phosphatase 5 (PP5) $\uparrow$		
	AKAP110-mediated activation of PKA $\uparrow$		
	HSP90 $\uparrow$		
$G\beta/\gamma$	$\beta_{1-5}$	PLC $\beta$ s $\uparrow$	$\beta_1 \gamma_1$ : retinal rod cells $\beta_3 \gamma_8$ : retinal cone cells $\beta_5$ : neurons and neuroendocrine organs $\beta_{5(L)}$ : retina Most cell types express multiple $\beta$ and $\gamma$ subtypes
	$\gamma_{1-12}$	Adenylyl cyclase I $\downarrow$	
		Adenylyl cyclases II, IV, VII $\uparrow$	
		PI-3 kinases $\uparrow$	
		$K^+$ channels (GIRK1,2,4) $\uparrow$	
		$Ca^{2+}$ (N-, P/Q-, R-type) channels $\downarrow$	
		c-Jun N-terminal kinase (JNK) $\uparrow$	
		Src kinases $\uparrow$	
		G protein-coupled receptor kinase recruitment to membrane $\uparrow$	
		Protein kinase D $\uparrow$	

### 1.2.1 Structural features of heterotrimeric G proteins

Unlike GPCRs, the crystal structures of heterotrimeric G-proteins in a variety of different conformations have been determined, and these structures form the basis of our understanding of the mechanisms of G protein signalling (Coleman et al., 1994; Coleman and Sprang, 1998; Mixon et al., 1995; Raw et al., 1997). G  $\alpha$  subunits contain two domains: a GTPase domain that is involved in the binding and hydrolysis of GTP and a helical domain that buries the GTP within the core of the protein (Mixon et al., 1995) (**Figure 1.4**). The GTPase domain is homologous to that of the family of monomeric G proteins and is composed of a six stranded  $\beta$ -sheet surrounded by five  $\alpha$  helices. The most highly conserved sequences in this domain are the five loops that contain the consensus sequence for guanine nucleotide binding: the diphosphate-binding (P-) loop (GXGESGKS), the  $Mg^{2+}$ -binding domain (RXXTXGI and DXXG) and the guanine ring- $\gamma$ -phosphate binding motifs (NKXD and TCAT). Comparison of the inactive (GDP bound) and active (GTP bound)  $G\alpha_{i1}$  crystal structures has revealed the presence of three flexible regions, designated switches I, II and III, which become more rigid and well ordered in the GTP-bound active structure (Lambright et al., 1994; Mixon et al., 1995) (**Figure 1.4 C-D**). The GTPase domain not only hydrolyses GTP but also contains sites for binding to the  $\beta\gamma$  dimer, GPCRs and downstream effector proteins.

The helical domain has the most divergent sequence among  $G\alpha$  subunits and consequently may play a role in both receptor/G protein coupling selectivity and G protein/effector selectivity. It is composed of six  $\alpha$ -helices that form a lid over the nucleotide binding site, burying bound nucleotides in the core of the protein. The helical domain has been shown to increase the affinity for nucleotides and increase the GTP hydrolysis activity of the  $G\alpha$  subunits (Liu et al., 1998; Remmers et al., 1999).

In the isolated G protein crystal structures solved thus far, the N- and C- termini of  $G\alpha$  were either removed from the protein or disordered. Consequently, less is known about the structure of these important regions. However, in two separate crystal structures of the heterotrimeric complex, the N-terminal helix is ordered by its interaction with the  $\beta$ -propeller domain of  $G\beta$  (Lambright et al., 1996; Wall et al., 1995) (**Figure 1.4B**). As discussed later, biochemical studies suggest that these terminal regions play a key role in the activation process and in directing specific receptor/G protein coupling interactions. The N-terminus is also the site of fatty-acid modifications on  $G\alpha$  subunits that regulate G protein localisation and protein-protein interactions. All of these proteins, except  $G\alpha_t$ , are modified post-translationally with the 16-carbon fatty acid palmitate attached by a reversible thioester bond to cysteines near the N-terminus (Smotrys and Linder, 2004). Mutations that prevent palmitoylation shift the localisation of myristoylated proteins from the membrane to the cytoplasm (Wise and Milligan, 1997). Members of the  $G\alpha_{i/o}$  family are also myristoylated, with the addition of the saturated 14-carbon fatty acid myristate to the N-terminal glycine following removal of the initiating methionine residue. This modification is irreversible (Chen, 2001). It is thought that myristoylation has an important role in the structure of the N-terminal helix of  $G\alpha$ . In the non-myristoylated protein, this region is disordered, but becomes ordered upon myristoylation in the  $G\alpha$ .GDP complex even without the binding of the  $G\beta\gamma$ -dimer (Medkova et al., 2002). Furthermore this myristoylated structure is unchanged upon binding of the  $G\beta\gamma$ -dimer. Myristoylation also affects the interaction between  $G\alpha$  and effectors (Preininger et al., 2003). For  $G\alpha_i$  subunits, a two-signal membrane trapping model has been suggested for anchoring of  $G\alpha$  subunits to the membrane. In this model, myristoylation is the first signal which leads to a transient interaction between the  $G\alpha$  subunit and the membrane. Palmitoylation is the second signal that serves to securely attach the protein to the membrane (Shahinian, 1995).

All six G $\beta$ -subunits are ~ 36 kDa and share 50-90 % sequence identity and have a  $\beta$ -propeller structure containing seven WD-40 repeats (Downes and Gautam, 1999) (**Figure 1.4 B-C**). Each blade of the propeller is composed of four anti-parallel  $\beta$ -strands, where one WD-40 sequence contributes the last three strands in one blade and the first strand in the next blade. The final blade contributes the last three strands in one blade and the first strand in the next blade. The remaining N-terminal residues adopt an  $\alpha$ -helical conformation that forms a coiled coil which is essential for interaction with G $\gamma$ , an interaction that is essential for the proper folding of G $\beta$  (Oldham, 2006; Sondek et al., 1996). Members of the G $\gamma$  family are all small proteins, between 7 and 8 kDa and share 30-80% sequence identity (Downes and Gautam, 1999). They are composed of two  $\alpha$  helices connected by a loop. The N-terminal helix interacts with the N-terminus of G $\beta$  whilst the C-terminal binds to blades 5 and 6 (Sondek et al., 1996). G $\gamma$  subunits undergo post-translational isoprenylation at their C-termini. This increases the affinity of the G $\beta\gamma$  dimer for the membrane (Higgins and Casey, 1996). The G $\beta\gamma$  dimer is a functional unit that is not dissociable except by denaturation. Most  $\beta$  subunits can interact with most but not all  $\gamma$  subunits. Several G $\beta\gamma$  dimers can interact with the same G $\alpha$  isoform suggesting that differential expression may be an important determinant of signalling specificity (Clapham and Neer, 1997). The G $\beta\gamma$  dimer may be a determinant of the membrane localisation of G $\alpha$  subunits.

The crystal structures of G protein heterotrimers highlight two sites of interaction between G $\alpha$  and G $\beta\gamma$  (Lambright et al., 1996; Mixon et al., 1995; Wall et al., 1995). The primary site is between switches I and II of G $\alpha$  and residues from blades 5 and 7 of G $\beta$ , and the second is an interaction between blade 1 of G $\beta$  and the N-terminus of G $\alpha$ . There is however, no evidence of a G $\alpha$ :G $\gamma$  interaction surface. Upon heterotrimer formation no perturbations in the structure of G $\beta\gamma$  were identified. Conversely G $\beta\gamma$  binding significantly

alters the conformation of  $G\alpha$ . By stabilising the two flexible loops, Switches I and II, and by forming a salt bridge between the P-loop and Switch I  $G\beta\gamma$  binding locks GDP into the nucleotide binding pocket. This reorganisation also disassembles the binding sites for  $Mg^{2+}$ .

## 1.3 Structural basis of receptor-G protein interactions

### 1.3.1 Conformational changes associated with receptor activation

As described above the only receptor for which crystal structures have been defined is the dark (inactive) conformation of rhodopsin. Consequently, these structures shed little light on the G protein coupling mechanism of GPCRs. However, they have provided a framework within which to interpret other biophysical studies on the conformational changes associated with receptor activation. Extensive site-directed spin-labelling (SDSL) studies of rhodopsin have shown that photo-activation primarily results in an outward movement of helix VI, thereby opening a crevice in the intracellular face of the receptor (Farrens et al., 1996). This outward movement appears to be essential for G protein activation, as disulfide and metal-ion cross-links between helices III and VI prevent light-stimulated nucleotide exchange in  $G\alpha_t$ . Similar movements have been identified upon activation of other receptors (Gether et al., 2002). For example, studies of  $\beta_2$  adrenergic receptors labelled with fluorescent probes at the cytoplasmic end of TM VI provide evidence that agonists induce a rotation or titling movement of the cytoplasmic end of TM VI similar to that observed in rhodopsin (Ghanouni et al., 2001). A key structural change involving the disruption of an ionic interaction between the highly conserved D(E)RY sequence at the cytoplasmic end of TM VI is observed upon activation of both rhodopsin and the  $\beta_2$  adrenoceptor (Yao et al., 2006). Cysteine crosslinking studies on the M3 muscarinic receptor provide evidence for the movement of the cytoplasmic ends of TM V

and TM VI toward each other upon agonist activation (Ward et al., 2006). Interestingly, studies using FRET have shown that partial agonists and inverse agonists impart a conformational change on the receptor that is distinct from that of a full agonist (Nikolaev et al., 2006; Vilardaga et al., 2005).

### 1.3.2 The receptor-G protein interface

The newly formed pocket in the cytoplasmic face of the receptor forms the binding site for the c-terminus of  $G\alpha$  which, as described below is the best characterised receptor contact site in G proteins. Structural information about this region is lacking from crystal structures as this region is missing or disordered in most of them. Experiments using alanine scanning mutagenesis, chimeric  $G\alpha$  subunits, chemical cross linking and tryptic proteolysis have also implicated residues in the  $\alpha 4/\beta 6$  loop at the C-terminus of  $G\alpha$ . Similarly, the N-terminal helix has also been shown to be involved with receptor interaction. The  $G\beta\gamma$  dimer also binds receptors and is required to stabilise the receptor-G protein interface, with the C-terminus of  $G\beta$  and the  $G\gamma$  subunit thought to be particularly important (Oldham, 2006). As described below, the intracellular loops of GPCRs are thought to form the primary interaction surface on the receptor. Computational techniques have enabled investigators to apply the extensive amount of biochemical and biophysical information to the high resolution structures of rhodopsin and  $G\alpha_t$  and develop a model for the complex between an active rhodopsin and a GDP bound (inactive)  $G\alpha_t$  (Ciarkowski et al., 2005; Fotiadis et al., 2006). However, according to one model, the cytoplasmic surface of the receptor is not large enough to accommodate both the  $G\alpha$  C-terminus in its binding pocket and the  $G\gamma$  C-terminus (Ciarkowski et al., 2005). One possible resolution is that receptors function as dimers (Javitch, 2004; Milligan, 2007), and increasing experimental evidence suggests that this is the case. Therefore, the functional complex between a receptor and G protein could be one receptor dimer coupling to one  $G\alpha\beta\gamma$  heterotrimer.

### 1.3.3 Structural basis of receptor G protein coupling selectivity

The G protein coupling profiles of most GPCRs have been elucidated in considerable detail with the use of various different experimental approaches (Wess, 1998; Wong, 2003). When activated by the appropriate ligands, most GPCRs can recognise and activate only a limited set of the many structurally similar G proteins expressed in a cell (Gudermann et al., 1997; Milligan, 1995). Not surprisingly, given the sequence similarity between  $G\alpha$  subunits within the same sub-family, receptors ultimately can be broadly classified into  $G\alpha_{i/o}$ ,  $G\alpha_s$  and  $G\alpha_{q/11}$  coupled receptors. However, it has also become clear that most GPCRs, although preferentially linked to a certain subfamily of G proteins, can also couple to other classes of G proteins, although often with reduced efficiency (Gudermann et al., 1997). It should be noted that G protein coupling specificity is relative rather than absolute. In most cases where sufficient data are available, it appears that receptors are able to interact with most or all members of their preferred G protein family, frequently with different efficacies (Gazi et al., 2003; Perez and Karnik, 2005; Senogles et al., 2004). Because all GPCRs and all heterotrimeric G proteins are thought to share a similar molecular architecture, it is likely that the overall geometry of different receptor/G protein complexes is generally conserved. However, the amino acids predicted to determine the coupling properties of a specific member of a given receptor subfamily are usually not well conserved among the other GPCRs that display a similar G protein coupling profile. In addition, receptors from different structural classes, sharing little or no sequence homology, appear to couple to the same set of G proteins. Despite this wealth of information concerning GPCRs and their cognate G protein partners, little is known about how GPCRs selectively couple to a single subtype of G protein  $\alpha$  subunit. This is particularly puzzling given that there is approaching a thousand GPCRs of diverse primary structures, yet there are only four subfamilies of G protein. It is not possible, then, to

predict the G protein coupling profile of a GPCR based on its primary sequence, unless it shares a very high degree of sequence homology with a receptor whose G protein coupling preference is already known. However, despite the wide diversity of GPCR sequences, the regions within the receptor critical for receptor G protein coupling are generally conserved.

The observation that purified  $G\alpha_{o1}$  subunits could be activated by the wasp venom mastoparan, a 14 amino acid residue peptide, suggests that G proteins can be activated by short amphiphilic structures (Wong, 2003). This activation was pertussis toxin sensitive. Furthermore, a structure-function relationship study using a variety of synthetic peptides with sequences distinct from mastoparan suggests that G proteins can be activated by a variety of cationic and hydrophobic peptides with no obvious similarity in primary sequence. The common feature of all of these activators appears to be an amphiphilic  $\alpha$ -helical structure with a cationic residue on one side and a hydrophobic side chain on the other. This was also demonstrated for  $G\alpha_s$  and  $G\alpha_q$  (Bluml et al., 1994; Sukumar et al., 1997). Synthetic peptides based on regions of GPCRs have also been shown to activate G proteins, however, the receptor/G protein coupling specificity of the GPCR is not necessarily exhibited by the peptide (Wong, 2003).

### 1.3.4 Receptor domains involved in G protein coupling

A wide body of work has tried to isolate domains within GPCRs that are important for receptor/G protein coupling. Initial studies performed on muscarinic receptors have been extended to many other classes of GPCRs. Taken together, these studies have shown that G protein coupling specificity is determined by multiple intracellular receptor regions (Wess, 1998; Wong, 2003). The most critical regions are the second intracellular loop (ICL 2) and the third intracellular loop (ICL 3) (**Figure 1.2**). A considerable body of

evidence suggests that these regions act in a cooperative fashion to dictate proper G protein recognition and efficient G protein activation. However, the membrane proximal region of the C-terminal tail and residues within the first intracellular loop may also modulate both the selectivity and efficiency of receptor/G protein interactions. A general principle that has emerged from these studies is that the relative contribution of different intracellular receptor domains to the selectivity of G protein recognition varies among different classes of GPCR and even between GPCRs that are from the same subfamily. Below I will summarise the vast body of work that has implicated the importance of these regions in G protein coupling.

#### **1.3.4.1 The second intracellular loop**

Studies with hybrid GPCRs have provided strong evidence that the ICL 2 represents one of the key regions regulating the selectivity of receptor/G protein interactions. Several examples are known in which the substitution of the ICL 2 together with at least one other cytoplasmic receptor region, such as the ICL 3 or the C-terminal tail from a donor receptor into a functionally different, but structurally similar, acceptor receptor can confer on the resulting chimeric receptor the G protein coupling profile of the donor receptor (Wess, 1998). Such results have been obtained with m1 muscarinic/ $\beta$ 1 adrenergic and mGluR1/mGluR3 glutamate hybrid receptors (Pin, 1994; Wong and Ross, 1994). Other studies have shown that substitution of the ICL 2 alone can be sufficient to confer a new functional activity on a recipient receptor. For example, replacement of the ICL 2 of the  $G_s$  coupled  $V_2$  vasopressin receptor with the corresponding sequence of the  $G_{\alpha_{q/11}}$  coupled  $V_{1a}$  receptor sequence yielded a receptor that gained productive coupling to  $G_{\alpha_{q/11}}$  (Liu and Wess, 1996). Similar approaches have been used on the  $D_2$  dopamine receptor and  $\beta_2$ -

adrenergic receptors. The substitution of the second intracellular loop of these receptors for that of the  $G\alpha_{q/11}$  coupled thrombin receptor results in the conferment of  $G\alpha_q$  coupling to the  $D_2$  dopamine and  $\beta_2$  adrenergic receptors, which do not usually couple to  $G\alpha_q$  efficiently (Berg et al., 2001; Verrall et al., 1997). Interestingly, a study has shown that the editing of 5-HT<sub>2C</sub> receptor mRNA can result in receptor isoforms that differ in their ICL 2 sequences. These isoforms vary considerably in their  $G_q$  coupling efficiencies. This not only demonstrates that mRNA editing may represent a mechanism by which receptor/G protein coupling is regulated but also highlights the importance of this region in receptor/G protein coupling specificity (Berg et al., 2001; Burns et al., 1997).

#### **1.3.4.2 The third intracellular loop**

A vast body of evidence has implicated this region as playing a key role in receptor/G protein coupling specificity, but, as for the second intracellular loop, the relative contribution of this region to receptor/G protein coupling differs between GPCRs. Early studies carried out with chimeric muscarinic and adrenergic receptors showed that the exchange of the i3 loop between functionally different receptors frequently leads to a reversal of G protein coupling profiles, but with reduced efficiency. Furthermore, several of these hybrid receptors were shown to have retained coupling to G proteins normally activated by the recipient receptor (Wess, 1998). Both of these findings show that whilst the third intracellular loop is important, other regions of the receptor must be present to fully account for the coupling properties of a given receptor.

The third intracellular loop differs considerably in size among different classes of GPCRs and can contain as many as 240 (m3 muscarinic receptor) or as few as 15 amino acids (N-formyl peptide receptor). Deletion mutagenesis studies have shown, however, that only

the N- and C- terminal 8-15 amino acids of the third intracellular loop appear to be critical for G-protein coupling (Strader et al., 1994). Indeed, mutations in the C terminal region of the third intracellular loop frequently lead to constitutively active receptors (Lefkowitz, 1993). The structural and functional characteristics of both the N and C-terminal domains of the third intracellular loop have been analysed in great detail by mutagenesis studies of different muscarinic subtypes. Both residues at the junction of transmembrane region V and VI are thought to form amphiphilic  $\alpha$  helices that are critical for G protein recognition (Altenbach et al., 1996). According to the model proposed by Baldwin et al. the functionally critical receptor surfaces present at the N and C-terminal domains of intracellular loop three are predicted to project into the interior of the helical bundle (Baldwin et al., 1997). Receptor activation is proposed to be accompanied by an outward movement of transmembrane domains III and VI leading to an opening of the intracellular receptor surface that may allow the G protein heterotrimer to access the functionally important residues at the third intracellular loop/ transmembranes domain junctions. Furthermore Hubbell et al. measured light-activated changes in rhodopsin. They employed internitroxide distance measurements between labelled residues at cytoplasmic ends of TM1 (where a nitroxide label was attached as a reference point) and TM II, and another labelled residue at the cytoplasmic end of TM VIII. Residues in TM II were displaced relative to the position of TM VIII upon light activation when compared to the position of the reference residue (Altenbach et al., 2001). This group used the same approach to show that distances between a labelled residue in TM I and TM VII increase upon light activation of rhodopsin, which is consistent with a 2 to 4 Å movement of TM VII away from TM I. Together, these studies suggest that conformational changes occur in several regions of rhodopsin's cytoplasmic face (Altenbach et al., 2001).

### 1.3.4.3 C-terminal tail and intracellular loop 1

Relatively few studies have shown that the first intracellular loop is implicated in G protein coupling. However, several studies have shown that the structural integrity of the first intracellular loop is critical for efficient receptor/G protein coupling. Furthermore, the length of this region is highly conserved among GPCRs (Wess, 1998) indicating that it may play an important structural role. Studies using chimeric receptors with the fMLP formyl peptide and the C5a receptor, both of which couple to  $G\alpha_{i/o}$  and  $G\alpha_{16}$  subunits, showed that the exchange of the first intracellular loop of the fMLP peptide receptor with that of the C5a receptor led to a chimeric receptor that coupled to  $G\alpha_{16}$  even in the absence of activating ligands (Amatruda et al., 1995). There is, then, evidence that the first intracellular loop can influence G protein coupling. However, it remains to be determined whether this is due to direct contacts with the G protein heterotrimer or due to indirect conformational effects, for example, on the orientation or accessibility of other regions such as the third intracellular loop.

Deletion mutagenesis studies have shown that most of the cytoplasmic C-terminal tail region except for the membrane proximal 8-16 amino acids is not required for efficient G-protein coupling. However, it was noted that several truncated receptors were able to couple to G proteins with improved efficacy or display increased basal activity (Wess, 1998). Moreover, biochemical studies with short synthetic peptides corresponding to C-terminal tail sequences as well as loss of function mutagenesis studies implicate this region as being directly involved in G protein coupling (Merkouris et al., 1996). Interestingly, truncation of the C-terminal tail of the Mel1<sub>c</sub> receptor, which couples to  $G\alpha_{i/o}$  only,

enabled the receptor to couple to  $G\alpha_{i/o}$  and  $G\alpha_{16}$  (Lai et al., 2002). Grafting this region onto the c-terminus of the  $MT_1$  or  $MT_2$  receptors, which couple to both  $G\alpha_{i/o}$  and  $G\alpha_{16}$ , disrupted the coupling to  $G\alpha_{16}$  but not  $G\alpha_{i/o}$ . This indicates that the C-terminal region of  $Mel_{1c}$  negatively regulates the coupling to  $G\alpha_{16}$  but not  $G\alpha_{i/o}$ .

In summary, there is no consensus sequence predictive of Receptor/G protein coupling specificity but regions of importance in receptor/G protein coupling specificity, such as ICL 3, are conserved across many and diverse GPCRs. It could be postulated then that it is the orientation and availability of these domains that determines G protein coupling specificity (Oldham, 2006; Wong, 2003). Perhaps in agreement with this is the observation that point mutations of the LH/RH receptor (2<sup>nd</sup> extracellular loop) (Gilchrist et al., 1996) and  $\alpha_2$ -adrenoceptor receptor (2<sup>nd</sup> transmembrane domain) (Surprenant et al., 1992) disrupt G protein coupling. Indeed the work of Suprenant et al. is particularly relevant to this thesis and requires further discussion. An aspartate residue in the 2<sup>nd</sup> transmembrane domain of the  $\alpha_2$ -adrenoceptor receptor ( $Asp^{79}$ ) that is highly conserved among GPCRs, was mutated to an asparagine. In cells transfected with the mutant receptor, agonists inhibited adenylyl cyclase and calcium currents but did not increase potassium currents. It was postulated that distinct G proteins couple adrenoceptors to potassium and calcium currents, and that the mutant adrenoceptor was unable to achieve the conformation necessary to activate the G protein  $\alpha$  subunits that mediate potassium channel activation (Surprenant et al., 1992). These results can be explained by the loss of fidelity of G protein coupling due to a change in conformation at the intracellular region and suggests that the requirements for conferring G protein specificity may be subtle. Furthermore, these results also highlight one of the caveats of investigating G protein coupling using mutagenesis. Since this result shows that a single mutation in a seemingly distinct region can disrupt the structure of a GPCR in such a way as to alter the G protein coupling profile of this receptor, it is therefore not unlikely that other mutations, for

example within regions that are known to be involved with G protein coupling could have similar effects on the overall structure of that GPCR. As a consequence it is difficult to distinguish between mutations that affect G protein coupling, because that particular residue makes direct contact with the G proteins or mutations that simply change the overall structure of the receptor. In support of a model where specific receptor conformations may be more or less favourable for coupling to specific G proteins, different agonists can affect which, and to what extent, G proteins are activated by a given receptor (Kenakin, 2003; Perez and Karnik, 2005; Urban et al., 2006a).

### **1.3.5 Regions of G protein $\alpha$ subunits predicted to interact with GPCRs**

The extreme C-terminus of  $G\alpha$  and, in particular, the last five residues, has been established as an important mediator of receptor/G protein interaction. This consensus was arrived at from numerous studies using diverse methodologies (Wess, 1998). The pertussis toxin catalysed ADP ribosylation of cysteine residue -4 results in the uncoupling of  $G\alpha_{i/o}$  proteins from receptors (Milligan, 1995). Numerous reports of mutations in this region that alter receptor-G protein specificity have also appeared. In addition, several investigators have generated sequence-specific C-terminal peptides or antibodies targeting the C-terminal domain to study receptor-G protein interaction (Milligan, 1995). Antisera raised against decapeptides corresponding to the C-terminal ten amino acids of  $G\alpha$  subunits have been used to study receptor-G protein interaction. Antisera recognising  $G\alpha$  C-terminal domains block receptor-G protein signalling. Sequence-specific C-terminal synthetic peptides have been shown to either: stabilise the active agonist bound form of the receptor and therefore mimic the G protein, or serve as competitive inhibitors of receptor-G protein interface (Gilchrist et al., 1998; Rasenick et al., 1994). The sequence homology

of  $G\alpha$  subunits is high, and consequently the overall structural similarity is also high. This has allowed the construction of chimeric  $G\alpha$  subunits that fold appropriately and are functional. It was shown that the presence of only some 3 to 5 amino acids from the extreme C-terminus of  $G\alpha$  was sufficient to determine the selectivity of receptor coupling (Conklin and Bourne, 1993; Kostenis et al., 1997). This finding has allowed the generation of chimeric  $G\alpha$  subunits in which the C-terminal five amino acids of  $G\alpha_s$  or forms of  $G\alpha_{i/o}$  are transplanted onto the backbone of  $G\alpha_q$  (Kostenis et al., 2005). This allows receptors that normally couple to  $G\alpha_s$  or forms of  $G\alpha_{i/o}$  and those that couple to  $G\alpha_q$  to all generate a  $[Ca^{2+}]$  output in response to agonist activation. Consequently, a single generic assay suitable to detect agonist activation of many GPCRs can be developed. This not only demonstrates the importance of this region for receptor-G protein coupling selectivity but illustrates the potential benefits that an understanding of this subject can bring.

The c-terminus is not the only region directing receptor-G protein interactions. Several  $G\alpha$  subunits possess identical or nearly identical residues within the extreme C-terminus yet exhibit differential coupling to receptors. For example, within the last 11 amino acids of  $G\alpha_{i1}$  and  $G\alpha_t$ , only a single residue is divergent, yet the 5-HT<sub>1B</sub> receptor fails to couple to  $G\alpha_t$  but couples to  $G\alpha_{i1}$ . It was shown that two residues within the  $\alpha4$  helix of  $G\alpha_{i1}$  are critical mediators of this specificity (Bae et al., 1999). Slessarevara et al. (2003) demonstrated that receptors use multiple and distinct domains on G protein  $\alpha$ -subunits for selective coupling. This study made use of  $G\alpha_{i1}/G\alpha_t$  and  $G\alpha_q/G\alpha_{i1}$  chimeras and monitored their differential coupling to the A1 adenosine, 5-HT<sub>1A</sub>, 5-HT<sub>1B</sub> and muscarinic M2 receptors. The findings indicate that whilst the C-terminal region of  $G\alpha$  subunits is indeed an important region for the interaction of receptor and G protein, the residues involved in G protein coupling differ among the receptors studied. Domains within the N-terminus,  $\alpha4$ -helix, and  $\alpha4$ -helix- $\alpha4/\alpha6$ -loop of  $G\alpha_{i1}$  are involved in 5-HT and M2 receptor interaction. However, the relative influence of these domains and the individual

residues involved in the receptor/ G protein interaction differ with individual receptors. These results suggest that coupling selectivity ultimately involves subtle and cooperative interactions among various domains on both the G-protein and the associated receptor (Slessareva et al., 2003).

### **1.3.6 Regions of G protein $\beta\gamma$ subunits predicted to interact with GPCRs**

In addition to the structural determinants on  $G\alpha$  subunits, specific isoforms of  $G\beta$  and  $G\gamma$  subunits have been shown to preferentially interact with specific receptors. For example, both  $G\beta_1\gamma_2$  and  $G\beta_5\gamma_2$  can couple  $G\alpha_q$  to endothelin B and  $M_1$ -muscarinic receptors, but only  $G\beta_1\gamma_2$  promotes endothelin B receptor binding to  $G\alpha_i$  (Lindorfer et al., 1998). Further work showed that  $G\beta_5\gamma_2$  specifically couples  $G\alpha_q$  to receptors (Fletcher, 1998; Hou et al., 2000). The  $G\gamma$  subunit also plays an important role in the determination of receptor G protein coupling specificity. For example, the  $M_2$ -muscarinic receptor does not interact with  $G\alpha_o$ .  $G\beta_1\gamma_2$  heterotrimers but  $G\beta_1\gamma_5$  and  $G\beta_1\gamma_7$  did mediate binding of  $G\alpha_o$  to this receptor (Hou et al., 2000). The principal determinant of this specificity is likely the C-terminal third of  $G\gamma$  as shown by studies with chimeric  $G\gamma$  subunits (Myung et al., 2006). However, the type of lipid modification also has an effect on receptor coupling as a geranylgeranyl moiety on  $G\gamma_1$  or  $G\gamma_2$  increased the affinity of the G protein for rhodopsin and the  $A_1$ -adenosine receptor respectively.

### 1.3.7 Strategies used to study receptor-G protein coupling

Receptor-G protein coupling selectivity is a fundamental step in GPCR signalling and, accordingly, a considerable number of studies using diverse experimental strategies have been directed at trying to elucidate its molecular basis. I will summarise these strategies below with particular reference to those used in this study.

The most frequently used approach is to study biochemical or physiological responses mediated by stimulation of a given GPCR in either native tissue or heterologous cell systems. The nature of the observed responses then allows investigators to draw conclusions about the identity of the receptor-activated G proteins. For example, robust increases in intracellular cAMP levels are most likely due to activation of  $G\alpha_s$  subunits, whereas a reduction is most likely due to activation of  $G\alpha_{i/o}$  subunits. Pertussis toxin, which catalyses the ADP-ribosylation of a cysteine at the c-terminus of  $G\alpha_{i/o}$  subunits preventing their functional interaction with the receptor, has also proved a useful tool. Responses, then, can either be divided into pertussis toxin sensitive ( $G\alpha_{i/o}$ ) responses or pertussis toxin insensitive (all other  $G\alpha$  family members). However, there are several drawbacks to dissecting receptor-G protein coupling using these methods. The first is that this method cannot distinguish between  $G\alpha$  subunits of the same family, for example  $G\alpha_{i1}$ ,  $2, 3$  and  $G\alpha_{o1}$ , are all sensitive to pertussis toxin, and could inhibit adenylate cyclase. Secondly, effector regulation is subject to various forms of feedback and cross-regulation. Furthermore, G protein subunits released on activation of the G protein heterotrimer may converge on the same effectors to have antagonistic or synergistic effects (Milligan, 1994; Wess, 1998).

### 1.3.7.1 [<sup>35</sup>S] GTP $\gamma$ S binding assays

To avoid the problems associated with measuring downstream signalling events it is possible to directly measure receptor mediated G protein activation. One method to do this is to measure guanine nucleotide exchange on the G $\alpha$  subunit using the [<sup>35</sup>S] GTP $\gamma$ S assay. [<sup>35</sup>S] GTP $\gamma$ S is a non-hydrolysable form of GTP and therefore resistant to the GTPase activity of the G $\alpha$  subunit. Thus uptake of the radiolabelled GTP analogue gives a direct measurement of nucleotide exchange. Guanine nucleotide exchange is a very early event in the signal transduction cascade, and is an attractive event to monitor because it is less subject to amplification or regulation by other cellular processes than more distal events (e.g. regulation of gene expression) that are required for reporter gene assays. Therefore, it provides an excellent measure of the basic pharmacological characteristics and the relative efficacy of a series of compounds at a GPCR that might often be compromised when measuring downstream effects. However, one drawback is that the signal-to-noise ratio of the assay is often quite low, particularly when looking at receptors that couple to G proteins other than those in the G $\alpha_{i/o}$  family due to the relative expression levels of different G proteins within cells and the high basal GTP turnover of G $\alpha_{i/o}$  subunits. This can be circumvented by using antibodies raised against individual G $\alpha$  subunits in an immunoprecipitation step. This effectively allows the selection of the G $\alpha$  subunit of interest and therefore improves the signal window (Milligan, 2003).

### 1.3.7.2 Immuno-neutralisation of G proteins

The well established technique of immunoneutralisation of G proteins takes advantage of the observation that antibodies directed against the C-terminal tail of G $\alpha$  subunits prevent functional interaction of the receptor with the G protein. Therefore, antibodies raised

against and specific for different  $G\alpha$  subunits can be used to dissect receptor/G protein signalling. However, this technique is unable to distinguish between G proteins with identical C-terminal sequences, for example  $G\alpha_{i1}/G\alpha_{i2}$  and  $G\alpha_q/G\alpha_{11}$  (Milligan, 1994).

### **1.3.7.3 Co-expression of receptors and G proteins and reconstitution experiments**

The transient or stable expression of both receptor and G protein into a heterologous cell system in which the receptor and G protein are not expressed is a commonly used approach to study receptor/G protein coupling efficiency (Senogles et al., 2004). The ability of a given receptor to activate different G proteins can be easily assessed. However, there are several caveats with this method. Firstly, the relative expression of receptor and G protein must be controlled since relative levels of these two proteins can affect the efficiency and perhaps the specificity of interaction (Kenakin, 1997). However, it is unlikely that all of the receptor-G protein interactions observed using this strategy represent physiologically relevant interactions. Secondly, all mammalian cell lines will already express an array of G proteins, although this problem can be overcome by several means. For example the receptor and G protein of interest can be expressed in a heterologous cell system without endogenous G protein, exemplified by the expression of mammalian  $\alpha$  and  $\beta\gamma$  subunits in insect Sf9 cell lines (Gazi et al., 2003; Grunewald et al., 1996). The use of Sf9 cells has the advantage that the endogenous insect cell G proteins are expressed at a very low level as compared to the introduced mammalian G protein. Another technique allowing the investigation of the coupling of a receptor to a particular  $G\alpha_{i/o}$  subunit is the use of pertussis-toxin resistant mutants of these  $G\alpha$  subunits. The pertussis toxin-resistant variant of the  $G\alpha$  subunit of interest can be expressed in a heterologous cell line along with the

receptor of interest. Subsequent treatment with pertussis toxin will render all endogenous  $G\alpha_{i/o}$  subunits unable to functionally interact with the receptor so that the interaction between the receptor and pertussis toxin resistant variant  $G\alpha_{i/o}$  can be studied in isolation (Senogles, 1994; Senogles et al., 2004; Wise et al., 1997).

#### 1.3.7.4 Receptor-G protein fusion proteins

Receptor G protein fusion proteins can be expressed from chimeric cDNAs in which the 5' end of G protein  $\alpha$ -subunits are linked directly to the 3' tail of a G protein-coupled receptor (**Figure 1.5**). Consequently, the stoichiometry of expression of the two protein partners should always be 1:1 irrespective of the cell system used for expression or the absolute levels of expression of the fusion protein. Furthermore, the receptor and G protein will have the same co-localisation within the cell. c Estimates of ligand efficacy vary frequently with levels of GPCR expression and thus are also sensitive to the stoichiometry of expression of GPCR, G protein and effector polypeptides (Hildebrandt, 2006; Milligan, 2002). Therefore, as long as the measure of agonist function is taken directly at a point of GPCR–G protein interaction, rather than at some downstream or temporally distant point, measurement of ligand intrinsic activity should be free from this constraint. The fusion protein approach, then, should ensure that measurements of agonist-binding affinity and  $EC_{50}$  for G-protein activation are directly comparable for the same receptor coupling to each G protein.

#### 1.3.7.5 Chimeric receptors

In the summary of domains important for receptor-G protein coupling, data was included from both mutagenesis studies and from the use of chimeric receptor and G proteins. However, a potential caveat of mutagenesis studies is that abolition or a change in receptor/G protein coupling could be due to an alteration of the overall folding of the receptor rather than that particular region being involved in G protein coupling (Wong, 2003). A perhaps more convincing strategy to identify the G protein coupling region is the use of chimeric receptors. In this approach, intracellular regions are exchanged between GPCRs of differing G protein coupling specificities (Wess, 2002; Wong, 2003). Substituting these regions of the 'donor receptor' onto the corresponding region in another 'acceptor receptor' should result in the acceptor receptor gaining the G protein coupling specificities of the donor receptor. A summary of work to date using chimeric receptors, including the region of the receptor exchanged, is displayed in **Table 1.2**. Studies using chimeric receptors derived from highly homologous receptors are perhaps the most relevant since disruption of receptor structure is likely to be minimal.

As described above the high homology of G protein  $\alpha$  subunits makes the use of chimeric receptors to highlight regions of G proteins important in receptor coupling particularly appealing. This technique has highlighted the c-terminus of  $G\alpha$  subunits as an important region governing receptor-G protein coupling selectivity as described in **section 1.3.6**.

**Table 1.2: Chimeric GPCRs that showed a change in G protein-coupling specificity.**

Chimeric receptors (R1-R2) were constructed with the indicated intracellular region of donor receptor (R2) substituted into the corresponding region of acceptor (R1). I2 = 2<sup>nd</sup> intracellular loop; I3 = 3<sup>rd</sup> intracellular loop; I3N = N-terminal region of the 3<sup>rd</sup> intracellular loop; IC3 = C-terminal region of the 3<sup>rd</sup> intracellular loop, C = C-terminal tail. All of the chimeric receptors presented have acquired the G protein selectivity of R2, while

the majority of those tested either retained the coupling to the acceptor receptor or became functionally promiscuous. No coupling = coupling not detectable with the assay system used: ND = not determined (Taken from Wong, 2003).

Acceptor receptor (R1)		Donor receptor (R2)			Chimeric receptor R1-R2: G protein selectivity		
receptor	G protein selectivity	receptor	Regions substituted	G protein selectivity	R2	R1	Other G proteins
$\alpha_2$ AR	$G\alpha_{i/o}$	$\beta_2$ AR	I3	$G\alpha_s$	+	ND	ND
mGluR <sub>3</sub>	$G\alpha_{i/o}$	mGluR <sub>1</sub>	I2+I3+C	$G\alpha_q$	+	ND	ND
D <sub>3</sub>	no coupling	D <sub>2</sub>	I3	$G\alpha_{i/o}$	+	ND	ND
D <sub>2</sub>	$G\alpha_{i/o}$	M <sub>1</sub>	I3	$G\alpha_q$	+	ND	ND
D <sub>2</sub>	no coupling	thrombin	I2	$G\alpha_q$	+	ND	no $G\alpha_s$
M <sub>2</sub>	$G\alpha_{i/o}$	M <sub>3</sub>	I2	$G\alpha_q$	+	ND	no $G\alpha_s$
M <sub>2</sub>	$G\alpha_{i/o}$	M <sub>3</sub>	I3	$G\alpha_q$	+	-	ND
M <sub>3</sub>	$G\alpha_q$	M <sub>2</sub>	I3	$G\alpha_{i/o}$	+	-	ND
M <sub>2</sub>	$G\alpha_{i/o}$	M <sub>3</sub>	I3N	$G\alpha_q$	+	+	ND
A <sub>1A</sub>	$G\alpha_{i/o}$	A <sub>2A</sub>	I3, I3N	$G\alpha_s$	+	+	ND
$\beta_2$ AR	$G\alpha_s$	$\alpha_2$ AR	I3N+I3C+C	$G\alpha_{i/o}$	+	+	ND
$\beta_2$ AR	$G\alpha_s$	$\alpha_1$ AR	I3, I3N	$G\alpha_q$	+	+	ND
$\beta_2$ AR	$G\alpha_s$	thrombin	I2	$G\alpha_q$	+	+	ND
PACAPR <sub>2</sub>	$G\alpha_s$	PAFR	I3	$G\alpha_q$	+	+	ND
VP <sub>2</sub>	$G\alpha_s$	VP <sub>1</sub>	I2	$G\alpha_q$	+	+	no $G\alpha_{i/o}$
VP <sub>1</sub>	$G\alpha_q$	VP <sub>2</sub>	I3	$G\alpha_s$	+	+	no $G\alpha_{i/o}$
M <sub>1</sub>	$G\alpha_q$	$\beta_1$ AR	I3, I3N	$G\alpha_s$	+	+	$G\alpha_{i/o}$ , $G\alpha_z$
M <sub>2</sub>	$G\alpha_{i/o}$ , $G\alpha_z$	$\beta_1$ AR	I3N	$G\alpha_s$	+	+	$G\alpha_q$
M <sub>1</sub>	$G\alpha_q$	$\beta_1$ AR	I2+I3N, I2+I3	$G\alpha_s$	+	-	no $G\alpha_{i/o}$ , $G\alpha_z$
M <sub>2</sub>	$G\alpha_{i/o}$ , $G\alpha_z$	$\beta_1$ AR	I2+I3N	$G\alpha_s$	+	-	no $G\alpha_{i/o}$ , $G\alpha_z$

## 1.3.8 Molecular basis of G protein activation

### 1.3.8.1 Receptor activation and GDP release

Activated receptors bind to G proteins and catalyze GDP release from  $G\alpha$ , which is the rate limiting step in G protein activation. Until GTP binds, a high affinity complex between the agonist-bound receptor and  $G\alpha$  subunit is formed. Based on the current models of this interaction, the nucleotide binding pocket is 30 Å away from the receptor (Bourne, 1997; Fotiadis et al., 2006). The conformational change induced by the receptor must cause GDP release over this distance and has been investigated by analysis of the affect of various mutations on the basal and receptor-catalyzed nucleotide exchange rates of the G protein. However, there is little direct evidence of specific receptor-mediated conformational changes within G proteins and the molecular mechanisms for receptor mediated nucleotide exchange. The  $\alpha 5$ -helix links the C-terminus of  $G\alpha$  to the  $\beta 6/\alpha 5$  loop containing the guanine ring-binding TCAT motif. Mutations in this motif greatly enhance GDP release (Posner et al., 1998). Indeed, an activating mutation A<sup>366</sup>S  $G\alpha_s$  causes pseudo-hypoparathyroidism in male patients and a homologous mutation in  $G\alpha_i$  also enhances GDP release (Iiri et al., 1994; Posner et al., 1998). Alanine scanning mutagenesis of  $G\alpha_i$  identified three residues on the inward face of the helix which when mutated substantially increased rates of basal and receptor-catalysed exchange and several residues on the outward face of this helix that decreased catalysed exchange (Marin et al., 2001). Interestingly, a flexible five glycine linker inserted between the extreme C-terminus and the  $\alpha 5$ -helix severely reduced receptor-mediated nucleotide exchange but did not effect binding to the receptor. However, G protein coupling was only minimally reduced when the length of this region was doubled but the rigidity of the contact between

the C-terminus and GDP-binding pocket was maintained (Natochin et al., 2001). A recent study using site-directed spin-labeling showed receptor-activation dependant alterations in the structure of the  $\alpha 5$ -helix at sites distant from the receptor-G protein interface (Oldham et al., 2006). These conformational changes were uncoupled from receptor activation by the insertion of a five glycine linker suggesting, then, that the rigidity of the connection between the C-terminus and the GDP binding pocket is important. The introduction of an isoleucine-to-proline mutation at the C-terminus of the  $\alpha 5$ -helix has been shown to reduce the stimulatory activity of D<sub>2</sub> dopamine receptor mimetic peptide on nucleotide exchange G $\alpha_{i1}$  (Nanoff et al., 2006) indicating that perturbations in this region are transmitted to the GDP binding pocket.

As for the  $\alpha 5$ -helix, the  $\beta 6$  strand may transmit receptor binding to the  $\alpha 4/\beta 6$  to the binding pocket at the  $\beta 6/\alpha 5$  loop. In accordance, mutations within this region have been shown to reduce receptor-catalyzed activation despite normal receptor binding (Onrust et al., 1997). Intramolecular contacts with the N-terminal region have also been implicated in nucleotide exchange. Mutations within this region or within regions interacting with the N-terminal  $\beta 1$  and  $\beta 3$  strands may perturb the hydrophobic core of the  $\alpha$  subunit, thereby reducing the affinity for GDP (Oldham, 2006). Two models have been proposed for receptor-mediated GDP release (**Figure 1.6**). The first uses the N-terminal helix of G $\alpha$  as a lever arm to pull the G $\beta\gamma$  away from G $\alpha$ . This would allow GDP release as Switches I and II are pulled away from the nucleotide binding pocket (Iiri et al., 1998). The second model proposes that the receptor uses the  $\alpha N$ -helix to force G $\beta\gamma$  into G $\alpha$ , allowing the N-terminus of G $\gamma$  to engage the helical domain of G $\alpha$ . This interaction may cause the interdomain gap between the helical and GTPase domains of G $\alpha$  to open, leading to GDP release (Cherfils and Chabre, 2003) For both of these models, it is proposed that the G $\beta\gamma$  dimer acts as a guanine nucleotide exchange factor. In support of this proposal, alanine

mutations at the switch interface of  $G\beta$  have been shown to prevent receptor-catalyzed nucleotide exchange, and mutations within the c-terminus of  $G\gamma$  have been shown to increase the rate of nucleotide exchange (Ford et al., 1998). Accordingly, a study using bioluminescence resonance energy transfer to probe structural rearrangements in  $\alpha_{2A}$ adrenoceptor- $G\alpha_i\beta_1\gamma_2$  complexes showed agonist activation of the receptor causes a rearrangement of the receptor-G protein complex. It was proposed that this conformational rearrangement causes the  $G\alpha$ - $G\beta\gamma$  interface to open, in turn causing the opening of the GTPase and helical domain through the interdomain linker region, resulting in GDP release (Gales et al., 2006). Glycine to proline mutations in each of the interdomain linkers of  $G\alpha_t$  enhances the basal nucleotide exchange rate of  $G\alpha$ , in agreement with this interdomain rearrangement (Majumdar et al., 2004).

All of the conformational changes described above are supported by data from both biochemical and mutagenesis studies. However, without the crystal structure of an activated receptor bound to a G protein heterotrimer, many questions remain about the orientation of these two proteins, the sites of interaction between them and the conformational changes that lead to GDP release. It was recently demonstrated that both light-activated rhodopsin and a soluble mimic of the active receptor form trapped intermediate complexes with a GDP-released "empty pocket" state of the heterotrimer in the absence of GTP (or  $GTP\gamma S$ ). The results suggested that activated receptor-mediated changes in the receptor-interacting regions of  $G\alpha$ , and not the absence of bound guanine nucleotide, are the predominant factors which dictate  $G\alpha$  conformation and dynamics in this activated receptor-bound state of the heterotrimer (Abdulaev et al., 2006).

### 1.3.8.2 GTP binding-mediated alteration of the receptor G protein complex

The concentration of GTP in the cell exceeds that of GDP by several fold, consequently the receptor-G protein complex is transient due to the rapid binding of GTP. The binding of GTP to the  $G\alpha$  subunit causes a structural rearrangement of  $G\alpha(\text{GTP})$ , and its orientation with both the  $G\beta\gamma$  dimer and the receptor. This rearrangement allows interaction with downstream effectors. Conformational rearrangements in the three switch regions between  $G\alpha_{i1}$  when bound to GDP or  $\text{GTP}\gamma\text{S}$  were revealed by crystal structures of these complexes (Coleman et al., 1994; Lambright et al., 1994; Mixon et al., 1995). This structural rearrangement was thought to eliminate the  $G\beta\gamma$  binding surface of the  $\alpha$  subunit therefore leading to subunit dissociation. However, studies monitoring the structural rearrangements of the receptor and the G protein heterotrimer using fluorescence and bioluminescence resonance energy transfer suggest that the receptor and G protein subunits may remain closely associated following receptor activation (Bunemann et al., 2003; Gales et al., 2006).

In addition to the conformational changes in the switch regions, GTP binding also causes a conformational change in the myristoylated N-terminus of  $G\alpha$ . Site-directed fluorescence labelling indicates that the myristoylated N-terminus moves into an even more hydrophobic environment, perhaps suggesting that the conformational changes associated with GTP binding expose an intramolecular binding site for the N-terminus (Preininger et al., 2003). The non-myristoylated N-terminus of  $G\alpha$  becomes disordered upon binding GTP.

### 1.3.8.3 G protein inactivation

Termination of the G protein signal is achieved upon the intrinsic hydrolysis of GTP to GDP by the  $G\alpha$  subunit and re-association or rearrangement of the heterotrimer. Again, structural insight into the mechanism of GTP hydrolysis was provided by crystal structures of the complexes  $G\alpha_{i1}.GDP$  and  $G\alpha_{i1}.AlF_4^-$  (Coleman et al., 1994). Aluminium fluoride is an activator of  $G\alpha$  subunits and binds along with GDP in the active site as a tetra-coordinate  $AlF_4^-$  ion. In the crystal structure of  $G\alpha_{i1}.GDP.AlF_4^-$ , the  $AlF_4^-$  ion is in a square planar configuration with the oxygen of the  $\beta$ -phosphate and a water molecule acting as transaxial ligands forming a tetragonal bipyramid. It was proposed that this conformation represents a transition state for the hydrolysis of GTP. The crystal structure of this transition state revealed several residues with important roles in the GTPase activity of  $G\alpha_{i1}$ . A conserved glutamine ( $Glu^{204}$ ) polarizes and orients the nucleophilic water molecule. Mutation of this glutamine to a leucine results in a GTPase-deficient  $G\alpha$  subunit that is effectively constitutively active (Landis et al., 1989). A conserved arginine ( $Arg^{178}$  in  $G\alpha_{i1}$ ) stabilises the transition state, by stabilising the developing negative charge on the leaving  $\gamma$  phosphate and facilitating its release. ADP ribosylation of this arginine by cholera toxin abolishes the GTPase activity of  $G\alpha_s$  and  $G\alpha_t$ , as does the mutation of this residue to a cysteine, both resulting in a constitutively active  $G\alpha$  subunit. Indeed, this mutation has been shown to cause sporadic endocrine tumours and McCune-Albright syndrome (Bourne, 1987; Weinstein and Shenker, 1993). Two mutations in the nucleotide binding pocket, a glycine to valine substitution in the P-loop, and a glycine to alanine mutation (Berghuis et al., 1996; Raw et al., 1997) in switch II stabilise a  $G\alpha_{i1}.(GDP.P_i)$  complex associated with substantial conformational change in switch II. An additional lysine-to-proline mutation in Switch I accelerates a conformational change in the Switch regions, but decreases the rate of GTP hydrolysis (Thomas et al., 2004). Consequently, the dynamics of the Switch regions may be critical for GTP hydrolysis.

The intrinsic GTP hydrolysis activity varies among  $G\alpha$  family members, where  $G\alpha_{i/o}$  family members ( $1.8-2.4 \text{ min}^{-1}$  at  $30 \text{ }^\circ\text{C}$ ) and  $G\alpha_s$  family members have a higher GTPase activity than members of the  $G\alpha_q$  ( $0.8 \text{ min}^{-1}$  at  $30 \text{ }^\circ\text{C}$ ) or  $G\alpha_{12}$  ( $0.2 \text{ min}^{-1}$  at  $30 \text{ }^\circ\text{C}$ ) families. Differences in the helical domains, N and C-termini may provide the structural basis for this observation (Cabrera-Vera et al., 2003).

#### 1.3.8.4 GTPase-activating proteins

It was noted that the intrinsic GTPase activity of many purified  $G\alpha$  subunits was much slower than the deactivation rates of G protein signalling *in vivo*. This suggested the influence of GTPase accelerating proteins (or GAPs). The first GAPs identified were the  $G\alpha$  effectors  $\text{PLC}\beta 1$  and  $\text{PDE}\gamma$  ( $G\alpha_t$ ) (Arshavsky and Bownds, 1992; Berstein et al., 1992). This illustrates that effectors, following activation by  $G\alpha$ , can negatively regulate the amplitude and duration of the G protein signal. However, in addition to effector mediated feedback inhibition another class of GAPs have been identified: the regulators of G-protein signalling (RGS). These proteins share a common 120 amino acid RGS domain that forms a bundle of nine  $\alpha$ -helices that bind to the switch regions of  $G\alpha$ . The RGS domain enhances the GTPase activity of  $G\alpha$  by stabilising the transition state conformation and orientating the  $G\alpha$  backbone to stabilise the nucleophilic water molecule (Tesmer et al., 1997a).

### 1.3.8.5 Interaction of activated G proteins with their downstream effectors

Once  $G\alpha$ .GTP has dissociated from or perhaps altered its conformational relationship with the  $G\beta\gamma$  dimer, it can interact directly with effector proteins to continue the signal cascade. The tissue distribution, effector molecules and known disease relevance of all  $G\alpha$  family members is summarized in **Table 1.1**. Each  $G\alpha$  family activates a distinct profile of effectors. The molecular basis of this divergence has not been completely elucidated but co-crystallization studies of  $G\alpha_s$  in a complex with the catalytic domains of adenylyate cyclase identified the  $\alpha 2$  helix and the  $\alpha 3$ - $\beta 5$  loop as being particularly important (Ghahremani et al., 1999; Tesmer et al., 1997b). Furthermore, within a  $G\alpha$  family, each different  $G\alpha$  subunit exhibits a different profile of effector activation. For example,  $G\alpha_{i2}$  is required for a dopamine  $D_{2S}$  receptor-mediated inhibition of forskolin-stimulated adenylyate cyclase activity, whereas  $G\alpha_{i3}$  is required to inhibit PDE $\beta$ -induced ( $G\alpha_s$  coupled) enhancement of adenylyate cyclase activity (Ghahremani et al., 1999). Thirdly, some  $G\alpha$  subunits couple only to one effector, such as  $G\alpha_t$  to cGMP phosphodiesterase.

Initially  $G\beta\gamma$  was thought to facilitate the completion of the G protein signal by passively binding to and hastening the return of the heterotrimer to the plasma membrane, thereby preventing noise or spontaneous  $G\alpha$  activation in the absence of receptor stimulation. It is now known that  $G\beta\gamma$  interacts with and influences several effectors including PLC $\beta$ , several isoforms of adenylyate cyclase, PI-3 kinases,  $Ca^{2+}$  channels and  $K^+$  channels (Oldham, 2006).

## 1.4 Receptor theory, agonist directed receptor trafficking and protean agonism

Receptors bind a ligand on the extracellular side and following activation by an agonist, conformational changes occur that allow the intracellular region of the GPCR to bind to and activate the heterotrimeric G protein. Pharmacological theory proposes that ligands can be characterised by the nature of their functional effects generated by their interaction with their target receptor. These effects are governed by two important properties: the affinity of the ligand for its receptor, and efficacy, the ability of the ligand once bound to elicit a response (Kenakin, 2001). This has led to the classification of receptor ligands as agonists, partial agonists, neutral antagonists or inverse agonists. According to this classification, full agonists possess sufficiently high intrinsic efficacy such that they maximally stimulate all cellular responses linked to a given receptor. Partial agonists possess lower degrees of intrinsic efficacy and therefore give sub-maximal responses. Initially, it was thought that an agonist ligand was the regulator to select or induce the active conformation of the receptor. The current model(s) of GPCR function uses the concept of allosterism, which was first described for ion channels and enzymes and subsequently applied to receptors. These ideas culminated in the ternary complex model for GPCRs, which was first published by De Lean and colleagues (De Lean et al., 1980). This model describes a receptor that, when activated by an agonist, moves laterally in the cell membrane to physically couple to a trimeric G protein. This introduced a novel concept in receptor models, namely that the sensitivity of the system (and potency of agonists) was subject to the availability of an external protein (i.e. a G protein). Supporting this model were data showing that physical complexes between receptors and G proteins could be isolated after addition of agonist to receptor systems (Limbird and Lefkowitz, 1978).

However, the observation that mutations in the third intracellular loop of the  $\beta_2$ -adrenoceptor resulted in its constitutive activation led to an appreciation that receptors can exist in the active state even without the effects of an agonist (Samama et al., 1993). This led to the revision of the ternary complex model, which postulated that receptor activation required the agonist-promoted formation of an active, “ternary” complex of agonist, receptor and G protein. The revised model was termed the two state model. This includes the explicit isomerisation of the receptor to the active ( $R^*$ ) state prior to coupling to G proteins. This model explains constitutive activation as a shift in the equilibrium between receptor molecules in the inactive state ( $R$ ) and the active states ( $R^*$ ), resulting in a higher proportion of receptor molecules in the  $R^*$  state. Conversely, inverse agonists have a higher affinity for, and will shift the equilibrium towards, the inactive state ( $R$ ). Therefore, inverse agonists will reduce the basal activity of a constitutively active receptor. Neutral antagonists bind with equal affinity to both  $R$  and  $R^*$  and therefore have no effect on the basal activity of constitutively active receptors. An extension of this two state model is termed the cubic ternary complex model and differs in that it allows G-proteins to bind to inactive receptors. This cubic ternary complex model implies the existence of a receptor conformation that can couple to its G-protein partner, but is unable to evoke a response, allowing a ligand with high affinity for this receptor conformation to behave as a neutral antagonist or inverse agonist (Weiss et al., 1996a; Weiss et al., 1996b; Weiss et al., 1996c).

It was assumed that the ability of the ligand to impart (or reduce) stimuli once that ligand is bound to the receptor is an inherent parameter that is constant for each ligand at a given receptor, irrespective of where that receptor is expressed. For example, a full agonist would be expected to activate all of the signalling pathways linked to a receptor to the same degree as the endogenous ligand for that receptor. Similarly, a ligand that antagonised one signalling pathway via a specific receptor should antagonise every pathway coupled to that receptor to the same extent. This assumption is still widely held and forms the basis of drug discovery today (Urban et al., 2006a). Most drug screening

programmes employ an experimental model system and it is assumed that, due to intrinsic system-independent efficacy, that the pharmacological characteristics of a drug seen in these experimental conditions can be extrapolated to *in vivo* systems. However, data demonstrating differential pharmacology of the same ligand at the same receptor through different signalling pathways has emerged over the last decade and are not consistent with this assumption (Kenakin, 2001; Perez and Karnik, 2005; Urban et al., 2006a). I will summarise these considerable and diverse data below.

#### **1.4.1 Examples of functional selectivity**

The capability of certain serotonergic ligands to differentially activate signal transduction pathways associated with the human serotonin 5-HT<sub>2A</sub> and 5-HT<sub>2c</sub> receptors was shown. It was observed that the relative efficacy of a series of ligands for each of the receptors differed depending upon whether PLC-mediated accumulation of IP or PLA<sub>2</sub>-mediated release of arachidonic acid (AA) was measured (Berg et al., 1998). Importantly, responses to the reference ligand were obtained along with each test ligand for each experiment. A cysteine to phenylalanine mutation in TM III of the  $\alpha_{1b}$ -adrenoceptor constitutively activates the receptor resulting in G protein coupling in the absence of agonist (Perez et al., 1996). However, this mutation results in the activation of the PLC pathway, and not phospholipase A<sub>2</sub>. Furthermore it was shown that these two pathways are coupled to two different G proteins (Perez et al., 1993). It was found that phenylethylamine ligands from full to partial agonists were able to recognise this selective active state. However, a series of structurally-distinct imidazoline agonists, such asoxymetazoline, did not change in either their signalling or binding characteristics. This same mutation has been shown to cause similar phenotypes in a cross-section of GPCRs that couple to different G-proteins for example the angiotensin receptor (Noda et al., 1996) and the bradykinin receptor (Ishii

et al., 1997). In fact, a large area around this residue in TM III seems responsible for active state isomerisation suggesting that this region is a possible switch region controlling key steps in the isomerisation from the inactive to active structure (Parnot et al., 2000).

## 1.4.2 Evidence from kinetic & binding studies

Using a series of weak to full  $\beta_2$ -adrenergic agonists Seifert et al. (2001) examined their ability to both stabilise the ternary complex and activate GTPase activity. No correlation was observed between the efficacy of ligands to stabilise the ternary complex and to activate GTPase suggesting that the receptor conformation that stabilises the ternary complex is different from that which can stabilise the ternary complex (Seifert et al., 2001). Several  $\beta_2$  adrenergic agonists were shown to display different order of efficacies in their ability to hydrolyse different purine nucleotides than was seen for their ability to activate adenylate cyclase in the presence of the different nucleotides (Seifert et al., 1999). Perhaps some of the most convincing evidence for multiple signalling states comes from biophysical studies using purified  $\beta_2$ -adrenergic receptors. The labelling of specific sites on the receptor with specific probes allows for the detection of changes in the bound fluorophore, such as fluorescence lifetime and emission. Therefore variations in receptor conformation can be detected (Ghanouni et al., 2001). Similarly, rapid kinetics of fluorescent neurokinin A (NKA) binding in parallel with intracellular calcium and cAMP measurements allowed the determination of multiple activation states in the tachykinin NK2 receptor (Palanche et al., 2001).

### **1.4.3 Evidence from reversal of efficacy (protean agonism)**

Protean agonists were predicted to exist from theoretical arguments based upon multiple active conformations of GPCRs (Kenakin, 2001). It was predicted that a protean agonist could act both as an agonist or an inverse agonist at the same GPCR. The reversal from agonism to inverse agonism would only occur when an agonist produces an active conformation of lower efficacy than a totally active conformation. It was shown that proxyfan, a high-affinity histamine H<sub>3</sub>-receptor ligand, acted as a protean agonist at recombinant H<sub>3</sub> receptors expressed in Chinese hamster ovary cells (Gbahou et al., 2003). However, using neurochemical and behavioural assays in rodents and cats, proxyfan displayed a spectrum of activity ranging from full agonism to full inverse agonism. Protean agonism, then, is a direct demonstration of the existence of alternative agonist active states different from the constitutively active state.

### **1.4.4 Evidence from differential phosphorylation, desensitisation, internalisation and palmitoylation**

In addition to multiple signalling states, there is also evidence to suggest that there are multiple deactivation states. Since different ligands can invoke different active conformations, it makes sense that the mechanism to deactivate these states may also be different from one another. Perhaps the most compelling and pharmaceutically-relevant example of this is the observation that DAMGO but not morphine could induce rapid phosphorylation and internalisation of the  $\mu$ -opioid receptor and that cAMP-dependent protein kinase could phosphorylate *in vitro* the  $\mu$ -opioid receptor in the presence of morphine but not DAMGO (Arden et al., 1995; Chakrabarti et al., 1998).

To explain these observations, the concept of agonist-directed trafficking was described. It is clear that GPCRs, like all proteins, can adopt numerous conformations according to thermal energy. What is not clear is how many of these conformations are capable of activating G proteins. As described in **section 1.3.2**, certain regions of a GPCR's intracellular surface, when available and in the correct conformation, are capable of activating G proteins. With this in mind, it would suggest that the inactive form of the receptor prevents access of G proteins to these regions. Therefore, any disruption to the GPCR tertiary structure, for example, exerted by the binding of a ligand, could make these regions available for G protein activation. It follows then that a receptor can adopt more than one activated R\* state. According to this model, each agonist is theoretically able to promote its own specific active receptor state leading to a limitless number of receptor conformations (Kenakin, 1995). However, a criticism of this theory is that some of these conformations may not be physiologically pertinent, i.e. several different conformations may have essentially the same physiological consequences. Leff et al. (1997) proposed an alternative model where the receptor might exist in three states, an inactive (R) and two active conformations (R\*,R\*\*), thereby still accounting for multiple G protein coupling but limiting the number of receptor conformations to those that are theoretically physiologically active (Leff et al., 1997). However, since even for the most well characterised GPCRs with rich pharmacology the number of ligands are limited, the difference between these two theories is debatable. The phenomenon of multiple signalling states of GPCRs has been described by a number of names including agonist directed trafficking, functional selectivity, biased agonism, protean agonism, differential engagement and stimulus trafficking.

## 1.5 Dopamine receptors

Dopamine is the predominant catecholamine neurotransmitter in the mammalian brain, where it controls a number of functions such as locomotor activity, emotion, cognition, food intake and endocrine regulation. It also acts in the periphery as a modulator of cardiovascular function, hormone secretion, renal function and gastrointestinal motility. The dopaminergic signalling pathways have been the focus of a vast body of research over the past forty years. This is due to its involvement in the wide ranging and important functions listed above and its dysregulation being linked to several pathological conditions. These include Parkinson's disease, schizophrenia, Tourette's syndrome and hyperprolactinemia (Missale et al., 1998). Dopamine receptor antagonists have been developed to block hallucinations and delusions that occur in schizophrenic patients, whereas dopamine receptor agonists are effective in alleviating the symptoms of Parkinson's disease. The treatment of diseases associated with dopamine imbalances is associated with severe side effects. The blockade of dopamine receptors can induce extrapyramidal effects similar to those resulting from dopamine depletion, and high doses of dopamine agonists can cause psychoses.

### 1.5.1 Classification of dopamine receptors

Initial pharmacological studies identified two distinct populations of dopamine receptor, one positively coupled to adenylyl cyclase ( $D_1$ ) and one which was not ( $D_2$ ). The cDNAs of five distinct dopamine receptor subtypes have been isolated and characterized and three novel subtypes have been characterised  $D_3$ ,  $D_4$  and  $D_5$ . However, all dopamine receptor

subtypes fall into one of the two initially recognised receptor categories both in terms of their structure and pharmacology. The D<sub>1</sub> and D<sub>5</sub> receptors share a very high homology in their transmembrane domains and ligand binding characteristics, and a similar homology is shared between D<sub>2</sub>, D<sub>3</sub> and D<sub>4</sub> receptors (Missale et al., 1998). The genomic organisation of the dopamine receptors suggests that they derive from the divergence of two gene families that mainly differ in the absence or presence of introns in their coding sequences. D<sub>1</sub>-like receptor genes do not contain introns in their coding regions, a characteristic shared with many G-protein coupled receptors. In contrast, the genes encoding the D<sub>2</sub>-like receptors are interrupted by introns (Jackson and Westlind-Danielsson, 1994; O'Dowd, 1993). Analysis of the structure of D<sub>2</sub> like receptors revealed that the D<sub>2</sub> receptor-coding region contains six introns, the D<sub>3</sub> coding region five and the D<sub>4</sub> receptor three (Missale et al., 1998). The presence of introns within the coding region allows the generation of splice variants, for example, the D<sub>2</sub> receptor has two main variants, called D<sub>2s</sub> and D<sub>2l</sub>, which are generated by alternative splicing of an 87bp exon between introns 4 and 5 (Gingrich and Caron, 1993). Splice variants of the D<sub>3</sub> receptor encoding non-functional proteins have also been identified. Analysis of the gene for human D<sub>4</sub> receptor revealed the existence of polymorphic variations within the coding sequence. A 48-bp sequence in the third cytoplasmic loop exists either as a direct repeat sequence, as a four fold repeat, or a seven fold repeat. D<sub>4</sub> receptors containing up to 11 repeats have been found. The D<sub>5</sub> receptor has two related pseudogenes on human chromosomes 1 and 2. They are 98 % identical to each other and 95 % identical to the human D<sub>5</sub> receptor and encode truncated, non-functional forms of the D<sub>5</sub> receptor.

## 1.5.2 Localisation of dopamine receptor subtypes

In the brain, the D<sub>1</sub> receptor is the most widespread dopamine receptor and is expressed at higher levels than any other dopamine receptor. Its expression has been demonstrated in the striatum, the nucleus accumbens, the olfactory tubercle, limbic system, hypothalamus and thalamus (Fremeau et al., 1991; Weiner et al., 1991). In comparison the D<sub>5</sub> receptor is much less widely expressed and has been detected in the hippocampus, thalamus and certain areas of the forebrain (Meador-Woodruff et al., 1992). The expression of D<sub>1</sub> and D<sub>5</sub> at both pre and post-synaptic locations has been demonstrated although the postsynaptic localisation is more prevalent (Levey et al., 1993). The D<sub>2</sub> receptor is found mainly in the striatum, in the olfactory tubule, and in the hypothalamus (Gurevich and Joyce, 1999; Jackson and Westlind-Danielsson, 1994). Co-localisation with the D<sub>1</sub> receptor is rare. Compared with the D<sub>2</sub> receptor, the D<sub>3</sub> receptor is expressed in roughly 10-fold lower density. The D<sub>3</sub> receptor has a specific distribution within limbic areas such as the ventromedial shell of the nucleus accumbens, but low levels of expression have been observed in the hippocampus and in various cortical layers. In the human brain it was demonstrated that D<sub>3</sub> mRNA was often expressed in D<sub>2</sub> mRNA positive neurons (Gurevich and Joyce, 1999; Landwehrmeyer et al., 1993). High dopamine D<sub>4</sub> expression has been demonstrated in the frontal cortex, amygdala, hippocampus, hypothalamus and mesencephalon. In the periphery, it has been shown that all dopamine receptor subtypes are present in the kidney and D<sub>4</sub> receptors are present in the heart (Missale et al., 1998).

### **1.5.3 Functions of dopamine receptors in the brain**

The effects of dopamine on motor activity have been extensively investigated, and the activation of D<sub>1</sub>, D<sub>2</sub> and D<sub>3</sub> receptors has been implicated. Activation of pre-synaptic D<sub>2</sub> autoreceptors decreases locomotor activity whereas post synaptic D<sub>2</sub> receptor activation increases locomotor activity. Conversely, the D<sub>3</sub> receptor seems to play a mainly inhibitory role in locomotor activity. (Jackson and Westlind-Danielsson, 1994; Missale et al., 1998). Activation D<sub>1</sub> receptors alone has been shown to have little effect on locomotor activity, but the concomitant activation of D<sub>1</sub> and D<sub>2</sub> receptors has been shown to be required for D<sub>2</sub> agonists to produce maximal locomotor stimulation. The mesolimbocortical dopamine pathway is implicated in reward and reinforcement mechanisms demonstrated by the observation that administration of psycho-stimulants and drugs of abuse elicit an increase in dopamine release in the mesolimbic areas. Pharmacological studies show that both D<sub>1</sub> and D<sub>2</sub> receptors are involved in this pathway. In the case of drug administration, it has been shown that both D<sub>1</sub> and D<sub>2</sub> receptors are involved in the reinforcing properties of different drugs of abuse, with D<sub>2</sub> receptors mediating the stimulant drug reinforcement and D<sub>1</sub> receptors playing a permissive role. The mesolimbic dopamine pathway also plays a role in learning and memory, again involving both D<sub>1</sub> and D<sub>2</sub> receptors (Missale et al., 1998).

### **1.5.4 Dopamine and disease**

Parkinson's disease is a neurodegenerative disorder with an insidious onset and a prolonged course over many years. The primary cause of the symptoms of this illness is the death of dopamine-producing neurons of the substantia nigra and the resultant depletion of dopamine in the striatum (Hornykiewicz, 1998). The therapeutic intervention

for Parkinson's disease is based on the assumption that activation of postsynaptically located dopamine receptors will provide some return of balance to the system. The preferred mode of treatment of the symptoms of this illness is with L-dopa, which is taken up by surviving dopamine neurons and converted to dopamine, which, in turn, can be stored and released. Loss of dopamine leads to changes in expression levels for both D<sub>1</sub> and D<sub>2</sub> receptors in the striatum and changes in dopamine-mediated activity. However, for many patients significant loss of effectiveness in L-dopa treatment and inability and inability to reverse dementia or depression occurs after five or more years of treatment (Joyce, 2001). Therefore dopamine agonists have an advantage over L-dopa treatment, since they will bypass the degenerating neurons and directly stimulate the intact, although denervated post synaptic receptors in the striatum. Furthermore, agonists that target specific dopamine receptor subtypes may have more specific therapeutic effects and perhaps target certain clinical symptoms. Within the basal ganglia D<sub>2</sub> and D<sub>3</sub> receptors and only extremely low levels of the D<sub>4</sub> receptor are expressed indicating that stimulation of D<sub>2</sub> and D<sub>3</sub> receptors prominently contributes to the antiparkinsonian effects of most of the compounds used (Gurevich and Joyce, 1999). Indeed relief of Parkinsonian symptoms is most consistently observed with drugs that target with D<sub>2</sub>-like receptors (Joyce, 2001).

The dopamine hypothesis of schizophrenia proposes that the symptoms result from disturbances in the normal dopaminergic transmission in the brain. These abnormalities affect two of the main dopamine pathways in the brain – the mesolimbic pathway and the mesocortical pathway- producing changes in brain activity (Lieberman, 2004). Increased dopaminergic transmission in the mesolimbic pathway is thought to cause the positive or psychotic symptoms of schizophrenia, which include delusions and hallucinations. Reduced activity in the mesocortical pathway, which projects into the frontal cortex, produces hypodopaminergic activity in these regions. This is believed to underlie the negative symptoms such as apathy, social withdrawal and poverty of thought. Evidence

for the key role of dopamine came initially from examining the effects of drugs that either stimulate or reduce dopaminergic activity. Psychostimulant drugs that increase dopamine release, such as amphetamine, have been shown to induce psychosis in healthy individuals following repeated administration. Similarly treatment with the dopamine precursor L-dopa induces psychotic symptoms in a high proportion of patients with Parkinson's disease. Conversely, both typical and atypical antipsychotics, which are effective in treating psychosis show antagonistic activity at D<sub>2</sub> receptors. In fact there is a strong correlation between the clinical efficacy of typical antipsychotics and their binding affinity for the D<sub>2</sub> receptor. Furthermore, a number of studies have implicated the D<sub>3</sub> receptor as being a potential target for antipsychotics (Joyce, 2001; Joyce and Millan, 2005). All dopaminergic antagonists used in the treatment of schizophrenia demonstrate high affinity for the D<sub>3</sub> receptor. Interestingly, the atypical antipsychotic clozapine has 7-fold higher affinity for the D<sub>2</sub> receptor as compared to the D<sub>3</sub> receptor (Guo et al., 1998). However, it has predominant actions through neurons expressing the D<sub>3</sub> receptor. Therefore occupancy of the D<sub>3</sub> receptor by antipsychotics cannot be excluded as a target site for therapeutic intervention. However, direct evidence for abnormal dopamine levels is less clear cut. For example, *in vivo* research using nuclear magnetic imaging has shown that patients with schizophrenia release more dopamine into synapses upon neuronal stimulation as compared to healthy individuals (Guillin et al., 2007). Increased levels of both D<sub>2</sub> and D<sub>3</sub> receptors have been detected in the caudate nucleus, putamen and nucleus accumbens, but this may be due to antipsychotic drug treatment. *In vivo* imaging studies using positron emission tomography (PET) and single-photon emission tomography (SPECT) in patients with schizophrenia have also proved inconsistent. Some studies reported increased D<sub>2</sub> receptor density in largely drug-naïve individuals with schizophrenia but others showed no differences between schizophrenia and control groups. Although dopaminergic dysfunction appears to play a key role in the pathophysiology of schizophrenia, it is increasingly

apparent that other neuro-transmitter pathways are also involved in the disorder (Joyce, 2001).

### **1.5.5 Dopamine receptor structure**

Analysis of the primary structure of the cloned dopamine receptors revealed that they are indeed members of the seven transmembrane domain GPCR family (Jackson and Westlind-Danielsson, 1994; Missale et al., 1998). The D<sub>2</sub>-like receptors possess moderate sequence homology with the D<sub>1</sub> like receptors. For example, the rat D<sub>1</sub> and D<sub>2</sub> receptors possess only 41% homology in transmembrane domains. In contrast, the D<sub>3</sub> receptor possesses 52 % homology with the D<sub>2</sub> receptor, with 75% homology in the transmembrane domains (Gingrich and Caron, 1993; Jackson and Westlind-Danielsson, 1994; Missale et al., 1998). The N-terminal region has a similar number of amino acids in all the receptor subtypes and carries a variable number of consensus N-glycosylation sites. The D<sub>1</sub> and D<sub>5</sub> receptors possess two such sites, one in the N-terminal and the other one in the second intracellular loop. The D<sub>2</sub> receptor has four potential glycosylation sites, the D<sub>3</sub> has three and the D<sub>4</sub> possesses only one. The C-terminal region is about seven times longer for D<sub>1</sub>-like receptors as compared to that of the D<sub>2</sub>-like receptors. In both cases this region is rich in threonine and serine residues and contains a cysteine residue that is the site of palmitoylation and conserved in many GPCRs. In the D<sub>1</sub>-like receptors this residue is located near the beginning of this region at end of TM VI. In the D<sub>2</sub>-like receptors the c-terminus ends with this region. Two cysteine residues in the 2<sup>nd</sup> and 3<sup>rd</sup> intracellular loops, which are conserved in all Class I GPCRs, have been suggested to form an intermolecular disulphide bridge to stabilise the receptor structure

D<sub>2</sub>-like receptors possess a long third intracellular loop, which is common to receptors interacting with the G $\alpha_{i/o}$  subfamily of G proteins to inhibit AC whereas the D<sub>1</sub>-like receptors are characterized by a short third loop as for many G $\alpha_s$  coupled receptors (Gingrich and Caron, 1993; Jackson and Westlind-Danielsson, 1994; Missale et al., 1998). The D<sub>2</sub> receptor exists as two alternatively spliced isoforms differing in the insertion of a stretch of 29 amino acids in the third intracellular loop (D<sub>2s</sub> and D<sub>2l</sub>). As described previously this region plays an important role in receptor/G protein coupling.

Site directed mutagenesis and protein modelling have suggested that the agonist-binding site occurs within the hydrophobic TM domains (Kalani et al., 2004; Shi and Javitch, 2002). Highly conserved residues within these domains define a narrow binding pocket that probably corresponds to the agonist-binding site. Important residues were predicted by computational modelling and confirmed by previous mutagenesis studies. For the dopamine D<sub>2</sub> receptor Asp<sup>114</sup> in TM III is an important residue. The carboxyl group of the aspartate forms a tight salt bridge (2.6 Å) with the primary amino group of dopamine. This residue is conserved over all five human dopamine receptors, as well as in all human biogenic amine receptors. Mutation studies have implicated this residue in the direct binding of the dopamine to D<sub>2</sub> (Kalani et al., 2004; Shi and Javitch, 2002). The residues Ser<sup>193</sup> and Ser<sup>197</sup> in TM V hydrogen-bond to the metahydroxyl and parahydroxyl groups, respectively, of the catechol ring of dopamine, playing an essential role in recognizing dopamine. These two residues are conserved over all five human dopamine receptors and have been shown to be involved in direct binding of ligand through mutation studies (Shi and Javitch, 2002). Ser<sup>194</sup> is also conserved over all five human dopamine receptors, and mutation studies indicate that it is involved in binding of the ligand. Ser<sup>194</sup> might serve as an alternate to Ser<sup>193</sup> in hydrogen bonding to the metahydroxyl group of the catechol for the slightly modified structure of the receptor that might result from activation. The residues Phe<sup>110</sup>, Met<sup>117</sup>, Cys<sup>118</sup> (TM III), Phe<sup>164</sup> (TM IV), Phe<sup>189</sup>, Val<sup>190</sup> (TM V), Trp<sup>386</sup>,

Phe<sup>390</sup>, and His<sup>394</sup> (TM VI) of the D<sub>21</sub> receptor are thought to form a mostly hydrophobic pocket for dopamine (Kalani et al., 2004). It was shown that Trp<sup>386</sup> and Phe<sup>390</sup> of the conserved WXXFF motif in TM VI are within the 4.5-Å binding pocket, but Phe<sup>389</sup> is 7.2 Å away from dopamine. Furthermore, it was proposed that the second extracellular loop has a critical role in contributing to the binding site for small molecular weight aminergic ligands, much in the same way as this loop dives down into the binding-site crevice and contacts retinal in rhodopsin (Shi and Javitch, 2004). As for all Class I GPCRs the DRY motif proximal to TM III plays a crucial role in receptor activation.

#### 1.5.5.1 Dopamine receptor oligomerisation

As described above the higher order organisation has been visualised by atomic force microscopy for mouse rhodopsin (Fotiadis et al., 2003). A considerable amount of evidence points to other GPCRs existing as dimers or oligomers. Accordingly, dopamine receptor oligomerisation has been demonstrated in a number of different studies, with examples of both homo-oligomerisation and hetero-oligomerisation. Homo-oligomerisation has been demonstrated for the D<sub>2</sub> receptor, with evidence provided by ligand binding studies, (Vivo et al., 2006) cysteine cross-linking (Guo et al., 2005), and by visualisation of oligomeric complexes by Western blotting (Lee et al., 2003b).

Furthermore, residues within TM IV were shown to be a key contact sites in this interaction (Guo et al., 2005; Javitch, 2004). Furthermore, in the cysteine cross linking study it was shown that the susceptibility of substituted cysteine residues within TM IV to crosslinking was differentially altered by the presence of agonists and inverse agonists. The TM IV dimer interface in the inverse agonist-bound conformation was consistent with the dimer of the inactive form of rhodopsin modelled with constraints from atomic force microscopy. Crosslinking of a different set of cysteines in TM IV was slowed by inverse agonists and accelerated in the presence of agonists; crosslinking of the latter set locks the

receptor in an active state. It was proposed that a conformational change at the TM IV dimer interface is part of the receptor activation mechanism (Guo et al., 2005). Similarly the homo-oligomerisation of dopamine D<sub>1</sub> receptors has been demonstrated (George et al., 1998) as has that of the D<sub>3</sub> receptor (Elmhurst et al., 2000). As described above, all the dopamine receptor subtypes have an overlapping localisation of expression. It is perhaps likely then that these highly homologous receptors will form heterodimers and accordingly D<sub>2</sub>/D<sub>3</sub> dopamine receptor hetero-oligomers has been demonstrated *in vitro* (Scarselli et al., 2001) as have D<sub>1</sub>/D<sub>2</sub> dopamine receptor oligomers (Dziedzicka-Wasylewska et al., 2006). Dopamine receptors have also been shown to form hetero-dimers or oligomers with other GPCRs. D<sub>2</sub> receptors have been shown to form heterodimers with the CB<sub>1</sub> cannabinoid receptor (Kearn et al., 2005), the A<sub>2A</sub> adenosine receptor (Canals et al., 2003) and the somatostatin receptor subtype SSTR5 (Rocheville et al., 2000). Similarly, D<sub>1</sub> has been shown to form heterodimers with the A<sub>1</sub> adenosine receptor (Gines et al., 2000). The functional consequences of these interactions, with particular focus on the signaling pathways of the D<sub>2</sub>-like receptors, will be discussed later.

### 1.5.6 Dopamine receptor pharmacology

As might be predicted from their sequence homology, the D<sub>1</sub>-like and D<sub>2</sub>-like dopamine receptors have pharmacological profiles that are distinct from each other. However, the individual members within D<sub>1</sub>-like or D<sub>2</sub>-like receptor families have pharmacological profiles that are extremely similar (Missale et al., 1998). The individual dopamine receptor subtypes, their principal signal transduction, and a list of selective antagonists and agonists are displayed in **Table 1.3**.

The pharmacological profile of the D<sub>5</sub> receptor is similar, yet distinct from that of the D<sub>1</sub> receptor. The most consistent difference is represented by dopamine itself which has a 10

fold higher affinity for the D<sub>5</sub> receptor as compared to that of D<sub>1</sub> (Missale et al., 1998). Analysis of the pharmacological profiles of the D<sub>2</sub>-like receptors shows that there are no compounds that discriminate between the short and the long variants of the D<sub>2</sub> receptor, although a marginal difference in the affinities of sulpiride and raclopride for the two isoforms has been described (Malmberg et al., 1993). The pharmacological profile of the D<sub>3</sub> receptor reveals that some agonists and antagonists can distinguish it from the D<sub>2</sub> receptor. Dopamine itself has a 20 times higher affinity at the D<sub>3</sub> as compared to the D<sub>2</sub> receptor (Sokoloff et al., 1990). With the use of chimeric D<sub>2</sub>/D<sub>3</sub> receptors, this difference has been related to the third intracellular loop (Robinson et al., 1994). Similarly, many agonists show a higher affinity for the D<sub>3</sub> receptor as compared to the D<sub>2</sub> receptor, although interestingly apomorphine does not. The inverse agonist/antagonist spiperone shows a 10 fold higher affinity for the D<sub>2</sub> receptor. The antagonists S33084, nafadotride and (+)S14297 have all been shown to have selectivity at the D<sub>3</sub> receptor (Millan et al., 1994; Millan et al., 2000; Missale et al., 1998). The pharmacological profile of the D<sub>4</sub> receptor closely resembles those of the D<sub>2</sub> and D<sub>3</sub> receptors, but specific differences have emerged. The most important feature distinguishing the D<sub>4</sub> from the D<sub>2</sub> and D<sub>3</sub> receptors is its high affinity for clozapine (Van Tol et al., 1991). Conversely, the antagonist raclopride shows lower affinity at D<sub>4</sub> receptor as compared to the D<sub>2</sub> and D<sub>3</sub>.

**Table 1.3: The dopamine receptor subtypes, their principle signal transduction pathway, and pharmacological profiles**

The selectivity of these agonists is less than two orders of magnitude. [<sup>3</sup>H] raclopride exhibits a similar high affinity for D<sub>2</sub> and D<sub>3</sub> receptors (low affinity for D<sub>4</sub>) but has been used to label D<sub>2</sub> receptors in the presence of a D<sub>3</sub>-selective antagonist (Alexander et al., 2006).

Nomenclature	D1	D2	D3	D4	D5
Other names	D <sub>1</sub> , D <sub>1A</sub>	D <sub>2</sub>	D <sub>3</sub>	D <sub>4</sub>	D <sub>5</sub> , D <sub>1B</sub>
Principal transduction	G $\alpha_s$ , G $\alpha_{olf}$	G $\alpha_{i/o}$	G $\alpha_{i/o}$	G $\alpha_{i/o}$	G $\alpha_s$ , G $\alpha_{olf}$
Selective agonists	R(+)-SKF81297, R(+)-SKF38393, dihydroxedine	(+)-PHNO	PD128907	PD168077	-
Selective antagonists	SCH23390, SKF83566, SCH39166	Raclopride, domperidone	S33084 (Millan et al., 2000), Nafadotride, (+)-S14297 (Millan et al., 1994), SB277011 (Reavill et al., 2000)	L745870, U101958 (Schlachter et al., 1997), L741742,	-

## 1.5.7 Signal transduction of dopamine receptors

### 1.5.7.1 Signal transduction of D<sub>1</sub>- like dopamine receptors

It has been shown in a variety of cell lines that the D<sub>1</sub> receptor robustly stimulates cAMP accumulation. D<sub>5</sub> has also been shown to be coupled to the stimulation of adenylate cyclase (Missale et al., 1998). It is generally assumed that the activation of adenylate cyclase by D<sub>1</sub>-like receptors is mediated by the G $\alpha_s$  subunit of G proteins. In the neostriatum, however, the brain region with the densest dopamine innervation and the highest expression of the D<sub>1</sub> receptor, expression of G $\alpha_s$  is very low but expression of the highly homologous G $\alpha_{olf}$  is high (Corvol et al., 2001; Zhuang et al., 2000). G $\alpha_{olf}$  null mutant mice exhibit little dopamine-stimulated adenylate cyclase and lack other functional and behavioural responses to D<sub>1</sub> dopamine receptor stimulation, including cocaine of D<sub>1</sub> agonist-induced locomotor activation and induction of c-fos expression (Corvol et al., 2001). However, there is evidence that D<sub>1</sub> can also couple to G $\alpha_z$  and G $\alpha_o$  (Sidhu et al., 1998). The selective concentration of adenylate cyclase subtype V in the neostriatum suggested that it mediates dopamine receptor signalling, a hypothesis confirmed with the creation of adenylate cyclase V null mutant mice in which neostriatal D<sub>1</sub> receptor-stimulated cAMP accumulation is markedly diminished (Iwamoto et al., 2003). The increase in intracellular cAMP mediated by the D<sub>1</sub> receptor via G $\alpha_{s/olf}$  has been linked to the activation of protein kinase A (PKA) (Neve et al., 2004). The PKA substrates that have been implicated in dopamine D<sub>1</sub>-like receptor mediated signalling include DARPP32 (a bifunctional signalling protein that inhibits protein phosphatase 1 and PKA), ion channels (for example the inhibition of K<sup>+</sup> currents through several types of inwardly rectifying channels). D<sub>1</sub> like receptors modulate intracellular calcium levels by a variety of

mechanisms; for example via the stimulation of PLC producing inositol 1,4,5 trisphosphate, which mobilizes intracellular calcium stores (Neve et al., 2004).

### 1.5.7.2 D<sub>2</sub>-like receptor signalling

#### Dopamine D<sub>2</sub>-like receptor G protein coupling

As mentioned above the D<sub>2</sub> dopamine receptor family consists of two isoforms, the short form (D<sub>2s</sub>) and the long form, the D<sub>2l</sub> receptor, which are alternatively spliced transcripts of the same gene. These isoforms differ only by the presence of an additional 29 amino acids and their expression is coincident in all tissues although the ratios differ between tissues (Missale et al., 1998). Localization studies of the two isoforms demonstrated that the D<sub>2l</sub> receptor is strongly expressed in neurons of the striatum and nucleus accumbens, and that the D<sub>2s</sub> receptor is found in the cell bodies and axons of the mesencephalon and hypothalamus (Khan et al., 1998). This suggests that the D<sub>2s</sub> receptor is predominantly a presynaptic auto receptor and that the D<sub>2l</sub> receptor is predominantly found post synaptically (Uziel et al., 2000). It is therefore likely that the D<sub>2</sub> isoforms have unique localisation and serve distinct functions.

The G-protein coupling specificity of the D<sub>2s</sub> receptor and D<sub>2l</sub> receptor remains controversial. A difference in coupling of these two receptors was initially suggested by pertussis toxin studies in JEG-3 cells (Montmayeur and Borrelli, 1991) and further study indicated that D<sub>2l</sub> interacts specifically with G $\alpha_{i2}$  (Montmayeur et al., 1993). A similar result was obtained by antisense ablation of  $\alpha_{i2}$  and  $\alpha_{o1}$  in GH4C1 cells stably transfected with one of the two receptor isoforms (Liu et al., 1994). However, an experiment using the expression of PTX insensitive mutant G $\alpha_{i1-3}$  subunits, again in GH4C1 cells, suggested that the D<sub>2s</sub> receptor signalled preferentially through the Cys<sup>352</sup>Ile G $\alpha_{i2}$  mutant whilst the D<sub>2l</sub>

receptor signalled through the Cys<sup>351</sup>Ile  $G\alpha_{i3}$  mutant (Senogles, 1994). In transfected fibroblast cells, CCL1.3,  $D_{21}$  receptors were found to couple to  $G\alpha_{i2}$  and  $G\alpha_{i3}$  but not  $G\alpha_{o1}$  or  $G\alpha_{i1}$  (O'Hara CM, 1996). However, in transfected NS20Y neuroblastoma cells,  $D_{21}$  receptors coupled to  $G\alpha_{o1}$ , but not to any other  $G\alpha_i$  subunits (Watts et al., 1998). Similarly, in AtT-20 cells,  $D_{2L}$  coupled to  $G\alpha_{o1}$  and to  $G\alpha_{i3}$ , whereas  $D_{2S}$  coupled to both  $G\alpha_{o1}$  and  $G\alpha_{i2}$  (Wolfe and Morris, 1999). In baculovirus-infected Sf9 cells co-transfected with  $D_{2S}$  and either  $G\alpha_{i1}$  or  $G\alpha_{i2}$ ,  $D_{2S}$  receptors were found to couple with higher efficacy to  $G\alpha_{i1}$  than they did to  $G\alpha_{i2}$  (Grunewald et al., 1996). Accumulating evidence from a number of studies now implicate  $G\alpha_{o1}$  as the subtype most robustly activated by  $D_{21}$  and  $D_{2S}$ . This is confirmed by a study showing  $D_2$ -like receptors predominantly couple to  $G\alpha_{o1}$  in mouse brain (Jiang et al., 2001). Studies using an array of agonists at both the  $D_{21}$  and  $D_{2S}$  receptors showed that different agonists conferred differential G protein coupling. It was concluded from this that the degree of selectivity of G-protein activation by the  $D_{21}$  receptor can depend of the conformation of the receptor stabilised by an agonist (Gazi et al., 2003).

The regions flanking each extremity of the loop adjacent to transmembrane domains V and VI have been shown to be fundamental to the coupling of receptor with G proteins.

However, the insert present in  $D_{21}$  does not affect these regions as it adds 29 amino acids at a position 31 residues C-terminal from transmembrane domain V. Mutagenesis was used to assess the role of residues within the insert region. Two mutants produced a modest change in coupling: in both cases it involved a negatively charged amino acid being substituted for a non-polar amino acid. The  $D_{21}$  insert is predicted to have a helical structure, and it was postulated that these substitutions might modify this structure (Guiramand et al., 1995). However, a more recent experiment substituted the insert region for a non-homologous region of identical length. It was demonstrated that this epitope substitution generated a functional receptor with no difference in down-stream signalling

as compared to the wild type D<sub>2L</sub> receptor (Kendall and Senogles, 2006). Therefore this indicates that the alternatively spliced insert region, itself, does not appear to play a direct role in signal transduction. Another study in HEK293 cells showed that two random point mutations of the D<sub>2S</sub> receptor changed the coupling specificity. While the wild-type D<sub>2S</sub> receptor couples predominantly to Cys<sup>352</sup>Ile Gα<sub>i2</sub>, the D<sub>2S</sub> receptor mutant Arg<sup>233</sup>Gly couples preferentially to Cys<sup>351</sup>Ile Gα<sub>i3</sub> and the D<sub>2S</sub> receptor mutant Ala<sup>234</sup>Tyr couples preferentially to Cys<sup>351</sup>Ile Gα<sub>i1</sub> (Senogles et al., 2004). This underlies the importance of this region of the third cytoplasmic loop is crucial for determining Gα<sub>i/o</sub> protein coupling selectivity.

The human D<sub>4</sub> receptor is similar to D<sub>2</sub> in that it activates multiple pertussis toxin-sensitive G proteins, including Gα<sub>i2</sub>, Gα<sub>i3</sub>, Gα<sub>o1</sub> (Li-Xin Liu, 1999). The rat D<sub>4</sub> receptor has been reported to couple preferentially to Gα<sub>z</sub> and the transducin subtype Gα<sub>t2</sub> (Yamaguchi et al., 1997). Although the D<sub>3</sub> and D<sub>2</sub> receptors show marked sequence homology and pharmacological similarity the D<sub>3</sub> receptor was initially reported not to couple to G-proteins as shown by the lack of a guanine nucleotide shift of agonist binding curves, and an inability to inhibit adenylyl cyclase in cell lines (Sokoloff et al., 1990; Tang et al., 1994). However, more recently it has been shown that the D<sub>3</sub> receptor does weakly inhibit adenylyl cyclase in some cell lines (Chio et al., 1994; Freedman et al., 1994; Potenza et al., 1994), with one group showing selective inhibition of adenylyl cyclase type V, but not types I or VI in HEK 293 cells (Robinson and Caron, 1997). A subsequent study using [<sup>35</sup>S] GTPγS binding to investigate the activation of G proteins coupled to D<sub>3</sub> and D<sub>2</sub> receptors stably expressed in CHO cells found that antibodies against the c-terminus of Gα<sub>i/o</sub> reduced dopamine-induced G protein activation for both D<sub>3</sub> and D<sub>2</sub> membranes, whereas Gα<sub>s</sub> antibodies had no effect at either site. In contrast, incubation with anti-Gα<sub>q/α11</sub> antibody did not affect dopamine-induced G protein activation at D<sub>2</sub> receptor but attenuated D<sub>3</sub>-induced G protein activation. This suggests that D<sub>3</sub> receptors may couple to

$G_{\alpha_q}/\alpha_{11}$  and would be consistent with the observation that pertussis toxin treatment, which inactivates only  $G_{i/o}$  proteins, only submaximally (80%) blocked dopamine-stimulated [ $^{35}$ S]GTP $\gamma$ S binding in CHO-D<sub>3</sub> cells (Newman-Tancredi et al., 1999). The efficient coupling of the dopamine D<sub>3</sub> receptor to  $G_{\alpha_{o1}}$  was demonstrated in SH-SY5Y cells but not HEK293 cells. The abundance of this G protein subunit was demonstrated in both cell lines and it was postulated that the presence of adenylate subtype V was required for coupling of the dopamine D<sub>3</sub> receptor to  $G_{\alpha_{o1}}$  (Zaworski et al., 1999).

Interestingly, the D<sub>3</sub> receptor has been shown to bind agonists with a high affinity that is relatively insensitive to GTP (Neve et al., 2004). The insensitivity of the D<sub>3</sub> receptor to GTP could reflect GTP-resistant coupling to G proteins or a receptor structure that is constrained in a conformation with high affinity for agonists regardless of interactions with G proteins. A study expressing the D<sub>3</sub> receptor in *E coli* and, therefore, in the absence of endogenous G proteins with which the receptor can interact showed that agonist binding was minimally affected by G protein coupling, pointing to a constrained receptor structure (Vanhouwe et al., 2000).

### **Investigations into the molecular basis of G protein coupling specificity using chimeric D<sub>2</sub>/D<sub>3</sub> receptors**

Dopamine D<sub>2</sub> and D<sub>3</sub> receptors are highly homologous making them extremely suitable for investigations into the structural basis of G protein selectivity using chimeric receptors.

An initial experiment showed that a chimeric dopamine receptor containing the third intracellular loop of the D<sub>2</sub> receptor retained D<sub>3</sub> like affinities for dopaminergic ligands but did not functionally couple to adenylyl cyclase (McAllister et al., 1993). However, a subsequent experiment showed that a chimeric D<sub>2</sub> receptor containing the third

intracellular loop of the D<sub>3</sub> receptor exhibited lower affinity for agonists but did not investigate coupling specificity (Robinson and Caron, 1996). A study using a D<sub>3</sub> receptor with the third intracellular loop of the human D<sub>2</sub> receptor showed that although the chimeric receptor retained D<sub>3</sub> receptor binding, the receptor was negatively coupled to adenylyl cyclase through a pertussis toxin sensitive pathway apparently mediated by the D<sub>2</sub> third intracellular loop. This response was not seen for D<sub>3</sub> receptors, and the inhibition seen with the chimera was less than that seen with the D<sub>2</sub> receptor, implying that additional sequences in the D<sub>2</sub> receptor contribute to normal G-protein coupling (Van Leeuwen et al., 1995). To determine which area of the D<sub>2</sub> dopamine receptor's third intracellular loop contributes to G-protein coupling, a study constructed reciprocal chimeric D<sub>2</sub>/D<sub>3</sub> receptors with fusion points near the centre of the third intracellular loop. Both of these chimeras were able to effectively inhibit adenylyl cyclase activity to almost the same extent as that seen with the D<sub>2</sub> receptor. This implies that both the N and C-terminal portions of the D<sub>2</sub> receptor ICL 3 are capable of independently supporting functional G<sub>i</sub> coupling although both may be required for maximal coupling. However, in this study no inhibition of adenylyl cyclase activity was seen in cells transfected with the D<sub>3</sub> receptor (Lachowicz and Sibley, 1997). Chimeras were constructed in which a twelve amino acid sequence located at the C-terminal portion of the third intracellular loop was exchanged between dopamine D<sub>2</sub> and D<sub>3</sub> receptors. Chimera constructions did not modify substantially the pharmacological profiles as compared to their respective wild-type receptors. However, the D<sub>2</sub> receptor chimera, containing the C-terminal portion of the third intracellular loop of the D<sub>3</sub> receptor, had a lower potency to inhibit cyclic AMP production. The reciprocal construction generated a D<sub>3</sub> receptor that was fully coupled to this second messenger in Chinese hamster ovary (CHO) cells pathway, whereas the native D<sub>3</sub> receptor was not. These results suggest that the sequence selected is important for specific coupling characteristics shown by these two dopamine receptor homologues (Filteau et al., 1999).

## **D<sub>2</sub>-like receptor downstream signalling**

The first signalling described pathway for the D<sub>2</sub>-like receptors was the inhibition of adenylate cyclase and therefore the inhibition of cAMP accumulation. As for D<sub>1</sub>-like receptors, the genetic deletion of adenylate cyclase V abolishes D<sub>2</sub> receptor mediated inhibition of adenylate cyclase in the mouse neostriatum. This null mutation also eliminates the locomotor inhibitory effects of D<sub>2</sub> receptor blocking anti-psychotic drugs, demonstrating the behavioural significance of this pathway (Lee et al., 2002). Therefore, current experimental evidence favours a D<sub>2</sub> → Gα<sub>o1</sub> → adenylate cyclase V pathway. As opposed to the effects of D<sub>1</sub>-like receptors, by decreasing the activity of adenylate cyclase and therefore the levels of intracellular cAMP, it is expected that D<sub>2</sub> receptor stimulation decreases PKA activity (Neve et al., 2004). For example, stimulation of D<sub>2</sub>-like autoreceptors reverses PKA-dependent phosphorylation of tyrosine hydroxylase at Ser<sup>40</sup>, a phosphorylation event that activates the enzyme (Lew et al., 1999). In addition to effects mediated by α subunits, many pathways modulated by D<sub>2</sub>-like receptor activation are mediated by βγ subunits released upon α subunit activation (Neve et al., 2004). D<sub>2</sub> stimulation exerts a powerful influence over K<sup>+</sup> currents; indeed, D<sub>2</sub> stimulation decreases cell excitability by increasing K<sup>+</sup> currents in most brain areas. All of the D<sub>2</sub>-like receptors activate a G protein-regulated inwardly rectifying potassium channel (GIRK or Kir3), a channel that carries one of several potassium currents modulated by dopamine in midbrain dopamine neurones and neostriatal D<sub>2</sub> receptor-expressing neurons with activation mediated by βγ subunits (Neve et al., 2004). The D<sub>3</sub> receptor was shown to be as efficient as D<sub>2</sub> receptors at coupling to GIRK channels in the rat mesencephalon (Kuzhikandathil et al., 1998). D<sub>2</sub> and D<sub>4</sub> receptors have been shown to co-precipitate with GIRK2 (Lavigne et al., 2002). It has been shown that dopamine release regulating D<sub>2</sub> autoreceptors mediate their effect via GIRK channels rather than by inhibition of adenylate cyclase (Cass and

Zahniser, 1991). All D<sub>2</sub>-like receptors decrease the activity of L, N and P/Q type Ca<sup>2+</sup> channels via pertussis toxin-sensitive G proteins. For example D<sub>2</sub> receptors inhibit N-type Ca<sup>2+</sup> channels in a pathway involving βγ subunits (Hernandez-Lopez et al., 2000). D<sub>2</sub>-receptors have been shown to activate MAP kinases, including both isoforms of the extracellular signal-regulated kinase (ERK). It has been demonstrated that the D<sub>3</sub> mainly utilizes the βγ pathway associated with Gα<sub>i</sub> activation, which involves the transactivation of EGFR in HEK-293 cells. In contrast, the α subunit of the G<sub>i</sub> heterotrimer plays a main role in D<sub>2</sub>-mediated ERK activation (Beom et al., 2004). This study indicated that dopaminergic neurons could regulate ERK activity more flexibly through alternative usage of either the D<sub>2</sub> or D<sub>3</sub> pathway depending on the cellular situation. The stimulation of dopamine D<sub>1</sub>, D<sub>2</sub>, D<sub>5</sub> but not D<sub>3</sub> and D<sub>4</sub> receptors has been shown to cause the robust translocation of β-arrestin to the plasma membrane (Cho et al., 2006; Kim et al., 2001). This suggests that desensitization of the D<sub>3</sub> receptor is weakly associated with G protein-coupled receptor kinase (GRK)/beta arrestin and indeed calveolin 1 directed internalisation. Further work from this same group showed that the D<sub>3</sub> receptor undergoes robust protein kinase C (PKC)-dependent sequestration that is accompanied by receptor phosphorylation and the desensitisation of signaling D<sub>3</sub>. Filamin A was shown to be essential for both the efficient signaling and sequestration of the D<sub>3</sub> receptor (Cho et al., 2007). In another study focusing on the dopamine D<sub>3</sub> presynaptic autoreceptor it has been suggested that the D<sub>3</sub> receptor, filamin A and beta arrestin form a signaling complex that is destabilised by agonist- or expression based increases in GRK2/3 activity. These findings suggest that the D<sub>3</sub> receptor, filamin A and beta-arrestin form a signaling complex that is destabilised by agonist or expression-mediated increases in GRK2/3 activity (Kim et al., 2005). D<sub>2</sub> receptors have been shown to activate a cytosolic, Gβγ stimulated form of phospholipase C (PLCβ1) resulting in reduced L type Ca<sup>2+</sup> currents (Kanterman et al., 1991). This pathway may contribute to D<sub>2</sub> receptor mediated activation of both ERK and CREB in neostriatal neurons. D<sub>2</sub>-like receptor activation in the neostriatum exerts variable

effects on Na<sup>+</sup> channels via several intracellular signalling pathways, perhaps dependent on the subtype of D<sub>2</sub>-like receptor expressed by a given cell. Heterologously expressed D<sub>2</sub>, D<sub>3</sub> and D<sub>4</sub> receptors have been shown to activate the widely expressed Na<sup>+</sup>/H<sup>+</sup> exchanger NHE1 (Neve et al., 2004). Glutaminergic neurotransmission is enhanced in D<sub>2</sub> receptor null mutant mice, probably reflecting the loss of both presynaptic control of glutamate release and post-synaptic inhibition of glutaminergic responses by the D<sub>2</sub> receptor (Cepeda et al., 2001). One possible mechanism for this effect is that D<sub>2</sub> stimulation results in changes in Na<sup>+</sup> and K<sup>+</sup> currents, resulting in cell hyperpolarisation and preventing the removal of the Mg<sup>2+</sup> blockade over these channels.

### **Dopamine receptor hetero-dimer/oligomerisation and consequences on cell signalling**

As discussed above, the D<sub>2</sub>-like dopamine receptor subtypes have been shown to form hetero-oligomeric complexes with other dopamine receptor subtypes and other GPCRs. The functional implications of these interactions will now be discussed. For example, there is considerable evidence, both behavioural and functional, for interactions between brain dopamine and adenosine systems and between dopamine and somatostatin. Receptor heterodimerisation is likely to be a molecular mechanism of these interactions (Agnati et al., 2003). Interestingly the formation of a hetero-oligomeric complex between the D<sub>2</sub> dopamine receptor and the CB<sub>1</sub> cannabinoid receptor results in a change in G protein coupling of the CB<sub>1</sub> receptor, normally a G $\alpha_{i/o}$  coupled receptor. In this case, D<sub>2</sub> receptor activation, simultaneously with CB<sub>1</sub> receptor stimulation, results in the receptor complex coupling to G $\alpha_s$  protein in preference to the expected G $\alpha_{i/o}$  proteins. The result of this interaction is an increase in the second messenger cAMP, reversing an initial synergistic inhibition of adenylate cyclase activity seen at sub-threshold concentrations of cannabinoid

agonist (O'Dowd et al., 2005). Scarselli et al. demonstrated that cells expressing D<sub>2</sub> and D<sub>3</sub> receptors exhibited 7-OH-DPAT-mediated reduction in adenylate cyclase VI activity far above that produced by wild type D<sub>2</sub> receptors. In cells transfected with D<sub>3</sub> receptors alone, no detectable decrease in adenylate cyclase VI activity was observed in response to dopamine agonists. The formation of D<sub>2</sub>/D<sub>3</sub> heterodimers may therefore give rise to novel receptors with unique pharmacological and physiological properties that are different from the activities produced by D<sub>2</sub> or D<sub>3</sub> receptors alone (Scarselli et al., 2001). It is clear then that the formation of heterodimers/hetero-oligomers may have significant effects on the downstream signalling of dopamine receptors. Consequently, dopamine receptor heterodimers may prove to be attractive targets for therapeutic intervention (Cepeda et al., 1993).

## 1.6 Project Aims

The dopamine D<sub>2</sub> and D<sub>3</sub> receptors are highly homologous GPCRs, with a similar pharmacology and over-lapping expression. They are also therapeutic targets for both the treatment of Parkinson's disease and schizophrenia. An understanding of their signalling pathways would therefore be beneficial to the treatment of these diseases. Despite these similarities, the G protein coupling specificities of these two receptors seem to be markedly different. The D<sub>2</sub> receptor has been shown to couple to all members of the G $\alpha_{i/o}$  family of G proteins, although the order of preference remains controversial. The promiscuity of the D<sub>2</sub> receptor in coupling to all four G $\alpha_{i/o}$  subunits, plus the rich pharmacology of this receptor make it an ideal subject for an investigation of agonist-directed G protein coupling. This then was the first aim of this study.

The D<sub>3</sub> receptor is also thought to couple to G $\alpha_{i/o}$  subunits, but with less efficiency. Several groups have described the selective coupling of D<sub>3</sub> to G $\alpha_{o1}$ , with one group suggesting the presence of adenylate cyclase V is required for efficient coupling. The

second aim of this study, then, was to investigate the G protein coupling specificities of both the D<sub>2</sub> and D<sub>3</sub> receptors. The high homology of these receptors makes them ideal for an investigation of receptor/G protein coupling specificity using chimeric receptors. As described in this introduction, this approach has been used with these receptors extensively, and these studies have highlighted the third intracellular loop as being particularly important for the coupling of the D<sub>2</sub> receptor to downstream effectors such as adenylate cyclase. It was of interest then to investigate whether this region is important for the differential G protein signalling of the two receptors.

In this introduction, I have described the G protein cycle, from the activation of a receptor by an agonist, the subsequent activation of and nucleotide exchange at its heterotrimeric G protein partner, the dissociation or rearrangement of the subunits with the heterotrimer and their coupling to their downstream effectors. The structural changes that occur within both the receptor and G protein have also been described. Functional assays which monitor receptor mediated G protein activation are integral to both basic research and the drug discovery process. Ligand-induced regulation of the binding of [<sup>35</sup>S] GTPγS is a widely used technique that allows the direct measurement of receptor mediated nucleotide exchange at a G protein α subunit. However, the cost and restrictions associated with the use of radiolabels makes this assay increasingly less attractive particularly for drug discovery. The final aim of this project was to develop a viable alternative to this assay, using antibodies that recognise the active GTP bound form of Gα.

**Figure 1.1: The G protein cycle**

The nature of the guanine nucleotide-bound  $G\alpha$  subunit controls the extent and temporal kinetics of G-protein signaling. Conversion of a G protein heterotrimer from the inactive, (GDP-bound), to active (GTP-bound) state is promoted by interaction with a guanine nucleotide exchange factor (GEF), the most common of which are members of the GPCR family. Subsequent conformational changes promote separation of the GTP-bound  $\alpha$ -subunit from the  $\beta\gamma$  complex, whereupon both elements of the G protein can regulate the activity of effector proteins that include second messenger generating enzymes and ion channels (see Table 1.1 for details). The intrinsic GTPase activity of the G protein  $\alpha$ -subunit hydrolyses the terminal phosphate of bound GTP and terminates function. This activity is accelerated by GTPase-activating proteins, the largest family of which are the regulators of G protein signaling (RGS) proteins. Reassociation of  $G\alpha$ -GDP with the  $\beta\gamma$  complex terminates effector regulation by the  $\beta\gamma$ -subunits (Table 1.1) and completes the cycle. Further interaction with a GEF is now required to reinitiate the cycle (Milligan and Kostenis, 2006).

Figure 1.1

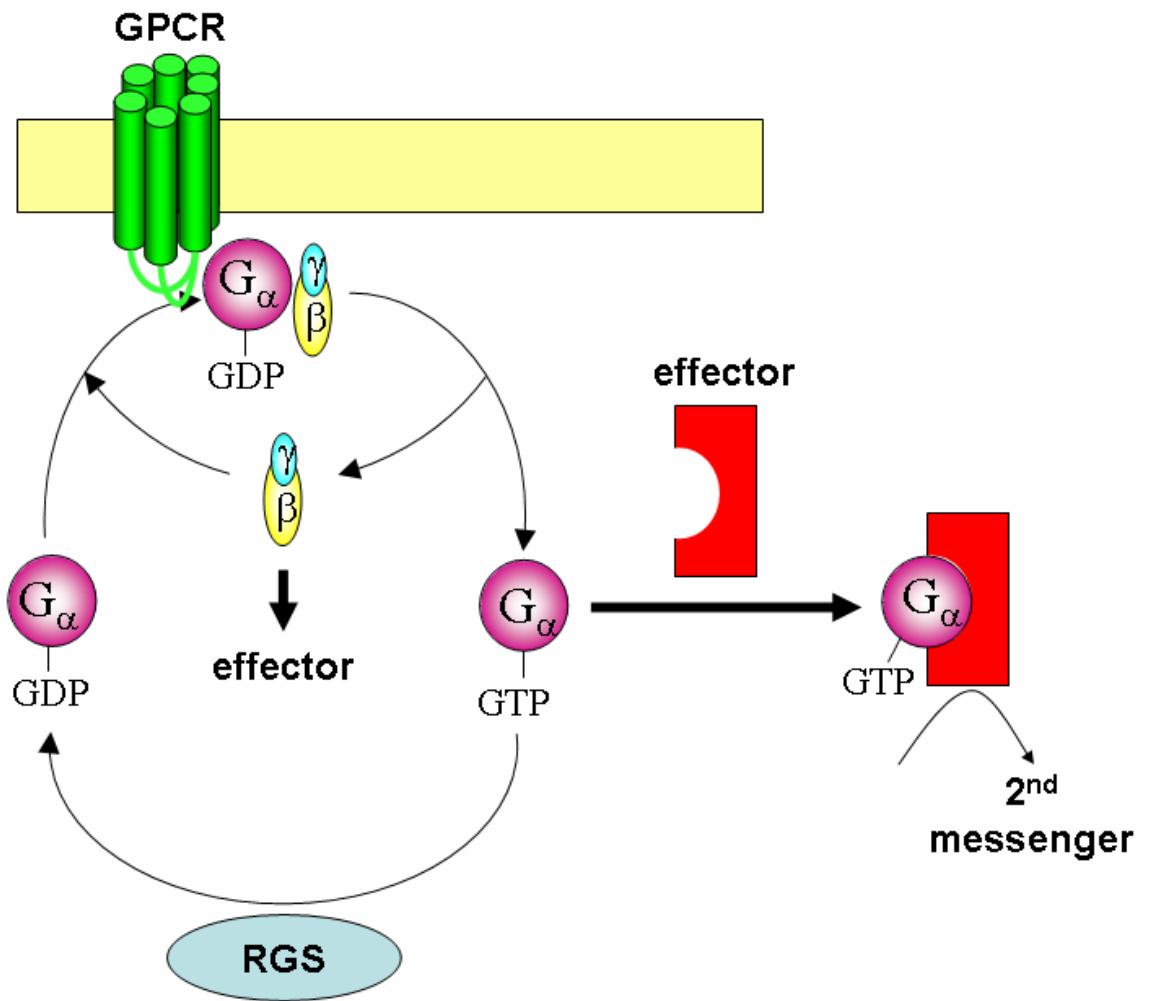


**Figure 1.2: The structure of G protein-coupled receptors (GPCRs)**

A schematic diagram of a G protein-coupled receptor (GPCR) is shown **(A)**, illustrating the extracellular N-terminal domain, the seven transmembrane domains (TM I-VII, red to blue) linked by alternating intracellular (ICL1-3) and extracellular (ECL 1-3) loops and the intracellular domain including helix VIII. The ribbon model of dark (inactive) rhodopsin **(B)** (1U19) shows the orientation of TMI-VII and 11-cis-retinal (grey spheres). Conserved side-chains important for G protein coupling are illustrated (magenta), including the E(D)RY motif adjacent to TM III (yellow) and Np<sub>xx</sub>Y<sub>x</sub><sub>5</sub>F motif on TM VII and VIII (blue and violet). The extracellular **(C)** and intracellular **(D)** faces of rhodopsin are shown. Receptor activation results in an outward movement of TM VI (yellow arrow), which opens a gap in the cytoplasmic face of the receptor, exposing residues critical for G protein activation, such as the E(D)RY motif on TM III (adapted from Oldham and Hamm, 2006).

**Figure 1.2**

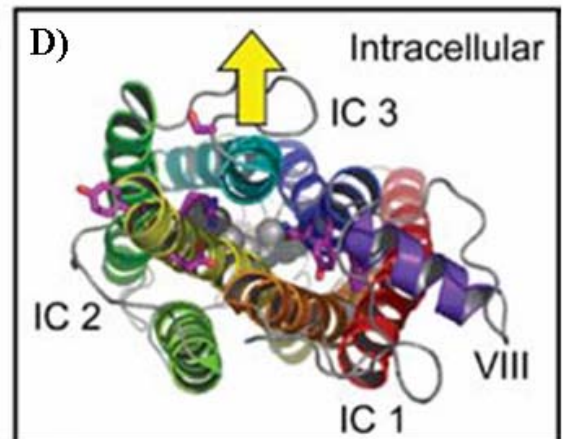
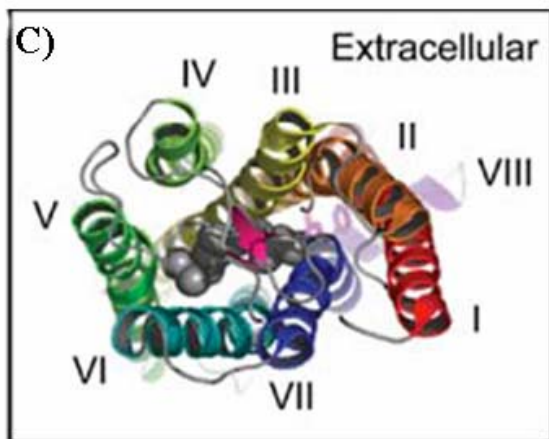
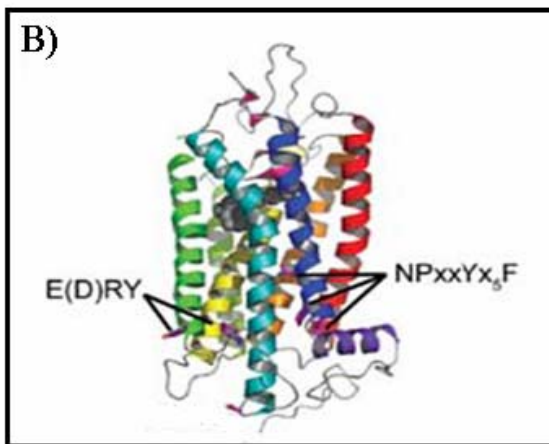
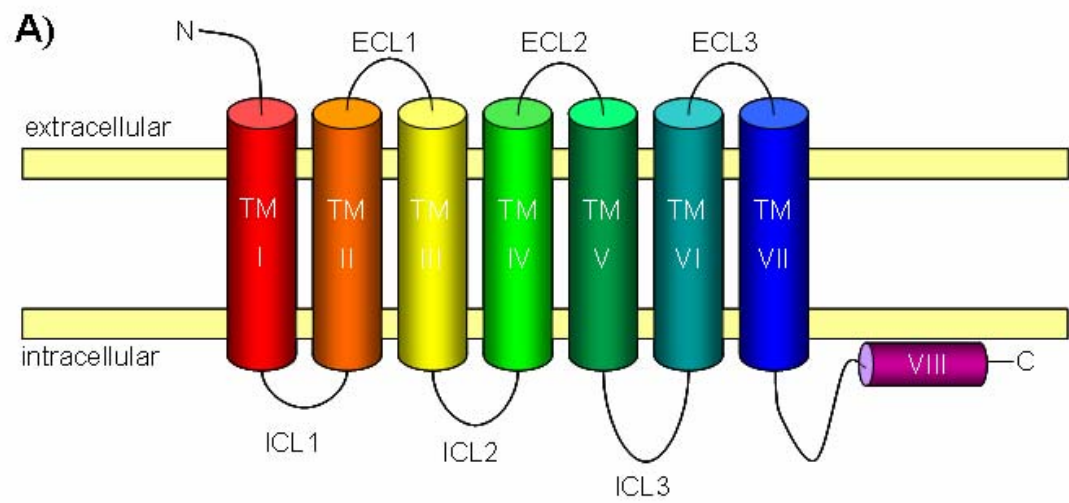


**Figure 1.3: Classification and diversity of GPCRs**

Three main families (I (A), II (B) and III (C)) can be easily recognized when comparing their amino-acid sequences. Receptors from different families share no sequence similarity, suggesting a remarkable example of molecular convergence. Family I (A) contains most GPCRs including receptors for: small ligands, where the binding site is localized within the seven TMs; for peptides whose binding site includes the N-terminal, the extracellular loops and the superior parts of TMs; for glycoprotein hormones where the binding site is mostly extracellular but at least with contact with extracellular loops 1 and 3. Family II (B) GPCRs have a similar morphology to family I GPCRs, but they do not share any sequence homology. Their ligands include high molecular weight hormones such as glucagon, secretin, VIP-PACAP and the Black widow spider toxin. Family III (C) contains glutamate receptors (mGluRs) and the  $\text{Ca}^{2+}$  sensing receptors. The ligand binding domain for family III GPCRs is located in the amino terminus, which is often described as being like a 'Venus fly trap' (George et al., 2002).

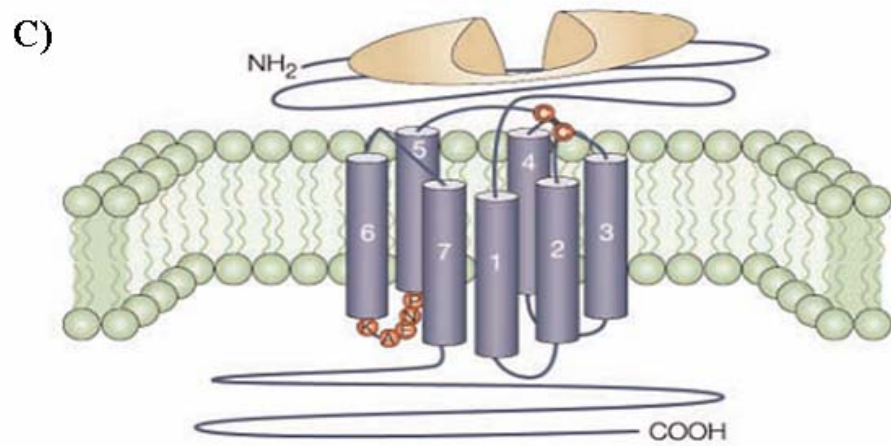
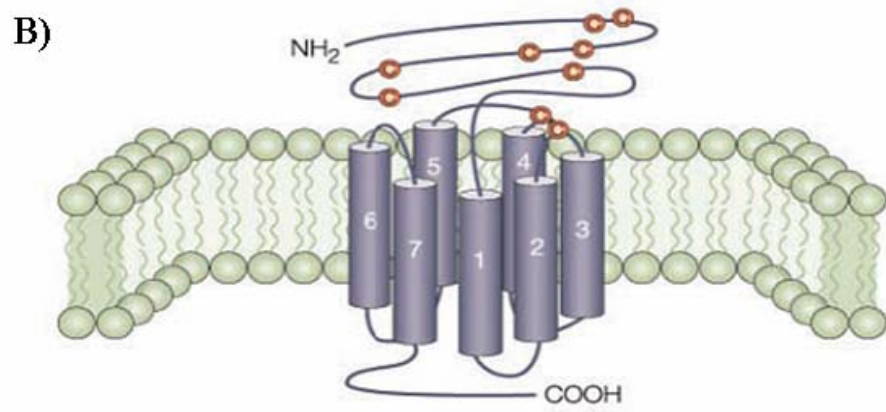
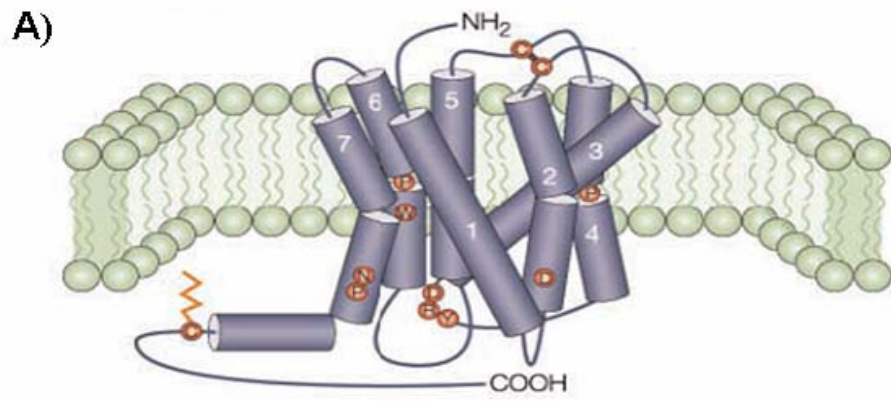


**Figure 1.4: Structure of the G protein heterotrimer**

(A) Sequence alignment of the N- and C- terminal regions of selected  $G\alpha$ -subunits.

Residues that are subject to N-linked myristoylation, thio-palmitoylation or N-linked palmitoylation are highlighted in orange, green and yellow, respectively. In each case, M (black) is the protein synthesis initiator, methionine, which is eliminated during protein synthesis. Residues comprising the N-terminal  $\alpha$ N helix are highlighted in red and residues at the extreme C-terminus of  $G\alpha$  are shown in blue. The  $\alpha$ N helix is required for binding  $\beta\gamma$ -subunits, and particular  $\beta\gamma$  contacts are boxed in black, the extreme C-terminus plays a key role in specific receptor recognition. In the secondary structure diagram below the aligned sequences,  $\beta\gamma$  and receptor interaction sites are highlighted in red and blue, respectively. Only selected domains of  $G\alpha$  are shown, and for simplicity the domains between  $\alpha$ A and the  $\alpha$ 2 helix have been omitted as indicated by the dotted line (Milligan and Kostenis, 2006). (B) The Ribbon model of  $G\alpha_i(\text{GDP})\beta_1\gamma_1$  heterotrimer (1GOT), where  $\alpha$  is blue,  $\beta$  is green and  $\gamma$  is gold. The three Switch regions in  $G\alpha$  are highlighted in yellow. GDP (red) is buried between the GTPase and helical domains of  $G\alpha$ . (C) The subunits have been rotated to show the intersubunit interface, which is primarily composed of the  $\alpha$ N-helix (truncated in this view) and Switch II on  $G\alpha$  and blades 1–3 on  $G\alpha$ . (D) When the GDP-bound (1TAG),  $\text{GTP}\gamma\text{S}$ -bound (1TND) and heterotrimeric (1GOT) structures of  $G\alpha$  are aligned, significant conformational differences are found in the three Switch regions (compare gray and colored backbone). The crystal structures indicate that, upon GTP binding (green backbone), the three Switch regions collapse toward the  $\gamma$ -phosphate of GTP. The  $G\alpha(\text{GDP})$  conformation is likely a short-lived transition state *in vivo* due to the large hydrophobic surface presented by this conformation of the Switch regions (blue backbone) (Oldham, 2006).

Figure 1.4

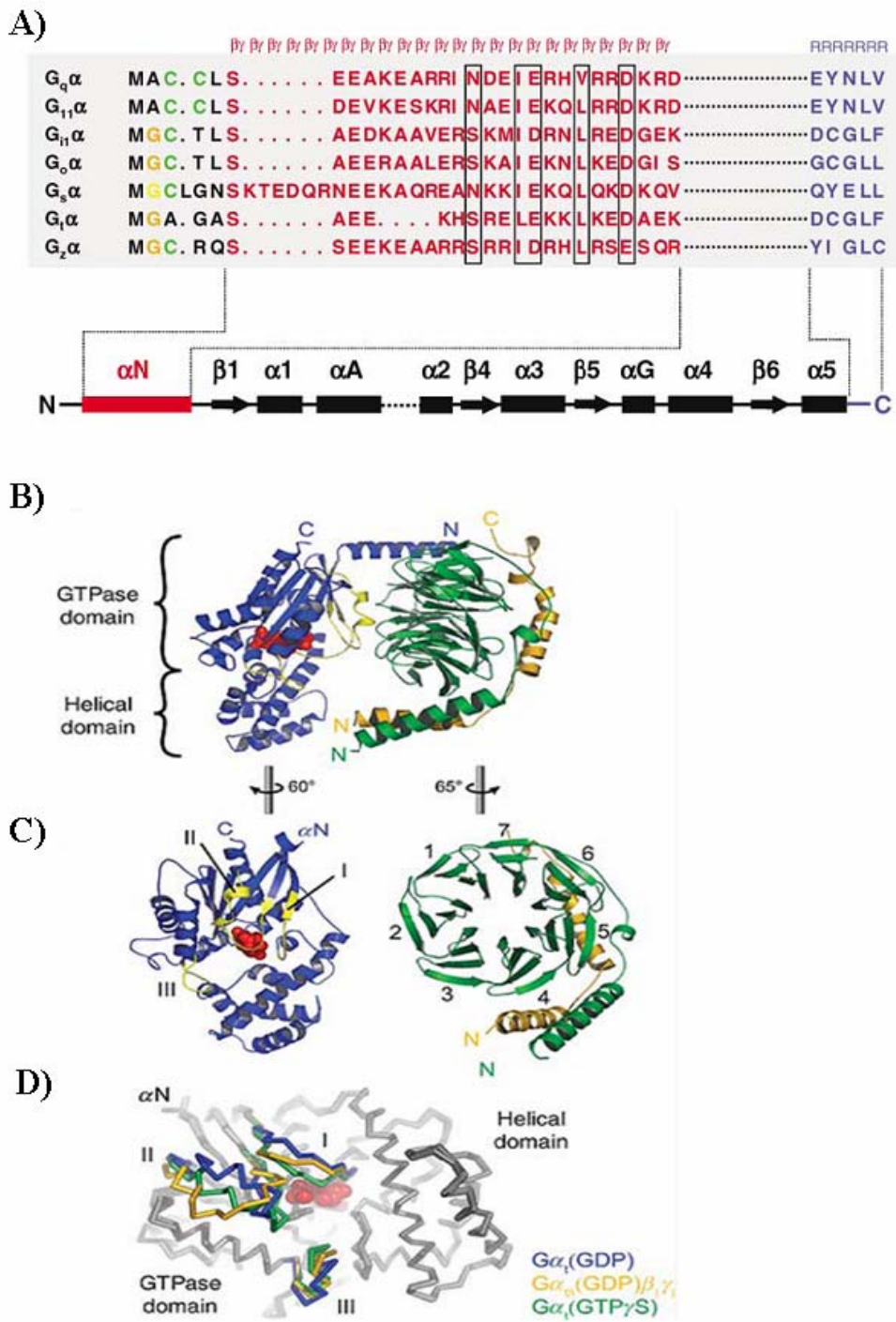


**Figure 1.5: GPCR-G protein fusion proteins**

Physical linkage of the N-terminal of a G-protein  $\alpha$ -subunit to the C-terminal tail of a GPCR from which the stop codon has been removed allows expression of a single polypeptide encoding the functions of both proteins.

**Figure 1.5**

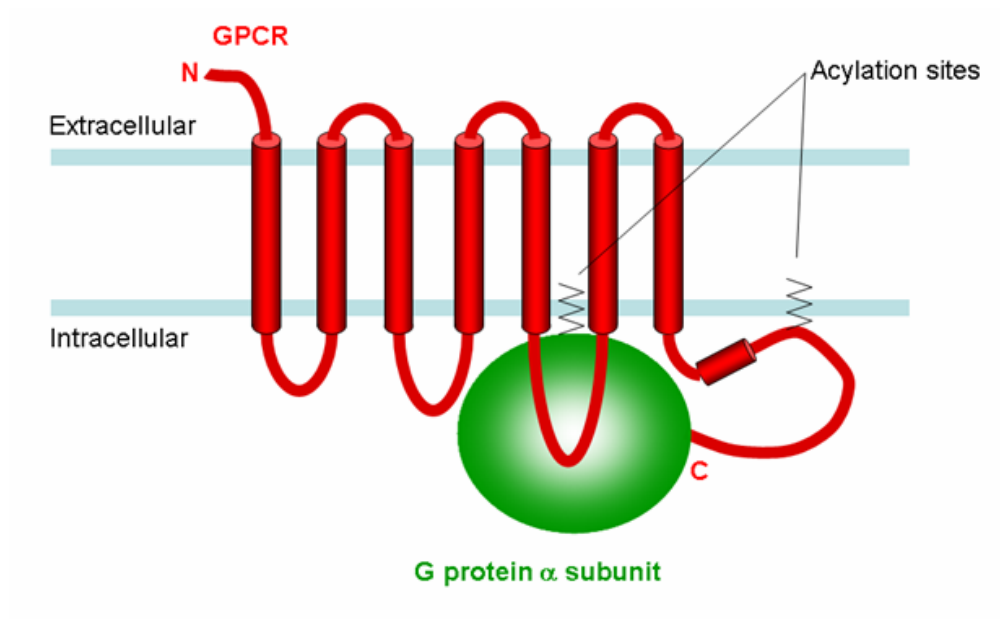


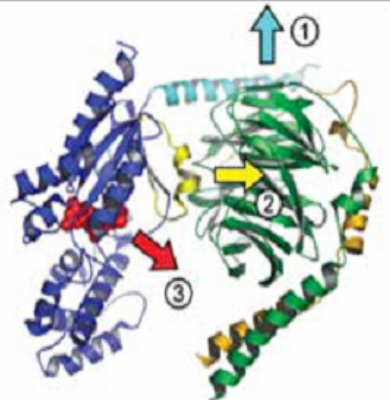
**Figure 1.6: Proposed mechanisms of GDP release**

Two models have been proposed in which the activated receptor may use  $G\beta\gamma$  to catalyze GDP release. In the lever-arm hypothesis (**A**), the receptor uses the  $\alpha$ N-helix as a lever to pull  $G\beta\gamma$  away from  $G\alpha$  (1), thereby prying Switch II away from the nucleotide-binding pocket (2) and causing GDP release (3). The alternative gear-shift model (**B**) requires that the receptor push  $G\beta\gamma$  closer to  $G\alpha$  (1). This allows the N-terminus of  $G\gamma$  to engage the helical domain (2), thus forcing the binding pocket open due to the reorientation of the two domains (3), leading to GDP release (4)(Oldham, 2006).

Figure 1.6

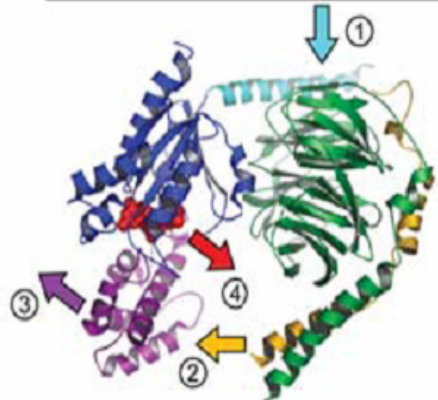
A)

Lever-arm



B)

Gear-shift



## **2 Materials and Methods**

### **2.1 Materials**

#### **2.1.1 General Reagents, enzymes and kits**

**Amersham Pharmacia Biotech UK Ltd., Little Chalfont, Buckinghamshire, UK**

Rainbow Markers

**BDH, Lutterworth, Leicestershire, UK**

22mm coverslips, microscope slides, sodium di-hydrogen orthophosphate, potassium hydroxide, potassium chloride, methanol, isopropanol

**Duchefa. Haarlem, The Netherlands**

Yeast extract, tryptone, agar

**Fisher Scientific UK Ltd, Loughborough, Leicestershire, UK**

Glycine, HEPES, sucrose, SDS, potassium di-hydrogen orthophosphate, calcium chloride, manganese chloride

**Invitrogen BV, Gronigen, The Netherlands**

NuPage Novex pre-cast 8-12 % Bis-tris gels, MOPS running buffer

**Konica Europe, Hohenbrunn, Germany**

X-ray film

**Melford Laboratories Ltd, Ipswich, Suffolk, UK**

Isopropyl- $\beta$ -D-thiogalactopyranoside (IPTG)

**Pierce, Perbio Science UK Ltd, Tattenhall, Cheshire, UK**

Supersignal West Pico chemiluminescent substrate

**Promega UK Ltd., Southampton, UK**

All restriction endonucleases, T4 DNA ligase, Pfu polymerase, Wizard Plus SV minipreps

**Qiagen, Crawley, West Sussex, UK**

QiaQuik PCR purification kit, QiaQuik gel extraction kit, Qiafilter maxiprep kit.

**Roche Diagnostics Ltd., Lewes, East Sussex, UK**

Complete EDTA free protease inhibitor tablets, 1Kb DNA ladder, Shrimp Alkaline Phosphatase

**Sigma-Aldrich Company Ltd., Poole Dorset, UK**

Magnesium chloride, sodium chloride, sodium hydroxide, sodium acetate, DTT, di-sodium orthophosphate, tris base, EDTA, bromophenol blue, Hoescht stain, rubidium chloride, Triton X-100, DMSO glycerol, tween 20, ethylene glycerol, formaldehyde, ampicillin, kanamycin, sodium azide, pertussis toxin

**Semat International, Hatfield, UK**

GF/C glass filters

**Thermoelctron, Ulm, Germany**

Oligonucleotides

**Thermo Shandon, Pittsburgh, PA, USA**

Immuno-mount

## **2.1.2 Pharmacological compounds**

**Sigma, Poole, Dorset, UK**

(+)-butaclamol, dopamine, (-)-quinpirole, *m*-tyramine, *p*-tyramine, *S*-(-)-3-(3-hydroxyphenyl)-*N*-propylpiperidine (*S*-(-)-PPP), *R*-(+)-3-PPP, *R*-(-)-10,11-dihydroxy-*N*-*n*-propylnorapomorphine (NPA), *R*(+)-7-Hydroxy-DPAT hydrobromide (7-OH-DPAT)

**Tocris, Bristol, UK**

Spiperone Hydrochloride

## **2.1.3 Radiochemicals**

**Amersham Pharmacia Biotech UK Ltd., Little Chalfont, Buckinghamshire, UK**

[<sup>3</sup>H]Spiperone (65-140 Ci/mmol)

**PerkinElmer Life and Analytical Sciences, Boston, MA**

[<sup>35</sup>S]GTPγS (1250 Ci/mmol)

## **2.1.4 Tissue Culture**

### **American Tissue Culture Collection, Rockville, USA**

HEK293T cells

### **Costar, Cambridge, M.A., USA**

5 mL, 10 mL, and 25 mL pipettes, 75 cm<sup>2</sup> and 125 cm<sup>2</sup> vented tissue culture flasks, 6 well plates, 100 cm<sup>2</sup> dishes

### **Invitrogen BV / Gibco, Groningen, The Netherlands**

Lipofectamine transfection reagent, Optimem-1, L-glutamine (200 mM), Flp-In T-Rex-293 cell line, Zeocin, Blasticidin, dialysed Fetal Bovine Serum, Penicillin-Streptomycin, DMEM (+L-glutamine, - pyruvate)

### **Qiagen, Crawley, West Sussex, UK**

Effectene transfection reagent

### **Roche Diagnostics Ltd., Lewes, East Sussex, UK**

Hygromycin B

### **Sigma-Aldrich Company Ltd., Poole, Dorset, UK**

DMEM, 0.25 % trypsin-EDTA, poly-D-lysine, Newborn Calf Serum

### **2.1.5 Antisera**

#### **Cambridge Research Biochemicals (CRB) Ltd., Billingham, Cleveland, UK**

Antisera were raised against peptides based on the C-terminal 10 amino acids of  $G\alpha_{i1/2}$ ,  $G\alpha_q$ ,  $G\alpha_s$  and were characterised in house.

#### **Applied Biosystems, Foster City, USA**

FMAT Blue® GAM (Goat anti-Mouse IgG) Conjugate, FMAT Blue® GAM (Goat anti-Rabbit IgG) Conjugate

#### **Amersham Pharmacia Biotech UK Ltd., Little Chalfont, Buckinghamshire, UK**

Sheep anti-mouse IgG-HRP conjugate, donkey anti-rabbit IgG-HRP conjugate

#### **Molecular Probes, Eugene, Oregon, USA**

Anti-mouse Alexa ® 594 IgG conjugate, antimouse Alexa ® 594 igG conjugate

## **2.2 Buffers and Reagents**

### **2.2.1 Buffers and Reagents for molecular biology**

#### **LB medium (Luria-Bertani Medium)**

Bacto-tyrptone 10 g

Bacto-yeast extract 5 g

NaCl 10 g

Dissolved in 950 ml of distilled H<sub>2</sub>O, pH adjusted to 7.0 with 5 M NaOH. Volume adjusted to 1 L with distilled H<sub>2</sub>O and sterilized by autoclaving for 20 mins at 15 lbs/sq.in.

### **LB media (Luria-Betrani Medium) containing agar (LBA)**

Was made as above except for the addition of 15 g/L of bacto-agar prior to autoclaving.

### **Ethidium Bromide (10 mg/ml)**

1 g of ethidium bromide was added to 100 ml of H<sub>2</sub>O and left stirring for several hours. Container was wrapped in magnesium foil and stored at room temperature.

### **Tris acetate (TAE) (50 x)**

242 g Tris base, 57.1 ml glacial acetic acid, 100 ml 0.5 M EDTA (pH8.0). This was made up to a final volume of one litre with distilled H<sub>2</sub>O. 10 ml of this stock was diluted in 490 ml of H<sub>2</sub>O as required to make 1x buffer.

### **Solution 1 for preparation of competent Bacteria**

1 M Potassium acetate, 1 M RbCl<sub>2</sub>, 1 M CaCl<sub>2</sub>, 1 M MnCl<sub>2</sub>, 80 % (w/v) glycerol

Final volume is made up with de-ionised water and pH adjusted to 5.8 with 100 mM

Acetic acid. The solution is filter sterilised by passage through a 0.22 micron filter and stored at 4 °C.

### **Solution 2 for preparation of competent bacteria**

100 mM MOPS pH 6.5, 1 M CaCl<sub>2</sub>, 1 M RbCl<sub>2</sub>, 80% (w/v) glycerol

Final volume is made up with de-ionised water and pH adjusted to 6.5 with 100 mM

concentrated HCl. The solution is filter sterilised by passage through a 0.22 micron filter and stored at 4 °C.

**Gel loading buffer**

0.25 % bromophenol blue, 40 % sucrose (w/v) dissolved in distilled H<sub>2</sub>O

**2.2.2 Buffers and Reagents for biochemical assays****Tris-EDTA buffer (TE)**

10 mM Tris Base, 0.1 mM EDTA dissolved in distilled H<sub>2</sub>O, pH 7.4

**Tris-EDTA-Magnesium chloride buffer (TEM)**

50 mM Tris base, 1 mM EDTA, 12.5 mM MgCl<sub>2</sub> dissolved in distilled H<sub>2</sub>O, pH7.4

**Phosphate Buffered Saline (PBS)**

140 mM NaCl, 2.7 mM KCl, 1.5 mM KH<sub>2</sub>PO<sub>4</sub>, 8 mM Na<sub>2</sub>HPO<sub>4</sub>, pH 7.4

**STE buffer**

10mM Tris-HCl, 150 mM NaCl, 1mM EDTA, pH 8.0

**GTPγS filtration / SPA assay buffer**

20 mM HEPES, 100 mM NaCl, 6 mM MgCl<sub>2</sub>, 40μM ascorbic acid pH 7.4

**GTPγS immunoprecipitation Assay buffer (10 x)**

200 mM Hepes, 30 mM MgCl<sub>2</sub>, 1 M NaCl, 2 mM Ascorbic acid pH 7.4

**GTPγS immunoprecipitation assay – solubisation buffer**

100 mM Tris, 200 mM NaCl, 1 mM EDTA, 1.25 % NP40, pH7.4

**GTP $\gamma$ S immunoprecipitation Assay- bead suspension buffer**

BSA (2 %), 0.1 % NaN<sub>3</sub> in distilled H<sub>2</sub>O

**Laemmli Buffer (2x)**

0.4 M DTT, 0.17 M SDS, 50 mM Tris, 5 M urea, 0.01 % (w/v) bromophenol blue

**2.3 Molecular Biology****2.3.1 LB plates**

LBA was made as detailed above. After autoclaving, medium was allowed to cool to 50°C before addition of a thermolabile antibiotic to the following final concentrations; ampicillin (100 µg/ml), kanamycin (50 µg/ml). Plates (10 cm Petri dishes) could then be poured directly from the flask, using about 25 ml of liquid per dish. Any air bubbles were removed by flaming the surface of the medium with a Bunsen burner before the agar has hardened. Once hardened, plates were inverted and stored at 4 °C

**2.3.2 Preparation of competent bacteria**

E coli strain XL1 Blue was used for all transformation procedures. A sample of XL1 Blue was taken via stabbing with a sterile pipette tip. This was streaked out onto a minimal agar plate and incubated at 37 °C overnight. A single colony was selected and used to inoculate a 5 ml LB culture, which was grown for 16 hours at 37°C in a rotary shaker. Next day this culture was used to inoculate 100 ml of L-Broth and grown until the optical density at 550 nm is 0.48 - approximately 90 minutes of incubation. After chilling on ice for 5 min the cells were spun at 1811 x g for 10 minutes at 4°C in 50 ml sterile falcon tube. Each pellet

was re-suspended in 20 ml of solution 1 by gentle pipetting, then chilled on ice for 5 minutes and spun as before. Each pellet was then resuspended in 2 ml of buffer 2 by gentle pipetting and chilled on ice for a further 15 minutes. Cells were then aliquoted in 220  $\mu$ l volumes and stored at -80 °C until required.

### **2.3.3 Transformation of competent cell with plasmid DNA**

220  $\mu$ l aliquots of competent XL1 Blue were taken from -80 °C storage and thawed on ice. Using a sterile pipette tip 50-100 ng of plasmid DNA in a volume of 2  $\mu$ l was added to a sterile 15 ml falcon tube containing 50  $\mu$ l of competent bacteria. Tubes were left on ice for 30 minutes. The tubes were then transferred to a water bath, which had been preheated to 42 °C and heat shocked for 60 seconds. Tubes were immediately transferred to ice and allowed to chill for 5 minutes before 450  $\mu$ l of LB was added to each tube. Cultures were incubated for 60 minutes at 37 °C in a rotary shaker. 200  $\mu$ l of each culture was spread on a LB Agar plate with appropriate antibiotic. Plates were inverted and left to incubate at 37 °C for 16 hours. Transformed colonies were selected and cultured overnight at 37 °C in 5 ml LB containing appropriate antibiotic.

### **2.3.4 Preparation of plasmid DNA**

#### **2.3.4.1 Miniprep**

Plasmid cDNA was prepared using the Promega Wizard™ Plus SV miniprep purification system. A 5 ml culture of transformed cells was grown overnight at 37 °C as described above. 1.5 ml of the culture was spun at 15,600 x g and the pellet resuspended in 250  $\mu$ l of resuspension buffer (50 mM Tris-HCL pH 7.5, 10mM EDTA, 100  $\mu$ g/ml RNase) followed by lysis with 250  $\mu$ l of lysis solution (0.2 M NaOH, 1% SDS). The resulting lysate was neutralised with 205  $\mu$ l of neutralisation solution (4.09 M guanidine

hydrochloride, 0.76 M potassium acetate, 2.12 M glacial acetic acid, pH 4.2) to precipitate any unwanted chromosomal DNA. This was removed by centrifugation (15,600 x g for 10 minutes) and the resulting supernatant was transferred to a DNA purification column wash solution (60 mM potassium acetate, 10mM Tris-HCl pH 7.5, 60 % ethanol). Finally, the cDNA was eluted from the column with 50µl of sterile water.

#### **2.3.4.2 Maxiprep**

To achieve a larger scale of purified DNA the Qiagen Plasmid Maxi system was used. This was performed according to the manufacturer's instruction; refer to Qiagen purification handbook (Qiagen, 1999). Briefly, a single colony was picked from a plate of transformed bacteria and used to inoculate a starter culture of 5 ml LB containing appropriate selective antibiotic. This was incubated for 8-9 hours in a rotary shaker at 37 °C. The entire starter culture was used to inoculate a 200 ml LB culture in a conical flask containing appropriate antibiotics. This was grown at 37 °C for 12-16 hours with vigorous shaking. Bacterial cells were harvested by centrifugation at 3468 x g using a Beckman JA-14 rotor for 15 minutes at 4 °C. The bacterial pellet was resuspended in 10 ml of chilled buffer P1 (50 mM Tris-HCl pH 8.0, 10 mM EDTA, 100 µg/ml RNase A) and lysed with 10 ml of chilled buffer P2 (200mM NaOH, 1 % SDS). The lysate was neutralised with 10 ml of cooled buffer P3 (3.0 M potassium acetate pH 5.5). The sample was then spun at 3220 x g for 30 minutes at 4°C. During this spin the Qiagen-tip 500 column was equilibrated with 10 ml of buffer QBT (750mM NaCl, 50 mM MOPS pH 7.0, 15% isopropanol). The supernatant was poured into the column, the column washed with 60 ml of buffer QC (1.0 NaCl, 50 mM MOPS pH 7.0, 15% isopropanol) and the DNA eluted from the column with 15 ml of buffer QF (1.25 M NaCl, 50 mM Tris-HCl pH 8.5, 15 % isopropanol). The DNA was precipitated by adding 10.5 ml of isopropanol and the mixture spun at 27216 x g for 30 min at 4°C. The resulting pellet was washed with 5 ml of 70% ethanol and then allowed to air dry. Finally the DNA was re-dissolved in 0.5-1.0 ml of sterile water.

### 2.3.5 Quantification of DNA

This was determined by spectrophotometric measurement of the amount of ultraviolet radiation absorbed by DNA bases. In routine DNA measurements the stock DNA was diluted by a factor of 100 in sterile distilled H<sub>2</sub>O. The absorbance unit being equal to 50 ug/ml of double stranded DNA (Maniatis et al., 1982). The sample concentration could then be determined using the following formula.

$$\text{Sample concentration} = \text{OD}_{260} \times \text{dilution factor (100)} \times 50\text{ug/ml}$$

The purity of the sample was then determined by measuring the absorbance at 280nm, the ratio  $\text{OD}_{260}/\text{OD}_{280}$  provided an estimate of purity with a value of 1.8 representing a pure preparation. Typically, DNA samples gave a ration in the range 1.6-2.0. This was adequate for all the procedures for which their use was required.

### 2.3.6 Digestion of DNA with restriction endonucleases

For all restriction endonucleases used, one unit of restriction endonuclease activity was capable of completely digesting 1ug of DNA in 60 minutes at the appropriate temperature. Volume activity of the enzymes (units/ $\mu$ l) ranges from 5-40. A typical reaction mixture is outlined below.

---

Plasmid DNA	1 $\mu\text{g}$ (1ul of 1ug/ $\mu\text{l}$ )
Restriction enzyme	1 $\mu\text{l}$ of each
10X buffer (determined by restriction enzymes used)	2 $\mu\text{l}$
Sterile distilled dH <sub>2</sub> O	x $\mu\text{l}$
<hr/>	
Final Volume	20 $\mu\text{l}$
<hr/>	

The reaction was then incubated at 37 °C in a water bath for 3-24 hours. All enzymes required an incubation temperature of 37 °C unless otherwise stated by the manufacturer.

### **2.3.7 Electrophoresis of agarose gels**

Digested DNA fragments were separated and analysed using agarose gel electrophoresis. A 1% agarose gel was prepared using 1 x TAE buffer and 0.6  $\mu\text{g}/\text{ml}$  ethidium into a horizontal gel tank (Life technologies, Gibco, Horizon 58 model). After the gel has set completely, enough 1 x TAE buffer was then added to cover the gel to a depth of 5 mm. DNA samples were mixed with a one sixth volume of gel loading buffer and loaded into the slots of the submerged gel. A voltage of 100 mA was applied across the gel. DNA bands stained with ethidium bromide could then be viewed by ultraviolet light, and photographed using an UV transilluminator.

### **2.3.8 Purification of DNA from agarose gels**

DNA bands of interest were located using an UV transilluminator and were excised from the agarose gel with a sterile disposable scalpel blade. Excised gel fragments were transferred to a sterile Eppendorf tube. Recovery and purification of the fragments was achieved by using the QIAquick gel extraction kit. Excised DNA fragments were dissolved in QIA quick buffer QG followed by addition of isopropanol. The solution was

loaded onto a QIAquick purification column, washed with an ethanol based wash solution (PE) and finally the DNA eluted from the column with sterile water.

### 2.3.9 Dephosphorylation of Vector DNA

Once plasmid DNA had been digested by restriction endonucleases it was then dephosphorylated to prevent re-ligation of vector DNA during the ligation reaction. This was performed using Shimp Alkaline Phosphatase (SAP) (Roche), following the manufacturers protocol. A typical reaction is outlined below

To inactivate restriction endonucleases the sample was heated at 65 °C for 15 min. The following reaction mix was then set up:

Digested vector DNA	20 µl
Phosphatase buffer 10X	5 µl
SAP	6 µl
Sterile dH <sub>2</sub> O	19 µl
Final Volume	50 µl

This mix was incubated at 37 °C for 1 hour. Heating the sample at 65 °C for 15 min then inactivated the enzyme.

### 2.3.10 Ligation of DNA fragments

Once plasmid DNA and PCR fragments had been digested and purified via the methods described above, the amount of DNA present in the samples was determined by ethidium bromide fluorescent quantification. Ligation of digested PCR fragments to the digested vector DNA was achieved using a T4 DNA ligase kit (Promega). For ligations with sticky ends the following reaction volumes were used:

Vector DNA	x $\mu$ l
Insert DNA	x $\mu$ l
T4 DNA Ligase	1 $\mu$ l
10 x ligase buffer	1 $\mu$ l
Sterile dH2O	x $\mu$ l
Final Volume	10 $\mu$ l

Approximately 200 ng of vector DNA was used per reaction. A vector to insert ratio of 1:3 was typically used, and multiple insert fragments could be used in a given ligation reaction. The reaction was left for 3 hours at room temperature or overnight at 4 °C and then 3  $\mu$ l transformed into competent bacteria.

### 2.3.11 Polymerase Chain Reaction

PCR reactions were established in a volume of 50  $\mu$ l containing 10ng of template DNA, 0.2 mM dNTPs (dATP, dCTP, dGTP, dTTP) 25 pmol of sense and anti-sense oligonucleotide primers, 1 x Pfu polymerase buffer and 1 unit of Pfu polymerase enzyme. Reactions were carried out on an Eppendorf gradient Thermocycler. PCR cycles used were:

Denaturation	Annealing	Extension	Cycles
95 °C , 1 min	50-60 °C, 1 min	72 °C , 2 min	30
95 °C , 1 min	50-60 °C, 1 min	72 °C, 10 min	1

### 2.3.12 PCR for Mutagenesis (introduction of mutations using QuikChange site directed mutagenesis kit)

Point mutations were introduced using QuikChange kit (Stratagen) according to the manufacturer's instructions

#### 2.3.12.1 Design of Primers

Primers had a length of between 25 to 45 bases, a melting temperature  $T_m$  greater than or equal to 78°C and a minimum GC content of 40%.

#### 2.3.12.2 PCR

The following reaction mixes were made:

DNA template	1 $\mu$ l (20 ng)	2.5 $\mu$ l (50 ng)	5 $\mu$ l (100 ng)	7.5 $\mu$ l (150 ng)
Forward primer (125 ng/ $\mu$ l)	1 $\mu$ l	1 $\mu$ l	1 $\mu$ l	1 $\mu$ l
Reverse primer (125 ng/ $\mu$ l)	1 $\mu$ l	1 $\mu$ l	1 $\mu$ l	1 $\mu$ l
Pfu DNA polymerase	1 $\mu$ l	1 $\mu$ l	1 $\mu$ l	1 $\mu$ l
Pfu buffer (10x)	5 $\mu$ l	5 $\mu$ l	5 $\mu$ l	5 $\mu$ l
dNTPs	1 $\mu$ l	1 $\mu$ l	1 $\mu$ l	1 $\mu$ l
Dimethylsulphoxide (DMSO)	1 $\mu$ l	1 $\mu$ l	1 $\mu$ l	1 $\mu$ l
Deionised H <sub>2</sub> O	39 $\mu$ l	37.5 $\mu$ l	35 $\mu$ l	32.5 $\mu$ l
Total Volume	50 $\mu$ l	50 $\mu$ l	50 $\mu$ l	50 $\mu$ l

Primers were heated to 95 °C for 2 minutes using a heating block before addition to reaction to reduce secondary structure. The reactions were carried out in a thermocycler with the following steps:

Rapid thermal ramp to 95 °C

Hold at 95 °C for 3 minutes

These conditions were used for 1 cycle

Hold at 95 °C for 30 seconds

Cool to 55 °C

Hold at 55 °C for 1 minute

Rapid thermal ramp to 68 °C

Hold at 68 °C for 24 minutes

These conditions were used for 18 cycles

Following this 1 µl of the restriction endonuclease *Dpn I* was added to each reaction and the tube incubated at 37 °C for 3 hours. This step was carried out to digest the methylated template DNA. Following this the mutagenesis reaction was transformed into bacterial cells.

## 2.4 Generation of Dopamine receptor constructs

### 2.4.1 Dopamine Receptor subcloning into pcDNA3

#### 2.4.1.1 D<sub>2</sub> Dopamine receptor subcloning into pcDNA3

cDNA of the long isoform of the human D<sub>2</sub> dopamine receptor (D<sub>2L</sub>) was obtained from A. Wise (GSK, Harlow, UK) in the vector pDEST12.2. D<sub>2L</sub> cDNA was amplified by PCR using the following primers:

sense;           5' AAA AGA ATC CGC CAC CAT GGA TCC ACT GAA TCT GTC C 3'  
antisense;       5' AAA ACT CGA GTC AGC AGT GGA GGA TCT TCA GGA AGG 3'

Underlined bases indicate the restriction sites *EcoRI* (sense) and *XhoI* (antisense). The resulting PCR fragment was digested with *EcoRI* and *XhoI* and inserted into pcDNA3.

#### 2.4.1.2 D<sub>3</sub> and chimeric D<sub>3/2</sub> Dopamine receptor subcloning into pcDNA3

cDNA of the human D<sub>3</sub> dopamine receptor and the chimeric D<sub>3/2</sub> dopamine receptor was obtained from A. Wise (GSK, Harlow, UK) in the vectors pRC and pcDNA3.1 respectively. The two cDNAs were amplified by PCR using the following primers:

Sense;           5' CCC AAG CTT ATG GCA TCT CTG AGT CAG CTG 3'  
Antisense;       5' AAA AAA AAC CAT GGA AGA CAG GAT CTT GAG GAA GGC 3'

Underlined bases indicate the restriction sites *HindIII* (sense) and *Xho I* (antisense). The resulting PCR fragment was digested with *HindIII* and *Xho I* and inserted into pcDNA3.

## 2.4.2 Construction of the Myc-Dopamine Receptor: G-protein $\alpha$ subunit fusion proteins

Pertussis toxin-resistant  $\alpha_{2A}$ -adrenoceptor–G-protein fusion proteins had been prepared as described previously (Wise and Milligan, 1997). Briefly, Cys<sup>351</sup> of rat  $G\alpha_{i1, i2, i3, o1}$  was mutated to isoleucine by site-directed mutagenesis and then used to create the  $\alpha_{2A}$ -adrenoceptor– $G\alpha$  fusion proteins using the porcine  $\alpha_{2A}$ -adrenoceptor in pcDNA3 as described by Wise and Milligan. These constructs were cloned into pcDNA3 using a created 5' *Kpn I* site and 3' *EcoRI* site with a *Nco I* site in between receptor and G-protein  $\alpha$  subunit cDNAs.

### 2.4.2.1 *Nco I* site removal from D<sub>21</sub> by mutagenesis

To create D<sub>21</sub>:G protein  $\alpha$  subunit proteins, the first step was to remove the *Nco I* site from within the D<sub>21</sub> cDNA by site directed mutagenesis using a QuikChange Mutagenesis kit (Stratagene, La Jolla, CA) and the following primers:

Sense;            5'-CC GAC CCG TCC CAT CAT GGT CTC CAC AG -3';

Antisense;        5'-CT GTG GAG ACC ATG ATG GGA CGG GTC GG -3'.

Bold letters indicate altered bases. The PCR product was then digested with *Dpn I* and transformed into bacteria.

### 2.4.2.2 *Nco I* site removal from $G\alpha_{o1}$ and $G\alpha_{i1}$ by mutagenesis

In a similar manner *Nco I* sites were removed from both the  $G\alpha_{i1}$  and  $G\alpha_{o1}$  cDNAs in the respective  $\alpha_{2A}$ -adrenoceptor- $G\alpha$  fusion protein cDNAs using the following primers:

$G\alpha_{i1}$ :

Sense; 5'-TT GCC ATC ATT AGA GCG ATG GGG AGA TTG AAA ATC G -3';

antisense; 5'-C GAT TTT CAA TCT CCC CAT CGC TCT AAT GAT GGC AA -3',

$G\alpha_{o1}$ :

Sense; 5'-CC ATT GTG CGG GCG ATG GAT ACT CTG GG -3';

Antisense; 5'-CC CAG AGT ATC CAT CGC CCG CAC AAT GG -3'.

### 2.4.2.3 Myc-D<sub>21</sub> (Nco I -)

Primers encoding the Myc epitope sequence were used to generate N-terminally tagged Myc-D<sub>21</sub> and remove the stop codon:

Sense; 5'- AGA ACG GGG TAC CTT ATG **GAA CAA CAA AAA CTT ATT TCT**

**GAA GAA GAT CTG** GAT CCA CTG AAT CTG TCC TGG TAT GAT G -3'

Antisense; 5'-AA AAA AAA CCAT GGA GTG GAG GAT CTT CAG GAAGGC -3'.

Underlined bases indicate introduced restriction sites (sense: *Kpn I*, antisense; *Nco I*), bases in bold indicate introduced N-terminal Myc tag. The PCR fragment was digested using *Kpn I* and *Nco I*.

#### 2.4.2.4 Myc-D<sub>3</sub> / D<sub>3/2</sub>

Primers encoding the Myc epitope sequence were used to generate N-terminally tagged Myc-D<sub>3</sub> and Myc-D<sub>3/2</sub> and remove the stop codon:

Sense;           5'-AAA AAA AG GTA CCA TGG AAC AAA AAC TTA TTT CTG  
**AAG AAG ATC TGG CAT CTC TGA GTC AGC TGA GTA GC**-3'

Antisense;      5' -AAA AAA AAC CAT GGA AGA CAG GAT CTT GAG GAA GGC -  
 3'

Underlined bases indicate introduced restriction sites (sense: *Kpn I*, antisense; *Nco I*), bases in bold indicate introduced N-terminal Myc tag. The PCR fragment was digested using *Kpn I* and *Nco I*.

#### 2.4.2.5 Construction of D<sub>21</sub>:G protein fusion proteins

The  $\alpha_{2A}$ -adrenoceptor-G $\alpha$  fusion proteins (*Nco I*-) were excised from pcDNA3 using *Kpn I* and *EcoRI*, digested with *Nco I*, and the G $\alpha$  subunit cDNA purified. The G $\alpha_i$  subunit cDNAs were then cloned into pcDNA3 with the Myc-D<sub>21</sub> Nco I (-) PCR fragment to create the four D<sub>21</sub> Dopamine Receptor:G-protein  $\alpha$  subunit fusion proteins.

### 2.4.2.6 Construction of D<sub>3</sub>:G protein fusion proteins and D<sub>3/2</sub> subunit cDNA fusion proteins

As for D<sub>21</sub>, G $\alpha$ <sub>i</sub> subunit cDNAs were purified and cloned into pcDNA3 with the Myc-D<sub>3</sub> or Myc-D<sub>3/2</sub> PCR fragment to create four D<sub>3</sub> receptor: G protein  $\alpha$  subunit fusion proteins and four chimeric D<sub>3/2</sub> receptor: G protein  $\alpha$  subunit fusion proteins.

## 2.4.3 Construction of Myc-D<sub>21</sub>-YFP fusion protein

### 2.4.3.1 Myc-D21

Primers encoding the Myc epitope sequence were used to generate N-terminally tagged Myc-D<sub>21</sub> and remove the stop codon:

Sense 5'-ACA GAC CCA AGC TTA TGG AAC AAA AAC TTA TTT CTG AAG  
AAG ATC TGG ATC CAC TGA ATC TGT CCT GG-3'

Antisense 5' 5' CGG GGT ACC GCA GTG GAG GAT CTT CAG GAA 3'

Underlined bases indicate introduced restriction sites (sense: *Hind III*, antisense; *Kpn I*), bases in bold indicate introduced N-terminal Myc tag. The PCR fragment was digested using *Hind III* and *KpnI*.

### 2.4.3.2 eYFP

eYFP cDNA was obtained from Clontech (USA). Primers were used to amplify eYFP cDNA with the desired 5' and 3' restriction sites

Sense: 5' CGG GGT ACC ATG GTG AGC AAG GGC GAG GAG 3'

Antisense: 5' TTT TCC TTT TGC GGC CGC TTA CTC GAT GTT GTG GCG GAT 3'

Underlines bases indicate introduced restriction sites (sense; *Kpn I*; antisense *Not I*). The PCR fragment was digested using *Kpn I* and *Not I*.

### 2.4.3.3 Generation of D<sub>21</sub>:eYFP fusion

pcDNA3 was digested using the restriction endonucleases *Hind III* and *Not I* and the Myc-D<sub>21</sub> and eYFP PCR fragments ligated into the sites.

## 2.5 G protein $\alpha$ subunit constructs

### 2.5.1 Generation of G protein mutants

#### 2.5.1.1 G $\alpha_{i1}$ L<sup>204</sup>Q mutation

Human G $\alpha_{i1}$  Q<sup>204</sup>L CDNA in the plasmid pcDNA3.1 was obtained from UMR cDNA Resource Center, (University of Missouri-Rolla, Rolla, USA). To change L<sup>204</sup>Q and give a

wild type human  $G\alpha_{i1}$  cDNA a QuikChange Mutagenesis kit was used as described above using the following primers.

Sense: 5'-TTT GAT GTG GGA GGT CAG AGA TCT GAG CGG AAG-3'

Antisense: 5'-CTT CCG CTC AGA TCT CTG ACC TCC CAC ATC AAA-3'

Bases in bold indicate changed bases.

### 2.5.1.2 $G\alpha_{i1}$ G<sup>203</sup>A mutation

To change G<sup>203</sup>A and give a constitutively inactive human  $G\alpha_{i1}$  mutant cDNA a QuickChange Mutagenesis kit was used as described above using the following primers and the wild type human  $G\alpha_{i1}$  in pcDNA3.1 as a template:

Sense; 5' CAT TTT AAA ATG TTT GAT GTG GGA GCT CAG AGA TCT CGG 3'

Antisense; 5' CCG AGA TCT CTG AGC TCC CAC ATC AAA CAT TTT AAA ATG

Bases in bold indicate changed bases.

### 2.5.1.3 Construction of G-protein alpha subunit / Fc fragment fusions

Constitutively active and inactive mutant  $G\alpha_{i1}$  cDNA was cloned into the vector  $\alpha$ FcMCS to give a G protein  $\alpha$  subunit: Fc fragment fusion protein cDNA.  $G\alpha_{i1}$  mutant cDNA was amplified using the following primers, removing a stop codon and inserting the relevant 5' and 3' restriction sites:

Sense: 5' AAAA AAG CTT ATG GCC TGC ACG CTG AGC

Antisense: 3' AAG GAA AAA AGC GGC CGC AAA GAG ACC ACA ATC TTT  
TAG ATT

Underlined bases indicate restriction sites (sense, *Hind III*; antisense: *Not I*)

PCR fragments were digested with *Hind III* and *Not I* and cloned into  $\alpha$ FcMCS which had been digested with the above restriction endonucleases.

## 2.6 Expression of $G\alpha_i$ family G-proteins in *E Coli*

cDNAs for all of four rat  $G\alpha_i$  family members ( $G\alpha_{i_{1,2,3,oi}}$ ) were previously subcloned into the prokaryotic expression vector pT7.7 and then transformed into the *E coli* strain BL21 DE3. (work performed in house by A. Wise) This is a strain of bacteria suitable for the expression of genes in the vector pT7.7. Glycerols of these transformed bacteria were stored at -80 °C until required. A scrape of the required glycerol was taken using a sterile pipette tip and cultured to a 5 ml scale for 16 hours at 37 °C in LB containing 100  $\mu$ g/ml ampicillin. 2.5 ml of each of these 5 ml cultures were transformed into 2 x 100ml LB containing 100  $\mu$ g/ml ampicillin and grown at 37 °C until an absorbance of 0.4 at 550 nm has been reached. One of the two cultures was then induced with 1mM IPTG and both cultures incubated at 30 °C for a further 4 hours. Cells were then harvested by centrifugation at 4000 rpm for 30 minutes at 3220 x g, supernatant discarded and pellets frozen at -80 °C. Cell pellets were thawed and resuspended in 20 ml STE buffer. Cells were lysed with two passes through a French press set at 950 PSI. Cell lysates were cleared by centrifugation at 10000 x g for fifteen minutes and the supernatant removed and kept on ice. Protein concentration was determined using a BCA assay and lysates stored in 1 ml aliquots at -80 °C.

## **2.7 Cell culture**

### **2.7.1 Routine cell culture**

For cell growth sterile pipettes and flasks were used for all manipulation, and all tissue culture work was carried out in a sterile flow cabinet. To initiate growth of a specific cell line, cells were brought up from liquid nitrogen storage and the aliquot was thawed rapidly at 37 °C. To remove DMSO the entire aliquot (1 mL) was then added to a sterile 15 ml falcon tube, 10 ml of appropriate growth media (prewarmed to 37 °C ) added and tube spun at 180 x g for 5 minutes. Supernatant was removed and cells resuspended in 10 ml of appropriate media and transferred to a 75 cm<sup>2</sup> flask.

### **2.7.2 Cell subculture**

Typically cells were grown to approximately 80-100% confluency before being subcultured into new flasks using the following procedure. Media was removed, 2 ml of trypsin solution added and flask incubated at 37 °C for 3 minutes. Cells were detached by administering a sharp slap to the side of the flask. 8 ml of appropriate media containing serum was added to halt the enzymatic action of trypsin. Cells were then spun at 180 x g at room temperature to pellet cells. The supernatant was discarded and cells resuspended in 5 ml media. The cells were then diluted as desired for further subculturing into 75cm<sup>2</sup> flasks.

### 2.7.3 Coating of coverslips and 24 well plates with poly-D-lysine

Coverslips were prepared by washing in 70 % ethanol, then washing several times with dH<sub>2</sub>O and then autoclaving in a sealed container. Coverslips were placed into the wells of a six well dish using sterile forceps, working in a flow cabinet. 2 ml poly-D-lysine (1 mg/ml in sterile dH<sub>2</sub>O) was added to each well, removed, and the procedure repeated. The coated plates were allowed to dry for 30 minutes in flow cabinet and then sealed and stored at 4 °C until required.

### 2.7.4 Transient transfection using lipofectamine

Transfections using lipofectamine were performed as per the manufacturer's instructions. Briefly, cells were grown to approximately 60-80 % confluency before transfection. 4-10 µg of DNA at a concentration of 0.1 µg/µl in sterile water was used for each 10 cm dish. The amount of DNA and lipofectamine used was dependent on the number of 10 cm dishes being transfected. Lipofectamine was diluted with optimem in a 1:30 ratio. DNA was also diluted with optimem to the same given volume. A typical transfection mix for one 10 cm dish is detailed below:

	Tube 1	Tube 2
DNA	40-80 µl	
Optimem-1	520-560 µl	580 µl
Lipofectamine <sup>TM</sup>	-	20 µl

The DNA-optimem and Lipofectamine-Optimem mixtures were combined and left to complex at room temperature for 30 minutes. Cells to be transfected had growth media removed and to ensure no traces of serum remained; 6 ml optimem was added to the dish.

This was left for 20 minutes at 37 °C and then removed. The Optimem / Lipofectamine / DNA mix was then diluted to an appropriate volume (6 ml total volume per 10 cm dish) and then added to the monolayer of cells. This was returned to the incubator for 4 hours, before the transfection reagents were removed and replaced with an appropriate volume of growth media. Cells were then allowed a further 48 hours of growth before harvesting for assays.

### **2.7.5 Transfections using Effectene® for immunocytochemistry experiments**

Effectene ® (Qiagen,) was used according to the manufacturer's instructions. When confluent, HEK293T cells were split in a 1:40 ratio and 2 ml was transferred into each well of 6 well plates containing coverslips. cDNA was diluted to 0.1 µg/µl. For each 6 well plate the following mix was used:

0.5 µg (5 µl) of Gα cDNA + 0.3 µg (3 µl) D<sub>21</sub> YFP cDNA = 0.80µg (8 µl) total

The final DNA mix was diluted with buffer EC to a total volume of 100 µl \* no. of 6 well plate wells. Enhancer ( 8 µl enhancer per 1 µg of total DNA for each transfection) was added. This was incubated at room temperature for 2-4 min. 10 µl Effectene reagent was added to the DNA-enhancer mixtures and mixed by pipetting up and down 5 times.

Samples were incubated at room temperature for 5-10 min to allow transfection complex formation. Fresh growth medium (1.6 ml) was added to each well. Growth medium (600 µl x no. of wells) was added to the tube containing the transfection complexes. This was mixed by pipetting up and down twice, and then immediately added to the cell monolayers.

## **2.7.6 Generation and maintenance of Flp-In T-REx cell lines**

### **inducibly expressing pertussis toxin insensitive G protein $\alpha$ subunits.**

Prior to transfection cells were maintained in Dulbecco's modified Eagle's medium without sodium pyruvate, 4500 mg/liter glucose, and L-glutamine supplemented with 10% (v/v) fetal calf serum, 1% antibiotic mixture, 15  $\mu$ g/ml blasticidin and Zeocin (100  $\mu$ g/ml final) at 37 °C in a humidified atmosphere of air/CO<sub>2</sub> (19:1). One day prior to transfection media was removed and replaced with media without zeocin or blasticidin (basal media).

To generate Flp-In T-REx HEK293 cells able to inducibly express the G protein  $\alpha$  subunit of interest, the cells were transfected with a mixture containing the pOG44 and desired G – protein  $\alpha$  subunit cDNA in the pcDNA5/FRT/TO vector in a ratio of 9:1 to give a total of 5  $\mu$ g DNA per 10 cm dish. Transfections were performed using lipofectamine as described above and basal media was used to stop the transfection. 24 hours after transfection cells were split in a ratio of 1:20. 48 hours after transfection the medium was changed to medium supplemented with 15  $\mu$ g/ml blasticidin and 100  $\mu$ g/ml hygromycin (selective medium) to initiate selection of stably transfected cells. Selective media was replaced every 4 days until foci could be identified. The entire polyclonal population was then pooled and screened for tetracycline regulated gene expression. Cells were plated in selective medium and expression of gene of interest induced by adding 1  $\mu$ g/ml tetracycline. Expression of relevant G protein was tested using Western Blotting.

### **2.7.7 Generation and maintenance double cell lines stably expressing Dopamine receptor and expressing pertussis toxin insensitive G protein $\alpha$ subunits from the inducible Flp-In locus**

To constitutively stably co-express the D<sub>2L</sub> receptor in Flp-In T-REx HEK293 cells able to inducibly express the G protein  $\alpha$  subunit of interest, the appropriate cells were further transfected with the receptor cDNA in pcDNA3 using lipofectamine<sup>TM</sup> as described above, and resistant cells were selected in the presence of 1 mg/ml G418. Resistant clones were picked, cultured, and screened for receptor expression using [<sup>3</sup>H] Spiperone saturation binding and G-protein expression using Western blotting.

### **2.7.8 Induction of inducible gene of interest in Flp-In T-REx cells**

Cells were grown in serum free media for 24 hours prior to induction. Typically expression of gene of interest was induced with 1  $\mu$ g / $\mu$ l tetracycline 48 hours prior to cell harvest.

### **2.7.9 Pertussis Toxin Treatment**

The ADP-ribosylation of a C-terminal cysteine for all G $\alpha_i$  subunits is catalysed by Pertussis toxin (from *Bordetella Pertussis*), preventing functional interaction between receptor and G protein and thus blocking receptor activation of the G protein. Cells were treated with 25 ng/ml pertussis toxin in appropriate growth media and incubated at 37 °C 16 hours prior to cell harvesting.

### **2.7.10 Cell harvesting**

Cells were washed 3 times with ice cold PBS, before resuspension in ice cold PBS and centrifugation at 450 x g. Supernatant was discarded and the resultant cell pellet was frozen at - 80°C until required.

### **2.7.11 Preparation of cell membranes**

Cells were harvested as above, frozen at -80°C for at least 1 hour and resuspended in 15 ml of TE buffer (10mM Tris, 0.1mM EDTA, pH7.4). Cell suspensions were then homogenised using an Ultra Turrax for 3 x 20 s. The homogenate was centrifuged at 1700×g for 10 min and the supernatant was collected and centrifuged at 48 000×g for 45 min at 4°C. The resulting pellet was resuspended in TE buffer and stored at -80°C in aliquots of 1ml. The protein concentration was determined by BCA protein quantification assay as described below.

## **2.8 Protein Biochemistry**

### **2.8.1 BCA protein quantification assay**

To determine the protein concentration in cell lysates bicinchonic acid (BCA) and copper sulphate solutions were used. Proteins reduce Cu(II) ions to Cu(I) in a concentration dependent manner. BCA is a highly specific chromogenic reagent for Cu(I) forming a purple complex with an absorbance maximum at 562 nm. The absorbance is directly

proportional to the protein concentration. The protein concentration was determined using known concentrations of BSA solutions as standard (0.2-2 mg/ml)

One part reagent B was added to 49 parts reagent A. 200  $\mu$ l of this solution was added to 10  $\mu$ l of each protein sample/standard in a 96 well plate. The absorbance was read after incubation at 37 °C for 30 min.

## **2.8.2 Preparation of samples for SDS gel electrophoresis**

Cell membranes were prepared as above, diluted to a 1 mg/ml protein concentration in TE buffer and then mixed 1:1 with Laemmli buffer and heated for 5 minutes at 85 °C before loading onto SDS-PAGE gels.

## **2.8.3 SDS polyacrylamide gel electrophoresis (SDS PAGE)**

Samples were prepared as above and resolved on NuPAGE ® Novex precast bis-tris gels (Invitrogen). The NuPage ® system is based upon a bis-tris HCl buffered (pH 6.4) polyacrylamide gel, containing a separating gel that operates at pH 7.0. Gels with a polyacrylamide concentration of 4-12% achieved the best separation of the proteins of interest and were used exclusively. To run the gels NuPage ® MOPS SDS running buffer was used. The gels were run at 200 V in the Xcell Sureblock™ mini-cell

## **2.8.4 Western blotting**

Following SDS-PAGE the proteins were electrophoretically transferred onto a nitrocellulose membrane at 30 V for 90 minutes in transfer buffer (0.2 M glycine, 25mM Tris, 20% (v/v) methanol) using the Xcell II™ blot module (Invitrogen). The membranes

were blocked with 5% (w/v) fat free milk in PBS/ 0.2% (v/v) Tween 20 for 2 hours at room temperature or 16 hours at 4 °C. The membranes were then incubated with the appropriate primary antibody in 5% (w/v) fat free milk PBS / 0.2% (v/v) Tween 20 overnight at 4 ° C or 2 hours at room temperature. After removing the primary antibody and washing the membrane 4 times for 5 minutes each with PBS/ PBS / 0.2% (v/v) Tween 20, the blots were treated with the appropriate HRP-conjugated secondary antibody in blocking buffer for 1 hour at room temperature. After repeating the washing step, the reactive proteins were visualised by enhanced chemiluminescence and exposure onto photosensitive film. For western blot analysis the following antibody dilutions were used unless specified otherwise:

#### Primary Antibodies;

Antigen Raised Against	Antibody	Dilution
C-terminal 10 amino acids of $G\alpha_{i1,2}$	SG3	1:2500
	1319 G	1:2500
C –terminal 10 amino acids of $G\alpha_{i3}$	I3D	1:2500
C –terminal 10 amino acids of $G\alpha_{o1}$	OC2	1:5000
C-terminal 10 amino acids of $G\alpha_q$	CQ5	1:5000
C-terminal 10 amino acids of $G\alpha_s$	CS2	1:2500

#### Secondary Antibodies;

	Dilution
HRP conjugated donkey $\alpha$ mouse	1:10,000
HRP conjugated donkey $\alpha$ mouse	1:10,000

## 2.9 Pharmacological Assays

### 2.9.1 Radioligand binding

#### 2.9.1.1 Saturation binding assays using [<sup>3</sup>H]-spiperone

Cell membranes (10 µg protein) were incubated in triplicate with [<sup>3</sup>H]-spiperone (0.001–2 nM) in a total volume of 1 ml buffer (20 mM HEPES, 6 mM MgCl<sub>2</sub>, 1 mM EDTA, 1 mM EGTA, pH 7.4). Non-specific binding was determined by the inclusion of 10 µM (+)-butaclamol. The reaction was initiated by the addition of membranes and the tubes were incubated at 25 °C for 3 hours. The reaction was terminated by rapid filtration using a Brandel cell harvester with three 5 ml washes of ice-cold PBS (140 mM NaCl, 10 mM KCl, 1.5 mM KH<sub>2</sub>PO<sub>4</sub>, 8 mM Na<sub>2</sub>HPO<sub>4</sub>). The filters were soaked in 3 ml scintillation fluid and radioactivity present was determined by liquid scintillation spectrometry.

#### 2.9.1.2 Agonist competition versus [<sup>3</sup>H]-spiperone binding

Cell membranes (10 µg protein) were incubated with 0.05 nM [<sup>3</sup>H]-spiperone and various concentrations of dopamine, in triplicate, in a final volume of 1 ml buffer (20 mM HEPES, 6 mM MgCl<sub>2</sub>, 1 mM EDTA, 1 mM EGTA, 40µM ascorbic acid, pH 7.4). Non-specific binding was determined by the inclusion of 10 µM (+)-butaclamol. The reactions were initiated, incubated and terminated as described above. The effect of guanine nucleotides on dopamine binding was assessed by the addition of 100 mM NaCl and 100 µM GTP to the buffer.

## 2.9.2 [<sup>35</sup>S] GTP $\gamma$ S binding assays

### 2.9.2.1 [<sup>35</sup>S] GTP $\gamma$ S binding assay with termination by filtration

Cell membranes (10  $\mu$ g) were incubated in 900  $\mu$ l buffer (20 mM HEPES, 100 mM NaCl, 6 mM MgCl<sub>2</sub>, 40  $\mu$ M ascorbic acid pH 7.4) containing 10  $\mu$ M GDP and various concentrations of agonist. All experiments were performed in triplicate. The reaction was initiated by the addition of cell membranes and incubated at 30 °C for 30 min. A 100  $\mu$ l volume of [<sup>35</sup>S]-GTP $\gamma$ S (0.1 nM final concentration) was then added and the incubation continued for a further 30 min. The reaction was terminated by rapid filtration with a Brandel cell harvester and three 4 ml washes with ice-cold PBS. Radioactivity was determined as described for saturation analysis. For antagonist dose-response assays an 'EC<sub>50</sub>' concentration of dopamine was added along with various concentrations of antagonist.

### 2.9.2.2 [<sup>35</sup>S] GTP $\gamma$ S binding assay with immunoprecipitation step

[<sup>35</sup>S]GTP $\gamma$ S-binding experiments were initiated by the addition of cell membranes containing 10 fMol of the various fusion constructs to an assay buffer (20 mM Hepes (pH 7.4), 3 mM MgCl<sub>2</sub>, 100 nM NaCl, 10  $\mu$ M GDP, 0.2 mM ascorbic acid, 50 nCi of [<sup>35</sup>S]GTP $\gamma$ S) in the presence or absence of dopamine. Non-specific binding was determined in the same conditions but with the addition of 100  $\mu$ M GTP $\gamma$ S. Reactions were incubated for 30 min at 30 °C and were terminated by the addition of 0.5 ml of ice-cold buffer, containing 20 mM Hepes (pH 7.4), 3 mM MgCl<sub>2</sub> and 100 mM NaCl. The samples were centrifuged at 16000 g for 15 min at 4 °C, and the resulting pellets were resuspended in solubilisation buffer (100 mM Tris, 200 mM NaCl, 1 mM EDTA, 1.25% Nonidet P-40) plus 0.2% SDS. Samples were precleared with Pansorbin, followed by

immunoprecipitation with relevant antiserum. Finally, the immunocomplexes were washed twice with solubilisation buffer, and bound [ $^{35}\text{S}$ ]GTP $\gamma$ S was measured by liquid-scintillation spectrometry.

### 2.9.2.3 [ $^{35}\text{S}$ ] GTP $\gamma$ S binding assay – scintillation proximity assay

[ $^{35}\text{S}$ ]GTP $\gamma$ S binding assays were performed at room temperature in 384-well format. Membranes (10  $\mu\text{g}/\text{point}$ ) were diluted to 0.4 mg/ml in assay buffer (20 mM HEPES, 100 mM NaCl, 10 mM MgCl<sub>2</sub>, pH 7.4) supplemented with saponin (10 mg/l) and preincubated with 10  $\mu\text{M}$  GDP and wheat germ agglutinin SPA beads (Amersham Biosciences) (0.5 mg) and incubated at room temperature for 45 min with agitation. Various concentrations of D<sub>2</sub> dopamine receptor agonists were added, followed by [ $^{35}\text{S}$ ]GTP $\gamma$ S (1170 Ci/mmol; Amersham Biosciences) at 0.3 nM (total volume of 46  $\mu\text{l}$ ), and binding was allowed to proceed at room temperature for four hours. Bound [ $^{35}\text{S}$ ]GTP $\gamma$ S was determined by scintillation counting on a ViewLux ultraHTS Microplate Imager (PerkinElmer).

### 2.9.3 Data analysis

Data were analysed using the computer program GraphPad Prism (GraphPad Software). [ $^3\text{H}$ ]Spiperone saturation binding curves were fitted best by a one binding site model from which the  $B_{\text{max}}$  (receptor expression level) and  $K_d$  (dissociation constant for [ $^3\text{H}$ ]spiperone) were derived. Data from competition experiments were fitted to two binding site and one binding site models, and the best fit was determined using an  $F$ -test. Concentration–response curves for agonist and inverse agonist effects on [ $^{35}\text{S}$ ]GTP $\gamma$ S binding were analysed by non-linear least squares regression analysis using a sigmoidal concentration /

response relationship with a Hill coefficient of 1 and  $EC_{50}$  and  $E_{max}$  (maximum effect) values were derived from this analysis.

## 2.10 Antibody Generation and Characterisation Protocols

### 2.10.1 Immunisation, hybridoma generation, tissue culture and antibody purification

Plasmid immunisation, rapid immunisation using recombinant  $G\alpha_{i1}$ , hybridoma generation and maintenance and antibody purification was all performed by I. Kinghorn (Antibody Technology Group, BioPharm and Protein Technology, Bioreagents & assay development, GlaxoSmithKline, Stevenage, UK)

#### 2.10.1.1 Immunisation

A myristoylated preparation of recombinant rat  $G\alpha_{i1}$ -subunit (25  $\mu$ g) was purchased from calbiochem (Merck KGaA, Darmstadt, Germany) this was incubated at RT °C with 100  $\mu$ M GTP $\gamma$ S in a buffer containing 100 mM NaCl, 20 mM HEPES, 3 mM MgCl<sub>2</sub>, 1 mM EDTA, 200 nM GDP, pH 8.0 for 30 minutes (Performed by B. Powney, Screening & Compound Profiling, GSK, UK) . Repetitive Immunisation at Multiple Sites (RIMMS) immunisations were carried out using a procedure simplified from (Bynum et al., 1999). Over a period of 11 days, 10 $\mu$ g protein (rGi1 + 10 $\mu$ M GTP $\gamma$ S) emulsified in Complete Freund's adjuvant and RIBI adjuvants (Sigma) were injected at 6 subcutaneous sites proximal to draining lymph nodes in 2 anaesthetised female SJL mice (Harlan, UK). After 6 and 11 days, mice were immunised with 5  $\mu$ g protein in RIBI adjuvant at 4 sites. Three days after the final boosts, a cell suspension harvested from popliteal, superficial inguinal, axillary and brachial lymph nodes was prepared. In a similar manner plasmid

immunisations were performed with gold particles coated with cDNA of Glu<sup>204</sup>Leu G $\alpha_{i1}$ , cloned into the vector  $\alpha$ FcMCS using a gene gun. As described in **section 2.5.1.3**, the stop codon of the Glu<sup>204</sup>Leu G $\alpha_{i1}$  gene was removed and therefore upon cloning into the multiple cloning site of  $\alpha$ FcMCS, the cDNA of a Glu<sup>204</sup>Leu G $\alpha_{i1}$  human Fc fragment fusion protein was generated.

### **2.10.1.2 Cell Fusion**

Lymph node cells were centrifuged with myeloma cells (P3X63/Ag8.653, Kearney) and fused using PEG1500 (Roche). The cell pellet following the fusion procedure was resuspended in JRH610 containing 10% hybridoma cloning factor (Sigma), 10% FCS (Hyclone), pen/strep, 1 x HAT (InVitrogen) and 1.35% methylcellulose (Sigma 4000cps). The fusion suspension was distributed between 5 Nunc omnitrays 4 Genetix Petriwell plates for selection and cloning in a single step. After 10-11 days culture, colonies were imaged and picked using an automated robotic colony picker (Genetix ClonepixFL, ). Individual monoclonal hybridoma colonies (1632) were deposited into Greiner 96 well plates containing 200  $\mu$ l/well of the above medium without methylcellulose and 1 x HT in place of HAT.

### **2.10.2 ELISA assay**

0.05 M carbonate-bicarbonate pH 9.6 buffer was made by adding 1 x carbonate-bicarbonate buffer capsule (Sigma) to 100ml of dH<sub>2</sub>O. An antigen solution of the appropriate concentration was made using this buffer. 200  $\mu$ l of this solution was added to each well of a 96 well microtitre plate, and the plate incubated for 16 hours at 4 °C. The antigen solution was then removed and the plate washed three times in PBS / 0.1% (v/v) Tween 20. To minimise non-specific binding a blocking step was included where 200  $\mu$ l PBS / 5% BSA was added to each well and incubated at room temperature for 1 hour, after

which washing was repeated as above. Primary antibodies were diluted in PBS / 0.1% (v/v) Tween 20 in a ratio of 1:3 sequentially to give a range of concentrations. 200 µl of the diluted antibody was added to each well, and plates incubated at 4 °C overnight. The negative control in all cases was a species matched, non specific immunoglobulin diluted in PBS / 0.1% (v/v) tween 20. Plates were then washed as above and the appropriate HRP conjugated secondary antibody added at a dilution of 1:1000 in PBS / 0.2 % Tween 20 and plates incubated for 1 hour at room temperature and then washed as above. 100 µl of SureBlue™ TMB HRP substrate per well (KPL, Gaithersburg, USA) was then added. Reaction was stopped by addition of 100 µl of 1N HCl, and plates read at a wavelength of 450 nm

### **2.10.3 FMAT assay for screening of hybridoma clones**

#### **2.10.3.1 Cell culture and transfection**

HEK293T cells were grown to 80-90% confluency in 225 cm<sup>3</sup> tissue culture flasks in DMEM +10% dialysed FCS (25 ml tissue culture media / flask). Transfections were performed using an in-house transfection reagent ‘Gemini (GSC103 DOPE)’ (GSK, Stevenage, UK). For each flask the following transfection mixtures were set up:

85 µg DNA                    +            12.25 ml Optimem

250 µl Gemini                +            12.25 ml Optimem

These two mixtures were combined and allowed to complex for 30 minutes at room temperature. The entire complex was then added to the flask of cells and mixed with the 25 mL of tissue culture media. Transfected cells were left at 37 °C in a humidified atmosphere of air / CO<sub>2</sub> (19:1) for 48 hours prior to cell harvest. Cells were then washed

once with 50 mL PBS / flask, and then harvested in 10 mL PBS-dissociation buffer / flask. Cells were pelleted by centrifugation at 450 x g. Supernatant was discarded and the resultant cell pellet was either resuspended in PBS / 1% BSA / 0.1% NaN<sub>3</sub> for immediate use in an FMAT assay, or resuspended in 10% DMSO / FBS and stored at -80 °C in 1 mL aliquots until required.

### **2.10.3.2 Thawing of frozen cell aliquots**

Frozen cell aliquots were thawed rapidly in a 37 °C water bath and washed once with PBS (4 °C) as described in section 2.10.2.2. The supernatant was discarded and the pellet was resuspended in PBS / 1% BSA / 0.1% NaN<sub>3</sub>.

### **2.10.4 General FMAT assay protocol**

Prior to use in the FMAT assay, the number of viable cells present in the PBS /1% BSA / 0.1% NaN<sub>3</sub> cell suspension was determined by counting using a Vi-Cell XR Cell Viability Analyzer (Beckman Coulter Inc., Fullerton, CA,USA). Typically the number of viable cells / ml was in the region of  $1 \times 10^7$ . Cells were resuspended to  $1 \times 10^5$  viable cells per ml. For the wild type  $G\alpha_{i1}$  transfected HEK293 cell preparations nucleotide (GTP $\gamma$ S or GDP $\beta$ S) was added to a final assay concentration of 100  $\mu$ M. The secondary antibodies, either donkey anti-rabbit FMAT blue ® or donkey anti-mouse FMAT blue ® (Applied Biosystems, Foster City, CA, U.S.A.), were added to a final dilution of 1:2000. 50  $\mu$ l of this solution was added per well of a 384 well FMAT ® plate to give 5,000 cells per well. This well contained 1  $\mu$ l of the appropriate primary antibody. The antibody dilutions used typically are displayed below.

Rabbit  $\alpha$ - $G\alpha_{i1/2}$  polyclonal antisera (1319 glycine, in house) - 1:500 in PBS

Mouse  $\alpha$ -FLAG monoclonal antisera (GSK, Stevenage, UK) – 1:500 in PBS

Plates were covered with aluminium foil, and left for at least 2 hours at room temperature. Bound fluorescence was detected using a FMAT 8200 high throughput screening system (Applied biosystems) and analysed using FMAT™ software.

#### **2.10.4.1 FMAT assay protocol specific for primary hybridoma screen**

FMAT assay protocol was performed as described in **2.10.4**. Hybridoma clone tissue culture supernatant (5  $\mu$ l) and HEK293 cell / FMAT donkey anti-mouse FMAT blue ® / PBS / 1% BSA / 0.1 % NaN<sub>3</sub> suspension were added to 384 well FMAT ® plates. All manipulations were carried out using an automated liquid handling robot based on a Beckman BiomekFx. Plates were read following at least 2 hours incubation at room temperature.

Bound fluorescence was detected using a FMAT 8200 high throughput screening system (Applied Biosystems, Foster City, CA, U.S.A.) taking advantage of the Zymark Twister® robotic plate handler and four input stacks. The FMAT software allows robotic plate handling to remove and load plates to and from the scanner.

#### **2.10.5 Hybridoma expansion and immunoglobulin purification**

Hybridomas from wells of interest were expanded into 24 well plates (Greiner, Stonehouse, Gloucestershire, UK), cryopreserved and subcloned in semisolid medium to ensure stability. To generate purified mAbs, hybridomas were expanded further into 2 x T225 cm<sup>2</sup> flasks in the above medium without HCF and HT and cells pelleted, resuspended in medium without serum and cultured until cell viability dropped to ca. 10%. Immunoglobulins were purified from the conditioned medium using immobilised Protein A (Prosep-A) and the Perbio buffer system according to manufacturers instructions. Purified mAbs were dialysed against and stored in PBS (Sigma). Isotypes were determined using a typing stick kit from Amersham Biosciences (All mAbs were IgG1 kappa).

## **2.10.6 Epitope Mapping of Antibodies using PepSet™ from Mimotopes**

### **2.10.6.1 Re-dissolving peptides in PepSet™**

A PepSet™ peptide Library of 86 16mer peptides corresponding to the entire sequence of Gα<sub>i1</sub> and overlapping by four amino acids was obtained from Mimotopes. Before use in an epitope mapping assay the supplied peptides must be dissolved and aliquoted into smaller volumes. The following procedure is based on a standard procedure outlined by the manufacturer. Peptides were reconstituted with 200 µl of 80% dimethyl sulfoxide (DMSO) / 20% degassed dH<sub>2</sub>O and tubes repeatedly inverted for 5 minutes. Tubes were then inspected to make sure peptide had totally dissolved. It was necessary to sonicate the entire pepset for 5 minutes in a sonication bath to completely dissolve all the peptides. 20ul of each peptide solution was then aliquoted into one well of a 96 well polypropylene deep well plate. Deep well plates were sealed and stored at -20 ° C until use.

### 2.10.6.2 Epitope Mapping Assay

Prior to use the peptide solutions created as above were diluted to a working strength of 1:1000 in a PBS / 0.1 % Tween 20 / 0.1% (w/v) NaN<sub>3</sub> solution. These solutions can be stored for one day at 4 °C or -20 °C for longer storage. Non-specific adsorption was blocked by adding 200 µl of blocking buffer( PBS, 5% fat free milk powder, 0.1% tween 20) to each well streptavidin coated 96 well plate (mimotopes) and incubation for 1 hour at room temperature. Plates were washed 4 times with PBS / 0.1% tween 20 and remaining buffer removed by vigorously slapping the plates well side down onto a benchtop covered with absorbent paper towels. 100 µl of diluted peptide solution was transferred into the corresponding well positions of the streptavidin coated plate. The plates were then placed on a shaker table and the reaction allowed to proceed for 1 hour at room temperature. After incubation the solution was flicked out and the washing procedure repeated as described above. Relevant antibodies were diluted 1:1000 in PBS/ 0.1% tween 20 / 0.1 % NaN<sub>3</sub>. 100 µl of this diluted serum was added to each of the wells of the plates containing captured peptides. Plates were placed on a shaker table and incubated with agitation for 16 hours at 4 ° C. The washing step was repeated as above. Bound antibody was detected using a suitable either anti-rabbit or anti-mouse HRP labelled secondary antibody at a final dilution of 1:2000 in PBS / 5% fat free milk powder / 0.1% tween 20. 100 µl of the dilute conjugate was dispensed into each well and incubated at room temperature for 1 hour. The washing step was repeated as above and finally the plates were washed twice with PBS. Presence of peroxidase was measured by adding 100 µl SureBlue™ TMB HRP substrate per well (KPL, Gaithersburg, USA). Reaction was stopped by addition of 100ul of 1N HCl, and plates read at a wavelength of 450nm

## **2.10.7 Immunocytochemistry**

### **2.10.7.1 Hoescht nuclear staining**

Cells were cultured and transfected as described in section 2.7.5. Cells were washed 1 x with room temperature PBS, and then incubated with hoescht stain (1:1000 dilution in PBS) for 15 minutes at 37 ° C in the incubator.

### **2.10.7.2 Immunocytochemistry**

Cells were washed 2 x with room temperature PBS (leaving PBS on for 5 mins each time). Fixation of cells was performed by incubation for 10 mins with 10% Formaldehyde in PBS solution at room temperature for exactly 10 minutes. Cells were then washed three times with ice cold PBS (leaving PBS on for 5 mins each time). Blocking and cell permeabilisation was achieved in one step with a 10 minute incubation in PBS + 3% marvel milk + 0.15% triton X100. Primary antibodies were diluted 1:1000 in PBS / 3% marvel milk / 0.15% triton X100. 500ul of this solution was spotted onto nescofilm and coverslips were placed cell side down onto this spot and incubated for 1 hour at room temperature. Coverslips were then returned to 6 well plates cell side up and washed 3 x with ice cold PBS as before. Secondary antibody was diluted as follows in PBS + 3% marvel milk + 0.15% triton X100:

$\alpha$ -mouse Alexa 594 – 1:400

$\alpha$ -rabbit Alexa 594 – 1:600

This was spotted onto nescofilm and coverslips applied as above and incubation was for 1 hour at room temperature. Cells were washed as above and then mounted onto slides using Immuno-Mount solution and stored at 4°C until use.

### **2.10.7.3 Modified Immuncytochemical method: Aluminium Fluoride Stimulated Whole Cell Assay**

All  $\text{AlF}_4^-$  protocols were performed in 6 well plates. Cells were washed using GTP $\gamma$ S buffer (50 mM Tris, 5 mM  $\text{MgCl}_2$ , 100 mM NaCl, 0.2 mM EGTA, pH 7.4), followed by incubation at room temperature for 1 hour with  $\text{AlF}_4^-$  solution (50 mM Tris, 5 mM  $\text{MgCl}_2$ , 100 mM NaCl, 0.2 mM EGTA, 10mM NaF, 0.03 mM  $\text{AlCl}_3$ , 3% fat Marvel milk (w/v), 0.2% Saponin (v/v)). Cover-slips were subsequently washed with PBS and fixed using 4% Formaldehyde in PBS. Cover-slips were washed three times with 4°C PBS. Cells were incubated with the relevant secondary antiserum for one hour at room temperature (PBS, 3% marvel milk (w/v), 0.2% saponin (v /v)). Finally, cells were washed with ice cold PBS and mounted using Immu-Mount for microscopy.

### **2.10.7.4 NPA stimulated GTP $\gamma$ S Whole Cell Assay**

All agonist stimulated assays were performed in 6 well plates. Cells were washed using GTP $\gamma$ S buffer (50 mM Tris, 5 mM  $\text{MgCl}_2$ , 100 mM NaCl, 0.2 mM EGTA). Cells were then incubated in GTP $\gamma$ S buffer + 0.2 % (v/v) Saponin / 3% (v/v) Marvel Milk / with 10  $\mu\text{M}$  GTP $\gamma$ S or 100  $\mu\text{M}$  GDP $\beta$ S and with or without 1  $\mu\text{M}$  NPA, with an appropriate concentration of primary antibody, for 1 hour at room temperature. Cover-slips were then washed with PBS and fixed using fixed using 4% Formaldehyde in PBS. The experiment was completed as for **section 1.10.7.4**.

### 2.10.8 Epifluorescence Microscopy

Formaldehyde fixed cells, expressing the Dopamine D<sub>21</sub> fusion protein and appropriate G protein  $\alpha$  subunit were imaged in 2D using an inverted Nikon TE2000-E microscope (Nikon Instruments, Melville, NY) equipped with a x 60, (NA=1.4), oil immersion Plan Fluor Apochromat lens, a z-axis linear encoder and a cooled digital Cool Snap-HQ CCD camera (RoperScientific/Photometrics, Tucson, AZ). Epifluorescence excitation light was generated by an ultra high point intensity 75 W xenon arc Optosource lamp (Cairn Research, Faversham, Kent, UK) coupled to a computer controlled Optoscan monochromator (Cairn Research, Faversham, Kent, UK). Monochromator was set to 500/5 nm and 575/12nm for the sequential excitation of eYFP and Alexa Fluor 594 respectively. excitation light was transmitted through the objective lens using the following single pass dichroics; Q515LP for eYFP and Q595LP for Alexa Fluor 594 and emitters; HQ535/30 nm for eYFP and HQ645/75 nm for Alexa Fluor 594. Using these filter sets, the fluorophores were easily separated with no bleed through. Images were collected using a Cool Snap-HQ digital camera operated in 12-bit mode. Computer control of all electronic hardware and camera acquisition was achieved using Metamorph software (version 6.3.7; Molecular Devices Corp.,Downing, PA). For one experiment exposure and intensity was set using the positive control condition and this used for all other conditions.

## 3 Protean agonism at the dopamine D<sub>2</sub> receptor

### 3.1 Introduction

There is a wealth of experimental evidence that some GPCRs can couple to multiple G protein  $\alpha$  subunits (Wess, 1998). Similarly, a large number of GPCRs are able to generate multiple intracellular signals, and for those with a rich pharmacology of synthetic small molecule ligands it has often been possible to observe differential pharmacology for particular end points (Perez and Karnik, 2005; Urban et al., 2006a). This has resulted in an appreciation, that instead of a receptor having a single active state, different ligands may stabilise different conformational states that differ from the constitutively active state (see **Fig 3.1A + B**) (Kenakin, 2003). With the expansion of the simple ‘active or inactive’ two state model, the proposed extended ternary complex (ETC) model which takes into account constitutive activity of receptors, the potential for an essentially infinite number of receptor states could be predicted (**Fig 3.1C**). In this model the multiplier  $\gamma$  confers a different affinity of the receptor for G proteins when the receptor is ligand bound. Therefore, every value of  $\gamma$  defines a new ligand-bound receptor state. Accordingly, differences in agonist pharmacology to regulate signals via different G proteins is frequently described as ‘agonist-directed trafficking’ (Kenakin, 1995; Urban et al., 2006a). The majority of these observations have focused on measuring the varying efficacy of ligands to regulate the production of two separate second messengers rather than directly measuring differential activation of two individual G proteins. It should be noted that in addition, although GPCRs are defined by their capacity to activate hetero-trimeric G proteins, a number of ligand-induced signals appear not to require G protein interactions. In the case of the  $\beta_2$  adrenoceptor for example, such separation of signal transduction has resulted in the identification of ligands that can be defined as inverse agonists for their effects on adenylyl

cyclase activity but as agonists for their capacity to stimulate phosphorylation of the ERK1/2 MAP kinases (Azzi et al., 2001; Galandrin and Bouvier, 2006). Ligands that display either positive or negative efficacy when assessed in different assays or in different experimental conditions are named protean ligands (Kenakin, 2001). In agreement with the idea of agonist directed trafficking, namely that different ligands stabilise different receptor conformations, it follows that for two distinct signalling pathways a ligand could be an agonist for one but an inverse agonist/ antagonist for another. Observation of this provides compelling evidence for multiple ligand stabilised receptor conformations.

The dopamine D<sub>21</sub> receptor is one of the most well studied and characterised GPCRs. As with a series of GPCRs that interact with members of the pertussis toxin sensitive G proteins, this receptor is able to promiscuously modulate signals via each of G $\alpha_{i1}$ , G $\alpha_{i2}$ , G $\alpha_{i3}$ , and G $\alpha_{o1}$  (Gazi et al., 2003). However, ligand pharmacology can be greatly influenced by the ratio of GPCR to G protein expression (Milligan, 2000) and this can be difficult to define in cells, particularly in comparisons between different G proteins. One method to overcome this is to employ GPCR-G protein fusions that ensure a fixed 1:1 stoichiometry of GPCR and G protein (Milligan et al., 2004). Another consideration is that pertussis toxin sensitive G proteins, in particular G $\alpha_{i2}$  and G $\alpha_{i3}$ , are expressed by all mammalian cells. It is therefore essential to develop some method by which the coupling of one particular G $\alpha_i$  subunit to the receptor of interest can be monitored. A strategy used previously is to employ variants of each of G $\alpha_{i1}$ , G $\alpha_{i2}$ , G $\alpha_{i3}$ , and G $\alpha_{o1}$  which have been rendered insensitive to the ADP-ribosyltransferase activity of pertussis toxin by mutation of the cysteine which is the site of modification to an isoleucine. In addition to the fusion proteins another strategy is to use cell lines stably expressing the D<sub>21</sub> receptor in which varying amounts of each Cys→Ile variant G protein  $\alpha$  subunit can be expressed in an entirely tetracycline-dependent manner. Flp-In™ T-REx host cell lines (Invitrogen) have a single Flp recombinase target (FRT) site located at a transcriptionally active genomic locus

that allows you to generate isogenic inducible expression cell lines using targeted integration. Using these two strategies, in which the relative levels of receptor and G protein expression can be controlled, I will demonstrate that S-(-)-3-(3-hydroxyphenyl)-N-propylpiperidine (S-(-)-3-PPP) is a protean ligand at the D<sub>21</sub> receptor, being an agonist for activation of G $\alpha_{o1}$  but an antagonist/inverse agonist at G $\alpha_{i1}$ , G $\alpha_{i2}$ , G $\alpha_{i3}$ . This observation provides evidence for the concept that the dopamine D<sub>21</sub> receptor can exist in multiple conformational states and indicates that it is possible to selectively direct the nature of D<sub>21</sub> receptor signalling by the use of synthetic ligands.

## 3.2 Results

### 3.2.1 Generation and characterisation of dopamine D<sub>21</sub> receptor:

#### Cys→Ile G protein alpha subunit fusion proteins

The promiscuous coupling of the dopamine D<sub>21</sub> receptor to all four pertussis toxin sensitive mutants ( $G\alpha_{i1}$ ,  $G\alpha_{i2}$ ,  $G\alpha_{i3}$ , and  $G\alpha_{o1}$ ) has been previously established.  $G\alpha_{i2}$  and  $G\alpha_{i3}$  are expressed endogenously by all cells, so to investigate any variations in the ability of ligands at the D<sub>21</sub> receptor to activate the different G protein  $\alpha$  subunits it was necessary to use a model system in which the specific interactions of the receptor with each individual G protein  $\alpha$  subunit could be investigated. Pertussis toxin mediated ADP-ribosylation occurs at a cysteine residue at the fourth position from the C-terminus (**Figure 3.2A**) on members of the  $G\alpha_i$  family. This abrogates functional contact between receptor and  $G\alpha_i$ , thus maintaining the G protein in its inactive formation. Consequently the interaction between receptor and endogenous  $G\alpha_i$  can be abolished. To allow study of a specific  $G\alpha_i$  subunit introduced into a cell, mutants of  $G\alpha_i$  with the C-terminal cysteine residue mutated to an isoleucine can be used. This mutation makes the G protein resistant to pertussis toxin catalysed ADP-riboyslation. Consequently, cells can be transfected with the pertussis toxin insensitive mutant  $G\alpha_i$  subunit of interest and then treated with pertussis toxin to ADP-ribosylate endogenous  $G\alpha_i$  subunits and ensure functional coupling only occurs between the introduced pertussis toxin insensitive mutant and the receptor of interest (**Figure 3.2B**). Another consideration when investigating the coupling of a receptor to different G-proteins is to control the relative expression levels of both receptor and G-protein. One solution to this is to use receptor-G-protein fusion proteins in which the Cys to Ile, pertussis toxin insensitive mutants of  $G\alpha_{i1}$ ,  $G\alpha_{i2}$ ,  $G\alpha_{i3}$  and  $G\alpha_{o1}$ , were linked in frame with the C-terminal tail of the human D<sub>21</sub> (**Figure 3.3**). This ensured that the

stoichiometry of receptor to G protein would be identical for each G protein studied and that the relative cellular distribution and orientation of receptor and G protein would be uniform.

### **3.2.1.1 Characterisation of dopamine D<sub>21</sub> receptor-Cys→Ile variant G protein $\alpha$ subunit fusion proteins**

Each fusion protein was expressed transiently in HEK293T cells, and 16 hours prior to cell harvest, these cells were treated with pertussis toxin (25 ng/ml). Following cell harvest membrane preparations were made. Saturation binding assays employing [<sup>3</sup>H] spiperone showed that each fusion protein was expressed to similar levels of around 1.5 pMol.mg<sup>-1</sup> of membrane protein and bound this ligand with a similar high affinity (**Table 3.1**). It should be noted that the levels of receptor expression sufficiently high that it is likely that depletion of [<sup>3</sup>H] spiperone will have occurred. Calculations suggest that after binding to the receptor the concentration of free ligand will have effectively decreased to 85% of the total added. This can result in the estimation of the K<sub>D</sub> (the affinity) being too high. However, experimentally ligand depletion of 10% is generally ignored, consequently the effect of ligand depletion in the above experiments will not have a dramatic effect on the values for ligand affinity obtained.

**Table 3.1: [<sup>3</sup>H] spiperone binds with similar and high affinity to various D<sub>21</sub> receptor-G protein fusions**

<b>Receptor: G Protein fusion</b>	<b>K<sub>d</sub>, nM (± S.E.M.)</b>	<b>B<sub>max</sub> fMol.mg<sup>-1</sup> (± S.E.M.)</b>
<b>D<sub>21</sub>Gα<sub>i1</sub></b>	<b>0.049 (0.003)</b>	<b>1500 (49)</b>
<b>D<sub>21</sub>Gα<sub>i2</sub></b>	<b>0.051 (0.003)</b>	<b>1415 (24)</b>
<b>D<sub>21</sub>Gα<sub>i3</sub></b>	<b>0.057 (0.002)</b>	<b>1976 (14)</b>
<b>D<sub>21</sub>Gα<sub>o1</sub></b>	<b>0.057 (0.006)</b>	<b>1508 (43)</b>

Experiments were performed in triplicate to n = 3

### 3.2.1.2 Increasing amounts of D<sub>21</sub>-Cys<sup>351</sup>Ile Gα<sub>o1</sub> lead to a proportional increase in [<sup>35</sup>S] GTPγS binding

HEK293T cells were transfected with cDNA encoding the D<sub>21</sub>-Cys<sup>351</sup>Ile Gα<sub>o1</sub> fusion protein, membrane preparations made and receptor binding site density estimated using [<sup>3</sup>H] spiperone (**Table 3.1**). Various amounts of membranes (and therefore varying amounts of receptor) were incubated with 10 μM GDP and with or without the presence of 10 μM dopamine using a [<sup>35</sup>S] GTPγS assay with an immunoprecipitation step. Antiserum raised against the C-terminal tail of Gα<sub>o1</sub> was used for the immunoprecipitation step. For D<sub>21</sub>-Cys<sup>351</sup>Ile Gα<sub>o1</sub> an increase in receptor added to the reaction from 1 to 25 fMol lead to a proportional increase in both basal and dopamine-stimulated [<sup>35</sup>S] GTPγS binding (**Figure 3.3B**). Basal levels of [<sup>35</sup>S] GTPγS binding could reflect constitutive activity of the dopamine receptor-Gα<sub>o1</sub> fusion, or perhaps the basal [<sup>35</sup>S] GTPγS loading of increasing amounts of Gα subunit added to the reaction.

### 3.2.2 The ligands *p*-tyramine and S-(-)-3-PPP only stimulate [<sup>35</sup>S] GTPγS binding at the D<sub>21</sub>-Cys<sup>351</sup>Ile Gα<sub>o1</sub> fusion protein

To test the ability of a selection of ligands to act at the D<sub>21</sub> receptor and stimulate each of the four Gα<sub>i</sub> subunits [<sup>35</sup>S] GTPγS binding was used. Dopamine stimulated [<sup>35</sup>S] GTPγS binding at all four G protein α subunits (**Figure 3.4**) with a significantly higher potency at D<sub>21</sub>-Cys<sup>351</sup>Ile Gα<sub>o1</sub> (**Table 3.2**). [<sup>35</sup>S]GTPγS binding was also stimulated for all fusion proteins by N-propylapomorphine (NPA), quinpirole, *m*-tyramine and R (+) 3-(3-hydroxyphenyl)-N-propylpiperidine (R-(+)-3-PPP), although, when compared to dopamine, only NPA was a full agonist at each construct. Again, with the exception of NPA and 7-OH DPAT, potency of the ligands was greatest for D<sub>21</sub>-Cys<sup>351</sup>Ile Gα<sub>o1</sub>. For the partial agonists *m*-tyramine and R (+) 3-(3-hydroxyphenyl)-N-propylpiperidine (R-(+)-3-PPP), a significantly higher efficacy in relation to a maximal dopamine stimulation for the D<sub>21</sub>-Cys<sup>351</sup>Ile Gα<sub>o1</sub> construct was observed. However, the ligands *p*-tyramine and S (-) 3-(3-hydroxyphenyl)-N-propylpiperidine (S-(-)-3-PPP) displayed agonism only at the D<sub>21</sub>-Cys<sup>351</sup>Ile Gα<sub>o1</sub> fusion protein. Whilst *p*-tyramine displayed greater agonist efficacy than S-(-)-3-PPP at the D<sub>21</sub>-Cys<sup>351</sup>Ile Gα<sub>o1</sub> fusion subsequent studies employed S-(-)-3-PPP since its potency as an agonist was 300 fold greater than *p*-tyramine (**Table 3.2**).

**Table 3.2: The potency and efficacy of ligands at D<sub>21</sub> receptor-G protein fusions**

	D <sub>21</sub> Gα <sub>i1</sub>		D <sub>21</sub> Gα <sub>i2</sub>		D <sub>21</sub> Gα <sub>i3</sub>		D <sub>21</sub> Gα <sub>o1</sub>	
	pEC <sub>50</sub> , (±S.E.M.)	E <sub>max</sub> , %DA (±S.E.M.)	pEC <sub>50</sub> (±S.E.M.)	E <sub>max</sub> , %DA (±S.E.M.)	pEC <sub>50</sub> (±S.E.M.)	E <sub>max</sub> , %DA (±S.E.M.)	pEC <sub>50</sub> (±S.E.M.)	E <sub>max</sub> , %DA (±S.E.M.)
<b>Dopamine</b>	<b>5.63</b> (0.05)	<b>100</b>	<b>5.25</b> (0.16)	<b>100</b>	<b>4.92</b> (0.15)	<b>100</b>	<b>6.15</b> (0.15)	<b>100</b>
<i>m</i> - <b>tyramine</b>	<b>4.81</b> (0.14)	<b>50</b> (2)	<b>4.92</b> (0.32)	<b>40</b> (13)	<b>4.97</b> (0.30)	<b>34</b> (2)	<b>5.38</b> (0.03)	<b>74</b> (3)
<i>p</i> - <b>tyramine</b>	na		na		na		<b>3.85</b> (0.20)	<b>53</b> (4)
<b>R-(+)-3-PPP</b>	<b>4.77</b> (0.06)	<b>61</b> (2)	<b>4.67</b> (0.30)	<b>33</b> (2)	<b>4.59</b> (0.23)	<b>41</b> (10)	<b>5.21</b> (0.02)	<b>82</b> (1)
<b>S-(-)-3-PPP</b>	na		na		na		<b>6.25</b> (0.09)	<b>21</b> (2)
<b>Quinpirole</b>	<b>5.53</b> (0.06)	<b>99</b> (1)	<b>4.72</b> (0.76)	<b>59</b> (27)	<b>5.62</b> (0.42)	<b>55</b> (15)	<b>6.12</b> (0.03)	<b>100</b> (4)
<b>NPA</b>	<b>7.84</b> (0.45)	<b>143</b> (6)	<b>7.64</b> (0.23)	<b>96</b> (18)	<b>7.48</b> (0.31)	<b>101</b> (17)	<b>7.86</b> (0.58)	<b>109</b> (5)
<b>7-OH DPAT</b>	<b>8.12</b> (0.13)	<b>34</b> (1)	na		<b>7.83</b> (0.30)	<b>21</b> (2)	<b>7.99</b> (0.21)	<b>51</b> (1)

Experiments were performed in triplicate to n = 3.

na = no significant dose dependent response observed

'% DA' refers to E<sub>max</sub> value of [<sup>35</sup>S] binding as compared to maximal dopamine

stimulation. The values of potency or efficacy for each ligand at the four different D<sub>21</sub>-

fusion proteins were compared using one way ANOVA with a Tukey's post test using

GraphPad Prism version 4. A significant difference was observed in pEC<sub>50</sub> between D<sub>3/2</sub>

receptor fusion proteins for dopamine; D<sub>2</sub>Gα<sub>o1</sub> > D<sub>2</sub>Gα<sub>i1</sub> > D<sub>2</sub>Gα<sub>i2</sub> = D<sub>3/2</sub>Gα<sub>i3</sub> (P<0.01)

### 3.2.3 S(-)-3-PPP only shows a high affinity binding site in competition with [<sup>3</sup>H] spiperone at D<sub>21</sub>-Cys<sup>351</sup>Ile Gα<sub>01</sub> fusion protein

To further characterise this apparent example of ligand directed trafficking, where S(-)-3-PPP favours coupling only to Gα<sub>01</sub>, it was important to investigate the relative affinity of S(-)-3-PPP for each of the four fusion proteins (**Figure 3.5**), using competition binding versus [<sup>3</sup>H] spiperone. The ability of dopamine to compete with [<sup>3</sup>H] spiperone to bind to the various D<sub>21</sub>-G-protein fusions was best fit by a two-site model in which between 30 and 50 % of the sites displayed higher affinity (pK<sub>h</sub> = 7.1-7.7) and the remainder lower affinity (pK<sub>l</sub> = 5.6-5.8) for dopamine. The presence of 100 μM GTP in such assays resulted in this competition becoming monophasic (pK<sub>iGTP</sub> = 5.5-5.9) in each case. For pK<sub>h</sub>, pK<sub>l</sub> and pK<sub>iGTP</sub> binding sites there was no significant difference in affinity between the four fusion constructs (**Table 3.3**). In contrast, the ability of S(-)-3-PPP to compete with [<sup>3</sup>H] spiperone was monophasic in the absence of GTP and essentially unaffected by the presence of GTP (pK = 6.2-6.5) for the D<sub>21</sub>-Gα<sub>i1</sub>, D<sub>21</sub>-Gα<sub>i2</sub>, D<sub>21</sub>-Gα<sub>i3</sub> Cys→Ile variant fusion proteins (**Figure 3.5**). However, a bi-phasic competition curve was observed for S(-)-3-PPP binding at the D<sub>21</sub>-Cys<sup>351</sup>Ile Gα<sub>01</sub> fusion protein (pK<sub>h</sub> = 8.4, pK<sub>l</sub> = 6.2). This was converted to a monophasic curve (pK = 6.3) in the presence of GTP (**Table 3.3**). These results are in agreement with observations from [<sup>35</sup>S]GTPγS binding studies showing that S(-)-3-PPP is a partial agonist at D<sub>21</sub>-Gα<sub>01</sub>. At D<sub>21</sub>-Gα<sub>i1</sub>, D<sub>21</sub>-Gα<sub>i2</sub>, D<sub>21</sub>-Gα<sub>i3</sub> fusion proteins S(-)-3-PPP still has a similar affinity for the receptor but does not show the high affinity state indicative of agonist action through these G protein alpha subunits. This suggests that at D<sub>21</sub>-Gα<sub>i1</sub>, D<sub>21</sub>-Gα<sub>i2</sub>, and D<sub>21</sub>-Gα<sub>i3</sub> S(-)-3-PPP is an antagonist or inverse agonist.

**Table 3.3: The binding characteristics of dopamine and S(-)-3-PPP with D<sub>21</sub> receptor-G protein fusions**

Receptor: G-protein fusion	D <sub>21</sub> -Gα <sub>i1</sub>		D <sub>21</sub> -Gα <sub>i2</sub>		D <sub>21</sub> -Gα <sub>i3</sub>		D <sub>21</sub> -Gα <sub>o1</sub>	
	Dopamine	S(-)-3- PPP	Dopamine	S(-)-3- PPP	Dopamine	S(-)-3- PPP	Dopamine	S(-)-3- PPP
pK <sub>h</sub> (±SEM)	7.12 (0.11)		7.20 (0.12)		7.52 (0.13)		7.67 (0.35)	8.44 (0.15)
pK <sub>I</sub> (±SEM)	5.75 (0.08)	6.27 (0.06)	5.63 (0.17)	6.47 (0.11)	5.58 (0.12)	6.26 (0.07)	5.82 (0.18)	6.24 (0.07)
%R <sub>h</sub>	44 (7)		55 (4)		36 (4)		29 (4)	29 (2)
pK <sub>iGTP</sub> (±SEM)	5.53 (0.01)	6.23 (0.02)	5.81 (0.01)	6.52 (0.11)	5.50 (0.11)	6.27 (0.11)	5.86 (0.07)	6.3 (0.01)

Experiments were performed in triplicate to n = 3.

One way ANOVA with Tukey's post-hoc test was performed using GraphPad Prism version 4. No significant differences in values of pK<sub>h</sub>, pK<sub>I</sub> or pK<sub>iGTP</sub> were observed for dopamine. For S(-)-3-PPP no significant differences in values of pK<sub>I</sub> or pK<sub>iGTP</sub> at each of the four fusion proteins were observed. However a high affinity binding site (pK<sub>h</sub>) for S(-)-3-PPP was observed only at the D<sub>21</sub>-Cys<sup>351</sup>Ile Gα<sub>o1</sub> fusion protein.

### 3.2.4 S(-)-3-PPP acts as an antagonist or inverse agonist at D<sub>21</sub>-Cys<sup>351</sup>Ile Gα<sub>i1</sub>, Gα<sub>i2</sub>, Gα<sub>i3</sub>, but as a partial agonist at D<sub>21</sub>-Cys<sup>351</sup>Ile Gα<sub>o1</sub>.

To further explore a possible 'protean' characteristic of S(-)-3-PPP at the D<sub>21</sub> receptor I compared effects at D<sub>21</sub>-Cys<sup>351</sup>Ile Gα<sub>o1</sub> and D<sub>21</sub>-Cys<sup>351</sup>Ile Gα<sub>i2</sub>. Increasing concentrations of

S-(-)-3-PPP inhibited the capacity of an  $EC_{50}$  concentration of dopamine to stimulate binding of [ $^{35}$ S] GTP $\gamma$ S to both fusion constructs with  $pIC_{50} = 4.68 \pm 0.07$  ( $D_{21}$ -Cys $^{351}$ Ile  $G\alpha_{i2}$ ) and  $5.09 \pm 0.12$  ( $D_{21}$ -Cys $^{351}$ Ile  $G\alpha_{o1}$ ) (**Figure 3.6A**). However, the maximal effect of S-(-)-3-PPP at  $D_{21}$ -Cys $^{351}$ Ile  $G\alpha_{o1}$  in this assay confirmed its partial agonist action at  $G\alpha_{o1}$ , because it failed to reduce binding of [ $^{35}$ S]GTP $\gamma$ S to the level observed in the absence of dopamine. By contrast, at  $D_{21}$ -Cys $^{352}$ Ile  $G\alpha_{i2}$  S-(-)-3-PPP completely blocked dopamine stimulation and, indeed, acted as an efficacious inverse agonist (**Figure 3.6B**). Spiperone is frequently described as an inverse agonist at the dopamine receptor and unsurprisingly acted as an effective inverse agonist at  $D_{21}$ -Cys $^{351}$ I  $G\alpha_{i2}$ . Furthermore, spiperone fully reversed the effect of dopamine at  $D_{21}$ -Cys $^{351}$ Ile  $G\alpha_{o1}$  (**Figure 3.6A**). Similar studies also demonstrated that both spiperone and S-(-)-3-PPP also acted as antagonists/inverse agonists at both  $D_{21}$ -Cys $^{351}$ Ile  $G\alpha_{i1}$  and  $D_{21}$ -Cys $^{351}$ Ile  $G\alpha_{i3}$  (**Figures 3.6C, 3.6D**).

### 3.2.5 Generation and characterisation of stable cell lines expressing $G\alpha_{i1}$ , $G\alpha_{i2}$ , $G\alpha_{i3}$ , and $G\alpha_{o1}$ in an inducible manner

As described above the fusion proteins are extremely useful tools to study receptor G-protein interactions since they define the receptor to G protein ratio as 1:1 for each G-protein. However, they are an inherently artificial system, and it was therefore important to investigate if S-(-)-3-PPP would behave as a protean agonist at the  $D_{21}$  receptor when coupling to different  $G\alpha_i$  subunits in a system expressing separated receptor and G protein. To achieve this, a series of HEK293 cell lines were generated based on the Flp-In T-REx system (**Figure 3.7**). This system allows the expression of a gene of interest from a single, defined chromosomal locus by addition of tetracycline. The Flp-In T-REx host cell line containing a single Flp recombinase target 'FRT' homologous recombination site and stably expressing the Tet Repressor gene, was co-transfected with the cDNAs of Pertussis

toxin resistant Cys to Ile mutants of  $G\alpha_{i1}$ ,  $G\alpha_{i2}$ ,  $G\alpha_{i3}$ ,  $G\alpha_{o1}$  in the vector pcDNA5/FRT/TO along with the Flp recombinase cDNA contained within the vector pOG44. This recombinase catalyses a homologous recombination event between the FRT site in the host genome and that of the pcDNA5/FRT/TO vector. Cells which have the Cys→Ile variant  $G\alpha_{i/o}$  cDNA of interest stably integrated into the FRT site were selected by antibiotic selection using hygromycin. Since all clones should, theoretically, be equivalent, clones were pooled and the polyclonal mix tested for ability to inducibly express the Cys→Ile  $G\alpha_{i/o}$  subunit of interest. Western blotting using antisera raised against the C-terminal tail of each  $G\alpha$  subunit showed inducible expression of  $G\alpha_{i1}$ ,  $G\alpha_{i2}$ ,  $G\alpha_{i3}$ ,  $G\alpha_{o1}$  only upon treatment with 1  $\mu\text{g/ml}$  of tetracycline 24 hours prior to cell harvest (**Figure 3.8**).

### **3.2.5.1 Generation and characterisation of cell lines stably and constitutively expressing dopamine $D_{21}$ receptor and expressing $G\alpha_{i1}$ , $G\alpha_{i2}$ , $G\alpha_{i3}$ , or $G\alpha_{o1}$ Cys→Ile mutants from the inducible Flp-In locus**

Using these cell lines, further cell lines were generated that stably and constitutively express dopamine  $D_{21}$  receptor, with the inducible expression of  $G\alpha_{i1}$ ,  $G\alpha_{i2}$ ,  $G\alpha_{i3}$ , or  $G\alpha_{o1}$  Cys→Ile mutants as described in the section 2.7.7. Consequently by treatment with pertussis toxin to cause ADP-ribosylation of endogenously expressed forms of ' $G\alpha_i$ ' I anticipated this would produce a system in which  $D_{21}$  mediated stimulation of [ $^{35}\text{S}$ ] GTP $\gamma$ S binding must reflect only activation of a single, defined G protein. Flp-In T-REx cells which inducibly express the  $G\alpha_{i1}$ ,  $i_2$ ,  $i_3$ , or  $o_1$  Cys → Ile pertussis toxin insensitive mutants were transfected with dopamine  $D_{21}$  receptor cDNA and stable cell lines generated. Clones generated were screened for receptor expression by radioligand binding using a single near saturating concentration of [ $^3\text{H}$ ] spiperone. Non-specific binding was estimated using 10  $\mu\text{M}$  (+)-butaclamol (**Figure 3.9**). Clones showing significant expression of receptor were frozen down in liquid nitrogen until required for further characterisation. One clone for

each of the four different  $G\alpha_i$  stable cell lines was selected as follows:  $D_{21} + G\alpha_{i1}$ ; clone 5,  $D_{21} + G\alpha_{i2}$ ; clone 15,  $D_{21} + G\alpha_{i3}$ ; clone 3,  $D_{21} + G\alpha_{o1}$ ; clone 4, and further characterised.

Initial studies confirmed expression of the G protein of interest in all cases in a ‘tetracycline-on’ fashion. At a 24 hours time point, maximal expression of each G protein was achieved by treatment with between 0.5 -1.0  $\mu\text{g}\cdot\text{ml}^{-1}$  tetracycline (**Figure 3.10**).

Levels of the  $D_{21}$  receptor constitutively expressed by each of the cell lines was not affected by tetracycline induced turn on of the G-proteins (**Table 3.4**).

**Table 3.4: Expression levels of the  $D_{21}$  receptor are unaffected by expression of various G proteins**

Experiments were performed in triplicate to  $n = 3$ .

An unpaired Student’s t-test ( $p > 0.05$ ) was performed using GraphPad Prism version 4. No significant differences in  $B_{\text{max}}$  values were observed in receptor expression with and without induction of G-protein expression for all cell lines.

$1\mu\text{g}\cdot\text{ml}^{-1}$ Tet.	-		+	
	<b>[<math>^3\text{H}</math>] Spiperone Binding</b>			
<b>Cell Line</b>	<b><math>B_{\text{max}}</math>, fMol.<math>\text{mg}^{-1}</math></b> ( $\pm$ S.E.M.)	<b><math>K_d</math>, nM</b> ( $\pm$ S.E.M.)	<b><math>B_{\text{max}}</math>, fMol.<math>\text{mg}^{-1}</math></b> ( $\pm$ S.E.M.)	<b><math>K_d</math>, nM</b> ( $\pm$ S.E.M.)
<b><math>D_2 + G\alpha_{i1}</math></b>	<b>988 (108)</b>	<b>0.02 (0.01)</b>	<b>1156 (261)</b>	<b>0.03 (0.01)</b>
<b><math>D_2 + G\alpha_{i2}</math></b>	<b>1448 (191)</b>	<b>0.02 (0.01)</b>	<b>1861 (225)</b>	<b>0.04 (0.01)</b>
<b><math>D_2 + G\alpha_{i3}</math></b>	<b>538 (52)</b>	<b>0.03 (0.01)</b>	<b>510 (120)</b>	<b>0.02 (0.02)</b>
<b><math>D_2 + G\alpha_{o1}</math></b>	<b>3790 (396)</b>	<b>0.06 (0.02)</b>	<b>3864 (249)</b>	<b>0.07 (0.02)</b>

### 3.2.6 S(-)-3-PPP stimulates the binding of [<sup>35</sup>S] GTPγS upon induction of Cys<sup>351</sup>Ile Gα<sub>o1</sub> expression but not Cys<sup>352</sup>Ile Gα<sub>i2</sub> expression

As could be expected, there was no capacity of dopamine to stimulate binding of [<sup>35</sup>S] GTPγS in membranes of pertussis toxin treated cells, where expression of Cys→Ile G protein α subunit was not induced by tetracycline treatment (**Figures 3.11A, 3.12A**). In equivalent membranes of cells where expression of Cys<sup>352</sup>Ile Gα<sub>i2</sub> was induced by tetracycline, dopamine produced a robust stimulation of [<sup>35</sup>S] GTPγS binding. This stimulation of [<sup>35</sup>S] GTPγS binding by dopamine was both substantial and concentration-dependent. The potency of dopamine (pEC<sub>50</sub> = 6.05 ± 0.11) was significantly higher than that seen at the D<sub>21</sub>-Cys<sup>352</sup>Ile Gα<sub>i2</sub> fusion protein (pEC<sub>50</sub> = 5.25 ± 0.16, un-paired Student's t-test, P<0.05) (**Table 3.2, Figure 3.4**). However, in the same membranes S(-)-3-PPP was unable to enhance [<sup>35</sup>S] GTPγS binding at all (**Figure 3.11B**). In membranes expressing the D<sub>21</sub> receptor and induced to express Cys<sup>351</sup>Ile Gα<sub>o1</sub> dopamine also stimulated [<sup>35</sup>S] GTPγS binding in a concentration-dependent manner. Again the potency of dopamine was significantly higher (pEC<sub>50</sub> = 7.56 ± 0.17) than recorded for the D<sub>21</sub>-Cys<sup>352</sup>Ile Gα<sub>i2</sub> fusion protein (pEC<sub>50</sub> = 6.15 ± 0.15, un-paired Student's t-test, P<0.01) (**Table 3.2, Figure 3.4**). S(-)-3-PPP also stimulated the binding of [<sup>35</sup>S] GTPγS in a concentration-dependent manner and behaved as a partial agonist (**Figure 3.12B**). The E<sub>max</sub> relative to maximal dopamine stimulation was 20%, similar to the value recorded in receptor-G protein fusion experiments (**Table 3.2, Figure 3.4**). The potency of S(-)-3-PPP (pEC<sub>50</sub> = 6.65 ± 0.10) was significantly higher than seen at the D<sub>21</sub>-Cys<sup>351</sup>Ile Gα<sub>o1</sub> fusion protein (pEC<sub>50</sub> = 6.25 ± 0.09, un-paired Student's t-test, P<0.05) (**Table 3.2, Figure 3.4**).

### 3.2.7 S-(-)-3-PPP shows a high affinity binding site in competition with [<sup>3</sup>H] spiperone binding but only in the presence of Cys<sup>351</sup>Ile Gα<sub>o1</sub> expression and not Cys<sup>352</sup>Ile Gα<sub>i2</sub> expression

In cells expressing the D<sub>21</sub> receptor and without induction of Cys<sup>352</sup>Ile Gα<sub>i2</sub> expression the competition of dopamine with [<sup>3</sup>H] spiperone gave a monophasic curve of low affinity (pK<sub>i</sub> ~5.4) that was unaffected by addition of 100 μM GTP (pK<sub>iGTP</sub> ~5) (**Figure 3.13A, Table 3.5**). However, with tetracycline induction of Cys<sup>352</sup>Ile Gα<sub>i2</sub> expression the competition of dopamine with [<sup>3</sup>H] spiperone produced a biphasic curve, with the appearance of a high affinity site (pK<sub>h</sub> ~7.6) which was eliminated by the presence of GTP. In contrast, both with and without tetracycline induction of Cys<sup>352</sup>Ile Gα<sub>i2</sub> expression the capacity of S-(-)-3-PPP to compete with [<sup>3</sup>H] spiperone was both monophasic and unaffected by the presence of GTP (pK ~ 5.8) (**Figure 3.13B, Table 3.5**). In equivalent membranes of pertussis toxin treated cells expressing D<sub>21</sub> and allowing the inducible expression of Gα<sub>o1</sub>, dopamine versus [<sup>3</sup>H] spiperone competition binding identified both high (pK<sub>h</sub> ~ 7.3, **Table 3.5**) and low (pK<sub>i</sub> ~ 4.6) affinity sites only following induction of Gα<sub>o1</sub> Cys<sup>351</sup>Ile expression (**Figure 3.14A**). In the presence of GTP the high affinity site was lost. In contrast to membranes expressing D<sub>21</sub> and Cys<sup>352</sup>Ile Gα<sub>i2</sub>, for membranes expressing D<sub>21</sub> and induced to express Cys<sup>351</sup>Ile Gα<sub>o1</sub>, S-(-)-3-PPP identified both high (pK<sub>h</sub> ~8.3) and low affinity (pK<sub>i</sub> ~ 6.4) states (**Figure 3.14B**). Again the high affinity site was lost in the presence of GTP. In view of the higher potency of dopamine at the D<sub>21</sub> receptor when expressed in membranes of the relevant Flp-In T-REx cell line with either Cys<sup>352</sup>Ile Gα<sub>i2</sub> or Gα<sub>o1</sub> Cys<sup>351</sup>Ile expression induced compared to that seen for the D<sub>21</sub>-Cys<sup>352</sup>Ile Gα<sub>i2</sub> or D<sub>21</sub>-Gα<sub>o1</sub> Cys<sup>351</sup>Ile fusion proteins, it is interesting to note that the affinities for dopamine are not generally significantly different at these two systems, and where significant difference

exists, the affinity is higher at the D<sub>21</sub>-fusion protein (Tables 3.3 + 3.5, un-paired Student's t-test, P<0.05).

**Table 3.5: The binding characteristics of dopamine and S-(-)-3-PPP at the D<sub>21</sub> receptor with and without the induction of Cys<sup>352</sup>Ile Gα<sub>12</sub> or Cys<sup>351</sup>Ile Gα<sub>01</sub>**

	<b>Gα<sub>12</sub></b>			
<b>Tet.</b>	-		+	
	<b>Dopamine</b>	<b>S-(-)-3-PPP</b>	<b>Dopamine</b>	<b>S-(-)-3-PPP</b>
<b>pK<sub>h</sub></b> (±SEM)			<b>7.56</b> (0.09)	
<b>pK<sub>i</sub></b> (±SEM)	<b>5.48</b> (0.18)	<b>5.90</b> (0.27)	<b>5.22</b> (0.13)	<b>5.75</b> (0.15)
<b>%R<sub>h</sub></b> (±SEM)			<b>30</b> (5)	
<b>pK<sub>iGTP</sub></b> (±SEM)	<b>4.94</b> (0.23)	<b>5.47</b> (0.12)	<b>5.14</b> (0.21)	<b>5.74</b> (0.05)
	<b>Gα<sub>01</sub></b>			
<b>Tet.</b>	-		+	
	<b>Dopamine</b>	<b>S-(-)-3-PPP</b>	<b>Dopamine</b>	<b>S-(-)-3-PPP</b>
<b>pK<sub>h</sub></b> (±SEM)			<b>7.32</b> (0.21)	<b>8.29</b> (0.3)
<b>pK<sub>i</sub></b> (±SEM)	<b>5.20</b> (0.16)	<b>6.27</b> (0.26)	<b>4.55</b> (0.13)	<b>6.40</b> (0.23)
<b>%R<sub>h</sub></b> (±SEM)			<b>50</b> (10)	<b>35</b> (3)
<b>pK<sub>iGTP</sub></b> (±SEM)	<b>4.94</b> (0.11)	<b>6.06</b> (0.13)	<b>5.04</b> (0.18)	<b>6.17</b> (0.13)

Experiments were performed in triplicate to n = 3

### 3.2.8 S-(-)-3-PPP acts as a partial agonist at the D<sub>21</sub> receptor upon induction of expression of Cys<sup>351</sup>Ile Gα<sub>01</sub> but as an antagonist upon induction of Cys<sup>352</sup>Ile Gα<sub>i2</sub> expression

The action of S-(-)-3-PPP and spiperone in cells expressing the D<sub>21</sub> receptor and expressing Cys<sup>352</sup>Ile Gα<sub>i2</sub> or Cys<sup>351</sup>Ile Gα<sub>01</sub> upon treatment with tetracycline was explored.

Stimulation of [<sup>35</sup>S] GTPγS binding by an EC<sub>50</sub> concentration of dopamine was completely reversed by both spiperone and S-(-)-3-PPP in membranes where expression of Cys<sup>352</sup>Ile Gα<sub>i2</sub> had been induced (**Figure 3.15A**). However, in membranes where Cys<sup>351</sup>Ile Gα<sub>01</sub> expression was induced, although spiperone again completely reversed dopamine stimulation of [<sup>35</sup>S] GTPγS binding, S-(-)-3-PPP produced only partial inhibition, consistent with its action as a partial agonist when D<sub>21</sub> is coupled to Gα<sub>01</sub> (**Figure 3.15B**).

### Figure 3.1: The multiple signalling states of GPCRs

#### A+B) Two views of GPCRs

A) The receptor has recognition capability for ligands but once ligand is bound the receptor becomes a uniform activation unit (single active state) that goes on to mediate the same GPCR activities in the cell for each of the four ligands indicated in the diagram by the arrows.

B) The receptor has bipolar recognition capability in that the binding of different ligands can lead to different receptor conformations leading to a texture with respect to the recognition properties of the receptor for cellular machinery. This signalling capability is more versatile and complex. For example, in this diagram, four different ligands binding to the receptor will each affect the ability of the receptor to couple to any of three different G-proteins (marked  $G_1$ ,  $G_2$ , and  $G_3$ ).

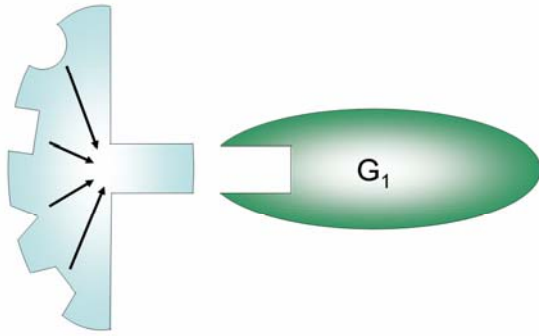
#### C) Extended Ternary Complex model showing a pleiotropic receptor interacting with two G-proteins; $G_1$ and $G_2$ .

In this model both unliganded forms of the receptor; active state ( $R_a$ ) and inactive state ( $R_i$ ) are shown.  $A$  represents the Ligand,  $G$  is the G protein,  $K_a$  is the affinity of the ligand for the inactive receptor state,  $\alpha K_a$  is the affinity of the ligand for the active receptor state,  $K_g$  is the affinity of the activated receptor for the G protein when the ligand is not bound,  $\gamma K_g$  is the affinity of the receptor for the G protein when ligand is bound and  $L$  is the allosteric constant for the receptor defined as  $[R_a]/[R_i]$ . Such a system will be controlled by the relative concentrations of the two G-protein types, the ability of the agonist to induce the receptor coupling to each G-protein ( $\gamma_1$  and  $\gamma_2$ ), the capability of the agonist to induce the receptor active state ( $\alpha$ ) and the natural constitutive activity of the receptor ( $L$ ).

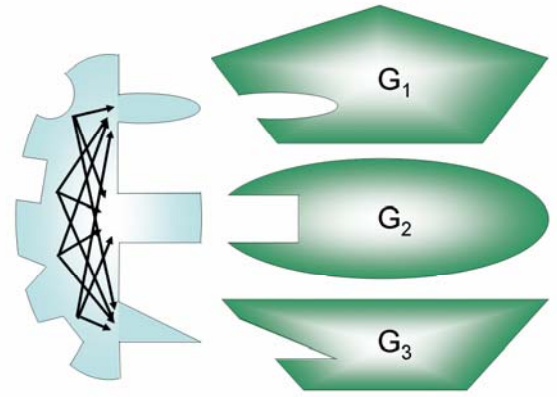
Consequently, differences in  $\gamma$  can lead to different agonist selective receptor states. Both diagrams adapted from (Kenakin, 2003)

Figure 3.1

A) Receptor as an on-off switch



B) Receptor as bipolar recognition unit



C) Extended Ternary Complex model for interaction of one receptor with two G-proteins

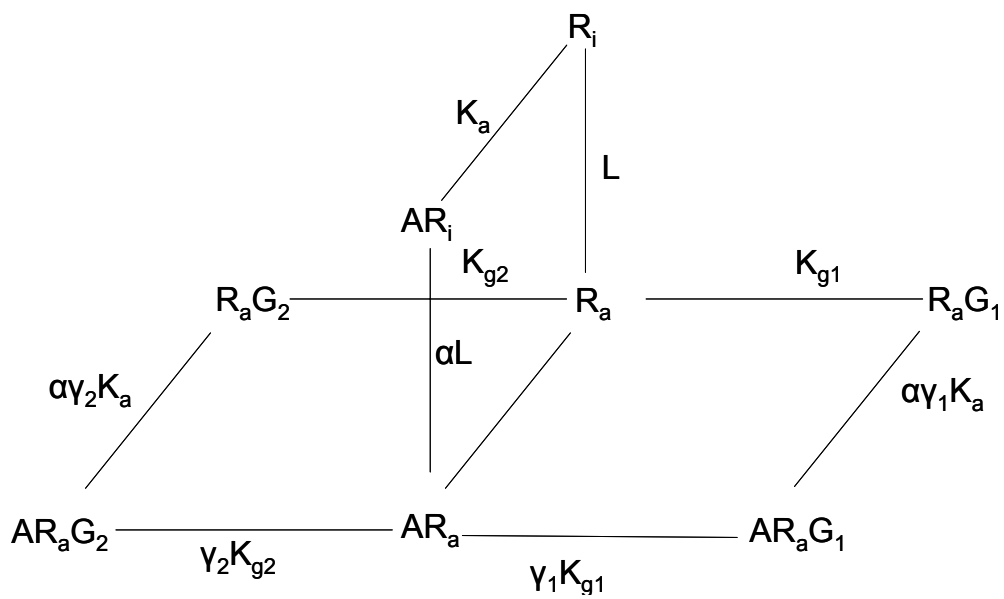


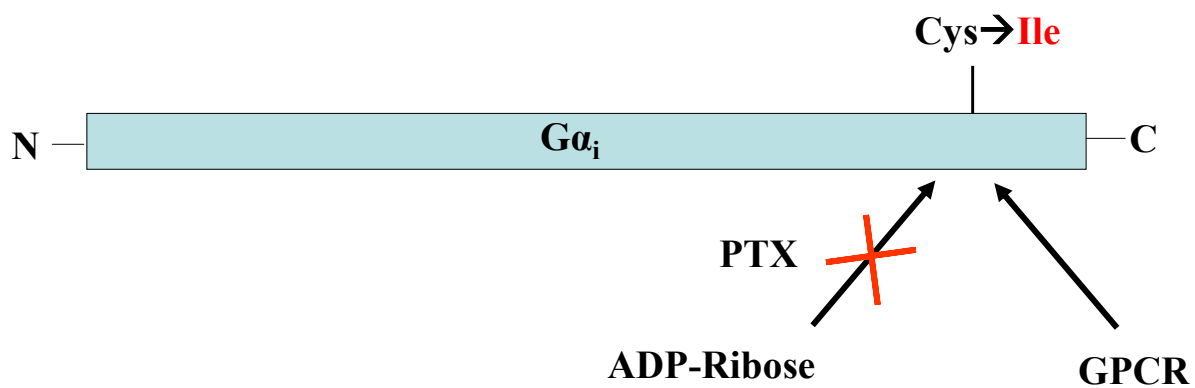
**Figure 3.2: The use of pertussis toxin insensitive variants of  $G_i$  family G-proteins to study specific interactions between a receptor and a  $G_i$  G-protein of interest.**

A) Pertussis toxin (PTX) catalyses the transfer of an ADP-ribose group from  $NAD^+$  to specific amino acid residues on  $G_i$  family G protein  $\alpha$  subunits. This occurs at a conserved cysteine residue four amino acids from the C-terminus and leads to receptor-G protein uncoupling. Mutation of this cysteine residue to isoleucine renders the G protein insensitive to pertussis toxin catalysed modification.

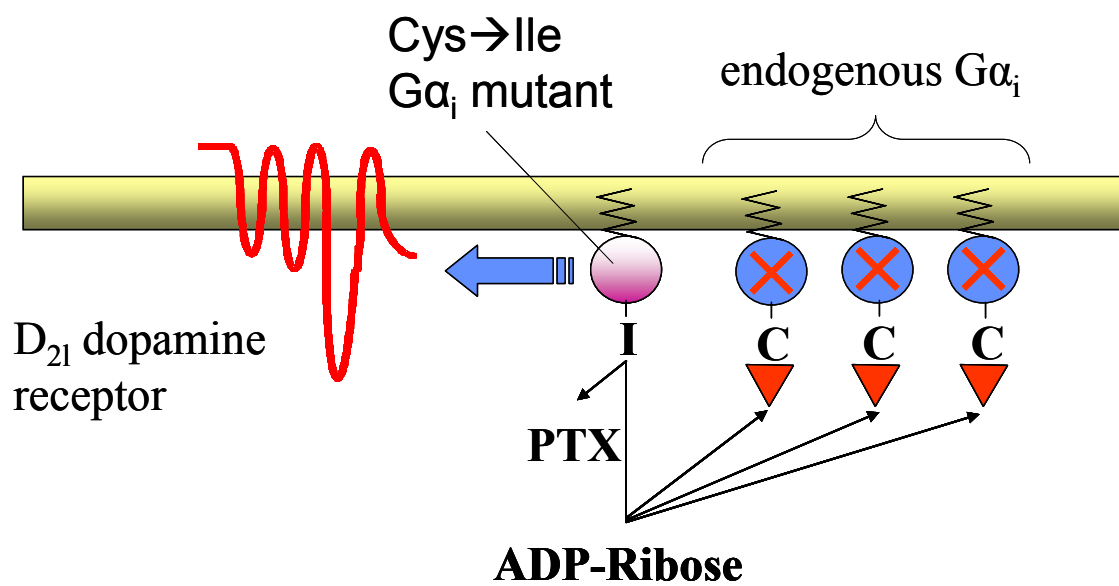
B) PTX-insensitive Cys $\rightarrow$ Ile mutants of the  $G\alpha_i$  family can be introduced into cells along with the receptor of interest (in this case dopamine  $D_{21}$ ). The interaction between the receptor and the Cys $\rightarrow$ Ile  $G\alpha_i$  can be studied in isolation following exposure of cells to PTX to eliminate any potential coupling to endogenous  $G_i$ -family G proteins.

Figure 3.2

A)



B)



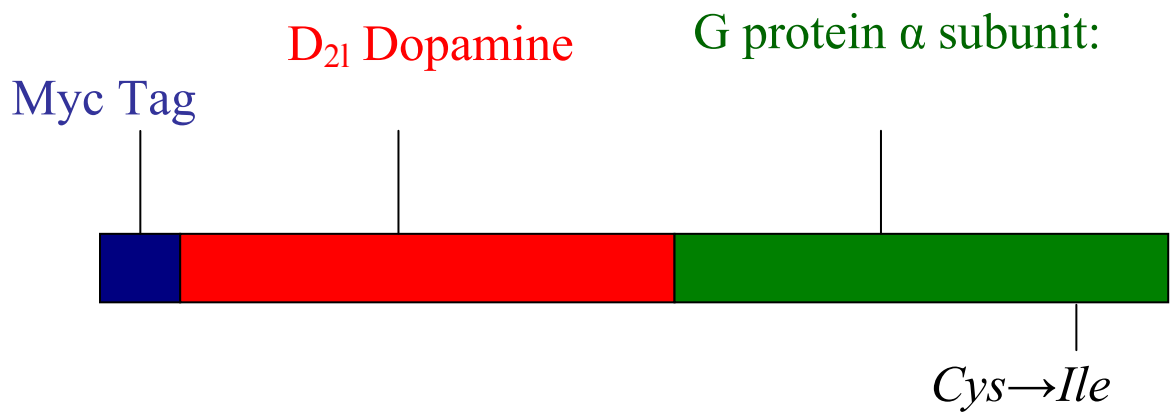
**Figure 3.3: Generation and characterisation of dopamine D<sub>2L</sub> receptor-Cys→Ile variant G protein  $\alpha$  subunit fusion proteins**

**A)** A series of fusion proteins were generated by linking Cys-Ile mutant, pertussis toxin-insensitive variants of G $\alpha_{i1}$ , G $\alpha_{i2}$ , G $\alpha_{i3}$  and G $\alpha_{o1}$  in frame with the C-terminal tail of the human D<sub>2L</sub> receptor.

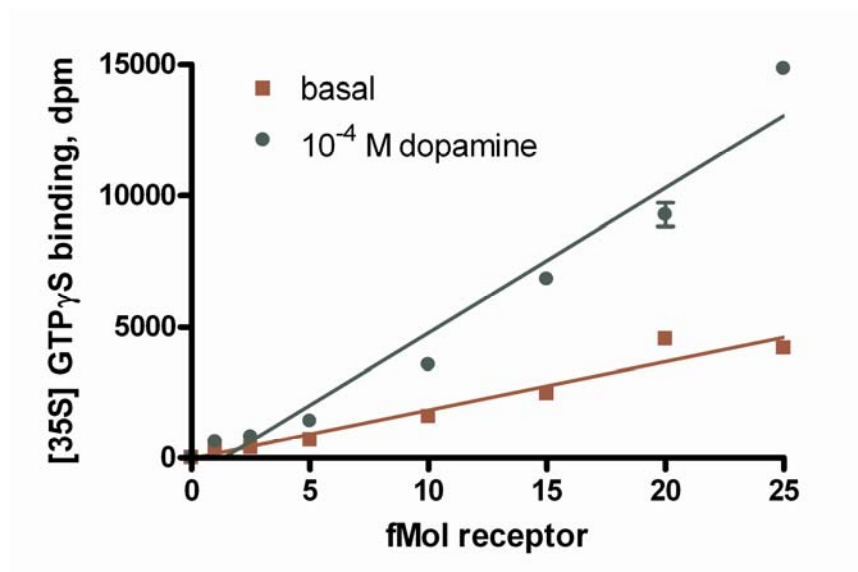
**B)** D<sub>2L</sub>-Cys<sup>351</sup>Ile-G $\alpha_{o1}$  was expressed transiently in HEK293 cells. Following pertussis toxin treatment (25ng/ml, 24 h) cells were harvested, membranes generated and fusion protein expression estimated using [<sup>3</sup>H] spiperone saturation binding (**Table 3**) [<sup>35</sup>S]GTP $\gamma$ S binding studies were performed in the absence and presence of 100 $\mu$ M dopamine and with varying amounts of receptor-G protein fusion protein (1-25 fMol per reaction).

Figure 3.3

A)



B)



**Figure 3.4: Characterisation of the actions of various D<sub>2</sub> agonists at D<sub>21</sub> receptor-G protein fusion proteins**

Each of the dopamine D<sub>21</sub> receptor-Cys→Ile variant Gα fusion proteins; (A) D<sub>21</sub>-Gα<sub>i1</sub>, (B) D<sub>21</sub>-Gα<sub>i2</sub>, (C) D<sub>21</sub>-Gα<sub>i3</sub>, (D) D<sub>21</sub>-Gα<sub>o1</sub> was expressed transiently in HEK293 cells.

Following pertussis toxin treatment (25ng/ml, 24 h) cells were harvested, membranes generated and [<sup>35</sup>S]GTPγS binding studies performed in the absence and presence of varying concentrations of a variety of ligands (dopamine (◆), m-tyramine (■), p-tyramine (□), R-(+)-3-PPP (▲), S-(-)-3PPP (△), quinpirole (▽), NPA (●), 7-OH DPAT(◇)) reported to have affinity and efficacy at dopamine D<sub>2</sub> receptors. Data are representative and full details are provided in **Table 3.2**.

Figure 3.4

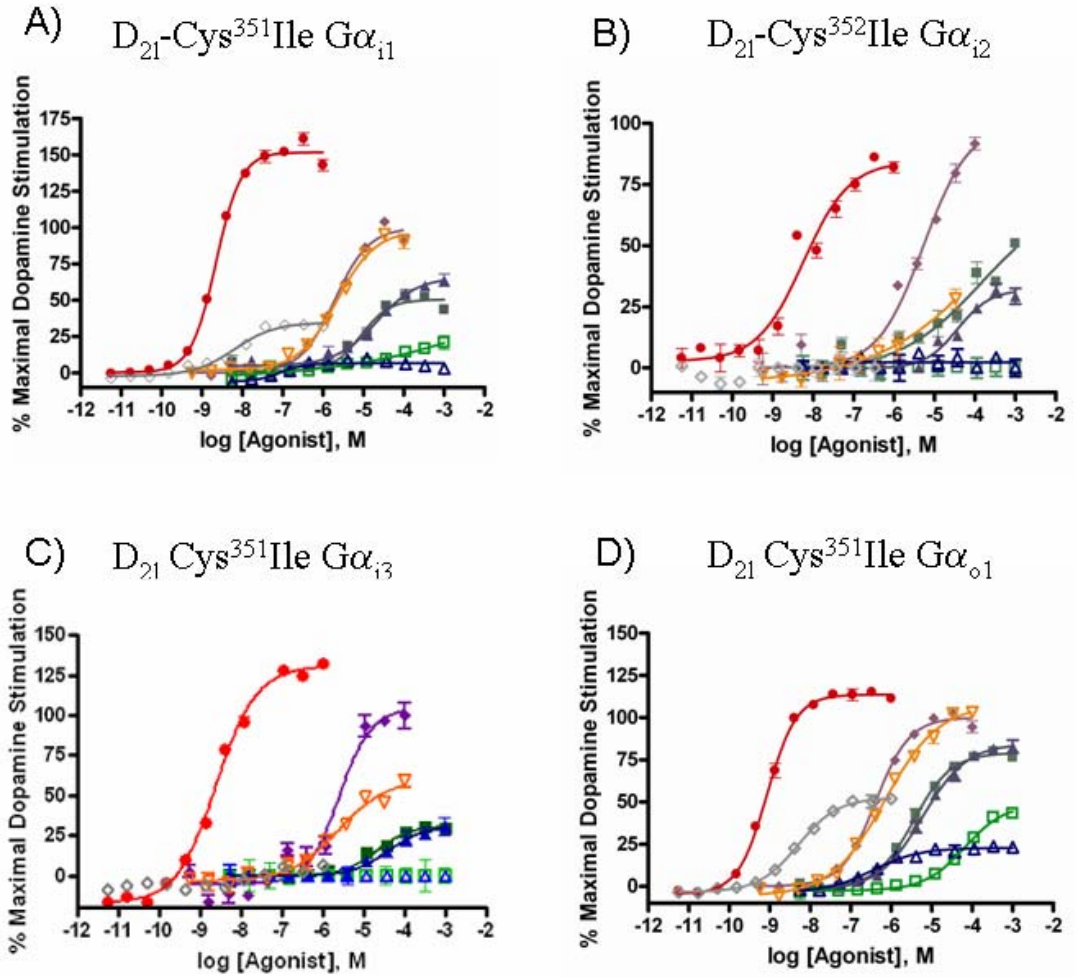


**Figure 3.5: In ligand binding studies S-(-)-3PPP displays both low and high affinity states only at the D<sub>21</sub>-Gα<sub>01</sub> fusion protein**

Membranes of pertussis toxin-treated HEK293 cells expressing (A) D<sub>21</sub>-Gα<sub>i1</sub>, (B) D<sub>21</sub>-Gα<sub>i2</sub>, (C) D<sub>21</sub>-Gα<sub>i3</sub>, (D) D<sub>21</sub>-Gα<sub>o1</sub> were used in competition binding studies employing 0.1 nM [<sup>3</sup>H] spiperone and varying concentrations of either (i) dopamine or (ii) S-(-)-3PPP. The assays were performed in the absence (green squares) or presence (red triangles) of 100 μM GTP. In the absence of GTP, both high and low affinity states for dopamine were observed for each fusion protein whereas this was only true for S-(-)-3PPP at the D<sub>21</sub>-Gα<sub>o1</sub> fusion protein. The presence of GTP converted each competition curve to a single monophasic state displaying low affinity for either dopamine or S-(-)-3PPP. Data are representative and full details are provided in **Table 3.3**. The curves are the best fit curves to one, or two site models (p<0.05) (F-test) using GraphPad Prism version 4.

Figure 3.5

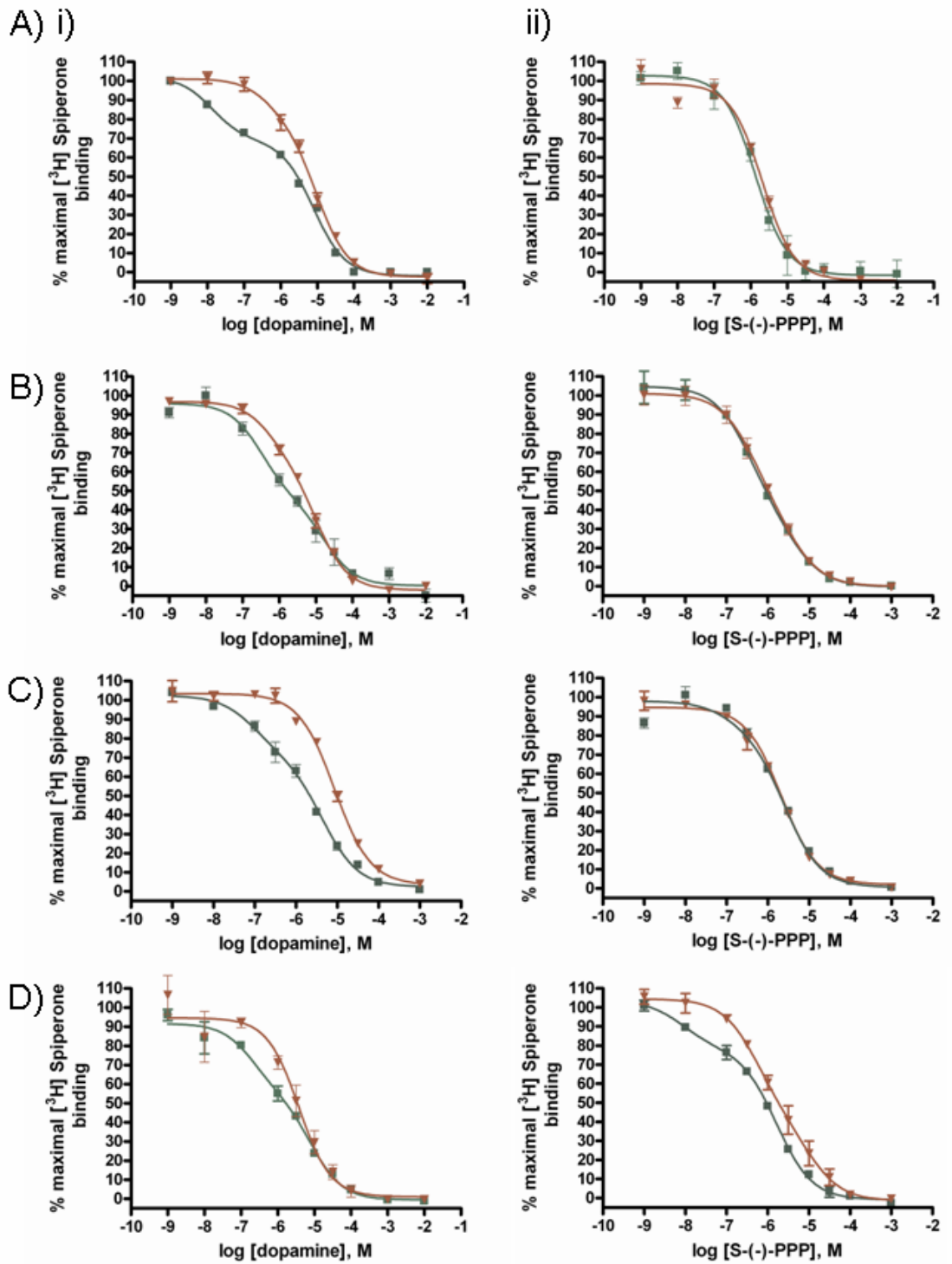
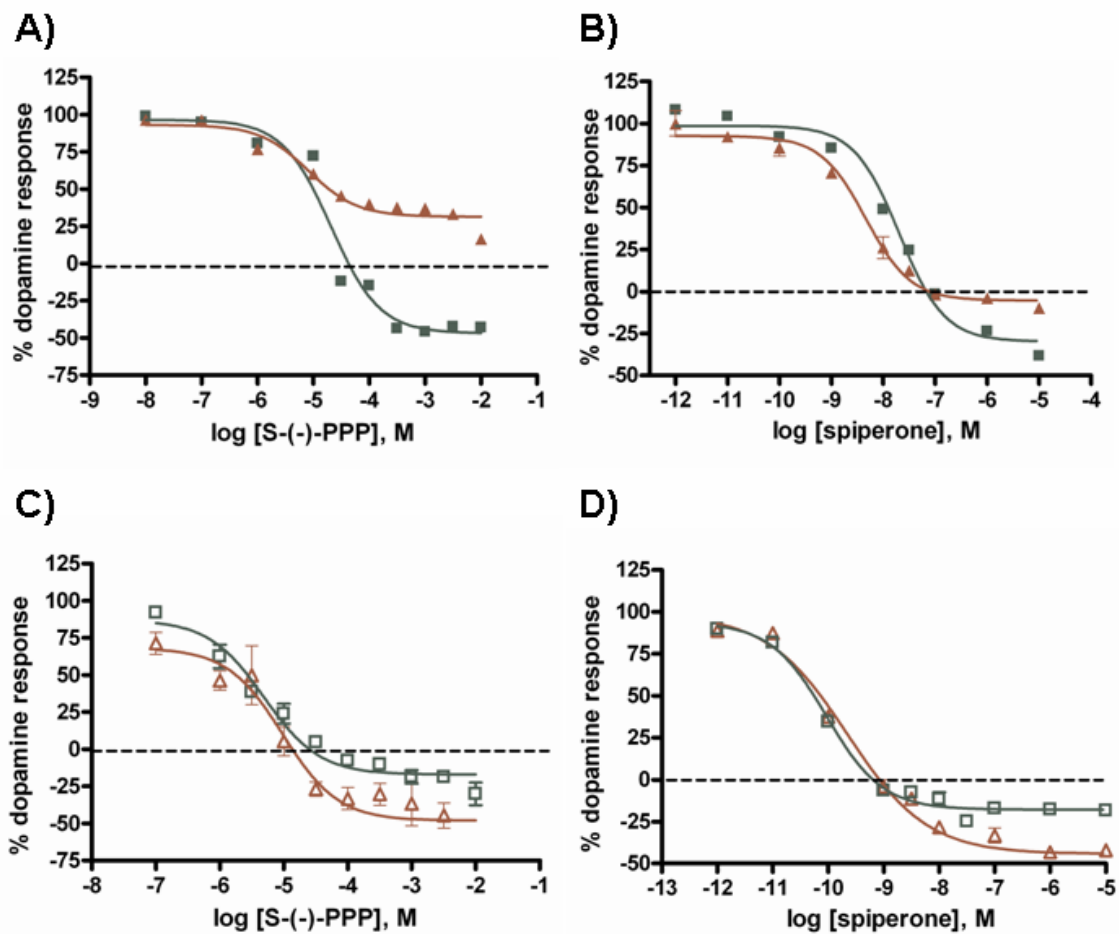


**Figure 3.6: S(-)-3PPP is an agonist at D<sub>21</sub>-Gα<sub>01</sub> but an antagonist/inverse agonist for the other D<sub>21</sub>-G protein fusion proteins**

**A, B.** Membranes from pertussis toxin-treated HEK293 cells expressing either D<sub>21</sub>-Gα<sub>01</sub> (**red triangles**) or D<sub>21</sub>-Gα<sub>i2</sub> (**green squares**) were used in [<sup>35</sup>S]GTPγS binding studies. Dopamine at an EC<sub>50</sub> concentration for each fusion (0.3μM D<sub>21</sub>-Gα<sub>01</sub>, 3μM D<sub>21</sub>-Gα<sub>i2</sub>) along with varying concentrations of either S(-)-3PPP (**A**) or spiperone (**B**) were employed. On the y-axis 100 is the stimulation produced by dopamine in the absence of a second ligand and 0 the basal activity in the absence of ligands.

**C, D.** Equivalent experiments to those of **A** and **B** were performed with membranes expressing D<sub>21</sub>-Gα<sub>i1</sub> (**open red triangles**) or D<sub>21</sub>-Gα<sub>i3</sub> (**open red squares**). **C.** Studies with S(-)-3PPP, **D,** studies with spiperone.

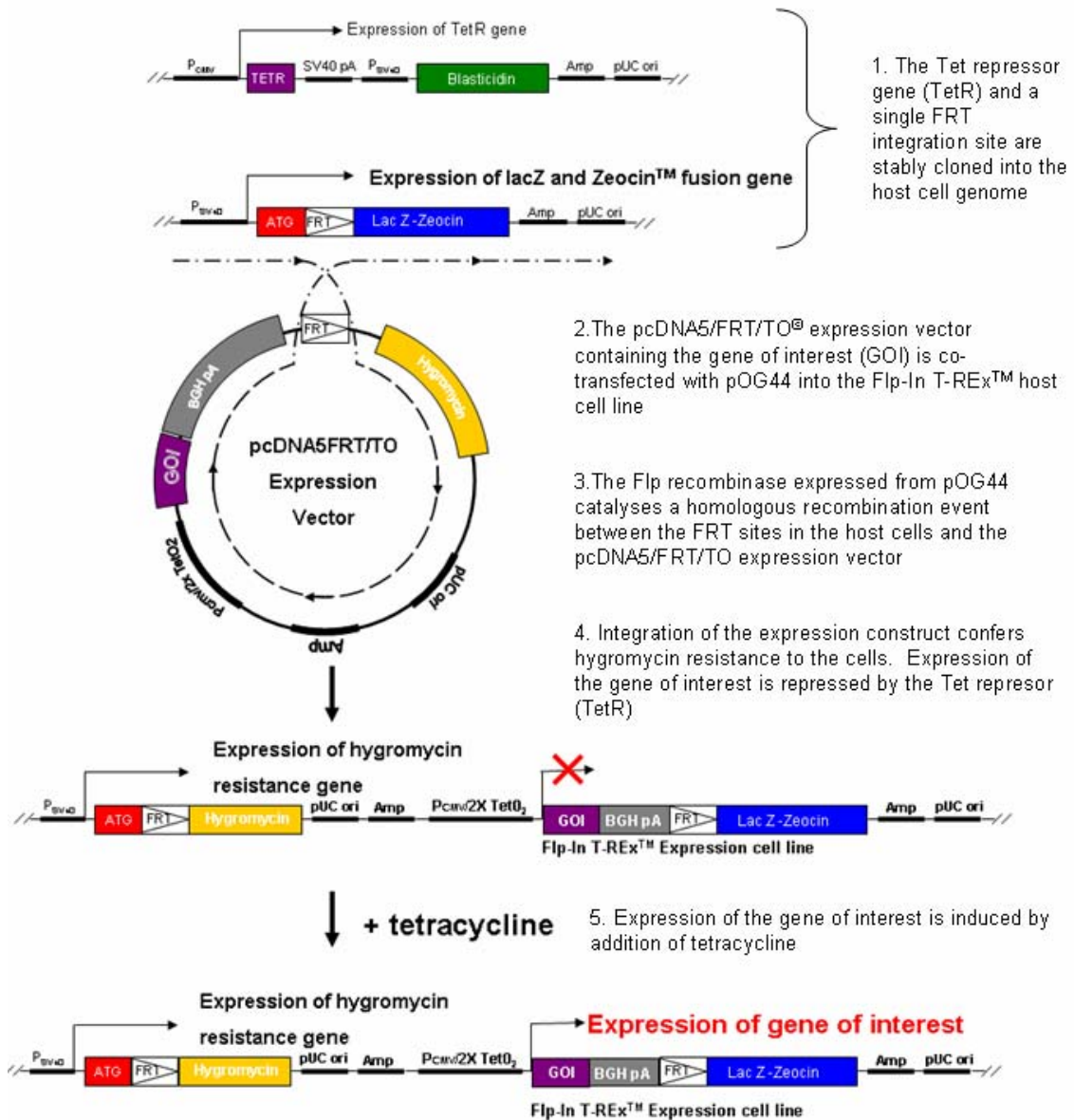
Figure 3.6



**Figure 3.7: The Flp-In™ T-REx™ HEK293 system can be used to express a gene of interest by induction of expression upon treatment of the cells with tetracycline**

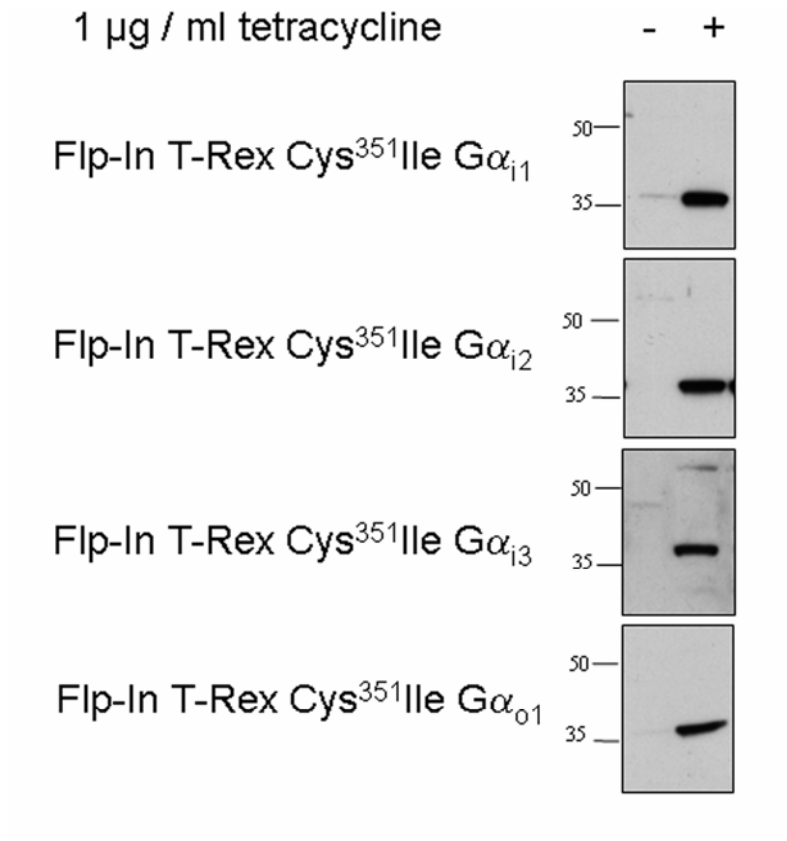
Schematic cartoon showing the cloning of a gene of interest (GOI) into a Flp-In™ T-REx™ HEK293 host cell line (Invitrogen), to generate a stable cell line where the GOI is expressed from a single location in the host genome upon induction of expression with tetracycline treatment of cells (diagram based on information from Invitrogen Flp-In. T-REx. Core Kit manual)

Figure 3.7



**Figure 3.8: Characterisation of Flp-In T-REx cells harbouring pertussis toxin-insensitive mutant G proteins at the Flp-In locus**

Flp-In T-REx cell lines were established with one of Cys<sup>351</sup>Ile G $\alpha_{i1}$ , Cys<sup>352</sup>Ile G $\alpha_{i2}$ , Cys<sup>351</sup>Ile G $\alpha_{i3}$  or Cys<sup>351</sup>Ile G $\alpha_{o1}$  cloned into the Flp-In locus. These cells were treated with tetracycline (1.0  $\mu$ g/ml for 24 h prior to cell harvest). Cell membranes were then prepared, resolved by SDS-PAGE and immunoblotted to detect G $\alpha_{i1}$ , G $\alpha_{i2}$ , G $\alpha_{i3}$  or G $\alpha_{o1}$ .

**Figure 3.8**

**Figure 3.9: Characterisation of Flp-In T-REx cells constitutively expressing the D<sub>21</sub> receptor and harbouring pertussis toxin-insensitive mutant G proteins at the inducible Flp-In locus**

Flp-In T-REx cell lines were established with one of Cys<sup>351</sup>Ile G $\alpha_{i1}$ , Cys<sup>351</sup>Ile G $\alpha_{i2}$ , Cys<sup>351</sup>Ile G $\alpha_{i3}$  or Cys<sup>351</sup>Ile G $\alpha_{o1}$  cloned into the Flp-In locus. These cells were further transfected to constitutively and stably express the D<sub>21</sub> receptor. A single, near saturating concentration of 1 nM [<sup>3</sup>H] spiperone was used to assess the relative constitutive expression levels of D<sub>21</sub> receptor of various clones generated from D<sub>21</sub> receptor cDNA transfection, with non-specific binding estimated using 10  $\mu$ M (+)-butaclamol. Only clones showing significant expression of D<sub>21</sub> receptor were retained and further characterised (**Table 3**).

Figure 3.9

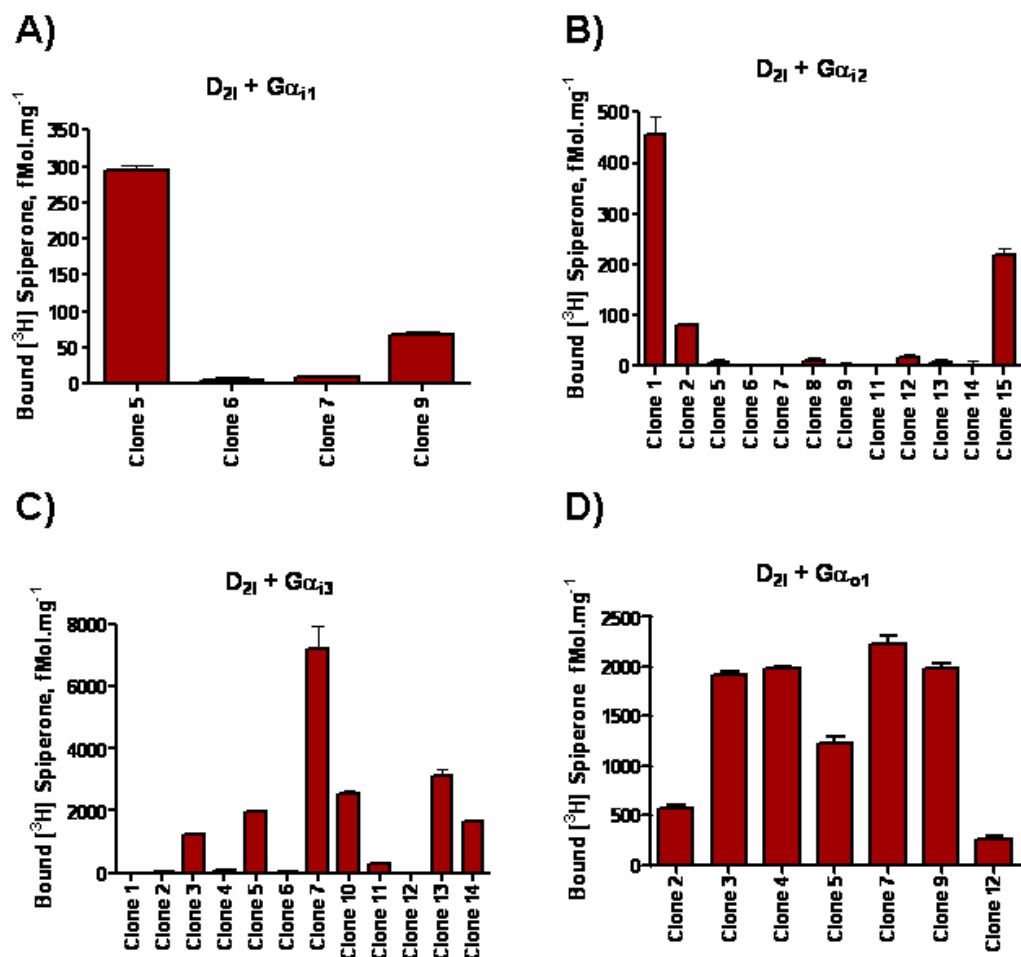


**Figure 3.10: Characterisation of Flp-In T-REx cells harbouring pertussis toxin-insensitive mutant G proteins at the Flp-In locus and constitutively and stably expressing the D<sub>21</sub> receptor**

Flp-In T-REx cell lines were established with one of Cys<sup>351</sup>Ile G $\alpha_{i1}$ , Cys<sup>352</sup>Ile G $\alpha_{i2}$ , Cys<sup>351</sup>Ile G $\alpha_{i3}$  or Cys<sup>351</sup>Ile G $\alpha_{o1}$  cloned into the Flp-In locus. These cells were further transfected to constitutively and stably express the D<sub>21</sub> receptor (see **Table 3.3 for details**). These cells were treated with concentrations of tetracycline (Tet) between 0 and 1.0  $\mu\text{g/ml}$  for 24 h. Cell membranes were then prepared, resolved by SDS-PAGE and immunoblotted to detect G $\alpha_{i1}$ , G $\alpha_{i2}$ , G $\alpha_{i3}$  or G $\alpha_{o1}$  (**A**). Densitometric scans were used to quantitate relative expression levels of the G proteins (**B**).

Figure 3.10

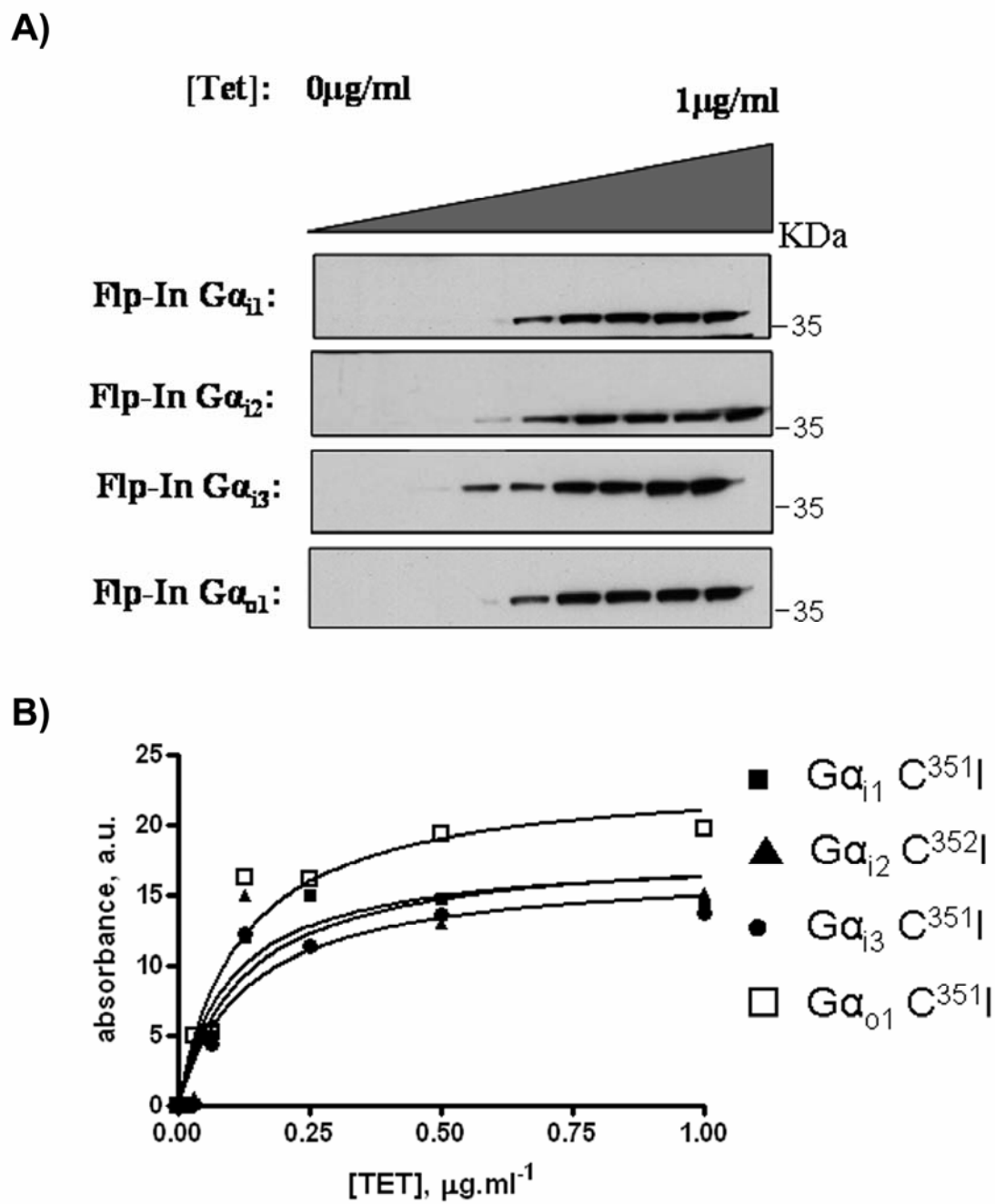
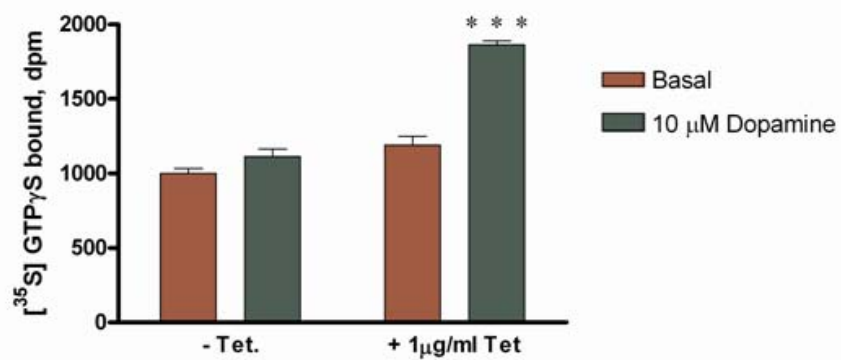


**Figure 3.11: D<sub>21</sub> receptor stimulates [<sup>35</sup>S] GTPγS binding to Cys<sup>352</sup>Ile Gα<sub>i2</sub> in membranes of pertussis toxin-treated Flp-In T-REx cells only when G protein expression is induced**

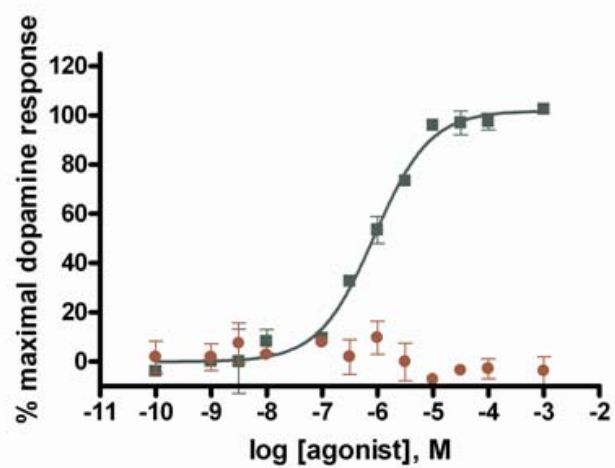
Flp-In T-REx HEK293 cells stably expressing the D<sub>21</sub> receptor and harbouring Cys<sup>352</sup>Ile Gα<sub>i2</sub> at the Flp-In locus were treated with or without 1 μg/ml tetracycline for 24 h. Both sets of cells were also treated with pertussis toxin. Membranes from these cells were (A), used to measure basal [<sup>35</sup>S]GTPγS binding and the effect of 10 μM dopamine on this, (B) to measure the ability of varying concentrations of dopamine (pEC<sub>50</sub> = 6.05±0.11) ( **green squares**) or S-(-)-3-PPP (**red circles**) to modulate [<sup>35</sup>S]GTPγS binding following induction of Cys<sup>352</sup>Ile Gα<sub>i2</sub>. An unpaired Student's t-test was performed using GraphPad Prism version 4. A highly significant difference between basal and dopamine stimulated [<sup>35</sup>S] GTPγS binding was observed upon induction of Cys<sup>351</sup>Ile Gα<sub>i2</sub> expression (P<0.001).

Figure 3.11

A)



B)

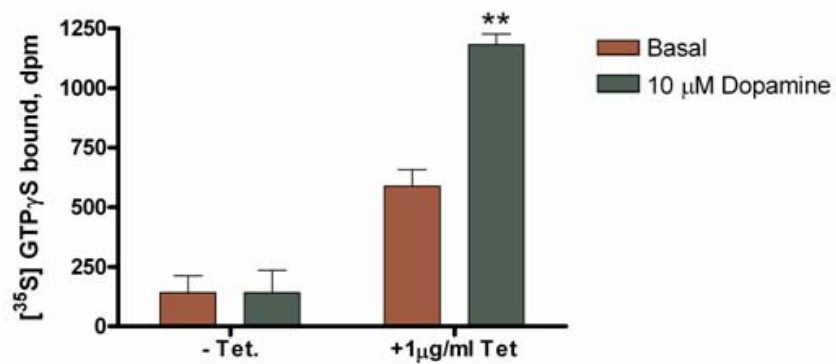


**Figure 3.12: D<sub>21</sub> receptor stimulates [<sup>35</sup>S] GTPγS binding to Cys<sup>351</sup>Ile Gα<sub>o1</sub> in membranes of pertussis toxin-treated Flp-In T-REx cells only when G protein expression is induced**

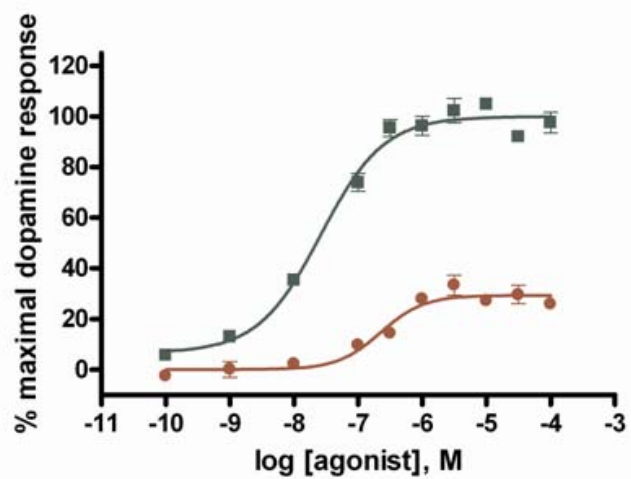
Flp-In T-REx HEK293 cells stably expressing the D<sub>21</sub> receptor and harbouring Cys<sup>351</sup>Ile Gα<sub>o1</sub> at the Flp-In locus were treated with or without 1 μg/ml tetracycline for 24 h. Both sets of cells were also treated with pertussis toxin (25ng/ml, 16 hours prior to cell harvest). Membranes from these cells were (A), used to measure basal [<sup>35</sup>S]GTPγS binding and the effect of 10 μM dopamine on this, (B) to measure the ability of varying concentration of dopamine (pEC<sub>50</sub> = 7.56 ± 0.17) (**green squares**) or S-(-)-3PPP (pEC<sub>50</sub> = 6.65 ± 0.10) (**red circles**) to modulate [<sup>35</sup>S]GTPγS binding following induction of Cys<sup>351</sup>Ile Gα<sub>o1</sub>. A very significant difference between basal and dopamine stimulated [<sup>35</sup>S] GTPγS binding was observed upon induction of Cys<sup>351</sup>Ile Gα<sub>o1</sub> expression (P<0.01).

Figure 3.12

A)



B)



**Figure 3.13: A high affinity binding site for dopamine but not for S-(-)-3PPP appears with induced expression of Cys<sup>352</sup>Ile G $\alpha_{i2}$**

Flp-In T-REx HEK293 cells stably expressing the D<sub>21</sub> receptor and harbouring Cys<sup>352</sup>Ile G $\alpha_{i2}$  at the Flp-In locus were treated with ( **filled symbols**) or without ( **open symbols**) tetracycline and pertussis toxin as in **Figure 3.10**. Membranes from these cells were employed in competition binding assays using 0.1 nM [<sup>3</sup>H]spiperone and varying concentrations of either dopamine (**A**) or S-(-)-3PPP (**B**) in the absence ( **red squares**) or presence ( **green circles**) of 100 $\mu$ M GTP. Data are representative and full details are provided in **Table 3.5**. The curves are the best fit curves to one, or two site models ( $p < 0.05$ ) (F-test) using GraphPad Prism version 4.

Figure 3.13

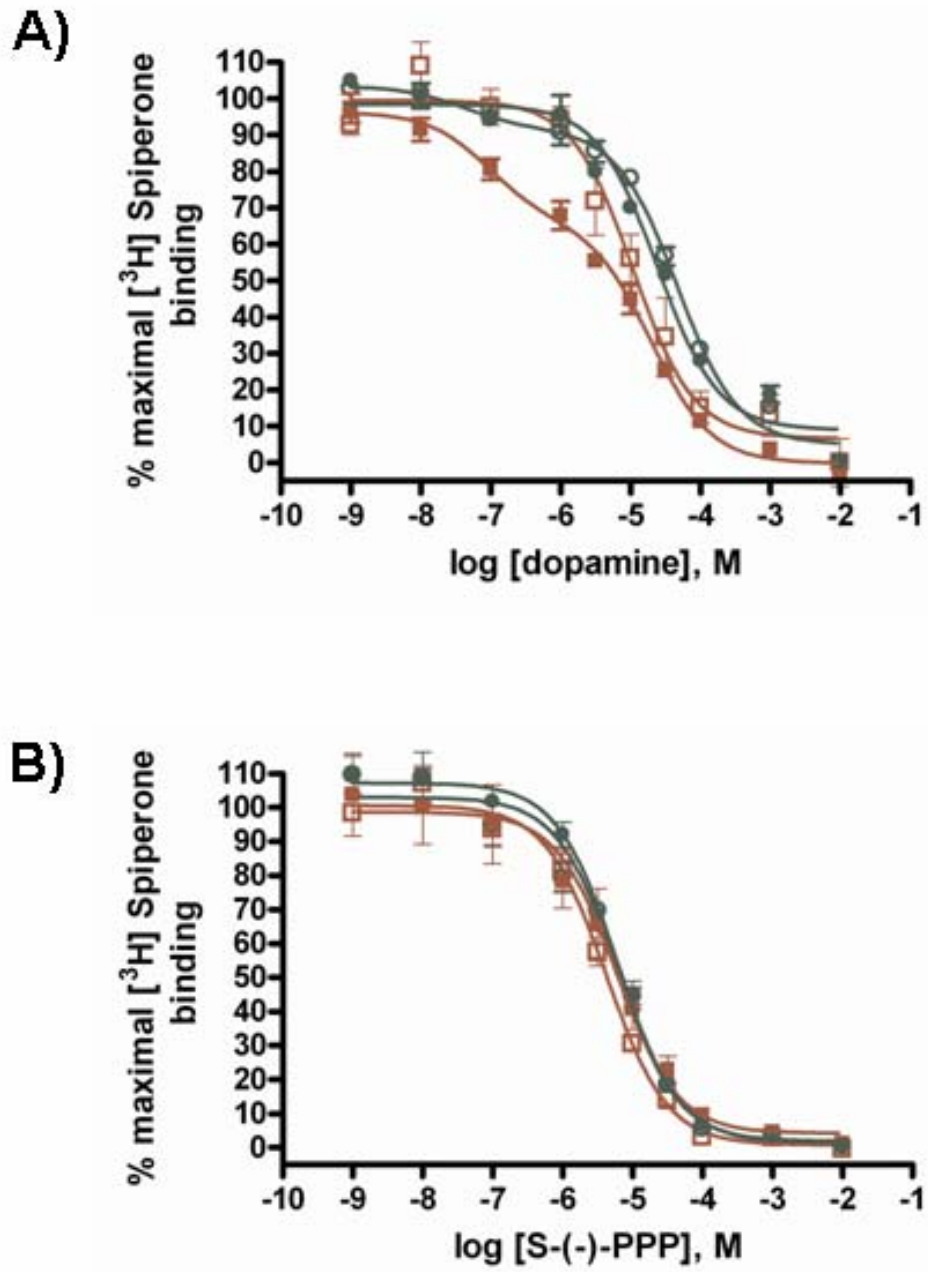


**Figure 3.14: A high affinity binding site for both dopamine and for S-(-)-3PPP appears with induced expression of Cys<sup>352</sup>Ile G $\alpha$ <sub>o1</sub>**

Flp-In T-REx HEK293 cells stably expressing the D<sub>21</sub> receptor and harbouring Cys<sup>352</sup>Ile G $\alpha$ <sub>o1</sub> at the Flp-In locus were treated with ( **filled symbols**) or without ( **open symbols**) tetracycline and pertussis toxin as in **Figure 3.11**. Membranes from these cells were employed in competition binding assays using 0.1 nM [<sup>3</sup>H]spiperone and varying concentrations on either dopamine (**A**) or S-(-)-3PPP (**B**) in the absence ( **red squares**) or presence ( **green circles**) of 100 $\mu$ M GTP.

Figure 3.14

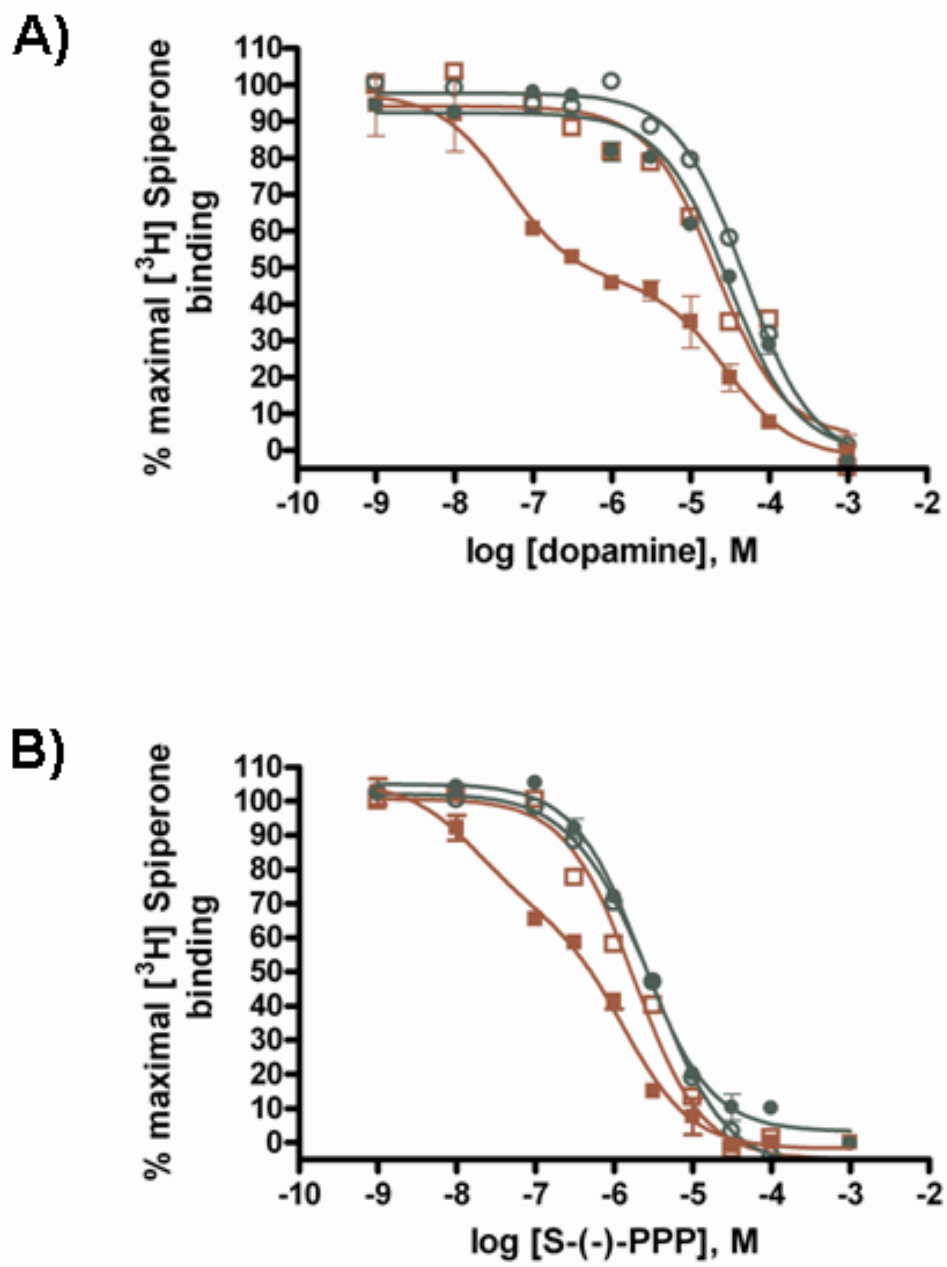
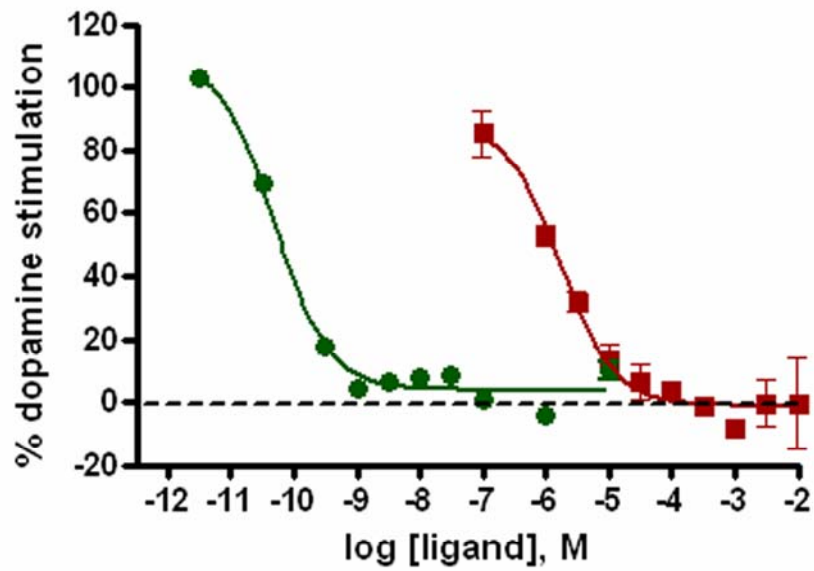


**Figure 3.15: S-(-)-3PPP is an antagonist of D<sub>21</sub>-mediated activation of Cys<sup>351</sup>Ile Gα<sub>i2</sub> but a partial agonist for Cys<sup>351</sup>Ile Gα<sub>o1</sub>**

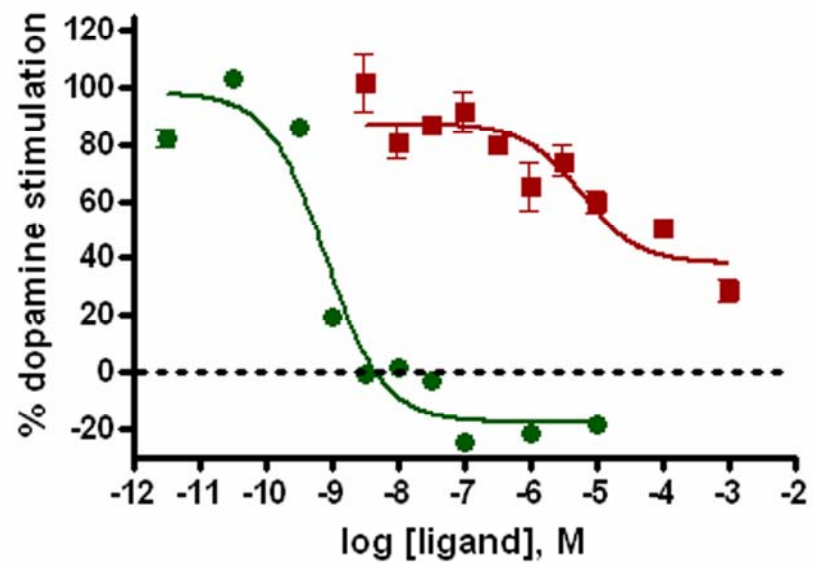
Flp-In T-REx HEK293 cells stably expressing the D<sub>21</sub> receptor and harbouring Cys<sup>352</sup>Ile Gα<sub>i2</sub> (A) or Cys<sup>352</sup>Ile Gα<sub>o1</sub> (B) at the Flp-In locus were treated with tetracycline and pertussis toxin as in **Figures 3.10, 3.11**. Dopamine at an EC<sub>50</sub> concentration for each cell line (0.1 μM D<sub>21</sub> + Cys<sup>352</sup>Ile Gα<sub>o1</sub>, 1 μM D<sub>21</sub> + Cys<sup>352</sup>Ile Gα<sub>i2</sub>) was used to stimulate [<sup>35</sup>S]GTPγS binding and the effects of varying concentrations of spiperone (**green circles**) or S-(-)-3PPP (**red squares**) or on this were assessed.

Figure 3.15

A)



B)



### 3.3 Discussion

There is now a large body of evidence for the existence of multiple receptor states. The labelling of specific sites on the purified  $\beta_2$  adrenoceptor with fluorescent probes has allowed the detection of changes in the bound fluorophore, and thereby elucidated variations in receptor conformations, and suggested that agonist binding and activation occur through a series of discrete conformational intermediates (Ghanouni et al., 2001; Swaminath et al., 2004). These discrete receptor conformations stabilised by different ligands can result in the ability of different ligands to control pairs of signal transduction pathways that are modulated by that GPCR (Perez and Karnik, 2005). An increasing body of data emerging over the past decade support this conclusion as certain ligands were shown to have quite diverse functional consequences at the same receptor (Clarke and Bond, 1998; Ghanouni et al., 2001; Gonzalez-Maeso et al., 2003; Kenakin, 1995). Such observations are important since they provide suggestions of mechanisms that may explain the differential functional properties of individual agonists that are selective for a single receptor, and furthermore give insights into the flexibility of GPCR structure.

There is a huge amount of evidence to suggest that many GPCRs can couple to multiple G protein  $\alpha$  subunits, from within the same sub family or even from distinct subfamilies (Wess, 1998). It could be predicted that different agonist-stabilised receptor conformations could differentially couple to a population of G proteins. A number of studies have identified differences in the potency or efficacy of agonist ligands to interact with more than one G protein. Of particular relevance to this study is work done with the  $D_{21}$  receptor, which was co-expressed with four different G-proteins in Sf9 cells using a baculovirus expression system. Functional interaction was demonstrated between the receptor and the four  $G_i$  G-proteins. Furthermore, it was demonstrated that different

agonists differentially activate the four G-proteins (Gazi et al., 2003). Members of the  $G\alpha_i$  subfamily are widely expressed, and are similar in sequence and therefore structure. It is hardly surprising then, that GPCRs can interact with and activate more than one member of this family if they are co-expressed. Consequently, efforts to study receptor-G-protein selectivity are hampered by the expression of a number of these G-proteins in all mammalian cells and tissues. As demonstrated by Gazi et al. (2003), one way to overcome this is to use insect cell systems (Clawges et al., 1997; Cordeaux et al., 2001; Gazi et al., 2003), where levels of expression, or the sequence conservation, of such G proteins is low. Consequently, mammalian G proteins can be introduced into such cells, along with the GPCR of interest and activation is then largely restricted to the exogenous G protein. However, to allow the use of mammalian cell lines an alternative has been to use pertussis toxin-resistant variants of these G-proteins (Ghahremani et al., 1999; Senogles et al., 2004; Wise et al., 1997) in which the Cys residue that is the target for pertussis toxin-mediated ADP ribosylation is altered to another amino acid and which retain the ability to interact with GPCRs. These mutants can be expressed in mammalian cells which are subsequently treated with pertussis toxin. The endogenously expressed forms of  $G\alpha_i$  become ADP-ribosylated and therefore are not able to functionally interact with the receptor. Previous detailed studies on  $G\alpha_{i1}$  replaced Cys with every other natural amino acid and assessed the impact on GPCR-mediated activation (Bahia et al., 1998) and similar studies were subsequently performed with  $G\alpha_{i3}$  (Dupuis et al., 1999).

Both pertussis toxin-resistant mutants and insect cell lines are extremely useful to investigate an interaction between a receptor and specific G protein  $\alpha$  subunit in isolation. However, relative expression levels of receptor and G protein must be controlled. It is well established that alterations in GPCR to G protein ratio can alter ligand function and receptor pharmacology (Milligan, 2000). Consequently to study differential agonist actions at different G proteins or, indeed, any aspect of receptor-G-protein selectivity it is

essential that this ratio is carefully controlled. This can, however, be a challenge. For example, in previous studies examining interactions between D<sub>21</sub> and different G protein  $\alpha$  subunits in insect Sf9 cells, receptor to G protein ratios ranging from 1:3 to 1:14 were reported for the different G proteins (Gazi et al., 2003).

In my work two methods have been used to meet this challenge. Firstly, the use of receptor-G-protein fusion proteins, so stoichiometry of receptor to G protein must be 1:1 (Milligan et al., 2004). Although an artificial system, GPCR-G protein fusions can greatly improve signal to background in [<sup>35</sup>S] GTP $\gamma$ S binding studies (Milligan et al., 2004). The second strategy used was the inducible expression of individual G proteins from a single, defined site of chromosomal integration in Flp-In T-REx HEK 293 cells (Canals et al., 2006; Milasta et al., 2006). Although the Flp-In T-REx HEK 293 cells cannot ensure exactly the same expression level for each G protein, each G protein is produced from the same chromosomal site and this overcomes potential differences in the effectiveness of expression level that might arise from expression from different sites of integration. In combination with both of the above strategies, pertussis toxin insensitive mutants were used. A standard Cys to Ile alteration was selected as Ile and other branched chain, hydrophobic amino acids preserved the efficacy of GPCR-G protein interactions (Bahia et al., 1998; Moon et al., 2001a; Moon et al., 2001b). This not only ensures for the receptor-G protein fusions and the inducible cell lines that receptor pharmacology for coupling to individual G $\alpha_i$  subunits can be investigated in isolation, but in the case of the Flp-In cell lines that G-protein expression can be induced into an essentially 'null' background. In summary then, two different techniques to investigate D<sub>21</sub> receptor G-protein coupling were developed, receptor-G-protein fusions in which the ratio of receptor to G protein is rigidly controlled and Flp-In T-REx stable cell lines in which receptor-G protein interactions could be investigated between the two proteins expressed as separate entities.

As could be expected, the majority of dopamine D<sub>2</sub> agonists stimulated [<sup>35</sup>S] GTPγS binding to all of the four receptor-G protein fusion proteins. This agrees with previous work suggesting that the D<sub>21</sub> receptor will promiscuously couple to all Gα<sub>i</sub> subfamily members (Gazi et al., 2003; Robinson and Caron, 1997; Senogles et al., 2004; Watts et al., 1998). However, in agreement with Gazi et al. (2003) there was a significant variation in potency and efficacy in coupling to each G protein. For example, dopamine showed a significantly higher potency at D<sub>21</sub>-Cys<sup>351</sup>Ile Gα<sub>o1</sub> in comparison with the other G<sub>i</sub> subunits. This is in agreement with a general consensus that Gα<sub>o1</sub> is the Gα<sub>o/i</sub> subunit that is most robustly activated by D<sub>21</sub> (Neve et al., 2004) and furthermore the G protein subtype that is predominantly coupled to D<sub>2</sub>-like receptors in mouse brain (Jiang et al., 2001). It could also be extrapolated then, that dopamine stabilises a structure which favours coupling to Gα<sub>o1</sub>. Similarly, for all partial agonists tested, potency and efficacy was significantly higher at D<sub>21</sub>-Cys<sup>351</sup>Ile Gα<sub>o1</sub>. However, the full agonist NPA showed no significant difference in efficacy in relation to maximal dopamine stimulation or potency at any of the Gα<sub>i/o</sub> subunits. This suggests that NPA stabilises a conformation of the receptor which does not discriminate between the four Gα<sub>i/o</sub> proteins. This, in comparison to the differential action of dopamine, for example, at the four different G proteins can be considered an example of agonist directed G protein coupling. In general, the potency of the ligands used was higher for activation of Gα<sub>o1</sub> than for Gα<sub>i2</sub>. There were not statistically valid differences between the values obtained for Gα<sub>i1</sub>, Gα<sub>i2</sub> and Gα<sub>i3</sub> for enough compounds to allow us to convincingly state rank-order potency differences (that might reflect selective stabilization of distinct states of the receptor) for interactions with Gα<sub>i1</sub> versus Gα<sub>i2</sub> for example. This may reflect that the amino acid sequence identities for Gα<sub>i1</sub>, Gα<sub>i2</sub> and Gα<sub>i3</sub> are all between 86% and 94%, whereas for each of these against Gα<sub>o</sub>, sequence identity lies between 70-73%. It might, therefore, be postulated that greater variation in ligand conformational states could be observed for interactions with Gα<sub>o</sub> versus the others rather than between Gα<sub>i1</sub>, Gα<sub>i2</sub> and Gα<sub>i3</sub>.

Most obvious, however, was the failure of *p*-tyramine and S-(-)-3-PPP to stimulate [<sup>35</sup>S] GTPγS binding to Cys<sup>351</sup>Ile Gα<sub>i1</sub>, Cys<sup>352</sup>Ile Gα<sub>i2</sub> and Cys<sup>351</sup>IleGα<sub>i3</sub> despite their action as partial agonists at Cys<sup>351</sup>Ile Gα<sub>o1</sub>. Subsequent studies were performed with S-(-)-3-PPP because the potency of *p*-tyramine was sufficiently low to limit its usefulness for detailed studies. S-(-)-3-PPP was able to fully inhibit dopamine stimulated [<sup>35</sup>S] GTPγS binding at Cys<sup>351</sup>Ile Gα<sub>i1</sub>, Cys<sup>352</sup>IleGα<sub>i2</sub> and Cys<sup>351</sup>Ile Gα<sub>i3</sub>, and, indeed, acted as an efficacious inverse agonist. However, consistent with its action as a partial agonist, even at maximally effective concentrations it was unable to fully block dopamine stimulated binding of [<sup>35</sup>S] GTPγS at Cys<sup>351</sup>Ile Gα<sub>o1</sub>, and the maximal level of inhibition was consistent with the direct measures of its partial activity. Consistent with these observations using fusion proteins, when receptor and Cys→Ile Gα mutants were expressed as separate entities in the Flp-In T-REx stable cell lines, S-(-)-3-PPP was unable to stimulate [<sup>35</sup>S] GTPγS binding at Cys<sup>352</sup>Ile Gα<sub>i2</sub>, but produced robust concentration-dependent [<sup>35</sup>S] GTPγS binding above basal levels at Cys<sup>351</sup>Ile Gα<sub>o1</sub>. As could be expected, S-(-)-3-PPP caused complete inhibition of dopamine stimulated [<sup>35</sup>S] GTPγS binding when the expression of Cys<sup>352</sup>Ile Gα<sub>i2</sub> was induced, but only partial inhibition when Cys<sup>351</sup>Ile Gα<sub>o1</sub> was induced, consistent with its action as a partial agonist for this pathway. It is interesting to note the higher potency observed at the D<sub>21</sub> receptor upon induction of expression of Gα<sub>i2</sub> or Gα<sub>o1</sub> in comparison to the equivalent D<sub>21</sub>-receptor fusion proteins. However, the affinity of dopamine or S-(-)-3PPP for the D<sub>21</sub> receptor in these two different models is similar. Since the ratio of receptor to G protein must be 1:1 in the fusion proteins, this indicates that in the Flp-In T-REx D<sub>21</sub> receptor plus either Gα<sub>i2</sub> or Gα<sub>o1</sub> cell lines there could be a receptor reserve accounting for this increase in potency.

This apparent protean effect was corroborated by competition binding studies, comparing the binding profiles of both dopamine and S(-)-3-PPP. Dopamine showed both high and low affinity states for all four G protein environments, consistent with its action as an agonist. In the presence of GTP the high affinity site was lost, consistent with the dissociation of the receptor from the GTP bound  $\alpha$  subunit. Conversely, S(-)-3-PPP only showed a high affinity site in the presence of Cys<sup>351</sup>Ile  $G\alpha_{o1}$  but not at any of the other the Cys $\rightarrow$ Ile  $G\alpha_i$  mutants. This was true for both the receptor-Cys $\rightarrow$ Ile G protein  $\alpha$  subunit mutant fusion proteins and for the cell lines where either expression Cys<sup>352</sup>Ile  $G\alpha_{i2}$  or Cys<sup>351</sup>Ile  $G\alpha_{o1}$  could be induced by tetracycline treatment. The Flp-In T-REx cell lines in particular showed clearly how the G protein environment has a significant effect on S(-)-3-PPP pharmacology. For both dopamine and S(-)-3-PPP, without the induction of G protein, where the receptor is in essentially a  $G\alpha_{i/o}$  'null' environment, competition binding was best fit by a monophasic, low affinity curve. However, with the induced expression of either Cys<sup>352</sup>Ile  $G\alpha_{i2}$  or Cys<sup>351</sup>Ile  $G\alpha_{o1}$  dopamine gained a GTP-sensitive high affinity binding site, whereas for S(-)-3-PPP a high affinity site was only seen in the presence of Cys<sup>351</sup>Ile  $G\alpha_{o1}$ .

It is interesting to note that in the case of the dopamine receptor-Cys $\rightarrow$ Ile G protein  $\alpha$  subunit mutant fusion proteins, as demonstrated by the action of spiperone, a higher constitutive activity is observed at the Cys<sup>351</sup>Ile  $G\alpha_{i2}$  fusion protein as compared to that observed when the D<sub>21</sub> receptor is coupled to Cys<sup>352</sup>Ile  $G\alpha_{o1}$ . It would appear then that the S(-)-3PPP is an inverse agonist at  $G\alpha_{i2}$  when there is high constitutive activity, but an agonist at  $G\alpha_{o1}$  where the observed constitutive activity negligible. This is consistent with the description of a protean agonist as described by Kenakin (Kenakin, 2001). However, for the work using the FlpIn T-REx stable cell lines where the receptor and G protein are expressed as separate polypeptides no such difference in constitutive activity is observed, and the action of S(-)-3PPP could better be described by the term functional selectivity.

This term describes the observation that many ligands can differentially activate signaling pathways mediated via a single G protein-coupled receptor in a manner that challenges the traditional definition of intrinsic efficacy. In this case then S-(-)-3PPP stabilises a conformation of the D<sub>2L</sub> receptor that selectively couples to G $\alpha_{o1}$ .

In conclusion then, data from both the binding and the [<sup>35</sup>S]GTP $\gamma$ S studies indicated that the D<sub>21</sub> generated a high affinity state for S-(-)-3-PPP and allowed G protein activation by this ligand only in the presence of G $\alpha_{o1}$ . This protean agonism or functional selectivity is a clear demonstration that different agonists at the D<sub>21</sub> receptor can stabilise different receptor conformations. Moreover, this may have implications for the physiological action of S-(-)-3-PPP. S-(-)-3-PPP has been described, using both biochemical and behavioural experiments, as an agonist at dopamine autoreceptors, but an antagonist at post-synaptic dopamine receptors (Arnt et al., 1983; Hjorth et al., 1983). Interestingly, the localisation of G $\alpha_{i/o}$  proteins has been shown to be different at post and pre-synaptic densities. In post synaptic densities G $\alpha_{i2}$  and G $\alpha_{i3}$  were shown to be more prevalent, whereas at pre-synaptic densities G $\alpha_{o1}$  was shown to be more prevalent (Aoki et al., 1992). It could be extrapolated then, that the differential antagonistic and agonistic effects of S-(-)-3-PPP at postsynaptic dopamine receptors and pre-synaptic dopamine receptors respectively, could lie at the different G protein environments of these two receptor populations as demonstrated by the results in this chapter.

In two studies with S-(-)-3-PPP, patients with schizophrenia showed improvements in both positive and negative symptoms, but a limited duration of effectiveness (Lahti et al., 1998). It has been postulated that this is due to the action of S-(-)-3-PPP as a D<sub>2</sub>-like dopamine receptor partial agonist and that this would have a ‘dopamine system stabilisation effect’ ie. normalisation of both dopamine hypo- and hyperactivity in the pathologically affected dopaminergic tracts observed in schizophrenic patients (Lieberman, 2004). Similarly, the

atypical antipsychotic aripiprazole (Abilify) which now has FDA approval for the treatment of schizophrenia, has also been characterised as a partial agonist at D<sub>2</sub> receptors and again to have a dopamine stabilisation effect (Burriss et al., 2002; Cosi et al., 2006). However, the intrinsic activity and potency of aripiprazole at the D<sub>2</sub> receptor is both cell line and assay dependent. For example, aripiprazole has been shown to be a partial agonist for inhibition of cAMP accumulation in a CHO cell line but an antagonist for [<sup>35</sup>S] GTPγS binding (Shapiro et al., 2003). Most significant, however, is the observation that, like S-(-)-3-PPP, the drug is reported to antagonise post-synaptic D<sub>2</sub> receptors but partially activate presynaptic autoreceptors (Kikuchi et al., 1995). In agreement with these findings, a recent paper demonstrated the differential signalling of aripiprazole for several D<sub>21</sub> mediated pathways (Urban et al., 2006b). These observations are consistent with aripiprazole, like S-(-)-3-PPP, having differential pharmacology at different signalling pathways, and it would be interesting to ascertain if aripiprazole has similar protean characteristics in terms of G protein coupling.

‘Protean’ effects of ligands have been demonstrated both *in vitro* at the β<sub>1</sub> and β<sub>2</sub> adrenergic receptors (Galandrin and Bouvier, 2006) and for functional *in vivo* end points at the histamine H<sub>3</sub> receptor (Gbahou et al., 2003). As suggested above, this concept may have relevance to the reported differences in clinical effects of ligands that appear to target the same receptor. The utility of fusion constructs for evaluating receptor signalling mechanisms for systems that are otherwise designed to be catalytic with a spare receptor reserve, for example, has been highlighted (Colquhoun, 1998; Hildebrandt, 2006). The invariant ratio of receptor to G protein α subunit overcomes differences in expression that can complicate comparisons among different receptors and G proteins. This is an attractive quality when investigating phenomena such as agonist directed trafficking and protean ligands. This is highlighted by recent work using the thromboxane A<sub>2</sub> receptor (TPα) fused to either Gα<sub>12</sub> or Gα<sub>13</sub> (Zhang et al., 2006). This study indicated that the

purported antagonist pinane thromboxane A<sub>2</sub> stimulated no response at the TP $\alpha$ - G $\alpha$ <sub>12</sub> fusion protein but was an agonist at the TP $\alpha$ - G $\alpha$ <sub>13</sub> fusion protein. Although not suggested by the authors, these results indicate that pinane thromboxane A<sub>2</sub> could well be a 'protean' agonist.

## **4 An investigation of the G protein-coupling specificity of D<sub>2</sub> and D<sub>3</sub> dopamine receptors**

### **4.1 Introduction**

The G protein coupling selectivity of dopamine D<sub>2</sub> receptors has been well studied, and it is now generally accepted that D<sub>2</sub> receptors couple efficiently and promiscuously to all four G $\alpha_{i/o}$  subtypes, although the relative order of preference remains controversial (Gazi et al., 2003; Jiang et al., 2001; Senogles et al., 2004; Watts et al., 1998). There has been a large amount of research directed at the elucidation of the signalling pathways of the D<sub>2</sub> dopamine receptor due to identification of this receptor as a therapeutic target for schizophrenia (Seeman, 2006). Similarly, there has been considerable interest in the D<sub>3</sub> receptor as a target for antipsychotic drugs (Joyce, 2001; Joyce and Millan, 2005; Sokoloff et al., 2006). Human dopamine D<sub>2</sub> and D<sub>3</sub> receptors have an overall amino acid similarity of 52% which increases to 78% if only transmembrane regions are considered (Sokoloff et al., 1990). Consequently D<sub>2</sub> and D<sub>3</sub> receptors exhibit a similar pharmacological profile (Ahlgren-Beckendorf and Levant, 2004). However, signal transduction by the D<sub>3</sub> receptor is less clearly understood than that of the D<sub>2</sub> receptor. Studies to elucidate cellular responses to D<sub>3</sub> receptor activation are hampered by the similar pharmacological profiles of D<sub>2</sub> and D<sub>3</sub>, the co-expression of these receptors in brain tissue and the lack of definitively selective pharmacological tools. It follows then, that the majority of data has been obtained by expression of the receptors in heterologous systems. This has led to a number of different and conflicting results. Initial reports indicated that the D<sub>3</sub> receptor expressed in a variety of cell systems did not exhibit a decrease in affinity for agonists in the presence of guanyl nucleotides as would be expected for a G protein coupled receptor (Freedman et al., 1994; Sokoloff et al., 1990; Tang et al., 1994). Consistent with this

observation, several studies reported that the D<sub>3</sub> receptor did not modulate adenylyate cyclase activity (Sokoloff et al., 1990; Tang et al., 1994)

However, subsequent studies using heterologous expression systems showed some pertussis toxin-sensitive inhibition of adenylyate cyclase (Cox et al., 1995; Griffon et al., 1997; Hall and Strange, 1999). Of particular note, in HEK293 cells or COS-7 cells, stimulation of D<sub>3</sub> receptors attenuated forskolin-stimulated adenylyate cyclase activity, but only when cells were co-transfected with the adenylyate cyclase V isozyme (Robinson and Caron, 1997). In agreement with this dopaminergic agonists dose-dependently stimulated [<sup>35</sup>S] GTPγS binding in Sf-9 insect cells (Alberts et al., 2000), Chinese hamster ovary (CHO) cells (Jurgen et al., 2000; Malmberg et al., 1998; Newman-Tancredi et al., 1999; Vanhauwe et al., 1999) and SH-SY5Y human neuroblastoma cells (Zaworski et al., 1999) in which the D<sub>3</sub> receptor was expressed. Furthermore, this effect was abolished by pertussis toxin, suggesting coupling to Gα<sub>i/o</sub> proteins. This first objective of this project, therefore, was to elucidate the intrinsic coupling specificities of both D<sub>21</sub> and D<sub>3</sub> dopamine receptors in parallel. As for the characterisation of agonist directed coupling at the D<sub>21</sub> receptor (chapter 3), the need to devise a model system in which the interaction between a specific receptor and G protein could be studied in isolation was crucial. To this end, pertussis-toxin resistant variants of Gα<sub>i/o</sub> G proteins were again employed. Similarly, it is also important to control the relative expression levels of both receptor and G protein. Again, both receptor-G protein fusion proteins and Flp-In T-REx cell lines in which the receptor was constitutively expressed and the G protein was expressed from the inducible Flp-In locus were utilised. In this chapter the use of these strategies confirmed the promiscuous coupling of the D<sub>21</sub> receptor to Gα<sub>i1</sub>, Gα<sub>i2</sub>, Gα<sub>i3</sub>, and Gα<sub>o1</sub>. Furthermore, the efficient and specific coupling of D<sub>3</sub> to Gα<sub>o1</sub> but not Gα<sub>i1</sub>, Gα<sub>i2</sub> and Gα<sub>i3</sub> was demonstrated.

The second aim of this project was to investigate the molecular basis of the differential G protein-coupling specificities of the dopamine D<sub>2</sub> and D<sub>3</sub> receptors. An accepted and widely-used approach that has led to a wealth of information about the molecular basis of receptor-G protein-coupling selectivity is to analyze hybrid receptors constructed between functionally distinct members of a GPCR subfamily (Wess, 1998). Perhaps due to the high homology of the D<sub>2</sub> and D<sub>3</sub> receptors, a number of investigations into coupling of D<sub>3</sub> receptors have been performed using D<sub>2</sub>/D<sub>3</sub> receptor chimera constructions (McAllister et al., 1993; Robinson and Caron, 1996; Robinson et al., 1994; Van Leeuwen et al., 1995). These studies indicated that the third intracellular loop of D<sub>2</sub> and D<sub>3</sub> receptors is important for the coupling to AC. However, in D<sub>3</sub>/D<sub>2</sub> receptor chimeras that fully coupled to inhibition of cAMP production, agonist binding to these chimeras was still resistant to the effect of GTP or its analogues (Van Leeuwen et al., 1995). A subsequent study identified more specific components of the third intracellular loop of the human dopamine D<sub>2</sub> receptor involved in the coupling of these receptors with adenylate cyclase (Filteau et al., 1999). This study used reciprocal chimera constructions between hD<sub>2</sub> and hD<sub>3</sub> dopamine receptors with the exchange of a divergent twelve amino acid section in the c-terminus of the third intracellular loop of each receptor. The chimeric D<sub>3</sub> receptor with a twelve amino acid section of D<sub>2</sub> (termed D<sub>3/2</sub>, **Figure 4.1**) gained coupling to adenylate cyclase. In this chapter, the same chimera has been used. As for the native D<sub>2</sub> and D<sub>3</sub> dopamine receptors, the G protein coupling specificity of this chimeric D<sub>3/2</sub> receptor was characterised, showing coupling to G $\alpha_{i1}$ , G $\alpha_{i2}$ , G $\alpha_{i3}$  and G $\alpha_{o1}$ . Therefore, the exchange of a twelve amino acid section of the third intracellular loop of D<sub>3</sub> with that of the D<sub>2</sub> receptor confers promiscuous D<sub>2</sub>-like coupling selectivity to the D<sub>3</sub> receptor.

## 4.2 Results

### 4.2.1 The use of a chimeric D<sub>3/2</sub> receptor to investigate regions of D<sub>21</sub> and D<sub>3</sub> important for G protein coupling selectivity

To investigate regions within the D<sub>21</sub> and D<sub>3</sub> receptors which are important in directing potential differences in G protein selectivity, an accepted approach is the use of chimeric receptors in which one region of a donor receptor is replaced with the equivalent region of the acceptor receptor. In this case the chimera used was a D<sub>3</sub> receptor with a twelve amino acid section of the C-terminus of the third intracellular loop (IC loop 3) replaced with the equivalent region of D<sub>2</sub> (**Figure 4.1**). The twelve amino acids are of entirely different sequence but are flanked by homologous regions to their C-terminal side close to transmembrane domain VI (TM VI) and N-terminal side. As in chapter 3, this study used heterologous expression in HEK293T cells as the model system. However, there is significant endogenous G protein  $\alpha$  subunit expression in HEK293T cells, so it was necessary to use systems which ensured the interaction between a receptor and one G protein subtype could be investigated in isolation. D<sub>2</sub>-like (i.e. both D<sub>2</sub> and D<sub>3</sub>) dopamine receptors have shown their down stream signalling to be pertussis toxin-sensitive and, therefore, that they couple to the G<sub>i</sub> subclass of G proteins. Consequently, to allow the investigation of coupling between a specific receptor and G protein, cells can be transfected with cDNA of both the dopamine receptor and a pertussis toxin insensitive mutant G $\alpha_{i/o}$  subunit of interest, and then treated with pertussis toxin 16 hours prior to cell harvest. This methodology has been described in detail in **chapter 3**.

## 4.2.2 Investigation of D2-like dopamine receptor coupling using transient co-transfection of receptor and pertussis toxin insensitive $G\alpha_{i/o}$ subunits

### 4.2.2.1 Determination of dopamine receptor levels in HEK293T cells transiently co-transfected with either $D_{21}$ , $D_3$ or $D_{3/2}$ cDNA and Cys<sup>352</sup>Ile $G\alpha_{i2}$ or Cys<sup>351</sup>Ile $G\alpha_{o1}$

HEK293T cells were co-transfected with a dopamine receptor ( $D_{21}$ ,  $D_3$  or  $D_{3/2}$ ) and either Cys<sup>352</sup>Ile  $G\alpha_{i2}$  or Cys<sup>351</sup>Ile  $G\alpha_{o1}$  and treated with or without pertussis toxin (25ng/ml) 16 hours prior to cell harvest. To allow a determination of the number of functionally competent (properly folded) receptors, the high affinity, radiolabeled dopaminergic antagonist, [<sup>3</sup>H] spiperone, was used. For saturation binding experiments, co-transfected HEK293T membranes (10  $\mu$ g) were incubated with a range of [<sup>3</sup>H] spiperone concentrations (0.001–2 nM). Non-specific binding was determined by the inclusion of 10  $\mu$ M (+)-butaclamol. Incubations were carried out for 3 hours at 25 ° C to achieve equilibrium-binding conditions, and bound radioactivity separated from free by filtration through GF/C filters. Ligand affinities were calculated using Prism (Graphpad).

In  $D_{21}$  co-transfections, a single high affinity site for [<sup>3</sup>H] spiperone was observed with  $K_d$  of approximately 0.04 nM (**Table 4.1**). Receptor density as indicated by the  $B_{max}$  value was approximately 3-4 pmol/mg membrane protein in all transfections. In both cases there was no significant difference in  $K_d$  or  $B_{max}$  between the same transfection with or without pertussis toxin treatment. However, although no difference in  $K_d$  was observed, a

significantly higher receptor density was observed for  $G\alpha_{o1}$  co-transfections as compared to  $G\alpha_{i2}$  transfections.

By contrast, [ $^3$ H] spiperone showed a lower affinity for dopamine  $D_3$  receptor co-transfections with a  $K_d$  of 0.1-0.15 nM, with receptor density similar to levels seen for  $D_{21}$  co-transfections. For the chimeric  $D_{3/2}$  receptor co-transfections, affinity for [ $^3$ H] spiperone was similar to that observed for the  $D_3$  receptor with a  $K_d$  of 0.1nM for all co-transfections.  $B_{max}$  values indicating receptor density were around four-fold lower than for both  $D_{21}$  and  $D_3$  at 0.5-1 pmol/mg (**Table 4.1**). Results indicate that the chimeric  $D_{3/2}$  receptor retains a 'D<sub>3</sub>-like' affinity for [ $^3$ H] spiperone, suggesting a functionally competent chimeric receptor. As for  $D_{21}$  co-transfections, a significantly higher value of  $B_{max}$  was observed in the  $G\alpha_{o1}$  co-transfections as compared to the equivalent  $G\alpha_{i2}$  co-transfections for both  $D_3$  and  $D_{3/2}$ . Again no significant difference in  $K_d$  or  $B_{max}$  was observed for the same transfection with or without pertussis toxin treatment. It is perhaps noteworthy, however, that in the case of the  $D_3$  receptor only, a significant difference in  $K_d$  between  $G\alpha_{i2}$  and  $G\alpha_{o1}$  for [ $^3$ H] spiperone was observed dependent on whether  $G\alpha_{i2}$  or  $G\alpha_{o1}$  was co-expressed.

#### **4.2.2.2 Estimation of $G\alpha$ subunit expression levels in HEK293T cells transiently co-transfected with either $D_{21}$ , $D_3$ or $D_{3/2}$ cDNA and Cys<sup>352</sup>Ile $G\alpha_{i2}$ or Cys<sup>351</sup>Ile $G\alpha_{o1}$**

G protein expression was measured for both Cys<sup>352</sup>Ile  $G\alpha_{i2}$  and Cys<sup>351</sup>Ile  $G\alpha_{o1}$  co-transfections by western blotting using antisera raised against the C-terminal decapeptide of the respective G protein  $\alpha$  subunits. HEK293T cell membranes transfected with

equivalent amounts of pcDNA3 vector were included as a control. SDS-PAGE was performed using 10  $\mu\text{g}$  of membrane protein loaded per lane onto a 4-12% bis-tris gel, and transferred to nitrocellulose. Western blots (**Figure 4.2**) show that both  $G\alpha_{i2}$  and  $G\alpha_{o1}$  were significantly over-expressed in all co-transfections with respect to the mock-transfected cells. There was significant variation in the levels of G protein  $\alpha$  subunit detected between co-transfections, but no significant difference observed between the same co-transfections with or without pertussis toxin treatment.

**Table 4.1:** [ $^3\text{H}$ ] spiperone binds with similar affinity to  $D_3$  and the chimeric  $D_{3/2}$  receptor when co-expressed with either  $\text{Cys}^{352}\text{Ile } G\alpha_{i2}$  or  $\text{Cys}^{351}\text{Ile } G\alpha_{o1}$

Co-Transfection				
Receptor	G protein	Pertussis Toxin, 25ng/ml	$K_d$ , nM ( $\pm$ S.E.M)	$B_{\text{max}}$ , fMol.mg $^{-1}$ ( $\pm$ S.E.M)
$D_{21}$	$\text{Cys}^{352}\text{Ile } G\alpha_{i2}$	-	0.04 (0.01)	3409 (150)
$D_{21}$	$\text{Cys}^{352}\text{Ile } G\alpha_{i2}$	+	0.03 (0.01)	3036 (96)
$D_{21}$	$\text{Cys}^{351}\text{Ile } G\alpha_{o1}$	-	0.06 (0.01)	4488 (160) **
$D_{21}$	$\text{Cys}^{351}\text{Ile } G\alpha_{o1}$	+	0.04 (0.01)	4815 (169) ***
$D_3$	$\text{Cys}^{352}\text{Ile } G\alpha_{i2}$	-	0.10 (0.01)	1857 (169)
$D_3$	$\text{Cys}^{352}\text{Ile } G\alpha_{i2}$	+	0.09 (0.01)	2429 (70)
$D_3$	$\text{Cys}^{351}\text{Ile } G\alpha_{o1}$	-	0.12 (0.01)	3079 (86) **
$D_3$	$\text{Cys}^{351}\text{Ile } G\alpha_{o1}$	+	0.15 (0.01) *	3345 (68) ***
$D_{3/2}$	$\text{Cys}^{352}\text{Ile } G\alpha_{i2}$	-	0.08 (0.01)	583 (21)
$D_{3/2}$	$\text{Cys}^{352}\text{Ile } G\alpha_{i2}$	+	0.14 (0.03)	509 (34)
$D_{3/2}$	$\text{Cys}^{351}\text{Ile } G\alpha_{o1}$	-	0.11 (0.02)	1117 (39) ***
$D_{3/2}$	$\text{Cys}^{351}\text{Ile } G\alpha_{o1}$	+	0.08 (0.01)	1255 (30) ***

Experiments were performed in triplicate to  $n = 3$

Differences in  $K_d$  and  $B_{max}$  were analysed using an unpaired Student's t-test ( $p < 0.05$ ). No significant differences in  $K_d$  or  $B_{max}$  were seen for the same transfection with or without pertussis toxin treatment.  $B_{max}$  and  $K_d$  values were compared between  $G\alpha_{i2}$  and  $G\alpha_{o1}$  co-transfections with the same receptor and pertussis toxin treatment condition.

Significant differences seen between  $G\alpha_{i2}$  and  $G\alpha_{o1}$  co-transfections are annotated below the value of  $B_{max}$  or  $K_d$  for the  $G\alpha_{o1}$  transfection as follows:

P < 0.05		N = 3	
P value	Definition	Summary	
< 0.001	extremely significant	***	
0.001 to 0.01	very significant	**	
0.01 to 0.05	significant	*	
> 0.05	not significant		

#### 4.2.2.3 Optimisation of [GDP] required in [<sup>35</sup>S]GTP $\gamma$ S assays using membranes expressing D<sub>3</sub> dopamine receptors

In order to study the functional coupling between receptor and G protein  $\alpha$  subunits a [<sup>35</sup>S] GTP $\gamma$ S binding assay was established incorporating an immunoprecipitation step using antisera raised against the C-terminal tail of  $G\alpha_{i2}$  or  $G\alpha_{o1}$  as described in section 2.9.2.2.

However, before embarking on detailed experiments it was important to optimise conditions for the assay with respect to the concentration of GDP used in the assay. Using membranes from D<sub>3</sub> + Cys<sup>351</sup>Ile  $G\alpha_{o1}$  co-transfections, reactions were set up with 10 fMol of receptor per reaction, various concentrations of GDP and with or without the addition of 10  $\mu$ M dopamine. In such experiments the largest signal window (**Figure 4.3**) (i.e. the stimulation of [<sup>35</sup>S] GTP $\gamma$ S binding above basal levels) was observed at 10  $\mu$ M GDP.

Consequently, GDP was used at a concentration of 10  $\mu$ M for all subsequent [<sup>35</sup>S] GTP $\gamma$ S assay experiments.

#### 4.2.2.4 Dopamine D<sub>21</sub> and the chimeric D<sub>3/2</sub> receptors couple efficiently to both Cys<sup>352</sup>Ile Gα<sub>i2</sub> and Cys<sup>351</sup>Ile Gα<sub>o1</sub> whilst the D<sub>3</sub> receptor only couples through Cys<sup>351</sup>Ile Gα<sub>o1</sub>.

As described previously, HEK293T cells were co-transfected with a dopamine receptor and either Cys<sup>352</sup>Ile Gα<sub>i2</sub> or Cys<sup>351</sup>Ile Gα<sub>o1</sub> cDNA, membranes made and functional coupling between receptor and G protein assayed using [<sup>35</sup>S]GTPγS binding. For Gα<sub>i2</sub> co-transfections a [<sup>35</sup>S] GTPγS assay was performed with an immunoprecipitation step using in-house antiserum raised against the C-terminal tail of Gα<sub>i1/2</sub>. Correspondingly, experiments using membranes from Cys<sup>351</sup>Ile Gα<sub>o1</sub> transfected cells were performed with an immunoprecipitation step using an in-house antiserum raised against the C-terminal tail of Gα<sub>o1</sub>. In all cases membranes containing equal amounts of receptor (10 fMol) were incubated with 10μM GDP with or without the presence of the endogenous dopamine receptor agonist dopamine. For Cys<sup>351</sup>Ile Gα<sub>o1</sub> co-transfections significant agonist-driven stimulation of [<sup>35</sup>S] GTPγS binding above basal levels was observed for D<sub>21</sub>, D<sub>3</sub> and chimeric D<sub>3/2</sub> co-transfections, indicating that all three receptors can couple efficiently to Gα<sub>o1</sub> (**Figure 4.4B**). However, for Cys<sup>352</sup>Ile Gα<sub>i2</sub> co-transfections, significant dopamine-stimulated [<sup>35</sup>S] GTPγS binding was seen for D<sub>21</sub> and D<sub>3/2</sub> but not for D<sub>3</sub> co-transfections (**Figure 4.4A**). This suggests that, under the conditions employed, D<sub>21</sub> coupled efficiently to both Gα<sub>i2</sub> and Gα<sub>o1</sub> whereas D<sub>3</sub> only couples to Gα<sub>o1</sub>. The chimeric D<sub>3/2</sub> receptor couples to both Gα<sub>i2</sub> and Gα<sub>o1</sub> indicating that it has acquired 'D2-like' G protein coupling promiscuity. However, it was also apparent that despite the same amount of receptor being added to each experiment there was significant differences between basal [<sup>35</sup>S] GTPγS loading between different receptors for the Gα<sub>o1</sub> and in a far more pronounced manner for the Gα<sub>i2</sub> co-transfections. For example, for membranes where D<sub>21</sub> was co-transfected with Cys<sup>352</sup>Ile Gα<sub>i2</sub> the basal level of [<sup>35</sup>S] GTPγS binding was around 200 dpm, increasing to

500 dpm (**Figure 4.4A**). By contrast, the basal level of [<sup>35</sup>S] GTP $\gamma$ S binding for the D<sub>3/2</sub> receptor was some 4000 dpm, increasing to 8000 dpm upon stimulation with dopamine. The amount of receptor added was the same in each case. This might be explained in two ways, firstly that the chimeric D<sub>3/2</sub> receptor is highly constitutively active and couples more efficiently to G $\alpha_{o1}$  than D<sub>21</sub>. However, a perhaps more likely explanation may reflect that the D<sub>3/2</sub> chimera was expressed at a four-fold (**Table 4.1**) lower level as compared to D<sub>21</sub> whereas the G protein expression was equivalent or higher (**Figure 4.2**). Consequently, although the amount of receptor added in each condition was the same, the amount of G protein would be much higher per reaction for the D<sub>3/2</sub> chimera.. It is important, therefore, to control relative levels of both G protein and receptor expression, in order to generate useful comparisons of the G protein-coupling selectivity of different receptors.

### **4.2.3 Generation of dopamine receptor-pertussis toxin-insensitive Cys $\rightarrow$ Ile variant G protein alpha subunit fusions**

In order to control relative levels of G protein and receptor expression, dopamine receptor: G protein fusion proteins were generated. Constraining receptor and G protein within a single fusion protein defines the stoichiometry of expression of the two entities as 1:1 and ensures their co-localisation following expression. As described previously in section 3.2.1, four dopamine D<sub>21</sub> receptor-Cys $\rightarrow$ Ile pertussis toxin-insensitive G  $\alpha$  subunit fusion proteins were constructed. Using the same methodology, eight further dopamine receptor-Cys  $\rightarrow$  Ile G  $\alpha$  subunit fusion proteins were generated (**Figure 4.5**), fusing each of the two remaining dopamine receptors (D<sub>3</sub>, D<sub>3/2</sub>) to each of the four Cys  $\rightarrow$  Ile pertussis toxin insensitive variants of the G<sub>i</sub> family G protein  $\alpha$  subunits (G $\alpha_{i1}$ , G $\alpha_{i2}$ , G $\alpha_{i3}$ , G $\alpha_{o1}$ ). After transfection and prior to cell harvest, HEK293T cells were treated with pertussis toxin to allow the interaction between the receptor and G protein within the fusion protein to be studied in isolation.

#### 4.2.3.1 Determination of the levels of dopamine receptor-G protein fusion protein expression using [<sup>3</sup>H] spiperone saturation binding

HEK293T cells were transiently transfected with each of the receptor-Cys → Ile G  $\alpha$  subunit fusion protein cDNAs, treated as above with pertussis toxin, cells harvested and membranes made. As for the transient co-transfection studies, receptor binding site density was assessed using [<sup>3</sup>H] spiperone saturation binding. Membranes (10  $\mu$ g) were incubated with a range of [<sup>3</sup>H] spiperone concentrations (0.001–2 nM). Non-specific binding was determined by the inclusion of 10  $\mu$ M (+)-butaclamol.

As for D<sub>21</sub> receptor plus G protein co-transfections, [<sup>3</sup>H] spiperone displayed a high affinity for the D<sub>21</sub>: G protein fusion proteins with a K<sub>d</sub> in the region of 0.04 nM. There was no significant difference in K<sub>d</sub> between all four D<sub>21</sub> fusion proteins. Receptor binding site density as indicated by B<sub>max</sub> values was approximately 1.5 pmol/mg membrane protein for all D<sub>21</sub> fusion proteins (**Table 3.1**). The D<sub>3</sub> receptor fusion proteins showed a lower affinity for [<sup>3</sup>H] spiperone with a K<sub>d</sub> of 0.12 nM (**Table 4.2**). Receptor binding site density was between 0.5 and 2 pmol/mg for each of the D<sub>3</sub> receptor fusion proteins, with the observed B<sub>max</sub> significantly higher at the D<sub>3</sub>-G $\alpha_{o1}$  fusion protein as compared to the other D<sub>3</sub> fusion proteins. The D<sub>3/2</sub> receptor fusion proteins showed a 'D<sub>3</sub>-like' affinity for [<sup>3</sup>H] spiperone with K<sub>d</sub> of some 0.12 nM. B<sub>max</sub> values of receptor density were between 0.5 and 1 pmol/ mg membrane protein. Significantly higher values of B<sub>max</sub> were observed at the D<sub>3/2</sub>-G $\alpha_{i1}$  and D<sub>3/2</sub>-G $\alpha_{o1}$  fusion proteins as compared to the other D<sub>3/2</sub> receptor fusion proteins.

**Table 4.2: [<sup>3</sup>H] spiperone binds with similar and high affinity to various D<sub>3</sub> or D<sub>3/2</sub> receptor-G protein fusions**

<b>Receptor: G Protein fusion</b>	<b>K<sub>d</sub>, nM (± S.E.M.)</b>	<b>B<sub>max</sub> fMol.mg<sup>-1</sup> (± S.E.M.)</b>
<b>D<sub>3</sub>Gα<sub>i1</sub></b>	0.08 (0.01)	641 (49)
<b>D<sub>3</sub>Gα<sub>i2</sub></b>	0.15 (0.02)	527 (21)
<b>D<sub>3</sub>Gα<sub>i3</sub></b>	0.12 (0.02)	563 (14)
<b>D<sub>3</sub>Gα<sub>o1</sub></b>	0.12 (0.01)	1985 (68) ***
<b>D<sub>3/2</sub>Gα<sub>i1</sub></b>	0.11 (0.01)	1328 (22) ***
<b>D<sub>3/2</sub>Gα<sub>i2</sub></b>	0.07 (0.01)	652 (17)
<b>D<sub>3/2</sub>Gα<sub>i3</sub></b>	0.11 (0.01)	446 (11)
<b>D<sub>3/2</sub>Gα<sub>o1</sub></b>	0.11 (0.01)	1472 (34) ***

Experiments were performed in triplicate to n = 3

\*\*\* - Differences in K<sub>d</sub> and B<sub>max</sub> for D<sub>3</sub> or D<sub>3/2</sub> receptor fusion proteins were analysed using a one way ANOVA with Tukey's post-hoc test using GraphPad Prism version 4. No significant difference in K<sub>d</sub> was observed for both D<sub>3</sub> and D<sub>3/2</sub> receptor fusion proteins. However, a significant difference in B<sub>max</sub> was observed between D<sub>3</sub> receptor fusion proteins with D<sub>3</sub>Gα<sub>o1</sub> > D<sub>3</sub>Gα<sub>i3</sub> = D<sub>3</sub>Gα<sub>i2</sub> = D<sub>3</sub>Gα<sub>i1</sub> (P<0.001), and between D<sub>3/2</sub> receptor fusion proteins with D<sub>3/2</sub>Gα<sub>o1</sub> = D<sub>3/2</sub>Gα<sub>i3</sub> > D<sub>3/2</sub>Gα<sub>i2</sub> = D<sub>3/2</sub>Gα<sub>i1</sub> (P<0.001).

#### 4.2.3.2 **Increasing amounts of dopamine receptor-Cys → Ile G protein $\alpha$ subunit fusion protein leads to a proportional increase in [<sup>35</sup>S] GTP $\gamma$ S binding**

HEK293T cells were transiently transfected with dopamine receptor-Cys<sup>351</sup>Ile G $\alpha_{o1}$  fusion proteins, cells treated with pertussis toxin and harvested. Cell membrane preparations were made and receptor binding site density estimated using [<sup>3</sup>H] spiperone binding as described earlier. Varying amounts of membrane (and therefore varying amounts of receptor) were incubated with 10  $\mu$ M GDP and with or without 10  $\mu$ M dopamine using the [<sup>35</sup>S] GTP $\gamma$ S assay with an immunoprecipitation step. An antiserum raised against the C-terminal tail of G $\alpha_{o1}$  was used for the immunoprecipitation step. For D<sub>21</sub>-Cys<sup>351</sup>Ile G $\alpha_{o1}$  (**Figure 3.3C**), D<sub>3</sub>-Cys<sup>351</sup>Ile G $\alpha_{o1}$  (**Figure 4.6A**) and D<sub>3/2</sub>-Cys<sup>351</sup>Ile G $\alpha_{o1}$  (**Figure 4.6B**) an increase in receptor per reaction lead to a linear increase in both basal and agonist stimulated [<sup>35</sup>S] GTP $\gamma$ S binding. Basal levels of [<sup>35</sup>S] GTP $\gamma$ S binding could reflect constitutive activity of the dopamine receptor-Cys<sup>351</sup>Ile G $\alpha_{o1}$  fusions, or perhaps the basal [<sup>35</sup>S] GTP $\gamma$ S loading (i.e. intrinsic guanine nucleotide exchange) of increasing amounts of G  $\alpha$  subunit added to the reaction.

#### 4.2.3.3 **D<sub>3</sub> receptor couples only to Cys<sup>351</sup>Ile G $\alpha_{o1}$ whereas the chimeric D<sub>3/2</sub> receptor couples through all four G protein $\alpha$ subunits**

To investigate the coupling selectivity of the D<sub>21</sub>, D<sub>3</sub> or the chimeric D<sub>3/2</sub> receptor for each of the four Cys→Ile G $\alpha_{i/o}$  subunits, HEK293T cells were transfected with dopamine receptor-Cys→Ile G protein  $\alpha$  subunit fusion protein cDNA. Cells were pertussis toxin treated (25 ng/ml for 16 hours), harvested and cell membrane preparations made. Cell

membranes (15 fMol of receptor/ reaction) were incubated with 10  $\mu$ M GDP, and with or without 10  $\mu$ M dopamine. A [ $^{35}$ S] GTP $\gamma$ S assay was performed with an immunoprecipitation step. For Cys $^{351}$ Ile G $\alpha_{i1}$  fusion protein membranes, and Cys $^{352}$ Ile G $\alpha_{i2}$  fusion protein membranes, an antiserum raised against the C-terminal tail of G $\alpha_i$  was used. For Cys $^{351}$ Ile G $\alpha_{i3}$  an antiserum raised against the C-terminal tail of G $\alpha_{i3}$  was employed. Similarly, an antiserum raised against the C-terminal tail of G $\alpha_{o1}$  was used for membranes expressing the Cys $^{351}$ Ile G $\alpha_{o1}$  fusion protein. For G $\alpha_{i1}$  fusion transfections, significant stimulation above basal was seen for D $_{21}$ -Cys $^{351}$ Ile G $\alpha_{i1}$  and the D $_{3/2}$ -Cys $^{351}$ Ile G $\alpha_{i1}$ , but not for D $_3$ -Cys $^{351}$ Ile G $\alpha_{i1}$  (**Figure 4.7A**). Similarly, for D $_{21}$ -Cys $^{352}$ Ile G $\alpha_{i2}$  significant stimulation above basal was observed in the presence of 10  $\mu$ M dopamine but not for D $_3$ -Cys $^{352}$ Ile G $\alpha_{i2}$ . Once again, significant coupling to G $\alpha_{i2}$  was regained for the D $_{3/2}$  chimera-Cys $^{352}$ Ile G $\alpha_{i2}$  fusion protein (**Figure 4.7B**). A similar pattern was seen with the dopamine receptor-Cys $^{351}$ Ile G $\alpha_{i3}$  fusion proteins, with both D $_{21}$  and D $_{3/2}$  fusion proteins showing significant agonist dependent stimulation. However, no stimulation above basal was seen with the D $_3$ -Cys $^{351}$ Ile G $\alpha_{i3}$  fusion membrane preparations (**Figure 4.7C**). By contrast, for each of the D $_{21}$ , D $_3$  and D $_{3/2}$ : G $\alpha_{o1}$  fusion protein preparations significant stimulation above basal levels of [ $^{35}$ S] GTP $\gamma$ S binding was observed in the presence of 10  $\mu$ M dopamine (**Figure 4.7D**). In summary then, it would seem that D $_{21}$  coupled promiscuously to all four G $_i$  subfamily members with dopamine-stimulated [ $^{35}$ S] GTP $\gamma$ S binding seen for G $\alpha_{i1}$ , G $\alpha_{i2}$ , G $\alpha_{i3}$ , G $\alpha_{o1}$  fusion proteins. The D $_3$  receptor coupled selectively and exclusively to G $\alpha_{o1}$  whilst the chimeric receptor showed ‘D $_2$ -like’ G protein coupling behaviour, and coupled to all four G $\alpha_i$  subunits. This pattern is in agreement with results from the receptor plus G protein co-transfection experiments (**section 4.2.5**).

#### 4.2.4 The action of various dopamine D<sub>2</sub>-like agonists at dopamine receptor: Cys→Ile G protein alpha subunit variant fusion proteins

To further characterise the dopamine receptor-G protein fusion proteins, the action of various, previously characterised dopamine D<sub>2</sub> receptor agonists was tested in membranes of HEK293T cells transfected with dopamine receptor-Cys → Ile G $\alpha$  subunit fusion protein cDNA, treated with pertussis toxin as above and harvested. As a general pattern, dopamine and NPA were able to stimulate [<sup>35</sup>S] GTP $\gamma$ S binding for all D<sub>2</sub>- Cys→Ile G $\alpha_{i/o}$  fusion proteins (**Figure 3.4D, Table 3.2**). However, for all of the agonists examined, stimulation of [<sup>35</sup>S] GTP $\gamma$ S binding through the D<sub>3</sub> receptor was only seen for the D<sub>3</sub>-Cys<sup>351</sup>Ile G $\alpha_{o1}$  fusion protein and not for the other three D<sub>3</sub>-G $\alpha_{i/o}$  Cys→Ile fusion proteins (**Figure 4.8 A-E, Table 4.3**). This supports the previous data indicating that D<sub>2</sub> is promiscuous and couples to all four G $\alpha_{i/o}$  subunits, whereas D<sub>3</sub> selectively and exclusively couples to G $\alpha_{o1}$ . Dopamine, NPA and quinpirole caused stimulation of [<sup>35</sup>S] GTP $\gamma$ S binding in all four of the D<sub>3/2</sub>-Cys →Ile G $\alpha_{i/o}$  fusion proteins in a concentration- dependent manner (**Figure 4.9A-D, Table 4.4**). This is in agreement with previous results showing that the chimeric receptor has a D<sub>2</sub>-like ability to couple promiscuously to all four G $\alpha_{i/o}$  subunits.

As a general pattern, agonists showed increased potency at D<sub>3</sub>-Cys<sup>351</sup>Ile G $\alpha_{o1}$  fusion proteins as compared to D<sub>2</sub>-Cys<sup>351</sup>Ile G $\alpha_{o1}$  fusion proteins, with dopamine, *m*-tyramine, *p*-tyramine, R-(+)-3PPP, S-(-)-3PPP, 7-OH DPAT, and quinpirole all showing significant increases in potency (**Figure 4.10 A, Table 3.2, Table 4.3**) (P<0.05, unpaired, two-tailed Students t-test). Similarly, in terms of efficacy, when compared to the maximal stimulation produced by the endogenous agonist dopamine at the given dopamine receptor-G $\alpha_{i/o}$  fusion protein, the values of E<sub>max</sub> for the agonists *p*-tyramine, S-(-)-3PPP, R-(+)-3PPP, 7-OH DPAT and quinpirole were significantly higher at D<sub>3</sub>- Cys<sup>351</sup>Ile G $\alpha_{o1}$  than D<sub>2</sub>-

Cys<sup>351</sup>Ile G $\alpha_{01}$  (**Figure 4.10 B, Table 3.2, Table 4.3**) ( $P < 0.05$ , un-paired, two-tailed Students t-test). However, NPA showed no significant difference in potency or  $E_{\max}$  between D<sub>21</sub>-Cys<sup>351</sup>Ile G $\alpha_{01}$  and D<sub>3</sub>-Cys<sup>351</sup>Ile G $\alpha_{01}$  fusion proteins.

The chimeric D<sub>3/2</sub>-Cys<sup>351</sup>Ile G $\alpha_{01}$  fusion protein showed pharmacology similar to the dopamine D<sub>3</sub>-Cys<sup>351</sup>Ile G $\alpha_{01}$  fusion protein for all agonists examined. Indeed, there was no significant difference between potency ( $pEC_{50}$ ) (**Figure 4.11 A**) or efficacy ( $E_{\max}$  relative to maximal dopamine stimulation) (**Figure 4.11 A, Table 4.3, Table 4.4**) ( $P < 0.05$ , unpaired, two-tailed Students t-test). All agonists produced a robust and concentration-dependent stimulation of [<sup>35</sup>S] GTP $\gamma$ S binding at both D<sub>3/2</sub>-Cys<sup>351</sup>Ile G $\alpha_{01}$  and D<sub>3/2</sub>-Cys<sup>351</sup>Ile G $\alpha_{i3}$ . Furthermore, there were no significant differences between the efficacy or potency of all agonists at these two dopamine D<sub>3/2</sub> receptor-fusion proteins (**Figure 4.12 A-B, Table 4.4**) ( $P < 0.05$ , unpaired, two-tailed Students t-test). For both the D<sub>3/2</sub>-Cys<sup>351</sup>Ile G $\alpha_{i1}$  and the D<sub>3/2</sub>-Cys<sup>352</sup>Ile G $\alpha_{i2}$  fusion proteins the agonists dopamine, NPA and quinpirole stimulated the binding of [<sup>35</sup>S] GTP $\gamma$ S in a robust and concentration-dependent manner. Furthermore, there were no significant differences between the potency or efficacy of dopamine and quinpirole at these two receptor-G protein fusion proteins (**Figure 4.12 C-D, Table 4.4**) ( $P < 0.05$ , unpaired, two-tailed Students t-test). It should be noted that the potency of both quinpirole and dopamine was significantly lower at D<sub>3/2</sub>-Cys<sup>351</sup>Ile G $\alpha_{i1}$  and D<sub>3/2</sub>-Cys<sup>352</sup>Ile G $\alpha_{i2}$  fusion proteins ( $pEC_{50} \sim 5.5$ ) when compared to the D<sub>3/2</sub>-Cys<sup>351</sup>Ile G $\alpha_{i3}$  or D<sub>3/2</sub>-Cys<sup>351</sup>Ile G $\alpha_{01}$  fusion proteins ( $pEC_{50} \sim 7.3$ ) indicating, perhaps, a lower efficiency of coupling to these  $\alpha$  subunits (**Table 4.4**).

The agonists *m*-tyramine and R-(+)-3PPP produced a concentration-dependent stimulation of [<sup>35</sup>S] GTP $\gamma$ S binding at D<sub>3/2</sub>-Cys<sup>352</sup>Ile G $\alpha_{i2}$  but not D<sub>3/2</sub>-Cys<sup>351</sup>Ile G $\alpha_{i1}$ . Conversely 7-OH DPAT stimulated [<sup>35</sup>S] GTP $\gamma$ S binding at D<sub>3/2</sub>-Cys<sup>351</sup>Ile G $\alpha_{i1}$  but not D<sub>3/2</sub>-Cys<sup>352</sup>Ile G $\alpha_{i2}$ . However, the partial agonists S-(-)-3PPP and *p*-tyramine failed to stimulate [<sup>35</sup>S]

GTP $\gamma$ S binding at either D<sub>3/2</sub>-Cys<sup>351</sup>Ile G $\alpha_{i1}$  or D<sub>3/2</sub>-Cys<sup>352</sup>Ile G $\alpha_{i2}$  (**Figure 4.9, Table 4.4**).

This is, perhaps, another example of agonist directed trafficking as described for the D<sub>21</sub> receptor in chapter 3.

There were differences, however, between the pattern of agonist action as described for D<sub>21</sub> and that seen at the chimeric dopamine receptor. For the D<sub>21</sub> receptor the ligands S(-)-3PPP and *p*-tyramine failed to stimulate activation of G $\alpha_{i1}$ , G $\alpha_{i2}$ , G $\alpha_{i3}$  (**Table 3.2, Figure 3.2**), whereas at the chimeric D<sub>3/2</sub> receptor these ligands produced a robust response at G $\alpha_{i3}$  and G $\alpha_{o1}$  (**Table 4.4, Figure 4.9 A-D**). Similarly the ligands *m*-tyramine and R-(+)-3PPP stimulated [<sup>35</sup>S] GTP $\gamma$ S binding to all four G $\alpha_{i/o}$  subunits with D<sub>21</sub> receptor fusions but only to G $\alpha_{i2}$ ,  $i_3$  and  $o_1$  with chimeric D<sub>3/2</sub> receptor fusions. Furthermore the rank order of potency of dopamine for the four different G $\alpha_{i/o}$  subunits differed between D<sub>21</sub> and D<sub>3/2</sub>. For the D<sub>21</sub> receptor the order of potency for dopamine was; D<sub>21</sub>-Cys<sup>351</sup>Ile G $\alpha_{i1}$  = D<sub>21</sub>-Cys<sup>352</sup>Ile G $\alpha_{i2}$  = D<sub>21</sub>-Cys<sup>351</sup>Ile G $\alpha_{i3}$  < D<sub>21</sub>-Cys<sup>351</sup>Ile G $\alpha_{o1}$ , whereas for D<sub>3/2</sub> it was; D<sub>3/2</sub>-Cys<sup>351</sup>Ile G $\alpha_{i1}$  = D<sub>3/2</sub>-Cys<sup>352</sup>Ile G $\alpha_{i2}$  < D<sub>3/2</sub>-Cys<sup>351</sup>Ile G $\alpha_{i3}$  = D<sub>3/2</sub>-Cys<sup>351</sup>Ile G $\alpha_{o1}$ .

In summary, from experiments using dopamine receptor-Cys  $\rightarrow$  Ile G $\alpha$  subunit fusion proteins, the chimeric D<sub>3/2</sub> dopamine receptor retains some 'D<sub>3</sub>-like' pharmacology in terms of affinity for [<sup>3</sup>H] spiperone, the efficacy of agonists at G $\alpha_{o1}$  and the potency of agonists at G $\alpha_{o1}$ . However, with the exchange of a twelve amino acid section of the 3<sup>rd</sup> intracellular loop of the D<sub>3</sub> receptor of the equivalent region of the D<sub>2</sub> receptor, the chimeric D<sub>3/2</sub> dopamine receptor has gained D<sub>21</sub>-like promiscuous coupling to the G $\alpha_i$  subfamily G proteins. Moreover, the pattern of agonist action in terms of rank-order of potencies or potential agonist directed trafficking differs between the D<sub>3/2</sub> and D<sub>21</sub> receptors.

**Table 4.3: The potency and efficacy of ligands at D<sub>3</sub> receptor-G protein fusions**

	D <sub>3</sub> Gα <sub>i1</sub>		D <sub>3</sub> Gα <sub>i2</sub>		D <sub>3</sub> Gα <sub>i3</sub>		D <sub>3</sub> Gα <sub>o1</sub>	
	pEC <sub>50</sub> , (±s.e.m)	E <sub>max</sub> , % DA (±s.e.m)	pEC <sub>50</sub> (±s.e.m)	E <sub>max</sub> , % DA (±s.e.m)	pEC <sub>50</sub> (±s.e.m)	E <sub>max</sub> , % DA (±s.e.m)	pEC <sub>50</sub> (±s.e.m)	E <sub>max</sub> , % DA (±s.e.m)
<b>Dopamine</b>	na		na		na		<b>7.60</b> (0.09)	<b>100</b>
<i>m</i> - <b>tyramine</b>	na		na		na		<b>6.64</b> (0.05)	<b>86</b> (6)
<i>p</i> - <b>tyramine</b>	na		na		na		<b>5.26</b> (0.09)	<b>84</b> (6)
<b>R-(+)-3-PPP</b>	na		na		na		<b>6.32</b> (0.01)	<b>96</b> (4)
<b>S-(-)-3-PPP</b>	na		na		na		<b>6.85</b> (0.12)	<b>63</b> (2)
<b>Quinpirole</b>	na		na		na		<b>7.69</b> (0.12)	<b>116</b> (2)
<b>NPA</b>	na		na		na		<b>8.13</b> (0.50)	<b>113</b> (3)
<b>7-OH DPAT</b>	na		na		na		<b>10.0</b> (0.08)	<b>68</b> (2)

Experiments were performed in triplicate to n = 3.

‘% DA’ refers to E<sub>max</sub> value of [<sup>35</sup>S] binding as compared to maximal dopamine

stimulation. The term ‘na’ refers to conditions in which no concentration-dependent

stimulation of [<sup>35</sup>S] GTPγS binding was observed.

**Table 4.4: The potency and efficacy of ligands at D<sub>3/2</sub> receptor-G protein fusions**

	D <sub>3/2</sub> Gα <sub>i1</sub>		D <sub>3/2</sub> Gα <sub>i2</sub>		D <sub>3/2</sub> Gα <sub>i3</sub>		D <sub>3/2</sub> Gα <sub>o1</sub>	
	pEC <sub>50</sub> , (±s.e.m)	E <sub>max</sub> , % DA (±s.e.m)	pEC <sub>50</sub> (±s.e.m)	E <sub>max</sub> , % DA (±s.e.m)	pEC <sub>50</sub> (±s.e.m)	E <sub>max</sub> , % DA (±s.e.m)	pEC <sub>50</sub> (±s.e.m)	E <sub>max</sub> , % DA (±s.e.m)
<b>Dopamine</b>	<b>5.32</b> (0.06)	<b>100</b>	<b>5.55</b> (0.18)	<b>100</b>	<b>7.24</b> (0.32)	<b>100</b>	<b>7.26</b> (0.12)	<b>100</b>
<i>m</i> -tyramine	na		<b>4.07</b> (0.16)	<b>53</b> (9)	<b>6.22</b> (0.17)	<b>81</b> (9)	<b>6.37</b> (0.09)	<b>79</b> (3)
<i>p</i> -tyramine	na		na		<b>5.53</b> (0.14)	<b>45</b> (5)	<b>5.22</b> (0.16)	<b>80</b> (1)
<b>R-(+)-3-PPP</b>	na		<b>4.09</b> (0.24)	<b>68</b> (11)	<b>6.08</b> (0.08)	<b>68</b> (7)	<b>5.98</b> (0.14)	<b>92</b> (4)
<b>S(-)-3-PPP</b>	na		na		<b>6.68</b> (0.36)	<b>40</b> (3)	<b>6.88</b> (0.10)	<b>50</b> (4)
<b>Quinpirole</b>	<b>5.60</b> (0.09)	<b>121</b> (13)	<b>5.34</b> (0.69)	<b>119</b> (3)	<b>7.42</b> (0.21)	<b>103</b> (4)	<b>7.61</b> (0.08)	<b>102</b> (3)
<b>NPA</b>	<b>9.38</b> (0.08)	<b>121</b> (12)	<b>8.55</b> (0.06)	<b>118</b> (1)	<b>9.28</b> (0.03)	<b>91</b> (3)	<b>9.14</b> (0.02)	<b>108</b> (2)
<b>7-OH DPAT</b>	<b>10.34</b> (0.19)	<b>76</b> (8)	na		<b>10.73</b> (0.88)	<b>34</b> (5)	<b>10.19</b> (0.03)	<b>64</b> (1)

Experiments were performed in triplicate to n = 3.

‘% DA’ refers to E<sub>max</sub> value of [<sup>35</sup>S] binding as compared to maximal dopamine stimulation. The term ‘na’ refers to conditions in which no concentration-dependent stimulation of [<sup>35</sup>S] GTPγS binding was observed. The potency of dopamine and quinpirole at the four different D<sub>3/2</sub> receptor-Gα subunit fusion-proteins were compared using a one-way ANOVA with Tukey’s post-hoc test using GraphPad Prism version 4. However, a significant difference was observed in pEC<sub>50</sub> between D<sub>3/2</sub> receptor fusion proteins for dopamine; D<sub>3/2</sub>Gα<sub>o1</sub> = D<sub>3/2</sub>Gα<sub>i3</sub> > D<sub>3/2</sub>Gα<sub>i2</sub> = D<sub>3/2</sub>Gα<sub>i1</sub> (P<0.001) and quinpirole; D<sub>3/2</sub>Gα<sub>o1</sub> = D<sub>3/2</sub>Gα<sub>i3</sub> > D<sub>3/2</sub>Gα<sub>i2</sub> = D<sub>3/2</sub>Gα<sub>i1</sub> (P<0.01).

#### 4.2.5 Generation and characterisation of cell lines stably and constitutively expressing D<sub>3</sub> or chimeric D<sub>3/2</sub> receptor and expressing Gα<sub>i1</sub>, Gα<sub>i2</sub>, Gα<sub>i3</sub>, or Gα<sub>o1</sub> Cys→Ile mutants from the inducible Flp-In locus

As for the Flp-In T-REx cell lines expressing pertussis toxin-insensitive Cys→Ile variants of Gα<sub>i1</sub>, <sub>2,3</sub> or <sub>o1</sub> at the inducible Flp-In locus and constitutively and stably expressing dopamine D<sub>21</sub> receptor (**section 3.2.7**), equivalent stable cell lines were generated constitutively expressing the dopamine D<sub>3</sub> receptor or D<sub>3/2</sub> chimeric receptor. Briefly Flp-In T-REx cells which inducibly express the Gα<sub>i1</sub>, <sub>i2</sub>, <sub>i3</sub>, or <sub>o1</sub> Cys→Ile pertussis-toxin insensitive mutants were transfected with dopamine D<sub>3</sub> or D<sub>3/2</sub> receptor cDNA and stable cell lines generated as described (**section 2.7.7**). Clones generated were screened for receptor expression by radioligand binding using a near saturating concentration of [<sup>3</sup>H] spiperone. Non-specific binding was estimated using 10 μM (+)-butaclamol. Clones showing significant expression of D<sub>3</sub> dopamine receptor (**Figure 4.13 A-D**) or chimeric D<sub>3/2</sub> dopamine receptor (**Figure 4.14 A-D**) were frozen down in liquid nitrogen until required for further characterisation. From experiments using both co-expression of receptor and pertussis toxin-insensitive G protein α subunits, or receptor-G protein fusion proteins it was clear that D<sub>21</sub> could couple promiscuously to all four Gα<sub>i/o</sub> subunits whereas D<sub>3</sub> coupled selectively to Gα<sub>o1</sub>. Consequently, for subsequent experiments characterising Flp-In T-REx cells expressing pertussis toxin-insensitive Gα subunits upon induction with tetracycline and constitutively expressing a dopamine receptor, it was decided to focus Cys<sup>351</sup>Ile Gα<sub>o1</sub> cell lines and one other from Cys<sup>351</sup>Ile Gα<sub>i1</sub>, Cys<sup>352</sup>Ile <sub>i2</sub>, Cys<sup>351</sup>Ile <sub>i3</sub>. Cys<sup>352</sup>Ile Gα<sub>i2</sub> cell lines were chosen to be consistent with the co-transfection work.

#### 4.2.6 Characterisation of Flp-In T-REx cells expressing Cys<sup>352</sup>Ile Gα<sub>i2</sub> or Cys<sup>351</sup>Ile Gα<sub>o1</sub> from the inducible Flp-In locus and constitutively expressing the D<sub>3</sub> dopamine receptor.

D<sub>3</sub> dopamine receptor expression levels both with and without the induction of G protein expression, were monitored using [<sup>3</sup>H] spiperone binding, with non-specific binding determined using 10 μM (+)-butaclamol. The D<sub>3</sub> receptor + Cys<sup>352</sup>Ile Gα<sub>i2</sub> cell line selected (D<sub>3</sub> Cys<sup>352</sup>Ile Gα<sub>i2</sub> clone 7) had a receptor expression level of approximately 0.2 pmol/mg membrane protein with no significant difference between expression with and without the induction of Gα<sub>i2</sub>. The D<sub>3</sub> + Cys<sup>351</sup>Ile Gα<sub>o1</sub> (D<sub>3</sub> Cys<sup>351</sup>Ile Gα<sub>o1</sub> clone 8) cell line had an expression level of around 1 pmol/mg without induction of Cys<sup>351</sup>Ile Gα<sub>o1</sub> and 1.5 pmol/mg upon induction of Cys<sup>351</sup>Ile Gα<sub>o1</sub>. For both the D<sub>3</sub> + Cys<sup>352</sup>Ile Gα<sub>i2</sub> and D<sub>3</sub> + Cys<sup>351</sup>Ile Gα<sub>o1</sub> cell lines, the affinity for [<sup>3</sup>H] spiperone was 0.1 nM (**Table 4.5**). As for both co-transfections and fusion proteins, a markedly lower affinity for [<sup>3</sup>H] spiperone was seen in D<sub>3</sub> receptor Flp-In cell lines than for the equivalent D<sub>21</sub> receptor Flp-In cell lines. Induction of G protein expression was monitored by western blotting using antisera raised against the C-terminal of the appropriate G protein (**Figure 4.15A**). For the D<sub>3</sub> receptor + Cys<sup>352</sup>Ile Gα<sub>i2</sub> cell line, significant levels of Gα<sub>i1/2</sub> were seen without induction of expression by tetracycline treatment. As in the case of the D<sub>21</sub> + Cys<sup>352</sup>Ile Gα<sub>i2</sub> double stable cell line this reflects high levels of endogenous Gα<sub>i2</sub> expression by HEK293 cells. A significant increase in Gα<sub>i2</sub> expression was, however, seen following treatment of the cells with 1 μg/ml tetracycline. This is consistent with the induced expression of the Cys<sup>351</sup>Ile Gα<sub>i2</sub> pertussis toxin-sensitive mutant. Without induction of G protein expression in the D<sub>3</sub> + Cys<sup>351</sup>Ile Gα<sub>o1</sub> cell line, no expression of Cys<sup>351</sup>Ile Gα<sub>o1</sub> (**Figure 4.15B**) was observed by western blotting, underlining the low expression of this G protein α subunit in HEK293 cells. Following treatment with tetracycline significant expression of Cys<sup>351</sup>Ile Gα<sub>o1</sub> was induced.

**Table 4.5: Expression levels of the D<sub>3</sub> receptor are unaffected by tetracycline-induced expression of Cys<sup>352</sup>Ile Gα<sub>i2</sub> or Cys<sup>351</sup>Ile Gα<sub>o1</sub> expression**

1µg/ml Tet.	-		+	
	<sup>3</sup> H Spiperone Binding			
Cell Line	B <sub>max</sub> , fMol.mg <sup>-1</sup> (± s.e.m.)	K <sub>d</sub> , nM (± s.e.m.)	B <sub>max</sub> , fMol.mg <sup>-1</sup> (± s.e.m.)	K <sub>d</sub> , nM (± s.e.m.)
<b>D<sub>3</sub> + Gα<sub>i2</sub></b> <b>(Clone 7)</b>	<b>199</b> <b>(27)</b>	<b>0.10</b> <b>(0.03)</b>	<b>247</b> <b>(21)</b>	<b>0.08</b> <b>(0.02)</b>
<b>D<sub>3</sub> + Gα<sub>o1</sub></b> <b>(Clone 8)</b>	<b>1555</b> <b>(227)</b>	<b>0.10</b> <b>(0.10)</b>	<b>1622</b> <b>(394)</b>	<b>0.13</b> <b>(0.01)</b>

Experiments were performed in triplicate to n = 3.

An unpaired Student's t-test was performed using GraphPad Prism version 4 (P<0.05). No significant difference in B<sub>max</sub> values were observed in receptor expression with and without induction of G protein expression.

**4.2.7 Agonist-dependent [<sup>35</sup>S] GTPγS binding is observed in membranes of the D<sub>3</sub> + Cys<sup>351</sup>Ile Gα<sub>o1</sub> cell line only upon induction of expression of Cys<sup>351</sup>Ile Gα<sub>o1</sub>. No stimulation of [<sup>35</sup>S] GTPγS binding above basal is observed in membranes of the D<sub>3</sub> + Cys<sup>352</sup>Ile Gα<sub>i2</sub> cell line with or without the induced expression of Cys<sup>352</sup>Ile Gα<sub>i2</sub>**

To further characterise the D<sub>3</sub> + Cys<sup>352</sup>Ile Gα<sub>i2</sub> and D<sub>3</sub> + Cys<sup>351</sup>Ile Gα<sub>o1</sub> cell lines the ability of a single concentration of dopamine to induce [<sup>35</sup>S] GTPγS binding for both, membranes (10 fMol of receptor) was investigated. A [<sup>35</sup>S] GTPγS binding assay was performed with or without 10 µM dopamine, and terminated by fast flow filtration onto GF/C filter paper. For the D<sub>3</sub> receptor plus Cys<sup>352</sup>Ile Gα<sub>i2</sub> cell line no stimulation of [<sup>35</sup>S] GTPγS binding was observed above basal with the addition of 10 µM dopamine, with or

without induction of Cys<sup>352</sup>Ile Gα<sub>i2</sub> expression (**Figure 4.16A**). This underlines the inability of the D<sub>3</sub> receptor to couple to Gα<sub>i2</sub> and is consistent with results using both transient co-transfection of receptor and G protein and receptor-G α subunit fusion proteins. There is however an increase in basal [<sup>35</sup>S] GTPγS levels upon induction of Cys<sup>352</sup>Ile Gα<sub>i2</sub>, which may reflect the intrinsic ability of G protein α subunits to load [<sup>35</sup>S] GTPγS. For the D<sub>3</sub> receptor plus Cys<sup>351</sup>Ile Gα<sub>o1</sub> cell line, agonist-dependent [<sup>35</sup>S] GTPγS binding above basal was seen only when Cys<sup>351</sup>Ile Gα<sub>o1</sub> expression was induced by tetracycline treatment. This underlines effective coupling of D<sub>3</sub> to Cys<sup>351</sup>Ile Gα<sub>o1</sub> as seen previously in experiments using both receptor and G protein co-transfections and receptor-G α subunits fusions. Again upon induction of Cys<sup>351</sup>Ile Gα<sub>o1</sub> expression, basal levels of [<sup>35</sup>S] GTPγS binding were observed to increase significantly (**Figure 4.16B**).

#### **4.2.8 Characterisation of Flp-In T-REx cells expressing Cys<sup>352</sup>Ile Gα<sub>i2</sub> or Cys<sup>351</sup>Ile Gα<sub>o1</sub> from the inducible Flp-In locus and constitutively expressing the chimeric D<sub>3/2</sub> dopamine receptor**

Expression levels of the chimeric D<sub>3/2</sub> dopamine receptor were monitored by [<sup>3</sup>H] spiperone binding, with non-specific binding determined with the addition of 10 μM (+)-butaclamol. For the selected cell line constitutively expressing D<sub>3/2</sub> plus Cys<sup>351</sup>Ile Gα<sub>i2</sub> the receptor was around 0.5 pMol/mg membrane protein (**Table 4.6**). For the selected cell line expressing D<sub>3/2</sub> plus Cys<sup>351</sup>Ile Gα<sub>o1</sub> receptor density was approximately 0.3 pMol/mg. In both cases the D<sub>3/2</sub> receptor showed D<sub>3</sub>-like affinity for [<sup>3</sup>H] spiperone with a K<sub>d</sub> of ~ 0.1 nM. For both cell lines no significant difference was seen for either receptor expression levels or affinity for [<sup>3</sup>H] spiperone with or without the induction of G protein α subunit expression.

**Table 4.6: Expression levels of the D<sub>3/2</sub> receptor are unaffected by tetracycline induced expression of Cys<sup>352</sup>Ile Gα<sub>i2</sub>**

<b>1μg/ml Tet.</b>	<b>-</b>		<b>+</b>	
	<b>[<sup>3</sup>H] Spiperone Binding</b>			
<b>Cell Line</b>	<b>B<sub>max</sub>, fMol.mg<sup>-1</sup></b> (± s.e.m.)	<b>K<sub>d</sub>, nM</b> (± s.e.m.)	<b>B<sub>max</sub>, fMol.mg<sup>-1</sup></b> (± s.e.m.)	<b>K<sub>d</sub>, nM</b> (± s.e.m.)
<b>D<sub>3/2</sub> + Gα<sub>i2</sub></b>	<b>491</b> <b>(180)</b>	<b>0.10</b> <b>(0.01)</b>	<b>681</b> <b>(64)</b>	<b>0.12</b> <b>(0.04)</b>
<b>D<sub>3/2</sub> + Gα<sub>o1</sub></b>	<b>256</b> <b>(41)</b>	<b>0.08</b> <b>(0.04)</b>	<b>291</b> <b>(40)</b>	<b>0.13</b> <b>(0.01)</b>

Experiments were performed in triplicate to n = 3.

An unpaired student's t-test was performed using GraphPad Prism version 4 (P<0.05). No significant differences in B<sub>max</sub> values were observed in receptor expression with and without induction of G protein expression.

#### 4.2.9 Agonist-dependent [<sup>35</sup>S] GTPγS binding is observed in membranes of the expressing D<sub>3/2</sub> upon induction of expression of Cys<sup>351</sup>Ile Gα<sub>o1</sub> or Cys<sup>352</sup>Ile Gα<sub>i2</sub>

For the cell line expressing the D<sub>3/2</sub> chimera and inducibly expressing Cys<sup>352</sup>Ile Gα<sub>i2</sub>, without the induction of Cys<sup>352</sup>Ile Gα<sub>i2</sub> expression, the addition of 10 μM dopamine was unable to stimulate [<sup>35</sup>S] GTPγS binding above basal levels (**Figure 4.17A**). However, upon induction of Gα<sub>i2</sub> expression a small but significant increase in basal levels of [<sup>35</sup>S] GTPγS binding was seen, reflecting an increase in G protein levels within the cell. Upon addition of 10 μM dopamine a significant stimulation of [<sup>35</sup>S] GTPγS binding was seen above basal levels. This reflects the ability of the chimeric D<sub>3/2</sub> receptor to couple to Cys<sup>352</sup>Ile Gα<sub>i2</sub>, and indicates that the chimeric receptor has a promiscuous, D<sub>2</sub>-like, G protein coupling as apposed to the selective coupling to Gα<sub>o1</sub> seen for D<sub>3</sub>. This is in agreement with both the experiments using both the co-expression of receptor and G protein α subunit or receptor-G protein fusion proteins.

For the cell line expressing the D<sub>3/2</sub> chimera and inducibly expressing Cys<sup>351</sup>Ile Gα<sub>o1</sub>, [<sup>35</sup>S] GTPγS binding was not stimulated above basal levels with the addition of 10 μM dopamine (**Figure 4.17B**). With induction of Cys<sup>351</sup>Ile Gα<sub>o1</sub> expression an increase in basal [<sup>35</sup>S] GTPγS binding was again seen, and upon addition of 10 μM dopamine there was a significant stimulation of [<sup>35</sup>S] GTPγS binding above basal, underlining the efficient coupling of the chimeric D<sub>3/2</sub> receptor to Gα<sub>o1</sub>.

**Figure 4.1: Schematic representation of the chimeric dopamine receptor (D<sub>3/2</sub>) consisting of a dopamine D<sub>3</sub> receptor with twelve amino acids in the c-terminus of intracellular loop 3 exchanged by the equivalent region in the D<sub>2</sub> receptor**

Human dopamine D<sub>2</sub> and D<sub>3</sub> receptors are shown, highlighting the 3<sup>rd</sup> intracellular loop and transmembrane domain VI (TM VI). A chimera was made where the highlighted sequence of the D<sub>3</sub> receptor was replaced by the equivalent region of the D<sub>2</sub> receptor (residues coloured red). The exchanged twelve amino acids are flanked by homologous regions to the c- and n-terminal sides. This chimera was generated by sequential site-directed mutagenesis and was the gift of A. Wise (GSK, Harlow, UK)

Figure 4.1

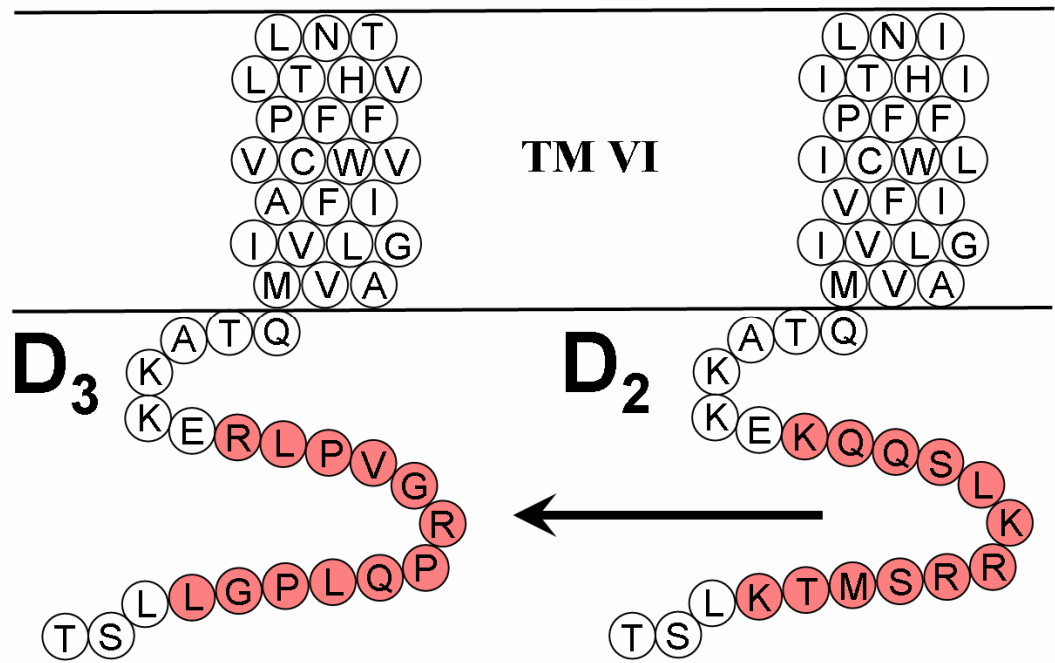


**Figure 4.2: Characterisation of HEK293T transiently co-transfected with pertussis toxin-insensitive Cys<sup>352</sup>Ile G $\alpha_{i2}$  or Cys<sup>351</sup>Ile G $\alpha_{o1}$  cDNA and dopamine receptor (D<sub>2l</sub>, D<sub>3</sub> or D<sub>3/2</sub>) cDNA.**

HEK293T cells were transiently co-transfected with pertussis toxin-insensitive Cys<sup>352</sup>Ile G $\alpha_{i2}$  or Cys<sup>351</sup>Ile G $\alpha_{o1}$  cDNA and dopamine receptor (D<sub>2l</sub>, D<sub>3</sub> or D<sub>3/2</sub>) cDNA. These cells were treated with or without pertussis toxin (25ng/ml) 16 hours prior to cell harvest. Cell membranes were then prepared, resolved by SDS-PAGE and immunoblotted to detect either G $\alpha_{i2}$  or G $\alpha_{o1}$ . Receptor expression levels were estimated using [<sup>3</sup>H] spiperone saturation binding (**Table 4.1**)

**Figure 4.2**

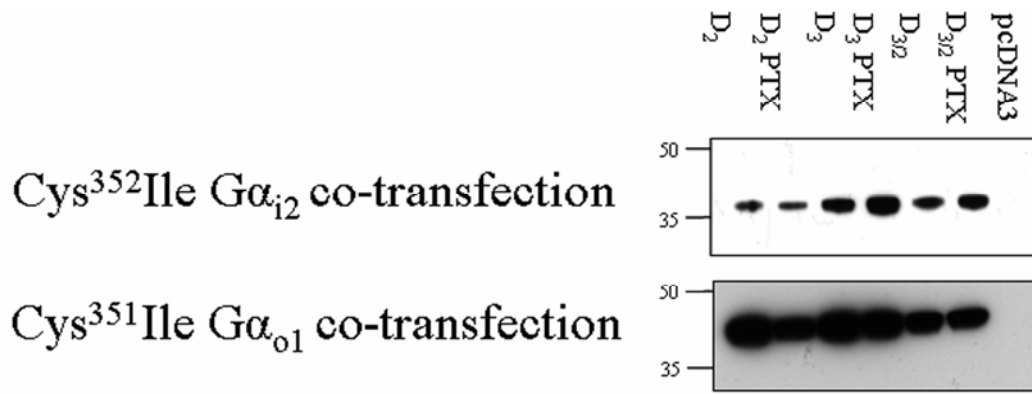


**Figure 4.3: 10  $\mu$ M GDP was the optimal concentration for [ $^{35}$ S] GTP $\gamma$ S assays using membranes from HEK293T cells co-transfected with dopamine D<sub>3</sub> receptor and Cys<sup>351</sup>Ile G $\alpha_{o1}$  cDNA**

HEK293T cells were transiently co-transfected with pertussis toxin-insensitive Cys<sup>351</sup>Ile G $\alpha_{o1}$  cDNA and D<sub>3</sub> dopamine receptor cDNA. These cells were treated with pertussis toxin (25ng/ml) 16 hours prior to cell harvest. Cell membranes were then prepared, resolved by SDS-PAGE and immunoblotted to detect either or G $\alpha_{i2}$  or G $\alpha_{o1}$ . Receptor expression levels were measured in [ $^3$ H] spiperone saturation binding studies. A [ $^{35}$ S] GTP $\gamma$ S assay was set up with 10 fMol of receptor, various concentrations of GDP and with or without the addition of 10 $\mu$ M dopamine. An immunoprecipitation step was included in the assay, using an in-house antiserum raised against the C-terminal tail of G $\alpha_{o1}$ .

Figure 4.3

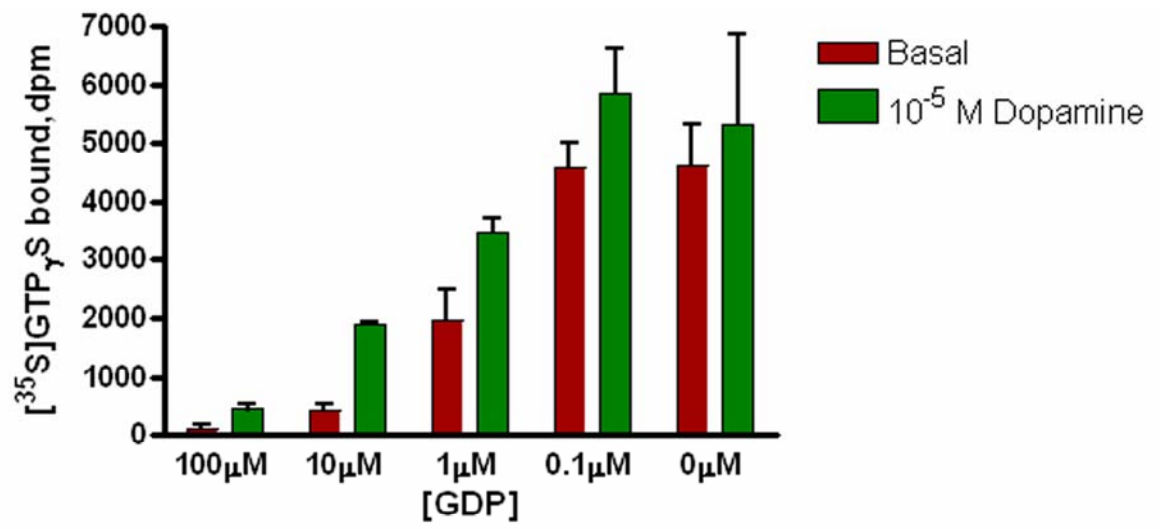


**Figure 4.4: The Chimeric D<sub>3/2</sub> dopamine receptor can couple to both Cys<sup>352</sup>Ile Gα<sub>i2</sub> and Cys<sup>351</sup>Ile Gα<sub>o1</sub>**

HEK293T were transiently co-transfected with a dopamine receptor (D<sub>21</sub>, D<sub>3</sub> or D<sub>3/2</sub>) cDNA and either Cys<sup>352</sup>Ile Gα<sub>i2</sub> (**A**) or Cys<sup>351</sup>Ile Gα<sub>o1</sub> (**B**). Cells were treated with or without pertussis toxin (25ng/ml) 16 hours prior to cell harvest. Membranes from these cells were used to measure basal [<sup>35</sup>S]GTPγS binding and the effect of 100 μM dopamine on this. A [<sup>35</sup>S] GTPγS protocol was used that included an immunoprecipitation step using in-house antisera raised against the C-terminal tail of Gα<sub>i2</sub> (**A**) or Gα<sub>o1</sub> (**B**). The significance of differences between basal and dopamine stimulated [<sup>35</sup>S] GTPγS binding was determined using an unpaired Students t-test (P<0.05), significant differences are noted as follows:

P < 0.05		N = 3	
P value	Definition	Summary	
< 0.001	extremely significant	***	
0.001 to 0.01	very significant	**	
0.01 to 0.05	significant	*	
> 0.05	not significant		

Figure 4.4

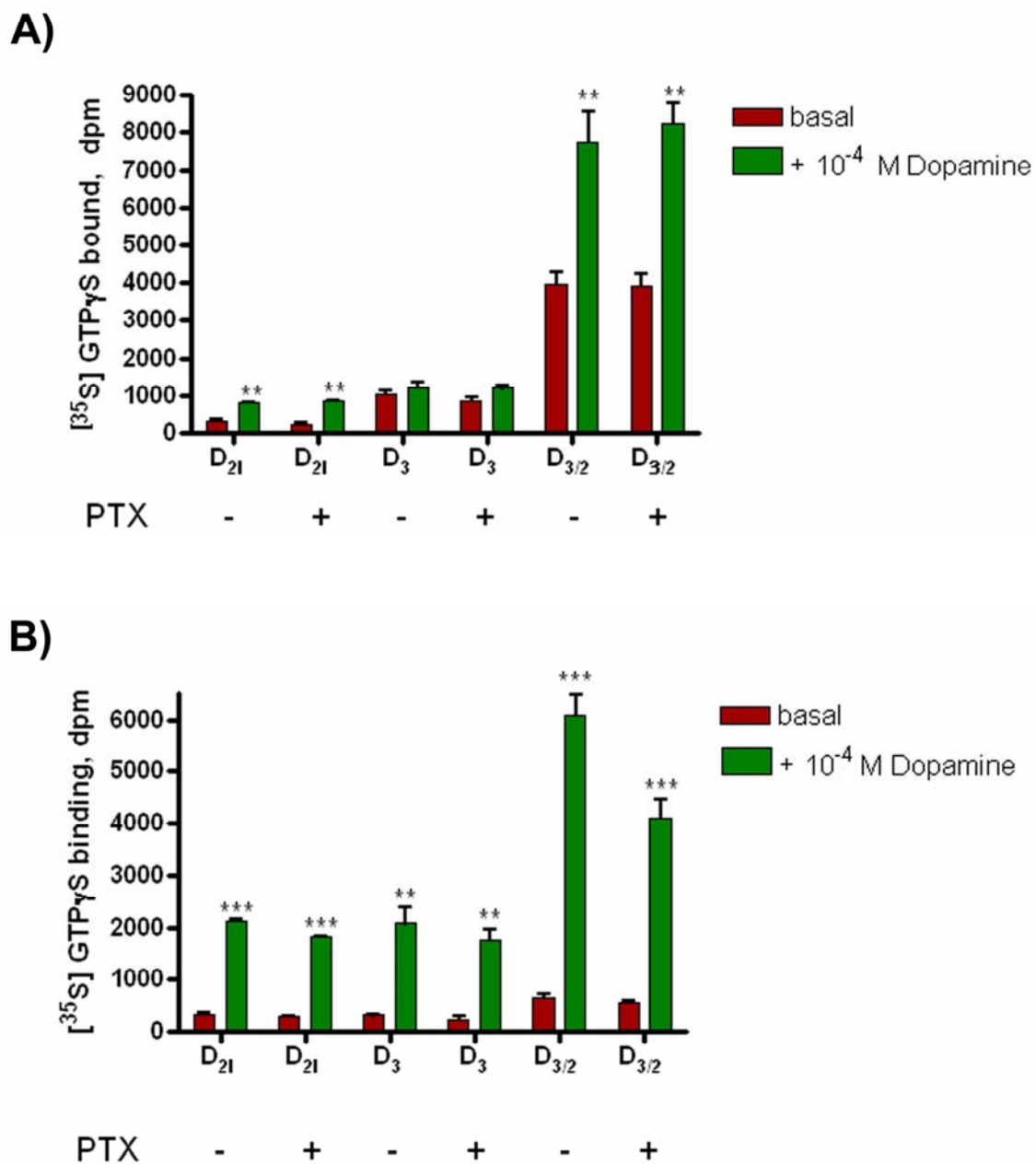


**Figure 4.5: Generation of dopamine D<sub>3</sub> receptor or chimeric D<sub>3/2</sub> receptor-Cys→Ile variant G protein  $\alpha$  subunit fusion proteins**

A series of fusion proteins were generated by linking Cys-Ile mutant, pertussis toxin-insensitive variants of G $\alpha_{i1}$ , G $\alpha_{i2}$ , G $\alpha_{i3}$  and G $\alpha_{o1}$  in frame with the C-terminal tail of the human D<sub>3</sub> receptor or the chimeric D<sub>3/2</sub> receptor.

Figure 4.5

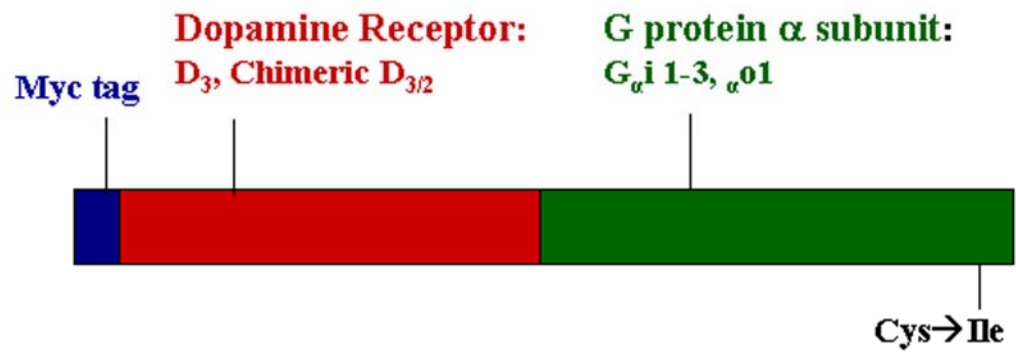


**Figure 4.6: Characterisation of dopamine D<sub>3</sub> receptor and chimeric D<sub>3/2</sub> receptor-Cys→Ile variant G protein  $\alpha$  subunit fusion proteins: addition of increasing amounts of fusion protein into [<sup>35</sup>S] GTP $\gamma$ S reactions results in a proportional increase in [<sup>35</sup>S] GTP $\gamma$ S bound**

D<sub>3</sub>-Cys<sup>351</sup>Ile-G $\alpha$ <sub>o1</sub> or D<sub>3/2</sub>-Cys<sup>351</sup>Ile-G $\alpha$ <sub>o1</sub> was expressed transiently in HEK293T cells. Following pertussis toxin treatment (25 ng/ml, 24 h) cells were harvested, membranes generated and fusion protein expression estimated using [<sup>3</sup>H] spiperone saturation binding (**Table 4.2**). [<sup>35</sup>S]GTP $\gamma$ S binding studies were performed in the absence and presence of 100  $\mu$ M dopamine and with varying amounts of receptor-G protein fusion protein (D<sub>3</sub>-Cys<sup>351</sup>Ile-G $\alpha$ <sub>o1</sub>: 1-50 fMol per reaction, D<sub>3/2</sub>-Cys<sup>351</sup>Ile-G $\alpha$ <sub>o1</sub>: 1-40 fMol per reaction).

Figure 4.6

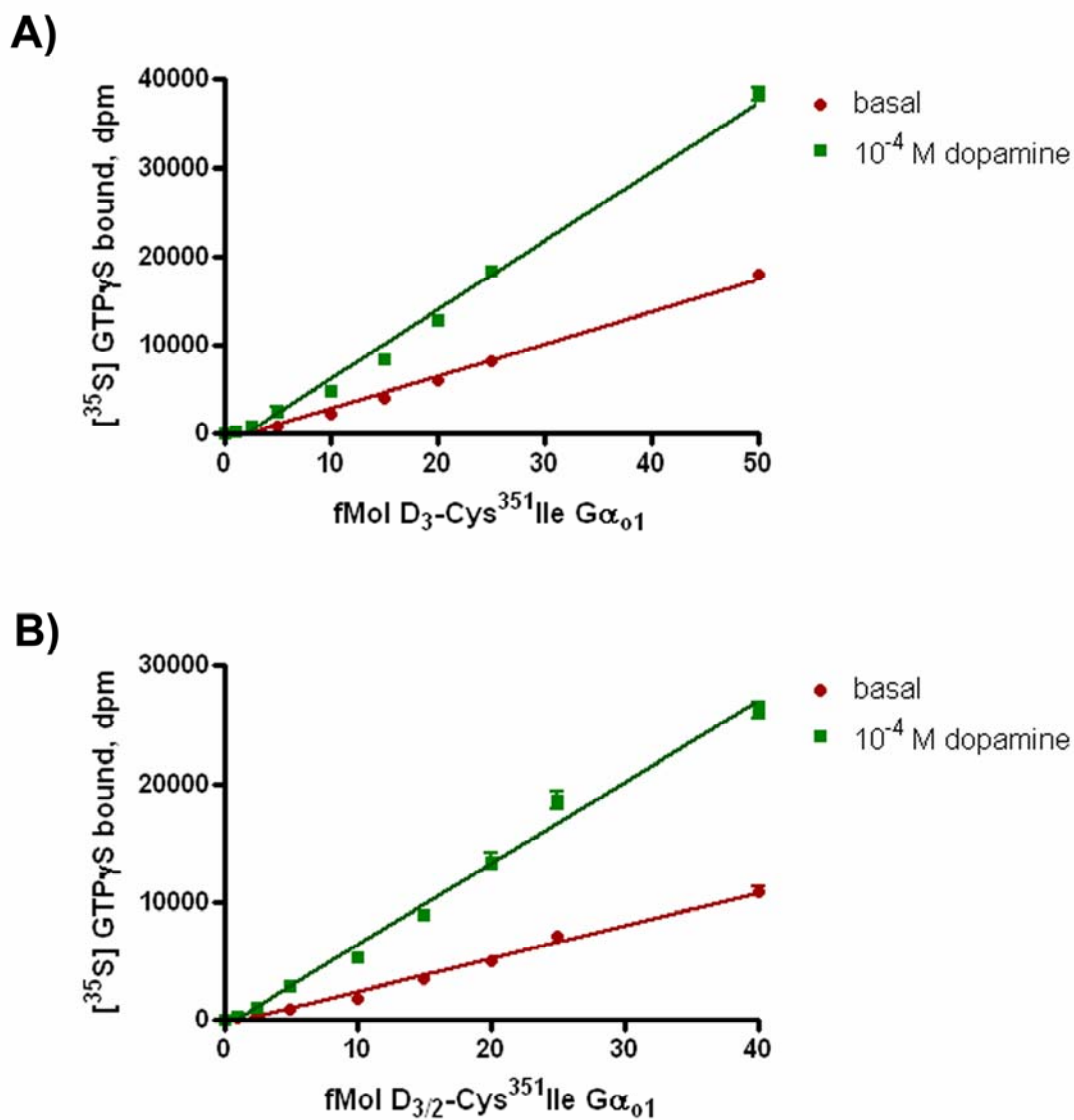


**Figure 4.7: Dopamine stimulated [<sup>35</sup>S] GTPγS binding above basal levels was observed only when the dopamine D<sub>3</sub> receptor was fused to Gα<sub>o1</sub>.**

HEK293T were transiently transfected with dopamine (D<sub>21</sub>, D<sub>3</sub> or D<sub>3/2</sub>) receptor-Cys→Ile G α subunit fusion protein cDNAs; **(A)** dopamine receptor-Cys<sup>351</sup>Ile Gα<sub>i1</sub>, **(B)** dopamine receptor-Cys<sup>352</sup>Ile Gα<sub>i2</sub> **(C)** dopamine receptor-Cys<sup>351</sup>Ile Gα<sub>i3</sub> **(D)** dopamine receptor-Cys<sup>351</sup>Ile Gα<sub>o1</sub>. Cells were treated with or without pertussis toxin 16 hours prior to cell harvest. Membranes from these cells were used to measure basal [<sup>35</sup>S]GTPγS binding and the effect of 100 μM dopamine on this. A [<sup>35</sup>S] GTPγS protocol was used that included an immunoprecipitation step using antisera raised against the C-terminal tail of Gα<sub>i1/2</sub> **(A + B)**, Gα<sub>i3</sub> **(C)** or Gα<sub>o1</sub> **(D)**. The significance of differences between basal and dopamine stimulated [<sup>35</sup>S] GTPγS binding was determined using an unpaired Students t-test (P<0.05), significant differences are notated as follows.

P < 0.05		N = 3	
P value	Definition	Summary	
< 0.001	extremely significant	***	
0.001 to 0.01	very significant	**	
0.01 to 0.05	significant	*	
> 0.05	not significant		

Figure 4.7

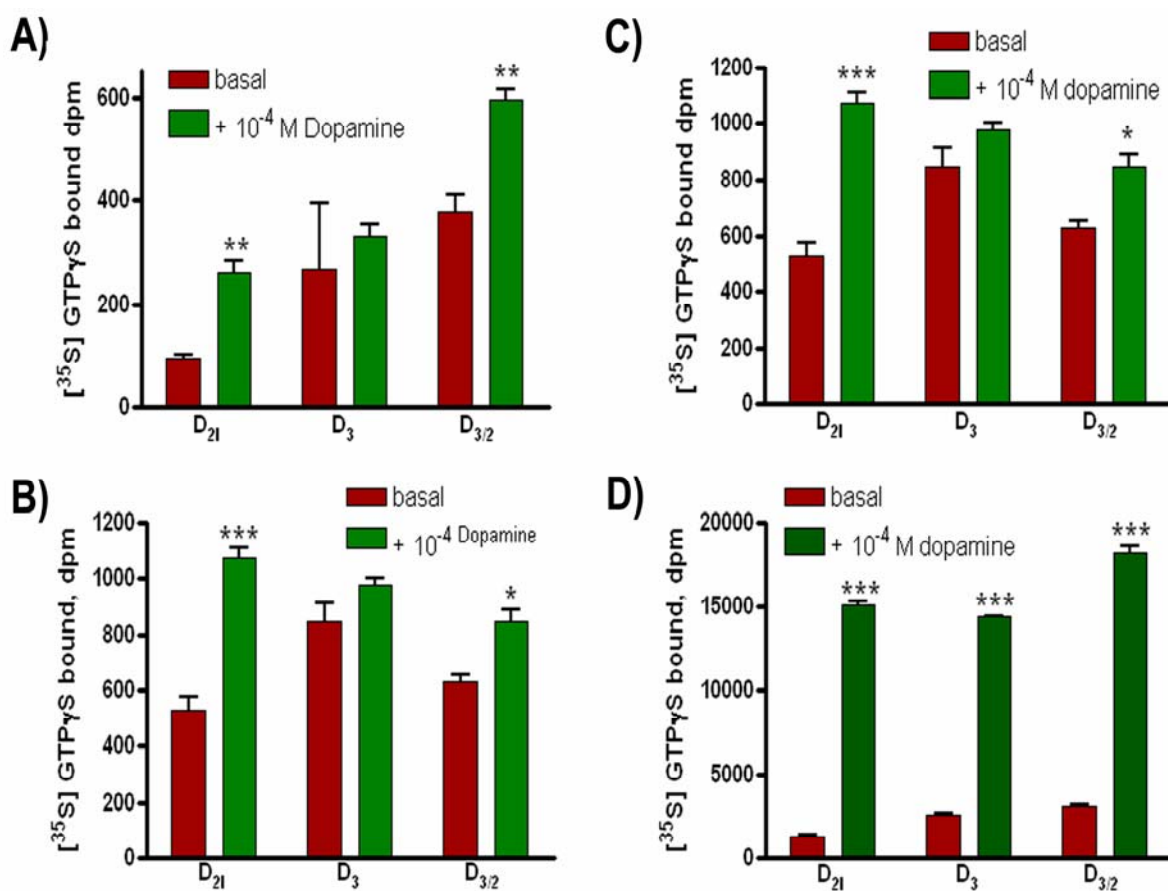


**Figure 4.8: G protein fusion proteins identify agonists at the D<sub>3</sub> receptor but only when coupled to G $\alpha$ <sub>01</sub>**

Each of the dopamine D<sub>3</sub> receptor-Cys→Ile variant G $\alpha$  fusion proteins; (A) D<sub>3</sub>-G $\alpha$ <sub>i1</sub>, (B) D<sub>3</sub>-G $\alpha$ <sub>i2</sub>, (C) D<sub>3</sub>-G $\alpha$ <sub>i3</sub>, (D + E) D<sub>3</sub>-G $\alpha$ <sub>o1</sub> was expressed transiently in HEK293 cells. (A-D) show data in terms of [<sup>35</sup>S] GTP $\gamma$ S bound as measured by fluorescence emitted following excitation of scintillant beads, arbitrary units (a.u.). (E) Shows data in terms of [<sup>35</sup>S] GTP $\gamma$ S bound as a % of maximal dopamine signal for D<sub>3</sub>-G $\alpha$ <sub>o1</sub> as agonists failed to generate a response for the other D<sub>3</sub>-G $\alpha$ <sub>i/o</sub> fusion proteins. Following pertussis toxin treatment (25ng/ml, 16 h) cells were harvested, membranes generated and [<sup>35</sup>S]GTP $\gamma$ S binding studies performed in the absence and presence of varying concentrations of a variety of ligands (dopamine (◆), m-tyramine (■), p-tyramine (□), R-(+)-3-PPP (▲), S-(-)-3PPP (△), quinpirole (▽), NPA (●), 7-OH DPAT(◇)) reported to have affinity and efficacy at dopamine D<sub>2</sub>-like receptors. Data are representative and full details are provided in **Table 4.3**.

Figure 4.8

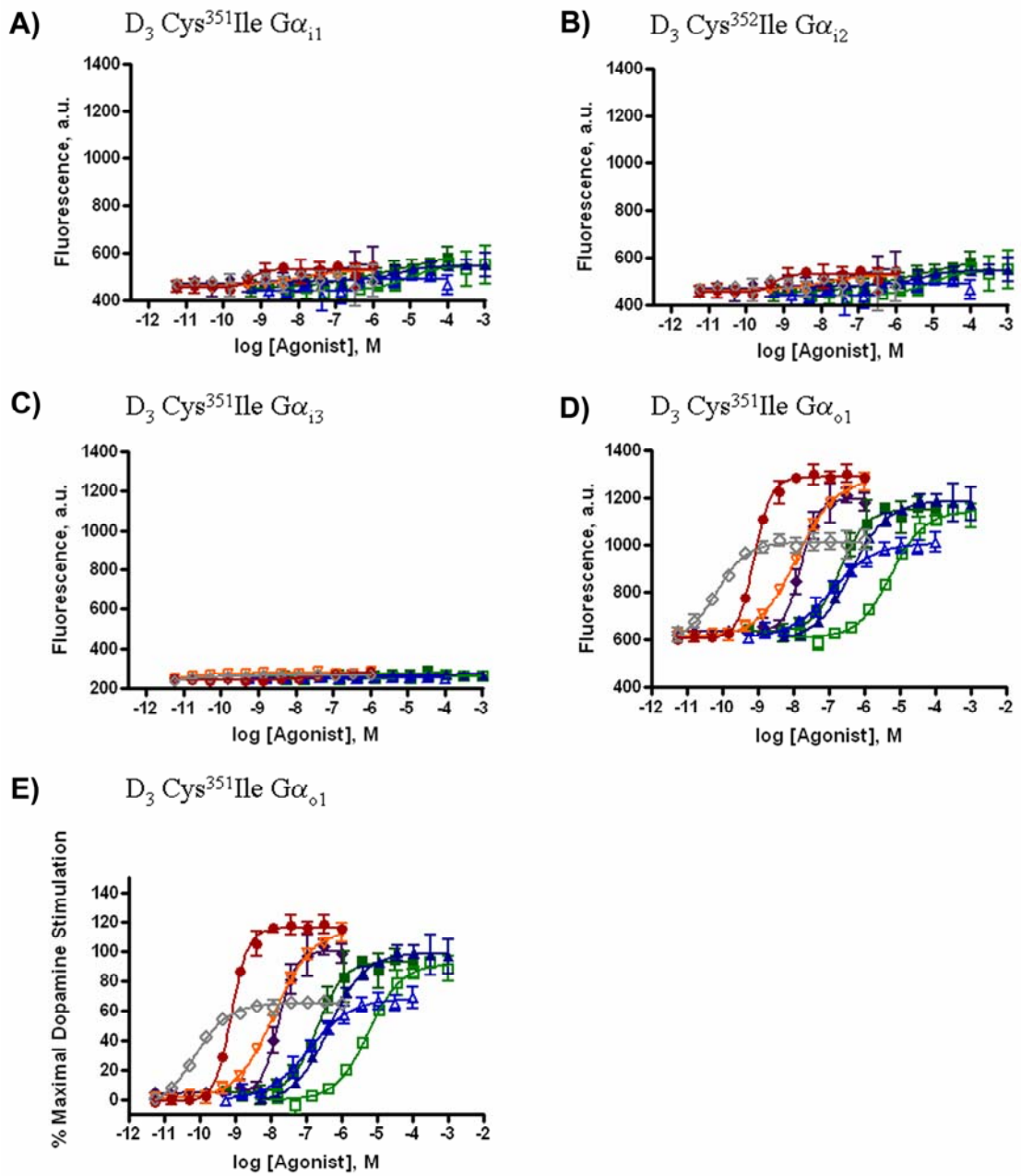


**Figure 4.9: G protein fusion proteins identify agonists at the D<sub>3/2</sub> receptor when coupled to all four pertussis-toxin resistant Gα<sub>i/o</sub> subunits**

Each of the dopamine D<sub>3/2</sub> receptor-Cys→Ile variant Gα fusion proteins; **(A)** D<sub>3/2</sub>-Gα<sub>i1</sub>, **(B)** D<sub>3/2</sub>-Gα<sub>i2</sub>, **(C)** D<sub>3/2</sub>-Gα<sub>i3</sub>, **(D + E)** D<sub>3/2</sub>-Gα<sub>o1</sub> was expressed transiently in HEK293 cells. Following pertussis toxin treatment (25ng/ml, 16 h) cells were harvested, membranes generated and [<sup>35</sup>S]GTPγS binding studies performed in the absence and presence of varying concentrations of a variety of ligands (dopamine (◆), m-tyramine (■), p-tyramine (□), R-(+)-3-PPP (▲), S-(-)-3PPP (△), quinpirole (▽), NPA (●), 7-OH DPAT(◇)) reported to have affinity and efficacy at dopamine D<sub>2</sub> like receptors. Data are representative and full details are provided in **Table 4.4**.

Figure 4.9

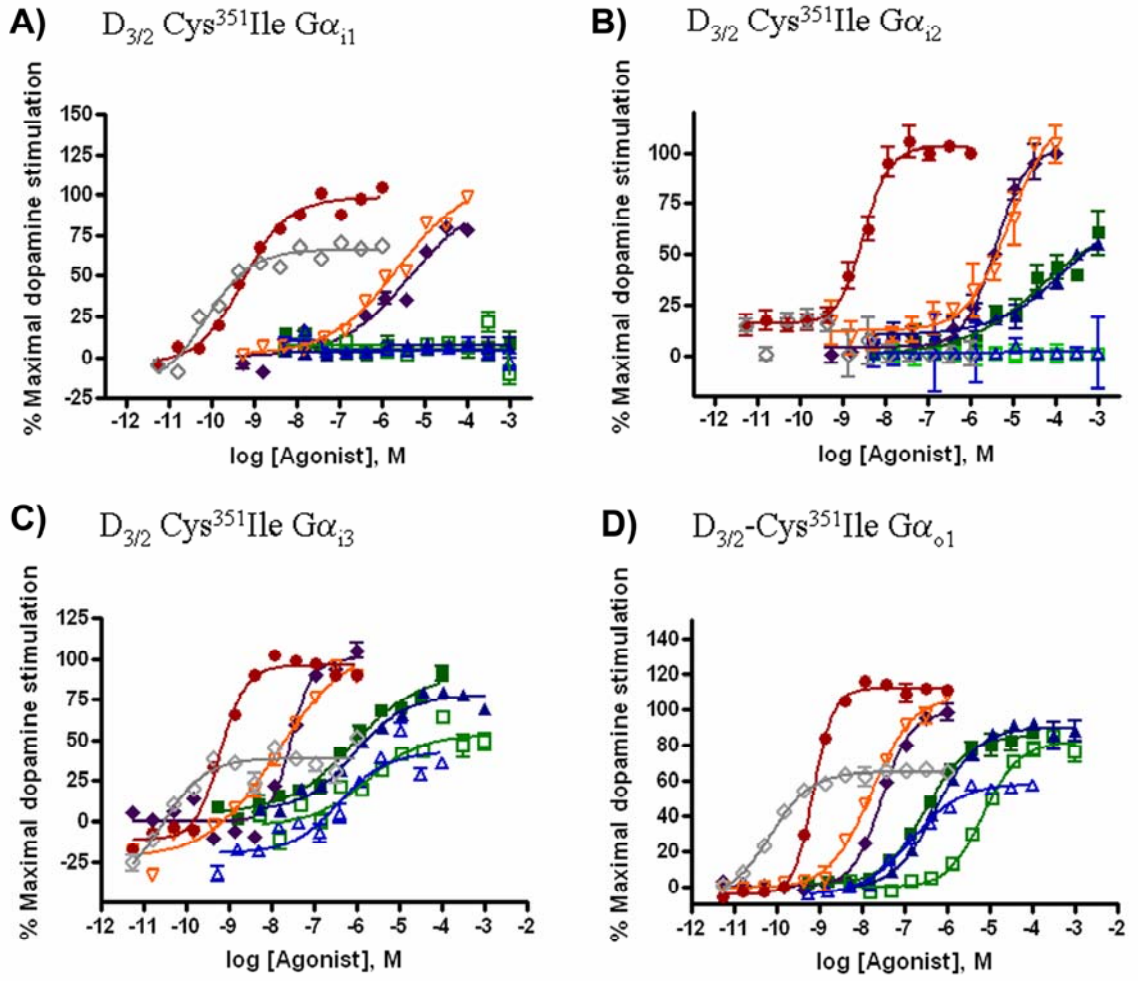


**Figure 4.10: Comparison of the potency and efficacy at the D<sub>21</sub>-G<sub>α<sub>01</sub></sub> fusion protein and D<sub>3</sub>-G<sub>α<sub>01</sub></sub> fusion protein receptor of various agonists reveals a trend towards both higher potency and efficacy at the D<sub>3</sub> receptor.**

The potencies (**A**) and efficacies (**B**) of various ligands at either the D<sub>21</sub>-G<sub>α<sub>01</sub></sub> fusion protein (**Figure 3.4D, Table 3.2**) or the D<sub>3</sub>-G<sub>α<sub>01</sub></sub> fusion protein (**Figure 4.8 E, Table 4.3**) were compared using an unpaired Students t-test (P<0.05). Significant differences are annotated as follows:

P < 0.05		N = 3
P value	Definition	Summary
< 0.001	extremely significant	***
0.001 to 0.01	very significant	**
0.01 to 0.05	significant	*
> 0.05	not significant	

Figure 4.10

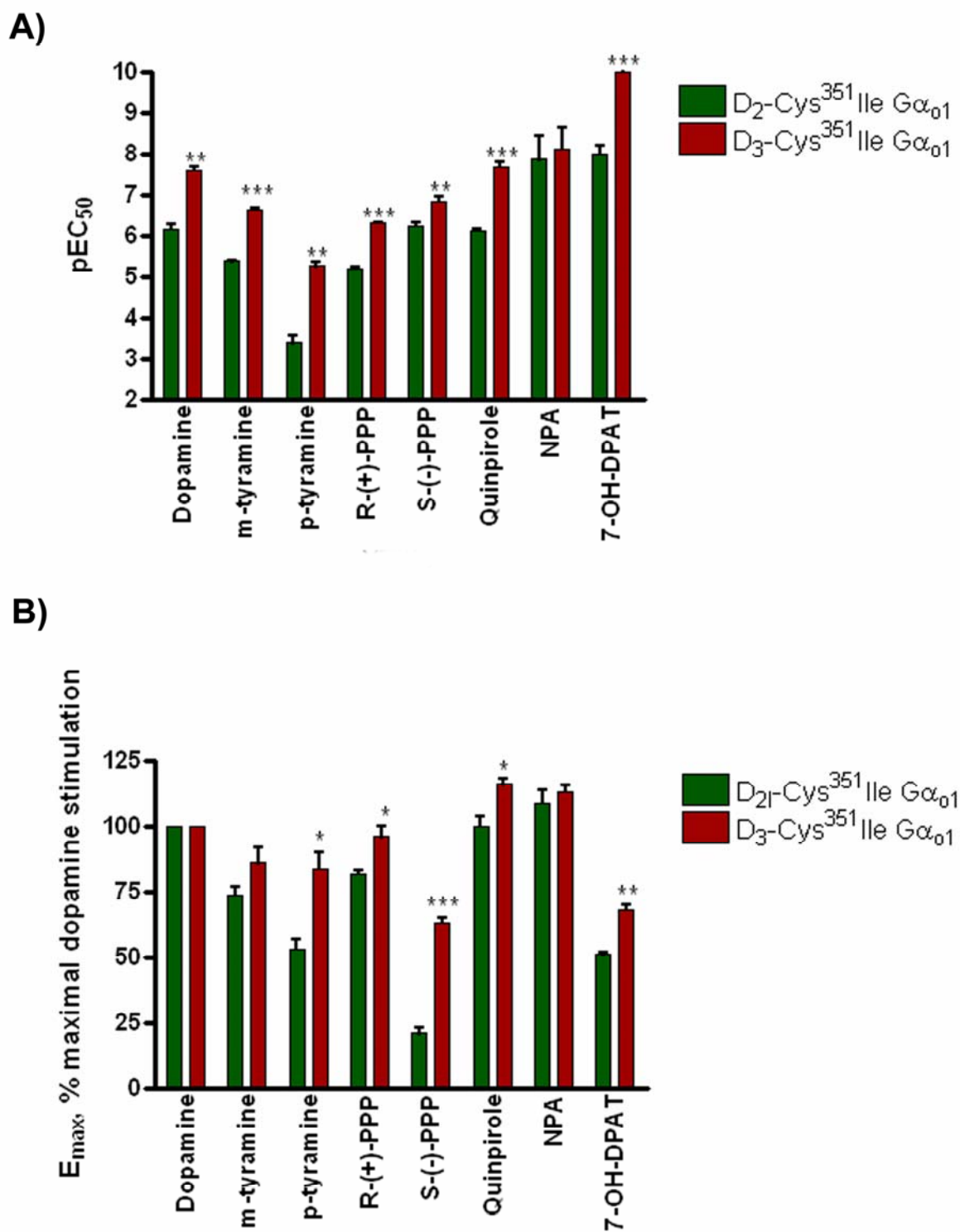


**Figure 4.11: Comparison of the potency and efficacy at the D<sub>3</sub>-Gα<sub>01</sub> fusion protein and D<sub>3/2</sub>-Gα<sub>01</sub> fusion protein of various agonists shows no significant differences in efficacy.**

The potencies (**A**) and efficacies (**B**) of various ligands at either the D<sub>3</sub>-Gα<sub>01</sub> fusion protein (**Figure 4.8 E, Table 4.3**) or the D<sub>3/2</sub>-Gα<sub>01</sub> fusion protein (**Figure 4.9 D, Table 4.4**) were compared using an unpaired Students t-test (P<0.05).

Figure 4.11

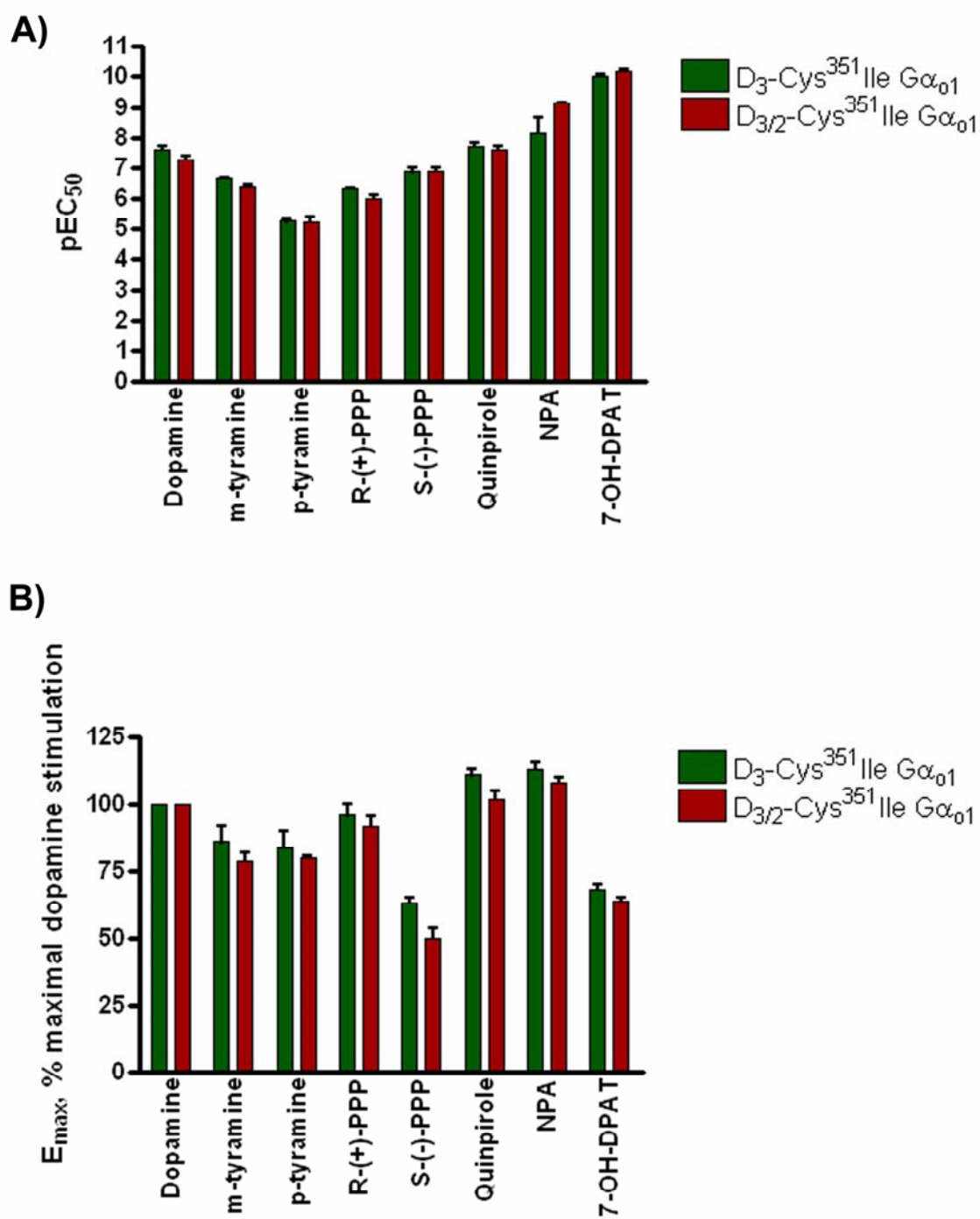


**Figure 4.12: Comparison of the potency and efficacy of various agonists at the D<sub>3/2</sub>-Gα<sub>i3</sub> and D<sub>3/2</sub>-Gα<sub>o1</sub> fusion proteins.**

The potencies (**A**) and efficacies (**B**) of various ligands at either the D<sub>3</sub>-Gα<sub>i3</sub> fusion protein (**Figure 4.8 C, Table 4.4**) or the D<sub>3/2</sub>-Gα<sub>o1</sub> fusion protein (**Figure 4.8 D, Table 4.4**) were compared using an unpaired Student's t-test (P<0.05). Similarly the potencies (**C**) and efficacies (**D**) of quinpirole, dopamine and NPA at either D<sub>3/2</sub>-Gα<sub>i1</sub> or D<sub>3/2</sub>-Gα<sub>i2</sub> were compared using an unpaired Students t-test (P<0.05)

Figure 4.12

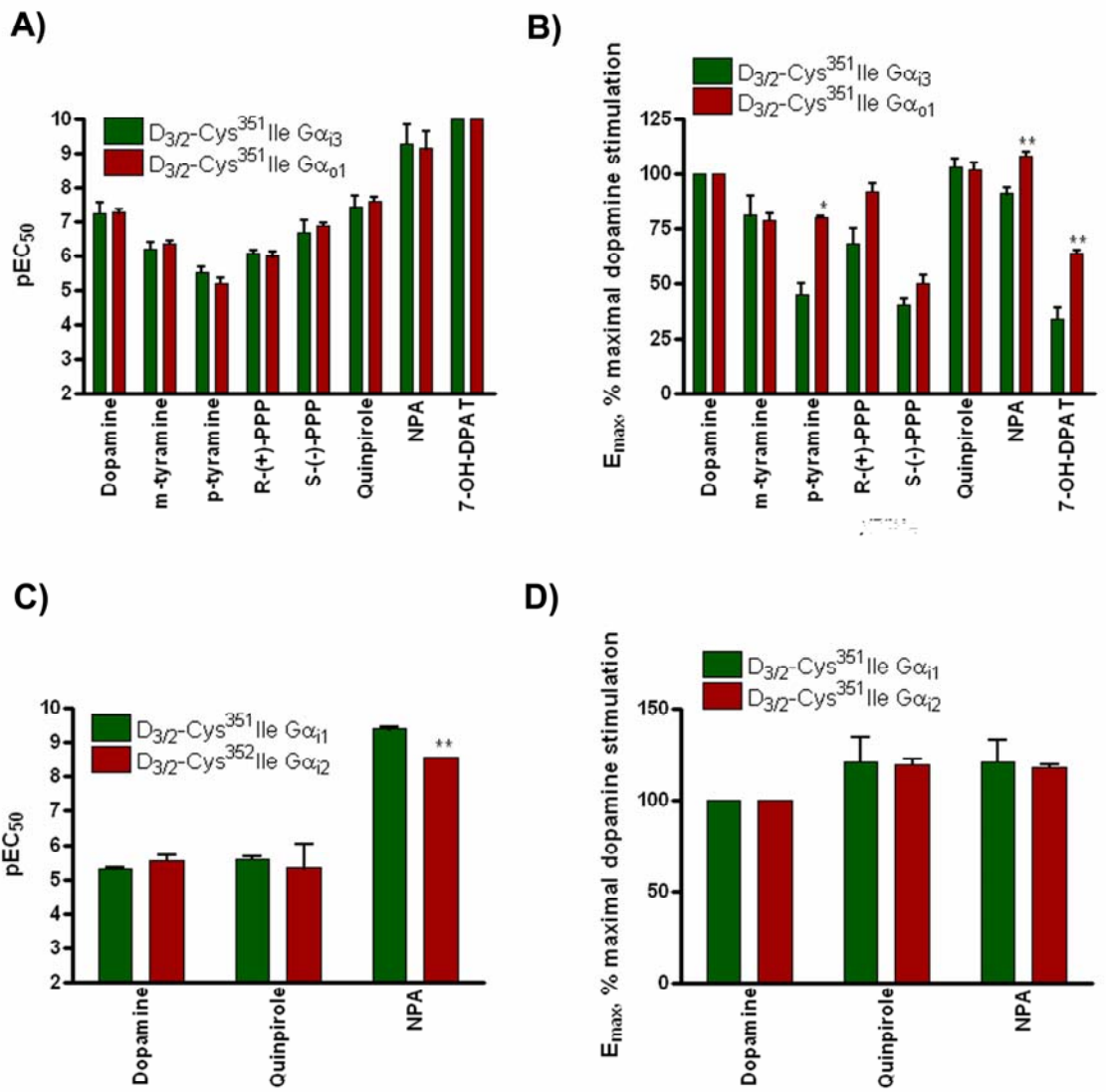


**Figure 4.13: Characterisation of Flp-In T-REx cells harbouring pertussis toxin-insensitive mutant G proteins at the Flp-In locus**

Flp-In T-REx cell lines were established with either (A) Cys<sup>351</sup>Ile G $\alpha_{i1}$ , (B) Cys<sup>352</sup>Ile G $\alpha_{i2}$ , (C) Cys<sup>351</sup>Ile G $\alpha_{i3}$  or (D) Cys<sup>351</sup>Ile G $\alpha_{o1}$  cloned into the Flp-In locus. These cells were further transfected to constitutively and stably express the D<sub>3</sub> receptor. Saturation [<sup>3</sup>H] spiperone binding was employed to assess the constitutive expression levels of D<sub>3</sub> receptor of various clones. A single, near-saturating concentration of 1 nM [<sup>3</sup>H] spiperone was used, with non-specific binding estimated using 10  $\mu$ M (+)-butaclamol. Only clones showing significant expression of D<sub>3</sub> receptor were retained and further characterised (**Table 4.3**).

Figure 4.13

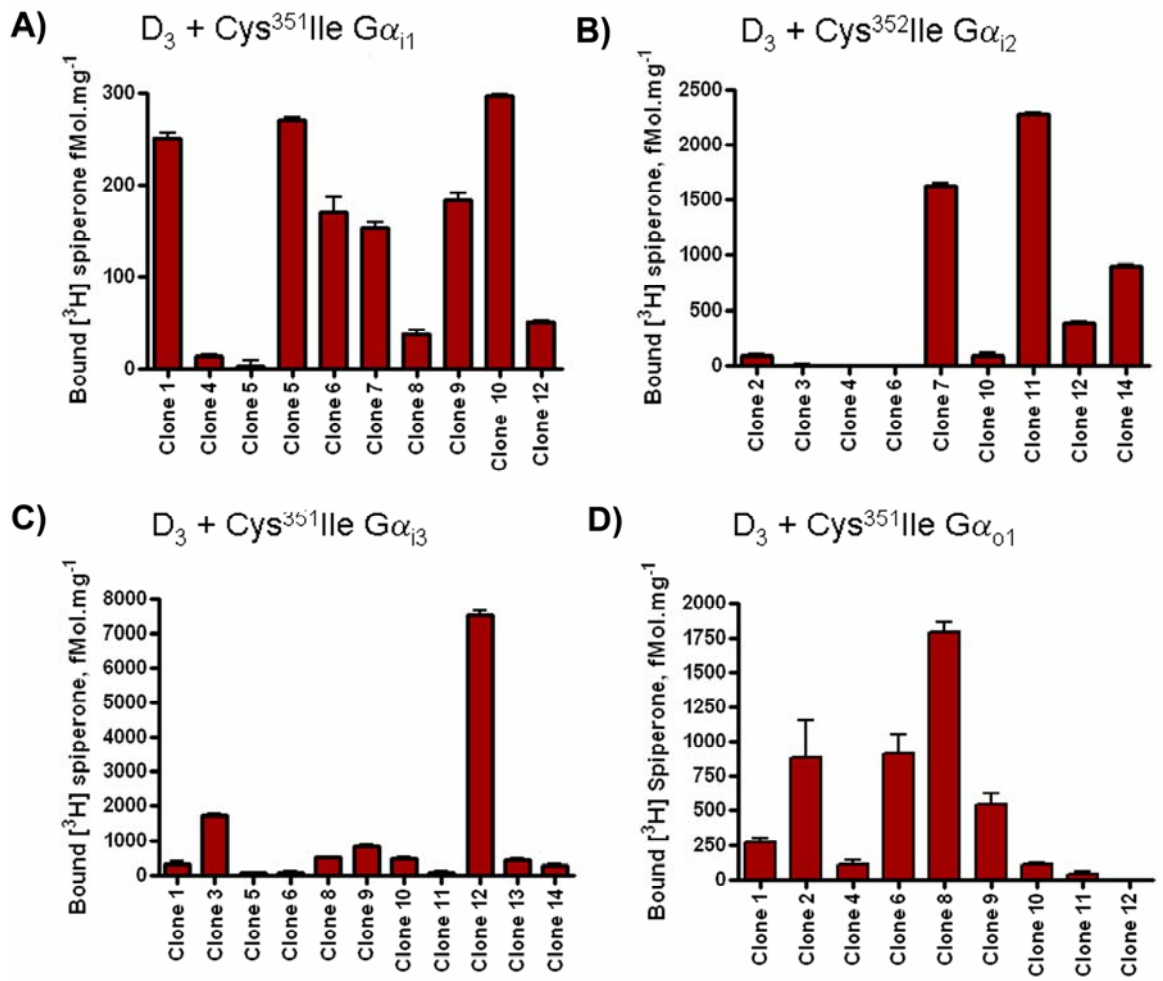


**Figure 4.14: Characterisation of Flp-In T-REx cells harbouring pertussis toxin-insensitive mutant G proteins at the Flp-In locus**

Flp-In T-REx cell lines were established with one of (A) Cys<sup>351</sup>Ile G $\alpha_{i1}$ , (B) Cys<sup>351</sup>Ile G $\alpha_{i2}$ , (C) Cys<sup>351</sup>Ile G $\alpha_{i3}$  or (D) Cys<sup>351</sup>Ile G $\alpha_{o1}$  cloned into the Flp-In locus. These cells were further transfected to constitutively and stably express the D<sub>3/2</sub> receptor. Saturation [<sup>3</sup>H] spiperone binding was employed to assess the constitutive expression levels of the D<sub>3/2</sub> chimera of various clones. A single near saturating concentration of 1 nM [<sup>3</sup>H] spiperone was used, with non-specific binding estimated using 10  $\mu$ M (+)-butaclamol. Only clones showing significant expression of D<sub>3/2</sub> receptor were retained and further characterised (Table 4.3).

Figure 4.14

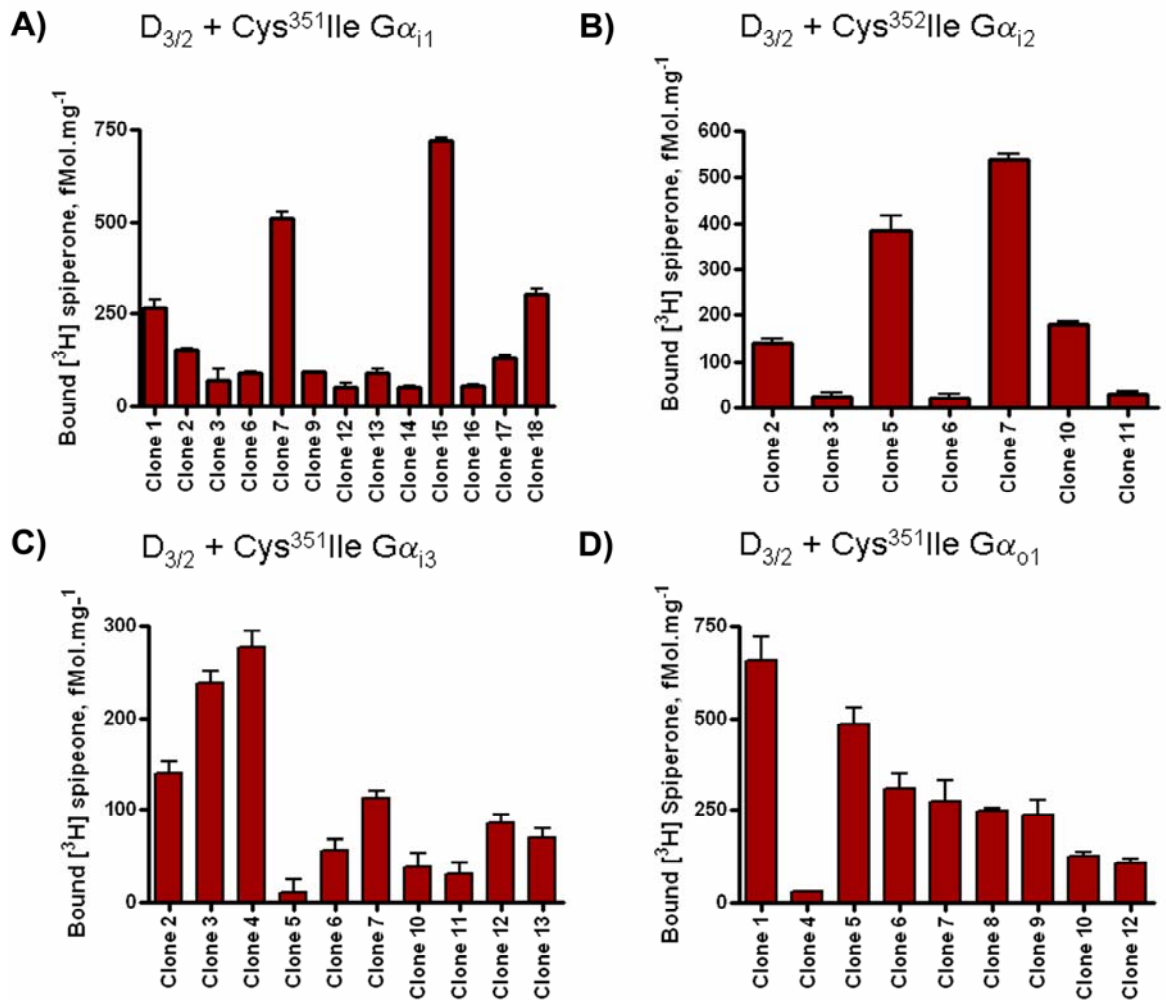
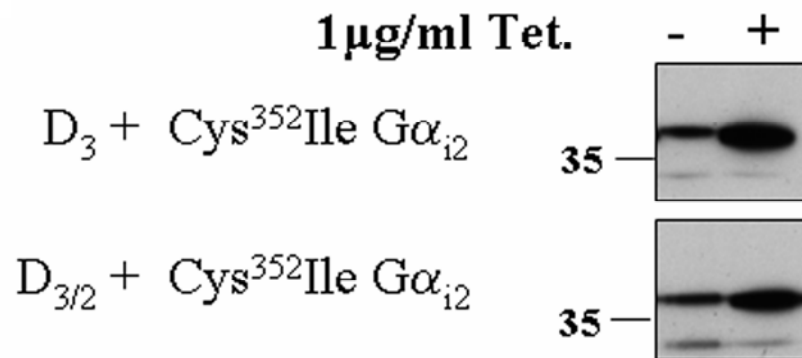


**Figure 4.15: Characterisation of Flp-In T-REx cells harbouring pertussis toxin-insensitive mutant G proteins at the Flp-In locus and constitutively expressing either the D<sub>3</sub> or D<sub>3/2</sub> receptor**

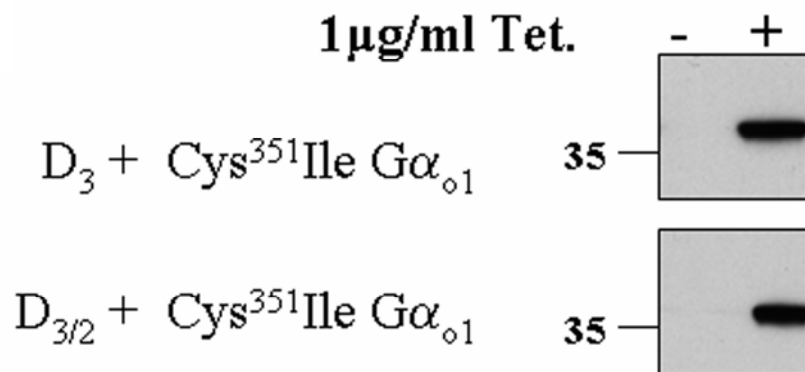
Flp-In T-REx cell lines were established with either Cys<sup>351</sup>Ile G $\alpha_{i2}$  or Cys<sup>351</sup>Ile G $\alpha_{o1}$  cloned into the Flp-In locus. These cells were further transfected to constitutively and stably express the D<sub>3</sub> receptor or chimeric D<sub>3/2</sub> receptor (see **Table 4.5 for details**). These cells were treated with or without tetracycline (Tet.) (1.0  $\mu$ g/ml for 24 h). Cell membranes were then prepared, resolved by SDS-PAGE and immunoblotted to detect either G $\alpha_{i2}$  (**A**) or G $\alpha_{o1}$  (**B**) (**upper panel**).

Figure 4.15

A)



B)

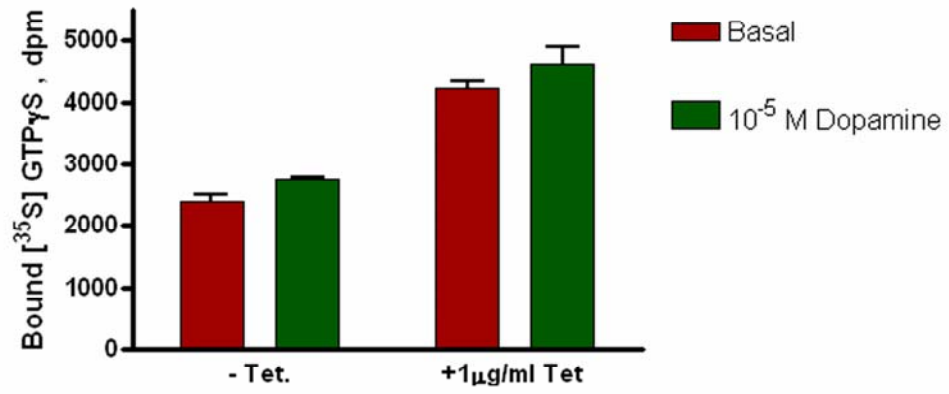


**Figure 4.16: Significant agonist-stimulated binding of [<sup>35</sup>S] GTP $\gamma$ S is observed in Flp-In T-REx HEK293 cells constitutively expressing the dopamine D<sub>3</sub> receptor, only upon expression of Cys<sup>351</sup>Ile G $\alpha$ <sub>o1</sub>**

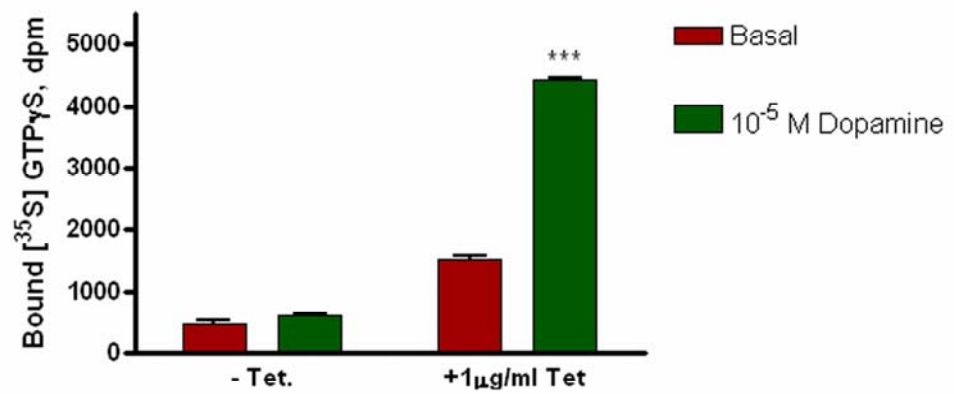
Flp-In T-REx HEK293 cells stably expressing the D<sub>3</sub> receptor and harbouring either Cys<sup>352</sup>Ile G $\alpha$ <sub>i2</sub> (A) or Cys<sup>351</sup>Ile G $\alpha$ <sub>o1</sub> (B) at the Flp-In locus were treated with or without 1  $\mu$ g/ml tetracycline for 24 h. Both sets of cells were also treated with pertussis toxin. Membranes from these cells were used to measure basal [<sup>35</sup>S] GTP $\gamma$ S binding and the effect of 10  $\mu$ M dopamine on this. A highly significant difference between basal and dopamine-stimulated [<sup>35</sup>S] GTP $\gamma$ S binding was observed upon induction of Cys<sup>351</sup>Ile G $\alpha$ <sub>o1</sub> expression (P<0.001, un-paired Students t-test).

Figure 4.16

A)



B)

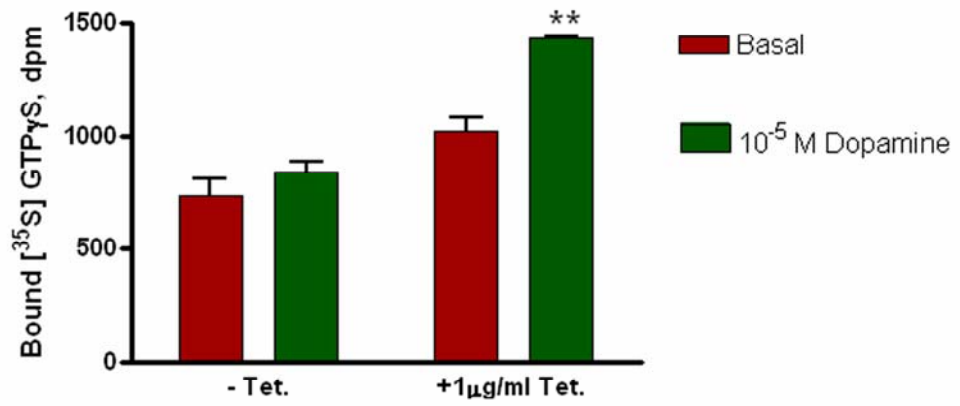


**Figure 4.17: Significant agonist-stimulated binding of [<sup>35</sup>S] GTPγS is observed in Flp-In T-REx HEK293 cells constitutively expressing the chimeric dopamine D<sub>3/2</sub> receptor, upon expression of Cys<sup>352</sup>Ile Gα<sub>i2</sub> and Cys<sup>351</sup>Ile Gα<sub>o1</sub>.**

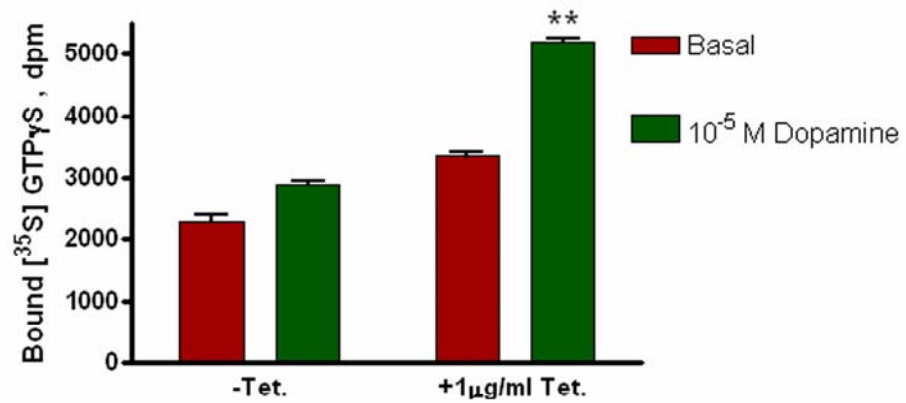
Flp-In T-REx HEK293 cells stably expressing the chimeric D<sub>3/2</sub> receptor and harbouring either Cys<sup>352</sup>Ile Gα<sub>i2</sub> (**A**) or Cys<sup>351</sup>Ile Gα<sub>o1</sub> (**B**) at the Flp-In locus were treated with or without 1 μg/ml tetracycline for 24 h. Both sets of cells were also treated with pertussis toxin. Membranes from these cells were used to measure basal [<sup>35</sup>S] GTPγS binding and the effect of 10 μM dopamine on this. A very significant difference between basal and dopamine stimulated [<sup>35</sup>S] GTPγS binding was observed upon induction of Cys<sup>352</sup>Ile Gα<sub>i2</sub> or Cys<sup>351</sup>Ile Gα<sub>o1</sub> expression (P<0.01, un-paired Student's t-test).

Figure 4.17

A)



B)



### 4.3 Discussion

Structurally, the D<sub>2</sub> and D<sub>3</sub> receptors exhibit 52% overall amino acid homology with the transmembrane domains exhibit 75% homology (Sokoloff et al., 1990). Since the transmembrane regions of the catecholamine receptors are believed to constitute the ligand binding sites the high homology of these domains explains the lack of compounds with high selectivity between D<sub>2</sub> and D<sub>3</sub> receptors. The G protein coupling of D<sub>2</sub> has been well characterised with a general consensus for promiscuous coupling to G $\alpha_{i1}$ , G $\alpha_{i2}$ , G $\alpha_{i3}$ , G $\alpha_{o1}$  (Gazi et al., 2003; Ghahremani et al., 1999; Jiang et al., 2001; Senogles, 1994; Watts et al., 1998). However, despite the high homology and similar pharmacology of D<sub>2</sub> and D<sub>3</sub> receptors, the coupling of D<sub>3</sub> has remained poorly characterised (Ahlgren-Beckendorf and Levant, 2004). The present study was based on the expression of D<sub>2</sub> and D<sub>3</sub> receptors and pertussis toxin resistant Cys $\rightarrow$ Ile G $\alpha_{i/o}$  subunits in the heterologous expression models based on HEK293 cells. This was combined with the use of receptor-G protein fusion proteins or Flp-In T-REx cell lines constitutively expressing dopamine receptor and expressing pertussis toxin resistant variant G  $\alpha$  subunits from the inducible Flp-In locus to control relative expression levels of receptor and G protein  $\alpha$  subunit. [<sup>35</sup>S] GTP $\gamma$ S binding was employed to directly monitor receptor-G protein coupling. These techniques allowed the characterisation, and direct comparison of the G protein coupling specificities of dopamine D<sub>2</sub> and D<sub>3</sub> receptors.

This study confirmed the promiscuous coupling D<sub>2</sub> to G $\alpha_{i1}$ , G $\alpha_{i2}$ , G $\alpha_{i3}$  and G $\alpha_{o1}$  already described by other studies (Gazi et al., 2003). Contrastingly, D<sub>3</sub> was shown to couple efficiently and selectively only to G $\alpha_{o1}$ . This is consistent with several studies which demonstrated the inhibition of adenylate cyclase by agonist stimulation of D<sub>3</sub> through a pertussis toxin sensitive, and therefore G $\alpha_{i/o}$  pathway (Robinson and Caron, 1997; Van

Leeuwen et al., 1995; Vanhauwe et al., 1999). Furthermore, studies using [<sup>35</sup>S] GTP $\gamma$ S binding have implicated coupling to pertussis toxin sensitive G $\alpha_{i/o}$  subunits, with two studies in particular showing efficient selective coupling to G $\alpha_{o1}$  (Beom et al., 2004; Zaworski et al., 1999) although Zaworski et al. postulated that efficient coupling to G $\alpha_{o1}$  required the expression of adenylyl cyclase subtype V. However, the study described in this chapter is the first to assess coupling to each of the four G $\alpha_{i/o}$  subunits directly.

Furthermore, constraining receptor to G protein expression stoichiometry in a 1:1 ratio with the use of receptor-G protein fusion proteins allowed a direct comparison between the coupling of D<sub>3</sub> to each G $\alpha_{i/o}$  subunit. In the previous chapter it was postulated that a greater variation in ligand conformational states exerted on the D<sub>21</sub> could be observed for interactions with G $\alpha_{o1}$  rather than between G $\alpha_{i1}$ , G $\alpha_{i2}$  and G $\alpha_{i3}$ . This may reflect the high amino acid homology between G $\alpha_{i1, 2}$  and  $3$  (85-90%) whereas for each of these against G $\alpha_{o1}$ , sequence identity is lower and lies between 70-73%. Similarly, the coupling of D<sub>3</sub> to G $\alpha_{o1}$  and not to other members of the G $\alpha_i$  subfamily may be a result of this relative dissimilarity between G $\alpha_{o1}$  and the other G $\alpha_i$  subunits. It could be said then that G $\alpha_{o1}$  is more promiscuous in its coupling to receptors than other G $\alpha_{i/o}$  subunits.

A comparison of the potencies and relative efficacies of various agonists at D<sub>21</sub> and D<sub>3</sub> revealed a trend towards higher potency and efficacy at the D<sub>3</sub> receptor. This could be explained by the observation of several groups that agonists such as dopamine quinpirole and 7 OH DPAT bind the D<sub>3</sub> receptor with a much higher affinity (by a factor of 20, 100 and 10 respectively) (Missale et al., 1998; Sokoloff et al., 1990). NPA however, showed no difference in potency at D<sub>2</sub> or D<sub>3</sub>. Again binding data for the highly related molecule apomorphine showed no difference in affinity for D<sub>2</sub> and D<sub>3</sub> (Sokoloff et al., 1990). The higher affinity for dopamine of D<sub>3</sub> relative to D<sub>2</sub>, and as shown in this study the higher potency of dopamine at the D<sub>3</sub> receptor, is consistent with its action as a presynaptic autoreceptor. The D<sub>3</sub> dopamine receptor, in addition to serving in a classical postsynaptic

sensory role, is also a presynaptic autoreceptor that is predominantly expressed in parts of the brain controlling behaviour, including that involved with emotion and movement (Joseph et al., 2002). Indeed, studies on the distribution of D<sub>3</sub> receptor in the brain show that it is expressed on virtually all dopaminergic neurons, strongly supporting the idea of the D<sub>3</sub> as an autoreceptor (Diaz et al., 2000; Gurevich and Joyce, 1999). Since the D<sub>3</sub> receptor has a higher affinity for dopamine than D<sub>2</sub> receptor the D<sub>3</sub> receptor may regulate dopamine release at lower dopamine concentrations than D<sub>2</sub>. Experiments with D<sub>3</sub> knock-out mice have shown this to be the case and that D<sub>3</sub> acts in the striatum/nucleus accumbens by modulating dopamine secretion rates rather than dopamine synthesis or dopamine transporter activity (Joseph et al., 2002). This presynaptic role is perhaps also consistent with the selective coupling of D<sub>3</sub> to G $\alpha_{o1}$ . Localisation of G $\alpha_{i/o}$  proteins has been shown to be different at post and pre-synaptic densities, with G $\alpha_{o1}$  shown to be more prevalent at pre-synaptic densities (Aoki et al., 1992). In agreement with this autoreceptor hypothesis, only a negligible fraction of plasma membrane D<sub>3</sub> receptors internalise as a result of persistent dopamine stimulation, even with increased GRK activity, so that the plasma membrane population of D<sub>3</sub> receptors remains relatively constant in order to provide continuous monitoring of ligand concentrations (Kim et al., 2005). As discussed in the previous chapter, S-(-)-3PPP has been shown to be an agonist at presynaptic dopamine receptors (Arnt et al., 1983; Hjorth et al., 1983), but an antagonist at post synaptic dopamine receptors. It is likely then that S-(-)-3PPP acts both through presynaptic dopamine D<sub>2</sub> and D<sub>3</sub> receptors coupled to G $\alpha_{o1}$ . Furthermore, S-(-)-3PPP has significantly higher potency and efficacy at the dopamine D<sub>3</sub> receptor as compared to that at the dopamine D<sub>2</sub> receptor, so perhaps S-(-)-3PPP is able to act through presynaptic D<sub>3</sub> receptors at a lower concentration. It would be interesting to assess the relative importance of the action of S-(-)-3PPP at dopamine D<sub>2</sub> versus D<sub>3</sub> presynaptic receptors.

There is considerable evidence that dopamine D<sub>2</sub> and D<sub>3</sub> receptors are co-localised within specific populations of cerebral neurons, both post-synaptically to dopaminergic projections and pre-synaptically on dopaminergic neurons themselves (Diaz et al., 2000; Gurevich and Joyce, 1999; Joseph et al., 2002; Joyce, 2001). This introduces the possibility that dopamine D<sub>2</sub> and D<sub>3</sub> receptors may form hetero-oligomeric complexes. In two separate studies it was demonstrated that several agonists exhibit a higher potency for inhibition of forskolin induced cAMP in membranes of cells where D<sub>21</sub> and D<sub>3</sub> had been co-transfected as compared to D<sub>21</sub> transfected alone (Maggio et al., 2003; Scarselli et al., 2001). Both of these studies were carried out in a system where D<sub>3</sub> was unable to couple to and inhibit a chimeric adenylate cyclase consisting of elements of ACV and ACVI. The authors argue that the agonists have a higher potency at D<sub>21</sub>/D<sub>3</sub> receptor heterodimers as compared to D<sub>21</sub> receptors. Immunoprecipitation studies provided further evidence of a D<sub>3</sub>/D<sub>2</sub> hetero-oligomer (Scarselli et al., 2001). My results show that agonists have a higher potency at D<sub>3</sub> receptors. The results of Maggio et al. (2003) could be explained by the agonist binding preferentially to the D<sub>3</sub> receptor in a D<sub>2</sub>/D<sub>3</sub> receptor heterodimer due to a demonstrated higher affinity. Furthermore, negative co-operativity in ligand binding across a D<sub>21</sub> dimer has been demonstrated (Vivo et al., 2006), and due to the relative homology between D<sub>2</sub> and D<sub>3</sub> it is perhaps likely that this would also occur for a D<sub>2</sub>/D<sub>3</sub> heterodimer. Cross-talk within a dimer, where one receptor can activate another receptor's G protein partner has been demonstrated using functional complementation of two non-functional opioid receptor-G protein fusions (Pascal and Milligan, 2005). It is possible then that D<sub>3</sub>, although unable to couple to adenylate cyclase, binds the agonist, and that this, by a crosstalk mechanism within the D<sub>2</sub>/D<sub>3</sub> dimer results in the activation of the G protein partner of D<sub>21</sub> resulting in the inhibition of the chimeric adenylate cyclase V/VI. My results suggest that this partner could be any one of G $\alpha_{i1}$ , G $\alpha_{i2}$  or G $\alpha_{i3}$  since D<sub>3</sub> can couple to G $\alpha_{o1}$ . It would be interesting to investigate this hypothesis using the functional complementation method used by Pascal and Milligan (2005). An alternative hypothesis is

that the D<sub>3</sub>/D<sub>2</sub> heterodimer recruits G proteins more efficiently, or couples to an alternative G protein as demonstrated for the dopamine D<sub>2</sub> receptor / cannabinoid CB<sub>1</sub> receptor heterodimer (Kearn et al., 2005). It is possible that in cells where both dopamine D<sub>2</sub> and D<sub>3</sub> receptors are co-expressed and co-localised that three populations of receptors could exist; D<sub>21</sub> homodimers, D<sub>3</sub> homodimers and D<sub>3</sub>/D<sub>2</sub> heterodimers. Furthermore, these different populations will have different pharmacologies and perhaps have different downstream signalling pathways. Consequently the action of dopamine or a dopaminergic ligand on a particular neuron may depend on the relative levels of each of the three different populations. Perhaps relevant to this idea, is the fact that both schizophrenia and cocaine abuse are associated with a marked elevation of mesolimbic D<sub>3</sub> receptors (Joyce, 2001; Segal et al., 1997; Staley and Mash, 1996). Taking into account the protean characteristic of S-(-)-3PPP at the D<sub>21</sub> receptor, as described in chapter 3, it would be interesting to look at the action of this ligand at a D<sub>3</sub>/D<sub>21</sub> heterodimer.

To understand the physiological actions of a G protein coupled receptor it is important to identify the specific G proteins with which this receptor can interact. A significant number of GPCRs have been shown to couple to multiple G protein subtypes. The molecular basis of this selectivity has been the focus of a great many studies (Wess, 1998; Wong, 2003). However, despite the wealth of information regarding the coupling specificities of a multitude of G protein coupled receptors, surprisingly little is known about how they exert this selectivity at a molecular level. No obvious sequence homology was observed even for GPCRs that couple to the same G protein subtype, and no consensus motif predictive of G protein coupling has been identified (Moller et al., 2001). A vast number of studies with many different GPCRs have shown that the selectivity of G protein recognition is determined by multiple intracellular receptor regions. The most critical regions are the second intracellular loop and the N and C terminal regions of the third intracellular loop (Wess, 1997).

In this chapter, the exchange of a twelve amino acid section of the D<sub>3</sub> receptor with the equivalent region of the D<sub>2</sub> receptor was seen to confer 'D<sub>2</sub>-like' promiscuous G protein coupling to the D<sub>3</sub> receptor. Indeed, with the exchange of this intracellular region, the D<sub>3/2</sub> chimera stimulated [<sup>35</sup>S] GTPγS binding to Gα<sub>i1</sub>, Gα<sub>i2</sub>, Gα<sub>i3</sub> and Gα<sub>o1</sub>, as opposed to the specific and selective coupling to Gα<sub>o1</sub> of D<sub>3</sub>. This is in agreement with a previous study using receptors transiently expressed in CHO cells. This showed that in that system the D<sub>3</sub> receptor was unable to inhibit adenylate cyclase whereas agonist stimulation of the D<sub>2</sub> receptor inhibited forskolin induced cAMP accumulation. An identical D<sub>3/2</sub> chimera to the one used in my study gained the ability to inhibit adenylate cyclase. In the reciprocal chimera, the potency of coupling with adenylate cyclase activity was reduced. It would seem then that this observed gain in the ability to couple to adenylate cyclase, with the exchange of a twelve amino acids in the C-terminal of intracellular loop of D<sub>2</sub> into D<sub>3</sub>, lies at the level of a gained ability to couple to one or a combination of Gα<sub>i1</sub>, Gα<sub>i2</sub>, and Gα<sub>i3</sub>. A characteristic of this twelve amino acid sequence is that nine amino acid residues carrying charged or polar groups in the D<sub>2</sub> sequence are replaced at equivalent positions by aliphatic or hydrophobic groups in the D<sub>3</sub> receptor. Furthermore the flanking sequences to this region (EKKATQ, close to TMVI, and the N-terminal TSL) are conserved in both receptors, so exchange of this region is unlikely to disrupt receptor structure. A vast body of evidence has shown that the C-terminal portion of the third intracellular loop of G protein coupled receptors is important for their coupling to G proteins (Wess, 1998). Furthermore, it has been suggested that the C-terminal portion of the third intracellular loop of G protein coupled receptors form a short α-helix that is extremely important for the interaction with heterotrimeric G proteins (Burstein et al., 1995; Wade et al., 1996). It is possible that proline residues present in this portion of the third intracellular loop of the D<sub>3</sub> receptor disrupt this α helical structure.

The affinity for the inverse agonist [<sup>3</sup>H] spiperone at the chimeric D<sub>3/2</sub> receptor is not significantly different from that of the wild-type D<sub>3</sub> receptor. This perhaps indicates that the exchange of the twelve amino acid section of D<sub>3</sub> with that of D<sub>2</sub> has not disrupted the binding domain of this ligand. Furthermore the potency of ligands when the chimera is coupled to Gα<sub>o1</sub> is not significantly different to that of D<sub>3</sub> coupled to Gα<sub>o1</sub>, again indicating that the binding affinity of these ligands is also not affected, in agreement with previous work (Filteau et al., 1999; McAllister et al., 1993). However, there is a marked decrease in potency of the full agonists dopamine and quinpirole when the chimera is coupled to Gα<sub>i1</sub> or Gα<sub>i2</sub> as compared to Gα<sub>i3</sub> or Gα<sub>o1</sub>, in effect the rank order of potency for dopamine could be described as: Gα<sub>i3</sub> = Gα<sub>o1</sub> >> Gα<sub>i1</sub> or Gα<sub>i2</sub>. This order of preference can, as for that of D<sub>2</sub> and D<sub>3</sub>, be related to the relative structural similarities of the Gα<sub>i/o</sub> subunits. Gα<sub>i3</sub> has a greater sequence similarity to Gα<sub>o1</sub> as compared to that of Gα<sub>i1</sub> or Gα<sub>i2</sub>, in the extreme c-terminus (**Figure 5.1**), a region shown to be important in receptor-G protein coupling (Slessareva et al., 2003; Wess, 1998).

The different rank order of dopamine potency observed at the D<sub>2</sub> receptor (Gα<sub>i1</sub> = Gα<sub>i2</sub> = Gα<sub>i3</sub> < Gα<sub>o1</sub>) as compared to that of the chimeric D<sub>3/2</sub> receptor, could point towards a difference in coupling specificity. This perhaps indicates that additional sites within the D<sub>2</sub> receptor confer G protein coupling specificity particularly in relation to coupling to Gα<sub>i1</sub> and Gα<sub>i2</sub>. In agreement with this, a previous study demonstrated that both N and C-terminal portions of the third intracellular loop were capable of supporting functional coupling of D<sub>2</sub> to adenylyl cyclase, but that both were required for maximal Gα<sub>i</sub> coupling (Lachowicz and Sibley, 1997). Indeed, the fact that the reciprocal chimera to the one used in this study showed only a reduction in the potency of coupling to adenylyl cyclase as compared to D<sub>2</sub> rather than a complete abolition of coupling, indicates the presence of additional G protein coupling domains within the D<sub>2</sub> receptor (Filteau et al., 1999).

It is interesting to note that a significantly higher receptor binding site density was identified in dopamine receptor plus  $G\alpha_{o1}$  co-transfections as compared to  $G\alpha_{i2}$  co-transfections. A similar pattern is could be seen in the  $D_3$  fusion proteins with a higher value of  $B_{max}$  for receptor- $G\alpha_{o1}$  fusions as compared to the others, but not for the  $D_2$  fusion proteins or the chimeric  $D_{3/2}$  fusions. Recent biophysical studies on recombinantly expressed receptors reconstituted with purified G proteins have supported the idea of the basic unit of signal transduction of the BLT1 leukotriene B4 receptor as a pentamer containing two receptors and the three subunits of a G protein hetero-trimer (Baneres and Parello, 2003; Milligan, 2007). One explanation for the higher receptor density observed with  $G\alpha_{o1}$  could be that  $D_2$ ,  $D_3$  and  $D_{3/2}$  may couple more efficiently to  $G\alpha_{o1}$ . This interaction, then, may stabilise the dimer more effectively than the other G protein  $\alpha$  subunits. However, in contrast, the levels of receptor was unaffected by the induction of  $G\alpha$  subunit expression in all Flp-In T-Rex stable cell lines, so the above pattern seen with the co-transfection of receptor and G protein may well be due to inconsistencies with transient transfection such as the relative qualities of DNA.

In summary then, the coupling specificities of dopamine receptors  $D_{21}$  and  $D_3$  have been characterised with  $D_{21}$  shown to couple to  $G\alpha_{i1}$ ,  $G\alpha_{i2}$ ,  $G\alpha_{i3}$  and  $G\alpha_{o1}$ .  $D_3$  was shown to selectively couple to  $G\alpha_{o1}$ . The use of a chimeric receptor has identified a twelve amino acid section in the C-terminus of the third intracellular loop of  $D_2$  to be important in directing coupling to  $G\alpha_{i1}$ ,  $G\alpha_{i2}$ , and  $G\alpha_{i3}$ . It would seem that  $G\alpha_{o1}$  is more promiscuous in its coupling to receptors than other  $G\alpha_i$  subunits, and perhaps has fewer requirements in receptor structure to become activated. It would be interesting to employ a system taking advantage of the differential signalling specificities of  $D_2$  and  $D_3$ , and use chimeric  $G\alpha_{i1}$  /  $G\alpha_{o1}$  subunits to determine the molecular basis of the relative promiscuity of  $G\alpha_{o1}$ .

## **5 The generation and characterisation of antibodies that identify only the active conformation of G<sub>i</sub>-family G protein $\alpha$ subunits**

### **5.1 Introduction**

Eighteen different G protein  $\alpha$  subunit subtypes have been identified. As discussed in both chapter 4 and chapter 5, the ability of a single GPCR to interact with various and different G protein  $\alpha$  subunits has been the subject of a large body of work and is now widely accepted (Wess, 1998; Wong, 2003). The dissection of the specificity of interactions between receptors, G proteins and effectors, requires tools to allow the selective identification of G proteins involved in a particular pathway. Early attempts to define the specificity of interactions between receptors and G proteins made considerable use of exotoxins produced by the bacteria *Vibrio cholerae* and *Bordetella pertussis*. As discussed in the previous chapters, pertussis toxin catalysed ADP ribosylation of the G $\alpha_{i/o}$  family of G protein  $\alpha$  subunits prevents functional coupling between receptors and these G proteins. Similarly, cholera toxin catalysed ADP-ribosylation of G<sub>s</sub> converts the G protein to an essentially irreversibly activated form which no longer required agonist occupation of a receptor to produce regulation of adenylyl cyclase. However, with the realisation that there could be multiple G-protein gene products which acted as substrates for these toxins expressed in a single cell or tissue, it became clear that more selective tools would be required to discriminate between receptor functions transmitted to effectors by the individual G proteins.

The isolation of cDNA sequences corresponding to G-protein  $\alpha$  subunits allowed the generation of antisera against short peptides which represent sections of the primary amino

acid sequence unique to specific G proteins. Antisera which are likely to be useful in the analysis of receptor-G protein interactions must be highly selective for individual G-protein  $\alpha$  subunits. Taking into account the high sequence homology of G protein  $\alpha$  subunits (**Figure 5.1, Table 5.1**) this restricts the choice of peptides to regions of relative dissimilarity. However, as demonstrated by my results in **chapters 3 and 4**, receptors can distinguish between G protein  $\alpha$  subunits from different sub-families and even between G protein  $\alpha$  subunits within the same sub-family, for example the selective coupling of  $D_3$  to  $G\alpha_{o1}$  and not the other members of the  $G\alpha_{i/o}$  sub-family. It is clear then that sections of G-protein subunits which can be deduced to play key roles in interactions with receptors and effectors are likely to be most appropriate for the development of antisera (Milligan, 1994; Mullaney and Milligan, 2004). Considerable evidence has identified the extreme C-terminal region of G-protein  $\alpha$  subunits as a key site for functional interactions between receptors and G proteins (Slessareva et al., 2003; Wess, 1998). On this basis antibodies generated against peptides corresponding to the last ten amino acids of individual G-protein  $\alpha$  subunits have been the most widely used to study functional interactions between receptors and G proteins (Milligan, 1994; Mullaney and Milligan, 2004). The relative dissimilarity of this region between various G protein  $\alpha$  subunits is illustrated in **Table 5.2**. The specificity of antisera generated in this manner towards different G protein  $\alpha$  subunits has been demonstrated, and anti- $G\alpha_{i1/2}$ ,  $G\alpha_{i3}$ ,  $G\alpha_{o1}$ ,  $G\alpha_s$  and  $G\alpha_{q/11}$  antisera have previously been generated and characterised (Milligan, 1993; Milligan, 1994; Mullaney and Milligan, 2004; Mullaney et al., 1995). The first aim of the work described in this chapter was the generation of antisera specific to  $G\alpha_{i1/2}$ ,  $G\alpha_s$  and  $G\alpha_{q/11}$ . As for previous studies antisera were raised against decapeptides corresponding to the C-terminal ten amino acids of these G protein  $\alpha$  subunits. It was essential to characterise the selectivity of these antisera towards the G protein  $\alpha$  subunits against which they were raised. This was achieved by the expression of the various G protein  $\alpha$  subunits in systems which essentially offer a null background for the specific G  $\alpha$  subunit of interest. This aspect of

antibody characterisation was achieved by Western blotting. Another application of antisera raised against the C-terminal tail of G  $\alpha$  subunits, and specific to individual G protein  $\alpha$  subunit subtypes has been their use in a modified form of a [ $^{35}\text{S}$ ] GTP $\gamma$ S assay (Milligan, 2003). This modified form of the [ $^{35}\text{S}$ ] GTP $\gamma$ S assay, like more conventional assays, allows the measurement of receptor mediated G protein activation by measuring the uptake of the non-hydrolysable [ $^{35}\text{S}$ ] GTP $\gamma$ S. However, by the inclusion of an immunoprecipitation step using antisera selective to the particular G protein of interest, this allows the enrichment of a particular [ $^{35}\text{S}$ ] GTP $\gamma$ S bound G protein  $\alpha$  subunit. This enrichment gives a reduced background of bound [ $^{35}\text{S}$ ] GTP $\gamma$ S, providing an enhanced signal window. This technique is particularly useful when investigating the coupling of receptors to G protein  $\alpha$  subunits other than those from the G $\alpha_{i/o}$  family. To further characterise the antisera generated in this project, their utility in a [ $^{35}\text{S}$ ] GTP $\gamma$ S assay with pulldown step was also assessed. The antisera generated would not only be useful reagents for use in this project, but if the immunisation program was successful, would be useful reagents for use in the industrial environment. Using these antisera for the modified [ $^{35}\text{S}$ ] GTP $\gamma$ S assay described above, in combination a technique such as the scintillation proximity assay (SPA), would allow the development of a high throughput [ $^{35}\text{S}$ ] GTP $\gamma$ S screening assay that could be used not only for G $\alpha_i$  but also G $\alpha_q$  and G $\alpha_s$  coupled receptors (Ferrer et al., 2003). In this chapter antisera raised against the C-terminal tail of G $\alpha_{i1/2}$ , G $\alpha_q$  and G $\alpha_s$  were shown to be selective towards the relevant G protein. Furthermore, the effective use of each antisera for the immunoprecipitation of the G protein against which they were raised was also demonstrated as part of a modified [ $^{35}\text{S}$ ] GTP $\gamma$ S assay.

GPCRs represent one of the largest gene families in the human genome (Milligan, 2003; Windh et al., 2002). They are the most tractable and effective set of targets for therapeutic drug design. Thus, screens for ligands that interact with GPCRs are integral to both basic research and the drug discovery process. Although recent studies have indicated that

GPCRs can provide information to cells that does not require activation of heterotrimeric G proteins (Seta et al., 2002), by definition all GPCRs must function, at least partially, via interaction and activation of G proteins. It is well established that the key step in this process is induced guanine nucleotide exchange on the G-protein  $\alpha$ -subunit. As demonstrated in chapters 4 and 5 the nucleotide exchange process can be monitored by measuring the binding of [ $^{35}\text{S}$ ] GTP $\gamma$ S. This technique has been successfully used in high throughput drug screening programs (Wise et al., 2003). However, from the perspective of the pharmaceutical industry the [ $^{35}\text{S}$ ] GTP $\gamma$ S assay has two drawbacks, both relating to use of radioactive isotopes. Firstly, the expense associated with the use and disposal of radioactive material make the [ $^{35}\text{S}$ ] GTP $\gamma$ S assay a less attractive technique for use in industry. However, a perhaps more limiting issue is that pharmaceutical companies have a defined quota for the disposal of radioactive material. This then limits the number of screening programs that can be performed using a [ $^{35}\text{S}$ ] GTP $\gamma$ S binding assay. There is therefore, an opportunity to develop an alternative, non-radioactive assay equivalent to the [ $^{35}\text{S}$ ] GTP $\gamma$ S assay. The aim of the final section of this study was to develop monoclonal antibodies that are selective against the active GTP-bound conformation of a G protein  $\alpha$  subunit. These monoclonal antibodies could then be used to develop a high throughput screening assay equivalent to the [ $^{35}\text{S}$ ] GTP $\gamma$ S assay. To allow integration of this study with the work on dopamine D<sub>2</sub>-like receptors described in chapters 3 and 4, it was decided to try to generate antibodies that recognise the GTP-bound form of G $\alpha_{i1}$ .

Upon activation by extracellular signals, the receptors catalyze the exchange of bound GDP for GTP at the G protein  $\alpha$  subunit. The GTP-bound form of the heterotrimer is unstable and heterolytically dissociates or undergoes a conformational rearrangement to form active GTP- $\alpha$  and  $\beta\gamma$  complexes. The structures of both the inactive (GDP bound) and active (GTP bound) conformations of G $\alpha_{i1}$  have been elucidated and this has provided information concerning the conformational changes occurring upon nucleotide exchange

and indeed the mechanism of GTP hydrolysis (Coleman and Sprang, 1998; Kleuss et al., 1994; Mixon et al., 1995; Wall et al., 1998). This work has also demonstrated specific roles in transition state stabilisation of two highly conserved residues. Glutamine<sup>204</sup> stabilises and orients the hydrolytic water in the trigonal-bipyrimidal transition state (**Figure 5.38**) Arginine<sup>178</sup> stabilises the negative charge at the equatorial oxygen atoms of the pentacoordinate  $\gamma$  phosphate intermediate (Coleman et al., 1994). Mutations of both of these residues, namely Arg<sup>178</sup>Cys and Glu<sup>204</sup>Leu, produce variants of  $G\alpha_{i1}$  which are effectively constitutively active. The interaction between the amide nitrogen of residue Gly<sup>203</sup> in the alpha 2 helix of  $G\alpha_{i1}$  and the gamma phosphate of GTP stabilises the active (GTP) bound conformation (Mixon et al., 1995). Mutation of glycine<sup>203</sup> to alanine prevents effective nucleotide exchange, and this variant is effectively constitutively inactive. Furthermore the complex Gly<sup>203</sup>Ala  $G\alpha_{i1}$ .GDP was shown to have an equivalent structure to wild type  $G\alpha_{i1}$ .GDP (Mixon et al., 1995).

This understanding of the different structural conformations of the inactive GDP bound and active GTP bound  $G\alpha_{i1}$  allowed the design of a strategy for the generation of antibodies selective towards the active conformation. Two immunisation strategies were used: The first was immunisation with recombinant human  $G\alpha_{i1}$  which had been pre-incubated with GTP $\gamma$ S to lock the protein into the active conformation. The second strategy was plasmid immunisation using cDNA of the constitutively active variant  $G\alpha_{i1}$  Glu<sup>204</sup>Leu. The technique of hybridoma production, combined with high throughput screening facilities available at GlaxoSmithKline (Stevenage, UK), allows the production and screening of many different monoclonal antibodies raised against an antigen (Harlow, 1988). Using the immunisation strategies described above it was most likely that the majority of antibodies would be selective towards  $G\alpha_{i1}$  but not show selectivity towards the inactive or active conformations. Therefore, design of an effective high throughput screen to recognise antibodies with the desired characteristics was crucial to this project.

To achieve this I made use of the non-hydrolysable nucleotide GTP $\gamma$ S, or the metabolically stable nucleotide GDP $\beta$ S to force G $\alpha_{i1}$  into active or inactive conformations. The constitutively active (Gln<sup>204</sup>Leu G $\alpha_{i1}$ ) or inactive mutants (Gly<sup>203</sup>Ala G $\alpha_{i1}$ ), described above, also proved effective tools for use in this screening process. This chapter describes the successful generation and characterisation of three separate monoclonal antibodies which are selective against the active (GTP bound) conformation of G $\alpha_{i1}$ . Further characterisation of these antibodies could result in the development of a non-radioactive assay equivalent to the [<sup>35</sup>S] GTP $\gamma$ S assay.

## 5.2 Results

### 5.2.1 Antisera raised against C-terminal decapeptide of G protein $\alpha$ subunits

To date, the most successful approach to generate selective probes for G protein  $\alpha$  subunits has been the generation of anti-peptide G protein  $\alpha$  subunit antisera. The sequence homology of G protein  $\alpha$  subunits is relatively high (**Table 5.1**). Previous studies have identified peptides generated corresponding to the C-terminal ten amino acids of G protein  $\alpha$  subunits to be effective in the generation of antisera selective to individual G protein  $\alpha$  subunit subtypes. The relative dissimilarity of this region among the selected G-protein subtypes is illustrated in **Table 5.2**. In order to generate useful probes selective for different G protein subtypes, antisera were generated against the decapeptides corresponding to the C-terminal ten amino acids of G $\alpha_t$ , G $\alpha_q$  and G $\alpha_s$  (**Table 5.3**). Antibodies were generated by CRL Cambridge Ltd (Cambridge, UK). Two animals were immunised for each decapeptide. The antiserum was been purified by affinity chromatography and therefore consists of antibodies specific to the antigen. The antibodies

were purified by eluting in a low pH buffer (glycine eluate pH 2.5) and then a high pH buffer (triethylammonium chloride (TEA) pH 11.5). The eluates were neutralised immediately and dialysed against phosphate buffered saline pH 7.4; therefore all the antibodies were supplied in PBS (with 0.01% sodium azide and 1% trehalose). The two different eluates supplied contain antibodies that have been eluted at high or low pH respectively therefore these may have different properties and therefore both eluates should be tested.

**Table 5.1: Percentage sequence homologies of various G protein  $\alpha$  subunits**

	<b>Gai2</b>	<b>Gai3</b>	<b>Gao1</b>	<b>Gao2</b>	<b>Gas-S</b>	<b>Gas-L</b>	<b>Gaq</b>	<b>Ga11</b>
<b>Gai1</b>	88	94	73	73	44	44	55	52
<b>Gai2</b>		86	70	70	43	44	51	51
<b>Gai3</b>			72	71	44	44	54	50
<b>Gao1</b>				94	46	46	51	51
<b>Gao2</b>					45	45	51	50
<b>Gas-S</b>						100	41	41
<b>Gas-L</b>							42	42
<b>Gaq</b>								89
<b>Ga11</b>								

**Table 5.2: The C-terminal ten amino acids of various G protein  $\alpha$  subunits.**

Residues coloured red and highlighted yellow indicate identical residues. Dark blue letters on a light blue background indicate conservative residues. Black letters on a green background indicate a block of similar residues. Green letters indicate weakly similar residues. Black letters indicate non-similar residues (Generated using Vector NTI suite, Invitrogen).

G $\alpha$ subunit	C-terminal 10 amino acids
$G\alpha_t$	KENLKDCGLF
$G\alpha_{i1}$	KNNLKDCGLF
$G\alpha_{i2}$	KNNLKDCGLF
$G\alpha_{i3}$	KNNLKECGLY
$G\alpha_{o1}$	ANNLRGCGLY
$G\alpha_s$	RMHLRQYELL
$G\alpha_{q/11}$	QLNLKEYNLV

**Table 5.3: Antisera against  $G\alpha_s$ ,  $G\alpha_{q/11}$  and  $G\alpha_{i1/2}$  were generated by CRL Laboratories Ltd. (Cambridge, UK) using the peptides below.**

The sequences of peptides shown correspond to the C-terminal ten amino acids of the listed G protein  $\alpha$  subunit. The N-terminal cysteine allows the coupling of the peptide to a carrier protein prior to immunisation. Each peptide was used to immunise two rabbits.

<b>Animal #</b>	<b>Peptide sequence</b>	<b>G-protein <math>\alpha</math> subunit</b>
<b>1314</b>	[C]RMHLRQYELL	$G\alpha_s$
<b>1315</b>	[C]RMHLRQYELL	$G\alpha_s$
<b>1316</b>	[C]QLNLKEYNLV	$G\alpha_{q/11}$
<b>1317</b>	[C]QLNLKEYNLV	$G\alpha_{q/11}$
<b>1318</b>	[C]KENLKDCGLF	$G\alpha_{t,i1,i2}$
<b>1319</b>	[C]KENLKDCGLF	$G\alpha_{t,i1,i2}$

## 5.2.2 Characterisation of antisera raised against the C-terminal ten amino acids of $G\alpha_t$

Antisera were successfully generated against a decapeptide corresponding to the C-terminal ten amino acids of  $G\alpha_t$ . The specificity towards the decapeptide was confirmed by CRL laboratories by ELISA. However, the selectivity of the antisera towards  $G\alpha_{i/2}$  had to be determined. Mammalian cell lines express an array of  $G\alpha$  subunits, with  $G\alpha_{i2}$  and  $G\alpha_{i3}$  appearing to be expressed in all cell types. To investigate the selectivity of these antisera for individual members of the  $G\alpha_i$  subfamily a system was needed in which the individual G protein  $\alpha$  subunits could be expressed in isolation. The successful expression of various G protein  $\alpha$  subunits in *E coli* has been described previously (Wise and Milligan, 1995). Briefly cDNA of  $G\alpha_{i1}$ ,  $G\alpha_{i2}$ ,  $G\alpha_{i3}$ , and  $G\alpha_{o1}$  was cloned into the expression vector pT7.7 and this subsequently transformed into the BL21 strain of *E coli*. Expression of the relevant  $G\alpha_{i/o}$  subunits was induced with the addition of IPTG. Protein was then separated by SDS PAGE and Western blotting performed using the various antisera generated in this project and compared with in-house antisera already characterised and known to be selective against various  $G\alpha$  subunit subtypes. An in-house antiserum (SG3) raised against the C-terminal ten amino acids of  $G\alpha_t$ , gave a single band between 35 and 50 kDa only for samples where the expression of  $G\alpha_{i1}$  or  $G\alpha_{i2}$  has been induced (**Figure 5.1A**). A faint band was seen where  $G\alpha_{i3}$  is induced indicating some cross reactivity with this subtype. The in-house antiserum I3B (raised against a decapeptide corresponding to the C-terminal tail of  $G\alpha_{i3}$ ) only gave a single band when the expression of  $G\alpha_{i3}$  was induced. The in-house antiserum, OC2, was raised against the C-terminal ten amino acids of  $G\alpha_{o1}$ . Using this antibody, a single band between 35 and 50 kDa was seen when the expression of  $G\alpha_{o1}$  was induced (**Figure 5.1A**). Furthermore, a

band was also seen for the sample where expression of  $G\alpha_{i3}$  was induced, highlighting the cross reactivity of this antibody with both  $G\alpha_{o1}$  and  $G\alpha_{i3}$ . This cross reactivity is perhaps not surprising given the high sequence similarity of the C-terminal ten amino acids of these two  $G\alpha$  subunits (**Table 5.2**). The glycine eluate of the antiserum raised against a decapeptide corresponding to the last ten amino acids of  $G\alpha_i$ , derived from animal 1318, gave a band between 35 and 50 kDa for samples in which expression of  $G\alpha_{i1}$ ,  $G\alpha_{i2}$ ,  $G\alpha_{i3}$  and  $G\alpha_{o1}$  was induced (**Figure 5.1B**). This indicates that this antiserum is not able to discriminate between all  $G\alpha$  subtypes within the  $G\alpha_i$  family. In contrast, the TEA eluate from animal 1318 and the glycine and TEA eluate from animal 1319 all showed selectivity for  $G\alpha_{i1}$  and  $G\alpha_{i2}$  only giving a single band between 35 and 50 kDa when the expression of these two subtypes were induced.

As part of an effort to further characterise these antisera, their ability to immunoprecipitate the [ $^{35}$ S]GTP $\gamma$ S bound forms of the relevant  $G\alpha$  subunits was assessed. To this end, a [ $^{35}$ S]GTP $\gamma$ S assay with an immunocapture step was performed using membranes from cells co-expressing the  $D_{21}$  receptor and  $G\alpha_{i1}$  and with or without the addition of 100  $\mu$ M dopamine. At the immunocapture step equivalent reactions were set up for both dopamine stimulated and unstimulated conditions using either the in-house  $G\alpha_{i1/2}$  selective antisera (SG3), or the glycine eluate of the antiserum from animal 1319 raised against the C-terminal decapeptide of  $G\alpha_i$ . The pulldown using the glycine eluate 1319 gave higher counts for both basal and dopamine-stimulated conditions as compared to the in-house antiserum (**Figure 5.2**).

Since the glycine eluate of the antiserum from animal 1318 had been shown to recognise  $G\alpha_{i1}$ ,  $G\alpha_{i2}$ ,  $G\alpha_{i3}$  and  $G\alpha_{o1}$  in Western blots, it was of interest to establish whether this antiserum could efficiently immunocapture a [ $^{35}$ S]GTP $\gamma$ S labelled subunit other than those of  $G\alpha_{i1/2}$ . A [ $^{35}$ S]GTP $\gamma$ S assay with an immunocapture step was performed using membranes from cells expressing the corticotrophin releasing factor (CRF) receptor fused

to  $G\alpha_{i3}$  (supplied by L. Jenkins, University of Glasgow) and with or without the addition of  $1\mu\text{M}$  sauvagine as agonist. The glycine eluate of antiserum from animal 1318 showed comparable counts to those seen when using the in-house antiserum (I3B) for both basal and agonist stimulated conditions (**Figure 5.3**). This shows then, that the glycine eluate from animal 1318 is capable of the immunoprecipitation of [ $^{35}\text{S}$ ] GTP $\gamma$ S-bound  $G\alpha_{i3}$ .

### 5.2.3 Characterisation of antisera generated against a decapeptide corresponding to the C-terminal decapeptide of $G\alpha_q$

Antisera were generated against a decapeptide corresponding to the C-terminal ten amino acids of  $G\alpha_q$  and affinity towards the decapeptide was confirmed in an ELISA (CRL laboratories). As for the antisera generated against  $G\alpha_t$  the selectivity of this interaction had to be confirmed. Again, a system where  $G\alpha_q$  could be expressed in a  $G\alpha_q$ -null background had to be used. In this case  $G\alpha_q/G\alpha_{11}$  null EF88 cells could be used (Stevens et al., 2001). EF88 cells were or were not transiently transfected with  $G\alpha_q$  (performed by Laura Ormiston, Molecular Pharmacology, University of Glasgow), membranes preparations made and proteins separated by SDS PAGE. Western blots were performed using the antisera raised against the C-terminal decapeptide of  $G\alpha_q$  and compared with an equivalent and previously characterised in-house antiserum (CQ5). The in-house antiserum CQ5 gave a single band between 35 and 50 kDa only in EF88 cell membranes where  $G\alpha_q$  had been transiently expressed (**Figure 5.4A**). Similarly, both the glycine and TEA eluates of antiserum from animals 1316 and 1317 (**Figures 5.4B-E**), gave a single band between 35 and 50 kDa, again only in EF88 cell membranes where  $G\alpha_q$  had been transiently expressed. This demonstrates the selectivity of these antisera towards  $G\alpha_q$ .

As for antisera raised against  $G\alpha_t$  it was of interest to establish whether this antiserum could efficiently immunocapture [ $^{35}\text{S}$ ] GTP $\gamma$ S bound  $G\alpha_{q/11}$ . A [ $^{35}\text{S}$ ] GTP $\gamma$ S assay with an immunocapture step was performed using membranes from EF88 cells co-expressing the  $\alpha_{1b}$ -adrenoceptor and  $G\alpha_{11}$  (supplied by L. Jenkins, University of Glasgow) and with or without the addition of 1 $\mu$ M phenylephrine. The glycine eluate of 1317 showed comparable counts to those seen when using the in-house antiserum (CQ5), for both basal and agonist-stimulated conditions (**Figure 5.5**). This shows then, that the glycine eluate of 1317 not only shows affinity for  $G\alpha_q$  on a western blot, but is capable of immunoprecipitation of [ $^{35}\text{S}$ ] GTP $\gamma$ S bound  $G\alpha_q$ . Furthermore, it showed a comparable efficiency of pulldown to an in-house antiserum raised against the C-terminal ten amino acids of  $G\alpha_q$ .

#### **5.2.4 Characterisation of antisera generated against a decapeptide corresponding to the C-terminal decapeptide of $G\alpha_s$**

Following the generation of antisera against the C-terminal tail of  $G\alpha_s$  their selectivity was confirmed both by Western blotting and immunoprecipitation.  $G\alpha_s$  is expressed in a wide range of mammalian cells and a  $G\alpha_s$  null cell line was not available. However, prolonged treatment with cholera toxin leads a decrease of  $G\alpha_s$  levels. Conversely, expression levels of  $G\alpha_s$  within a cell can be increased by transiently transfecting cells with  $G\alpha_s$  cDNA. Accordingly, to characterise the above antisera, HEK293T cells were transfected with cDNA corresponding to the long isoform of  $G\alpha_s$  or a mock transfection was performed using an equivalent amount of the empty vector pcDNA3. Of the cells which were mock transfected, one sample was subjected to a prolonged treatment with cholera toxin. Cells were harvested and membrane preparations made. Membrane protein was separated by

SDS PAGE and western blots performed using antisera generated against the C-terminal decapeptide of  $G\alpha_s$ . The in-house antiserum CS2 showed two bands between 35 and 50 kDa corresponding to the long and short isoforms of  $G\alpha_s$  for all membrane preparations. However, the intensity of these bands varied between the three preparations. As compared to the mock, un-treated HEK293T cells, the bands were more intense for the sample where  $G\alpha_s$  had been transiently transfected, and less intense where the cells had been treated with cholera toxin (**Figure 5.6A**). Similarly, the antisera generated in this project, namely the glycine and TEA eluates from animal 1314, showed a similar pattern. Indeed, as compared to the in-house antiserum the bands were of a higher intensity and with no non-specific bands (**Figure 5.6B-C**). The antisera generated in this project against the C-terminal tail ten amino acids of  $G\alpha_s$  showed selectivity towards  $G\alpha_s$  and are equivalent, if not better, than an in-house antibody previously generated against the same decapeptide.

The ability of this antiserum to efficiently immunocapture [ $^{35}\text{S}$ ] GTP $\gamma$ S  $G\alpha_s$  was tested. A [ $^{35}\text{S}$ ] GTP $\gamma$ S assay with an immunocapture step was performed using membranes from cells co-expressing the corticotrophin releasing factor (CRF) receptor and  $G\alpha_s$  and with or without the addition of 1 $\mu$ M sauvagine. The glycine eluate of 1314 showed comparable counts to those seen when using the in-house antiserum CS2 for both basal and agonist-stimulated conditions (**Figure 5.7**). This shows then, that the glycine eluate of 1314 not only shows affinity for  $G\alpha_s$  on a western blot, but is capable of immunoprecipitating [ $^{35}\text{S}$ ] GTP $\gamma$ S bound  $G\alpha_s$ . In conclusion then, antisera were raised against decapeptides of corresponding to the C-terminal ten amino acids of  $G\alpha_q$ ,  $G\alpha_s$  and  $G\alpha_t$ .

### **5.2.5 Generation of antibodies selective to the active conformation of $G\alpha_{i1}$ :**

The second aim of this chapter was the generation of antibodies that selectively recognise the active (GTP bound) conformation of the  $G\alpha_{i1}$  subunit. To achieve this goal two immunisation strategies were used; plasmid immunisation, or repetitive immunisation at multiple sites (RIMMS) using recombinant human  $G\alpha_{i1}$  which had been 'preloaded' with the non-hydrolysable GTP analogue GTP $\gamma$ S to force the  $G\alpha$  subunit into the active, GTP bound, conformation. For the plasmid immunisation strategy, cDNA of a constitutively active mutant of  $G\alpha_{i1}$ , Glu<sup>204</sup>Leu  $G\alpha_{i1}$ , was cloned into the vector  $\alpha$ FcMCS. The stop codon of the Glu<sup>204</sup>Leu  $G\alpha_{i1}$  gene was removed and therefore upon cloning into the multiple cloning site of  $\alpha$ FcMCS, a Glu<sup>204</sup>Leu  $G\alpha_{i1}$  human Fc fragment fusion protein was generated. Gold particles were coated with this cDNA and plasmid immunisation performed using a gene gun. For the RIMMS procedure, recombinant human  $G\alpha_{i1}$  was incubated with 100  $\mu$ M GTP $\gamma$ S, to 'load' the  $G\alpha_{i1}$  protein with GTP $\gamma$ S and to force the protein into its active conformation and animals immunised using a procedure modified from (Bynum et al., 1999). Both of these immunisation procedures were performed by I. Kinghorn (Antibody Generation, Biological Reagents and Assay Development (BRAD), GSK).

### **5.2.6 Outline of hybridoma generation**

The generation of monoclonal antibodies using the production of hybridomas is a well used and characterised procedure. In this project, as for the immunisation procedures all hybridoma generation and culture, as well as antibody purification was performed by I.

Kinghorn (Ab generation BRAD, GSK). I will, therefore, only include a brief and general outline of the steps involved in hybridoma production to put the subsequent screening and characterisation of antibodies into context. For a more detailed summary of the immunisation procedures and hybridoma generation procedures refer to section **2.10**. The antibody generation strategy is described by **Figure 5.8**. Periodic test bleeds collected from immunised animals can be checked for the desired antibodies. The test bleed will yield small samples of polyclonal sera. These sera should be tested in assays that will detect the presence of antibodies specific for the antigen. It is not worthwhile to fuse antibody secreting cells from animals that do not have a useable titre of antibodies in their serum. Antibody producing cells can be removed from the animal and fused with myeloma cells by centrifugation. Hybridoma clones are generated using selective medium preventing the growth of myeloma cells. Hybridoma cells secrete antibodies into the tissue culture medium in which they are grown. Consequently, samples of this tissue culture medium for all selected clones can be screened for antibodies with the desired characteristics. Cells from positive clones are then grown and single cells cloned. These single cell clones are then screened again and the final hybridoma can be expanded and frozen down.

### **5.2.7 The FMAT assay system**

The success of hybridoma production depends on the production of useful antibodies with the desired characteristics and is dependent on the strength of the immune response and the development of a robust screening method. Consequently, prior to the immunisation of animals it was necessary to have a robust screening method in place. The assay format

decided upon was a whole cell FMAT assay. The FMAT or 'Fluorometric Microvolume Assay Technology' is a system developed by Applied Biosystems (Foster city, CA, USA). The FMAT 8200 high throughput screening system provides a platform that is perfectly suited for hybridoma screening. The FMAT system is a macroconfocal scanner that visualizes and quantifies both cell-and bead-bound fluorescence. Consequently then, cells which express the antigen of interest can be incubated with hybridoma supernatant plus the relevant secondary antibody conjugated with the FMAT blue ® dye (**Figure 5.9**). The FMAT Blue® dye is a far-red emitting dye in the 650 nm range light generated from a 633 nm helium/neon laser scans an area of 1 mm<sup>2</sup> with a depth of focus of ~100 µm from the bottom of each well. Because the depth of focus is relatively small with respect to the remaining volume of the well, the majority of the unbound fluorophore remains undetected and need not be washed away. The FMAT™ software is then able to subtract the remaining background fluorescence from the fluorescence immobilized on the cells or beads. As a result, all assays performed with the FMAT system are 'mix-and-read' and do not require wash steps. The integrated plate handler allows for walk-away screening for up to sixty 96- or 384-well plates.

#### **5.2.7.1 Development and characterization of a whole cell FMAT assay to allow screening of hybridomas producing antibodies that are selective against the active conformation (GTP bound) conformation of Gα1**

The FMAT assay technology using whole cells expressing the desired antigen has been used successfully in previous antibody generation programmes to screen for hybridomas secreting antibodies with the desired selectivity. For these programmes the antigen was generally expressed on the extracellular surface in contrast to the desired antigen in this screen, a Gα subunit which has an intracellular localisation. It was necessary then, to

develop a method of permeabilising the cell to allow access of the antibody to this antigen. HEK293T cells were transiently transfected with cDNA of either  $G\alpha_{i1}$  (wild type), Gly<sup>203</sup>Ala  $G\alpha_{i1}$  (inactive mutant), Glu<sup>204</sup>Leu  $G\alpha_{i1}$  (active mutant) or GPR55 (FLAG N-terminus) as a negative control. Transfected cells were permeabilised by four different techniques, the relevant FMAT blue ® secondary antibody could be added to a dilution of 1:2000, and then added to each well of a 96 well FMAT™ plate into the bottom of which a sample of the desired primary antibody was aliquot. This general protocol is described by the diagram in **Figure 5.9**. Following each permeabilisation step cells were washed and assayed in PBS + 1% BSA + 0.1% NaN<sub>3</sub> + Triton X 100. Cell viability following each of the permeabilisation methods was measured prior to assay reading. For these experiments the polyclonal antiserum: glycine 1319 characterized in **section 5.2.2** was used. This antiserum recognizes the C-terminal ten amino acids of  $G\alpha_{i1/2}$  but would not be anticipated to discriminate between the inactive or active variants of  $G\alpha_{i1}$ , or indeed the GTP or GDP bound conformations of the wild type. Conversely, as a proof of concept, the FMAT assay was performed using an anti-FLAG antibody, and would only be anticipated to give a high signal for cells transfected with FLAG-GPR55

Following cell permeabilisation using the sodium azide method, in which cells were washed, resuspended and assayed in PBS +1% BSA + 0.1% NaN<sub>3</sub>, the proportion of viable cells was 80 %. Using the polyclonal anti- $G\alpha_{i1/2}$  antiserum, a high signal was seen for all conditions with cells transfected with  $G\alpha_{i1}$  cDNA compared to the negative control of cells transfected with FLAG-GPR55. The FMAT assay performed with a final polyclonal anti- $G\alpha_{i1/2}$  antiserum dilution of 1:500 gave an approximately 40 fold higher signal (200,000 counts) for positive conditions where  $G\alpha_{i1}$  was expressed as compared to the negative, GPR55 transfection condition (**Figure 5.10A**). In the Cytofix / Cytoperm method, cells were incubated with Cytofix/Cytoperm for 10 minutes at 4 °C. Cells then were washed twice with CytoPerm before the assay step. In the hERG fixation method

cells were resuspended in 4 % (w/v) neutral buffer formalin for 10 min at 4 °C prior to the assay step. In both cases (**Figure 5.10B + C**), a similar high signal was seen for  $G\alpha_{i1}$  transfected cells in the experiments using the anti- $G\alpha_{i1/2}$  antiserum as compared to the FLAG-GPR55 transfected negative control but cell viability was reduced to <10%. In a Modified Kruzik's method (Kruzik et.al 2005), cells were permeabilised in 4% (w/v) neutral buffer formalin for 15 min at room temperature. Methanol was added directly to fixative to a final concentration of 80 % and cells incubated for a further 5-10 minutes at room temperature. This protocol resulted in an even lower cell viability (<1%) (**Figure 5.10D**), and although higher counts were observed for  $G\alpha_{i1}$  transfection conditions compared to the FLAG-GPR55 transfection condition when the anti- $G\alpha_{i1/2}$  antisera was used, the signal window was much reduced as compared to that seen for the equivalent experiment using the sodium azide permeabilisation method.

High cell viability is important since the FMAT<sup>TM</sup> software contains an algorithm to select for fluorescence bound only to viable cells. Consequently, a permeabilisation procedure that maintains high cell viability is advantageous. In addition, the relative simplicity of the sodium azide method compared to the other permeabilisation methods made it the most attractive for subsequent optimisation and eventual use in the antibody screening assay.

This work was performed by Dion Daniels (BRAD, GSK, UK) and Ben Powney (Screening & Compound Profiling, GSK, UK).

#### **5.2.7.2 A whole cell FMAT assay for screening of hybridomas was stable for 23 hours**

To allow for efficient screening of a large number of hybridoma supernatants it was necessary for the assay to be carried out in 384 well plates. Furthermore, to allow the hybridoma screen to be performed overnight without supervision, the assay must be stable

for a 24 hour period. HEK293T cells were transiently transfected with cDNA of either wild type  $G\alpha_{i1}$  or the constitutively active variant  $Gln^{204}Leu G\alpha_{i1}$  and as a negative control cells were transfected with cDNA of FLAG-GPR55. Cells were resuspended in permeabilisation buffer (PBS + 1% BSA + 0.1%  $NaN_3$ ) with or without the addition of 10  $\mu M$   $GTP\gamma S$  and with the addition of FMAT blue ® anti-rabbit secondary antibody. This cell suspension was added to a well of a 384 well plate already containing 1  $\mu l$  of anti- $G\alpha_{i1/2}$  antiserum (glycine 1319). This plate was left at room temperature for 2 hours or 23 hours prior to reading. For the 2 hour read, a high signal (~600,000 counts) was observed for conditions in which  $G\alpha_{i1}$  had been transfected into cells as compared to the negative control, FLAG-GPR55 transfected cells (~ 20000 counts) (**Figure 5.11A**),. For the 23 hour read, a high signal was observed for the  $G\alpha_{i1}$  transfected cells (~2,000,000 counts) and a negligible signal seen for the FLAG-GPR55 control transfection (100,000 counts) (**Figure 5.11B**). As expected using the anti- $G\alpha_{i1/2}$  antiserum raised against the C-terminal ten amino acids of  $G\alpha_t$ , there was no difference between the signal observed for wild type  $G\alpha_{i1}$  transfections and transfections of the constitutively active variant  $Gln^{204}Leu G\alpha_{i1}$  or with the addition of 10  $\mu M$   $GTP\gamma S$ . As described by **Table 5.4**  $Z'$  is a simple statistical parameter for use in evaluation and validation of high throughput screening. By calculation of the  $Z'$  number for each positive  $G\alpha_{i1}$  transfection condition in comparison to the negative GPR55 transfection condition a measurement of the robustness of the assay was gained. For all conditions in both the 2 hour and 23 hour read the  $Z'$  value was greater than 0.6 (**Figure 5.12A + B**). Therefore, the assay was robust in a 384 well format, and that the large signal window of the assay was stable for at least 23 hours following cell addition. These characteristics made it suitable for hybridoma screening. This work was performed by Dion Daniels (BRAD, GSK, UK) and Ben Powney (S & CP, GSK, UK).

**Table 5.4: A simple characterisation of a high throughput screening assay by calculation of Z'.**

$Z' = 1 - \frac{3SD \text{ of sample} + 3SD \text{ of control}}{\text{mean of sample} - \text{mean of control}}$		
<b>Z-factor value</b>	<b>Structure of assay</b>	<b>Related to screening</b>
<b>1</b>	SD = 0 (no variation)	An idea assay
<b><math>1 &gt; Z \geq 0.5</math></b>	Separation band is large	An excellent assay
<b><math>0.5 &gt; Z &gt; 0</math></b>	Separation band is small	A double assay
<b>0</b>	No separation band, the sample signal variation and control signal variation bands touch	A “yes/no” type assay
<b>&lt;0</b>	No separation band, the sample signal variation and control signal variation bands overlap	Screening essentially impossible

SD = standard deviation. In the case of the FMAT assay control refers to the negative control conditions (Zhang et al., 1999).

**5.2.7.3 Frozen cells could be used in a whole cell FMAT assay for screening of hybridomas producing antibodies that are selective against the active conformation (GTP bound) conformation of Gα<sub>i1</sub>:**

To allow the preparation of all reagents needed for the screen prior to hybridoma screening it would be advantageous if stocks of appropriately transfected cells could be frozen down in advance and then brought up and defrosted when required. Cells were transfected with cDNA of either wild type Gα<sub>i1</sub>, the constitutively active variant Gln<sup>204</sup>Leu Gα<sub>i1</sub> or a mock transfection was performed using an equivalent amount of the empty vector pcDNA3.

Cells were counted and aliquots from each condition were either left on ice or re-suspended in foetal calf serum and frozen at  $-80\text{ }^{\circ}\text{C}$  for 2 hours. Frozen cells were then thawed rapidly in a  $37\text{ }^{\circ}\text{C}$  bath, washed twice in PBS ( $4\text{ }^{\circ}\text{C}$ ) and an FMAT assay performed as in section 5.2.8.2 using both frozen and fresh cells. Again, within the same treatment condition, there was little difference between signals observed for wild type and active variant  $G\alpha_{i1}$  transfections (**Figure 5.13**). Furthermore, there was no difference observed between counts for the fresh and frozen cells for each transfected cell condition. The robust signal window observed is highlighted by a  $Z'$  value of  $>0.6$  observed for each positive condition in comparison to the negative mock transfection condition (**Figure 5.12**). This experiment demonstrates that a robust assay for screening hybridomas selective against  $G\alpha_{i1}$  can be performed using pre-frozen aliquots of transiently transfected cells.

### **5.2.8 Test bleed ELISAs against recombinant $G\alpha_{i1}$**

Following the successful demonstration of a viable FMAT assay to screen hybridoma clones the immunisation programme was started. Two mice were immunised for each immunisation strategy, either plasmid immunisation or the protein RIMMS protocol described above. To check the strength of the immune response, and indeed the success of the immunisation, test bleeds were taken from each animal. A set of serial dilutions was made of each test bleed and as a positive control the polyclonal anti- $G\alpha_{i1}$  antiserum (Glycine 1319). These were dispensed onto 96 well plates coated with  $rG\alpha_{i1}$  ( $0.1\text{ }\mu\text{g}$  / well). The secondary antibody used was either a HRP conjugated anti-mouse or anti-rabbit antibody as appropriate. For the  $rG\alpha_{i1}$  RIMMS for both animal 120 and 121 a small but

significant signal was observed (**Figure 5.13A**), although this signal was three times smaller than the maximum signal observed for the anti-G $\alpha_{i1}$  antiserum (**Figure 5.13C**). This is perhaps not surprising since the concentration of antibody in the test bleed is likely to be many times lower than that seen for the purified anti-G $\alpha_{i1/2}$  antiserum. It is notable, however, that for the plasmid immunisations, no signal was observed (**Figure 5.13B**). This indicates that this immunisation strategy was unsuccessful.

### 5.2.9 Test bleed ELISAs against human IgG

To confirm that the plasmid immunisation did not stimulate an immune response, ELISAs were performed using the test bleeds from the plasmid immunised animals. A Gln<sup>204</sup>Leu G $\alpha_{i1}$ -human Fc fragment fusion protein was generated. Consequently, an immune response should be generated not only against Gln<sup>204</sup>Leu G $\alpha_{i1}$  but also against the Fc fragment. Again serial dilutions of the test bleeds from the plasmid immunised animals were made and these dispensed into 96 well plates pre-coated with human IgG. As a positive control a bleed from a plasmid immunised animal from another immunisation program again using a human Fc fragment fusion protein which had shown a strong immune response was used (supplied by I. Kinghorn, GSK). As a negative control, a test bleed from an unrelated program using a RIMMS protocol, which should therefore show no affinity for human IgG was used (supplied by I. Kinghorn). The positive control gave strong signal, and as expected the negative control gave no specific signal (**Figure 5.14**). In comparison to the positive control no signal was observed for the test bleeds from the G $\alpha_{i1}$ -Fc plasmid immunisation. This suggests that the plasmid immunisation program was unsuccessful and failed to generate an immune response.

## 5.2.10 Hybridoma Screen

### 5.2.10.1 Conditions for hybridoma screen

Following the positive response seen for the test bleed ELISAs from the rG $\alpha_{i1}$  immunisation protocol, it was decided to continue with the hybridoma generation program as described above, both with animals from the protein immunisation and the plasmid immunisation. Hybridoma clones were picked and grown up in 96 well plates. Screening was to be performed in 384 well plates. To allow complete automation of the screening process, including the dispensing of hybridoma supernatant from 96 well to 384 well plates the screen had to be set up to allow one supernatant to be screened in four wells of a 384 well plate. This meant that four conditions would have to be chosen to identify hybridomas producing antibody that was selective against the active (GTP bound) conformation of G $\alpha_{i1}$ . To achieve this the following conditions were set up: 1) HEK293T cells transfected with wild type G $\alpha_{i1}$  cDNA, and incubated with 100  $\mu$ M GTP $\gamma$ S to force the majority of expressed G $\alpha_{i1}$  into the active GTP bound conformation. 2) HEK293T cells transfected with constitutively active Gln<sup>204</sup>Leu G $\alpha_{i1}$  3) HEK293T cells transfected with wild type G $\alpha_{i1}$  cDNA, and incubated with 100  $\mu$ M GDP $\beta$ S to force the majority of expressed G $\alpha_{i1}$  into the inactive GDP bound conformation. 4) HEK293T cells mock transfected with pcDNA3 (**Figure 5.15**). As in preliminary assays cells were permeabilised by incubation in PBS + 1% BSA + 1% NaN<sub>3</sub>. FMAT blue ® anti-mouse secondary was used at a final dilution of 1:2000. A hybridoma producing antibody that is selective against G $\alpha_{i1}$  in the active GTP bound conformation should show a high signal against both the GTP $\gamma$ S loaded G $\alpha_{i1}$  wild type condition and also the Gln<sup>204</sup>Leu G $\alpha_{i1}$  condition, but not against the GDP $\beta$ S loaded or mock transfection conditions.

Furthermore, the inclusion of a wild type  $G\alpha_{i1}$  loaded with GTP $\gamma$ S condition should prevent the identification of false positive clones which simply pick up the mutation of Gln<sup>204</sup>Leu rather than the associated conformational change. It could be expected that the majority of hybridomas will produce antibody which is selective against  $G\alpha_{i1}$  but does not distinguish between the active and inactive conformations.

#### **5.2.10.2 Primary hybridoma screen: identification of 3 hybridoma showing selectivity towards the active (GTP bound) conformation of $G\alpha_{i1}$**

A total of 1632 hybridoma clones were screened originating both from the r $G\alpha_{i1}$  rapid immunisation and the plasmid immunisation strategies. Positive clones were identified using the FMAT™ software. This gave a visual representation of fluorescent signal/cell number, and allows easy identification of positive clones. To confirm this identification, an Excel spreadsheet (Microsoft) was designed to identify both clones which recognise  $G\alpha_{i1}$ , but do not show any selectivity between the inactive and active state and those which are conformation selective. In both cases a ratio of signal of the positive versus the negative conditions that was greater than or equal to 2 was highlighted as a positive result. For clones showing non-conformational selectivity a higher signal was observed for the three conditions in which HEK293T cells had been transfected with either  $G\alpha_{i1}$  wild type or Gln<sup>204</sup>Leu  $G\alpha_{i1}$  compared to that seen for the mock-transfected HEK293T cells. As could be expected, the majority of positive clones simply displayed selectivity towards the  $G\alpha_{i1}$  transfected conditions as compared to the mock-transfection (see **Table 5.5**). The large number of clones displaying this profile is perhaps again indicative that expression levels of both the wild type and constitutively active forms of  $G\alpha_{i1}$  were equivalent. However, three hybridoma clones (8D11, 6F12, 8A6) showed a profile indicative of selectivity towards the active or GTP bound conformation of  $G\alpha_{i1}$  (**Figure 5.16**). In all

cases the signal observed for either HEK293T cells expressing wild type  $G\alpha_{i1}$  preloaded with  $GTP\gamma S$  or cells expressing the constitutively active mutant  $Gln^{204}Leu G\alpha_{i1}$  was considerably higher than that observed for cells expressing wild type  $G\alpha_{i1}$  preloaded with  $GDP\beta S$  or the mock-transfected cells. It should be noted that for all three of the above hybridoma clones the observed signal for cells expressing wild type  $G\alpha_{i1}$  loaded with  $GDP\beta S$  was higher than that observed for mock transfected cells. This increased level of signal must be due to the increased level of  $G\alpha_{i1}$  expressed within the cell. This could be explained by two scenarios; firstly that the antibody has an affinity for the GDP bound (inactive) state of the receptor, albeit lower than that observed for the GTP bound (active) state, or secondly that the concentration of  $GDP\beta S$  used was not sufficient to force the entire population of  $G\alpha_{i1}$  into the inactive conformation. However, the 'signal window' observed between the  $GTP\gamma S$  loaded condition and the  $GDP\beta S$  loaded condition was large enough to warrant further characterisation of these three hybridoma clones.

**Table 5.5: Summary of results from initial hybridoma screen**

Clones showing selectivity towards  $G\alpha_{i1}$  had higher counts for conditions in which  $G\alpha_{i1}$  was expressed as compared to the mock transfection condition. Clones showing selectivity towards the active conformation of  $G\alpha_{i1}$  had higher counts for the  $G\alpha_{i1} + 100\mu M GTP\gamma S$  or the  $Gln^{204}Leu G\alpha_{i1}$  as compared to the  $G\alpha_{i1} + 100\mu M GDP\beta S$  or mock transfection conditions

<b>Number. of clones screened</b>	<b>Number of clones showing selectivity to <math>G\alpha_{i1}</math></b>	<b>Number of clones showing selectivity towards active conformation of <math>G\alpha_{i1}</math></b>
<b>1632</b>	<b>34</b>	<b>3</b>

### 5.2.10.3 Secondary hybridoma screen: Confirmation that three hybridomas show selectivity towards the active (GTP bound) conformation of $G\alpha_{i1}$

Clones, which showed selectivity towards  $G\alpha_{i1}$  transfected conditions, were subsequently sub-cultured. This included the three clones with putative selectivity towards the active conformation of  $G\alpha_{i1}$ . All other hybridoma clones were discarded. To confirm the results of the primary screen, a secondary screen was again set up using the same conditions as for the primary screen. However, for the secondary screen the experiment was performed in triplicate to  $N = 3$ . Again, the majority of clones showed no selectivity towards the active or inactive conformation of  $G\alpha_{i1}$ , but simply showed high counts in conditions where  $G\alpha_{i1}$  was expressed and negligible counts for the mock transfection condition (**Figure 5.17 A-D**). The three clones which were identified as being selective towards the active conformation of  $G\alpha_{i1}$  again showed higher counts in conditions where  $G\alpha_{i1}$  was in an active conformation as opposed to those seen for the condition in which  $G\alpha_{i1}$  was in the inactive (GDP $\beta$ S loaded) conformation (clones 8A5, (**Figure 5.17D**), 8D11 (**Figure 5.17D**), 6F12 (**Figure 5.17C**)). However, in comparison to the primary screen the difference between observed signal for active and inactive  $G\alpha_{i1}$  conditions was not as great. Indeed, in the primary screen the observed fold difference between the conditions in which  $G\alpha_{i1}$  would be in the active conformation as compared to the inactive conformation was around 10 fold as compared to a  $< 2$  fold difference in the secondary screen. However, the signal observed for the mock transfection remained extremely low (**Figure 5.17 A-D**). The higher counts observed in the condition where expressed  $G\alpha_{i1}$  was preloaded with GDP $\beta$ S indicated that these antibodies may still have significant affinity for the inactive conformation of  $G\alpha_{i1}$ . However, this pattern could also be seen if the concentration of GDP $\beta$ S used was insufficient to ensure all expressed  $G\alpha_{i1}$  was forced into an inactive GTP bound state.

#### 5.2.10.4 FMAT screen of sub-cloned hybridoma

In the initial generation and culture of individual hybridoma clones, a Clonepix robot was used to 'pick' individual clones from a polyclonal mix grown on a semisolid medium see **section 2.10**). Whilst this method saved a considerable amount of time, and consequently, allowed the generation and screening of many more hybridoma clones, it is not 100 % accurate and if colonies were growing close to each other might result in a clone actually being a mixed polyclonal population. If hybridoma producing non-conformation selective antibodies become a more prevalent members of this polyclonal population then the signal window observed between conditions in which  $G\alpha_{i1}$  was in an active state compared to the inactive state would decrease.

Hybridoma which had been shown to produce antibodies selective to the active conformation of  $G\alpha_{i1}$  (8A5, 8D11, 6F12), were re-cloned, individual colonies picked and cultured. Hybridoma tissue culture supernatant was again screened using the FMAT assay as in **section 5.2.11**. A mix of clones was again seen with some showing higher counts for conditions in which  $G\alpha_{i1}$  was in the active conformation. However, non-conformation selective clones were also observed (**Table 5.6**). It was disappointing to note then, that despite the re-cloning of these hybridoma and the removal of clones which produced non-conformation selective antibody the signal window was not significantly improved (**Figure 5.18A-C**). The clones which showed the largest signal window between  $G\alpha_{i1}$  in the active conformation and those in the inactive conformation were retained, subcultured and aliquots frozen down. All other clones were discarded. Retained clones were cultured on a large scale and antibody purified from the resulting supernatant. Two non-conformation selective antibody producing hybridoma clones (6B4 and 8F5), were also retained and cultured to a large scale and antibody purified from the resulting supernatant (**Figure 5.17 A-D**)

**Table 5.6: Summary of results from screen of sub-cloned hybridoma**

Clones showing selectivity towards  $G\alpha_{i1}$  had higher counts for conditions in which  $G\alpha_{i1}$  was expressed as compared to the mock transfection condition (**Figure 5.16**). Clones showing selectivity towards the active conformation of  $G\alpha_{i1}$  had higher counts for the  $G\alpha_{i1}$  + 100 $\mu$ M GTP $\gamma$ S or the Gln<sup>204</sup>Leu  $G\alpha_{i1}$  as compared to the  $G\alpha_{i1}$  + 100 $\mu$ M GDP $\beta$ S or mock transfection conditions

<b>Parental clone</b>	<b>Number. of clones screened</b>	<b>Number of clones showing selectivity to <math>G\alpha_{i1}</math></b>	<b>Number of clones showing selectivity towards active conformation of <math>G\alpha_{i1}</math></b>
<b>8A5</b>	<b>24</b>	<b>23</b>	<b>9</b>
<b>8D11</b>	<b>48</b>	<b>48</b>	<b>36</b>
<b>6F12</b>	<b>48</b>	<b>48</b>	<b>38</b>

#### **5.2.10.5 Titration experiment using purified antibody from each conformation selective hybridoma**

Using each purified antibody described in the previous section an ELISA-like experiment was set up. A sequential 1 in 3 set of twelve dilutions were made of each antibody. These were added into the wells of FMAT 384 well plates. Similar to the FMAT screens used previously the five following conditions were set up: HEK293T cells transiently expressing wild type  $G\alpha_{i1}$  were permeabilised in FMAT buffer and preloaded with either

10 $\mu$ M GTP $\gamma$ S (1) or 10 $\mu$ M GDP $\beta$ S (2). HEK293T cells transiently expressing either the constitutively active variant Gln<sup>204</sup>Leu G $\alpha_{i1}$  (3) or the constitutively inactive variant Gly<sup>203</sup>Ala G $\alpha_{i1}$  (4) were permeabilised in FMAT buffer but not pre-incubated with guanine nucleotide. Finally, cells were mock-transfected with the empty vector pcDNA3 and permeabilised as above (5). An FMAT assay was performed with each of these cell suspensions was added to the dilution sets of the five antibodies. The non-conformation selective antibodies 8A5 and 6B4 (**Figure 5.19 A-B**) showed little difference in counts between wild type G $\alpha_{i1}$  loaded with GTP $\gamma$ S or GDP $\beta$ S at all dilutions. In both cases, counts for the Gln<sup>204</sup>Leu G $\alpha_{i1}$  constitutively active variant were marginally lower than the counts observed for the wild type G $\alpha_{i1}$  conditions. Similarly, the counts observed for the Gly<sup>203</sup>Ala G $\alpha_{i1}$  inactive variant were markedly lower than those observed for the wild type G $\alpha_{i1}$  conditions. In both cases, this is most likely due to lower relative amounts of G $\alpha_{i1}$  variant expressed as compared to the wild type G $\alpha_{i1}$  transfected cells. The putative conformation-selective antibodies (8A6/1H1, 8D11/1C1, 6F12/1E5, **Figure 5.20 A-C**) all showed higher counts for wild type G $\alpha_{i1}$  loaded with GTP $\gamma$ S as compared to GDP $\beta$ S. However, this was titre dependent with the largest 'signal window' observed at approximately 0.1  $\mu$ g/ml initial antibody protein concentration for all antibodies. Counts observed for the Gln<sup>204</sup>Leu G $\alpha_{i1}$  constitutively active mutant expressing cells were high and similar to those observed for the condition in which wild type G $\alpha_{i1}$  was preloaded with GTP $\gamma$ S. However, for the cells expressing the inactive variant Gly<sup>203</sup>Ala G $\alpha_{i1}$  the observed counts were extremely low. Indeed for the antibodies 8A6/1H1 (**Figure 5.20 A**) and 8D11/ 1C1 (**Figure 5.20 B**) the observed counts were 10 fold lower than those observed for the constitutively active variant Gln<sup>204</sup>Leu G $\alpha_{i1}$  or indeed wild type G $\alpha_{i1}$  loaded with GTP $\gamma$ S. For the antibody 6F12/1E5 (**Figure 5.20 C**), a three fold difference was observed. In all cases this difference was large enough that it could not simply be explained by the lower relative expression of G $\alpha_{i1}$  (**Figure 5.19A-B**). For all antibodies the observed counts for the mock-transfection were markedly lower (**Figures 5.19, 5.20**). The best signal

window observed between wild-type  $G\alpha_{i1}$  loaded with  $GTP\gamma S$  and  $GDP\beta S$  was a modest two fold. This is strikingly smaller than the ten fold difference observed between the active and inactive variants of  $G\alpha_{i1}$ . This suggests that either the concentration of  $GDP\beta S$  used was not sufficient to force the entire population of  $G\alpha_{i1}$  into an inactive conformation, or that the conformation of  $G\alpha_{i1}$  bound to  $GDP\beta S$  is different to that of the constitutively inactive variant Gly<sup>203</sup>Ala  $G\alpha_{i1}$ . Since the cells are in a non-stimulated state, it would be expected that the majority of expressed  $G\alpha_{i1}$  would be in the GDP bound conformation.

### **5.2.11 Non-conformation selective antibodies show selectivity to $G\alpha_{i1}$ .**

#### **Conformation selective antibodies do not pick up $G\alpha_{i1}$ , $G\alpha_{i2}$ , $G\alpha_{i3}$ or $G\alpha_{o1}$ when denatured on a SDS-PAGE gel**

From the FMAT hybridoma screen and subsequent FMAT assays hybridoma clones were identified producing either antibodies selective towards the active GTP bound conformation of  $G\alpha_{i1}$  or antibodies simply selective towards  $G\alpha_{i1}$  but having equal affinity for both the GDP and GTP bound forms of  $G\alpha_{i1}$ . To further characterise these antibodies their specificity towards the other members of the  $G\alpha_{i/o}$  family was tested. To achieve this each of  $G\alpha_{i1}$ ,  $G\alpha_{i2}$ ,  $G\alpha_{i3}$  and  $G\alpha_{o1}$  were expressed in the BL21 strain of *E coli* which had been transformed with the vector pT7.7 into which the cDNA of each  $G\alpha_{i/o}$  subunit had been cloned. Expression of each  $G\alpha_{i/o}$  subunit was induced with the addition of IPTG and protein was separated by SDS PAGE. Western blotting was performed using the antibodies from each of the selected hybridoma clones. The polyclonal anti- $G\alpha_{i1/2}$  antiserum raised against the last ten amino acids of  $G_t$  (1319 Glycine) was used as a positive control. The conformation selective antibodies failed to pick up  $G\alpha_{i1}$ ,  $G\alpha_{i2}$ ,  $G\alpha_{i3}$  and  $G\alpha_{o1}$  when denatured on a SDS PAGE gel (**Figure 5.22A-C**). This is not surprising, since if they are conformation selective it is most likely than they recognise a three dimensional epitope which would be lost if the protein was denatured. Interestingly, the

non-conformation selective antibodies (6B4 and 8A5) recognised only  $G\alpha_{i1}$  and no other members of the  $G\alpha_{i/o}$  subfamily when denatured on a western blot (**Figure 5.21 A-B**). This was surprising given the high sequence homology of  $G\alpha_{i/o}$  subfamily members (**Table 5.1**) particularly between  $G\alpha_{i1}$  and  $G\alpha_{i3}$ . It follows then, that the epitope(s) recognised by these antibodies is likely to lie within regions of divergent amino acid sequence between  $G\alpha_{i1}$  and the other  $G\alpha_{i/o}$  subunits. Given the design of the assay and what is known about expression of members of the  $G\alpha_{i/o}$  subfamily it is perhaps not surprising that antibodies with these characteristics were generated.  $G\alpha_{i2}$  and  $G\alpha_{i3}$  are widely expressed in the majority of cell types including HEK293 cells. Since antibodies were selected which gave a low signal in the mock transfected HEK293 condition, it is likely that antibodies which showed an affinity for  $G\alpha_{i2}$  or  $G\alpha_{i3}$  and therefore relatively high counts for the mock-transfection condition were discarded. The anti- $G\alpha_{i1/2}$  polyclonal antisera recognised  $G\alpha_{i1}$ ,  $G\alpha_{i2}$  and to a lesser extent  $G\alpha_{i3}$ , demonstrating the expression of these  $G\alpha_{i/o}$  subunits (**Figure 5.21 C**). Coomassie stained blots demonstrate the equal amounts of protein loaded for each condition (**Figures 5.21 and 5.22**).

### **5.2.12 Immunocytochemistry using antibodies selective against the active conformation of $G\alpha_{i1}$**

The FMAT screen identified three hybridoma clones producing antibodies which were selective towards the active, GTP bound, form of  $G\alpha_{i1}$ . As part of an effort to characterise these antibodies further it was important to demonstrate this selectivity in another experimental format. The use of these antibodies for immunocytochemistry was an obvious approach to use. Firstly because, as for the FMAT assay,  $G\alpha_{i1}$  could be expressed and remain in a native form retaining the putative three dimensional epitope recognised by these antibodies. Secondly, immunocytochemistry is a widely used and useful technique,

and therefore an appropriate choice to demonstrate the potential utility of these antibodies. HEK293T cells were grown on poly-D-lysine coated coverslips and transiently transfected with cDNA of the D<sub>21</sub>-YFP fusion protein plus one of either wild type Gα<sub>i1</sub>, the constitutively active variant Gln<sup>204</sup>Leu Gα<sub>i1</sub>, or the constitutively inactive variant Gly<sup>203</sup>Ala Gα<sub>i1</sub>. Immunocytochemistry was performed as in **section 2.10.5.2**. The co-transfection of D<sub>21</sub>-YFP with the relevant variant of Gα<sub>i1</sub> allowed the identification of successfully transfected cells. For the antibody 8A6/1H1 successfully transfected cells, as indicated by the localisation of D<sub>21</sub>-YFP at the cell membrane, were observed for all transfections (**Figure 5.23 A-C i**). However, a signal from the antibody was only observed for the active variant Gln<sup>204</sup>Leu Gα<sub>i1</sub> co-transfection. As might be expected, the distribution of Gln<sup>204</sup>Leu Gα<sub>i1</sub> was at or in close proximity to the cell membrane (**Figure 5.23B**). For both the inactive variant Gly<sup>203</sup>Ala Gα<sub>i1</sub> and indeed the wild type Gα<sub>i1</sub> co-transfections no signal was observed (**Figure 5.23A, C**). This pattern was observed for both the remaining conformation selective antibodies 6F12/1E5 and 8D11/1C1 (**Figures 5.24 and 5.25**). It is of note that the wild type Gα<sub>i1</sub> gave no signal for any of the three conformation selective antibodies. It is likely that Gα<sub>i1</sub> in a non-stimulated cell would be in the GDP bound conformation, and therefore would have no affinity for the conformation selective antibodies. It follows then that when used for immunocytochemistry, all of the putative conformation selective antibodies show little affinity for the GDP bound inactive form of Gα<sub>i1</sub> and high affinity for the active form. In the FMAT assay, the signal observed for the GDPβS loaded wild type Gα<sub>i1</sub> condition was lower than that observed for the GTPγS loaded Gα<sub>i1</sub> condition (**Figure 5.20**). However, in contrast with the results from the experiments using immunocytochemistry, the signal was clearly higher than that observed for cells expressing the inactive variant Gly<sup>203</sup>Ala Gα<sub>i1</sub> or indeed the mock-transfected cells. This discrepancy must lie within physical differences in the two methodologies. The FMAT assay is a 'mix and read' assay whereas the immunocytochemical protocol included wash steps between both primary and secondary antibody application. These wash steps

may remove antibody bound with lower affinity to the GDP bound form as compared to the GTP bound form, thus improving the signal window. It would seem then that, for the conformation selective antibodies, the relative signal observed for the GTP bound and GDP bound forms of  $G\alpha_{i1}$  and therefore the signal window is assay dependent. This has obvious implications for the choice of assay format to allow the design of a robust high throughput assay that is equivalent to the [ $^{35}\text{S}$ ] GTP $\gamma$ S assay, the ultimate aim of this study.

### **5.2.13 Immunocytochemistry using antibodies not selective for the active conformation of $G\alpha_{i1}$**

In parallel with the immunocytochemistry using antibodies selective against the active GTP bound form of  $G\alpha_{i1}$ , equivalent experiments were performed using the antibodies generated by the hybridoma screen that do not distinguish between GTP and GDP forms of  $G\alpha_{i1}$  (6B4 and 8F5, **Figures 5.26 and 5.27**) and the polyclonal antiserum raised against the C-terminal ten amino acids of  $G\alpha_{i1}$  (1319 Glycine, **Figure 5.28**). These experiments had two purposes; firstly to demonstrate the effective use of these antibodies in this methodology, and secondly to provide a control indicating the relative expression levels of the three variants of  $G\alpha_{i1}$  used in this experiment. The anti- $G\alpha_{i1/2}$  polyclonal antiserum gave a signal of equivalent intensity for all  $G\alpha_{i1}$  co-transfections, indicating that each of wild type  $G\alpha_{i1}$ , Gly<sup>203</sup>Ala  $G\alpha_{i1}$  and Gln<sup>204</sup>Leu  $G\alpha_{i1}$  were expressed to equivalent levels (**Figure 5.28**). This underlined that, when immunocytochemistry was performed using the conformation selective antibodies, the specific signal observed for the Gln<sup>204</sup>Leu  $G\alpha_{i1}$  co-transfected cells only, was indeed due to the selectivity of these antibodies towards the active form of  $G\alpha_{i1}$  rather than a difference in expression levels. The signal observed in the mock-transfected cells was of a much lower intensity. Both of the non-conformation selective antibodies originating from the hybridoma screen also showed a signal of equal intensity for all  $G\alpha_{i1}$  variant co-transfections. This again underlined the equal expression

levels of  $G\alpha_{i1}$  variants between all co-transfections. In agreement with the results of FMAT assay, these antibodies did not distinguish between the active and inactive forms of  $G\alpha_{i1}$ . It is interesting to note that there was no observed signal in the pcDNA3 condition, in contrast to the polyclonal antisera which showed a small signal for this condition (**Figures 5.26D, 5.27.D, 5.28D**). Although, due to differences in concentration of antisera/antibody used may make comparison difficult, this low signal may reflect the specificity of both 6B4 and 8A5 antibody towards  $G\alpha_{i1}$  over the other members of the  $G\alpha_{i/o}$  subfamily (**Figure 5.21**).

### 5.2.14 Epitope mapping of anti- $G\alpha_{i1}$ antibodies

Using both FMAT and immunocytochemical methods I have identified and characterised antibodies which are selective against the active (GTP bound) form of  $G\alpha_{i1}$ . It would be of interest to identify the epitope that these antibodies recognise. This could provide information on the conformational changes undergone by  $G\alpha_{i1}$  upon activation and nucleotide exchange. The strategy used to identify potential epitopes was epitope mapping using a library of 86 16mer peptides overlapping by 4 amino acids and corresponding to the full amino acid sequence of human  $G\alpha_{i1}$  (the peptides and residues of  $G\alpha_{i1}$  that they correspond to are listed in **Appendix 1**). This 'Pepset™' library was supplied by Mimotopes Ltd, Australia. The epitope mapping experiments were performed as described in section 2.10.4. The polyclonal anti- $G\alpha_{i1/2}$  antiserum raised against the C-terminal ten amino acids of  $G\alpha_{i1}$ , as could be expected, gave a strong signal at peptide 86 (residues 339-354) (**Figure 5.29 A**). This peptide was the only peptide to contain the C-terminal ten amino acids of  $G\alpha_{i1}$  against which this antiserum was raised. The antiserum also gave a strong signal at peptide 20. However, this strong signal was seen for all antibodies tested (**Figures 5.29 and 5.30**), and so is almost certainly an artefact, perhaps indicating that this peptide has a property which makes it an attractive binding partner for all

antibodies/antisera. For the conformation selective antibodies 6F12/1E5 and 8D11/1C1 and the non-conformation selective antibody 6B4 (**Figures 5.30 A-B, 5.29 B**), no signal was observed for any peptide other than peptide 20. In the case of the conformation selective antibodies this is perhaps not surprising since the epitope may be a three dimensional one with contact points on amino acids that are in close proximity in the activated form of  $G\alpha_{i1}$  but not necessarily in close proximity in the linear amino acid sequence. The fact that these antibodies did not pick up denatured  $G\alpha_{i1}$  protein on a Western blot is in agreement with this hypothesis. It is interesting that the non-conformation-selective antibody, 6B4, did not show any affinity for the 16mer peptides (**Figure 5.29 B**). This indicates that either this antibody recognises an epitope that was missed due to the peptide set overlapping by 4 amino acids rather than 1 amino acid or that, as for the conformation selective antibodies, it recognises a three dimensional epitope. If this antibody does recognise a three dimensional epitope it is interesting that a specific interaction was observed with  $G\alpha_{i1}$  which had been denatured by SDS PAGE. A small proportion of the protein on a SDS PAGE gel will retain some three dimensional structure, which may be recognised by the antibody. The conformation selective antibody 8A6/1H1 gave a signal higher than background for peptides 33, 64, 65. (**Figure 5.30 C**) However, the signals observed at these peptides were lower when compared to the non-specific signal observed for peptide 20. This is perhaps indicative that these signals are non-specific interactions. These peptides were mapped to the structure of both the inactive (GDP bound) structure and the active (GTP bound) structure of  $G\alpha_{i1}$  (work performed by T. Houslay, BRC, University of Glasgow, data not shown). All peptides contained amino acids both on the surface of  $G\alpha_{i1}$  and within the molecule. Comparison of both the inactive and active structures revealed no obvious regions corresponding to peptides 33 (residues 129-144), 64 (residues 253-268) and 65 (residues 257-272) which become closer in proximity or revealed upon activation. The non-conformation selective antibody 8A5 gave small signals at peptides 47 (residues 185-200) and 56 (residues 221-236) (**Figure 5.29C**).

Again these were considerably smaller in magnitude than the signal observed for the non-specific interaction with peptide 20. Again these peptides were mapped to the structure of GTP and GDP bound  $G\alpha_{i1}$  and both peptides contained amino acids present at surface of the protein and concealed within the interior of the protein (data not shown). For both antibody 8A5 and 8A6/1H1 then, peptides were identified using epitope mapping using the Pepset™ library that perhaps correspond to the epitope of these antibodies. However, it is difficult to distinguish those peptides that correspond to the real epitope and those which are simply non-specific interactions. Furthermore, the identification of amino acids within these peptides which comprise the actual epitopes cannot be identified using this method. As a general conclusion epitope mapping using a set over overlapping peptides corresponding to the amino acid sequence of  $G\alpha_{i1}$  successfully identified the linear epitope against which a polyclonal antiserum was raised. However, the negative or inconclusive results obtained for all antibodies originating from the hybridoma screen, indicate that this method may not be appropriate for the identification of the epitopes recognised by conformation selective antibodies.

### **5.2.15 Further characterisation of conformation selective antibodies**

The above work describes the full extent of the characterisation of three antibodies selective towards the active (GTP bound) state of  $G\alpha_{i1}$  that I performed during the course of my studies. However, a number of obvious questions regarding these antibodies remained unanswered. To this end, whilst writing up this work, I was fortunate to supervise a Master's student (David Henderson, Biotechnology Msc., University of Glasgow). David performed a number of key experiments which gave a clearer picture of the characteristics of these antibodies and also highlight their potential utility in the development of a label-free, non-radioactive assay for G protein activation by agonist

ligands. For this reason, inclusion of this work is beneficial to the reader, and a summary is included below.

#### **5.2.15.1 The three conformation-selective antibodies show affinity for the constitutively active mutants of $G\alpha_{i2}$ and $G\alpha_{o1}$ but not $G\alpha_q$ or $G\alpha_s$**

$G\alpha_{i1}$  is highly related in sequence, and therefore presumably in structure, to each of  $G\alpha_{i2}$ ,  $G\alpha_{i3}$  and  $G\alpha_{o1}$  but substantial less to  $G\alpha_s$  and  $G\alpha_{q/11}$ . We therefore next assessed the capacity of the conformation-selective antibodies to identify wild type and constitutively active mutants of  $G\alpha_{i2}$  and  $G\alpha_{o1}$ . These antibodies did not recognise wild type  $G\alpha_{i2}$  or  $G\alpha_{o1}$  but did identify both Gln<sup>205</sup>Leu  $G\alpha_{i2}$  and Gln<sup>204</sup>Leu  $G\alpha_{o1}$  (**Figures 5.31 A-D, 5.32 A-D**). As controls we confirmed expression of both wild type  $G\alpha_{i2}$  and  $G\alpha_{o1}$  in parallel immunocytochemistry experiments using rabbit polyclonal anti-peptide antisera against the corresponding C-terminal decapeptide sequences (**Figures 5.31 A-D, 5.31 A-D**).

Conversely, none of the conformational-selective antibodies were able to identify either constitutively active (Gln<sup>227</sup>Leu  $G\alpha_s$ , Gln<sup>209</sup>Leu  $G\alpha_q$ ) or constitutively inactive (Gly<sup>226</sup>Ala  $G\alpha_s$ , Gly<sup>208</sup>Ala  $G\alpha_q$ ) forms of  $G\alpha_s$  and  $G\alpha_q$  although in all cases staining with rabbit polyclonal anti-peptide antisera against the corresponding C-terminal decapeptide sequences was able to confirm expression of the relevant polypeptide (**Figures 5.33 A-D, 5.35 A-D**).

### 5.2.15.2 The conformation-selective antibody 6F12 1E5 shows no affinity for the constitutively active mutant Arg<sup>178</sup>Cys Gα<sub>i2</sub>

Immunocytochemistry experiments were performed using HEK293T cells transiently expressing the constitutively active mutants Arg<sup>178</sup>Cys Gα<sub>i2</sub> (**Figure 5.35A**) and Gln<sup>204</sup>Leu Gα<sub>i2</sub> (**Figure 5.35B**). As controls, parallel experiments were performed on HEK293T cells expressing wild type Gα<sub>i2</sub> (**Figure 5.35C**) or mock transfected cells (**Figure 5.37D**).

Although as seen in previous experiments the antibodies showed affinity for the active mutant Gln<sup>204</sup>Leu Gα<sub>i2</sub> (**Figure 5.35B**), they did not recognise the active mutant Arg<sup>178</sup>Cys Gα<sub>i2</sub>. Comparable expression of all Gα<sub>i2</sub> variants was confirmed using the anti-Gα<sub>i1/2</sub> polyclonal antiserum 1319 Glycine.

### 5.2.15.3

### 5.2.15.4 The three conformation-selective antibodies show affinity for the active complex wild type Gα<sub>i2</sub>.GDP.AIF<sub>4</sub><sup>-</sup>, where AIF<sub>4</sub><sup>-</sup> is a mimic of the γ phosphate of GTP

AIF<sub>4</sub><sup>-</sup> is a substitute for and mimic of the γ phosphate of GTP (**Figure 5.36A and B**). As such addition of AIF<sub>4</sub><sup>-</sup> (10 μM AlCl<sub>3</sub> + 10 mM NaF) to HEK293T cells transiently expressing wild type Gα<sub>i2</sub> resulted in recognition of Gα<sub>i2</sub> by each of the three conformation-selective antibodies. (**Figure 5.37**)

### 5.2.15.5 The three conformation-selective antibodies show affinity for agonist activated G protein subunits in a whole cell GTP $\gamma$ S experiment

Finally we wished to assess if the conformation-selective antibodies would recognise agonist-activated G protein  $\alpha$  subunits. HEK293T cells transiently transfected to co-express dopamine D<sub>21</sub>-eYFP and wild type G $\alpha_{i2}$  were exposed to the dopaminergic agonist nor-apomorphine (1  $\mu$ M) in the presence of 10  $\mu$ M GTP $\gamma$ S, saponin (0.2% w/v) and an assay buffer (50 mM Tris, 5 mM MgCl<sub>2</sub>, 100 mM NaCl, 0.2 mM EGTA) previously used by others to develop an in cell [<sup>35</sup>S] GTP $\gamma$ S assay (Rios et al., 2006). In these conditions the conformation-selective antibodies identified G $\alpha_{i2}$  only in samples stimulated by agonist (**Figure 5.38A-D**). These data indicate that the conformation selective antibodies described herein may be used to develop label-free, non radioactive assays for G protein activation by agonist ligands.

**Figure 5.1: Characterisation of antisera raised against the C-terminal decapeptide of  $G\alpha_t$ .**

**A) The glycine eluate of the antiserum from animal 1318 recognises  $G\alpha_{i1}$ ,  $G\alpha_{i2}$ ,  $G\alpha_{i3}$ , and  $G\alpha_{o1}$ .**

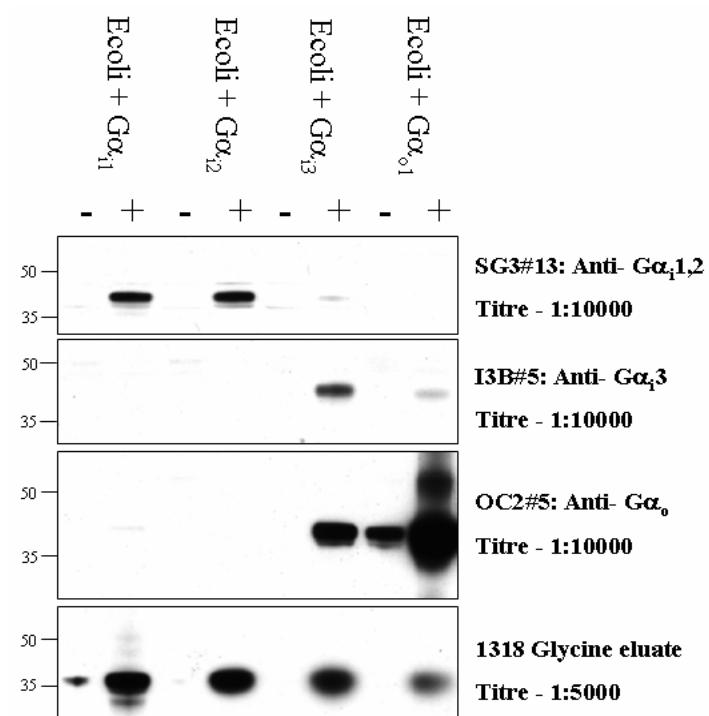
Chemically competent BL21 *E coli* cells were transformed with the vector pT7.7 containing the cDNA of the relevant G  $\alpha$  subunit. Expression of G  $\alpha$  subunit was induced with the addition of 1  $\mu\text{g}$  / ml IPTG. Cells were lysed using a French press and protein concentration estimated using a BCA assay. Lysate proteins (0.5  $\mu\text{g}$  / well) were separated by SDS PAGE and Western blots performed using the glycine 1318 antiserum raised against the C-terminal of  $G\alpha_t$ . In-house antisera raised against the C-terminal decapeptide of  $G\alpha_{i1/2}$ ,  $G\alpha_{i3}$  or  $G\alpha_{o1}$  were used as controls, to demonstrate the expression of the relevant  $G\alpha_i$  subunit in each sample.

**B) The TEA eluate of the antiserum from animal 1318 and the Glycine eluate from animal 1319 recognise  $G\alpha_{i1}$  and  $G\alpha_{i2}$  but not  $G\alpha_{i3}$  or  $G\alpha_{o1}$ .**

As above  $G\alpha_{i1}$ ,  $G\alpha_{i2}$ ,  $G\alpha_{i3}$ , and  $G\alpha_{o1}$  expression in BL21 *E coli* was or was not induced with the addition of 1  $\mu\text{g}/\text{ml}$  IPTG. Cell lysates made and protein (0.5  $\mu\text{g}$  / well) separated by SDS PAGE. Westerns were performed using antisera raised against the C-terminal decapeptide of  $G\alpha_t$ . The in-house antiserum SG3 raised against the C-terminal tail of  $G\alpha_t$  was used a positive control.

**Figure 5.1**

A)



B)

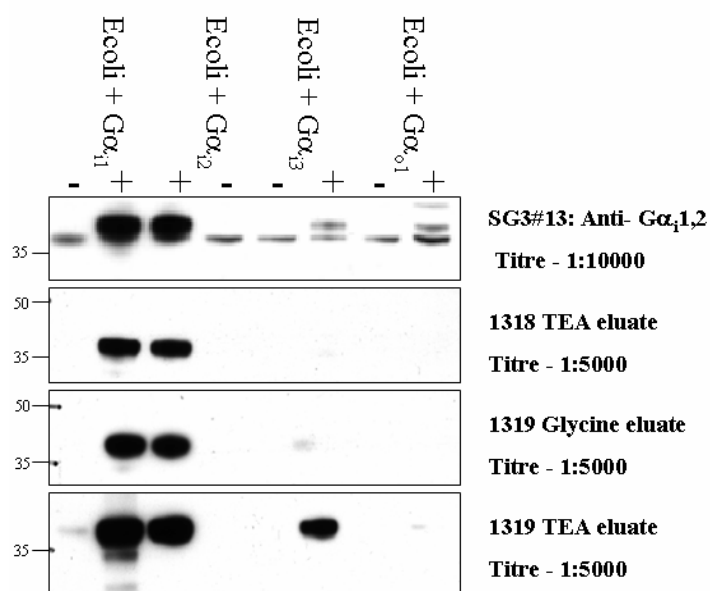


**Figure 5.2: The glycine eluate of antiserum from animal 1319 was used successfully to immunoprecipitate  $G\alpha_{i2}$  as part of a [ $^{35}$ S] GTP $\gamma$ S binding assay with immunoprecipitation step**

HEK293T cells were transiently co-transfected with cDNA of the dopamine D<sub>21</sub> receptor and the pertussis toxin-insensitive variant Cys<sup>352</sup>Ile  $G\alpha_{i2}$ . Cells were treated with pertussis toxin (25 ng/ml) 16 hours prior to cell harvest. Membrane preparations were made and membrane protein concentration estimated. Receptor binding site density was estimated using [ $^3$ H] spiperone saturation binding (**Table 4.1**). [ $^{35}$ S] GTP $\gamma$ S binding reactions were set up as described in **2.9.2.2**, following the protocol for the [ $^{35}$ S] GTP $\gamma$ S binding assay with immunoprecipitation step. [ $^{35}$ S] GTP $\gamma$ S binding was stimulated with the addition of 100  $\mu$ M dopamine. To assess the ability of the Glycine eluate of the antiserum 1319 to immunoprecipitate  $G\alpha_{i2}$  this antiserum was used for the immunoprecipitation step. As a comparison, an equivalent reaction was set up using the in-house antiserum (SG3) raised against the C-terminal tail of  $G\alpha_t$ . Experiment was performed in triplicate.

Figure 5.2

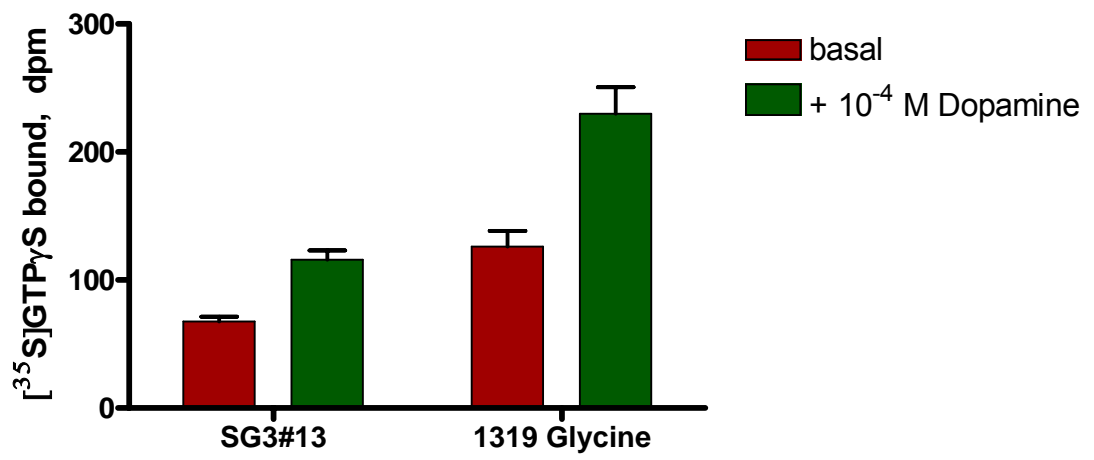


**Figure 5.3: The glycine eluate of antiserum from animal 1318 was used to immunoprecipitate  $G\alpha_{i3}$  as part of a [ $^{35}$ S] GTP $\gamma$ S binding assay with immunoprecipitation step**

HEK293T cells were transiently co-transfected with cDNAs of a CRF receptor- $G\alpha_{i3}$  fusion protein. [ $^{35}$ S] GTP $\gamma$ S binding reactions were set up as described in 2.9.2.2, following the protocol for the [ $^{35}$ S] GTP $\gamma$ S binding assay with immunoprecipitation step. [ $^{35}$ S] GTP $\gamma$ S binding was stimulated with the addition of 1  $\mu$ M sauvagine. To assess the ability of the glycine eluate of the antiserum 1319 to immunoprecipitate  $G\alpha_{i3}$  this antibody was used in the immunoprecipitation step. As a comparison, an equivalent reaction was set up using in-house antisera (I3C) raised against the C-terminal tail of  $G\alpha_{i3}$ . Experiments were performed in triplicate.

Figure 5.3

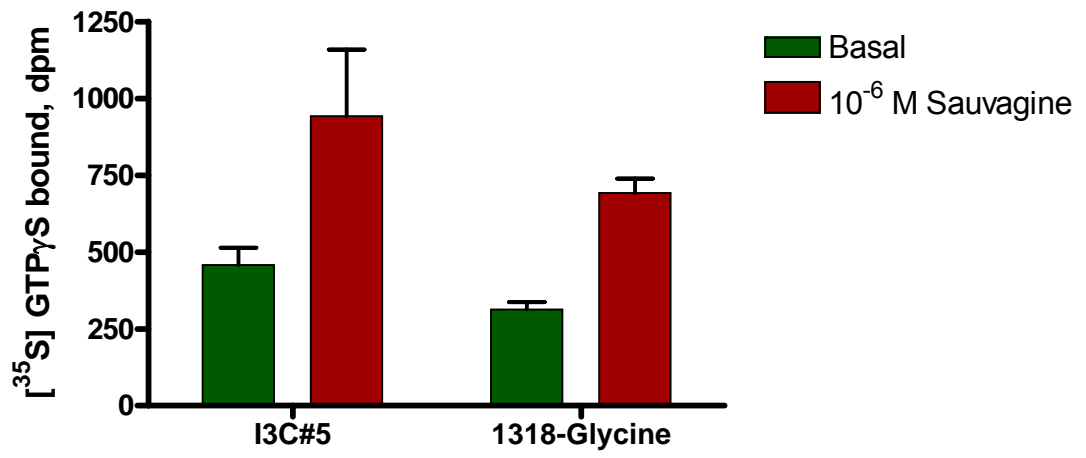


**Figure 5.4: Antisera from animals 1316 and 1317 raised against the C-terminal decapeptide of  $G\alpha_q$  selectively recognise  $G\alpha_q$  when this  $G\alpha$  subunit is transiently expressed in  $G\alpha_{q/11}$  null EF88 cells.**

EF88  $G\alpha_{q/11}$  (-/-) cells were or were not transiently transfected with  $G\alpha_q$  cDNA. Cells were harvested and membrane preparations were made. Membrane protein (0.5  $\mu\text{g}/\text{well}$ ) were separated using SDS PAGE and Western blots performed using both TEA and glycine eluates of purified antisera from animal 1316 (**B-C**) and 1317 (**D-E**) raised against the C-terminal decapeptide of  $G\alpha_q$ . In-house antisera (CQ5) raised against the C-terminal decapeptide of  $G\alpha_q$  was used a positive control (**A**).

**Figure 5.4**

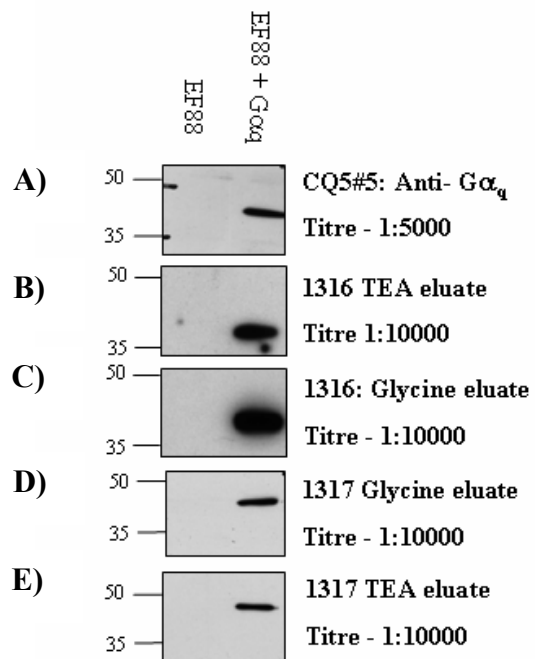


**Figure 5.5: The glycine eluate of antiserum from animal 1317 was used to immunoprecipitate  $G\alpha_{11}$  as part of a [ $^{35}\text{S}$ ] GTP $\gamma$ S binding assay with immunoprecipitation step.**

EF88 cells were transiently co-transfected with cDNA of the  $\alpha_{1b}$  adrenoceptor and  $G\alpha_{11}$ . [ $^{35}\text{S}$ ] GTP $\gamma$ S binding reactions were set up as described in **2.9.2.2**, following the protocol for the [ $^{35}\text{S}$ ] GTP $\gamma$ S binding assay with immunoprecipitation step. [ $^{35}\text{S}$ ] GTP $\gamma$ S binding was stimulated with the addition of 1  $\mu\text{M}$  phenylephrine. To assess the ability of the Glycine eluate of the antisera 1317 to immunoprecipitate  $G\alpha_q$  this antibody was used in the immunoprecipitation step. As a comparison, an equivalent reaction was set up using in-house antisera (CQ5) raised against the C-terminal tail of  $G\alpha_{q/11}$ . Experiments were performed in triplicate.

Figure 5.5

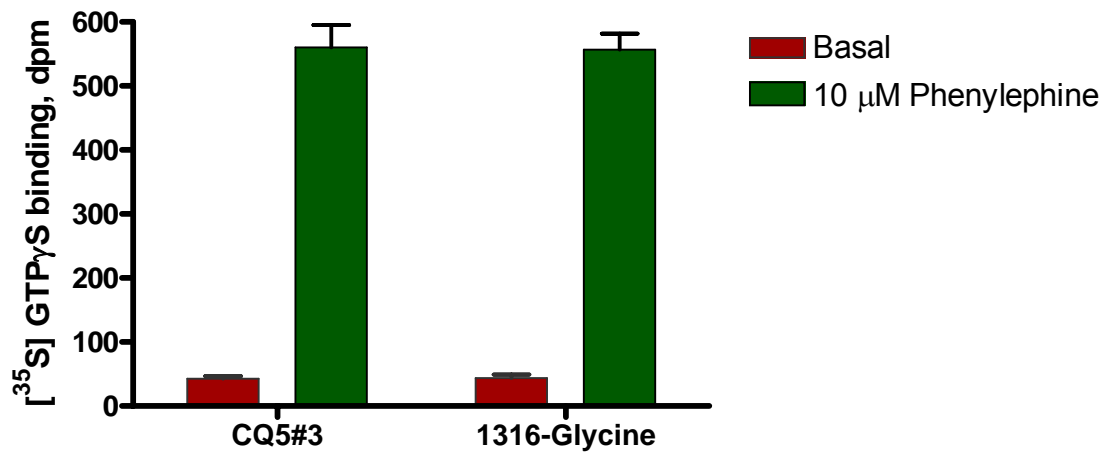


**Figure 5.6: Antiserum from animal 1314, raised against the C-terminal decapeptide of  $G\alpha_s$ , shows a cholera toxin-induced down-regulation of  $G\alpha_s$  in HEK293T cells**

HEK293T cells were either treated with cholera toxin (0.1  $\mu\text{g}$  / ml, 24 hrs prior to cell harvest) or not and membrane preparations made. HEK293T cells were also transiently transfected with cDNA of the long isoform of  $G\alpha_s$ , cells harvested and membrane preparations made. Membrane protein (0.5  $\mu\text{g}$  / well) was separated by SDS PAGE and Western blots performed using both Glycine (**B**) and TEA (**C**) eluates of antiserum raised against the C-terminal decapeptide of  $G\alpha_s$  from animal 1314. An in-house antiserum raised against the C-terminal decapeptide of  $G\alpha_s$  was used as a positive control (**A**).

**Figure 5.6**

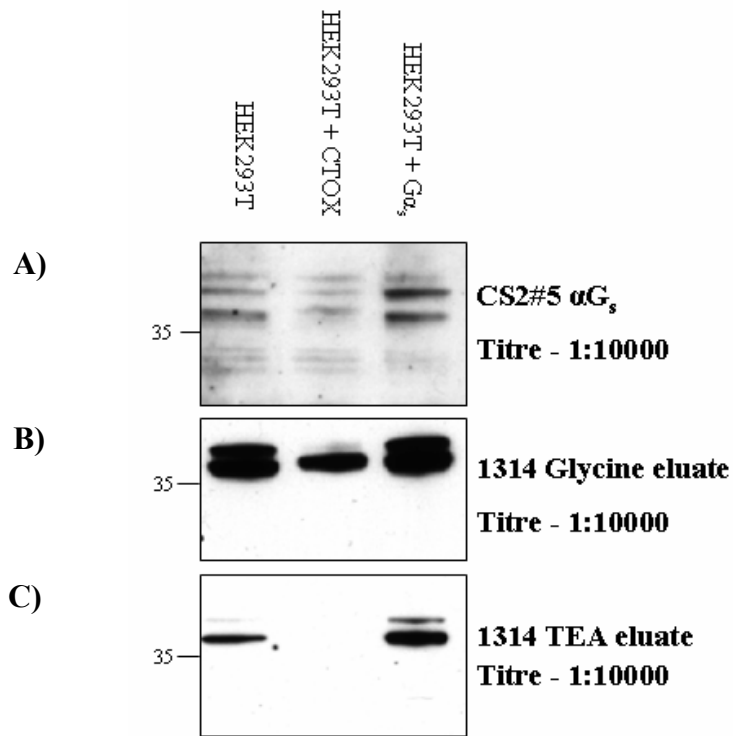


**Figure 5.7: The glycine eluate antiserum from animal 1314 was used to immunoprecipitate  $G\alpha_s$  as part of a [ $^{35}$ S] GTP $\gamma$ S binding assay with immunoprecipitation step**

HEK293T cells were transiently co-transfected with cDNA of the CRF- $G\alpha_s$  fusion protein. [ $^{35}$ S] GTP $\gamma$ S binding reactions were set up as described in 2.2.9.2, following the protocol for the [ $^{35}$ S] GTP $\gamma$ S binding assay with immunoprecipitation step. [ $^{35}$ S] GTP $\gamma$ S binding was stimulated with the addition of 10  $\mu$ M sauvagine. To assess the ability of the Glycine eluate of the antiserum 1314 to immunoprecipitate  $G\alpha_s$  this antibody was used in the immunoprecipitation step. As a comparison, an equivalent reaction was set up using in-house antisera (CS2) raised against the C-terminal tail of  $G\alpha_s$ . Experiments were performed in triplicate.

Figure 5.7

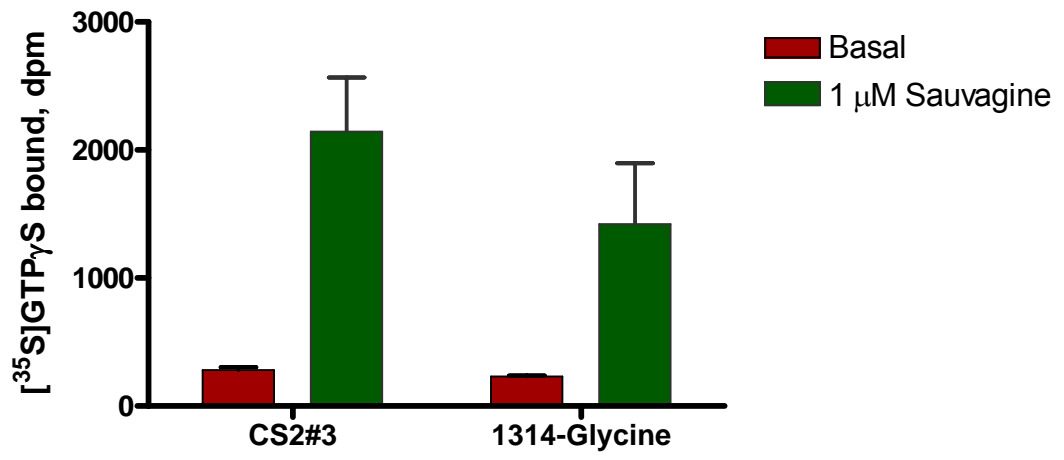


**Figure 5.8: Outline of the various stages of hybridoma generation. Adapted from 'Antibodies: A Laboratory Manual' (Harlow, 1988)**



**Figure 5.9: Schematic diagram of FMAT assay for the screening of hybridoma raised against  $G\alpha_{i1}$**

HEK293T cells were transfected with cDNA of human  $G\alpha_{i1}$ . These cells were then permeabilised (**section 5.2.11**). The relevant FMAT blue® secondary antibody was added to this cell suspension to a final dilution of 1:2000. The cell suspension was then added to each well of an FMAT plate containing the antibody/hybridoma clone tissue culture supernatant of interest. Following an incubation time of 2 hours the plate was read on an 8200 Cellular Detection System. The FMAT Blue® dye is a far-red emitting dye in the 650 nm range.

The 8200 Cellular Detection System scans the bottom of microtiter plates at a depth of focus of 100  $\mu\text{m}$ . The use of a red 633 nm HeNe laser greatly diminishes the autofluorescence from test materials and cells, resulting in low background noise. Any fluorescence that is not bound to a cell or bead that has settled to the bottom of the assay plate will be undetected, eliminating the need for wash steps. Reagents are added simultaneously which diminishes incubation and reagent addition steps and increases productivity. Consequently, antibodies that are selective against  $G\alpha_{i1}$  will give a high fluorescent signal for cells that express  $G\alpha_{i1}$ .

**Figure 5.9**

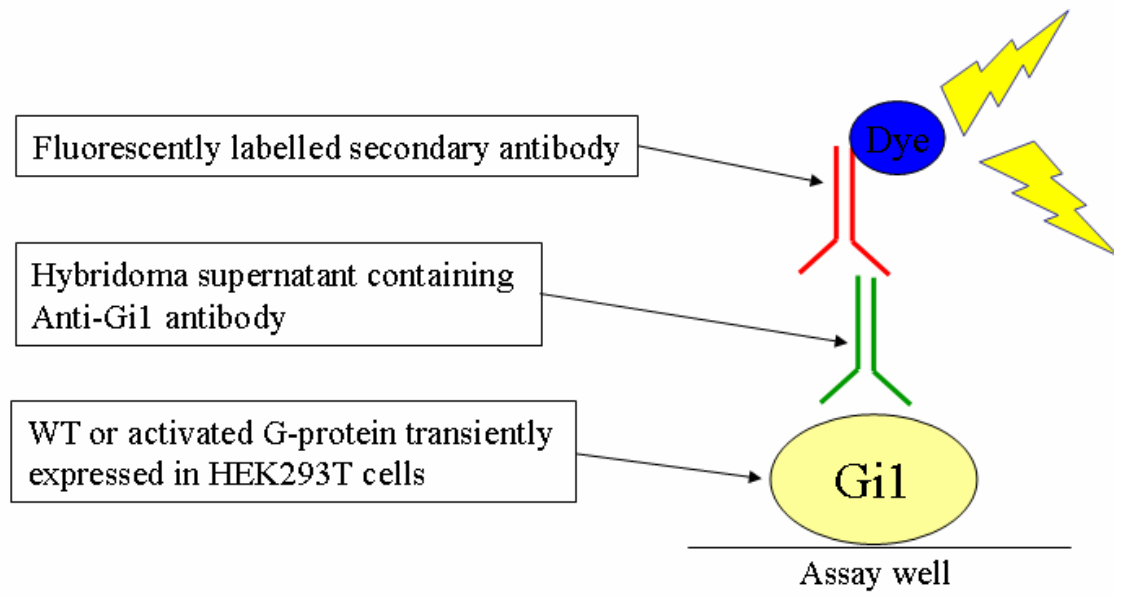


**Figure 5.10: Permeabilisation of cells using a PBS / 1% BSA / 0.1% sodium azide buffer proved the most effective method for use in an FMAT assay to screen for hybridoma producing antibodies selective against the active conformation of  $G\alpha_{i1}$ .**

HEK293T cells were transfected with either cDNA of wild-type  $G\alpha_{i1}$ , the inactive variant Gly<sup>203</sup>Ala ( $G\alpha_{i1}$  G<sup>203</sup>A), or the active variant Gln<sup>204</sup>Leu ( $G\alpha_{i1}$  Q<sup>204</sup>L). As a control cells were transfected with the cDNA of FLAG-GPR55. Cells were permeabilised using: **A)** PBS / 1% BSA / 0.1% NaN<sub>3</sub> buffer, **B)** a Cytofix / Cytoperm method, **C)** a hERG fixation method, **D)** a modified Kruzik's method (see section 5.1.11 for details). Using these permeabilised cell suspensions an FMAT assay was performed as in section 2.10.3.

Briefly a donkey anti-rabbit FMAT blue ® secondary antibody or a donkey anti-mouse FMAT blue ® secondary antibody was added to each cell suspension to a final dilution of 1:2000. These cell suspensions were then added to wells of a 96 well FMAT ® plate containing 1 µl of either an anti- $G\alpha_{i1/2}$  polyclonal antisera (1319G) (**i**) or an anti-FLAG monoclonal antibody (**ii**). Plates were incubated in the dark for 2 hours at room temperature and then fluorescence detected using an 8200 Cellular Detection System (Applied Biosystems). (Experiment performed by D. Daniels and B. Powney, GSK, Stevenage, UK)

Figure 5.10

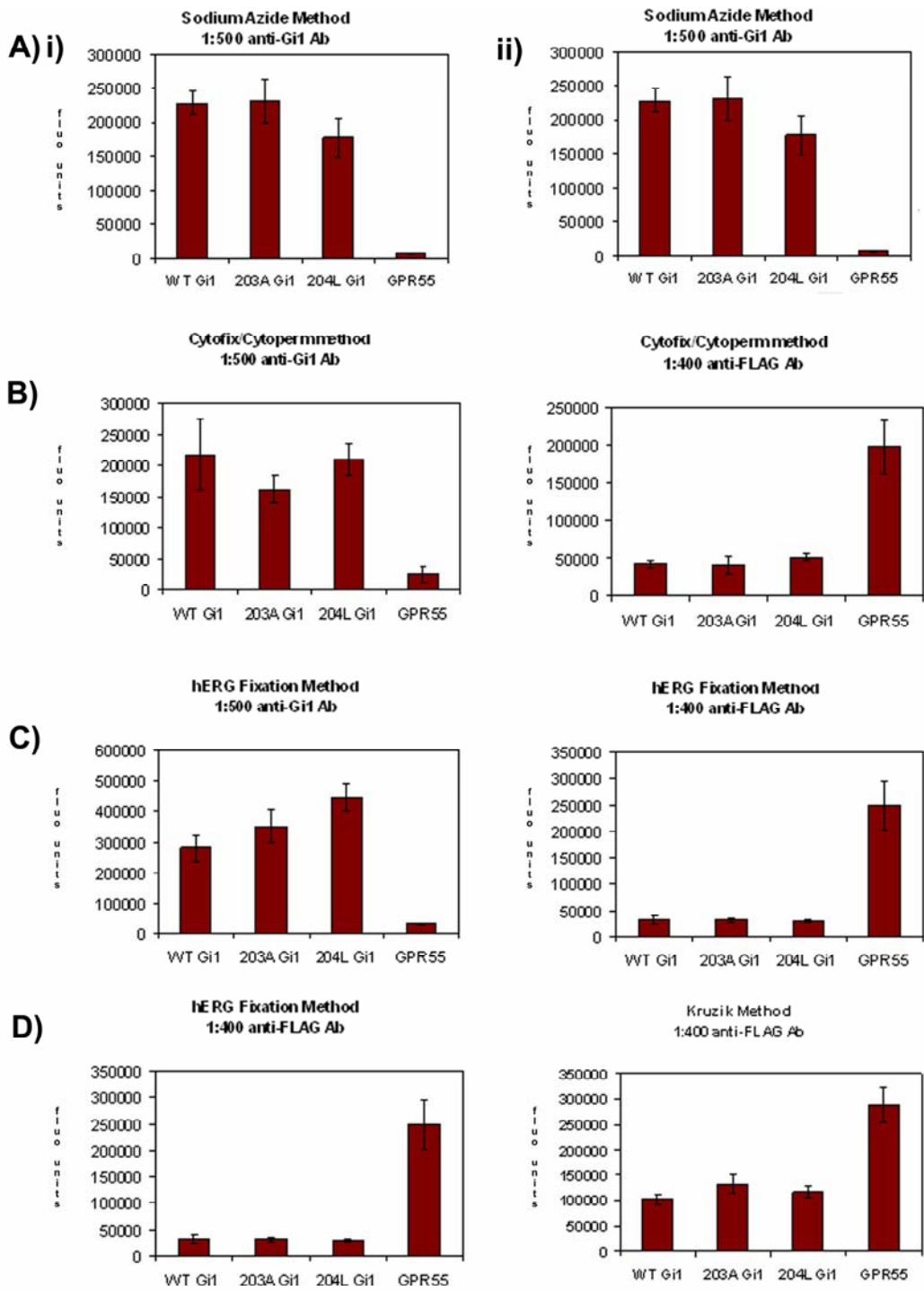


**Figure 5.11: An FMAT assay using a polyclonal antiserum raised against the C-terminal tail of  $G\alpha_{i1/2}$  remains robust after a 23 hour incubation**

HEK293T cells were transiently transfected with cDNA of either wild type  $G\alpha_{i1}$  (WT) or the constitutively active variant Gln<sup>204</sup>Leu  $G\alpha_{i1}$  (204L). As a control cells were transfected with cDNA of FLAG-GPR55 construct. Cells were resuspended in permeabilisation buffer (PBS + 1% BSA + 0.1% NaN<sub>3</sub>) with or without the addition of 10  $\mu$ M GTP $\gamma$ S and with the addition of FMAT blue ® anti-rabbit secondary antibody. This cell suspension was added to a well of a 384 well plate already containing 1  $\mu$ l of anti- $G\alpha_{i1/2}$  antisera (glycine eluate of 1319). This plate was left in the dark at room temperature for 2 hours (**A**) or 23 hours (**B**) prior to reading. Experiments were performed in triplicate.

Figure 5.11

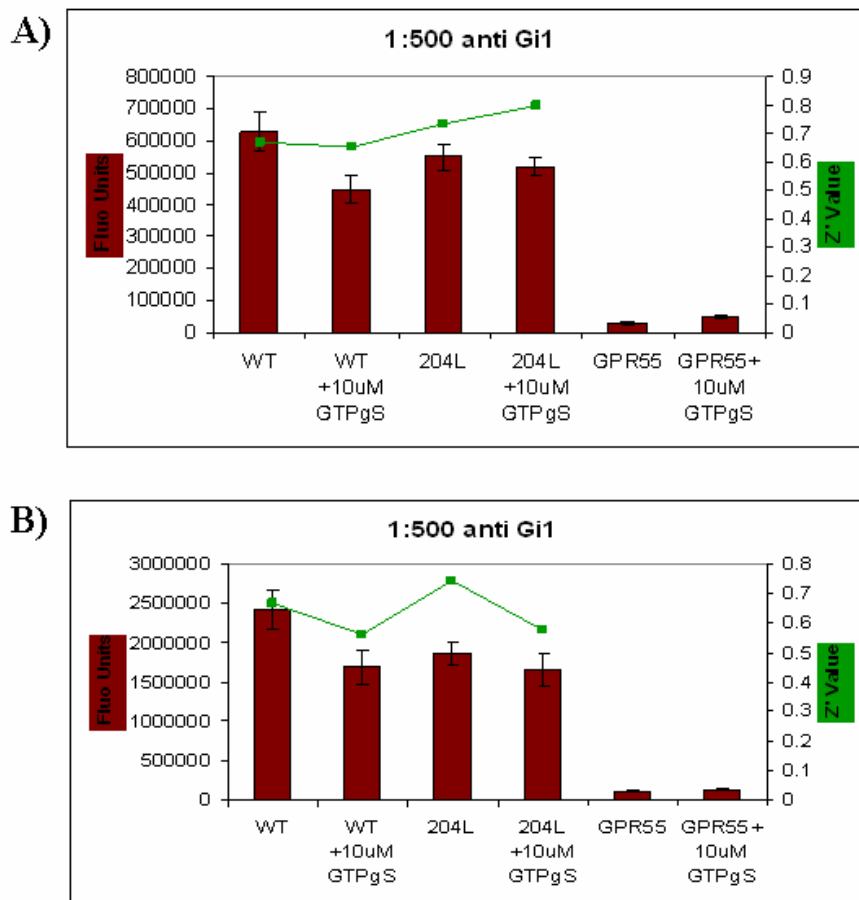


**Figure 5.12: The storage of aliquots of pre-transfected HEK293T cells at -80 °C prior to use in FMAT assay has no effect on fluorescent signal or robustness of assay**

Cells were transfected with cDNA of either wild type  $G\alpha_{i1}$  or the constitutively active variant Gln<sup>204</sup>Leu  $G\alpha_{i1}$ . A mock transfection was performed using an equivalent amount of the empty vector pcDNA3. 48 hours following transfection, cells were harvested and washed twice with PBS (room temperature). Cells were counted and aliquots from each condition were either left on ice or resuspended in foetal calf serum and frozen at -80 °C for 2 hours. Frozen cells were then thawed rapidly in a 37 °C bath, washed twice in PBS (4 °C) and both frozen and fresh cells resuspended in PBS + 1% BSA + 1% NaN<sub>3</sub> plus FMAT blue ® anti-rabbit secondary. This cell suspension was added to wells of a 384 well FMAT plate containing 1 µl of an anti- $G\alpha_{i1/2}$  antisera (glycine eluate 1319) diluted to 1:500

Figure 5.12

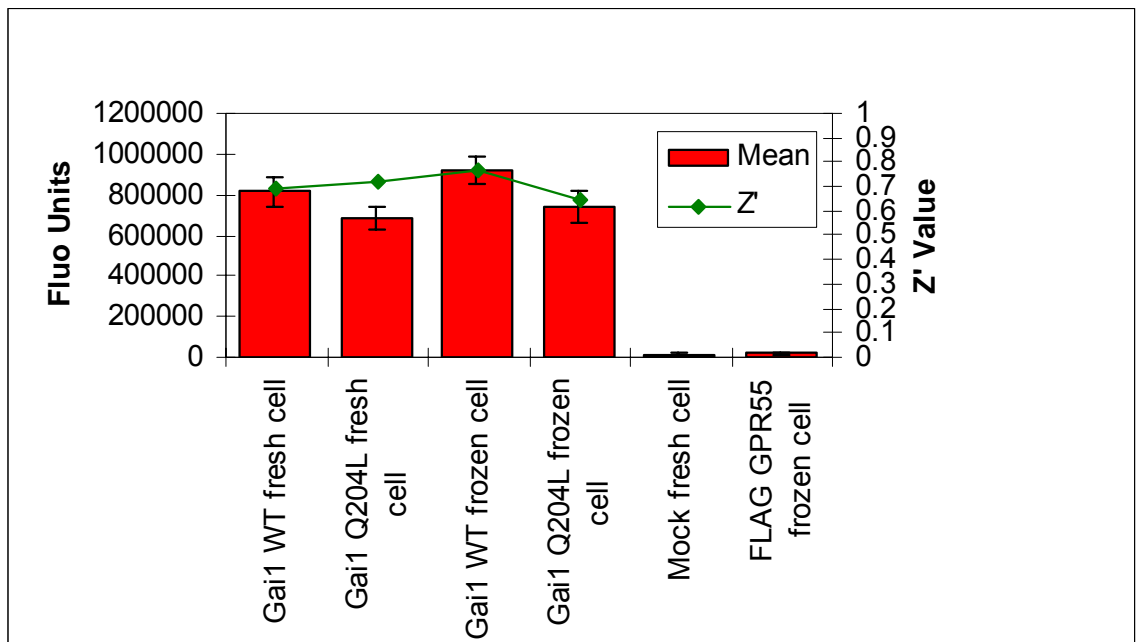


**Figure 5.13: ELISA using test bleeds from both rG $\alpha_{i1}$  rapid immunisation and plasmid immunisation strategies against rG $\alpha_{i1}$ . All animals immunised with rG $\alpha_{i1}$  showed an affinity for rG $\alpha_{i1}$ . No signal above background was observed for test bleeds from plasmid immunised animals.**

Two mice were immunised for each immunisation strategy, either plasmid immunisation using cDNA of the active variant Gln<sup>204</sup>Leu G $\alpha_{i1}$  (B) or the rapid immunisation protocol (A) as discussed in section 5.2.5. Test bleeds were taken from each animal (protein RIMMS: animals 120 and 121, plasmid immunisations, animals 122 1 and 122 2) and sets of serial dilutions were made of each test bleed and, as a positive control, a polyclonal anti-G $\alpha_{i1}$  antiserum (Glycine 1319) (C). These were dispensed onto 96 well plates coated with rG $\alpha_{i1}$  (0.1  $\mu$ g / well). The secondary antibody used was either a HRP conjugated anti-mouse or anti-rabbit antibody used at a final dilution of 1:5000.

Figure 5.13

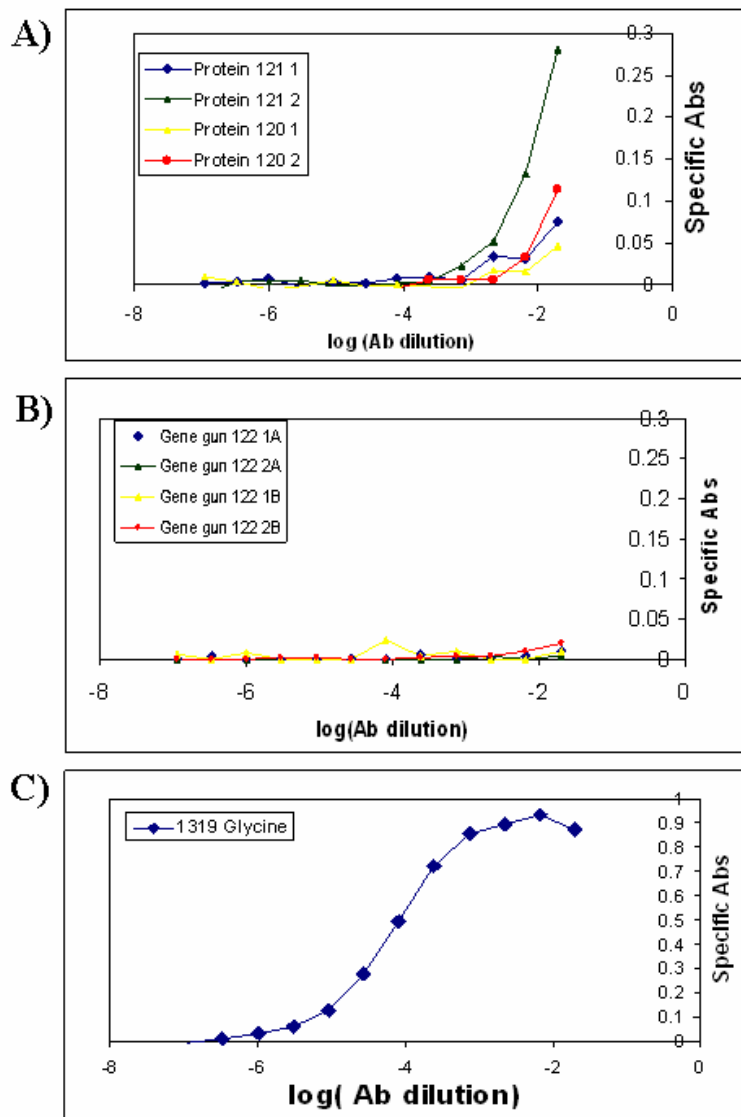


**Figure 5.14: ELISA using test bleeds from plasmid immunisation strategies against human IgG. No signal above background was observed for test bleeds from plasmid immunised animals.**

Serial dilutions of the test bleeds from the plasmid immunised animals (animals 122 1 and 122 2) were made and these dispensed onto 96 well plates pre-coated with human IgG. As a positive control, a bleed from a plasmid immunised animal from another immunisation program again using a human Fc fragment fusion protein which had shown a strong immune response was used (animal 116 1) (supplied by I. Kinghorn, GSK). As a negative control a test bleed from an unrelated program using a protein RIMMS protocol, which should therefore show no affinity for human IgG was used (animal 110 1) (supplied by I. Kinghorn).

Figure 5.14

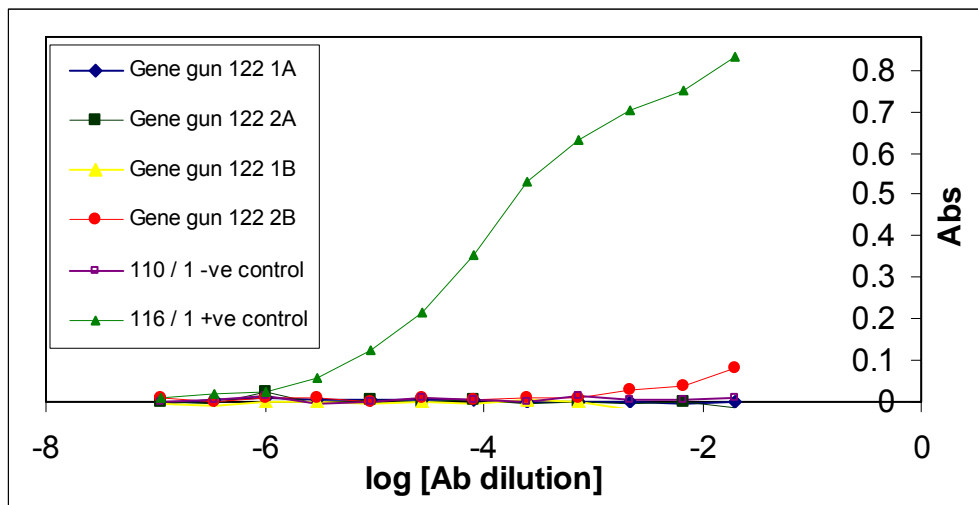


**Figure 5.15: Diagram illustrating the four conditions used in the whole cell FMAT assay to screen each hybridoma clone tissue culture supernatant.**

The conditions are as follows:

- 1) HEK293T cells transfected with wild type  $G\alpha_{i1}$  cDNA, permeabilised in PBS + 1% BSA + 0.1%  $\text{NaN}_3$  (FMAT Buffer), and incubated with 100  $\mu\text{M}$   $\text{GTP}\gamma\text{S}$  to force majority of expressed  $G\alpha_{i1}$  into active GTP bound conformation.
- 2) HEK293T cells transfected with constitutively active  $G\alpha_{i1}$  Q<sup>204</sup>L cDNA, permeabilised in PBS + 1% BSA + 0.1%  $\text{NaN}_3$  (FMAT Buffer).
- 3) HEK293T cells transfected with wild type  $G\alpha_{i1}$  cDNA, permeabilised in PBS + 1% BSA + 0.1%  $\text{NaN}_3$  (FMAT Buffer), and incubated with 100  $\mu\text{M}$   $\text{GDP}\beta\text{S}$  to force majority of expressed  $G\alpha_{i1}$  into inactive GDP bound conformation.
- 4) HEK293T cells mock transfected with pcDNA3, permeabilised in PBS + 1% BSA + 0.1%  $\text{NaN}_3$  (FMAT Buffer)

Figure 5.15

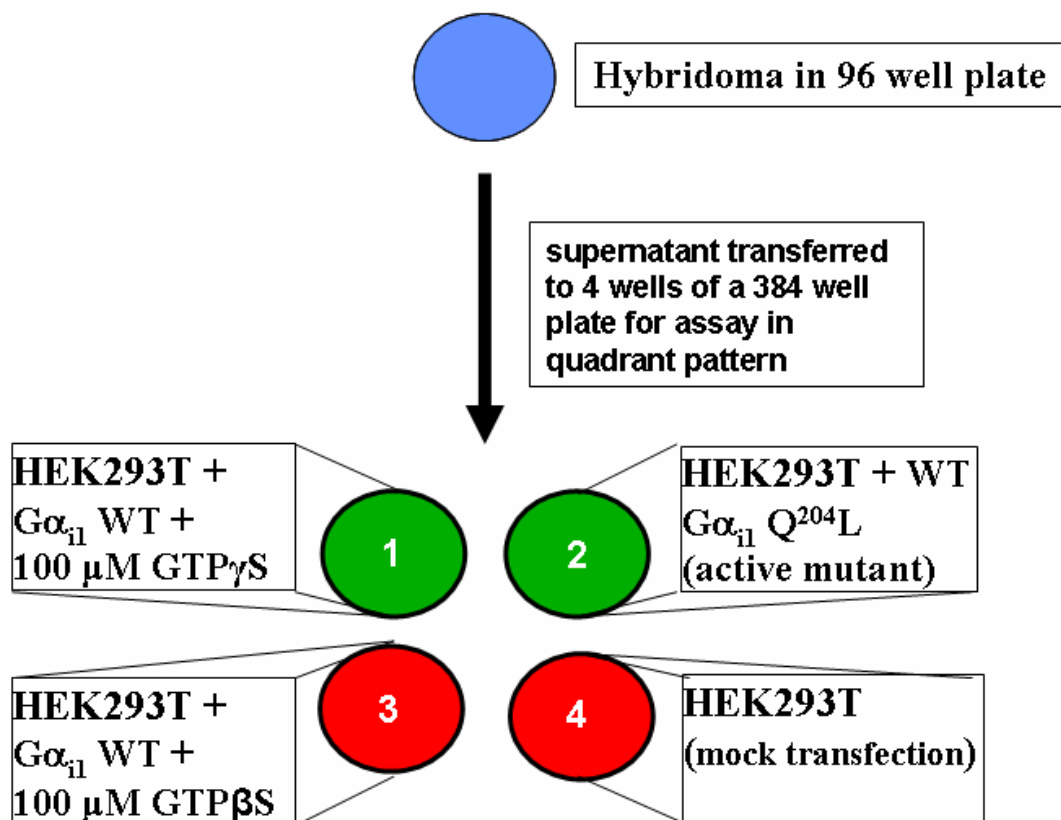


**Figure 5.16: Initial hybridoma screen identifies three hybridoma clones producing antibody which showed selectivity towards the active conformation of  $G\alpha_{i1}$**

1824 hybridoma clones were screened using the FMAT assay described in **Figure 5.9**.

The conditions used were as described in **Figure 5.15**: Briefly HEK293T cells were transfected with wild type  $G\alpha_{i1}$  cDNA, and incubated with 100  $\mu$ M GTP $\gamma$ S (**GTP**) or 100  $\mu$ M GDP $\beta$ S (**GDP**), transfected with the active mutant Gln<sup>204</sup>Leu  $G\alpha_{i1}$  cDNA (**Q204L**) or mock transfected with pcDNA3 (**MOCK**). Three hybridoma clones were identified as having selectivity towards the active (GTP bound) conformation of  $G\alpha_{i1}$ : 8A5 (**A**), 8D11 (**B**) and 6F12 (**C**)

Figure 5.16

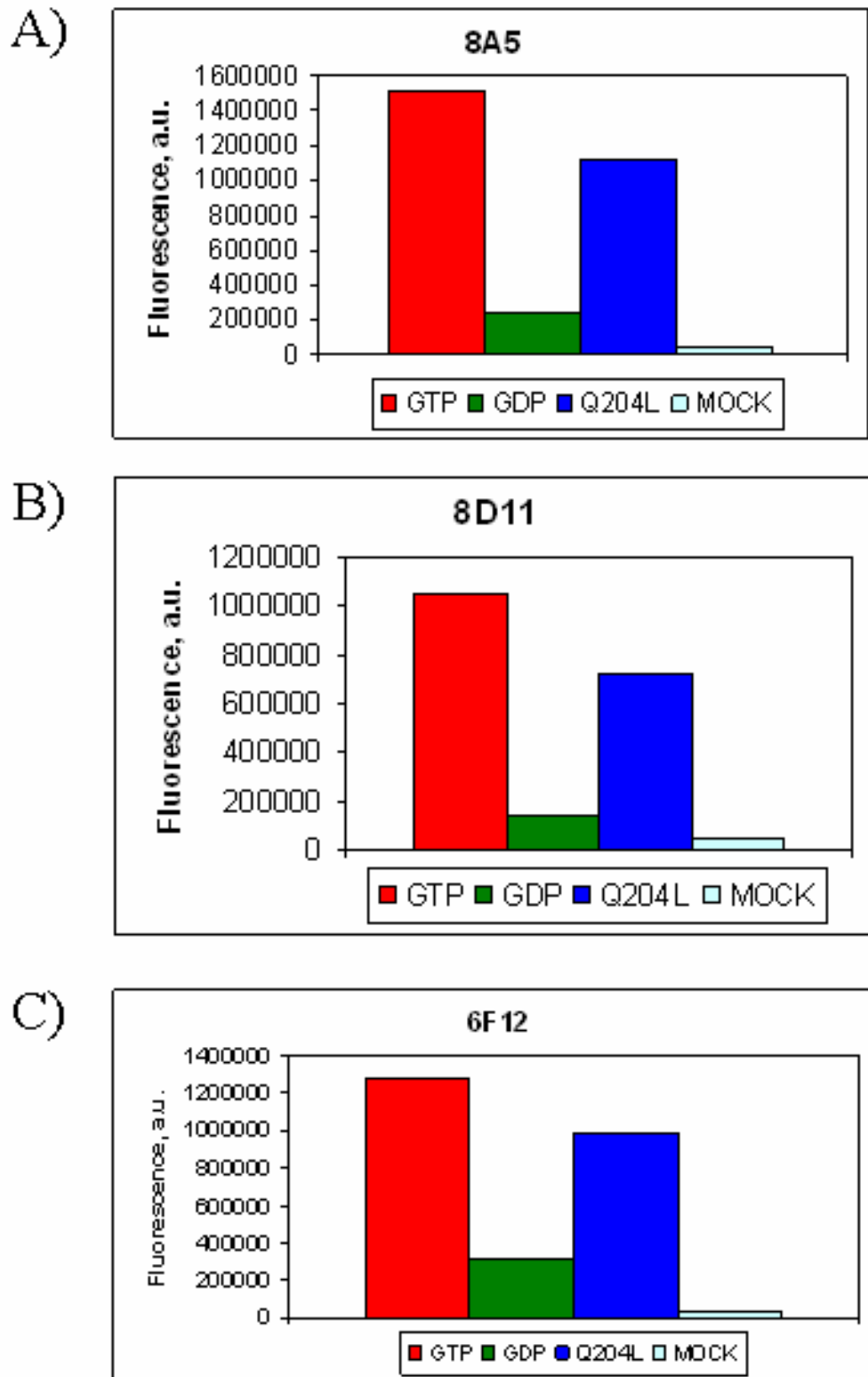


**Figure 5.17: Secondary FMAT screen of hybridoma clones: The three clones identified as showing selectivity towards the active (GTP bound) conformation of  $G\alpha_{i1}$  showed a similar selectivity upon repetition of the screen**

Hybridoma clones that, in the primary FMAT screen, showed high counts for the conditions in which  $G\alpha_{i1}$  was expressed as compared to the mock transfected cells were retained and sub-cultured. To confirm the results obtained in the primary screen, tissue culture supernatant from these clones was again screened using the FMAT whole cell assay. The conditions used were as described in **Figure 5.15**: Briefly HEK293T cells were transfected with wild type  $G\alpha_{i1}$  cDNA, and incubated with 100  $\mu$ M GTP $\gamma$ S (**GTP**) or 100  $\mu$ M GDP $\beta$ S (**GDP**), transfected with the active mutant Gln<sup>204</sup>Leu  $G\alpha_{i1}$  cDNA (**Q204L**) or mock transfected with pcDNA3 (**MOCK**). The experiment was performed in triplicate to N = 3. Each separate figure (**A-D**) refers to one FMAT plate, the three conformation selective clones identified in the primary screen were 6F12 (**C**) and 8A5, 8D11 (**D**)

Figure 5.17

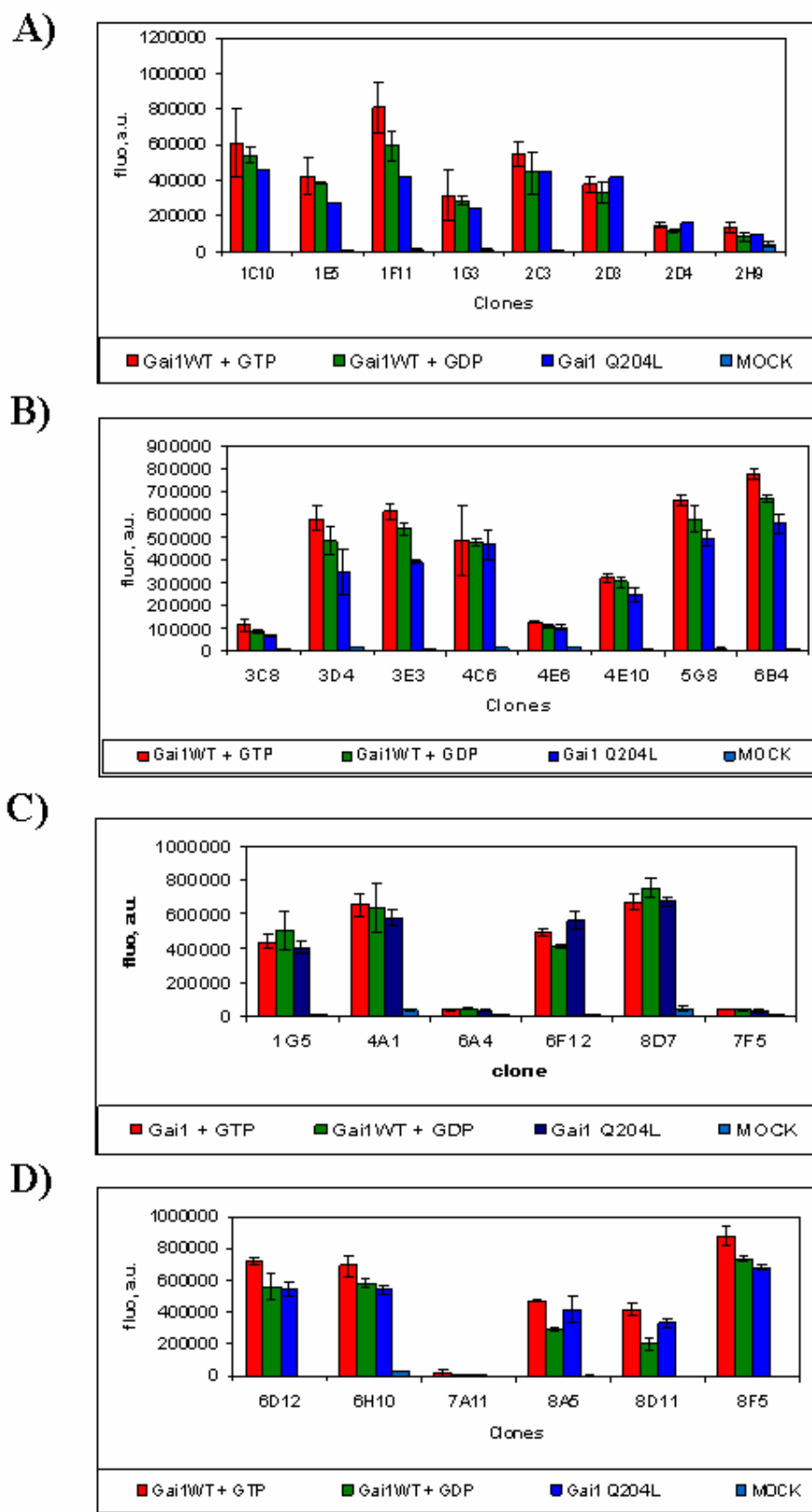


**Figure 5.18: FMAT screen of hybridoma clones following re-cloning of the three clones identified as showing selectivity towards the active (GTP bound) conformation of  $G\alpha_{i1}$ : Displayed are daughter clones that showed the best profile, selected from each of the three parental hybridoma cell lines.**

Each of the hybridoma cell lines that produced an antibody selective for the active GTP bound conformation of  $G\alpha_{i1}$  (8A5, 6F12, 8D11) were re-cloned. Using hybridoma clone tissue culture supernatant from all of the clones created by this re-cloning process, an FMAT screen was performed using the same conditions as for the primary FMAT hybridoma screen. A summary of data from all clones screened is displayed in **Table 5.6**. The data for the clone showing the best profile for each parental cell line is displayed as follows: **A)** 8A5 1C1 **B)** 6F12 1E5 **C)** 8D11 1H1.

Figure 5.18

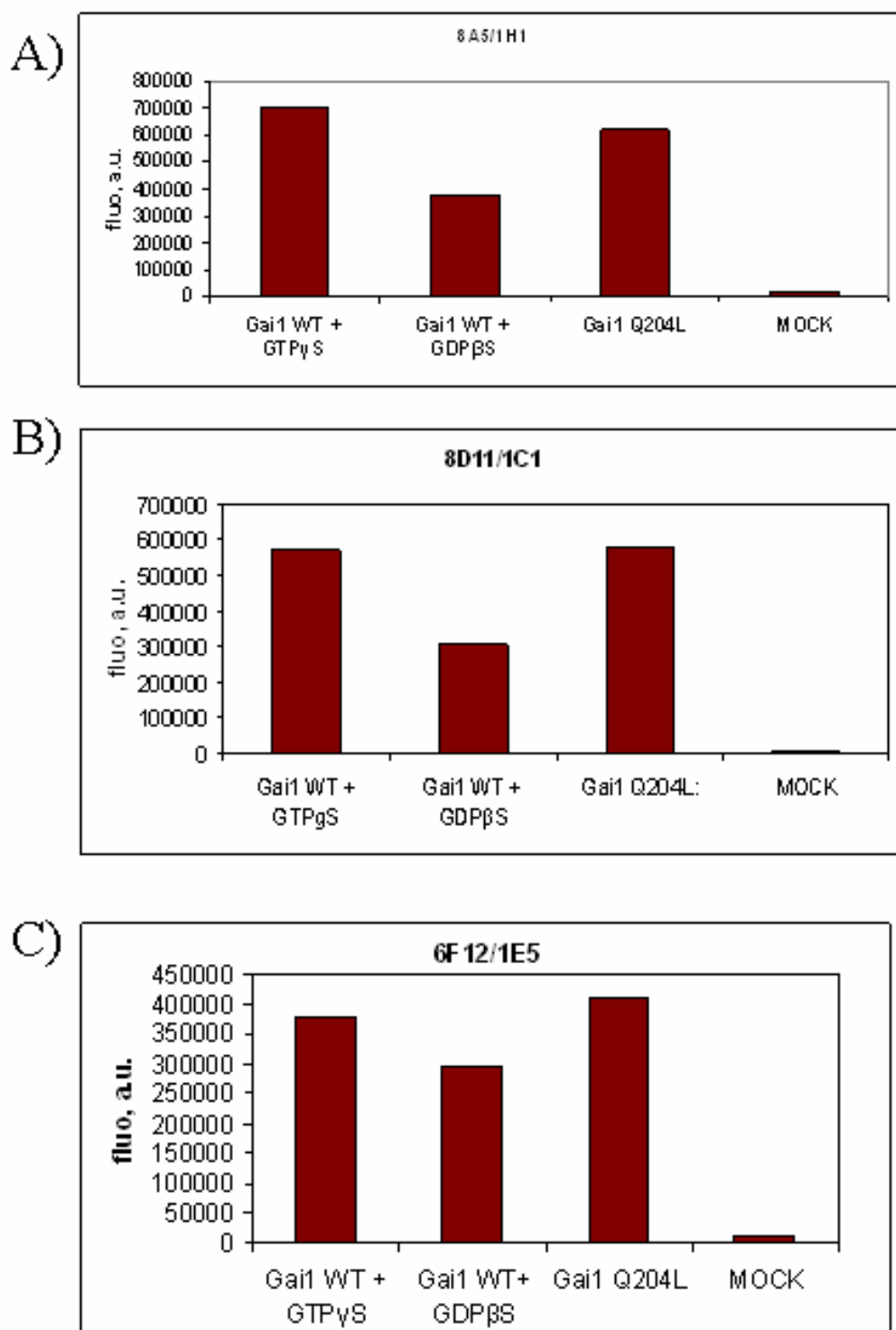


**Figure 5.19: Titration experiment using purified non-conformation selective antibodies produced by hybridoma clones 8F5 and 6B4**

Similar to the FMAT screens used previously the five following conditions were set up: HEK293T cells transiently expressing wild type  $G\alpha_{i1}$  preloaded with either 10  $\mu$ M GTP $\gamma$ S or 10  $\mu$ M GDP $\beta$ S, HEK293T cells expressing either the constitutively active variant Gln<sup>204</sup>Leu  $G\alpha_{i1}$  or the constitutively inactive variant Glu<sup>203</sup>Ala  $G\alpha_{i1}$  or cells mock-transfected with the empty vector pcDNA3. FMAT blue anti-mouse <sup>®</sup> antibody was added to the cell suspensions to a final dilution of 1 in 2000. Each of these cell suspensions was added to serial 1 in 3 dilution sets of either 6B4 (**A**) or 8F5 (**B**). Plates were incubated in the dark for 2 hours at room temperature and then fluorescence detected using an 8200 Cellular Detection System (Applied Biosystems).

Figure 19

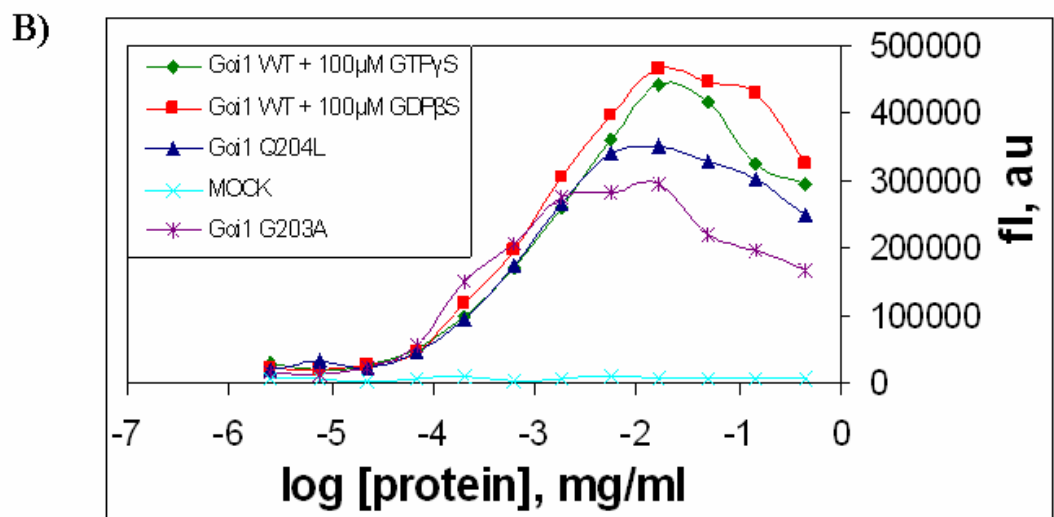
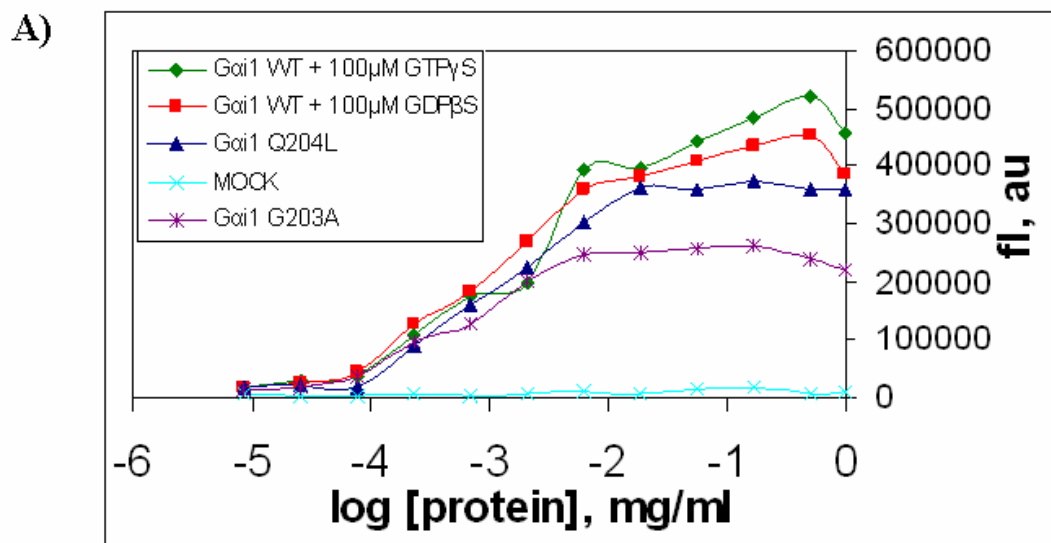


**Figure 5.20: Titration experiment using purified conformation selective antibodies produced by hybridoma clones 8A5/1C1, 6F12/1E5 and 8D11/1H1**

As for figure 5.20 the five following conditions were set up: HEK293T cells transiently expressing wild type  $G\alpha_{i1}$  preloaded with either 10  $\mu$ M GTP $\gamma$ S or 10  $\mu$ M GDP $\beta$ S, HEK293T cells expressing either the constitutively active variant Gln<sup>204</sup>Leu  $G\alpha_{i1}$  or the constitutively inactive variant Gla<sup>203</sup>Ala  $G\alpha_{i1}$  or cells mock-transfected with the empty vector pcDNA3. FMAT blue anti-mouse <sup>®</sup> antibody was added to the cell suspensions to a final dilution of 1 in 2000. Each of these cell suspensions was added to serial 1 in 3 dilution sets of either 8A5/1C1 (**A**), 6F12/1E5 (**B**) or 8D11/1H1 (**C**). Plates were incubated in the dark for 2 hours at room temperature and then fluorescence detected using an 8200 Cellular Detection System (Applied Biosystems).

Figure 5.20

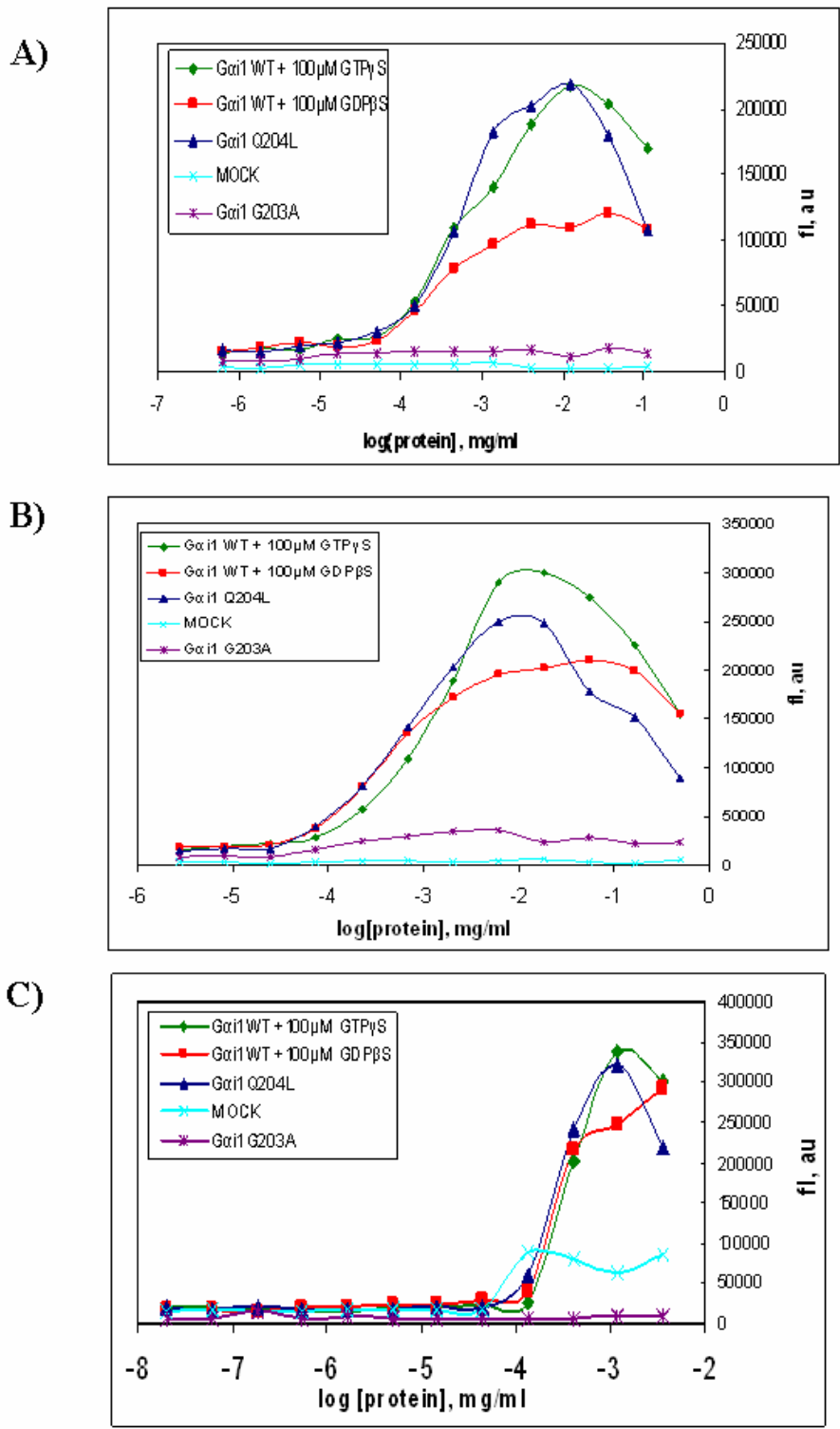


**Figure 5.21: Non-conformation selective antibodies 6B4 and 8F5 selectively recognise  $G\alpha_{i1}$  over other members of the  $G\alpha_{i/o}$  family on a Western blot.**

Chemically competent BL21 *E coli* cells were transformed with the vector pT7.7 containing the cDNA of the relevant  $G\alpha$  subunit. Expression of  $G\alpha$  subunit was induced with the addition of  $1\mu\text{g} / \text{ml}$  IPTG. Cell lysate proteins ( $0.5\mu\text{g} / \text{well}$ ) were separated by SDS PAGE and Western blots performed using the non-conformation selective antibodies 6B4 (**A-i**) and 8F5 (**B-i**). An in-house antiserum raised against the C-terminal decapeptide of  $G\alpha_{i1/2}$  (**C-i**), was used as a control. To assess the relative amount of protein loaded for each sample the nitrocellulose blots were stained with Coomassie stain. (**A-ii to C-ii**).

Figure 5.21

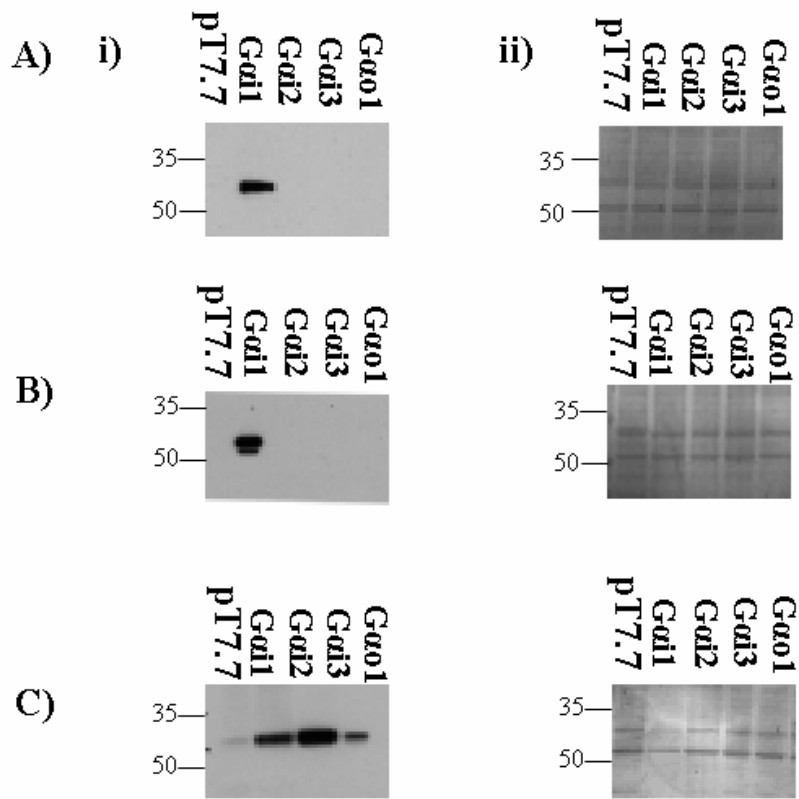


**Figure 5.22: Conformation selective antibodies 8A5/1C1, 6F12/1E5 and 8D11/1H1 do not recognise members of the  $G\alpha_{i/o}$  family denatured by SDS PAGE.**

In parallel with experiments described in **Figure 5.22**, chemically competent BL21 *E coli* cells were transformed with the vector pT7.7 containing the cDNA of the relevant G  $\alpha$  subunit. Expression of G  $\alpha$  subunit was induced with the addition of 1  $\mu$ g / ml IPTG. Cell lysate proteins (0.5  $\mu$ g / well) were separated by SDS PAGE and Western blots performed using the conformation selective antibodies 8A5/1C1 (**A-i**), 6F12/1E5 (**B-i**) and 8D11/1H1 (**C-i**). To assess the relative amount of protein loaded for each sample the nitrocellulose blots were stained with Coomassie stain. (**A-ii to C-ii**)

Figure 5.22

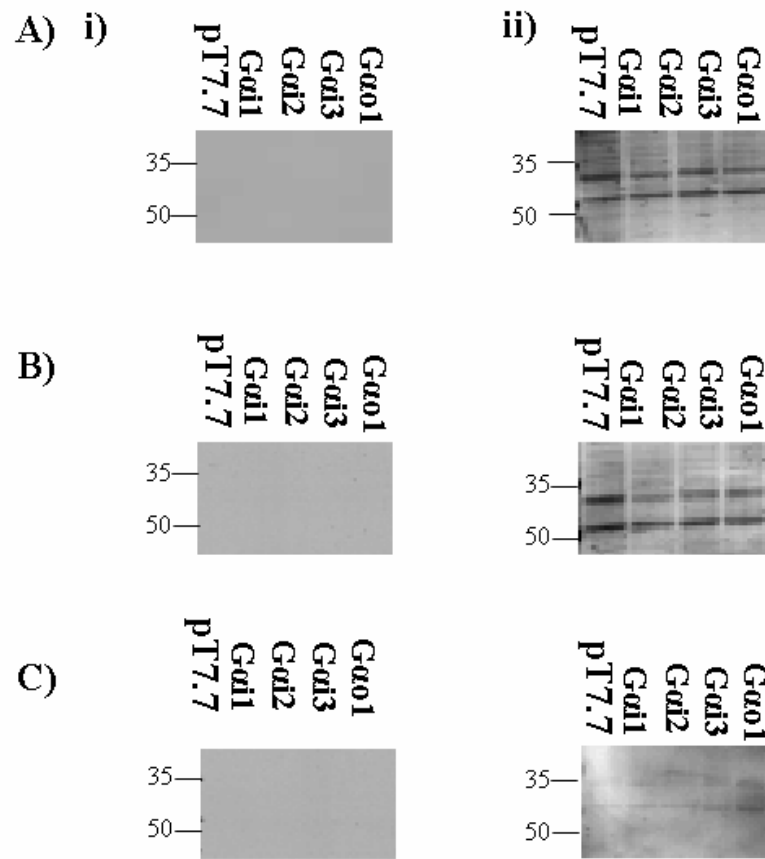


**Figure 5.23: Immunocytochemistry using the conformation selective antibody****8A6/1H1**

HEK293T cells were grown on poly-D-lysine coated coverslips. These cells were co-transfected with cDNA of the D<sub>21</sub>-YFP fusion protein and either wild type G $\alpha_{i1}$  (**A**), Gln<sup>204</sup>Leu G $\alpha_{i1}$  active variant (**B**), or the inactive variant Gly<sup>203</sup>Ala G $\alpha_{i1}$  (**C**).

Immunocytochemistry was performed as in section **2.10.7**. Nuclear staining was performed using Hoescht stain. The conformation selective antibody 8A6/1H1 was used at a final dilution of 1:100. The fluorescently labelled secondary antibody anti-mouse Alexa Fluor 594 was used at a final concentration of 1:400. Fluorescence detected from i) D<sub>21</sub>-eYFP, ii) Alexa Fluor 594, iii) Hoescht stain are shown. Scale marker represents 10  $\mu$ M.

**Figure 5.23**

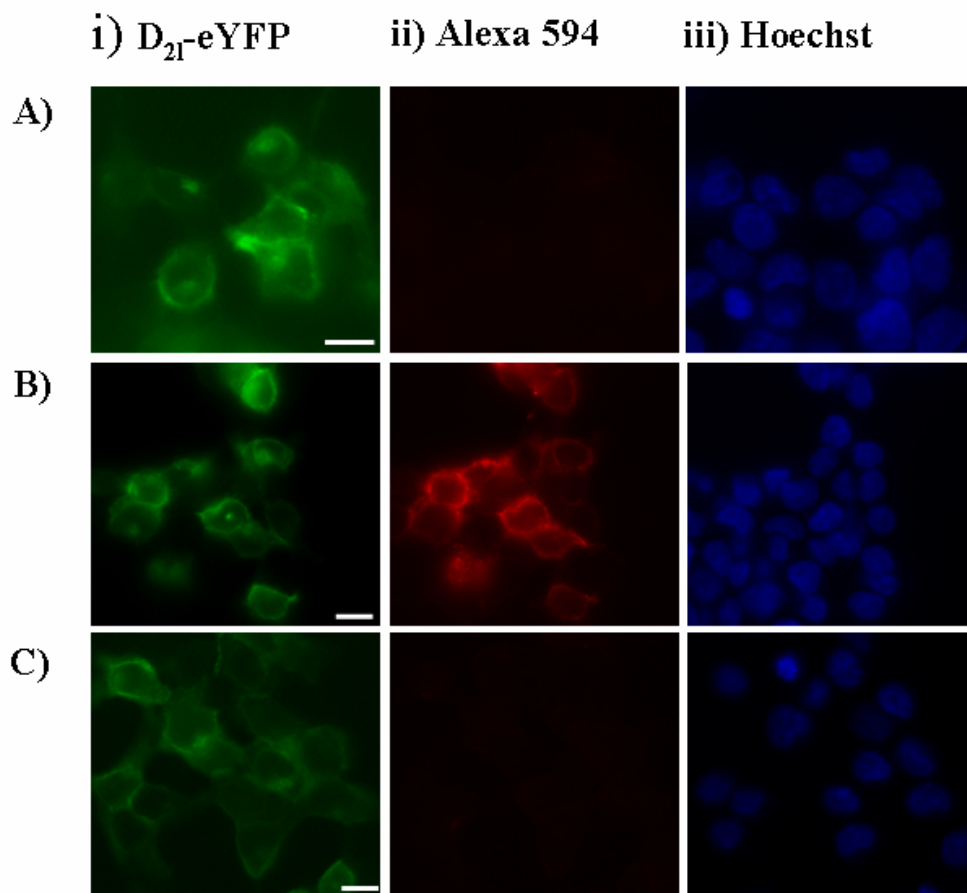


**Figure 5.24: Immunocytochemistry using the conformation selective antibody****6F12/1E5**

In parallel with the experiment described by **Figure 5.23**, HEK293T cells were grown on poly-D-lysine coated coverslips. These cells were co-transfected with cDNA of the D<sub>21</sub>-YFP fusion protein and either wild type G $\alpha_{i1}$  (**A**), Gln<sup>204</sup>Leu G $\alpha_{i1}$  (**B**) active variant or the inactive variant Gly<sup>203</sup>Ala G $\alpha_{i1}$  (**C**). Immunocytochemistry was performed as in section **2.10.7**. Nuclear staining was performed using Hoescht stain. The conformation selective antibody 8A6/1H1 was used at a final dilution of 1:100. The fluorescently labelled secondary antibody anti-mouse Alexa Fluor 594 was used at a final concentration of 1:400. Fluorescence detected from i) D<sub>21</sub>-eYFP, ii) Alexa Fluor 594, iii) Hoescht stain are shown. Scale marker represents 10  $\mu$ M.

Figure 5.24

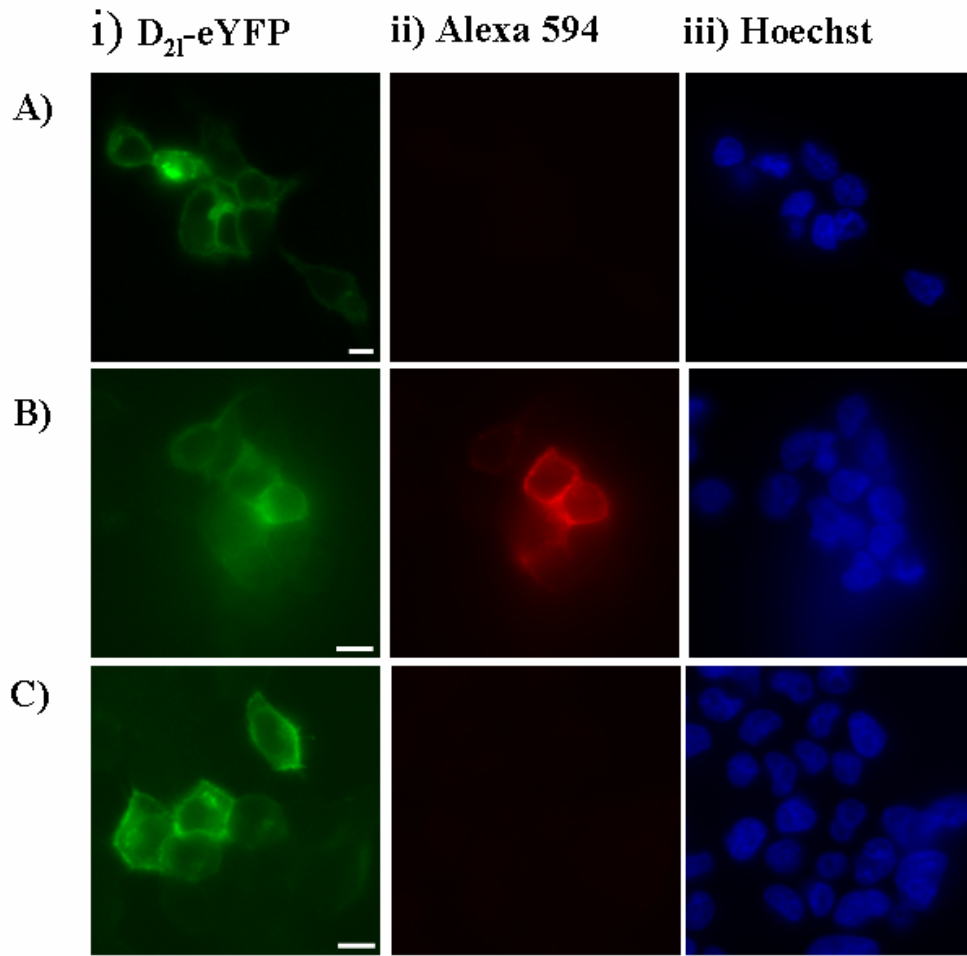


**Figure 5.25: Immunocytochemistry using the conformation selective antibody 8D11/1C1**

In parallel with the experiment described by **Figure 5.23**, HEK293T cells were grown on poly-D-lysine coated coverslips. These cells were co-transfected with cDNA of the D<sub>21</sub>-YFP fusion protein and either wild type G $\alpha_{i1}$  (**A**), Gln<sup>204</sup>Leu G $\alpha_{i1}$  (**B**) active variant or the inactive variant Gly<sup>203</sup>Ala G $\alpha_{i1}$  (**C**). Immunocytochemistry was performed as in section **2.10.7**. Nuclear staining was performed using Hoescht stain. The conformation selective antibody 8D11/1C1 was used at a final dilution of 1:100. The fluorescently labelled secondary antibody anti-mouse Alexa Fluor 594 was used at a final concentration of 1:400. Fluorescence detected from **i**) D<sub>21</sub>-YFP, **ii**) Alexa Fluor 594, **iii**) Hoescht stain are shown. Scale marker represents 10  $\mu$ M.

**Figure 5.25**

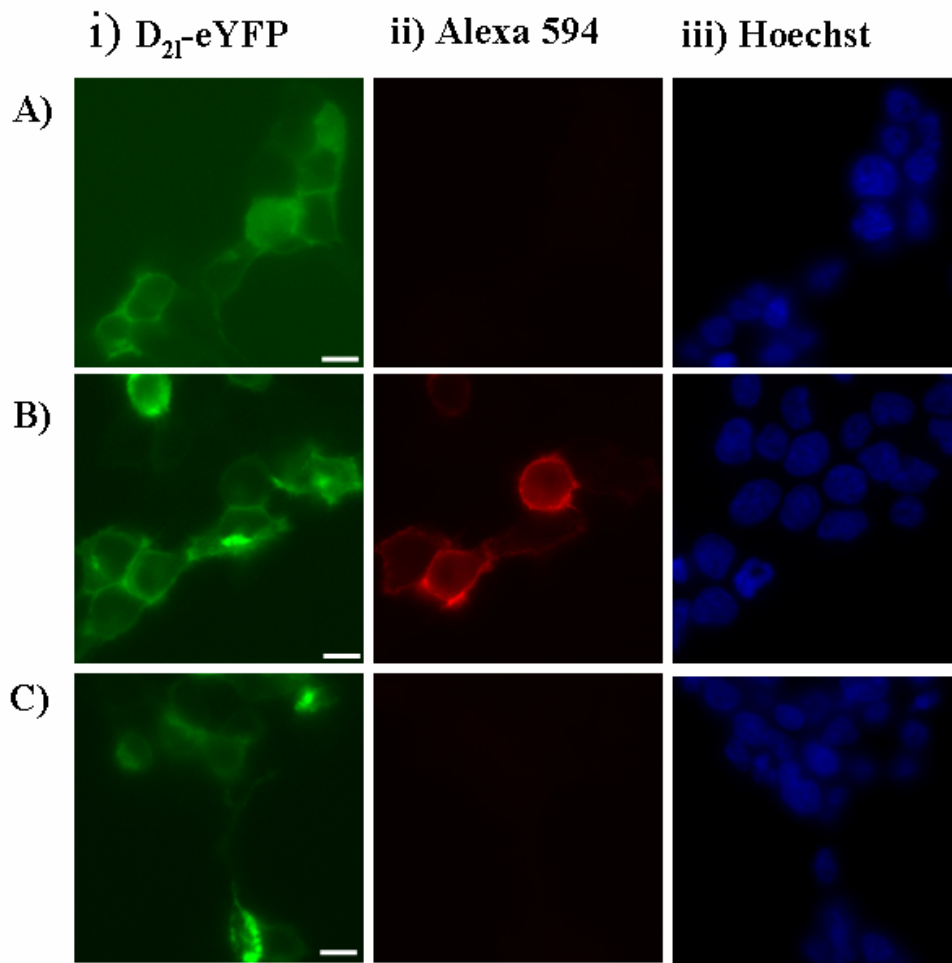


**Figure 5.26: Immunocytochemistry using the non-conformation-selective antibody 6B4**

In parallel with the experiment described by **Figure 5.23**, HEK293T cells were grown on poly-D-lysine coated coverslips. These cells were co-transfected with cDNA of the D<sub>21</sub>-eYFP fusion protein and either wild type G $\alpha_{i1}$  (**A**), Gln<sup>204</sup>Leu G $\alpha_{i1}$  (**B**) active variant or the inactive variant Gly<sup>203</sup>Ala G $\alpha_{i1}$  (**C**). As a control HEK293T cells were co-transfected with the vector pcDNA3 (**D**). Immunocytochemistry was performed as in section **2.10.7**.

Nuclear staining was performed using Hoescht stain. The non-conformation selective antibody 6B4 was used at a final dilution of 1:100. The fluorescently labelled secondary antibody anti-mouse Alexa Fluor 594 was used at a final concentration of 1:400.

Fluorescence detected from **i**) D21-YFP, **ii**) Alexa Fluor 594, **iii**) Hoescht stain are shown.

Scale marker represents 10  $\mu$ M.

Figure 5.26

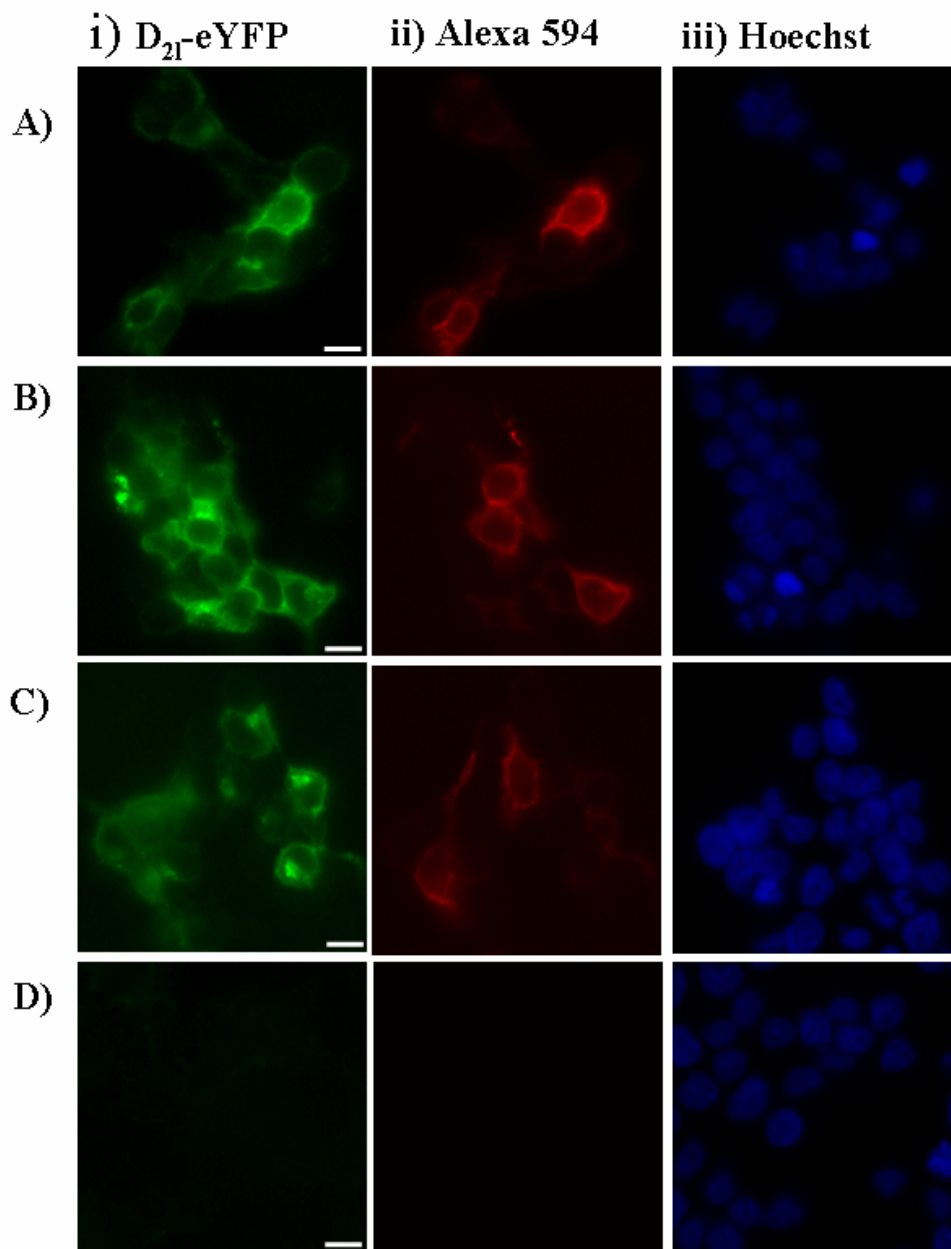


**Figure 5.27: Immunocytochemistry using the non-conformation selective antibody 8F5**

In parallel with the experiments described by **Figure 5.23**, HEK293T cells were grown on poly-D-lysine coated coverslips. These cells were co-transfected with cDNA of the D<sub>21</sub>-YFP fusion protein and either wild type G $\alpha_{i1}$  (**A**), Gln<sup>204</sup>Leu G $\alpha_{i1}$  active variant (**B**), or the inactive variant Gly<sup>203</sup>Ala G $\alpha_{i1}$  (**C**). As a control HEK293T cells were co-transfected with the vector pcDNA3 (**D**). Immunocytochemistry was performed as in section **2.10.7**.

Nuclear staining was performed using Hoescht stain. The non-conformation selective antibody 8F5 was used at a final dilution of 1:100. The fluorescently labelled secondary antibody anti-mouse Alexa Fluor 594 was used at a final concentration of 1:400.

Fluorescence detected from **i**) D<sub>21</sub>-YFP, **ii**) Alexa Fluor 594, **iii**) Hoescht stain are shown.

Scale marker represents 10  $\mu$ M.

**Figure 5.27**

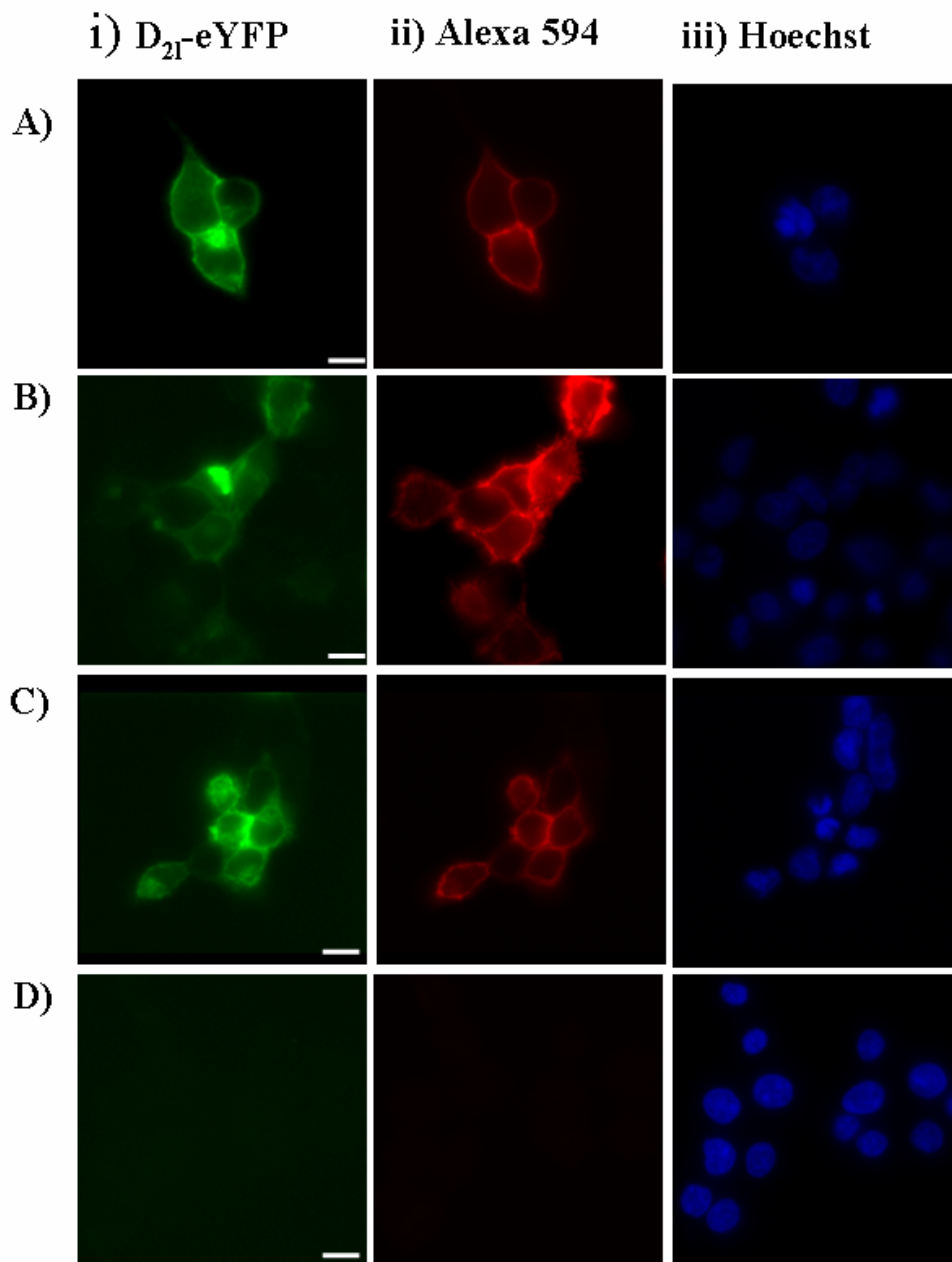


**Figure 5.28: Immunocytochemistry using an anti- $G\alpha_{i1/2}$  polyclonal antiserum raised against a decapeptide corresponding to the C-terminal ten amino acids of  $G\alpha_t$  (1319 Glycine)**

In parallel with the experiments described by **Figure 5.23**, HEK293T cells were grown on poly-D-lysine coated coverslips. These cells were co-transfected with cDNA of the D<sub>21</sub>-YFP fusion protein and either wild type  $G\alpha_{i1}$  (**A**), Gln<sup>204</sup>Leu  $G\alpha_{i1}$  active variant (**B**) or the inactive variant Gly<sup>203</sup>Ala  $G\alpha_{i1}$  (**C**). As a control HEK293T cells were co-transfected with cDNA of the D<sub>21</sub>-YFP fusion protein and pcDNA3 (**D**). Immunocytochemistry was performed as in section **2.10.7**. Nuclear staining was performed using Hoescht stain. The polyclonal antiserum 1319 glycine was used at a final dilution of 1:500. The fluorescently labelled secondary antibody anti-rabbit Alexa Fluor 594 was used at a final concentration of 1:600. Fluorescence detected from **i**) D<sub>21</sub>-YFP, **ii**) Alexa Fluor 594, **iii**) Hoescht stain are shown. Scale marker represents 10  $\mu$ M.

Figure 5.28

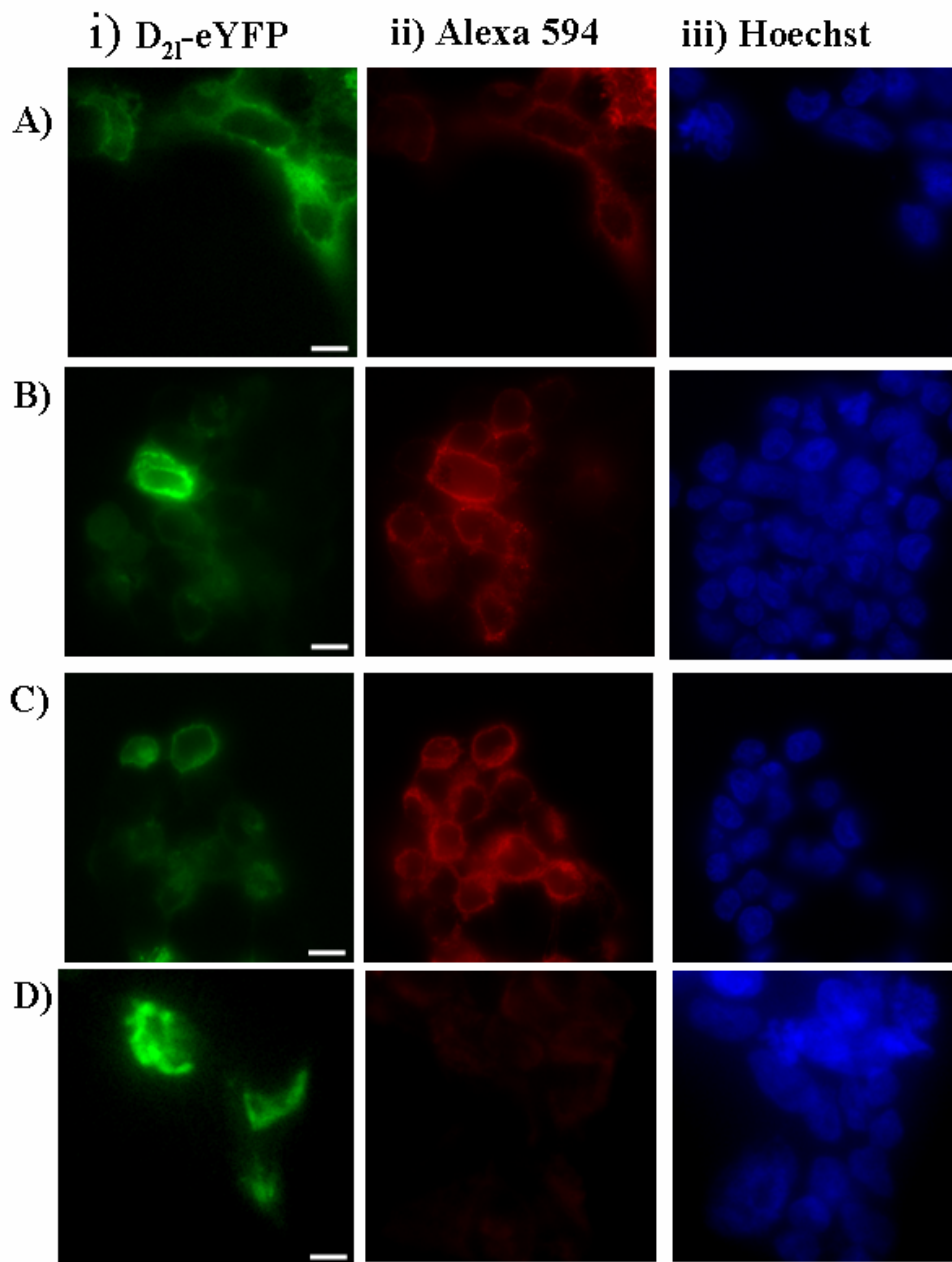


**Figure 5.29: Epitope mapping of non-conformation selective antibodies using a set of overlapping 16mer peptides corresponding to the amino acid sequence of human  $G\alpha_{i1}$**

A set of 16mer peptides overlapping by 4 amino acids and corresponding to the entire amino acid sequence of  $G\alpha_{i1}$  were generated by Mimotopes Ltd. The epitope mapping experiments were performed as described in section **2.10.6**. 100  $\mu$ l of peptide solution added to wells of a streptavidin coated 96 well plate. Following a 1 hour incubation, the biotinylated peptides were bound to the streptavidin coated plate. The peptide solution was removed and replaced with a 1:1000 dilution of antibody in PBS/ 0.1% Tween 20/ 0.1%  $\text{NaN}_3$ . Antibodies used were as follows: 6B4 (**B**) and 8F5 (**C**). The polyclonal antiserum 1319 Glycine raised against the C-terminal ten amino acids of  $G\alpha_{i1/2}$  was used as a positive control (**A**). HRP conjugated secondary antibody was used at a dilution of 1:2000 in PBS/ 0.1% Tween 20/ 0.1%  $\text{NaN}_3$ . The presence of peroxidase, indicating a specific interaction between a given peptide and the primary antibody, was detected using the substrate Sureblue™ TMB.

Figure 5.29

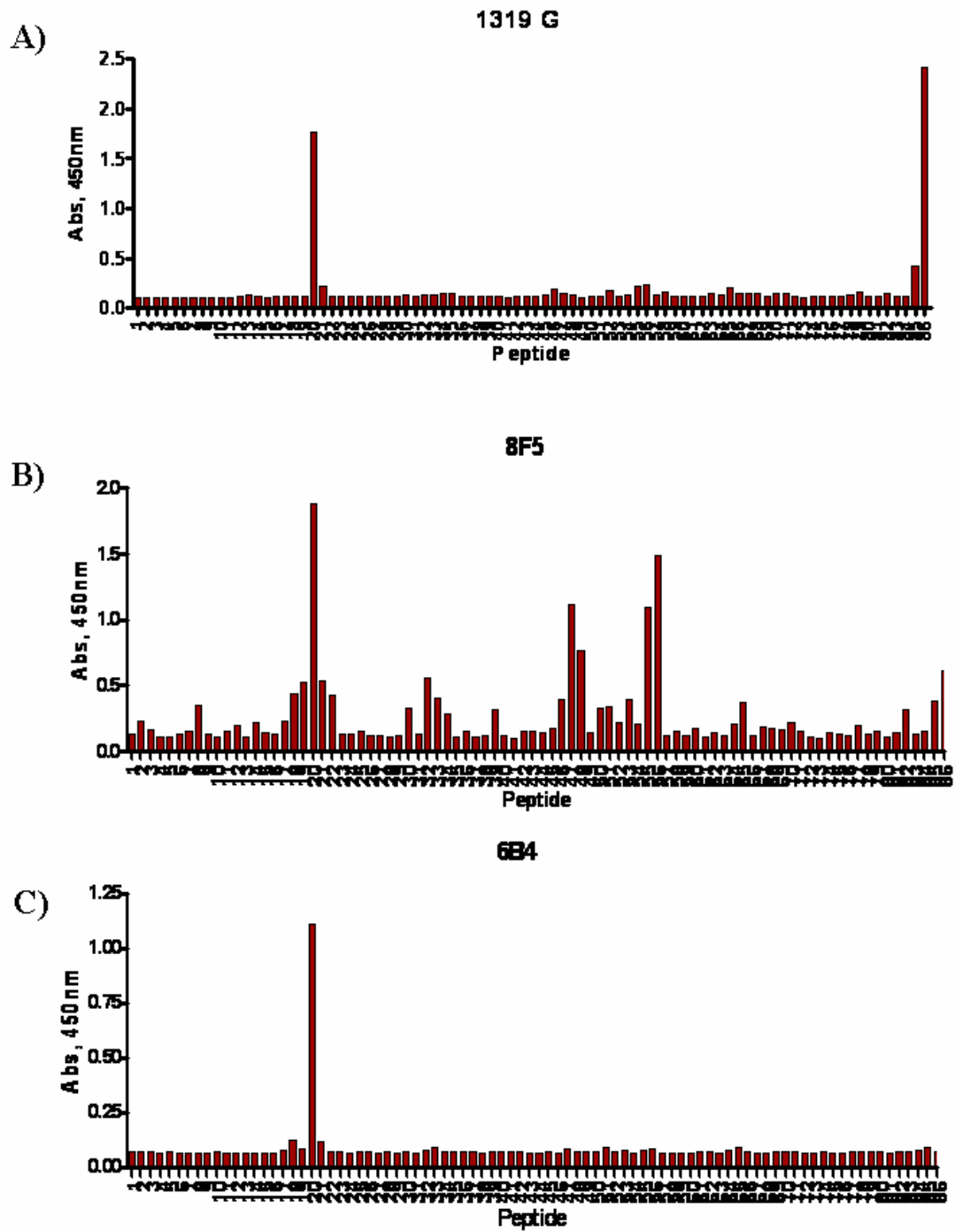


**Figure 5.30: Epitope mapping of conformation selective antibodies using a set of overlapping 16mer peptides corresponding to the amino acid sequence of human G $\alpha_{i1}$**

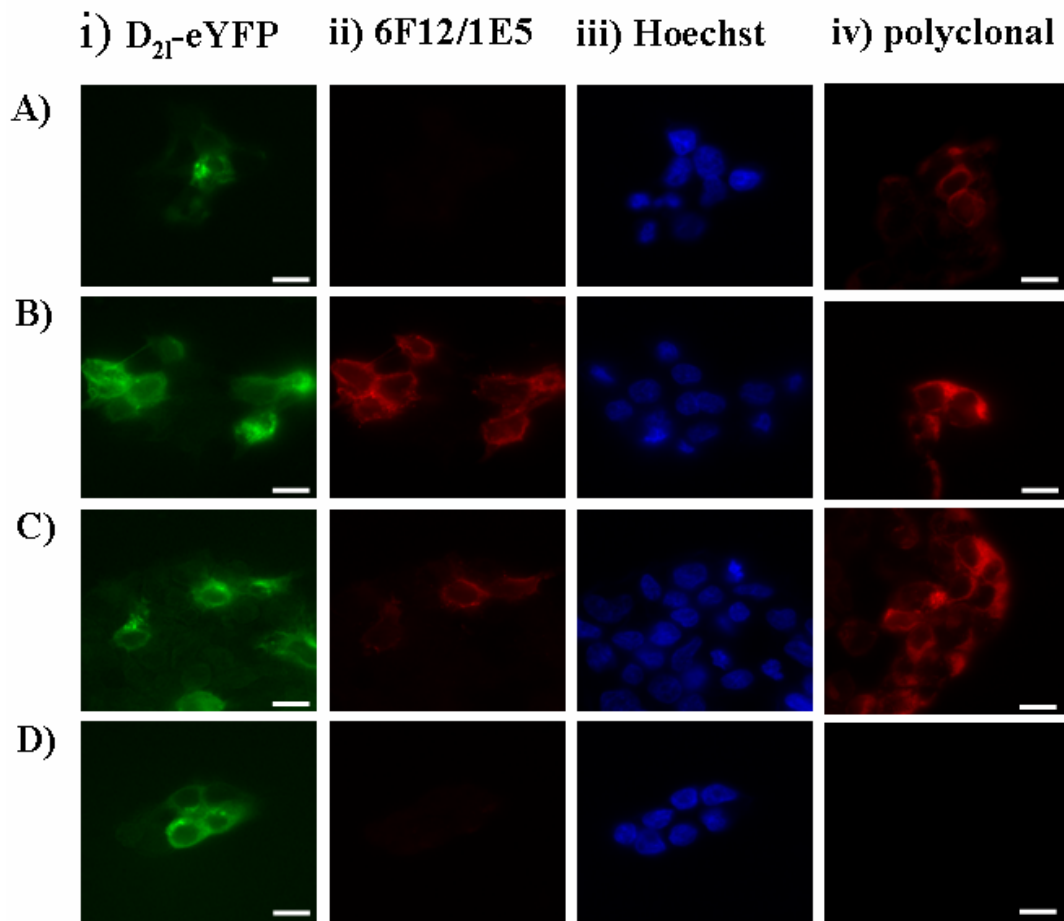
The epitope mapping experiments were performed as described in **Figure 5.29**.

Antibodies used were as follows: 8A5/1H1 (**A**), 8D11/1C1 (**B**) and 6F12/1E5 (**C**) at a 1:1000 dilution HRP conjugated secondary antibody was used at a dilution of 1:2000 in PBS/ 0.1% Tween 20 / 0.1% NaN<sub>3</sub>. The presence of peroxidase, indicating a specific interaction between a given peptide and the primary antibody, was detected using the substrate Sureblue™ TMB.



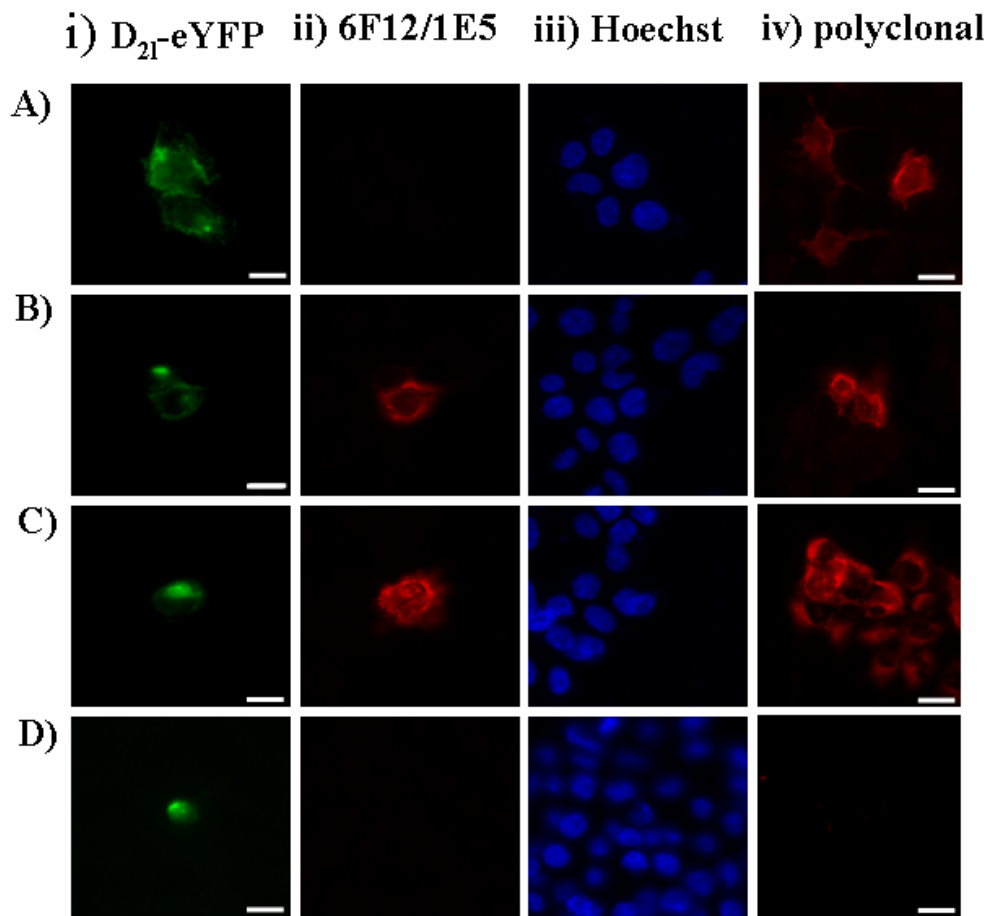
**Figure 5.31: The conformation-selective antibody 6F12/1E5 shows selectivity for the constitutively active mutant Gln<sup>205</sup>Leu G $\alpha$ <sub>i2</sub>**

HEK293T cells were grown on poly-D-lysine coated coverslips. These cells were co-transfected with cDNA of the D<sub>21</sub>-YFP fusion protein and either wild type G $\alpha$ <sub>i2</sub> (**A**), G $\alpha$ <sub>i2</sub> Gln<sup>205</sup>Leu active variant (**B**) or the active variant Gln<sup>204</sup>Leu G $\alpha$ <sub>i1</sub> (**C**). As a control HEK293T cells were co-transfected with cDNA of the D<sub>21</sub>-YFP fusion protein and pcDNA3 (**D**). Immunocytochemistry was performed as in section 2.10.7. Nuclear staining was performed using Hoescht stain. The conformation selective antibody 6F12/1E5 was used at a final dilution of 1:200. The fluorescently labelled secondary antibody anti-mouse Alexa Fluor 594 was used at a final concentration of 1:400. Fluorescence detected from (i) D<sub>21</sub>-YFP, (ii) Alexa Fluor 594 bound to 6F12/1E5, (iii) Hoescht stain are shown. To demonstrate expression of transfected G $\alpha$  protein a parallel immunocytochemistry experiment was performed using the rabbit polyclonal anti-peptide antiserum raised against the corresponding C-terminal decapeptide sequences of G $\alpha$ <sub>i1/2</sub> (**iv**). Scale marker represents 10  $\mu$ M.

**Figure 5.31**

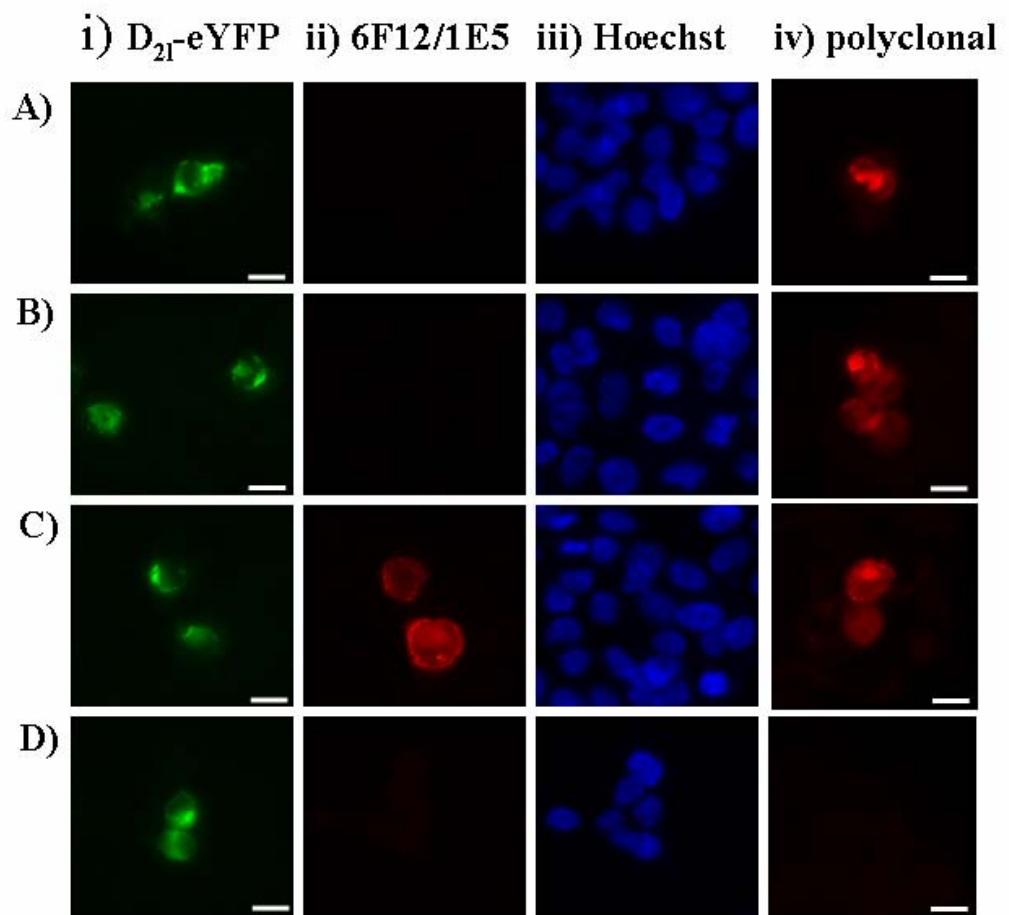
**Figure 5.32: The conformation-selective antibody 6F12/1E5 shows selectivity for the constitutively active mutant Gln<sup>204</sup>Leu G $\alpha$ <sub>o1</sub>**

HEK293T cells were grown on poly-D-lysine coated coverslips. These cells were co-transfected with cDNA of the D<sub>21</sub>-YFP fusion protein and either wild type G $\alpha$ <sub>o1</sub> (**A**), Gln<sup>204</sup>Leu G $\alpha$ <sub>o1</sub> active variant (**B**) or the active variant Gln<sup>204</sup>Leu G $\alpha$ <sub>i1</sub> (**C**). As a control HEK293T cells were co-transfected with cDNA of the D<sub>21</sub>-YFP fusion protein and pcDNA3 (**D**). Immunocytochemistry was performed as in section **2.10.5**. Nuclear staining was performed using Hoescht stain. The conformation selective antibody 6F12/1E5 was used at a final dilution of 1:200. The fluorescently labelled secondary antibody anti-mouse Alexa Fluor 594 was used at a final concentration of 1:400. Fluorescence detected from (**i**) D<sub>21</sub>-YFP, (**ii**) Alexa Fluor 594 bound to 6F12/1E5, (**iii**) Hoescht stain are shown. To demonstrate expression of transfected G $\alpha$  protein a parallel immunocytochemistry experiment was performed using rabbit polyclonal anti-peptide antisera against the corresponding C-terminal decapeptide sequences of G $\alpha$ <sub>i1/2</sub> or G $\alpha$ <sub>o1</sub> (**iv**). Scale marker represents 10  $\mu$ M.

**Figure 5.32**

**Figure 5.33: The conformation-selective antibody 6F12/1E5 does not show selectivity for the constitutively active mutant Gln<sup>227</sup>Leu Gα<sub>s</sub>**

HEK293T cells were grown on poly-D-lysine coated coverslips. These cells were co-transfected with cDNA of the D<sub>21</sub>-YFP fusion protein and either Gly<sup>226</sup>Ala Gα<sub>s</sub> inactive variant (**A**), Gln<sup>227</sup>Leu Gα<sub>s</sub> active variant (**B**), or the active variant Gln<sup>204</sup>Leu Gα<sub>i1</sub> (**C**). As a control HEK293T cells were co-transfected with cDNA of the D<sub>21</sub>-YFP fusion protein and pcDNA3 (**D**). Immunocytochemistry was performed as in section 2.10.5. Nuclear staining was performed using Hoescht stain. The conformation selective antibody 6F12/1E5 was used at a final dilution of 1:200. The fluorescently labelled secondary antibody anti-mouse Alexa Fluor 594 was used at a final concentration of 1:400. Fluorescence detected from (i) D<sub>21</sub>-YFP, (ii) Alexa Fluor 594 bound to 6F12/1E5, (iii) Hoescht stain are shown. To demonstrate expression of transfected Gα protein a parallel immunocytochemistry experiment was performed using rabbit polyclonal anti-peptide antisera raised against the corresponding C-terminal decapeptide sequences of Gα<sub>i1/2</sub> or Gα<sub>s</sub> (**iv**). Scale marker represents 10 μM.

**Figure 5.33**

**Figure 5.34: The conformation-selective antibody 6B12/1E5 does not show selectivity for the constitutively active mutant Q<sup>209</sup>L Gα<sub>q</sub>**

HEK293T cells were grown on poly-D-lysine coated coverslips. These cells were co-transfected with cDNA of the D<sub>21</sub>-YFP fusion protein and either Gly<sup>208</sup>Ala Gα<sub>q</sub> inactive variant (**A**), Gln<sup>209</sup>Leu Gα<sub>q</sub> active variant (**B**), or the active variant Gln<sup>204</sup>Leu Gα<sub>i1</sub> (**C**). As a control HEK293T cells were co-transfected with cDNA of the D<sub>21</sub>-YFP fusion protein and pcDNA3 (**D**). Immunocytochemistry was performed as in section 2.10.5. Nuclear staining was performed using Hoescht stain. The conformation selective antibody 6F12/1E5 was used at a final dilution of 1:200. The fluorescently labelled secondary antibody anti-mouse Alexa Fluor 594 was used at a final concentration of 1:400. Fluorescence detected from (i) D<sub>21</sub>-YFP, (ii) Alexa Fluor 594 bound to 6F12/1E5, (iii) Hoescht stain are shown. To demonstrate expression of transfected Gα protein a parallel immunocytochemistry experiment was performed using rabbit polyclonal anti-peptide antisera raised against the corresponding C-terminal decapeptide sequences of Gα<sub>i1/2</sub> or Gα<sub>q</sub> (**iv**). Scale marker represents 10 μM.

**Figure 5.34**

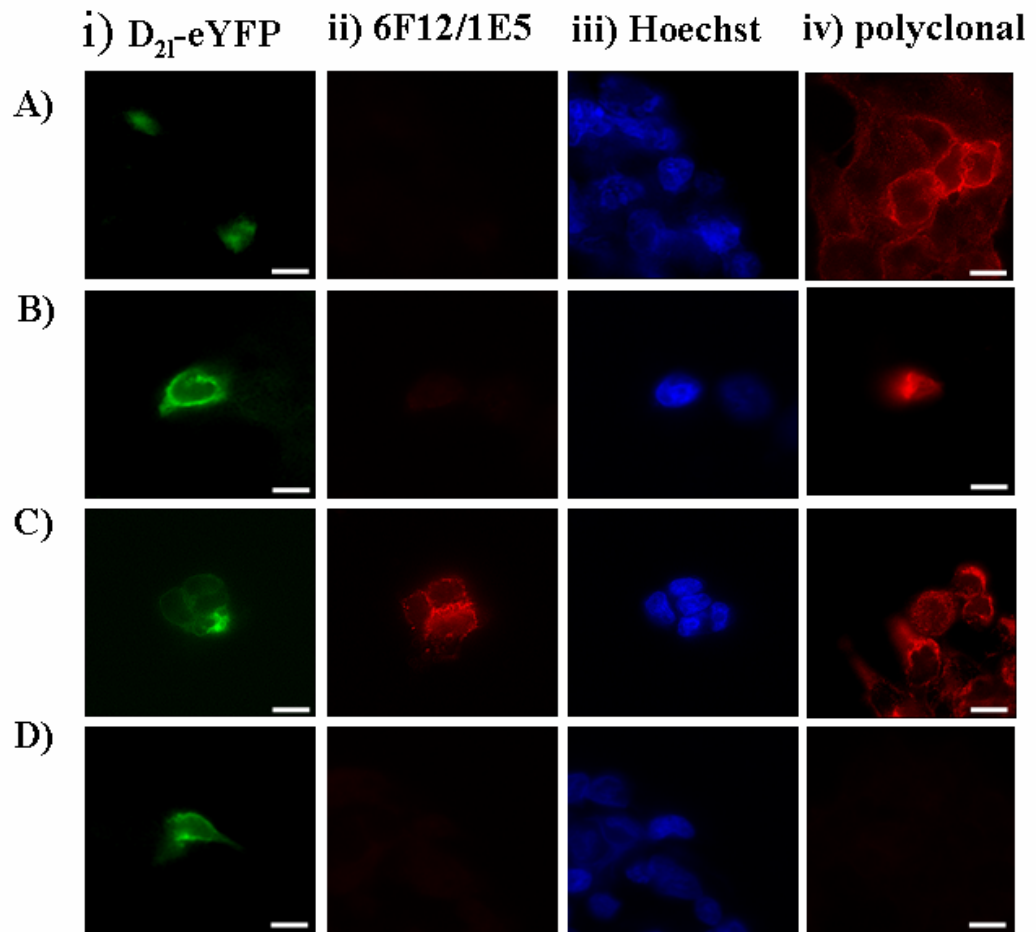


**Figure 5.35: The conformation-selective antibody 6F12/1E5 does not show selectivity for the constitutively active mutant R<sup>178</sup>C G $\alpha$ <sub>i2</sub>**

HEK293T cells were grown on poly-D-lysine coated coverslips. These cells were co-transfected with cDNA of the D<sub>21</sub>-YFP fusion protein and either Gln<sup>204</sup>Leu G $\alpha$ <sub>i2</sub> active variant (**A**), Arg<sup>178</sup>Cys G $\alpha$ <sub>i2</sub> active variant (**B**), or the wild type G $\alpha$ <sub>i2</sub> (**C**). As a control HEK293T cells were co-transfected with cDNA of the D<sub>21</sub>-YFP fusion protein and pcDNA3 (**D**). Immunocytochemistry was performed as in section 2.10.5. Nuclear staining was performed using Hoescht stain. The non-conformation selective antibody 6F12/1E5 was used at a final dilution of 1:200. The fluorescently labelled secondary antibody anti-mouse Alexa Fluor 594 was used at a final concentration of 1:400. Fluorescence detected from (i) D<sub>21</sub>-YFP, (ii) Alexa Fluor 594 bound to 6F12/1E5, (iii) Hoescht stain are shown. To demonstrate expression of transfected G $\alpha$  protein a parallel immunocytochemistry experiment was performed using the rabbit polyclonal anti-peptide antiserum raised against the corresponding C-terminal decapeptide sequences of G $\alpha$ <sub>i1/2</sub> (iv). Scale marker represents 10  $\mu$ M.

**Figure 5.35**

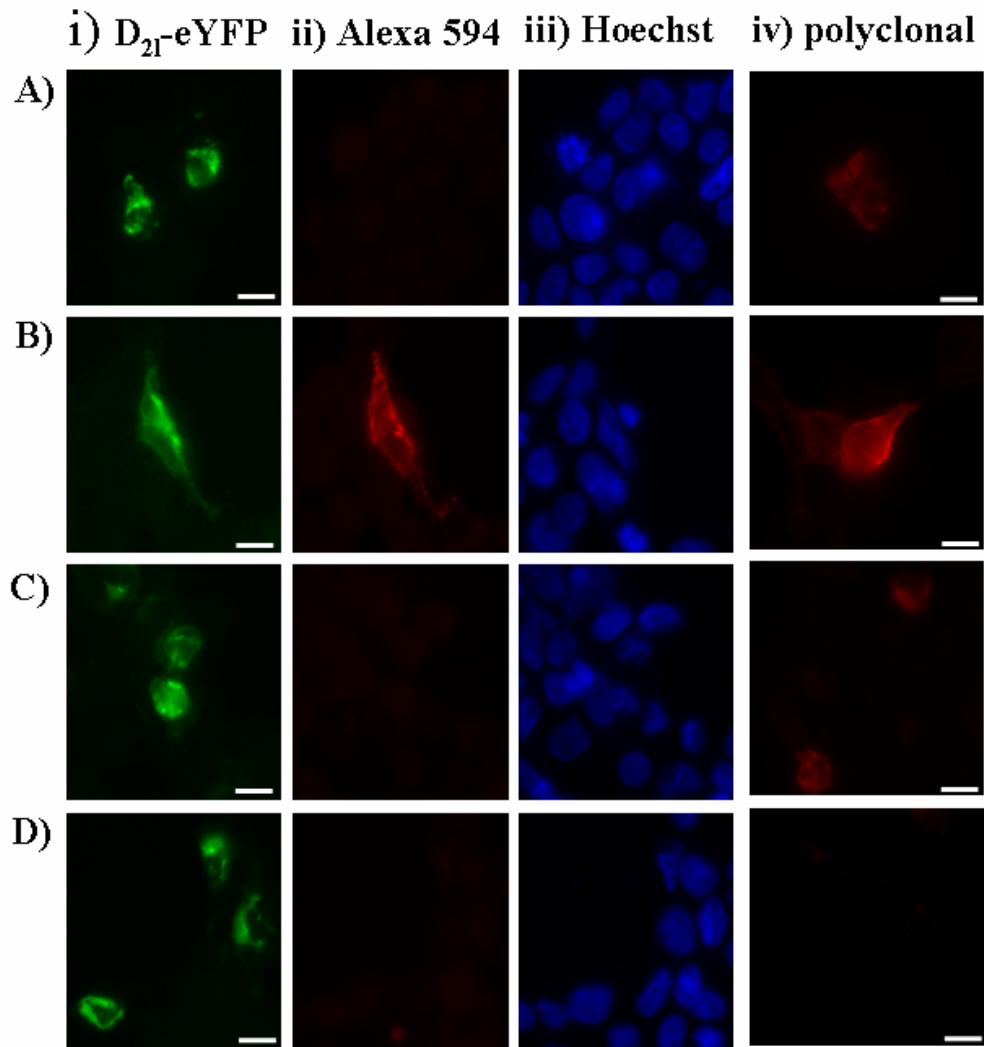
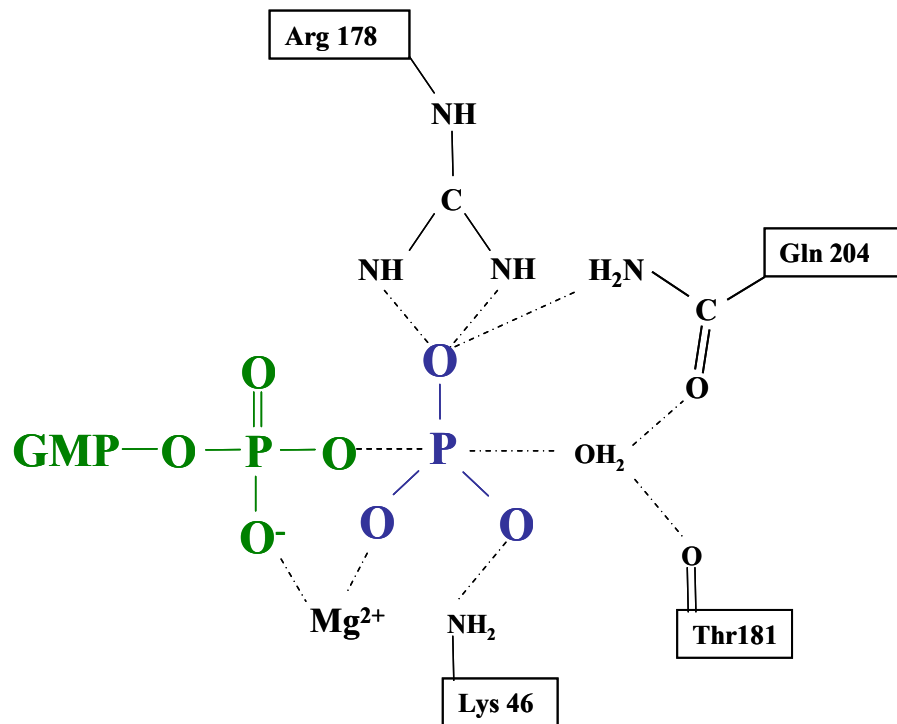


**Figure 5.36:  $\text{AlF}_4^-$  is a substitute for and mimic of the  $\gamma$  phosphate of GTP**

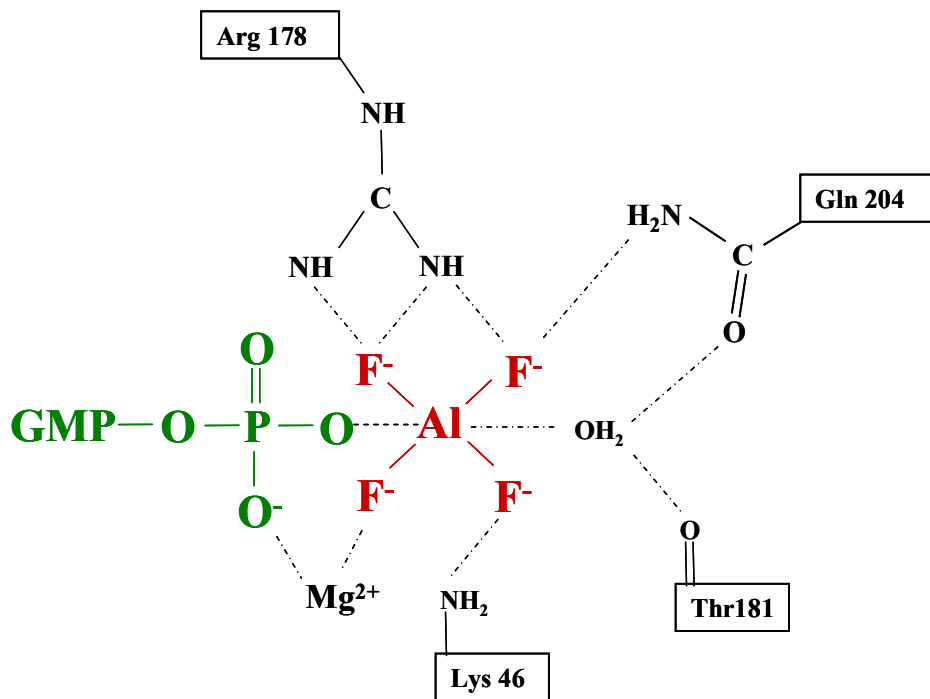
- A) **Schematic showing the co-ordination sphere of  $\text{AlF}_4^-$  involving  $\text{Arg}^{178}$ ,  $\text{Gln}^{204}$  the magnesium ion and other active site residues.**
- B) **Model of the active site of  $\text{G}\alpha_{i1}$  at the transition state of the phosphorolysis reaction, based on the structure of the  $\text{GDP}\cdot\text{AlF}_4^-$  complex.** The phosphorous atom of a trigonal ' $\text{PO}_3$ ' group was centred on the aluminium ion of the  $\text{AlF}_4^-$  with the planes of the  $\text{PO}_3$  group co-incident with that of  $\text{AlF}_4^-$ . The  $\text{PO}_3$  group was rotated to achieve a O-Mg distance similar to that observed for the F30-Mg contact in the  $\text{AlF}_4^-$  complex. This model is otherwise identical to the  $\text{GDP}\cdot\text{AlF}_4^-$  complex (both diagrams adapted from (Coleman et al., 1994).

Figure 5.36

A)



B)



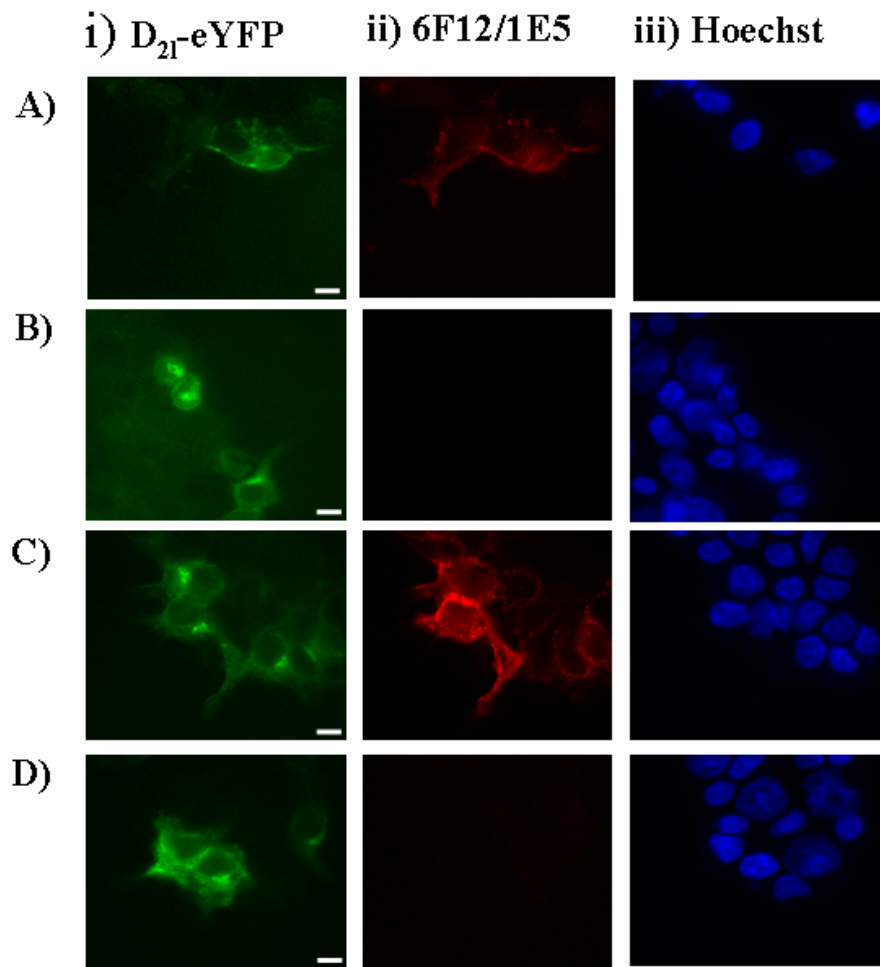
**Figure 5.37: The conformation-selective antibody 6F12/1E5 recognises the complex  $G\alpha_{i2}.GDP.AIF_4^-$**

HEK293T cells were grown on poly-D-lysine coated coverslips. These cells were co-transfected with cDNA of the D<sub>21</sub>-YFP fusion protein and either wild type  $G\alpha_{i2}$  (**A** and **B**), or the active variant Gln<sup>205</sup>Leu  $G\alpha_{i2}$  (**C**). As a control HEK293T cells were co-transfected with cDNA of the D<sub>21</sub>-YFP fusion protein and pcDNA3 (**D**). Cells transfected with cDNA of wild type  $G\alpha_{i2}$  were incubated with (**A**) or without (**B**) the addition of  $AIF_4^-$  (10  $\mu$ M  $AlCl_3$  + 10 mM NaF). Immunocytochemistry was performed as in section 2.10.5.

Nuclear staining was performed using Hoescht stain. The conformation selective antibody 6F12/1E5 was used at a final dilution of 1:200. The fluorescently labelled secondary antibody anti-mouse Alexa Fluor 594 was used at a final concentration of 1:400.

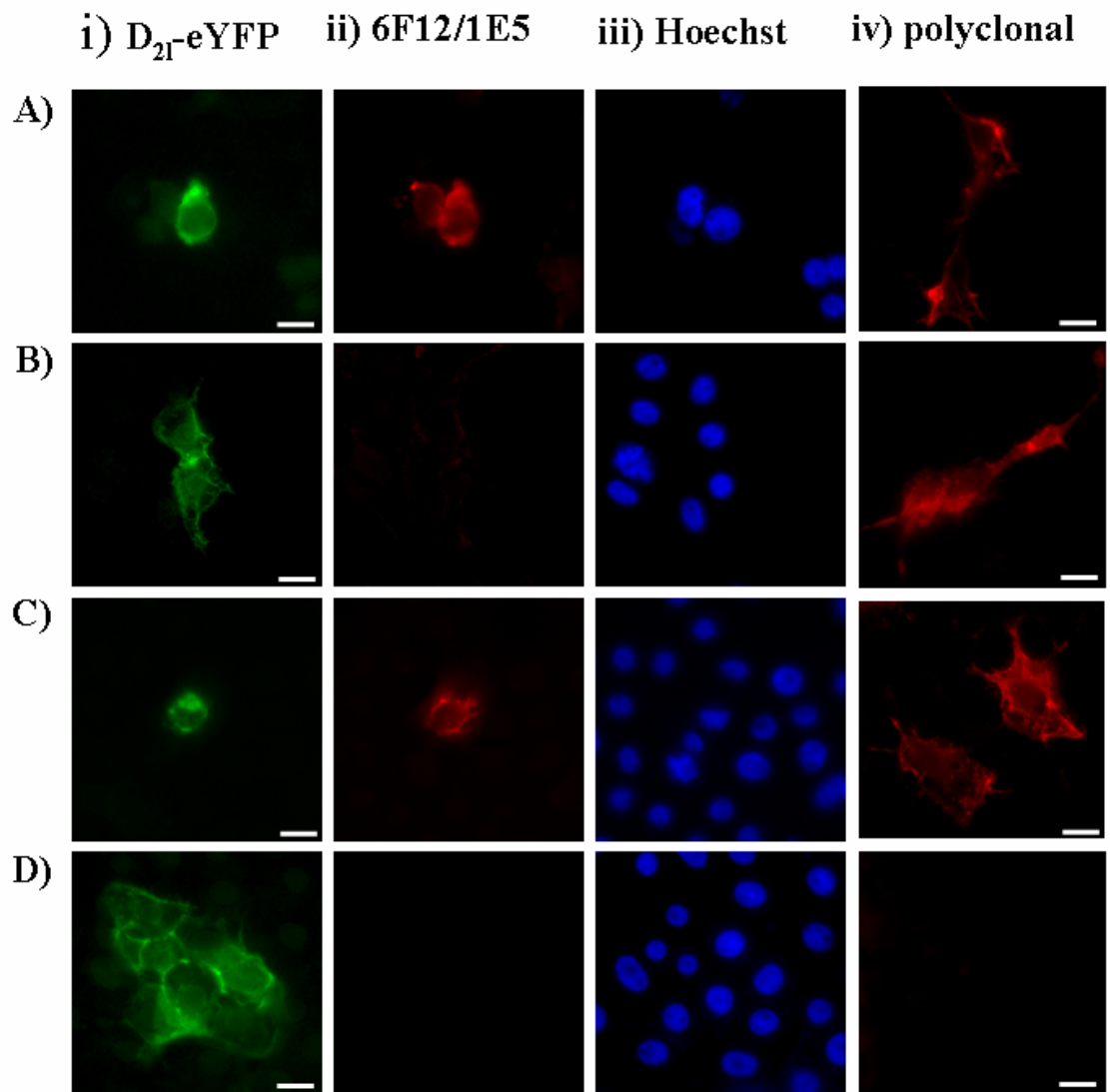
Fluorescence detected from (i) D21-YFP, (ii) Alexa Fluor 594 bound to 6F12/1E5, (iii) Hoescht stain are shown. Scale marker represents 10  $\mu$ M.

**Figure 5.37**



**Figure 5.38: The conformation-selective antibody 6F12/1E5 recognises the agonist induced complex  $G\alpha_{i2}.GTP\gamma S$**

HEK293T cells were grown on poly-D-lysine coated coverslips. These cells were co-transfected with cDNA of the D<sub>21</sub>-YFP fusion protein and either wild type  $G\alpha_{i1}$  (**A** and **B**), or the active variant Gln<sup>205</sup>Leu  $G\alpha_{i1}$  (**C**). As a control HEK293T cells were co-transfected with cDNA of the D<sub>21</sub>-YFP fusion protein and pcDNA3 (**D**). Cells transfected with cDNA of wild type  $G\alpha_{i1}$  were incubated with (**A**) or without (**B**) the addition of dopamine D<sub>2</sub> receptor agonist nor-apomorphine (1  $\mu$ M). Immunocytochemistry was performed as in section 2.5.10. Nuclear staining was performed using Hoescht stain. The conformation selective antibody 6F12/1E5 was used at a final dilution of 1:200. The fluorescently labelled secondary antibody anti-mouse Alexa Fluor 594 was used at a final concentration of 1:400. Fluorescence detected from (**i**) D21-YFP, (**ii**) Alexa Fluor 594 bound to 6F12/1E5, (**iii**) Hoescht stain are shown. To demonstrate expression of transfected  $G\alpha$  protein a parallel immunocytochemistry experiment was performed using rabbit polyclonal anti-peptide antiserum against the C-terminal decapeptide sequence of  $G\alpha_{i1/2}$  (**iv**). Scale marker represents 10  $\mu$ M.

**Figure 5.38**

### 5.3 Discussion

Characterisation of antisera raised against the C-terminal ten amino acids of  $G\alpha_t$ ,  $G\alpha_q$  and  $G\alpha_s$  revealed the successful generation of antisera selective for each G-protein  $\alpha$  subunit. Indeed, the antisera characterised in this study compared favourably with antisera for  $G\alpha_{i1/2}$ ,  $G\alpha_q$  and  $G\alpha_s$  previously generated in-house against the same decapeptide antigens (Milligan, 1994). The selectivity of each antiserum towards the G protein  $\alpha$  subunit against which it was raised was demonstrated using Western blotting. To achieve this, the relevant G protein  $\alpha$  subunit was expressed in an essentially null background for the G protein  $\alpha$  subunit of interest. As demonstrated in previous work, expression of  $G\alpha_{i1}$ ,  $G\alpha_{i2}$ , and  $G\alpha_{i3}$ , and  $G\alpha_{o1}$  in *E coli* allowed the characterisation of antisera raised against the C-terminal tail of  $G\alpha_t$  (Milligan, 1994). Three out of four antisera eluates tested showed selectivity towards  $G\alpha_{i1/2}$  but not  $G\alpha_{i3}$  or  $G\alpha_{o1}$ . The C-terminal ten amino acids of  $G\alpha_t$ ,  $G\alpha_{i1}$  and  $G\alpha_{i2}$  differ only by one amino acid change whereas the sequences of the equivalent regions of  $G\alpha_{i3}$  and  $G\alpha_{o1}$  differ from that of  $G\alpha_t$  by two and four amino acid residues respectively. This would indicate that the substitution of these amino acids has a significant effect on the structure of the decapeptide. As discussed in section 5.1, the C-terminal of G protein  $\alpha$  subunits has been implicated as an important region for the selective interaction with receptors (Slessareva et al., 2003; Wess, 1998). It is possible then that the selectivity demonstrated by the antisera towards  $G\alpha_{i1/2}$  and not  $G\alpha_{i3}$  or  $G\alpha_{o1}$  is due to the same difference in structure of the ten C-terminal amino acids that forms the basis of receptor-G protein selectivity as demonstrated for dopamine  $D_2$ -like receptors in chapter 4. Conversely, however, in the case of the dopamine  $D_3$  selectivity towards the  $G\alpha_{o1}$  subunit over other members of the  $G\alpha_{i/o}$  family was observed. Furthermore, whilst Slessareva et al identified the C-terminal of  $G\alpha$  subunits as being an important region for

receptor coupling specificity, it was observed that different receptors interacted with different amino acids within this region (Slessareva et al., 2003). Interestingly one antiserum eluate raised against the decapeptide corresponding to the C-terminal ten amino acids of  $G\alpha_t$  recognised  $G\alpha_{i1}$ ,  $G\alpha_{i2}$ ,  $G\alpha_{i3}$  and  $G\alpha_{o1}$ . This suggests that within the structure of peptides corresponding to the C-terminal tail of these  $G\alpha$  subunits there must be elements which are conserved, and that these are the structural elements forming the epitope for this antiserum. It is tempting to speculate that these conserved structural elements are those recognised by more promiscuous receptors, for example  $D_{21}$  which interacts functionally with all members of the  $G\alpha_{i/o}$  family (**Chapter 3**).

The expression of  $G\alpha_q$  in the  $G\alpha_{q/11}$  null EF88 cell line demonstrated the selectivity of antisera raised against the C-terminal ten amino acids of  $G\alpha_q$ . Prolonged treatment of HEK293T cells with cholera toxin to knockdown levels of endogenous  $G\alpha_s$  allowed the characterisation of antisera raised against the C-terminal of  $G\alpha_s$ . This characterisation revealed antisera which are selective against  $G\alpha_s$ . The use of antisera raised against the C-terminal ten amino acids in a [ $^{35}$ S] GTP $\gamma$ S assay with an immunoprecipitation step has been well documented (Milligan, 2003). This immunocapture step allows the [ $^{35}$ S] GTP $\gamma$ S bound G protein  $\alpha$  subunit of interest to be isolated and enriched, improving the signal window between basal and agonist stimulated conditions. All antisera generated for this project against  $G\alpha$  subunit C-terminal decapeptides showed a similar efficiency in the immunoprecipitation of the [ $^{35}$ S] GTP $\gamma$ S bound form of the relevant G  $\alpha$  subunit in comparison to previously-characterised in-house antisera. The majority of published reports using a [ $^{35}$ S]GTP $\gamma$ S assay with immunocapture step have used heterologous cell systems. However, this approach has been usefully applied to membranes from native tissues. Indeed, this approach has been used in hippocampal and cortical membranes from wild-type mice and both muscarinic  $M_1$  and  $M_3$  acetylcholine receptor knockout mice to demonstrate the predominant role of the  $M_1$  receptor in these locations and to explore the

extent of  $M_1$  receptor reserve (Porter et al., 2002). As described in chapters 3 and 4, many receptors can couple to multiple G protein  $\alpha$  subunit subtypes. [ $^{35}\text{S}$ ] GTP $\gamma$ S binding with an immunocapture step could be a suitable assay with which to investigate receptor-G protein coupling specificity. By performing a [ $^{35}\text{S}$ ] GTP $\gamma$ S assay including pulldown of different G protein  $\alpha$  subunits, this would allow analysis of the agonist stimulation over basal observed for each. This could allow dissection of the G-protein coupling specificity for each receptor. However, this method could lead to potentially erroneous conclusions. Consideration must be given towards the variation of relative efficiencies of immunoprecipitation between different antisera. For example using this method, it was shown that the muscarinic  $M_3$  receptor activates  $G\alpha_{i1}$  and  $G\alpha_{q/11}$ , with comparable signal seen for each G protein  $\alpha$  subunit. However, there is a widespread appreciation that the  $M_3$  receptor couples preferentially to  $G\alpha_q$ , so the above result is unlikely to reflect effective selection of both these GPCRs (Akam et al., 2001; Milligan, 2003). The titre of antisera used in an immunocapture step is likely to be high. My results demonstrated cross reactivity of antisera with G protein  $\alpha$  subunits other than the ones which they were raised against, namely, an antisera raised against the C-terminal tail of  $G\alpha_{o1}$  showed cross reactivity with  $G\alpha_{i3}$ . Conclusions about receptor-G protein selectivity, especially between G-proteins of high sequence homology reached when using this methodology should be viewed with caution. Antisera raised against the C-terminal tail of  $G\alpha$  subunits have been used to investigate receptor-G protein coupling specificity (Milligan, 1994; Newman-Tancredi et al., 1999; Newman-Tancredi et al., 2002). Due to the importance of the C-terminal region of  $G\alpha$  subunits for receptor coupling, antisera raised against this region are able to functionally un-couple the receptor and a specific G protein. Indeed, experiments using antisera raised against  $G\alpha_{i/o}$  and  $G\alpha_{q/11}$  in this manner, showed selective coupling of  $D_{21}$  receptors to  $G\alpha_{i/o}$ , and coupling of  $D_3$  to  $G\alpha_{i/o}$  and to a lesser extent  $G\alpha_{q/11}$  (Newman-Tancredi et al., 1999). However, as with the immunocapture assay, the relative affinity of different antisera for the relevant G protein and their cross reactivity at high titres are both

potential caveats of this approach. The polyclonal anti-G $\alpha_{i1/2}$  antiserum raised against the C-terminal ten amino acids of G $\alpha_t$  (1319 glycine) has been used throughout this chapter and in both **chapters 3 and 4**.

Assays using radiolabelled markers, such as [ $^{35}\text{S}$ ] GTP $\gamma$ S binding to measure nucleotide exchange or [ $\gamma$ - $^{32}\text{P}$ ]GTP to measure GTPase activity have been used extensively to measure receptor mediated G protein activation (Milligan, 2003; Ward and Milligan, 2005). However, the expense associated with the use of radiolabelled markers, especially in an industrial setting makes these approaches increasingly unattractive. Other approaches such as monitoring calcium mobilisation or intracellular cAMP levels have been utilised in high-throughput screening assays (Wise et al., 2002). However, guanine nucleotide exchange is a very early event in the signal transduction cascade, and is an attractive event to monitor because it is less subject to amplification or regulation by other cellular processes than the more distal events described above. It can thus provide excellent measures of the basic pharmacological characteristics and the relative efficacy of a series of compounds at a GPCR that might often be compromised when using reporter gene analyses, for example. The premise of this study then, was to develop an alternative non-radioactive assay equivalent to the [ $^{35}\text{S}$ ] GTP $\gamma$ S assay. The approach used in this study was the generation of antibodies that selectively recognise the active (GTP bound conformation) of G  $\alpha$  subunits. Accordingly, an immunisation programme was initiated in which recombinant G $\alpha_{i1}$  was loaded with GTP $\gamma$ S and used to immunise mice. Antibody producing plasma cells from these animals were used to generate hybridomas. 1824 hybridoma clones were generated and screened. Initial screens employed FMAT technology to identify clones with the appropriate characteristics. From these screens three hybridoma clones were identified that produce antibodies with the desired selective recognition of the active (GTP bound) form of G $\alpha_{i1}$ . All three hybridoma clones produced antibody which showed a higher signal for conditions in which HEK293T cells expressing

wild type  $G\alpha_{i1}$  had been preloaded with  $GTP\gamma S$  (and therefore in the activated conformation) than was seen for the same cells preloaded with  $GDP\beta S$ . Furthermore, all three antibodies displayed marked selectivity for the condition in which HEK293T cells were transfected with the constitutively active  $Gln^{204}Leu G\alpha_{i1}$  mutant which mimics the active state. Subsequent FMAT experiments using purified antibodies confirmed these results. Furthermore, all three antibodies failed to interact significantly with the constitutively inactive  $Gly^{203}Ala G\alpha_{i1}$ , a mutant that is unable to exchange guanine nucleotide and therefore unable to adopt the active state. To confirm the selectivity of these three antibodies for activated  $G\alpha_{i1}$  a series of immunocytochemistry-based experiments was performed. Again, all three antibodies showed selectivity towards the active  $Gln^{204}Leu G\alpha_{i1}$  variant and showed little interaction with the inactive  $Gly^{203}Ala G\alpha_{i1}$  variant. Furthermore, the antibodies showed no interaction with wild type  $G\alpha_{i1}$  in an unstimulated condition. Without receptor mediated stimulation the majority of expressed  $G\alpha_{i1}$  will be in the inactive, GDP bound conformation. The large difference in signal observed for this condition and that of the active  $Gln^{204}Leu G\alpha_{i1}$  is significant since it demonstrates the apparent high selectivity of the antibodies for the GTP bound versus GDP bound conformation. This high selectivity makes them potentially useful reagents to form the basis of an assay to monitor receptor mediated G protein activation.

In an effort to characterise these antibodies further, Western blots were performed on lysates of *E coli* transformed to express the  $\alpha$  subunits of  $G\alpha_{i1}$ ,  $G\alpha_{i2}$ ,  $G\alpha_{i3}$  and  $G\alpha_{o1}$ . Perhaps unsurprisingly, these conformational selective antibodies were unable to recognise denatured protein. The majority of hybridoma generated by the immunisation programme, when screened using the FMAT assay, produced antibody selective towards conditions in which  $G\alpha_{i1}$  was expressed, but showed no selectivity between the activated and inactive conformation of  $G\alpha_{i1}$ . Two of these antibodies were also characterised in Western blots and showed selectivity towards the  $G\alpha_{i1}$  over the other  $G\alpha_{i/o}$  subunits. Given the high

sequence homology of  $G\alpha_{i1}$  with  $G\alpha_{i2}$  and  $G\alpha_{i3}$  (88% and 94% respectively, see **Figure 5.1**) this indicates that the epitope recognised by these antibodies is within regions of relative dissimilarity between these three G protein  $\alpha$  subunits. Efforts to determine the epitope recognised by the conformation selective antibodies using an overlapping set of peptides corresponding to the sequence of  $G\alpha_{i1}$  were unsuccessful. This again is not surprising given the conformation dependent nature of their selectivity. It is likely that the epitope recognised is three dimensional and could include residues from disparate regions of the amino acid sequence.

Without knowledge of the epitope recognised by the three conformational selective antibodies the information they can give about the conformational changes associated with the activation of  $G\alpha_{i1}$  is limited. The structures of both the inactive (GDP bound) and active (GTP bound) conformations of  $G\alpha_{i1}$  have been elucidated and this has provided information concerning the conformational changes occurring upon nucleotide exchange and, indeed, the mechanism of GTP hydrolysis (Coleman and Sprang, 1998; Kleuss et al., 1994; Mixon et al., 1995; Wall et al., 1998). Upon GTP hydrolysis switch I and switch II segments become disordered and linker II connecting the Ras and alpha helical domains moves, altering the structures of potential effector and beta gamma binding regions.

Contacts between the alpha helical and Ras domains are weakened, possibly facilitating the release of guanosine diphosphate (GDP). The amino and carboxyl termini, which contain receptor and beta gamma binding determinants, are disordered in the complex with GTP, but are organised into a compact microdomain on GTP hydrolysis (Mixon et al., 1995).

This work highlighted the importance of the residues Arg<sup>178</sup> and Gln<sup>204</sup> for stabilisation of the transition state reached during GTP hydrolysis. It is significant that the three antisera showed selectivity towards the constitutively active variant Gln<sup>204</sup>Leu. This indicates that the structure of this active mutant must be analogous to that of the active (GTP $\gamma$ S bound) form of  $G\alpha_{i1}$ . A functional study that found that an equivalent mutation in  $G\alpha_t$  (Gln<sup>200</sup>Leu)

exhibited compromised GTPase activity, but instead of simply being locked in a GTP bound state 35-45% of the protein was in a GDP-Pi bound state (Majumdar et al., 2006). It was concluded that the mutation reveals G $\alpha$  subunit states that occur subsequent to GTP hydrolysis but are still capable of fully stimulating effector activity. It could be extrapolated then that the structure of this Gln<sup>204</sup>Leu mutant has a structure highly similar to that of the GTP bound form. This is confirmed by the results from the antibody studies in this chapter. Consequently, despite the limitations of not knowing their epitope, the three antibodies can give useful information concerning the conformation of G $\alpha_{i1}$ . Similarly, the mutation of residue Gly<sup>203</sup> to an Ala has been shown to prevent nucleotide exchange thus this variant is unable to adopt the active state (Mixon et al., 1995). The lack of interaction of the three conformation selective antibodies with this mutant is consistent with this observation.

Alterations in the conformation of G $\alpha$  subunits associated with their activation and the concomitant exchange of GDP for GTP have been detected previously by the incorporation of fluorescence resonance energy competent transfer sensors into the  $\alpha$  subunit and the  $\beta\gamma$  complex (Frank et al., 2005). However, this approach requires substantial modifications to the polypeptides. Use of the conformation selective antibodies generated in this study allow study on the native G $\alpha$  subunit and consequently has a significant advantage over the FRET approach. Various residues have been identified as important in the G protein both for the mechanism of receptor catalysed activation of heterotrimeric G proteins and as described above the mechanism of GTP hydrolysis. It would be interesting to see if the conformational selective antibodies show affinity for these various mutants. An obvious example was the Arg<sup>178</sup>Cys variant, which has, like the Gln<sup>204</sup>Leu mutation, been shown to produce a constitutively active state (Majumdar et al., 2006). Indeed, as for the Gln<sup>204</sup>Leu mutation it has been hypothesised that the Arg<sup>178</sup>Cys mutation stabilises a conformational state subsequent to GTP hydrolysis with a structure that still allows full stimulation of

effector activity. However, work described in this chapter suggests that the conformation selective antibodies do not interact with this mutant, suggesting that its structure is significantly different from that of the Gln<sup>204</sup>Leu mutant. This may relate to the different roles of these arginine and glutamine residues in the mechanism of GTP hydrolysis. Gln<sup>204</sup> stabilises and orients the hydrolytic water in the trigonal-bipyrimidal transition state (**Figure 5.38**) Arg<sup>178</sup> stabilises the negative charge at the equatorial oxygen atoms of the pentacoordinate  $\gamma$  phosphate intermediate (Coleman et al., 1994). A recent study identified amino acids involved in the binding of GRK2 with a mutagenesis strategy in a background of three different activated forms  $G\alpha_q$ . Interestingly it was shown that the  $G\alpha_q$  mutations had different phenotypes depending on which activated background was used,  $AlF_4^-$ , Gln<sup>209</sup>Leu or Arg<sup>183</sup>Cys. This is consistent with the Gln<sup>209</sup>Leu and Arg<sup>183</sup>Cys having a different structure (Day et al., 2004).

Similarly, mutation of Gly<sup>42</sup> to a Val diminishes the GTPase activity of  $G\alpha_{i1}$  due to the steric bulk of Val pushing Gln<sup>204</sup> into a catalytically incompetent conformation (Raw et al., 1997). Again, it would be interesting to see if the antibodies have a high affinity for this constitutively active variant.

In a similar vein, use of the above mutants or wild type  $G\alpha_{i1}$  complexed with various non-hydrolysable analogues of GTP has allowed the elucidation of structures thought to be snapshots of transition states involved in GTP hydrolysis (Berghuis et al., 1996; Raw et al., 1997). For example the Gly<sup>203</sup>Ala  $G\alpha_{i1}$  mutant complexed with GTP $\gamma$ S was thought to give a structure that was hypothesised to be similar, but not identical to the transient ternary complex of  $G\alpha_{i1}$  catalysed GTP hydrolysis (Berghuis et al., 1996). It would be interesting to probe this structure with the conformation selective antibodies.

A key experiment was to test these antibodies in a condition in which  $\text{AlF}_4^-$  was added to cells expressing a wild type GDP-bound G protein.  $\text{AlF}_4^-$  is a substitute for, and can mimic the  $\gamma$  phosphate of GTP, promoting an active conformation. However it was argued that, the geometry and coordination of the  $\text{GDP}.\text{AlF}_4^-$  complex, the structural changes within the catalytic site and the guanine nucleotide exchange kinetics indicate that  $\text{GDP}.\text{AlF}_4^-$  is not a GTP analogue but rather mimics the trigonal-bipyrimidal species presumed to appear at or near the transition state of the GTP hydrolysis reaction (Coleman et al., 1994). Our results showed that the antibodies recognised the complex  $\text{G}\alpha_{i1}.\text{GDP}.\text{AlF}_4^-$ , confirming that this complex has a conformation equivalent or highly similar to the active GTP bound conformation of  $\text{G}\alpha_{i1}$ . In conclusion then, the conformation selective antibodies could be a useful tool in determining changes in  $\text{G}\alpha_{i1}$  structure associated with nucleotide exchange and GTP hydrolysis. Furthermore, A variety of human tumors have been associated with mutations of either the switch II glutamine (corresponding to  $\text{G}\alpha_{i1} \text{Q}^{204}$ ) or the arginine finger (corresponding to  $\text{G}\alpha_{i1} \text{R}^{178}$ ) both in  $\text{G}\alpha_i$  and  $\text{G}\alpha_s$  (Bourne, 1987; Landis et al., 1989; Weinstein and Shenker, 1993). It follows then, that these conformation selective antibodies could be useful in the screening of potentially cancerous tissue for these mutations.

The characterisation of the conformation selective antibodies was further investigated with regard to their selectivity towards the active (GTP bound) conformations of other  $\text{G}\alpha$  subunits. Specific binding was also observed for the  $\text{Gln}\rightarrow\text{Leu}$  active mutants of  $\text{G}\alpha_{i2}$  and  $\text{G}\alpha_{o1}$ . However, the antibodies showed affinity for neither the equivalent wild type  $\text{G}\alpha$  subunits when expressed in an un-stimulated condition or the equivalent  $\text{Gly}\rightarrow\text{Ala}$  constitutively inactive mutants. Furthermore, the antibodies did not recognise equivalent active mutants of  $\text{G}\alpha_q$  and  $\text{G}\alpha_s$ . Considering the high sequence homology of  $\text{G}\alpha_{i1}$ ,  $\text{G}\alpha_{i2}$ ,  $\text{G}\alpha_{i3}$  and  $\text{G}\alpha_{o1}$  (**Figure 5.1**) it could be expected that they have a similar overall structure. It could be expected, therefore, that the conformation selective antibodies would recognise

the active structures of all  $G\alpha_{i/o}$  family  $\alpha$  subunits. The sequence homology of  $G\alpha_{i1}$  with  $G\alpha_q$  and  $G\alpha_s$  is considerably lower (44% and 55% respectively). Consequently it is less likely that these conformation selective antibodies would recognise the active conformations of these  $G\alpha$  subunits, since the structure of these  $G\alpha$  subunits is likely to be significantly different from that of  $G\alpha_{i1}$ .

A key role of RGS (Regulators of G protein Signalling) proteins is binding to the G-protein  $G\alpha$ -subunit and acting as GTPase-activating proteins (GAPs), thereby rapidly terminating G protein-coupled receptor (GPCR) signalling. In 1997, Tesmer and colleagues reported a 2.8 Å resolution crystal structure of the RGS protein, RGS4, complexed with  $G\alpha_{i1}$ - $Mg^{2+}$ -GDP- $AlF_4^-$  (Tesmer et al., 1997a). As described above this complex the  $GDP.AlF_4^-$  mimics the transition state of GTP during its hydrolysis to GDP, inducing the conformation of  $G\alpha_{i1}$  thought to be stabilized by RGS-binding. The contacts of RGS4 with  $G\alpha_{i1}$  on the surface of  $G\alpha_{i1}$  are formed by residues in the three Switch regions of  $G\alpha_{i1}$ : residues 179–185 in Switch I, residues 204–213 in Switch II, and residues 235–237 in Switch III. Of these regions, Switch I of  $G\alpha_{i1}$  interacts with three-fourths of the RGS4-binding pocket. Two surface residues of Switch I (Thr<sup>182</sup> and Gly<sup>183</sup>) appear to be essential for high-affinity  $G\alpha$ -RGS interaction (Fu et al., 2004; Tesmer et al., 1997a). Peptides corresponding to this region have been shown to inhibit RGS function (Roof et al., 2006). Since the conformation-selective antibodies also recognize the  $G\alpha_{i1}.GDP.AlF_4^-$  complex it would be interesting to see if these antibodies recognise a similar region to RGS4. As for early experiments using antisera raised against the C-terminal tail of  $G\alpha$  subunits to ablate the functional interaction between receptor and G protein, the conformation-selective antibodies could block the action of RGS proteins. This would not only give information about the epitope that is recognised by the antibodies, but highlights further possibilities of their use.

The ultimate aim of this study was the production of reagents suitable for, and the design of, a high throughput assay to monitor receptor mediated G protein activation. To this end then, the most important experiment was a demonstration of whether the antibodies could recognise agonist-induced receptor-mediated activation of G  $\alpha$  subunits. The design of the immunocytochemistry-based experiments described in this chapter provided a good basis for this experiment. The co-transfection of cDNA of wild type G $\alpha_{i1}$  with the D<sub>21</sub>-eYFP fusion protein allowed easy identification of successfully transfected cells. These transfected cells were exposed to the dopaminergic agonist nor-apomorphine in the presence of 10  $\mu$ M GTP $\gamma$ S to lock activated G $\alpha_{i1}$  in the active conformation. D<sub>21</sub> couples to G $\alpha_{i1}$ , G $\alpha_{i2}$ , G $\alpha_{i3}$  and G $\alpha_{o1}$  and has a wide and well characterised pharmacology, making it ideal for these preliminary experiments. In these conditions the conformation-selective antibodies identified G $\alpha_{i2}$  only in samples stimulated by agonist. These data indicate that the conformation selective antibodies described herein may be useful reagents with which to develop a non-radioactive assay for G protein activation by agonist ligands. However, an obvious extension to this experiment would be to include a condition in which the action of nor-apomorphine is blocked using a D<sub>21</sub> antagonist or inverse agonist such as spiperone. This would be a further demonstration that these antibodies would indeed be useful pharmacological tools.

In two different studies, antibodies sensitive to the different conformation of GPCRs have been developed (Gupta et al., 2007; Mancina et al., 2007). In the first study antibodies directed against the mid portion of the N-terminus were shown to have enhanced recognition of active state receptors (Gupta et al., 2007). This technique was applied to G $\alpha_i$ -coupled,  $\mu$ -opioid,  $\delta$ -opioid, CB1 cannabinoid,  $\alpha_{2A}$ -adrenergic as well as G $\alpha_s$ -( $\beta_2$ -adrenergic) and G $\alpha_q$ -coupled (AT1 angiotensin) receptors. It was shown that these antibodies accurately differentiate ligands with varying efficacies and can be used to

investigate the extent and duration of activation of endogenous receptors. Indeed, it was found that peripheral morphine administration led to a time-dependent increase in antibody binding in the striatum and prefrontal cortex with a peak at about 30 min. This study then demonstrates the utility of conformation selective antibodies for the monitoring of receptor pharmacology. Similarly conformation selective antibodies against the 5-HT<sub>2C</sub> serotonin receptor were generated using a hybridoma generation strategy similar to the one described in this chapter. Monoclonal antibodies specific to 5-HT<sub>2c</sub> were generated by immunising mice with 5-HT<sub>2c</sub> expressed and purified in *E coli*. As in this study, antibodies of various specificities were generated including two that are specific to the 5-HT (agonist) bound form as compared to the ketanserin (inverse agonist) bound form.

However, the above studies would require a different antibody for each receptor. Since there are only 16 known G protein  $\alpha$  subunits, antibodies recognising the active conformation of G protein  $\alpha$  subunits could be used to study the interaction between numerous GPCRs and one G protein. This makes them a more powerful and useful tool. Indeed, the fact that the antibodies characterised in this assay recognise the active form of all members of the G $\alpha_{i1}$  family make them an even more versatile tool. It would, therefore, be interesting to examine if the antibodies selective for the active conformation of G $\alpha_{i1}$  could be used to investigate the extent and duration of activation of endogenous G proteins.

## 6 General discussion

Receptor efficacy, that is how strongly a ligand activates a receptor, was thought to be independent of the system used and the response measured. However, this concept has been challenged by the recognition of inverse agonists – compounds with negative efficacy – and the recognition that distinct signalling pathways mediated by the same receptor do not show the same pattern of agonist dependence (Perez and Karnik, 2005; Urban et al., 2006a). This second observation has been given various names such as protean agonism or agonist directed trafficking of receptor stimulus. The possibility that agonists could selectively activate different G proteins was one possible explanation for this phenomenon, although evidence for this hypothesis was indirect (Berg et al., 1998). In the present study I investigated the activation of different members of the  $G\alpha_{i/o}$  family by different agonists at the dopamine  $D_{21}$  receptor. The majority of  $D_2$  agonists tested activated all  $G\alpha_{i/o}$  subunits, although as a general pattern most agonists tended to activate  $G\alpha_{o1}$  better than  $G\alpha_{i1-3}$ . However, S-(-)-3PPP and p-tyramine were only able to activate  $G\alpha_{o1}$ . Subsequent experiments using both [ $^{35}$ S] GTP $\gamma$ S binding and the monitoring of high affinity agonist binding showed that in contrast to its action as an agonist at  $G\alpha_{o1}$ , S-(-)-3PPP was an inverse agonist/antagonist at  $G\alpha_{i1}$ ,  $G\alpha_{i2}$ ,  $G\alpha_{i3}$ . This clearly establishes S-(-)-3PPP as a protean agonist. The use of receptor-G protein fusion proteins ensured that the ratio of receptor to G protein was constant and that the receptor and G protein had the same cellular localisation. This study then provides direct evidence that different agonists at the same receptor can induce differential G protein coupling. S-(-)-3PPP was shown to have differential effects on pre- and post-synaptic functions *in vivo* (Arnt et al., 1983). However, in 1983, the existence of five different dopamine receptor subtypes was not yet known, so a repetition of this work with receptor knock out models and/or improved pharmacological agents would be worthwhile. The antibodies generated and characterised

in chapter 5, which are selective against the active conformation of  $G\alpha_{i/o}$  would perhaps be useful tools to visualise pre- and postsynaptic  $G\alpha_{i/o}$  activation. Furthermore distinct effector mechanisms have been proposed for  $G\alpha_i$  and  $G\alpha_o$  signalling, with inhibition of voltage gated  $Ca^{2+}$  and activation of GIRK channels respectively (Sowell et al., 1997; Valenzuela et al., 1997). It would be interesting therefore, to investigate the action of S-(-)-3PPP by physiological studies in a  $D_2$  regulated neuronal system. Aripiprazole, an atypical antipsychotic, has been shown to display a pattern of differential efficacy through  $D_2$  mediated signalling pathways, that is startlingly similar to that of S-(-)-3PPP. As for S-(-)-3PPP, aripiprazole has been shown to have partial agonist and antagonist activity functions at the  $D_2$  receptor depending on the end point studied (Urban et al., 2006b). Furthermore, this drug has also been shown to be an antagonist at the post-synaptic principal and an agonist at pre-synaptic densities (Kikuchi et al., 1995). This suggests that functionally selective ligands or protean agonists may provide a new area for the development of novel therapeutics for psychoses and other disorders. However, the actions of aripiprazole have been proposed to originate solely from its partial agonist properties, and indeed other partial agonists at the dopamine  $D_2$  receptor such as bifeprunox and, interestingly, the principle metabolite of clozapine - N-desmethyl-clozapine - have been shown to have antipsychotic properties (Lieberman, 2004; Millan et al., 2007). Consequently it would be interesting to conduct an equivalent study to the one performed in chapter 3 using aripiprazole and these other  $D_2$  partial agonists.

The demonstration of S-(-)-3PPP as a protean agonist conforms with a growing body of evidence that the efficacy of a ligand at one receptor and for one signalling pathway cannot be extrapolated to other signalling pathways at the same receptor. Drug screening programmes often use heterologous expression systems to monitor the action of ligands at a certain receptor with the expectation that the efficacy detected in this system is consistent

with that observed *in vivo*. However, as shown by the actions of S-(-)-3PPP at the D<sub>21</sub> receptor, efficacy can be pathway, and therefore cell or tissue specific.

The study comparing the coupling specificities of the D<sub>2</sub> and D<sub>3</sub> receptors showed that whilst the D<sub>2</sub> receptor could promiscuously couple to G $\alpha_{i1}$ , G $\alpha_{i2}$ , G $\alpha_{i3}$  and G $\alpha_{o1}$ , the D<sub>3</sub> receptor coupled only to G $\alpha_{o1}$ . Furthermore, the exchange of a twelve amino acid section at the c-terminus of the third intracellular loop of the D<sub>3</sub> receptor with an equivalent region of the D<sub>2</sub> receptor gave a chimeric D<sub>3</sub>/D<sub>2</sub> receptor that gained a D<sub>2</sub>-like ability to couple to all four G $\alpha_{i/o}$  subunits. However, the order of potency observed for dopamine at the D<sub>2</sub> and chimeric D<sub>3/2</sub> receptor coupled to the different G $\alpha$  subunits was distinct. At the D<sub>2</sub> receptor the order of potency was as follows G $\alpha_{o1}$  > G $\alpha_{i1}$   $\geq$  G $\alpha_{i3}$  = G $\alpha_{i2}$  whereas for the chimeric D<sub>3/2</sub> receptor the order was G $\alpha_{i3}$  = G $\alpha_{o1}$  > G $\alpha_{i2}$  = G $\alpha_{i1}$ . This difference suggests that other regions within D<sub>2</sub> are important for G protein coupling, particularly to G $\alpha_{i1}$  and G $\alpha_{i2}$ . There is evidence to suggest that this is the case, and the N-terminus of the third intracellular loop has been implicated as a particularly important region. A recent study by Nanoff et al. used a peptide derived from this region to activate both G $\alpha_{i1}$  and G $\alpha_{o1}$  directly (Nanoff et al., 2006). Similarly a previous study constructed reciprocal chimeric D<sub>2</sub>/D<sub>3</sub> receptors with fusion points near the center of the third intracellular loop. Both of the D<sub>2</sub>/D<sub>3</sub> receptor chimeras were able to effectively inhibit adenylate cyclase activity to almost the same extent as that seen with the D<sub>2</sub> receptor whereas the D<sub>3</sub> receptor was without effect (Lachowicz and Sibley, 1997). These results suggest that the D<sub>2</sub> receptor possesses two independent domains for G-protein coupling and inhibition of adenylate cyclase activity. A logical future experiment then would be to investigate other regions within the D<sub>2</sub> receptor that direct its coupling to G $\alpha_{i1}$ , G $\alpha_{i2}$  and G $\alpha_{i3}$  with particular focus on the N-terminal region of the second intracellular loop. It would also be of interest to attempt to define the residues within the twelve amino acid section of the third intracellular loop that are important for coupling to each of the G $\alpha_{i/o}$  subunits. Work by Slessareva et al.

demonstrated that multiple and distinct regions of both the receptor and the G protein can direct G protein coupling (Slessareva et al., 2003). Furthermore it was shown, for the receptors and G proteins investigated in their study, that although regions such as the c-terminus of the G protein are universally important for receptor G protein coupling the individual residues involved differed for each receptor-G protein pair. It would be interesting to perform a similar study with the D<sub>2</sub> and D<sub>3</sub> receptors as models.

From both the investigation into the coupling specificity of the D<sub>2</sub> and D<sub>3</sub> receptors, and the study of agonist-directed coupling at the D<sub>21</sub> receptor, it could be concluded that the G $\alpha_{o1}$  subunit is more promiscuous in its ability to couple to both dopamine receptor subtypes, in conformations stabilised by all agonists tested. An investigation into the molecular basis of this coupling specificity would be worthwhile. In both the agonist directed trafficking study and the investigation of the G protein coupling specificities of the D<sub>2</sub> and D<sub>3</sub> receptors I have described two models with which the molecular basis of G $\alpha_{o1}$  coupling could be explored. Firstly, G $\alpha_{o1}$  couples to the D<sub>21</sub> receptor even when this receptor is bound to S-(-)-3PPP. In contrast G $\alpha_{i1}$ , G $\alpha_{i2}$  and G $\alpha_{i3}$  do not. Consequently, a study using mutagenesis or chimeric G proteins, in which regions of G $\alpha_{o1}$  are exchanged with equivalent regions of G $\alpha_{i1}$ , G $\alpha_{i2}$  and G $\alpha_{i3}$  could lead to the identification of important regions within G $\alpha_{o1}$  and the other G $\alpha_i$  subunits which govern their coupling specificity. Similarly the promiscuous coupling of G $\alpha_{o1}$  to both D<sub>2</sub> and D<sub>3</sub> in comparison to the selective coupling of G $\alpha_{i1, 2, 3}$  to D<sub>2</sub> provides another model with which to investigate this coupling specificity. Again chimeric G proteins could be useful to define the molecular basis of this difference. A simple extension of this study could be the use of chimeric G $\alpha_i$ /G $\alpha_q$  subunits described by Kostenis and Milligan (Kostenis et al., 2005). Chimeric G proteins in which the C-terminal 5 amino acids of G $\alpha_q$  are replaced by those of G $\alpha_{i1/2}$  or G $\alpha_{o1}$  allow G $\alpha_i$  coupled receptors to couple to this chimeric G protein and hence activate PLC- $\beta$  (Kostenis et al., 1997). It could be predicted then that whilst D<sub>2</sub> could

couple to a chimeric G protein in which the last five amino acids of  $G\alpha_q$  had been replaced by  $G\alpha_{i1}$  or  $G\alpha_{o1}$ ,  $D_3$  would perhaps only couple to the  $G\alpha_q/G\alpha_{o1}$  chimera. Furthermore, this could determine whether replacement of this region would be sufficient for the coupling of  $D_3$  to  $G\alpha_{o1}$  or whether other regions of  $G\alpha_{o1}$  are also required.

It is worth mentioning that the two models described above differ by the mode in which receptor-G protein coupling is determined. The basis of agonist directed trafficking or protean agonism is that the different agonists stabilise different receptor conformations, which in turn differentially couple to downstream signalling pathways (Kenakin, 2001). Accordingly, for the model making use of differential coupling of the  $D_2$  receptor to  $G\alpha_{i/o}$  subunits the orientation or availability of regions within the receptor provides the basis of G protein coupling specificity. For example, ligands such as dopamine and NPA which promote the coupling of the  $D_2$  receptor to all four  $G\alpha_{i/o}$  subunits, must stabilise a conformation of the receptor in which regions of the receptor that are essential for the interactions between receptor and  $G\alpha_{i1,2}$  and  $G\alpha_{i3}$  to occur are available. However, S(-)-3PPP must stabilise a conformation in which these critical regions are obscured and so preventing coupling to  $G\alpha_{i1}$ ,  $G\alpha_{i2}$ , and  $G\alpha_{i3}$ . For coupling of the  $D_2$  receptor to  $G\alpha_{o1}$ , these regions must not be necessary, or can exist in various orientations. Biophysical studies akin to those performed by Ghanouni et al. could provide information about the different conformations of the receptor stabilised by an agonist such as NPA in comparison with the protean agonist S(-)-3PPP (Ghanouni et al., 2001; Swaminath et al., 2004). Kendall et al. demonstrated that the substitution of the entire insert region of the  $D_{2l}$  receptor with an equivalent length, yet non-homologous, protein sequence resulted in a receptor which was indistinguishable from the wild type receptor (Kendall and Senogles, 2006). It is likely that this region has an effect on the overall conformation of the receptor and is another example of how changing the conformation of a receptor can alter G protein coupling specificity. In contrast, the ability of  $D_2$  to couple to  $G\alpha_{i1, 2, 3}$  and  $G\alpha_{o1}$ , but  $D_3$  to only

couple to  $G\alpha_{o1}$  is most likely determined by regions within the  $D_2$  receptor that are not present in the  $D_3$  receptor. Studies using chimeric  $D_3$  receptors, which contain regions of  $D_2$ , and which gain a  $D_2$  like ability to couple to  $G\alpha_{i1}$ , 2 and 3 (this study) or downstream effectors support this theory (Filteau et al., 1999; Lachowicz and Sibley, 1997; Robinson and Caron, 1996; Robinson et al., 1994).

Receptor-G protein fusion proteins proved useful tools in both of the above investigations. Their use ensured a 1:1 ratio of receptor to G protein. Therefore, they allowed the analysis and comparison of both efficacy and potency of different ligands at the same receptor and the same ligand at different receptors. Furthermore, they eliminated factors such as receptor reserve which may hamper such investigations (Hildebrandt, 2006; Milligan et al., 2004). They also eliminate membrane compartmentalization as a reason why one particular G protein is activated and the other is not. A recent study demonstrating agonist directed trafficking at the thromboxane A2 receptor is a further example of their utility (Zhang et al., 2006) It is interesting to note the higher potency of dopamine observed at the  $D_{21}$  receptor in cell lines where  $G\alpha_{i2}$  or  $G\alpha_{o1}$  was expressed from the inducible Flp-In locus as compared to that observed for the equivalent  $D_2$ - $G\alpha$  subunit fusion proteins. This difference indicates the presence of receptor reserve. Both the dopamine receptor-G protein fusion proteins and the cell lines in which dopamine receptor is constitutively expressed and the expression of pertussis toxin resistant  $G\alpha$  subunits can be induced from the Flp-In locus could be useful tools to investigate this phenomenon. Performing agonist dose-response experiments in the presence of increasing concentrations of an irreversible  $D_2$  antagonist, such as N-(p-isothiocyanatophenethyl)piperone (NIPS), it could be expected that different results would be obtained for fusion proteins and the Flp-In stable cell line. In the case of the fusion protein I would expect a decrease in  $E_{max}$  but no change in potency with increasing concentrations of the irreversible inhibitor. However, for the Flp-In stable cell lines, where spare receptor is present I would expect a decrease in

potency but no change in  $E_{\max}$  with increasing concentrations of irreversible inhibitor until a ratio of G protein to receptor-not-bound-to-irreversible-inhibitor of 1:1 is reached and there is no longer spare receptor. After this point it could be expected that, as for the fusion protein, a decrease in  $E_{\max}$  but no change in potency with increasing concentrations of the irreversible inhibitor would be observed. In the characterisation of the Flp-In stable cell lines, it was shown that the amount of G protein expressed could be controlled by treating cells with variable amounts of tetracycline. It would be interesting then to monitor the effect that increasing amounts of G protein could have on the potency and efficacy of agonists at the constitutively expressed  $D_{21}$  receptor. For example, would an increase in G protein effectively cause a decrease in receptor reserve and therefore a decrease in potency?

The majority of agonists used in this study, including the endogenous ligand dopamine, showed a higher potency at the  $D_3$  receptor coupled to  $G\alpha_{o1}$  than the  $D_{21}$  receptor coupled to  $G\alpha_{o1}$ . There is increasingly strong evidence that the  $D_3$  receptor represents an attractive target for antipsychotic agents. It is interesting then, that S-(-)-3PPP, a prototypical antipsychotic drug has both a higher potency and efficacy at the  $D_3$  receptor. It follows then, that future studies using aripiprazole and other partial agonists should be extended to include their action at the  $D_3$  receptor.

In all species, the  $D_3$  receptor is generally less abundant than the  $D_2$  receptor but with a high concentration in the limbic region of the striatum, in a post-synaptic location. The  $D_3$  receptor is also thought to have a role as an autoreceptor and is expressed by dopaminergic neurons of the substantia nigra (Joyce and Millan, 2005). Furthermore, there is anatomical and functional evidence that dopamine  $D_2$  and  $D_3$  receptors are co-localized in specific populations of cerebral neurones, both post-synaptically and pre-synaptically (Joyce, 2001; Segal et al., 1997). The existence of  $D_2/D_3$  heterodimers has been demonstrated *in vitro*

(Maggio et al., 2003). It is likely that these heterodimers represent another target for therapeutic intervention. It would be worthwhile, to investigate the pharmacology and G protein coupling specificities of these hetero-oligomers, taking into account the differences in both the pharmacology and G protein coupling specificities of these two dopamine receptor subtypes. This could be investigated using functional complementation of two non-functional receptor-G protein fusion proteins. However, another approach would be to make use of the stable cell lines generated in this study in which pertussis toxin insensitive variant  $G\alpha$  subunits are expressed from the inducible Flp-In locus (**Figure 6.1A**). A single stable cell line could express both the  $D_2$  and  $D_3$  receptors, with tetracycline controlled expression of  $G\alpha$  subunit. Although the pharmacology of the  $D_2$  and  $D_3$  receptors are similar, both  $D_2$  and  $D_3$  selective agonists and antagonists have recently been described. For example, the selective  $D_3$  receptor antagonists SB277,011 and the exceptionally potent S33084 have been thoroughly characterized *in vitro* and *in vivo* (Joyce and Millan, 2005; Millan et al., 2000; Stemp et al., 2000). The use of S33084 and SB277,011, then, in parallel with the preferential  $D_2$  versus  $D_3$  receptor antagonists L741,626 and S23199, is currently the best approach for pharmacological identification of the roles of  $D_3$  versus  $D_2$  receptors in functional models (Chaperon et al., 2003; Millan et al., 2007). Using these  $D_3$  selective antagonists and agonists with the inducible cell lines described above the pharmacology and G protein coupling specificity of the  $D_2/D_3$  heterodimer could be dissected. Furthermore, these studies could be extended to experimental models in which either expression of the  $D_2$  or  $D_3$  receptor can be induced from the Flp-In locus and the other dopamine receptor subtype and a pertussis toxin insensitive mutant  $G\alpha_{i/o}$  subunit can be constitutively expressed (**Figure 6.1B**). Using this system the pharmacology and coupling specificity of the  $D_2/D_3$  heterodimer could easily be compared with that of  $D_2$  or  $D_3$  homodimers. Both of the above systems would have the added advantage of receptor and G proteins expressed as separate polypeptides, instead of the useful, but inherently artificial, receptor-G protein fusion proteins used in the

dimerscreen™ method. Two obvious questions to be answered in this study would be does the D<sub>2</sub>/D<sub>3</sub> heterodimer gain a D<sub>3</sub>-like high affinity (and therefore potency) for dopamine, and can this heterodimer couple to G $\alpha_{i1-3}$  and G $\alpha_{o1}$ ? It is perhaps of note that heterodimerisation has been shown to cause a switch in G protein coupling specificity whereupon a G $\alpha_{i/o}$  coupled GPCR (CB<sub>1</sub>) gains coupling to G $\alpha_s$  upon dimerisation with the dopamine D<sub>2</sub> receptor (Kearn et al., 2005). These studies could be extended to characterise the action of S-(-)-3PPP, aripiprazole and other D<sub>2</sub> partial agonists at the D<sub>2</sub>/D<sub>3</sub> heterodimer.

The characterisation of antisera raised against decapeptides corresponding to the C-terminal tail of G $\alpha_t$ , G $\alpha_s$  and G $\alpha_q$  was described. I demonstrated their selectivity towards the G protein against which they were raised and their utility in a [<sup>35</sup>S] GTP $\gamma$ S assay with an immunocapture step, making these antisera useful and highly selective tools for investigations into GPCR research. The final part of chapter 5 describes the successful generation and characterisation of antibodies selective against the active (GTP bound) conformation of G $\alpha$  subunits. The ultimate aim of this project was to use these antibodies in an assay, equivalent to the [<sup>35</sup>S] GTP $\gamma$ S assay, which would monitor receptor-mediated G protein activation. To this end, perhaps the most significant result was that these antibodies selectively recognised the GTP $\gamma$ S.G $\alpha_{i1}$  complex formed following the activation of the dopamine D<sub>21</sub> receptor by the agonist nor-apomorphine. This shows that, not only can the antibodies recognise the constitutively active G $\alpha_{i/o}$  subunit variants but can also recognise the activated form of the wild-type G $\alpha$  subunit and are, therefore, potentially useful tools with which to develop a functional assay. Although, immunocytochemistry has been a useful technique with which to characterise these antibodies it is certainly not a high-throughput process. The next stage, then, would be to attempt to develop a high-throughput assay using these antibodies. Given the success of the immunocytochemical experiments, an assay based on this methodology would be perhaps the most successful.

The ArrayScan® HCS Reader (Cellomics Inc., Thermo-Fisher, Waltham, MA, USA) is an automated fluorescence microscopic imaging system designed for high content screening and high content analysis. This perhaps would be a suitable format with which to design an assay. Sovago et al. describe autoradiographic mapping of dopamine-D<sub>2</sub>/D<sub>3</sub> receptor stimulated [<sup>35</sup>S] GTPγS binding in the human brain (Sovago et al., 2005). It would of interest to see if these antibodies would provide an alternative to this useful technique.

The demonstration that the antibodies could recognise one constitutively active mutant of Gα<sub>i2</sub> (Q<sup>205</sup>L) but not another (R<sup>179</sup>C) suggests that, although their epitope was not determined, these conformation-selective antibodies could provide interesting information about the structural changes occurring upon G protein activation. Furthermore, since the antibodies, like RGS proteins and effectors, interact with the active form of the G-protein, it would be worthwhile to see if these antibodies can interfere with these interactions.

The work by Mancina et al. demonstrated that, simply immunising mice with purified serotonin receptor and by following a hybridoma generation procedure equivalent to the one used in this study, antibodies selective to the agonist-bound conformation of the receptor can be generated (Mancina et al., 2007). One of the unsolved, and perhaps unknowable, questions from the immunisation procedure used to generate the active Gα<sub>i/o</sub> selective antibodies is whether preincubation of the G protein with GTPγS was necessary or even useful. Although GTPγS binds Gα subunits with a high affinity and is non-hydrolysable, this binding is not irreversible. Perhaps then, the success of the antibody generation programme was due simply to the number of hybridoma generated and the design of a robust screen that allowed selection of antibodies with the desired characteristics. In the introduction to this body of work, I described the current understanding of the conformational changes undergone by both receptor and G protein following receptor activation by an agonist. Antibodies have been generated that are

selective against the active (agonist bound) form of the receptor (Gupta et al., 2007; Mancina et al., 2007) and the active (GTP bound) form of  $G\alpha_{i/o}$  subunits (this study). With the design of the correct screen and the use of a suitable antigen and antibody production using the generation of hybridoma, antibodies selective against other events in the GPCR-G protein cycle could be generated.

One aspect of GPCR function that could be investigated is dimerisation / oligomerisation. Although many different techniques have been used to demonstrate the quaternary structure of GPCRs, antibodies specific for a receptor homo or hetero-oligomer would be a useful tool and a direct demonstration of this higher order structure. A technique described in a recent paper by Guo et al. (2005) provides a route by which this could be achieved. In this paper the heterodimer interface in the dopamine  $D_{2s}$  receptor was mapped over the entire length of TM IV by cross-linking substituted cysteines (**Figure 6.2 A**). Using this method it was demonstrated that the rearrangement of the dimer interface is a critical component of receptor activation. The TM IV dimer interface in the inverse-agonist bound conformation is consistent with the dimer of the inactive form of rhodopsin modelled with constraints from atomic force microscopy (Fotiadis et al., 2003). Crosslinking of another set of a different set of cysteines in TM IV effectively locks the receptor in an active state (Guo et al., 2005). Therefore, the paper demonstrates the stabilisation of a  $D_{2s}$  homo-dimer by cysteine cross-linking. Furthermore, both the inactive and active conformations can be stabilised by cysteine-cross linking. If these two species could be purified they would represent two different antigens. Unfortunately, a negative condition with which to screen generated antibodies, where homo-dimerisation is prevented, does not exist. However, as described in chapter 1 the  $D_2$  and  $D_3$  receptors are highly homologous, particularly within the transmembrane domains. It is likely then that equivalent cysteine linkages can be made between  $D_2$  and  $D_3$  receptors in a hetero-dimer. If this was the case a screen could be designed in which the positive condition would be  $D_2$

and D<sub>3</sub> receptors expressed in the same cell and the negative condition would be a mixture of cells expressing either D<sub>2</sub> or D<sub>3</sub> receptors only (**Figure 6.2 C + D**). D<sub>2</sub>/D<sub>3</sub> heterodimers have been demonstrated *in vitro* (Maggio et al., 2003), and it has been suggested that they may represent important therapeutic targets for the treatment of schizophrenia (Joyce and Millan, 2005). Antibodies selective against a D<sub>2</sub>/D<sub>3</sub> heterodimer would be useful in the visualisation of this species in native tissue.

Historically, and as demonstrated in this study, antibodies selective against individual G $\alpha$  subunits have been important tools with which to investigate receptor-G protein coupling (Milligan, 1994). However, the generation of antibodies selective against the active conformation of both GPCRs (Gupta et al., 2007; Mancina et al., 2007) and G  $\alpha$  subunits (this study) will have an extremely important role in future investigations into GPCR function.

**Figure 6.1****Two possible methods for investigation of D<sub>2</sub>/D<sub>3</sub> heterodimers taking advantage of the Flp-In TREx expression system**

**A)** In this model both the D<sub>2</sub> and D<sub>3</sub> receptors are constitutively expressed and the pertussis toxin resistant variant of either G $\alpha_{i1,2,3}$  or  $\alpha_{o1}$  is expressed from the inducible Flp-In locus. Using this model then the pharmacology and G protein coupling specificity of the D<sub>2</sub>/D<sub>3</sub> heterodimer can be dissected using the D<sub>2</sub> and D<sub>3</sub> selective antagonists shown in the presence of each G $\alpha_{i/o}$  subtype.

**B)** An alternative model, which still takes advantage of the Flp-In TREx system, is described where the D<sub>2</sub> receptor and the pertussis toxin resistant variant of either G $\alpha_{i1,2,3}$  or  $\alpha_{o1}$  are constitutively expressed and D<sub>3</sub> is expressed from the inducible Flp-In locus. Using this model the pharmacology and G protein coupling of the D<sub>2</sub> homodimer can be compared with that easily compared with that of the D<sub>2</sub>/D<sub>3</sub> heterodimer, simply by inducing expression of the D<sub>3</sub> receptor upon treatment with tetracycline (Tet.)

Figure 6.1

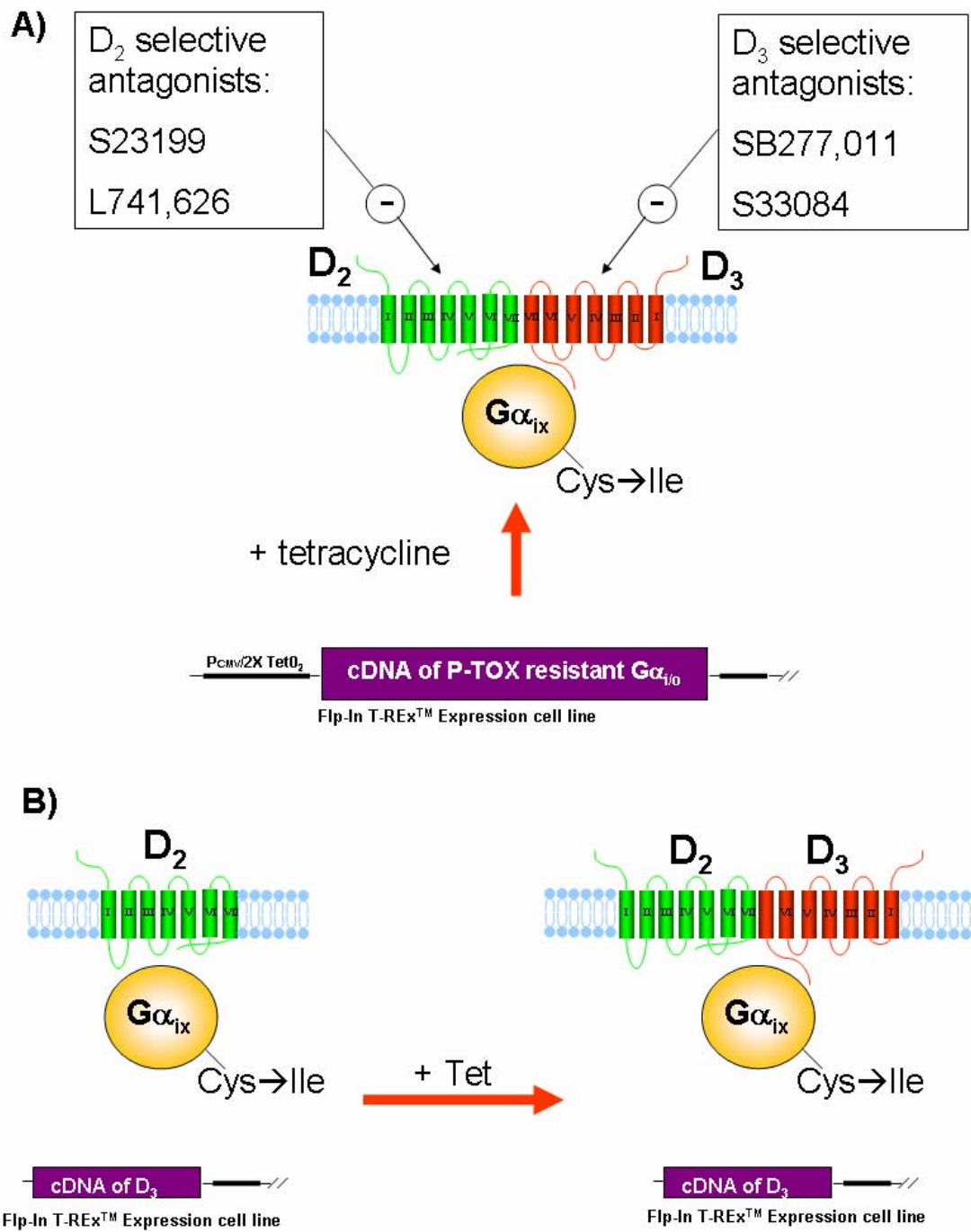


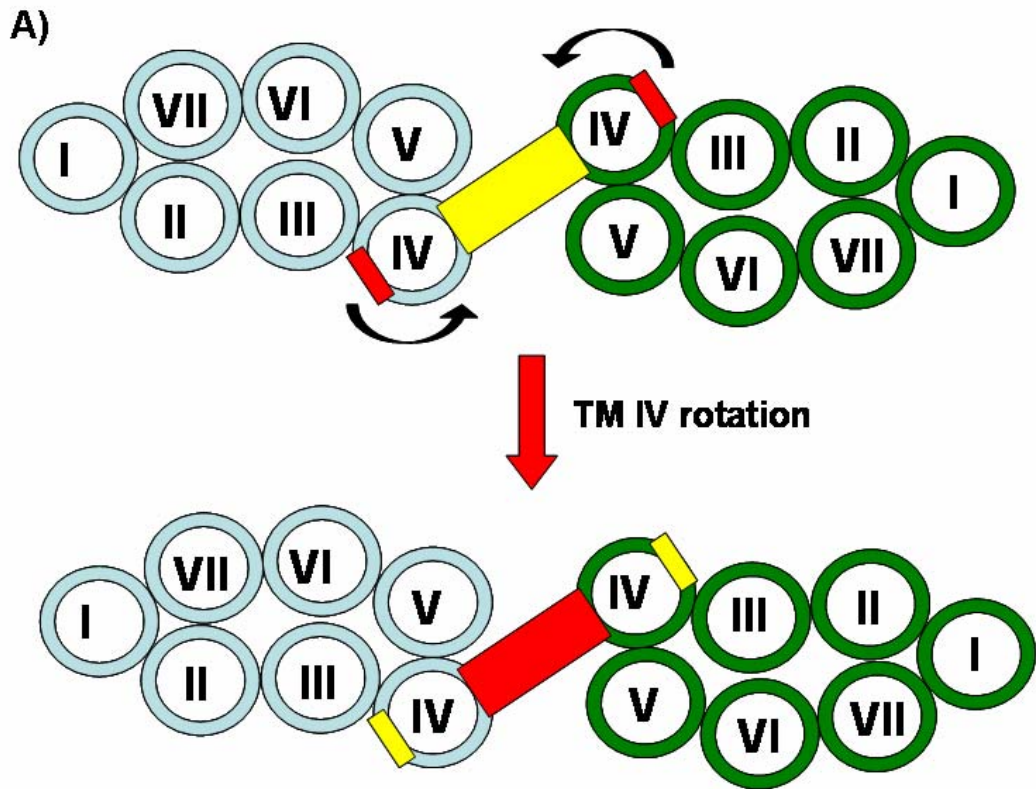
**Figure 6.2**

**An illustration of potential dimer interface rearrangements following receptor activation and the potential use of these cysteine cross-linked and stabilized conformations as antigens with which to generate antibodies selective against D<sub>2</sub>/D<sub>3</sub> heterodimers**

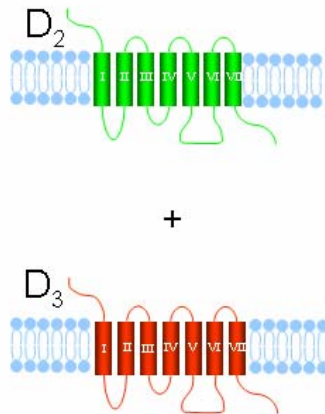
The entire homodimer interface of the D<sub>2</sub> receptor was mapped over the entire length of TM IV. In the inactive (inverse agonist) bound conformation cysteine linkages were made between one set of cysteine residues (yellow, **A**). However in the agonist bound conformation another set of cysteine residues were linked (red). This suggests that a conformational change at the TM IV interface is part of receptor activation. Given the high homology of D<sub>2</sub> and D<sub>3</sub> receptors it is likely that similar rearrangements may occur in a D<sub>2</sub>/D<sub>3</sub> heterodimer. These cysteine linked species then could be used as antigens for the generation of antibodies specific to this heterodimer (Taken from Guo et al., 2005).

An effective screen for antibodies with the correct selectivity would be needed, with both negative and positive conditions. Expression of either D<sub>2</sub> or D<sub>3</sub> in a heterologous cell line would generate only D<sub>2</sub> or D<sub>3</sub> homodimers, these then would be negative conditions (**B**). Co-expression of D<sub>2</sub> and D<sub>3</sub> within the same cell would generate D<sub>2</sub>/D<sub>3</sub> heterodimers, as well as D<sub>3</sub> and D<sub>2</sub> homodimers. This would be the positive control (**C**).

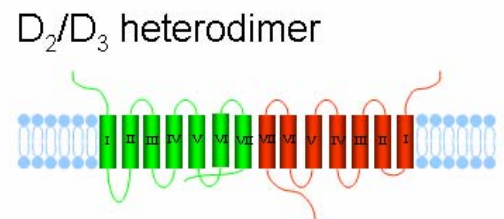
Figure 6.2



B)



C)



## Appendices

Sequence and residue number of peptides from Pepset™ corresponding to sequence of human  $G\alpha_{i1}$  (supplied by Mimotopes Ltd. Aus)

Peptide	Peptide Sequence	Corresponding residues of human $G\alpha_{i1}$	
		First residue	Last residue
1	H- MGCTLSAEDKAAVERSGSG -NH2	1	16
2	Biotin- SGGLSAEDKAAVERSKMID -NH2	5	20
3	Biotin- SGSGDKAAVERSKMIDRNLR -NH2	9	24
4	Biotin- SGSGVERSKMIDRNLRDGE -NH2	13	28
5	Biotin- SGSGKMIDRNLRDGEKAAR -NH2	17	32
6	Biotin- SGSGRNLRDGEKAAREVKL -NH2	21	36
7	Biotin- SGSGEDGEKAAREVKLLLLG -NH2	25	40
8	Biotin- SGSGKAAREVKLLLLGAGES -NH2	29	44
9	Biotin- SGSGEVKLLLLGAGESGKST -NH2	33	48
10	Biotin- SGSGLLLGAGESGKSTIVKQ -NH2	37	52
11	Biotin- SGSGAGESGKSTIVKQMKII -NH2	41	56
12	Biotin- SGSGGKSTIVKQMKIIHEAG -NH2	45	60
13	Biotin- SGSGIVKQMKIIHEAGYSEE -NH2	49	64
14	Biotin- SGSGMKIIHEAGYSEEECKQ -NH2	53	68
15	Biotin- SGSGHEAGYSEEECKQYKAV -NH2	57	72
16	Biotin- SGSGYSEEECKQYKAVVYSN -NH2	61	76
17	Biotin- SGSGECKQYKAVVYSNTIQS -NH2	65	80
18	Biotin- SGSGYKAVVYSNTIQSIIAI -NH2	69	84
19	Biotin- SGSGVYSNTIQSIIAIRAM -NH2	73	88
20	Biotin- SGSGTIQSIIAIRAMGRLLK -NH2	77	92
21	Biotin- SGSGIIAIRAMGRLLKIDFG -NH2	81	96
22	Biotin- SGSGIRAMGRLLKIDFGDSAR -NH2	85	100
23	Biotin- SGSGGRLKIDFGDSARADDA -NH2	89	104
24	Biotin- SGSGIDFGDSARADDARQLF -NH2	93	108
25	Biotin- SGSGDSARADDARQLFVLAG -NH2	97	112
26	Biotin- SGSGADDARQLFVLAGAAEE -NH2	101	116
27	Biotin- SGSGRQLFVLAGAAEEGFMT -NH2	105	120
28	Biotin- SGSGVLAGAAEEGFMTAELA -NH2	109	124
29	Biotin- SGSGAAEEGFMTAELAGVIK -NH2	113	128
30	Biotin- SGSGGFMTAELAGVIKRLWK -NH2	117	132
31	Biotin- SGSGAELAGVIKRLWKDSGV -NH2	121	136
32	Biotin- SGSGGVKRLWKDSGVQACF -NH2	125	140
33	Biotin- SGSGRLWKDSGVQACFNRSR -NH2	129	144
34	Biotin- SGSGDSGVQACFNRSREYQL -NH2	133	148
35	Biotin- SGSGQACFNRSREYQLNDSA -NH2	137	152
36	Biotin- SGSGNRSREYQLNDSAAYYL -NH2	141	156
37	Biotin- SGSGEYQLNDSAAYYLNLDL -NH2	145	160
38	Biotin- SGSGNDSAAYYLNLDLDRIAQ -NH2	149	164
39	Biotin- SGSGAYYLNLDLDRIAQPNYI -NH2	153	168

40	Biotin- SSGNDLDRIAQPNIPTQQ -NH2	157	172
41	Biotin- SSGRIAQPNIPTQQDVL R -NH2	161	176
42	Biotin- SSGPNIPTQQDVL RTRVK -NH2	165	180
43	Biotin- SSGPTQQDVL RTRVKT TGI -NH2	169	184
44	Biotin- SSGDVL RTRVKT TGI VETH -NH2	173	188
45	Biotin- SSGTRVKT TGI VETH FTFK -NH2	177	192
46	Biotin- SSGTTGI VETH FTFK DLHF -NH2	181	196
47	Biotin- SSGVETH FTFK DLHF KMF D -NH2	185	200
48	Biotin- SSGFTFK DLHF KMF D VGGQ -NH2	189	204
49	Biotin- SSGDLHF KMF D VGGQ RSE R -NH2	193	208
50	Biotin- SSGKMF D VGGQ RSE R KKI -NH2	197	212
51	Biotin- SSGVGGQ RSE R KKI HCF E -NH2	201	216
52	Biotin- SSGRSE R KKI HCF EGVTA -NH2	205	220
53	Biotin- SSGKKKI HCF EGVTA IIFC -NH2	209	224
54	Biotin- SSGHCF EGVTA IIFC VALS -NH2	213	228
55	Biotin- SSGGVTA IIFC VALS DYDL -NH2	217	232
56	Biotin- SSGIIFC VALS DYDL VLA E -NH2	221	236
57	Biotin- SSGVALS DYDL VLA E DEEM -NH2	225	240
58	Biotin- SSGDYDL VLA E DEEM NRMH -NH2	229	244
59	Biotin- SSGVLA E DEEM NRMHESMK -NH2	233	248
60	Biotin- SSGDEEM NRMHESMK LFDS -NH2	237	252
61	Biotin- SSGNRMHESMK LFDS ICNN -NH2	241	256
62	Biotin- SSGESMK LFDS ICNN KWFT -NH2	245	260
63	Biotin- SSGSLFDS ICNN KWFT DTSI -NH2	249	264
64	Biotin- SSGICNN KWFT DTSI ILFL -NH2	253	268
65	Biotin- SSGKWF T DTSI ILFL NKKD -NH2	257	272
66	Biotin- SSGDTSI ILFL NKKD LFEE -NH2	261	276
67	Biotin- SSGILFL NKKD LFEE KIKK -NH2	265	280
68	Biotin- SSGNKKD LFEE KIKK SPLT -NH2	269	284
69	Biotin- SSGLFEE KIKK SPLT ICYP -NH2	273	288
70	Biotin- SSGKIKK SPLT ICYP EYAG -NH2	277	292
71	Biotin- SSGSPLT ICYP EYAGSNTY -NH2	281	296
72	Biotin- SSGICYPEYAGSNTY EEEA -NH2	285	300
73	Biotin- SSGEYAGSNTY EEEA AAYIQ -NH2	289	304
74	Biotin- SSGSNTY EEEA AAYIQ QFE -NH2	293	308
75	Biotin- SSGEEA AAYIQ QFE DLNK -NH2	297	312
76	Biotin- SSGAYIQ QFE DLNK RKDT -NH2	301	316
77	Biotin- SSGCQFE DLNK RKDT KEIY -NH2	305	320
78	Biotin- SSGDLNK RKDT KEIY THFT -NH2	309	324
79	Biotin- SSGRKDT KEIY THFT CATD -NH2	313	328
80	Biotin- SSGKEIY THFT CATD TKNV -NH2	317	332
81	Biotin- SSGTHFT CATD TKNV QFVF -NH2	321	336
82	Biotin- SSGCATD TKNV QFVF DAVT -NH2	325	340
83	Biotin- SSGTKNV QFVF DAVT DVII -NH2	329	344
84	Biotin- SSGQFVF DAVT DVII KNNL -NH2	333	348
85	Biotin- SSGDAVT DVII KNNL KDCG -NH2	337	352
86	Biotin- SSGVTDVII KNNL KDCGLF -OH	339	354

## List of References

Abdulaev NG, Ngo T, Ramon E, Brabazon DM, Marino JP and Ridge KD (2006) The Receptor-Bound "Empty Pocket" State of the Heterotrimeric G-Protein  $\alpha$ -Subunit Is Conformationally Dynamic. *Biochemistry* 45(43):12986-12997.

Agnati LF, Ferre S, Lluís C, Franco R and Fuxe K (2003) Molecular Mechanisms and Therapeutical Implications of Intramembrane Receptor/Receptor Interactions among Heptahelical Receptors with Examples from the Striatopallidal GABA Neurons. *Pharmacol Rev* 55(3):509-550.

Ahlgren-Beckendorf JA and Levant B (2004) Signaling Mechanisms of the D<sub>3</sub> Dopamine Receptor. *Journal of Receptors and Signal Transduction* 24(3):117-130.

Akam EC, Challiss RAJ and Nahorski SR (2001) Gq/11 and Gi/o activation profiles in CHO cells expressing human muscarinic acetylcholine receptors: dependence on agonist as well as receptor-subtype. *Br J Pharmacol* 132(4):950-958.

Alberts GL, Pregoner JF and Im WB (2000) Advantages of heterologous expression of human D<sub>2</sub> dopamine receptors in human neuroblastoma SH-SY5Y over human embryonic kidney 293 cells. *Br J Pharmacol* 131(3):514-520.

Alexander SPH, Mathie A and Peters JA (2006) Guide to Receptors and Channels. *Br J Pharmacol* 147(S3):S32.

Altenbach C, Cai K, Klein-Seetharaman J, Khorana HG and Hubbell WL (2001) Structure and Function in Rhodopsin: Mapping Light-Dependent Changes in Distance between Residue 65 in Helix TM1 and Residues in the Sequence 306-319 at the Cytoplasmic End of Helix TM7 and in Helix H8. *Biochemistry* 40(51):15483-15492.

Altenbach C, Yang K, Farrens DL, Farahbakhsh ZT, Khorana HG and Hubbell WL (1996) Structural Features and Light-Dependent Changes in the Cytoplasmic Interhelical E-F

J. Robert Lane, 2007

Loop Region of Rhodopsin: A Site-Directed Spin-Labeling Study. *Biochemistry* 35(38):12470-12478.

Amatruda TT, III, Dragas-Graonic S, Holmes R and Perez HD (1995) Signal Transduction by the Formyl Peptide Receptor. *J Biol Chem* 270(47):28010-28013.

Angers S, Salahpour A and Bouvier M (2002) DIMERIZATION: An Emerging Concept for G Protein-Coupled Receptor Ontogeny and Function. *Annual Review of Pharmacology and Toxicology* 42(1):409-435.

Aoki C, Go CG, Wu K and Siekevitz P (1992) Light and electron microscopic localization of [alpha] subunits of GTP-binding proteins, G<sub>0</sub> and G<sub>1</sub>, in the cerebral cortex and hippocampus of rat brain. *Brain Research* 596(1-2):189-201.

Arden JR, Segredo V, Wang Z, Lamah J and Sadee W (1995) Phosphorylation and Agonist-Specific Intracellular Trafficking of an Epitope-Tagged  $\mu$ -Opioid Receptor Expressed in HEK 293 Cells. *Journal of Neurochemistry* 65(4):1636-1645.

Arnt J, Bäckström KP, Christensen AV, Hyttel J, Larsen JJ and Svendsen O (1983) Dopamine receptor agonistic and antagonistic effects of 3-PPP enantiomers. *Psychopharmacology* 81(3):199-207.

Arshavsky VY and Bownds MD (1992) Regulation of deactivation of photoreceptor G protein by its target enzyme and cGMP. *Nature* 357(6377):416-417.

Azzi M, Pineyro G, Pontier S, Parent S, Ansanay H and Bouvier M (2001) Allosteric Effects of G Protein Overexpression on the Binding of beta -Adrenergic Ligands with Distinct Inverse Efficacies. *Mol Pharmacol* 60(5):999-1007.

Bae H, Cabrera-Vera TM, Depree KM, Graber SG and Hamm HE (1999) Two Amino Acids within the alpha 4 Helix of Galpha i1 Mediate Coupling with 5-Hydroxytryptamine<sub>1B</sub> Receptors. *J Biol Chem* 274(21):14963-14971.

Bahia DS, Wise A, Fanelli F, Lee M, Rees S and Milligan G (1998) Hydrophobicity of Residue<sup>351</sup> of the G Protein G<sub>i1</sub> Determines the Extent of Activation by the  $\alpha_{2A}$ -Adrenoceptor. *Biochemistry* 37(33):11555-11562.

J. Robert Lane, 2007

Baldwin JM, Schertler GFX and Unger VM (1997) An alpha-carbon template for the transmembrane helices in the rhodopsin family of G-protein-coupled receptors. *Journal of Molecular Biology* 272(1):144-164.

Baneres J-L and Parello J (2003) Structure-based Analysis of GPCR Function: Evidence for a Novel Pentameric Assembly between the Dimeric Leukotriene B4 Receptor BLT1 and the G-protein. *Journal of Molecular Biology* 329(4):815-829.

Beom S, Cheong D, Torres G, Caron MG and Kim K-M (2004) Comparative Studies of Molecular Mechanisms of Dopamine D2 and D3 Receptors for the Activation of Extracellular Signal-regulated Kinase. *J Biol Chem* 279(27):28304-28314.

Berg KA, Cropper JD, Niswender CM, Sanders-Bush E, Emeson RB and Clarke WP (2001) RNA-editing of the 5-HT<sub>2C</sub> receptor alters agonist-receptor-effector coupling specificity. *Br J Pharmacol* 134(2):386-392.

Berg KA, Maayani S, Goldfarb J, Scaramellini C, Leff P and Clarke WP (1998) Effector Pathway-Dependent Relative Efficacy at Serotonin Type 2A and 2C Receptors: Evidence for Agonist-Directed Trafficking of Receptor Stimulus. *Mol Pharmacol* 54(1):94-104.

Berghuis AM, Lee E, Raw AS, Gilman AG and Sprang SR (1996) Structure of the GDP-Pi complex of Gly203-->Ala Gi[alpha]1: a mimic of the ternary product complex of G[alpha]-catalyzed GTP hydrolysis. *Structure* 4(11):1277-1290.

Berstein G, Blank JL, Smrcka AV, Higashijima T, Sternweis PC, Exton JH and Ross EM (1992) Reconstitution of agonist-stimulated phosphatidylinositol 4,5- bisphosphate hydrolysis using purified m1 muscarinic receptor, Gq/11, and phospholipase C-beta 1. *J Biol Chem* 267(12):8081-8088.

Bluml K, Mutschler E and Wess J (1994) Functional role of a cytoplasmic aromatic amino acid in muscarinic receptor-mediated activation of phospholipase C. *J Biol Chem* 269(15):11537-11541.

Bockaert J and Pin JP (1999) Molecular tinkering of G protein-coupled receptors: an evolutionary success. *EMBO J* 18(7):1723-1729.

J. Robert Lane, 2007

Bourne HR (1987) Discovery of a new oncogene in pituitary tumours? *Nature* 330(6148):517-518.

Bourne HR (1997) How receptors talk to trimeric G proteins. *Current Opinion in Cell Biology* 9(2):134-142.

Bunemann M, Frank M and Lohse MJ (2003) From The Cover: Gi protein activation in intact cells involves subunit rearrangement rather than dissociation. *PNAS* 100(26):16077-16082.

Burns CM, Chu H, Rueter SM, Hutchinson LK, Canton H, Sanders-Bush E and Emeson RB (1997) Regulation of serotonin-2C receptor G-protein coupling by RNA editing. *Nature* 387(6630):303-308.

Burris KD, Molski TF, Xu C, Ryan E, Tottori K, Kikuchi T, Yocca FD and Molinoff PB (2002) Aripiprazole, a Novel Antipsychotic, Is a High-Affinity Partial Agonist at Human Dopamine D2 Receptors. *J Pharmacol Exp Ther* 302(1):381-389.

Burstein ES, Spalding TA, Hill-Eubanks D and Brann MR (1995) Structure-Function of Muscarinic Receptor Coupling to G Proteins. *J Biol Chem* 270(7):3141-3146.

Bynum J, Andrews JL, Ellis B, Kull FCJ, Austin EA and Kilpatrick KE (1999) Development of class-switched, affinity-matured monoclonal antibodies following a 7-day immunization schedule. *Hybridoma* 18(5):407-411.

Cabrera-Vera TM, Vanhauwe J, Thomas TO, Medkova M, Preininger A, Mazzoni MR and Hamm HE (2003) Insights into G Protein Structure, Function, and Regulation. *Endocr Rev* 24(6):765-781.

Canals M, Jenkins L, Kellett E and Milligan G (2006) Up-regulation of the Angiotensin II Type 1 Receptor by the MAS Proto-oncogene Is Due to Constitutive Activation of Gq/G11 by MAS. *J Biol Chem* 281(24):16757-16767.

Canals M, Marcellino D, Fanelli F, Ciruela F, de Benedetti P, Goldberg SR, Neve K, Fuxe K, Agnati LF, Woods AS, Ferre S, Lluís C, Bouvier M and Franco R (2003) Adenosine A2A-Dopamine D2 Receptor-Receptor Heteromerization: QUALITATIVE AND

J. Robert Lane, 2007

QUANTITATIVE ASSESSMENT BY FLUORESCENCE AND BIOLUMINESCENCE ENERGY TRANSFER. *J Biol Chem* 278(47):46741-46749.

Cass WA and Zahniser NR (1991) Potassium channel blockers inhibit D2 dopamine, but not A1 adenosine, receptor-mediated inhibition of striatal dopamine release. *J Neurochem* 57(1):147-152.

Cepeda C, Buchwald NA and Levine MS (1993) Neuromodulatory Actions of Dopamine in the Neostriatum are Dependent Upon the Excitatory Amino Acid Receptor Subtypes Activated. *PNAS* 90(20):9576-9580.

Cepeda C, Hurst RS, Altemus KL, Flores-Hernandez J, Calvert CR, Jokel ES, Grandy DK, Low MJ, Rubinstein M, Ariano MA and Levine MS (2001) Facilitated Glutamatergic Transmission in the Striatum of D2 Dopamine Receptor-Deficient Mice. *J Neurophysiol* 85(2):659-670.

Chakrabarti S, Law P-Y and Loh HH (1998) Distinct Differences Between Morphine- and [d-Ala<sup>2</sup>,N-MePhe<sup>4</sup>,Gly-ol<sup>5</sup>]-Enkephalin-  $\mu$ -Opioid Receptor Complexes Demonstrated by Cyclic AMP-Dependent Protein Kinase Phosphorylation. *Journal of Neurochemistry* 71(1):231-239.

Chaperon F, Tricklebank MD, Unger L and Neijt HC (2003) Evidence for regulation of body temperature in rats by dopamine D2 receptor and possible influence of D1 but not D3 and D4 receptors. *Neuropharmacology* 44(8):1047-1053.

Chen CA, Manning, D.R. (2001) Regulation of G proteins by covalent modification. *Oncogene* 20(13):1643-1652.

Cherfils J and Chabre M (2003) Activation of G-protein G[alpha] subunits by receptors through G[alpha]-G[beta] and G[alpha]-G[gamma] interactions. *Trends in Biochemical Sciences* 28(1):13-17.

Chio CL, Lajiness ME and Huff RM (1994) Activation of heterologously expressed D3 dopamine receptors: comparison with D2 dopamine receptors. *Mol Pharmacol* 45(1):51-60.

J. Robert Lane, 2007

Cho D-I, Beom S, Tol HHMV, Caron MG and Kim K-M (2006) Characterization of the desensitization properties of five dopamine receptor subtypes and alternatively spliced variants of dopamine D2 and D4 receptors. *Biochemical and Biophysical Research Communications* 350(3):634-640.

Cho E-Y, Cho D-I, Park JH, Kurose H, Caron MG and Kim K-M (2007) Roles of Protein Kinase C and Actin-Binding Protein 280 in the Regulation of Intracellular Trafficking of Dopamine D3 Receptor. *Mol Endocrinol* 21(9):2242-2254.

Ciarkowski J, Witt M and Ślusarz R (2005) A hypothesis for GPCR activation. *Journal of Molecular Modeling* V11(4):407-415.

Clapham DE and Neer EJ (1997) G PROTEIN  $\beta\gamma$  SUBUNITS. *Annual Review of Pharmacology and Toxicology* 37(1):167-203.

Clarke WP and Bond RA (1998) The elusive nature of intrinsic efficacy. *Trends in Pharmacological Sciences* 19(7):270-276.

Clawges HM, Depree KM, Parker EM and Graber SG (1997) Human 5-HT<sub>1</sub> Receptor Subtypes Exhibit Distinct G Protein Coupling Behaviors in Membranes from Sf9 Cells. *Biochemistry* 36(42):12930-12938.

Coleman DE, Berghuis AM, Lee E, Linder ME, Gilman AG and Sprang SR (1994) Structures of active conformations of Gi alpha 1 and the mechanism of GTP hydrolysis. *Science* 265(5177):1405-1412.

Coleman DE and Sprang SR (1998) Crystal Structures of the G Protein Gi $\alpha$ 1 Complexed with GDP and Mg<sup>2+</sup>: A Crystallographic Titration Experiment. *Biochemistry* 37(41):14376-14385.

Colquhoun D (1998) Binding, gating, affinity and efficacy: The interpretation of structure-activity relationships for agonists and of the effects of mutating receptors. 125(5):923-947.

Conklin BR and Bourne HR (1993) Structural elements of G[alpha] subunits that interact with G[beta][gamma], receptors, and effectors. *Cell* 73(4):631-641.

J. Robert Lane, 2007

Cordeaux Y, Nickolls SA, Flood LA, Graber SG and Strange PG (2001) Agonist Regulation of D2 Dopamine Receptor/G Protein Interaction. EVIDENCE FOR AGONIST SELECTION OF G PROTEIN SUBTYPE. *J Biol Chem* 276(31):28667-28675.

Corvol JC, Studler JM, Schonn JS, Girault JA and Herve D (2001)  $G\alpha_{olf}$  is necessary for coupling D1 and A2a receptors to adenylyl cyclase in the striatum. *Journal of Neurochemistry* 76(5):1585-1588.

Cosi C, Carilla-Durand E, Assie MB, Ormiere AM, Maraval M, Leduc N and Newman-Tancredi A (2006) Partial agonist properties of the antipsychotics SSR181507, aripiprazole and bifeprunox at dopamine D2 receptors: G protein activation and prolactin release. *European Journal of Pharmacology* 535(1-3):135-144.

Cox B, Rosser MP, Kozlowski MR, Duwe KM, Neve RL and Neve KA (1995) Regulation and functional characterization of a rat recombinant dopamine D3 receptor. *Synapse* 21(1):1-9.

Davies A, Gowen BE, Krebs AM, Schertler GFX and Saibil HR (2001) Three-dimensional structure of an invertebrate rhodopsin and basis for ordered alignment in the photoreceptor membrane. *Journal of Molecular Biology* 314(3):455-463.

Day PW, Tesmer JJG, Sterne-Marr R, Freeman LC, Benovic JL and Wedegaertner PB (2004) Characterization of the GRK2 Binding Site of G $\{\alpha\}$ q. *J Biol Chem* 279(51):53643-53652.

De Lean A, Stadel JM and Lefkowitz RJ (1980) A ternary complex model explains the agonist-specific binding properties of the adenylyl cyclase-coupled beta-adrenergic receptor. *J Biol Chem* 255(15):7108-7117.

Diaz J, Pilon C, Le Foll B, Gros C, Triller A, Schwartz J-C and Sokoloff P (2000) Dopamine D3 Receptors Expressed by All Mesencephalic Dopamine Neurons. *J Neurosci* 20(23):8677-8684.

Downes GB and Gautam N (1999) The G Protein Subunit Gene Families. *Genomics* 62(3):544-552.

J. Robert Lane, 2007

Dupuis DS, Tardif S, Wurch T, Colpaert FC and Pauwels PJ (1999) Modulation of 5-HT<sub>1A</sub> receptor signalling by point-mutation of cysteine351 in the rat G $\alpha$ o protein. *Neuropharmacology* 38(7):1035-1041.

Dziedzicka-Wasylewska M, Faron-Gorecka A, Andrecka J, Polit A, Kusmider M and Wasylewski Z (2006) Fluorescence Studies Reveal Heterodimerization of Dopamine D<sub>1</sub> and D<sub>2</sub> Receptors in the Plasma Membrane. *Biochemistry* 45(29):8751-8759.

Ellis J, Pediani JD, Canals M, Milasta S and Milligan G (2006) Orexin-1 Receptor-Cannabinoid CB<sub>1</sub> Receptor Heterodimerization Results in Both Ligand-dependent and -independent Coordinated Alterations of Receptor Localization and Function. *J Biol Chem* 281(50):38812-38824.

Elmhurst JL, Xie Z, O'Dowd BF and George SR (2000) The splice variant D<sub>3</sub>nf reduces ligand binding to the D<sub>3</sub> dopamine receptor: evidence for heterooligomerization. *Molecular Brain Research* 80(1):63-74.

Ernst OP, Meyer CK, Marin EP, Henklein P, Fu W-Y, Sakmar TP and Hofmann KP (2000) Mutation of the Fourth Cytoplasmic Loop of Rhodopsin Affects Binding of Transducin and Peptides Derived from the Carboxyl-terminal Sequences of Transducin alpha and gamma Subunits. *J Biol Chem* 275(3):1937-1943.

Farrens DL, Altenbach C, Yang K, Hubbell WL and Khorana HG (1996) Requirement of Rigid-Body Motion of Transmembrane Helices for Light Activation of Rhodopsin. *Science* 274(5288):768-770.

Ferrer M, Kolodin GD, Zuck P, Peltier R, Berry K, Mandala SM, Rosen H, Ota H, Ozaki S, Inglese J and Strulovici B (2003) A Fully Automated [<sup>35</sup>S]GTPγS Scintillation Proximity Assay for the High-Throughput Screening of Gi-Linked G Protein-Coupled Receptors. *ASSAY and Drug Development Technologies* 1(2):261-273.

Filteau F, Veilleux F and Levesque D (1999) Effects of reciprocal chimeras between the C-terminal portion of third intracellular loops of the human dopamine D<sub>2</sub> and D<sub>3</sub> receptors. *FEBS Letters* 447(2-3):251-256.

J. Robert Lane, 2007

Fletcher JE, Lindorfer, M.A., DeFilippo, J.M., Yasuda, H., Guilmard, M., Garrison, J.C. (1998) The G protein beta5 subunit interacts selectively with the Gq alpha subunit. *J Biol Chem* 273(1):636-644.

Ford CE, Skiba NP, Bae H, Daaka Y, Reuveny E, Shekter LR, Rosal R, Weng G, Yang C-S, Iyengar R, Miller RJ, Jan LY, Lefkowitz RJ and Hamm HE (1998) Molecular Basis for Interactions of G Protein {beta} Subunits with Effectors. *Science* 280(5367):1271-1274.

Fotiadis D, Jastrzebska B, Philippsen A, Muller DJ, Palczewski K and Engel A (2006) Structure of the rhodopsin dimer: a working model for G-protein-coupled receptors. *Current Opinion in Structural Biology* 16(2):252-259.

Fotiadis D, Liang Y, Filipek S, Saperstein DA, Engel A and Palczewski K (2003) Atomic-force microscopy: Rhodopsin dimers in native disc membranes. *Nature* 421(6919):127-128.

Fotiadis D, Liang Y, Filipek S, Saperstein DA, Engel A and Palczewski K (2004) The G protein-coupled receptor rhodopsin in the native membrane. *FEBS Letters* 564(3):281-288.

Frank M, Thumer L, Lohse MJ and Bunemann M (2005) G Protein Activation without Subunit Dissociation Depends on a G{alpha}i-specific Region. *J Biol Chem* 280(26):24584-24590.

Freedman JE, Waszczak BL, Cox RF, June-Chih L and Gabriela JG (1994) The dopamine D3 receptor and 7-OH-DPAT. *Trends in Pharmacological Sciences* 15(6):173-173.

Freneau RT, Jr., Duncan GE, Fornaretto M, Dearry A and Gingrich JA (1991) Localization of D1 Dopamine Receptor mRNA in Brain Supports a Role in Cognitive, Affective, and Neuroendocrine Aspects of Dopaminergic Neurotransmission. *PNAS* 88(9):3772-3776.

Fu Y, Zhong H, Nanamori M, Mortensen RM, Huang X, Lan K, Neubig RR and David PS (2004) RGS-Insensitive G-Protein Mutations to Study the Role of Endogenous RGS Proteins, in *Methods in Enzymology* pp 229-243, Academic Press.

J. Robert Lane, 2007

Galandrin S and Bouvier M (2006) Distinct Signaling Profiles of beta1 and beta2 Adrenergic Receptor Ligands toward Adenylyl Cyclase and Mitogen-Activated Protein Kinase Reveals the Pluridimensionality of Efficacy. *Mol Pharmacol* 70(5):1575-1584.

Gales C, Van Durm JJJ, Schaak S, Pontier S, Percherancier Y, Audet M, Paris H and Bouvier M (2006) Probing the activation-promoted structural rearrangements in preassembled receptor-G protein complexes. *Nat Struct Mol Biol* 13(9):778-786.

Gazi L, Nickolls SA and Strange PG (2003) Functional coupling of the human dopamine D2 receptor with G[alpha]i1, G[alpha]i2, G[alpha]i3 and G[alpha]o G proteins: evidence for agonist regulation of G protein selectivity. *J Biol Chem* 278(5):775-786.

Gbahou F, Rouleau A, Morisset S, Parmentier R, Crochet S, Lin J-S, Ligneau X, Tardivel-Lacombe J, Stark H, Schunack W, Ganellin CR, Schwartz J-C and Arrang J-M (2003) Protean agonism at histamine H3 receptors in vitro and in vivo. *PNAS* 100(19):11086-11091.

George SR, Fan T, Xie Z, Tse R, Tam V, Varghese G and O'Dowd BF (2000) Oligomerization of {micro}- and delta -Opioid Receptors. GENERATION OF NOVEL FUNCTIONAL PROPERTIES. *J Biol Chem* 275(34):26128-26135.

George SR, Lee SP, Varghese G, Zeman PR, Seeman P, Ng GYK and O'Dowd BF (1998) A Transmembrane Domain-derived Peptide Inhibits D1 Dopamine Receptor Function without Affecting Receptor Oligomerization. *J Biol Chem* 273(46):30244-30248.

George SR, O'Dowd BF and Lee SP (2002) G-protein Coupled Receptor Oligomerisation And Its Potential For Drug Discovery. *Nature Reviews Drug Discovery* 1(10):808-820.

Gether U, Asmar F, Meinild AK and Rasmussen SGF (2002) Structural Basis for Activation of G-Protein-Coupled Receptors. *Pharmacology and Toxicology* 91(6):304-312.

Ghahremani MH, Cheng P, Lembo PMC and Albert PR (1999) Distinct Roles for Galpha i2, Galpha i3, and Gbeta gamma in Modulation of Forskolin- or Gs-mediated cAMP Accumulation and Calcium Mobilization by Dopamine D2S Receptors. *J Biol Chem* 274(14):9238-9245.

J. Robert Lane, 2007

Ghanouni P, Steenhuis JJ, Farrens DL and Kobilka BK (2001) Agonist-induced conformational changes in the G-protein-coupling domain of the beta 2 adrenergic receptor. *PNAS* 98(11):5997-6002.

Gilchrist A, Mazzoni MR, Dineen B, Dice A, Linden J, Proctor WR, Lupica CR, Dunwiddie TV and Hamm HE (1998) Antagonists of the Receptor-G Protein Interface Block Gi-coupled Signal Transduction. *J Biol Chem* 273(24):14912-14919.

Gilchrist RL, Ryu K-S, Ji I and Ji TH (1996) The Luteinizing Hormone/Chorionic Gonadotropin Receptor Has Distinct Transmembrane Conductors for cAMP and Inositol Phosphate Signals. *J Biol Chem* 271(32):19283-19287.

Gines S, Hillion J, Torvinen M, Le Crom S, Casado V, Canela EI, Rondin S, Lew JY, Watson S, Zoli M, Agnati LF, Verniera P, Lluís C, Ferre S, Fuxe K and Franco R (2000) Dopamine D1 and adenosine A1 receptors form functionally interacting heteromeric complexes. *PNAS* 97(15):8606-8611.

Gingrich JA and Caron MG (1993) Recent Advances in the Molecular Biology of Dopamine Receptors. *Annual Review of Neuroscience* 16(1):299-321.

Gonzalez-Maeso J, Wise A, Green A and Koenig JA (2003) Agonist-induced desensitization and endocytosis of heterodimeric GABAB receptors in CHO-K1 cells. *European Journal of Pharmacology* 481(1):15-23.

Griffon N, Pilon C, Sautel F, Schwartz J-C and Sokoloff P (1997) Two Intracellular Signaling Pathways for the Dopamine D3 Receptor: Opposite and Synergistic Interactions with Cyclic AMP. *Journal of Neurochemistry* 68(1):1-9.

Grunewald S, Reilander H and Michel H (1996) In Vivo Reconstitution of Dopamine D2S Receptor-Mediated G Protein Activation in Baculovirus-Infected Insect Cells: Preferred Coupling to Gi1 versus Gi2. *Biochemistry* 35(48):15162-15173.

Gudermann T, Schoneberg T and Schultz G (1997) FUNCTIONAL AND STRUCTURAL COMPLEXITY OF SIGNAL TRANSDUCTION VIA G-PROTEIN-COUPLED RECEPTORS. *Annual Review of Neuroscience* 20(1):399-427.

J. Robert Lane, 2007

Guillin O, AbiDargham A, Laruelle M and Anissa AbiDargham and Olivier G (2007) Neurobiology of Dopamine in Schizophrenia, in *International Review of Neurobiology* pp 1-39, Academic Press.

Guiramand J, Montmayeur J-P, Ceraline J, Bhatia M and Borrelli E (1995) Alternative Splicing of the Dopamine D2 Receptor Directs Specificity of Coupling to G-proteins. *Journal of Biological Chemistry* 270(13):7354-7358.

Guo N, Vincent SR and Fibiger HC (1998) Phenotypic characterization of neuroleptic-sensitive neurons in the forebrain: contrasting targets of haloperidol and clozapine. *Neuropsychopharmacology* 19(2):133-145.

Guo W, Shi L, Filizola M, Weinstein H and Javitch JA (2005) From The Cover: Crosstalk in G protein-coupled receptors: Changes at the transmembrane homodimer interface determine activation. *PNAS* 102(48):17495-17500.

Gupta A, Decaillet FM, Gomes I, Tkalych O, Heimann AS, Ferro ES and Devi LA (2007) Conformation State-sensitive Antibodies to G-protein-coupled Receptors. *J Biol Chem* 282(8):5116-5124.

Gurevich EV and Joyce JN (1999) Distribution of Dopamine D3 Receptor Expressing Neurons in the Human Forebrain: Comparison with D2 Receptor Expressing Neurons. *Neuropsychopharmacology* 20:60–80.

Hall DA and Strange PG (1999) Comparison of the ability of dopamine receptor agonists to inhibit forskolin-stimulated adenosine 3'5'-cyclic monophosphate (cAMP) accumulation via D2L (long isoform) and D3 receptors expressed in Chinese hamster ovary (CHO) cells. *Biochemical Pharmacology* 58(2):285-289.

Hall RA and Lefkowitz RJ (2002) Regulation of G Protein-Coupled Receptor Signaling by Scaffold Proteins. *Circ Res* 91(8):672-680.

Harlow E, Lane, D. (1988) *Antibodies - A Laboratory Manual* Cold Spring Harbour Laboratory Press

Hernandez-Lopez S, Tkatch T, Perez-Garci E, Galarraga E, Bargas J, Hamm H and Surmeier DJ (2000) D2 Dopamine Receptors in Striatal Medium Spiny Neurons Reduce L-

J. Robert Lane, 2007

Type Ca<sup>2+</sup> Currents and Excitability via a Novel PLC $\beta$ 1-IP3-Calcineurin-Signaling Cascade. *J Neurosci* 20(24):8987-8995.

Higgins JB and Casey PJ (1996) The role of prenylation in G-protein assembly and function. *Cellular Signalling* 8(6):433-437.

Hildebrandt JD (2006) Bring Your Own G Protein. *Mol Pharmacol* 69(4):1079-1082.

Hjorth S, Carlsson A, Clark D, Svensson K, Wikström H, Sanchez D, Lindberg P, Hacksell U, Arvidsson LE, Johansson A and Nilsson JLG (1983) Central dopamine receptor agonist and antagonist actions of the enantiomers of 3-PPP. *Psychopharmacology* 81(2):89-99.

Hornykiewicz O (1998) Biochemical aspects of Parkinson's disease. *Neurology* 51:S2-9.

Hou Y, Azpiazu I, Smrcka A and Gautam N (2000) Selective Role of G Protein gamma Subunits in Receptor Interaction. *J Biol Chem* 275(50):38961-38964.

Iri T, Farfel Z and Bourne HR (1998) G-protein diseases furnish a model for the turn-on switch. *Nature* 394(6688):35-38.

Iri T, Herzmark P, Nakamoto JM, Van Dop C and Bourne HR (1994) Rapid GDP release from Gs[alpha] in patients with gain and loss of endocrine function. *Nature* 371(6493):164-168.

Ishii I, Izumi T, Tsukamoto H, Umeyama H, Ui M and Shimizu T (1997) Alanine Exchanges of Polar Amino Acids in the Transmembrane Domains of a Platelet-activating Factor Receptor Generate Both Constitutively Active and Inactive Mutants. *J Biol Chem* 272(12):7846-7854.

Iwamoto T, Okumura S, Iwatsubo K, Kawabe J-I, Ohtsu K, Sakai I, Hashimoto Y, Izumitani A, Sango K, Ajiki K, Toya Y, Umemura S, Goshima Y, Arai N, Vatner SF and Ishikawa Y (2003) Motor Dysfunction in Type 5 Adenylyl Cyclase-null Mice. *J Biol Chem* 278(19):16936-16940.

Jackson DM and Westlind-Danielsson A (1994) Dopamine receptors: Molecular biology, biochemistry and behavioural aspects. *Pharmacology & Therapeutics* 64(2):291-370.

J. Robert Lane, 2007

Javitch JA (2004) The Ants Go Marching Two by Two: Oligomeric Structure of G-Protein-Coupled Receptors. *Mol Pharmacol* 66(5):1077-1082.

Jiang M, Spicher K, Boulay G, Wang Y and Birnbaumer L (2001) Most central nervous system D2 dopamine receptors are coupled to their effectors by Go. *PNAS* 98(6):3577-3582.

Joseph JD, Wang YM, Miles PR, Budygin EA, Picetti R, Gainetdinov RR, Caron MG and Wightman RM (2002) Dopamine autoreceptor regulation of release and uptake in mouse brain slices in the absence of D3 receptors. *Neuroscience* 112(1):39-49.

Joyce JN (2001) Dopamine D3 receptor as a therapeutic target for antipsychotic and antiparkinsonian drugs. *Pharmacology & Therapeutics* 90(2-3):231-259.

Joyce JN and Millan MJ (2005) Dopamine D3 receptor antagonists as therapeutic agents. *Drug Discovery Today* 10(13):917-925.

Jurgen FMV, Martine E, Danielle van de W, Mirek J and Josée EL (2000) Effects of recent and reference antipsychotic agents at human dopamine D2 and D3 receptor signaling in Chinese hamster ovary cells. *Psychopharmacology* V150(4):383-390.

Kalani MYS, Vaidehi N, Hall SE, Trabanino RJ, Freddolino PL, Kalani MA, Floriano WB, Kam VWT and Goddard WA, III (2004) The predicted 3D structure of the human D2 dopamine receptor and the binding site and binding affinities for agonists and antagonists. *PNAS* 101(11):3815-3820.

Kanterman RY, Mahan LC, Briley EM, Monsma FJ, Jr., Sibley DR, Axelrod J and Felder CC (1991) Transfected D2 dopamine receptors mediate the potentiation of arachidonic acid release in Chinese hamster ovary cells. *Mol Pharmacol* 39(3):364-369.

Kearn CS, Blake-Palmer K, Daniel E, Mackie K and Glass M (2005) Concurrent Stimulation of Cannabinoid CB1 and Dopamine D2 Receptors Enhances Heterodimer Formation: A Mechanism for Receptor Cross-Talk? *Mol Pharmacol* 67(5):1697-1704.

Kenakin T (1995) Agonist-receptor efficacy II: agonist trafficking of receptor signals. *Trends in Pharmacological Sciences* 16(7):232-238.

J. Robert Lane, 2007

Kenakin T (1997) Differences between natural and recombinant G protein-coupled receptor systems with varying receptor/G protein stoichiometry. *Trends in Pharmacological Sciences* 18(12):456-464.

Kenakin T (2001) Inverse, protean, and ligand-selective agonism: matters of receptor conformation. *FASEB J* 15(3):598-611.

Kenakin T (2003) Ligand-selective receptor conformations revisited: the promise and the problem. *Trends in Pharmacological Sciences* 24(7):346-354.

Kendall RT and Senogles SE (2006) Investigation of the alternatively spliced insert region of the D2L dopamine receptor by epitope substitution. *Neuroscience Letters* 393(2-3):155-159.

Khan ZU, Mrzljak L, Gutierrez A, de la Calle A and Goldman-Rakic PS (1998) Prominence of the dopamine D2 short isoform in dopaminergic pathways. *PNAS* 95(13):7731-7736.

Kikuchi T, Tottori K, Uwahodo Y, Hirose T, Miwa T, Oshiro Y and Morita S (1995) 7-(4-[4-(2,3-Dichlorophenyl)-1-piperazinyl] butyloxy)-3,4-dihydro-2(1H)-quinolinone (OPC-14597), a new putative antipsychotic drug with both presynaptic dopamine autoreceptor agonistic activity and postsynaptic D2 receptor antagonistic activity. *J Pharmacol Exp Ther* 274(1):329-336.

Kim K-M, Gainetdinov RR, Laporte SA, Caron MG and Barak LS (2005) G Protein-coupled Receptor Kinase Regulates Dopamine D3 Receptor Signaling by Modulating the Stability of a Receptor-Filamin- $\beta$ -Arrestin Complex: A CASE OF AUTORECEPTOR REGULATION. *J Biol Chem* 280(13):12774-12780.

Kim K-M, Valenzano KJ, Robinson SR, Yao WD, Barak LS and Caron MG (2001) Differential Regulation of the Dopamine D2 and D3 Receptors by G Protein-coupled Receptor Kinases and  $\beta$ -Arrestins. *J Biol Chem* 276(40):37409-37414.

Kleuss C, Raw AS, Lee E, Sprang SR and Gilman AG (1994) Mechanism of GTP Hydrolysis by G-Protein  $\alpha$  Subunits. *PNAS* 91(21):9828-9831.

J. Robert Lane, 2007

Kostenis E, Conklin BR and Wess J (1997) Molecular Basis of Receptor/G Protein Coupling Selectivity Studied by Coexpression of Wild Type and Mutant m2 Muscarinic Receptors with Mutant G $\beta$ 1;q Subunits. *Biochemistry* 36(6):1487-1495.

Kostenis E, Waelbroeck M and Milligan G (2005) Techniques: Promiscuous G[alpha] proteins in basic research and drug discovery. *Trends in Pharmacological Sciences* 26(11):595-602.

Kuzhikandathil EV, Yu W and Oxford GS (1998) Human Dopamine D3 and D2L Receptors Couple to Inward Rectifier Potassium Channels in Mammalian Cell Lines. *Molecular and Cellular Neuroscience* 12(6):390-402.

Lachowicz JE and Sibley DR (1997) Chimeric D2/D3 Dopamine Receptor Coupling to Adenylyl Cyclase. *Biochemical and Biophysical Research Communications* 237(2):394-399.

Lahti AC, Weiler MA, Corey PK, Lahti RA, Carlsson A and Tamminga CA (1998) Antipsychotic Properties of the Partial Dopamine Agonist (-)-3-(3-Hydroxyphenyl)-N-n-Propylpiperidine (Preclamol) in Schizophrenia. *Biological Psychiatry* 43(1):2-11.

Lai FPL, Mody SM, Yung LY, Kam JYM, Pang CS, Pang SF and Wong YH (2002) Molecular determinants for the differential coupling of G $\beta$ 1;16 to the melatonin MT1, MT2 and Xenopus Mel1c receptors. *Journal of Neurochemistry* 80(5):736-745.

Lambright DG, Noel JP, Hamm HE and Sigler PB (1994) Structural determinants for activation of the [alpha]-subunit of a heterotrimeric G protein. *Nature* 369(6482):621-628.

Lambright DG, Sondek J, Bohm A, Skiba NP, Hamm HE and Sigler PB (1996) The 2.0 A crystal structure of a heterotrimeric G protein. *Nature* 379(6563):311-319.

Landis CA, Masters SB, Spada A, Pace AM, Bourne HR and Vallar L (1989) GTPase inhibiting mutations activate the [alpha] chain of Gs and stimulate adenylyl cyclase in human pituitary tumours. *Nature* 340(6236):692-696.

Landwehrmeyer B, Mengod G and Palacios JM (1993) Dopamine D3 receptor mRNA and binding sites in human brain. *Brain Res Mol Brain Res* 18(1-2):187-192.

J. Robert Lane, 2007

Lavigne N, Ethier N, Oak JN, Pei L, Liu F, Trieu P, Rebois RV, Bouvier M, Hebert TE and Van Tol HHM (2002) G Protein-coupled Receptors Form Stable Complexes with Inwardly Rectifying Potassium Channels and Adenylyl Cyclase. *J Biol Chem* 277(48):46010-46019.

Lee K-W, Hong J-H, Choi IY, Che Y, Lee J-K, Yang S-D, Song C-W, Kang HS, Lee J-H, Noh JS, Shin H-S and Han P-L (2002) Impaired D2 Dopamine Receptor Function in Mice Lacking Type 5 Adenylyl Cyclase. *J Neurosci* 22(18):7931-7940.

Lee SP, O'Dowd BF and George SR (2003a) Homo- and hetero-oligomerization of G protein-coupled receptors. *Life Sciences* 74(2-3):173-180.

Lee SP, O'Dowd BF, Rajaram RD, Nguyen T and George SR (2003b) D2 Dopamine Receptor Homodimerization Is Mediated by Multiple Sites of Interaction, Including an Intermolecular Interaction Involving Transmembrane Domain 4. *Biochemistry* 42(37):11023-11031.

Leff P, Scaramellini C, Law C and McKechnie K (1997) A three-state receptor model of agonist action. *Trends in Pharmacological Sciences* 18(10):355-362.

Lefkowitz RJ, Cotecchia, S., Samama, P., Costa, T. (1993) Constitutive activity of receptors coupled to guanine nucleotide regulatory proteins. *Trends Pharmacol Sci* 14(8):303-307.

Levey AI, Hersch SM, Rye DB, Sunahara RK, Niznik HB, Kitt CA, Price DL, Maggio R, Brann MR and Ciliax BJ (1993) Localization of D1 and D2 Dopamine Receptors in Brain with Subtype- Specific Antibodies. *PNAS* 90(19):8861-8865.

Lew JY, Garcia-Espana A, Lee KY, Carr KD, Goldstein M, Haycock JW and Meller E (1999) Increased Site-Specific Phosphorylation of Tyrosine Hydroxylase Accompanies Stimulation of Enzymatic Activity Induced by Cessation of Dopamine Neuronal Activity. *Mol Pharmacol* 55(2):202-209.

Li-Xin Liu LHBAMGDRSLAC (1999) D2S, D2L, D3, and D4 dopamine receptors couple to a voltage-dependent potassium current in N18TG2 × mesencephalon hybrid cell (MES-23.5) via distinct G proteins. *Synapse* 31(2):108-118.

J. Robert Lane, 2007

Lieberman JA (2004) Dopamine Partial Agonists: A New Class of Antipsychotic. *CNS Drugs* 18:251-267.

Limbird LE, , and Lefkowitz RJ (1978) Agonist-induced increase in apparent beta-adrenergic receptor size. *PNAS* 75(1):228-232.

Lindorfer MA, Myung C-S, Savino Y, Yasuda H, Khazan R and Garrison JC (1998) Differential Activity of the G Protein beta 5gamma 2 Subunit at Receptors and Effectors. *J Biol Chem* 273(51):34429-34436.

Liu J and Wess J (1996) Different Single Receptor Domains Determine the Distinct G Protein Coupling Profiles of Members of the Vasopressin Receptor Family. *J Biol Chem* 271(15):8772-8778.

Liu W, Clark WA, Sharma P and Northup JK (1998) Mechanism of Allosteric Regulation of the Rod cGMP Phosphodiesterase Activity by the Helical Domain of Transducin alpha Subunit. *J Biol Chem* 273(51):34284-34292.

Liu YF, Jakobs KH, Rasenick MM and Albert PR (1994) G protein specificity in receptor-effector coupling. Analysis of the roles of G<sub>0</sub> and G<sub>i2</sub> in GH4C1 pituitary cells. *J Biol Chem* 269(19):13880-13886.

Lundstrom K (2006) Latest Development in Drug Discovery on G Protein-coupled Receptors. *Current Protein and Peptide Science* 7:465-470.

Maggio R, Scarselli M, Novi F, Millan MJ and Corsini GU (2003) Potent activation of dopamine D<sub>3</sub>/D<sub>2</sub> heterodimers by the antiparkinsonian agents, S32504, pramipexole and ropinirole. *Journal of Neurochemistry* 87(3):631-641.

Majumdar S, Ramachandran S and Cerione RA (2004) Perturbing the Linker Regions of the {alpha}-Subunit of Transducin: A New Class of Constitutively Active GTP-Binding Proteins. *J Biol Chem* 279(38):40137-40145.

Majumdar S, Ramachandran S and Cerione RA (2006) New Insights into the Role of Conserved, Essential Residues in the GTP Binding/GTP Hydrolytic Cycle of Large G Proteins. *J Biol Chem* 281(14):9219-9226.

J. Robert Lane, 2007

Malmberg A, Jackson DM, Eriksson A and Mohell N (1993) Unique binding characteristics of antipsychotic agents interacting with human dopamine D2A, D2B, and D3 receptors. *Mol Pharmacol* 43(5):749-754.

Malmberg A, Mikaelis A and Mohell N (1998) Agonist and Inverse Agonist Activity at the Dopamine D3 Receptor Measured by Guanosine 5'-[gamma -Thio]Triphosphate-[35S] Binding. *J Pharmacol Exp Ther* 285(1):119-126.

Mancia F, Brenner-Morton S, Siegel R, Assur Z, Sun Y, Schieren I, Mendelsohn M, Axel R and Hendrickson WA (2007) Production and characterization of monoclonal antibodies sensitive to conformation in the 5HT2c serotonin receptor. *PNAS* 104(11):4303-4308.

Maniatis T, Fritsch EF and Sambrook J (1982) *Molecular Cloning, A Laboratory Manual*.

Marin EP, Krishna AG and Sakmar TP (2001) Rapid Activation of Transducin by Mutations Distant from the Nucleotide-binding Site. Evidence For A Mechanistic Model of Receptor-Catalysed Nucleotide Exchange By G Proteins. *J Biol Chem* 276(29):27400-27405.

McAllister G, Knowles MR, Patel S, Marwood R, Emms F, Seabrook GR, Graziano M, Borkowski D, Hey PJ and Freedman SB (1993) Characterisation of a chimeric hD3/D2 dopamine receptor expressed in CHO cells. *FEBS Letters* 324(1):81-86.

Meador-Woodruff JH, Mansour A, Grandy DK, Damask SP, Civelli O and Watson SJJ (1992) Distribution of D5 dopamine receptor mRNA in rat brain. *Neurosci Lett* 145(2):209-212.

Medkova M, Preininger AM, Yu NJ, Hubbell WL and Hamm HE (2002) Conformational Changes in the Amino-Terminal Helix of the G Protein  $\alpha_{\text{L}}\beta\gamma_{\text{11}}$  Following Dissociation From G beta gamma Subunit and Activation. *Biochemistry* 41(31):9962-9972.

Merkouris M, Dragatsis I, Megaritis G, Konidakis G, Zioudrou C, Milligan G and Georgoussi Z (1996) Identification of the critical domains of the delta-opioid receptor involved in G protein coupling using site-specific synthetic peptides. *Mol Pharmacol* 50(4):985-993.

J. Robert Lane, 2007

Milasta S, Padiani J, Appelbe S, Trim S, Wyatt M, Cox P, Fidock M and Milligan G (2006) Interactions between the Mas-Related Receptors MrgD and MrgE Alter Signalling and Trafficking of MrgD. *Mol Pharmacol* 69(2):479-491.

Millan MJ, Audinot V, Rivet JM, Gobert A, Vian J, Prost JF, Spedding M and Peglion JL (1994) S 14297, a novel selective ligand at cloned human dopamine D3 receptors, blocks 7-OH-DPAT-induced hypothermia in rats. *Eur J Pharmacol* 260(2-3):R3-5.

Millan MJ, Gobert A, Newman-Tancredi A, Lejeune F, Cussac D, Rivet J-M, Audinot V, Dubuffet T and Lavielle G (2000) S33084, a Novel, Potent, Selective, and Competitive Antagonist at Dopamine D3-Receptors: I. Receptorial, Electrophysiological and Neurochemical Profile Compared with GR218,231 and L741,626. *J Pharmacol Exp Ther* 293(3):1048-1062.

Millan MJ, Iob L, Péglion J-L and Dekeyne A (2007) Discriminative stimulus properties of S32504, a novel D3/D2 receptor agonist and antiparkinson agent, in rats: attenuation by the antipsychotics, aripiprazole, bifeprunox, N-desmethylozapine, and by selective antagonists at dopamine D2 but not D3 receptors. *Psychopharmacology* 191(3):767-782.

Milligan G (1993) Regional distribution and quantitative measurement of the phosphoinositidase C-linked guanine nucleotide binding proteins G11 alpha and Gq alpha in rat brain. *J Neurochem* 61(3):845-851.

Milligan G (1994) Specificity and functional applications of antipeptide antisera which identify G-protein alpha subunits. *Methods Enzymology* 237:268-283.

Milligan G (2000) Altering the relative stoichiometry of receptors, G-proteins and effectors: effects on agonist function, in *The pharmacology of functional, biochemical, and recombinant receptor systems* (Angus TKaJA ed) pp 363-389, Springer Verlag KG.

Milligan G (2002) The Use of Receptor G-Protein Fusion Proteins for the Study of Ligand Activity. *Receptors and Channels* 8:309-317.

Milligan G (2003) Principles: Extending the utility of [<sup>35</sup>S]GTP[γ]S binding assays. *Trends in Pharmacological Sciences* 24(2):87-90.

J. Robert Lane, 2007

Milligan G (2007) G protein-coupled receptor dimerisation: Molecular basis and relevance to function. *Biochimica et Biophysica Acta (BBA) - Biomembranes* 1768(4):825-835.

Milligan G, Feng GJ, Ward RJ, Sartania N, Ramsay D, McLean AJ and Carrillo JJ (2004) G Protein-Coupled Receptor Fusion Proteins in Drug Discovery. *Current Pharmaceutical Design* 10:1989-2001.

Milligan G and Kostenis E (2006) Heterotrimeric G-proteins: a short history. *Br J Pharmacol* 147(S1):S46-S55.

Milligan G, Shah, B.H., Mullaney, I., Grassie, M.A.. (1995) Biochemical approaches to examine the specificity of interactions between receptors and guanine nucleotide binding proteins. *J Recept Signal Transduct Res* 15(1-4):253-265.

Missale C, Nash SR, Robinson SW, Jaber M and Caron MG (1998) Dopamine Receptors: From Structure to Function. *Physiol Rev* 78(1):189-225.

Mixon MB, Lee E, Coleman DE, Berghuis AM, Gilman AG and Sprang SR (1995) Tertiary and Quaternary Structural Changes in G $\alpha$  Induced by GTP Hydrolysis. *Science* 270(5238):954-960.

Molinari P, Ambrosio C, Riitano D, Sbraccia M, Gro MC and Costa T (2003) Promiscuous Coupling at Receptor-G $\alpha$  Fusion Proteins. THE RECEPTOR OF ONE COVALENT COMPLEX INTERACTS WITH THE  $\alpha$ -SUBUNIT OF ANOTHER. *J Biol Chem* 278(18):15778-15788.

Moller S, Vilo J and Croning MDR (2001) Prediction of the coupling specificity of G protein coupled receptors to their G proteins. *Bioinformatics* 17(suppl\_1):S174-181.

Montmayeur J and Borrelli E (1991) Transcription Mediated by a cAMP-Responsive Promoter Element is Reduced Upon Activation of Dopamine D2 Receptors. *PNAS* 88(8):3135-3139.

Montmayeur JP, Guiramand J and Borrelli E (1993) Preferential coupling between dopamine D2 receptors and G-proteins. *Mol Endocrinol* 7(2):161-170.

J. Robert Lane, 2007

Moon H-E, Cavalli A, Bahia DS, Hoffmann M, Massotte D and Milligan G (2001a) The human  $\delta$  opioid receptor activates  $G_{i1}\alpha$  more efficiently than  $G_{o1}\alpha$ . *Journal of Neurochemistry* 76(6):1805-1813.

Moon HE, Bahia DS, Cavalli A, Hoffmann M and Milligan G (2001b) Control of the efficiency of agonist-induced information transfer and stability of the ternary complex containing the [ $\delta$ ] opioid receptor and the [ $\alpha$ ] subunit of  $G_{i1}$  by mutation of a receptor/G protein contact interface. *Neuropharmacology* 41(3):321-330.

Mullaney I and Milligan G (2004) Identification and quantitation of G-protein alpha-subunits. *Methods Mol Biol* 259:207-224.

Mullaney I, Shah BH, Wise A and Milligan G (1995) Expression of the Human  $\beta_2$ -Adrenoceptor in NCB20 Cells Results in Agonist Activation of Adenylyl Cyclase and Agonist-Mediated Selective Down-Regulation of  $G_{s\beta_1}$ . *Journal of Neurochemistry* 65(2):545-553.

Myung C-S, Lim WK, DeFilippo JM, Yasuda H, Neubig RR and Garrison JC (2006) Regions in the G Protein  $\gamma$  Subunit Important for Interaction with Receptors and Effectors. *Mol Pharmacol* 69(3):877-887.

Nanoff C, Koppensteiner R, Yang Q, Fuerst E, Ahorn H and Freissmuth M (2006) The Carboxyl Terminus of the G  $\alpha$ -Subunit Is the Latch for Triggered Activation of Heterotrimeric G Proteins. *Mol Pharmacol* 69(1):397-405.

Natochin M, Moussaif M and Artemyev NO (2001) Probing the mechanism of rhodopsin-catalyzed transducin activation. *Journal of Neurochemistry* 77(1):202-210.

Neve KA, Seamans JK and Trantham-Davidson H (2004) Dopamine Receptor Signaling. *Journal of Receptors and Signal Transduction* 24(3):165-205.

Newman-Tancredi A, Cussac D, Audinot V, Pasteau V, Gavaudan S and Millan MJ (1999) G Protein Activation by Human Dopamine D<sub>3</sub> Receptors in High-Expressing Chinese Hamster Ovary Cells: A Guanosine-5'-O-(3-[<sup>35</sup>S]thio)-Triphosphate Binding and Antibody Study. *Mol Pharmacol* 55(3):564-574.

J. Robert Lane, 2007

Newman-Tancredi A, Cussac D, Marini L and Millan MJ (2002) Antibody Capture Assay Reveals Bell-Shaped Concentration-Response Isotherms for h5-HT<sub>1A</sub> Receptor-Mediated Galpha i3 Activation: Conformational Selection by High-Efficacy Agonists, and Relationship to Trafficking of Receptor Signaling. *Mol Pharmacol* 62(3):590-601.

Nikolaev VO, Hoffmann C, Bunemann M, Lohse MJ and Vilardaga J-P (2006) Molecular Basis of Partial Agonism at the Neurotransmitter {alpha}2A-Adrenergic Receptor and Gi-protein Heterotrimer. *J Biol Chem* 281(34):24506-24511.

Noda K, Feng YH, Liu Xp, Saad Y, Husain A and Karnik SS (1996) The Active State of the AT<sub>1</sub> Angiotensin Receptor Is Generated by Angiotensin II Induction. *Biochemistry* 35(51):16435-16442.

O'Dowd BF (1993) Structures of dopamine receptors. *J Neurochem* 60(3):804-814.

O'Dowd BF, Ji X, Alijaniam M, Rajaram RD, Kong MMC, Rashid A, Nguyen T and George SR (2005) Dopamine Receptor Oligomerization Visualized in Living Cells. *J Biol Chem* 280(44):37225-37235.

O'Hara CM TL, Taussig R, Todd RD, O'Malley KL. (1996) Dopamine D<sub>2L</sub> receptor couples to G alpha i2 and G alpha i3 but not G alpha i1, leading to the inhibition of adenylate cyclase in transfected cell lines. *J Pharmacol Exp Ther* 278(1):354-360.

Oldham WM, Hamm, H.E. (2006) Structural basis of function in heterotrimeric G proteins. *Q Rev Biophys* 39(2):117-166.

Oldham WM, Van Eps N, Preininger AM, Hubbell WL and Hamm HE (2006) Mechanism of the receptor-catalyzed activation of heterotrimeric G proteins. *Nat Struct Mol Biol* 13(9):772-777.

Onrust R, Herzmark P, Chi P, Garcia PD, Lichtarge O, Kingsley C and Bourne HR (1997) Receptor and beta gamma Binding Sites in the alpha Subunit of the Retinal G Protein Transducin. *Science* 275(5298):381-384.

Palanche T, Ilien B, Zoffmann S, Reck M-P, Bucher B, Edelstein SJ and Galzi J-L (2001) The Neurokinin A Receptor Activates Calcium and cAMP Responses through Distinct Conformational States. *J Biol Chem* 276(37):34853-34861.

J. Robert Lane, 2007

Palczewski K, Kumasaka T, Hori T, Behnke CA, Motoshima H, Fox BA, Trong IL, Teller DC, Okada T, Stenkamp RE, Yamamoto M and Miyano M (2000) Crystal Structure of Rhodopsin: A G Protein-Coupled Receptor. *Science* 289(5480):739-745.

Parnot C, Bardin S, Miserey-Lenkei S, Guedin D, Corvol P and Clauser E (2000) Systematic identification of mutations that constitutively activate the angiotensin II type 1A receptor by screening a randomly mutated cDNA library with an original pharmacological bioassay. *PNAS* 97(13):7615-7620.

Pascal G and Milligan G (2005) Functional Complementation and the Analysis of Opioid Receptor Homodimerization. *Mol Pharmacol* 68(3):905-915.

Perez DM, DeYoung MB and Graham RM (1993) Coupling of expressed alpha 1B- and alpha 1D-adrenergic receptor to multiple signaling pathways is both G protein and cell type specific. *Mol Pharmacol* 44(4):784-795.

Perez DM, Hwa J, Gaivin R, Mathur M, Brown F and Graham RM (1996) Constitutive activation of a single effector pathway: evidence for multiple activation states of a G protein-coupled receptor. *Mol Pharmacol* 49(1):112-122.

Perez DM and Karnik SS (2005) Multiple Signaling States of G-Protein-Coupled Receptors. *Pharmacol Rev* 57(2):147-161.

Pin JP, Joly C., Heinemann S.F., Bockaert J. (1994) Domains involved in the specificity of G protein activation in phospholipase C-coupled metabotropic glutamate receptors. *EMBO J* 13(2):342-348.

Porter AC, Bymaster FP, DeLapp NW, Yamada M, Wess J, Hamilton SE, Nathanson NM and Felder CC (2002) M1 muscarinic receptor signaling in mouse hippocampus and cortex. *Brain Research* 944(1-2):82-89.

Posner BA, Mixon MB, Wall MA, Sprang SR and Gilman AG (1998) The A326S Mutant of G $\alpha$ 1 as an Approximation of the Receptor-bound State. *J Biol Chem* 273(34):21752-21758.

J. Robert Lane, 2007

Potenza MN, Graminski GF, Schmauss C and Lerner MR (1994) Functional expression and characterization of human D2 and D3 dopamine receptors. *J Neurosci* 14(3):1463-1476.

Preininger AM, VanEps N, Yu NJ, Medkova M, Hubbell WL and Hamm HE (2003) The Myristoylated Amino Terminus of G $\alpha$ 1 Plays a Critical Role in the Structure and Function of G $\alpha$ 1 Subunits in Solution. *Biochemistry* 42(26):7931-7941.

Rasenick MM, Watanabe M, Lazarevic MB, Hatta S and Hamm HE (1994) Synthetic peptides as probes for G protein function. Carboxyl-terminal G alpha s peptides mimic Gs and evoke high affinity agonist binding to beta-adrenergic receptors. *J Biol Chem* 269(34):21519-21525.

Raw AS, Coleman DE, Gilman AG and Sprang SR (1997) Structural and Biochemical Characterization of the GTP $\gamma$ S-, GDP.Pi-, and GDP-Bound Forms of a GTPase-Deficient Gly<sup>42</sup>Val Mutant of G $\alpha$ 1. *Biochemistry* 36(50):15660-15669.

Reavill C, Taylor SG, Wood MD, Ashmeade T, Austin NE, Avenell KY, Boyfield I, Branch CL, Cilia J, Coldwell MC, Hadley MS, Hunter AJ, Jeffrey P, Jewitt F, Johnson CN, Jones DNC, Medhurst AD, Middlemiss DN, Nash DJ, Riley GJ, Routledge C, Stemp G, Thewlis KM, Trail B, Vong AKK and Hagan JJ (2000) Pharmacological Actions of a Novel, High-Affinity, and Selective Human Dopamine D3 Receptor Antagonist, SB-277011-A. *J Pharmacol Exp Ther* 294(3):1154-1165.

Remmers AE, Engel C, Liu M and Neubig RR (1999) Interdomain Interactions Regulate GDP Release from Heterotrimeric G Proteins. *Biochemistry* 38(42):13795-13800.

Rios C, Gomes I and Devi LA (2006) [ $\mu$ ] opioid and CB1 cannabinoid receptor interactions: reciprocal inhibition of receptor signaling and neuritogenesis. *Br J Pharmacol* 148(4):387-395.

Robinson SW and Caron MG (1996) Chimeric D2/D3 Dopamine Receptors Efficiently Inhibit Adenylyl Cyclase in HEK 293 Cells. *Journal of Neurochemistry* 67(1):212-219.

Robinson SW and Caron MG (1997) Selective Inhibition of Adenylyl Cyclase Type V by the Dopamine D3 Receptor. *Mol Pharmacol* 52(3):508-514.

J. Robert Lane, 2007

Robinson SW, Jarvie KR and Caron MG (1994) High affinity agonist binding to the dopamine D3 receptor: chimeric receptors delineate a role for intracellular domains. *Molecular Pharmacology* 46(2):352-356.

Rocheville M, Lange DC, Kumar U, Patel SC, Patel RC and Patel YC (2000) Receptors for Dopamine and Somatostatin: Formation of Hetero-Oligomers with Enhanced Functional Activity. *Science* 288(5463):154-157.

Roof RA, Jin Y, Roman DL, Sunahara RK, Ishii M, Mosberg HI and Neubig RR (2006) Mechanism of Action and Structural Requirements of Constrained Peptide Inhibitors of RGS Proteins. *Chemical Biology & Drug Design* 67(4):266-274.

Samama P, Cotecchia S, Costa T and Lefkowitz RJ (1993) A mutation-induced activated state of the beta 2-adrenergic receptor. Extending the ternary complex model. *J Biol Chem* 268(7):4625-4636.

Scarselli M, Novi F, Schallmach E, Lin R, Baragli A, Colzi A, Griffon N, Corsini GU, Sokoloff P, Levenson R, Vogel Z and Maggio R (2001) D2/D3 Dopamine Receptor Heterodimers Exhibit Unique Functional Properties. *J Biol Chem* 276(32):30308-30314.

Schlachter SK, Poel TJ, Lawson CF, Dinh DM, Lajiness ME, Romero AG, Rees SA, Duncan JN and Smith MW (1997) Substituted 4-aminopiperidines having high in vitro affinity and selectivity for the cloned human dopamine D4 receptor. *European Journal of Pharmacology* 322(2-3):283-286.

Seeman P (2006) Targeting the dopamine D2 receptor in schizophrenia. *Expert Opinion on Therapeutic Targets* 10(4):515-531.

Segal DM, Moraes CT and Mash DC (1997) Up-regulation of D3 dopamine receptor mRNA in the nucleus accumbens of human cocaine fatalities. *Molecular Brain Research* 45(2):335-339.

Seifert R, Gether U, Wenzel-Seifert K and Kobilka BK (1999) Effects of Guanine, Inosine, and Xanthine Nucleotides on beta 2-Adrenergic Receptor/Gs Interactions: Evidence for Multiple Receptor Conformations. *Mol Pharmacol* 56(2):348-358.

J. Robert Lane, 2007

Seifert R, Wenzel-Seifert K, Gether U and Kobilka BK (2001) Functional Differences between Full and Partial Agonists: Evidence for Ligand-Specific Receptor Conformations. *J Pharmacol Exp Ther* 297(3):1218-1226.

Senogles SE (1994) The D2 dopamine receptor isoforms signal through distinct Gi alpha proteins to inhibit adenylyl cyclase. A study with site-directed mutant Gi alpha proteins. *Journal of Biological Chemistry* 269(37):23120-23127.

Senogles SE, Heimert TL, Odife ER and Quasney MW (2004) A Region of the Third Intracellular Loop of the Short Form of the D2 Dopamine Receptor Dictates Gi Coupling Specificity. *J Biol Chem* 279(3):1601-1606.

Seta K, Nanamori M, Modrall JG, Neubig RR and Sadoshima J (2002) AT1 Receptor Mutant Lacking Heterotrimeric G Protein Coupling Activates the Src-Ras-ERK Pathway without Nuclear Translocation of ERKs. *J Biol Chem* 277(11):9268-9277.

Shahinian S, Silvius, J.R. (1995) lipid-modified protein sequence motifs exhibit long-lived anchorage to lipid bilayer membranes. *Biochemistry* 34(11):3813-3822.

Shapiro D, Renock S, Arrington E, Chiodo L, Liu L, Sibley D, Roth B and Mailman R (2003) Aripiprazole, a novel atypical antipsychotic drug with a unique and robust pharmacology. *Neuropsychopharmacology* 28(8):1400-1411.

Shi L and Javitch JA (2002) The Binding Site of Aminergic G Protein-Coupled Receptors: The Transmembrane Segments and Second Extracellular Loop. *Annual Review of Pharmacology and Toxicology* 42(1):437-467.

Shi L and Javitch JA (2004) The second extracellular loop of the dopamine D2 receptor lines the binding-site crevice. *PNAS* 101(2):440-445.

Sidhu A, Kimura K, Uh M, White BH and Patel S (1998) Multiple Coupling of Human D5 Dopamine Receptors to Guanine Nucleotide Binding Proteins Gs and Gz. *Journal of Neurochemistry* 70(6):2459-2467.

Slessareva JE, Ma H, Depree KM, Flood LA, Bae H, Cabrera-Vera TM, Hamm HE and Graber SG (2003) Closely Related G-protein-coupled Receptors Use Multiple and Distinct

J. Robert Lane, 2007

Domains on G-protein  $\alpha$ -Subunits for Selective Coupling. *J Biol Chem* 278(50):50530-50536.

Smotryz JE and Linder ME (2004) Palmitoylation of Intracellular Signalling Proteins: Regulation and Function. *Annual Review of Biochemistry* 73(1):559-587.

Sokoloff P, Diaz J, Foll BL, Guillin O, Leriche L, Bezard E and Gross C (2006) The Dopamine D3 Receptor: A Therapeutic Target for the Treatment of Neuropsychiatric Disorders. *CNS & Neurological Disorders - Drug Targets (Formerly Current Drug Targets - CNS and Neurological Disorders)* 5:25-43.

Sokoloff P, Giros B, Martres M-P, Bouthenet M-L and Schwartz J-C (1990) Molecular cloning and characterization of a novel dopamine receptor (D3) as a target for neuroleptics. *Nature* 347(6289):146-151.

Sondek J, Bohm A, Lambright DG, Hamm HE and Sigler PB (1996) Crystal structure of a G $\alpha$  protein [ $\beta$ ][ $\gamma$ ]dimer at 2.1 Å resolution. *Nature* 379(6563):369-374.

Sovago J, Makkai B, Gulyas B and Hall H (2005) Autoradiographic mapping of dopamine-D2/D3 receptor stimulated [<sup>35</sup>S]GTP $\gamma$ S binding in the human brain. *European Journal of Neuroscience* 22(1):65-71.

Sowell MO, Ye C, Ricupero DA, Hansen S, Quinn SJ, Vassilev PM and Mortensen RM (1997) Targeted inactivation of  $\alpha_2$  or  $\alpha_3$  disrupts activation of the cardiac muscarinic K<sup>+</sup> channel, IK<sub>ACh</sub>, in intact cells. *PNAS* 94(15):7921-7926.

Staley JK and Mash DC (1996) Adaptive Increase in D3 Dopamine Receptors in the Brain Reward Circuits of Human Cocaine Fatalities. *J Neurosci* 16(19):6100-6106.

Stemp G, Ashmeade T, Branch CL, Hadley MS, Hunter AJ, Johnson CN, Nash DJ, Thewlis KM, Vong AKK, Austin NE, Jeffrey P, Avenell KY, Boyfield I, Hagan JJ, Middlemiss DN, Reavill C, Riley GJ, Routledge C and Wood M (2000) Design and Synthesis of trans-N-[4-[2-(6-Cyano-1,2,3,4-tetrahydroisoquinolin-2-yl)ethyl]cyclohexyl]-4-quinolinecarboxamide (SB-277011): A Potent and Selective Dopamine D3 Receptor Antagonist with High Oral Bioavailability and CNS Penetration in the Rat. *J Med Chem* 43(9):1878-1885.

J. Robert Lane, 2007

Stevens PA, Pediani J, Carrillo JJ and Milligan G (2001) Coordinated Agonist Regulation of Receptor and G Protein Palmitoylation and Functional Rescue of Palmitoylation-deficient Mutants of the G Protein G11alpha following Fusion to the alpha 1b-Adrenoreceptor. PALMITOYLATION OF G11alpha IS NOT REQUIRED FOR INTERACTION WITH beta {middle dot} gamma COMPLEX. *J Biol Chem* 276(38):35883-35890.

Strader CD, Fong TM, Tota MR, Underwood D and Dixon RAF (1994) Structure and Function of G Protein-Coupled Receptors. *Annual Review of Biochemistry* 63(1):101-132.

Sukumar M, Ross EM and Higashijima T (1997) A Gs-Selective Analog of the Receptor-Mimetic Peptide Mastoparan Binds to Gs in a Kinked Helical Conformation. *Biochemistry* 36(12):3632-3639.

Surprenant A, Horstman DA, Akbarali H and Limbird LE (1992) A point mutation of the alpha 2-adrenoceptor that blocks coupling to potassium but not calcium currents. *Science* 257(5072):977-980.

Swaminath G, Xiang Y, Lee TW, Steenhuis J, Parnot C and Kobilka BK (2004) Sequential Binding of Agonists to the {beta}2 Adrenoceptor: KINETIC EVIDENCE FOR INTERMEDIATE CONFORMATIONAL STATES. *J Biol Chem* 279(1):686-691.

Tang L, Todd RD, Heller A and O'Malley KL (1994) Pharmacological and functional characterization of D2, D3 and D4 dopamine receptors in fibroblast and dopaminergic cell lines [published erratum appears in *J Pharmacol Exp Ther* 1994 Sep;270(3):1397]. *J Pharmacol Exp Ther* 268(1):495-502.

Teller DC, Okada T, Behnke CA, Palczewski K and Stenkamp RE (2001) Advances in determination of a high-resolution three-dimensional structure of rhodopsin, a model of G-protein-coupled receptors (GPCRs). *Biochemistry* 40(26):7761-7772.

Tesmer JJG, Berman DM, Gilman AG and Sprang SR (1997a) Structure of RGS4 Bound to AlF4--Activated Gi[alpha]1: Stabilization of the Transition State for GTP Hydrolysis. *Cell* 89(2):251-261.

J. Robert Lane, 2007

Tesmer JJG, Sunahara RK, Gilman AG and Sprang SR (1997b) Crystal Structure of the Catalytic Domains of Adenylyl Cyclase in a Complex with Gs{alpha}GTPS. *Science* 278(5345):1907-1916.

Thomas CJ, Du X, Li P, Wang Y, Ross EM and Sprang SR (2004) Uncoupling conformational change from GTP hydrolysis in a heterotrimeric G protein {alpha}-subunit. *PNAS* 101(20):7560-7565.

Urban JD, Clarke WP, von Zastrow M, Nichols DE, Kobilka BK, Weinstein H, Javitch JA, Roth BL, Christopoulos A, Sexton P, Miller K, Spedding M and Mailman RB (2006a) Functional selectivity and classical concepts of quantitative pharmacology. *J Pharmacol Exp Ther*:jpet.106.104463.

Urban JD, Vargas GA, von Zastrow M and Mailman RB (2006b) Aripiprazole has Functionally Selective Actions at Dopamine D2 Receptor-Mediated Signaling Pathways. *Neuropsychopharmacology*.

Usiello A, Baik J-H, Rouge-Pont F, Picetti R, Dierich A, LeMeur M, Piazza PV and Borrelli E (2000) Distinct functions of the two isoforms of dopamine D2 receptors. *Nature* 408(6809):199-203.

Valenzuela D, Han X, Mende U, Fankhauser C, Mashimo H, Huang P, Pfeiffer J, Neer EJ and Fishman MC (1997) G $\alpha_o$  is necessary for muscarinic regulation of Ca<sup>2+</sup> channels in mouse heart. *PNAS* 94(5):1727-1732.

Van Leeuwen DH, Eisenstein J, O'Malley K and MacKenzie RG (1995) Characterization of a chimeric human dopamine D3/D2 receptor functionally coupled to adenylyl cyclase in Chinese hamster ovary cells. *Molecular Pharmacology* 48(2):344-351.

Van Tol HHM, Bunzow JR, Guan H-C, Sunahara RK, Seeman P, Niznik HB and Civelli O (1991) Cloning of the gene for a human dopamine D4 receptor with high affinity for the antipsychotic clozapine. *Nature* 350(6319):610-614.

Vanhauwe JFM, Fraeyman N, Francken BJB, Luyten WHML and Leysen JE (1999) Comparison of the Ligand Binding and Signaling Properties of Human Dopamine D2 and D3 Receptors in Chinese Hamster Ovary Cells. *J Pharmacol Exp Ther* 290(2):908-916.

J. Robert Lane, 2007

Vanhouwe JFM, Josson K, Luyten WHML, Driessen AJ and Leysen JE (2000) G-Protein Sensitivity of Ligand Binding to Human Dopamine D2 and D3 Receptors Expressed in *Escherichia coli*: Clues for a Constrained D3 Receptor Structure. *J Pharmacol Exp Ther* 295(1):274-283.

Vassilatis DK, Hohmann JG, Zeng H, Li F, Ranchalis JE, Mortrud MT, Brown A, Rodriguez SS, Weller JR, Wright AC, Bergmann JE and Gaitanaris GA (2003) The G protein-coupled receptor repertoires of human and mouse. *PNAS* 100(8):4903-4908.

Verrall S, Ishii M, Chen M, Wang L, Tram T and Coughlin SR (1997) The Thrombin Receptor Second Cytoplasmic Loop Confers Coupling to Gq-like G Proteins in Chimeric Receptors. Additional Evidence For A Common Transmembrane Signalling And G Protein Coupling Mechanism in G Protein-Coupled Receptors. *J Biol Chem* 272(11):6898-6902.

Villardaga J-P, Steinmeyer R, Harms GS and Lohse MJ (2005) Molecular basis of inverse agonism in a G protein-coupled receptor. *Nat Chem Biol* 1(1):25-28.

Vivo M, Lin H and Strange PG (2006) Investigation of Cooperativity in the Binding of Ligands to the D2 Dopamine Receptor. *Mol Pharmacol* 69(1):226-235.

Wade SM, Scribner MK, Dalman HM, Taylor JM and Neubig RR (1996) Structural requirements for G(o) activation by receptor-derived peptides: activation and modulation domains of the alpha 2-adrenergic receptor i3c region. *Mol Pharmacol* 50(2):351-358.

Wall MA, Coleman DE, Lee E, Iniguez-Lluhi JA, Posner BA, Gilman AG and Sprang SR (1995) The structure of the G protein heterotrimer Gi[alpha]1[beta]1[gamma]2. *Cell* 83(6):1047-1058.

Wall MA, Posner BA and Sprang SR (1998) Structural basis of activity and subunit recognition in G protein heterotrimers. *Structure* 6(9):1169-1183.

Ward RJ and Milligan G (2005) A Key Serine for the GTPase-Activating Protein Function of Regulator of G Protein Signaling Proteins Is Not a General Target for 14-3-3 Interactions. *Mol Pharmacol* 68(6):1821-1830.

Ward SDC, Hamdan FF, Bloodworth LM, Siddiqui NA, Li JH and Wess J (2006) Use of an in Situ Disulfide Cross-Linking Strategy To Study the Dynamic Properties of the

J. Robert Lane, 2007

Cytoplasmic End of Transmembrane Domain VI of the M<sub>3</sub> Muscarinic Acetylcholine Receptor. *Biochemistry* 45(3):676-685.

Watts VJ, Wiens BL, Cumbay MG, Vu MN, Neve RL and Neve KA (1998) Selective Activation of Galpha o by D2L Dopamine Receptors in NS20Y Neuroblastoma Cells. *J Neurosci* 18(21):8692-8699.

Weiner DM, Levey AI, Sunahara RK, Niznik HB, O'Dowd BF, Seeman P and Brann MP (1991) D1 and D2 Dopamine Receptor mRNA in Rat Brain. *PNAS* 88(5):1859-1863.

Weinstein LS and Shenker A (1993) G protein mutations in human disease. *Clinical Biochemistry* 26(5):333-338.

Weiss JM, Morgan PH, Lutz MW and Kenakin TP (1996a) The Cubic Ternary Complex Receptor-Occupancy Model I. Model Description. *Journal of Theoretical Biology* 178(2):151-167.

Weiss JM, Morgan PH, Lutz MW and Kenakin TP (1996b) The Cubic Ternary Complex Receptor-Occupancy Model II. Understanding Apparent Affinity. *Journal of Theoretical Biology* 178(2):169-182.

Weiss JM, Morgan PH, Lutz MW and Kenakin TP (1996c) The Cubic Ternary Complex Receptor-Occupancy Model III. Resurrecting Efficacy. *Journal of Theoretical Biology* 181(4):381-397.

Wess J (1998) Molecular Basis of Receptor/G-Protein-Coupling Selectivity. *Pharmacology & Therapeutics* 80(3):231-264.

Wess J (2002) Considerations in the design and use of chimeric G protein-coupled receptors. *Methods Enzymol* 343:295-312.

Windh RT, Manning DR and Ravi Iyengar and John DH (2002) Analysis of G protein activation in Sf9 and mammalian cells by agonist-promoted [35S] GT[gamma]S Binding, in *Methods in Enzymology* pp 3-14, Academic Press.

Wise A, Foord SM, Fraser NJ, Barnes AA, Elshourbagy N, Eilert M, Ignar DM, Murdock PR, Stepkowski K, Green A, Brown AJ, Dowell SJ, Szekeres PG, Hassall DG, Marshall

J. Robert Lane, 2007

FH, Wilson S and Pike NB (2003) Molecular Identification of High and Low Affinity Receptors for Nicotinic Acid. *J Biol Chem* 278(11):9869-9874.

Wise A, Gearing K and Rees S (2002) Target validation of G-protein coupled receptors. *Drug Discovery Today* 7(4):235-246.

Wise A, Jupe SC and Rees S (2004) The Identification of Ligands at Orphan G-Protein Coupled Receptors. *Annual Review of Pharmacology and Toxicology* 44(1):43-66.

Wise A and Milligan G (1995) High level expression of mammalian G protein alpha subunit Gq subtypes in Escherichia coli. *Biochem Soc Trans* 23(1).

Wise A and Milligan G (1997) Rescue of Functional Interactions between the alpha 2A-Adrenoceptor and Acylation-resistant Forms of Gi1 alpha by Expressing the Proteins from Chimeric Open Reading Frames. *J Biol Chem* 272(39):24673-24678.

Wise A, Watson-Koken MA, Rees S, Lee M and G. M (1997) Interactions of the alpha2A-adrenoceptor with multiple Gi-family G-proteins: studies with pertussis toxin-resistant G-protein mutants. *Biochem J* 321(3):721-728.

Wolfe SE and Morris SJ (1999) Dopamine D2 Receptor Isoforms Expressed in AtT20 Cells Differentially Couple to G Proteins to Acutely Inhibit High Voltage-Activated Calcium Channels. *Journal of Neurochemistry* 73(6):2375-2382.

Wong S-F (2003) G Protein Selectivity Is Regulated by Multiple Intracellular Regions of GPCRs. *Neurosignals* 12(1):1-12.

Wong SK and Ross EM (1994) Chimeric muscarinic cholinergic:beta-adrenergic receptors that are functionally promiscuous among G proteins. *J Biol Chem* 269(29):18968-18976.

Yamaguchi I, Harmon SK, Todd RD and O'Malley KL (1997) The Rat D4 Dopamine Receptor Couples to Cone Transducin (Galpha t2) to Inhibit Forskolin-stimulated cAMP Accumulation. *J Biol Chem* 272(26):16599-16602.

Yao X, Parnot C, Deupi X, Ratnala VRP, Swaminath G, Farrens D and Kobilka B (2006) Coupling ligand structure to specific conformational switches in the [beta]2-adrenoceptor. *Nat Chem Biol* 2(8):417-422.

J. Robert Lane, 2007

Zaworski PG, Alberts GL, Pregoner JF, Im WB, Slightom JL and Gill GS (1999) Efficient functional coupling of the human D3 dopamine receptor to Go subtype of G proteins in SH-SY5Y cells. *J Biol Chem* 274(6):1181-1188.

Zhang J-H, Chung TDY and Oldenburg KR (1999) A Simple Statistical Parameter for Use in Evaluation and Validation of High Throughput Screening Assays. *J Biomol Screen* 4(2):67-73.

Zhang L, DiLizio C, Kim D, Smyth EM and Manning DR (2006) The G12 Family of G Proteins as a Reporter of Thromboxane A2 Receptor Activity. *Mol Pharmacol* 69(4):1433-1440.

Zhuang X, Belluscio L and Hen R (2000) GOLFAalpha Mediates Dopamine D1 Receptor Signaling. *J Neurosci* 20(16):91RC-.

## **Additional Material**

The following paper is based on work performed as part of this thesis